ANALYSIS AND CONTROL OF POWER SYSTEM HARMONICS

A THESIS

Submitted in partial fulfilment of the requirements for the award of the degree

of

DOCTOR OF PHILOSOPHY

in

ELECTRONICS AND COMPUTER ENGINEERING

by

ASHEESH KUMAR SINGH

DEPARTMENT OF ELECTRONICS AND COMPUTER ENGINEERING
INDIAN INSTITUTE OF TECHNOLOGY ROORKEE
ROORKEE-247 667 (INDIA)

DECEMBER, 2006

INDIAN INSTITUTE OF TECHNOLOGY ROORKEE
ROORKEE

CANDIDATE'S DECLARATION

I hereby certify that the work which is being presented in the thesis entitled **ANALYSIS AND CONTROL OF POWER SYSTEM HARMONICS** in partial fulfilment of the requirements for the award of the Degree of Doctor of Philosophy and submitted in the Department of Electronics and Computer Engineering, Indian Institute of Technology Roorkee, Roorkee is an authentic record of my own work carried out during a period from July 2003 to December 2006, under the supervision of Dr. R. Mitra, Professor, Department of Electronics & Computer Engineering and Dr. G. K. Singh, Professor, Department of Electrical Engineering, Indian Institute of Technology Roorkee, Roorkee.

The matter presented in this thesis has not been submitted by me for the award of any other degree of this or any other Institute.

Ashish

(ASHEESH KUMAR SINGH)

This is to certify that the above statement made by the candidate is correct to the best of our knowledge.

Dr. G. K. Singh
Professor
Department of Electrical Engineering
Indian Institute of Technology Roorkee, Roorkee

Dr. R. Mitra
Professor
Department of Electronics & Computer Engineering
Indian Institute of Technology Roorkee, Roorkee

Date:- 28.12.2006

The Ph.D. Viva-Voce Examination of **Shri Asheesh Kumar Singh** Research Scholar has been held on ..April 12, 2007...

Signature of Supervisors

Signature of External Examiner

ABSTRACT

The conventional power supply systems are designed to operate with sinusoidal waveforms, with the aim to maintain the voltage level at equipment terminal within certain limits. Ideally electrical energy must be supplied at a single constant frequency and specified voltage levels of constant magnitudes. However, this situation is difficult to achieve in practice. The undesirable deviation from a perfect sinusoidal waveform (variations in the voltage magnitude and /or the frequency) is generally expressed in terms of power quality. Power quality (PQ) is the combination of voltage quality and current quality. Voltage quality is concerned with deviations of the voltage from the ideal. The ideal voltage is a single frequency sine wave of constant amplitude and frequency. Current quality is the complementary term to voltage quality with the additional requirement that the current sine wave is in phase with the voltage sine wave. Any compromise with either attribute is a power quality concern.

Globally, increasing trend of liberalization of the energy market and privatization of the power supply industry has made the quality of electrical power an important feature of consumer goods on the market. Deficient quality of electrical power supply results in performance degradation of equipment. In general, the foremost power quality issues can be identified as waveform distortion due to harmonics, voltage unbalance, voltage dips, voltage swells /over-voltages, transients, flicker, and frequency variations etc. Among these, voltage unbalance and harmonics distortion are probably the most degenerative conditions to power quality because of being a steady state condition.

Voltage unbalance is a condition in which the three phase voltages differ in amplitude or are displaced from their normal 120 degree phase relationship or both. The nature of the unbalance includes unequal voltage magnitudes at the fundamental system frequency, under-voltage or over-voltage, fundamental phase angle deviation, and unequal levels of harmonic distortion between the phases. The voltage unbalance is inherent to electrical system

due to unequal phase impedances and unbalanced load distribution and it can exist anywhere in a power distribution system. Power system operation under unbalanced conditions putting worries for the power system engineers.

Rectifiers are widely used in power conversion industries for converting AC power to DC power. However, these rectifiers generate a large amount of current harmonic components back to the input utility side, due to their nonlinear nature. In case of unbalanced voltage supply, these rectifiers produce non-characteristic harmonics and changes in characteristic harmonic pattern. In general, it can contribute for high DC distortion, over-voltages, highly unbalanced currents, protection relay malfunction etc.

The harmonic distortion, and the means of keeping it under control, is a growing concern. This is primarily due to the increase in the number and application of nonlinear power-electronic equipments used in the control of power apparatus and the presence of sensitive electronic equipment. In electrical power systems, the harmful effects of harmonics are very real and they cause various problems in power systems. The control or mitigation of the harmonic distortion may be realized through the use of harmonic filters. Traditionally, passive LC filters have been used to eliminate line current harmonics, to increase the power factor, and thus improving the quality of power system. However, these are tuned to specific loads and are unsuitable for use in power systems with widely varying load currents. Furthermore, their operation depends on the electricity network impedance and the characteristics of the nonlinear load. An undesirable parallel resonance could occur between the source impedance and the shunt filter, at a specific frequency. Accordingly, active power filters (APFs) have been researched, developed and gradually recognized as a feasible solution to the problems caused by nonlinear loads.

APFs are used to eliminate the undesirable harmonics and reactive power components of load currents by injecting equal but opposite compensation currents. One of the most popular active power filters is the shunt active power filter. It is a current controlled device, connected in parallel with the nonlinear load. Classically, a shunt APF is controlled in such a way as to inject harmonic and reactive compensation currents based on calculated reference currents. The injected currents are meant to 'cancel' the harmonic and reactive currents drawn by the non-linear loads.

An increasingly attractive alternative is to use so-called intelligent control schemes involving tools such as expert systems, neural networks, or fuzzy logic. Artificial intelligence (AI) is one of the major fields developed since past four decades, and is popular due to its ability to handle complex problems at difficult situations. The AI techniques like fuzzy logic have already been utilized for harmonic minimization and power quality improvement.

The design of APF under 'fixed load' conditions is the most important observation from the work reported by various authors, though the load is continuously and randomly varying, in practical situations. Therefore, it is considered to design an APF for variable load conditions.

In view of these, there is strong motivation to undertake a thorough and systematic study on effects of power system voltage unbalance on the harmonics injected by an AC-DC rectifier load (nonlinear load), and its impact on AC-DC rectifier performance, and to develop a simple, robust fuzzy logic based active power filter to control the harmonics under variable load conditions.

The first part of this thesis reviews two typical power quality attributes viz. supply voltage unbalance and power system harmonics in terms of their causes and effects. Experimental survey of harmonics injected by various home appliances, equipments and devices is carried out to quantify and compare their individual and combined harmonic distortion.

In second part, a comprehensive study about the impact of source voltage unbalance on the performance of a three-phase AC-DC rectifier has been presented. The study includes the effect of source voltage unbalance on harmonic distortion of different input and output characteristics of the rectifier. Also, the harmonics injected by the rectifier load are investigated in terms of variation in magnitude of different characteristic and non-characteristic harmonics with variable degree of unbalance.

In final part, a simple fuzzy logic based robust active power filter to minimize the harmonics for wide range of variations of load current under stochastic conditions, is proposed, which is found very simple and also capable of maintaining the compensated line currents balanced, irrespective of the unbalance in the load currents. The proposed methodology is extensively tested for wide range of variable loads under stochastic conditions and results are found to be quite satisfactory to mitigate harmonics and reactive power components from the utility current.

ACKNOWLEDGEMENT

I am obliged to express my gratitude to those without whom my work would have been much more difficult or even impossible, to accomplish.

I am deeply indebted to my supervisors Dr. R. Mitra and Dr. G. K. Singh for their invaluable guidance, continuous encouragement, perceptiveness and unlimited support towards accomplishing this work. Despite his busy schedule, Dr. R. Mitra has always shared adequate time for discussions and evaluations in order to complete my project. The valuable discussions with Dr. G. K. Singh gave me many important impulses that contributed considerably to both my technical and personal development. His insightful and gentle guidance gave me a clearer perspective on the scientific process that constitutes research. The discussions, encouragement, sound advice, and critiques made by them were essence to the progress of this work and I feel privileged to have been able to work with them.

I would like to express my gratitude to Dr. S. N. Tiwari and Dr. S. C. Saxena, for their initial motivation and help towards pursuing my doctoral study.

I am thankful to Dr. Vijay Kumar for his constantly help and stimulating support. I am grateful to all members of the department in providing a good working environment. Also, my appreciation goes to Dr. R. K. Arya for his friendship, encouragement, and numerous fruitful discussions. I thankfully acknowledge my friends Anil K. Singh, Solomon Raju and N.P. Patidar for their instant help, and cooperation. I also wish to thank my family for helping me get through the difficult times, and for all the emotional support, companionship, and caring they provided.

Most importantly, I am grateful to my teachers and parents, for everything they have done to shape my life. To them I dedicate this thesis.

(Asheesh Kumar Singh)

CONTENTS

LIST OF FIGURES

LIST OF TABLES

LIST OF ABBREVIATIONS

AC	Alternating Current
ACW	Anti Clock Wise
AF	Attenuation Factor
APF	Active Power Filter
CB	Circuit Breaker
CIGRE	Conseil International des Grands Reseaux Electriques
CW	Clock Wise
DC	Direcct Current
DF	Diversity Factor
DPF	Displacement Power Factor
FFT	Fast Fourier Transform
Fig.	Figure
FLC	Fuzzy Logic Controller
HDD	Hard Disc Drive
HVDC	High Voltage Direct Current
Hz	Hertz
IEC	International Electrotechnical Commission
IEEE	Institute of Electrical and Electronics Engineers
IM	Induction Motor
KVAr	Kilo Volt Ampere reactive

LVUR	Line Voltage Unbalance Rate
MF	Membership Function
NEMA	National Equipment Manufacturer's Association
OV	Over Voltage
PC	Personal Computer
PI	Proportional Integral
PQ	Power Quality
PTHDUF	Phase Total Harmonic Distortion Unbalance Factor
PVUR	Phase Voltage Unbalance Rate
PWM	Pulse Width Modulation
RAF	Ripple Attenuation Factor
RMS	Root Mean Square
THD_I	Total Harmonic Distortion of current
THD_V	Total Harmonic Distortion of voltage
UPS	Uninterruptible Power Supply
UV	Under Voltage
VUF	Voltage Unbalance Factor

LIST OF SYMBOLS

$\cos\varphi$	Displacement Power Factor
C_{DC}	DC link capacitor
D	Distortion (harmonic) power requirement of non-linear loads
I_{sa}*, I_{sb}*, I_{sc}*	Estimated reference currents of phase *A*, *B*, and *C*
I_{sa}, I_{sb}, I_{sc}	Actual sensed currents of phase *A*, *B*, and *C*
I_{max}	Peak value of the supply current
I_L	load current
I_{S_1}	source fundamental current
I_{F_1}	fundamental filter current
L_F	Filter Inductance
m_a	Amplitude modulation factor
m_f	Frequency modulation ratio
n	Order of the harmonics
N	Multiplicity of PC load
P_L	Fundamental active power consumption of load
P_L^H	Harmonic active power consumption of load
P_{Loss}	Power losses of inverter
P_{INV}	Real power supplied by APF inverter

P_{Load}	Net active power consumption of load
P_S	Active power supplied by source
Q_L	Fundamental reactive power consumption of load
Q_L^H	Harmonic reactive power consumption of load
Q_S	Reactive power supplied by source
Q_{Load}	Net reactive power consumption of load
Q_{F_1}	Three-phase reactive power delivered by the APF
S	Apparent power
$V_{DC_{ref}}$	Reference DC link voltage
V_S	Source voltage
V_F	Voltage generated at AC side of PWM converter of the APF
ω	Frequency (rad. /sec.)
φ	Displacement power factor angle
∂_{V_F}, ∂_{I_F}	Phase angles of the fundamental components of voltage and current
V_2	Negative sequence voltage component
V_1	Positive sequence voltage component
V_{ab}, V_{bc}, V_{ca}	Line voltages
V_{an}, V_{bn}, V_{cn}	Individual phase voltages

CHAPTER I

INTRODUCTION

1.1 GENERAL

The aims of the electric power system are to supply electrical energy to terminals of electrical equipment, and to maintain the voltage at the equipment terminals within certain limits. For decades, research and education have been concentrated on the first aim. In an ideal ac power system, energy is supplied at a single constant frequency and specified voltage levels of constant magnitudes. However, this situation is difficult to achieve in practice. The undesirable deviation from a perfect sinusoidal waveform (variations in the magnitude and /or the frequency) is generally expressed in terms of power quality. Due to advances in power system components, the concern for the quality of electric power is increasing very rapidly. The last decade has seen a significant change in components of power systems from being largely linear to partially nonlinear. This change has meant that sensitivity of equipment to disturbances has increased and, therefore, the quality of power is of much concern. Power quality problems encompass a wide range of disturbances that can disrupt the operation of sensitive industrial loads and cause a loss of production. The following power quality problems have been identified [1, 2]:

- Voltage unbalance;
- Voltage and current harmonic distortion;
- Short interruptions;
- Voltage dips;
- Voltage swells /over-voltages;
- Voltage and current transients;
- Voltage flicker;
- Power frequency variations.

Among all power line disturbances, voltage unbalance and harmonics distortion are probably the most degenerative condition to power quality because of being a steady state condition. The power quality problems resulting from power system harmonics have been getting more and more attention by researchers.

Due to the unequal mutual coupling, unbalanced loading, blown fuses on three-phase capacitor banks, abnormal operating conditions during switching, open delta transformer connections, power system would have to operate under unbalanced conditions putting worries for the power system engineers. The three phase AC-DC rectifiers are the most utilized in industrial and commercial applications for economic reasons even though this rectifier employed in power electronic equipment has a poor power factor and generates much harmonics, due to its nonlinear nature. In case of unbalanced voltage supply, these rectifiers produce non-characteristic harmonics and changes in characteristic harmonic pattern. In general, it can contribute for high DC distortion, over-voltages, highly unbalanced currents, protection relay malfunction etc.

Harmonic mitigation is the reduction of harmonic voltage or current distortion. Due to the increased use of nonlinear loads in the power system, large amounts of distorted current and voltage waveforms exist. These nonlinear devices present a two-fold problem with regard to harmonics. Not only do they produce harmonics, but they also are typically more sensitive to the resulting distortion than more traditional power system devices. As the usage of these power-electronic equipment increases, users and utilities are becoming more concerned about the harmful effects of harmonics. The research has been underway for last three decades to have a control over the harmonics and to supply the consumers with reliable and clean fundamental frequency, sinusoidal electric power that does not represents a damaging threat to their equipments. To reduce harmonic distortion, both passive and active compensation techniques (filters) can be implemented.

Traditionally, passive LC filters have been used to eliminate line current harmonics and to increase the power factor. Passive harmonic filters are made of inductive, capacitive, and resistive elements. They are employed either to shunt the harmonic currents off the line or to block their flow between parts of the system by tuning the elements to create a resonance at a selected harmonic frequency (frequencies). When passive filters are connected in series with the power line, they are designed to have large impedance at a certain harmonic frequency. This will isolate the harmonics produced by the loads from reaching the supply system. However, when they are connected in parallel with the power line, they provide a low impedance path for selected harmonic currents to pass to ground, thus preventing them from entering the supply system. Passive LC tuned filters are the most common type of passive filters. In practical applications, passive filters have, however, the following disadvantages:

- They can not compensate for frequency variations;
- Their operation depends on the electricity supply network impedance and the characteristics of the nonlinear loads;
- When the harmonic current components increase, the filter may be overloaded;
- The components of passive filters have ageing and tuning problems;
- Their dimensions and weights are large;
- Parallel resonance between the power system and the passive filter causes amplification of harmonic currents on the source side at a special frequency.

In order to overcome these problems, active power filters (APFs) have been researched and developed, which have gradually been recognized as a feasible solution to the problems created by nonlinear loads. They are used to eliminate the unwanted harmonics and compensate power factor by injecting equal but opposite compensation currents. Active power harmonic filtering is a relatively new technology for eliminating harmonics which is based on sophisticated power electronics devices. An active power filter consists of one or more power electronic converters, which utilize power semiconductor devices controlled by integrated circuits. The use of active power filters to eliminate the harmonics before they enter a supply system is the optimal method of dealing with the harmonics problem. While they do not have the shortcomings of the passive filter, active power filters have some interesting features outlined as follows:

- They can address more than one harmonic at a time and can compensate for other power quality problems such as load imbalance and flicker. They are particularly useful for large, distorting loads fed from relatively weak points on the power system;
- They are capable of reducing the effect of distorted current /voltage waveforms as well as compensating the fundamental displacement component of current drawn by nonlinear loads;

- Because of high controllability and quick response of semiconductor devices, they have faster response than the conventional passive filters;
- They primarily utilize power semiconductor devices rather than conventional reactive components. This results in reduced overall size of a compensator and expected lower capital cost in future due to the continuously downward trend in the price of the solid state switches;

However, the active power filter technology adds to complexity of circuitry (power circuit and control). There will also be some losses associated with the semiconductor switches. Active power filters have proved to be an important and flexible alternative with fast control response to provide compensation for current and voltage harmonics in power distribution system. Depending on the particular application or electrical problem to be solved, APFs can be implemented as shunt type, series type or a combination of shunt and series APFs. The shunts APFs compensate load current harmonics by injecting equal-but-opposite harmonic compensating currents.

1.2 LITERATURE REVIEW

Voltage unbalance is a condition in which the three phase voltages differ in amplitude or are displaced from their normal 120 degree phase relationship or both. The nature of the unbalance includes unequal voltage magnitudes at the fundamental system frequency, under-voltage or over-voltage, fundamental phase angle deviation, and unequal levels of harmonic distortion between the phases. Unbalanced voltages can exist anywhere in a power distribution system. System voltages at the point of utilization can be unbalanced for several reasons. Unbalance is caused by induction furnaces, single-phase loads, displacement of commutation angles in semiconductor devices and non-symmetrical systems impedances.

In general, distribution system voltage unbalance can be attributed to asymmetrical transformer winding impedances, open wye and open delta transformer banks, blown fuses of three-phase capacitor banks, asymmetrical transmission impedances possibly caused by incomplete transposition of transmission lines, unequal transformer tap settings, large single-phase distribution transformer, unequal impedance in conductors of power supply wiring, unbalanced distribution of single-phase loads such as lighting, heavy reactive single-phase loads such as welders, to name a few. Within a user facility, unbalanced voltages can be caused by unbalanced and overloaded equipment and high impedance connections such as bad or loose contacts.

Since past few years, the three phase AC-DC rectifiers are finding great industrial utility and have a wide range of applications, from small rectifiers to large high voltage direct current (HVDC) transmission systems. They are used for electro-chemical process, many kinds of motor drives, traction equipments, controlled power supplies, and many other applications. The static power converters are nonlinear in nature and consequently they generate harmonics into the supply. As a result, the power factor of the converters is usually poor and varies with the load. These converters are designed on the basis of balanced three-phase supply at the fundamental frequency having small voltage and current ripple components permitting the reduction of filtering components resulting in decrease of input losses and magnetic noise in input transformers where used. These advantages can be fully realized only when the three-phase input source voltage is balanced. Due to unbalanced input voltage supply conditions, there is deterioration of rectifier input and output characteristics leading to appearance of non-characteristic harmonics and changes in characteristic harmonics in the input port to the rectifier and undesirable harmonic distortion in the output.

In practical systems, the supply is usually unbalanced to a certain extent, and the problems of harmonic generations are complicated. There is already a body of literature on problem of harmonic generation due to power system unbalance [3, 4]. Reeve et al. [3, 4] investigated the effects of commutation intervals on the harmonic generation at the fixed value of delay angle. Phadke and Harlow [5] also studied the problem of unbalance due to the errors in the delay angle but for a typical delay angle of 90 degree. All previous works were devoted to the mechanisms of harmonic generation only. A methodology to evaluate power system unbalance in the presence of harmonic distortion is proposed in [6]. Analysis of three-phase AC-DC converters under unbalance supply conditions is depicted in [7]. Authors in [8] have presented an analytical method for calculating harmonic currents of a three-phase bridge uncontrolled rectifier with dc filter. The proposed method is based on the frequency domain method and rectifier switching functions. Analytical equations for the harmonic currents on both the dc and ac sides are derived. The results are validated by comparison, with the results of time-domain simulation. Maswood et al. [9] have analyzed the effect of input voltage unbalances on the rectifier input current and on the filter KVA rating. They have also examined the effect of voltage unbalance on the rectifier output voltage, and have proposed a practical solution to eliminate the triplen input current harmonics. Yacamini and Oliveira [10] have described a method of calculating harmonics associated with non-ideal supply conditions. Jouanne and Banerjee [11] have presented a comprehensive summary of the causes and effects of voltage unbalance and have discussed the related standards, definitions and mitigation techniques.

Enjeti and Ziogas [12] have given a method to provide the closed-form expressions for all harmonics under balanced and unbalanced operating conditions. A technique for obtaining the sequence impedance and the equivalent circuit of a power converter at fundamental frequency is described by Hu [13], whose results can be used in the analysis of power converters under unbalanced supply. Another method, based on asymmetrical firing angle, to cancel the second harmonic at the converter output under unbalanced voltage supply was presented by Ngandui [14]. In [15], the effect of unbalance on the harmonics injected by a six-pulse converter drive is studied. In all of these mentioned papers, the authors deal with the modeling of converters through two different points of view, namely time domain analysis and frequency domain analysis. There may be several possible voltage unbalance conditions in a power system, such as three-phase, two-phase and single-phase under-voltage under-voltage magnitude unbalance; two-phase and single-phase angle unbalance; and three-phase, two-phase and single-phase over-voltage magnitude unbalance etc [16].

APFs are an up-to-date, dynamic and adjustable solution to power quality problems, which provide the compensation of harmonics, reactive power and /or neutral currents in ac network [17]. They are used to eliminate the unwanted harmonics and reactive power component of load current by injecting equal but opposite compensation currents. Active power filters are used in industrial and commercial sectors for over two decades. The development of control strategies became the key impetus of the rapid evolution of various APF techniques. Different topologies and control strategies [17-21] have been proposed and practiced, in the past. The common goal of all these strategies is to improve dynamic response of the controller in order to obtain better compensation.

Two fundamental approaches for improving power quality with APF are correction in time-domain [17] and correction in frequency-domain [18]. The advantage of time-domain method is fast response for on-line application without complicated control circuitry. The advantage occurs because time-domain control strategies operate on instantaneous values of the distorted signals rather than on at least one period time delay, as in frequency-domain methods so that the required computational time can be relatively small. The shortcoming of this method is that, in order to obtain optimum results, relatively high switching frequencies are needed, which leads to excessive switching losses in the semiconductor devices. Compensation in frequency-domain is based on the principle of Fourier analysis and periodicity of the distorted voltage or current waveform to be corrected. The basic principle is that FFT is applied to the sensed voltage /current signal. Compensating harmonic components are separated by eliminating the fundamental component and inverse of Fourier transform is applied to derive compensating reference in this domain [17, 18]. The main disadvantage of this technique is the accompanying time-delay sampling and computation of Fourier coefficients. This makes it difficult for real-time application with dynamically varying loads. It is, therefore, only suitable for slowly varying load conditions.

The voltage source shunt APF is the most common type among various topologies of APFs, due to its simple configuration and straight forward installation procedure. The operation of shunt APF is based on injection of harmonic and reactive compensation currents exactly in counter-phase to the load current harmonics, resulting in elimination of harmonic content of the line (supply) current. Thus the mains has to supply only fundamental current.

An increasingly attractive alternative is to use so-called intelligent control schemes involving tools such as expert systems, neural networks, or fuzzy logic. Artificial intelligence is one of the major fields developed since past four decades, and is popular due to its ability to handle complex problem at difficult situations. Artificial intelligence has already been applied to a wide range of power quality [22], power system [23], and power quality applications [24, 25]. A survey of various intelligent techniques is available in [23]. Research on the theory and application of fuzzy logic, one of the alternatives to artificial intelligence, has been growing since its first introduction in mid-1960's [26]. Use of fuzzy logic for harmonic minimization and power quality improvement is not a new issue rather various authors have introduced some innovative methodologies using these tools. A survey of various works using fuzzy logic in power systems is available in [27].

The most important observation from the works reported by various authors for power quality improvement is the design of active power filter under 'fixed load' conditions. However, in practical life, load is not fixed. Hence, there is the need to design an active power filter, which is capable of maintaining the THD according to the specifications decided by universally accepted IEEE norms [28], under variable load conditions.

In view of these, there is strong motivation to undertake a thorough and systematic study on effects of power system voltage unbalance on the harmonics injected by an AC-DC rectifier load (nonlinear load), and its impact on AC-DC rectifier performance, and to develop a simple, robust fuzzy logic based active power filter to control the harmonics under variable load conditions.

1.3 AUTHOR'S CONTRIBUTION

In view of the work revealed by the literature survey made on power system harmonics due to voltage unbalance, and control strategies to mitigate the power system harmonics, an attempt has been made to establish the following contribution in present investigation:

(i) A thorough and systematic research review on the power system harmonics depicting a brief history of power system harmonics; definition of power system harmonics; harmonic sources and its identification; effect of power system harmonics; power system harmonic analysis, and mitigation of harmonics etc;

(ii) Experimental survey of harmonics injected by various home appliances, equipments and devices, which are causing distortion in power system leading to poor supply quality;

(iii) A detailed study on the effect of power system voltage unbalance on the harmonics injected by an AC-DC rectifier load. The variation of different characteristic and non-characteristic harmonics with the degree of unbalance is investigated. The study also includes the effect of source voltage unbalance on harmonic distortion of different input and output characteristics of the rectifier. Since, the voltage sequence components play an important role in describing a more clear view of degree of voltage unbalance, an attempt has been made to identify the impact of sequence voltage components on total harmonic distortion and individual harmonic components in different phases. To describe the unbalance in Total Harmonic Distortion of current (THD_I) in three different phases, a new term "Phase Total Harmonic Distortion Unbalance Factor" (PTHDUF) is introduced;

(iv) Development of a fuzzy-expert system to control the performance of shunt active power filters. The suggested control strategy is simple, cost-effective, efficient, reliable and easily adaptable for randomly and dynamically variable load currents. It provides harmonic current and reactive power compensation simultaneously. With the help of proposed APF control method, this system provides almost unity power factor operation of non-linear loads with harmonic current sources, reactive, and unbalanced components.

1.4 ORGANIZATION OF THE THESIS

The text of the thesis is distributed in six chapters. An outline of each chapter is presented below:

In **Chapter I**, an overview of the impact of power system voltage unbalance on AC-DC rectifier performance, mitigation of power system harmonics is given. An exhaustive survey of shunt active power filter, and the scope of the present work, is followed by the contribution of the author and the format of the thesis.

In **Chapter II**, a detailed research review on the power system harmonics depicting a brief history of power system harmonics; definition of power system harmonics; harmonic sources and its identification; effect of power system harmonics; power system harmonic analysis, and mitigation of harmonics etc. is presented.

Chapter III deals with the survey of various appliances, equipments and devices, which are injecting distortion in power system. Their harmonic contribution together with the harmonic spectrum is measured for some nonlinear loads, which are used very commonly in daily life. Purpose of this survey is to quantify the harmonics generated by different nonlinear loads, to identify the trend of existing level of harmonic distortion and to increase the awareness and concern about the power quality.

Chapter IV is devoted to in-depth study of source voltage unbalance, which is one of many power quality problems. Types, causes and effects of source voltage unbalance in addition to various definitions of voltage unbalance measurement are discussed. A detailed analytical study on the effect of various possible voltage unbalance conditions in the supply system on the harmonics injected by a three-phase AC-DC rectifier is carried out. Different case studies are performed to find out the importance of sequence voltage components in voltage unbalance analysis and an attempt has been made to find out the answer of the question- 'how the composition of voltage unbalance affects the performance?' .

Chapter V presents the development of a new fuzzy logic controller based robust active power filter to minimize the harmonics for wide range of variations of load current under stochastic conditions.

Finally, **Chapter VI** summarizes the main conclusions from the thesis and suggests the areas of future work to complete the research.

Sincere attempts have been made to refer to the original source of references, which are appended at the end.

Based on the research work, one paper has been published in Electric Power Systems Research. Four papers are under review in IEEE Trans. Power Delivery, International Journal of Electrical Power and Energy Systems and Electric Power Systems Research. In addition, three papers has already published in IEEE sponsored Conferences.

Paper Published in Referred Journals /Conferences

1. Singh, G. K., Singh, A. K., and Mitra, R., 'A Simple Fuzzy Logic Based Robust Active Power Filter for Harmonics Minimization under Random Load Variation', Electric Power Systems Research (in Press- doi:10.1016/j.epsr.2006.09.006).
2. Singh, A. K., Singh, G. K., and Mitra, R., 'Some Observations on AC-DC Rectifier Performance under Source Voltage Unbalance', IEEE Conf. The 38th North American Power Symposium (ISBN: 1-4244-0228-X /06), NAPS-2006, September 17-19, 2006, Carbondale, USA, pp. 309-312.
3. Singh, A. K., Singh, G. K., and Mitra, R., 'Impact of Source Voltage Unbalance on AC-DC Rectifier Performance', IEEE Conf. The Second International Conference on Power Electronics Systems and Applications (ISBN: 962-367-544-5, IEEE catalogue no.: 06EX1618), PESA06, November 12-14, 2006, Hong Kong, pp. 96-101.
4. Singh, A. K., Singh, G. K., and Mitra, R., 'Evaluation of Harmonic Distortion under Unbalanced Supply Conditions', IEEE International Conference on Industrial Technology (ISBN: 1-4244-0726-5, IEEE catalogue no.: 06TH8924C), ICIT 2006, December 15-17, 2006, Mumbai, INDIA, pp. 2569-2574.

CHAPTER II

POWER SYSTEM HARMONICS - AN OVERVIEW

2.1 INTRODUCTORY REMARKS

Harmonics have existed in power systems since the very early stage of ac system development. The issue has, however, recently added significance by the simultaneous setting of two trends: the electric utility's increased concern to improve power factor to avoid penalty, and the wide-ranging addition of power electronic equipments in modern industry seeking higher system reliability and efficiency. The electric utility's increased use of capacitor banks attempting an improved power factor and large-scale addition of nonlinear devices has resulted in the distortion of the steady state ac current and voltage waveform called 'harmonics' or 'power system harmonics'. Harmonics can be defined as the undesirable spectral components of a distorted periodic waveform whose frequencies are integer (non-integer, in case of inter-harmonics) multiples of the fundamental frequency. The effects of these harmonics are failure of electrical /electronic components, overheating of neutral wires, transformer heating, and failure of power factor correction capacitors, losses in power generation and transmission, interference with protection, control and communication networks as well as customer loads.

In addition to their fast proliferation in various areas, electronic equipment has undergone great technological transformation becoming more powerful, versatile and smaller, they have also become more demanding in terms of power quality needed for them to function. Conventional power supply systems are designed to operate with sinusoidal waveforms. Electric utilities further strive to supply consumers with reliable and good quality fundamental-frequency sinusoidal electric power that is not damaging to their equipments.

These three contravening situations have set the basis for paying considerable attention to the quality of electric power and seriously addressing the issue of current and voltage distortion, a major form of which is harmonic distortion. This chapter, therefore, deals with a state-of-the-art discussion on power system harmonics, highlighting the analytical and technical considerations as well as various issues addressed in the literature towards the practical realization of this technology to supply consumers with reliable and acceptable quality electric power.

2.2 A BRIEF HISTORY OF POWER SYSTEM HARMONICS

The problem of power system harmonics is not new. To put the subject in historical perspective, it is necessary to go back the 18th and 19th centuries when various mathematician in general and Fourier in particular set up the basis for harmonic calculations [29]. A brief history of the power system harmonics [30], and first engineering publications and events that dealt with non-sinusoidal voltage and current waveform is given in [31]. In 1894, for the first time word 'harmonic' was used in paper written by Houston and Kennelly [32]. Without use of equations, this paper presents the basic properties of periodic curves in a concise manner. Indeed, this paper meant to popularize the concept of harmonics, explains that a superposition of such series of harmonics upon a plain sinusoidal fundamental wave will produce such a resultant (non-sinusoidal) wave. The lack of even harmonics in any practical ac circuit as well as the effect of the 3rd harmonic on the waveform and peak value of an alternating voltage is demonstrated using simple graphical interpretations.

In 1907, the concept of Harmonic Phasor Cancellation Technique was proposed by Adams [33], which became the most effective tool for building alternators with minimal distortion of voltage and current waveforms. The resonance question started to be well understood by a larger engineering population only in the early 1900's [34, 35]. The reasons for slow progress in the comprehension of the ac phenomena, especially the current and voltage distortion related ones are detailed by Lincoln in 1913 [36]. He puts the blame on two items: the unavailability of a ready and inexpensive method of determining wave shapes, and extremely limited practical experience.

With reference to power system harmonics, it was largely in Germany in the 1920s and 1930s when the subject of waveform distortion caused by static converters was developed. The most influential source of converter theory published during that period in the English language is the book by Rissik [37]. A classical paper on harmonic generation by static converters was written by Read in 1945 [38] and is still used by the designers today. During the 1950s and 10960s, the study of converter harmonics was advanced in the field of high voltage dc transmission. During this period a large number of papers were published. These are summarized in a book by Kimbark [39], which contains over 60 references in the field of power system harmonics. An extensive bibliography was produced in IEEE Power System Harmonics Working Group Report in 1984 [40].

Utilities recognized the consequences of harmonics in 1920s and 1930s when distorted voltage and current waveforms were observed on transmission lines. Concern over harmonic distortion has ebbed and flowed during the history of electric power systems. Steinmetz [41] published a book in 1916 that devoted considerable attention to the study of harmonics in three-phase power systems. His main concern was 3rd harmonic currents caused by saturated iron in transformers and machines, and he was the first to propose delta connections for blocking 3rd harmonic currents. Later, with the advent of rural electrification and telephone service, power and telephone circuits were often placed on common rights-of-way. Harmonic currents produced by transformer magnetizing currents caused inductive interference with open-wire telephone systems. The interference was so severe at times that the voice communication was impossible. The problem was studied and alleviated by filtering and by placing design limits on transformer magnetizing currents. Today, the most common sources of harmonics are power electronic loads such as adjustable-speed drives (ASDs) and switch-mode power supplies [42].

Significant efforts have been made in the past two decades to improve the management of harmonics in power systems. Standards [28, 43] for harmonic control have been established. Sophisticated instruments for harmonic measurements are readily available. The area of power system harmonic analysis has also experienced significant developments and well-accepted component models, simulation methods and analytical procedures for conducting harmonic studies have been established. Harmonic studies are becoming an important component of power analysis and design.

2.3 DEFINITION OF POWER SYSTEM HARMONICS

Harmonics can be defined as a sinusoidal component of a periodic wave having a frequency that is an integral multiple of the fundamental frequency. A distorted periodic wave of any conceivable shape can be composed by using different harmonic frequencies with different amplitudes. Conversely, any distorted periodic wave can be decomposed into a fundamental wave and a set of harmonic waves. This decomposition process is called Fourier analysis. With this technique, the effects of nonlinear elements in power systems can be systematically analyzed.

Non-characteristic harmonics are those that are not integer multiples of the fundamental power frequency, and are usually called 'Inter-harmonics'. A major source of inter-harmonics is the cycloconverter [44]. One special subset of inter-harmonics is called 'Sub-harmonics'. Sub-harmonics have frequency values that are less than that of the fundamental frequency. Lighting flicker is one indication of the presence of sub-harmonics. A well-known source of flicker is the arc furnace [45]. Sub-harmonics do not have any official definition but they are a special case of inter-harmonics for frequency components less than the fundamental. The mathematical definitions of harmonic, interharmonic and sub-harmonic are given in Table 2.1.

Table-2.1: Mathematical Definitions of Harmonic, Inter-harmonic and Sub-harmonic

Term	Definition	Remark
Harmonic	$f = n * f_1$	n is an integer > 0
DC	$f = 0\ Hz$	$f = n * f_1$, where $n = 0$
Interharmonic	$f \neq n * f_1$	n is an integer > 0
Sub-harmonic	$0 < f < f_1$	-
here, f_1 is the fundamental (main) frequency		

The inter-harmonics create some new additional problems like sub-synchronous oscillations, light flicker, voltage fluctuations etc besides the typical problems caused by the harmonics (overheating, useful life reduction etc.). The presence of inter-harmonic components strongly increases difficulties both in modeling and measuring of the distorted waveforms. This is mainly due to the variability of the frequency and amplitude of inter-harmonics and consequently, of the waveform periodicity, and to a great sensitivity to the spectral leakage phenomenon. The detailed study about the inter-harmonics is given in [46-57].

In [47], impact of induction furnace inter-harmonics on distribution systems is given. The basic characteristic of the induction furnace load and experience with an actual case study is described. Several alternatives for addressing the problem are presented, including modifications to induction furnaces, reconfiguration of the power supply, and flickering action. The impact of utilities deregulation on the identification and mitigation of such problems is also discussed. Sharaf and Abu-Azab [48] have addressed a novel low cost parallel capacitor compensation scheme, employing time-dependent loads controlled by a pulse width modulated two loops dynamic controller to ensure enhanced power quality, reduced supply system harmonics, increased energy utilization and reduced source energy. In [49], Zhezhelenko et al have presented a new approach to investigation of harmonics in power supply systems and have recommended the use of Fourier transform instead of Fourier series expansion for the analysis of inter-harmonics, because it allows a spectrum composition of inter-harmonics by the known characteristics of nonlinear harsh loads. Paper [50] proposes a new frequency domain approach for obtaining harmonics, inter-harmonics and unbalances of arc furnaces. The model is based on the calculation of zero crossings along a reference period by means of the solution of a set of non-linear equations. This model has been integrated in an iterative harmonic analysis where harmonic balance equations have been extended to treat inter-harmonic frequencies. Newton's method is applied to solve the current zero crossing of the model as well as the harmonic balance equations. Jacobian matrix presents a sparse structure for very fast calculation. Paper [51] reports the results obtained for the simultaneous measurement of inter-harmonics and flicker in a low voltage distribution system and the effect of harmonic distortion on the voltage tolerance of equipment. Authors also conclude that the voltage tolerance of equipment depends on the harmonic distortion in voltage supply, with equipment being more sensitive to low order harmonics. In [52], harmonic and inter-harmonic estimation of non-stationary signal is presented based on wavelet transform. Non-stationary signal, harmonics and inter-harmonics is decomposed into sub-band frequency using discrete wavelet transform. Here the wavelet filter uses Daubechies wavelet. Authors in paper [53] have proposed a method to standardize the harmonics and inter-harmonic measurement by the IEC [58, 59]. This method utilizes Discrete Fourier Transform (DFT) performed over a rectangular time window of exactly 10 cycles for 50 Hz or 12 cycles for 60 Hz systems, corresponding in both cases to 200 ms approximately. They have suggested applying Phase Locked Loop or other line frequency synchronization techniques to reduce the errors in frequency components due to spectral leakage effects. In [54] by De-Rosa et al, the inter-harmonic generation process has been addressed with reference to high power adjustable-speed drives (ASDs) based on double stage conversion systems using line commutated PWM inverters. Formulas to forecast the inter-harmonic frequencies have been developed and a proper symbolism has been proposed to recognize the inter-harmonic origins. Numerical analysis has been performed for ASDs for all possible frequencies, giving a comprehensive insight in the complex behavior of inter-harmonic component frequencies. Some characteristic aspects, such as the degeneration of inter-harmonic components in harmonics or the overlapping of a couple of inter-harmonics of different origins, have been highlighted. Testa in his paper [55] has addressed the issues related to the inter-harmonic modeling and simulation. Starting from the basic mathematical aspects, attention has been given to the inter-harmonic frequency and amplitude variability. The classical model developed for harmonic modeling is extended to include inter-harmonics with particular attention to the problem of frequency resolution and of computational burden. Researchers in [56] have analyzed the problems in inter-harmonic definition, detection and measurement. They have provided several practical recommendations for inter-harmonics. Hume et al [57] has presented a fast and accurate method for the direct calculation of non-characteristic frequencies occurring around HVDC links. The technique calculates small signal linearized frequency cross coupling interrelationships for both converters about a base operating point, modeling the coupling with matrix transfers. The full system consisting of ac and dc systems is modeled by connecting all individual transfers together with the appropriate system equations and nodal analysis. The returned sub-synchronous frequencies and the effect of switching instant variation are discussed. The method is validated against time-domain simulation, for two different asynchronous links. The significant findings of the studies may be summarized as follows:

- The presence of inter-harmonics introduces analysis and measurement difficulties due to the change of waveform periodicity and to inter-harmonic small amplitudes, which mean high sensitivity to de-synchronization problem;
- Inter-harmonics near fundamental or harmonics could cause light flicker. But these components are not easy to detect due to leakage or resolution limit;
- There are some genuine inter-harmonic sources. When ac-dc-ac type device connects two different frequencies, it may introduce inter-harmonics. The frequencies of inter-harmonics are determined by the topology of the converter (pulse number) and the output frequency. When waveform appears modulated, there is good chance that inter-harmonics exist;
- Hanning windowing is compatible with inter-harmonic grouping and improves sensibly the result accuracy;
- The synchronized process technique, as those based on Phase Locked Loop, is sensitive to uncertainty in the estimation of the actual fundamental frequency; only

averaging the instantaneous estimated values and utilizing the Hanning window gives reliable results;

- The desynchronized process technique based on harmonic filtering gives very accurate and stable results together with considerable advantages in terms of FFT utilization without re-sampling, with sampling frequency chosen with reference only to the rated value of the system fundamental frequency, independently from its time fluctuations;
- Non-stationary signal is a major source producing non-integral bins, but they are not real inter-harmonics. They are attributed to the violation of basic DFT assumption: stationary and periodical;
- In order to identify inter-harmonics correctly, the window size should be selected to ensure that frequency resolution is the common divider of all components in the signal.
- The voltage-current correlation, wave shape check or inter-harmonic-harmonic co-existence, may help to recognize if the non-integral components are real inter-harmonics;
- Zero-padding is helpful for spectrum readability improvement. It can be used to locate the inter-harmonic frequency;
- If inter-harmonics do exist, the voltage and current spectra should show correlation;
- Inter-harmonics usually co-exist with harmonics;
- Use of long window size if applicable will be advantageous to locate the inter-harmonics;
- If magnitude of a signal appears modulated, it is very likely that the signal contains inter-harmonics;
- The 5 Hz resolution and group harmonic /inter-harmonic concept as recommended by the IEC [58] and IEEE [59] might not be sufficient for inter-harmonic detection especially for those inter-harmonics that cause flickers.

2.4 HARMONIC SOURCES AND ITS IDENTIFICATION

Generally, sources of harmonics can be classified as [60]:

(i) Power electronic equipment including variable speed drives, uninterruptible power supplies UPS's, rectifiers, switched mode power supplies and SCR-controlled systems;

(ii) Arcing equipment including arc furnaces as well as fluorescent and mercury lights;

(iii) Saturable devices such as transformers, motors and generators.

Identification of harmonic sources in a power system has been a challenging task for many years. Several methodologies for detecting harmonic sources have been applied to calculate the harmonic contributions at the point of common coupling. The most common tool to solve this problem is the harmonic power direction based method [61-63] in which the symmetrical balanced or unbalanced and symmetrical three-phase harmonic power flows are detected. Another group of practical methods for harmonic source detection is to measure the utility and customer harmonic impedances and then calculate the harmonic sources behind the impedances. There are number of variations of this method [64-67]. Although this type of method is theoretically sound, it is very difficult to implement because the impedances can only be determined with the help of disturbances. Such disturbances are not readily available from the system or are expensive to generate with intrusive means. Reference [68] presents a projection and superposition method to detect harmonic contributions between supply and customer sides. Most of them use the Norton's model to express the harmonic equivalent circuit, and the analysis is focused on the equivalent harmonic current source. Chen et al [69] have used the Thevenin's equivalent circuit to express the harmonic equivalent systems and find out the relationship between the harmonic impedance and harmonic voltage sources through the one point measurements at the point of common coupling. Critical impedance is introduced to measure the harmonic equivalent voltage source which is called critical impedance method. The method can detect which side has more contributions on harmonic distortion at point of common coupling. In [70], authors have proposed a new method to determine whether the utility or the customer side has more contribution to the harmonic currents measured at the point of common coupling. The method is based on the idea that the direction of harmonic reactive power, instead of active power, is more reliable indicator on the location of dominant harmonic sources. The method needs approximate impedance information. Paper [71] describes a reverse power flow procedure to identify the sources of harmonic signals in electric power systems.

A harmonic power flow study is a technique whereby line currents and bus voltages at harmonic frequencies are calculated. This procedure may be Newton-Raphson based technique [72-75] or a technique based on the injection current response of the network [74, 75]. In each of these methods, the signal level at harmonic sources must be known, estimated or calculated. However, if the source of harmonic signal is not known, a practical engineering question may be to identify the location and type of harmonic source. The author in his paper [71] has used least square estimators to identify the location of harmonic sources. The identification is based on the fact that in a linear transmission network, active power associated with voltage and current of the same frequency is conserved. The author further concludes that inaccuracies occur due to losses, estimation errors and modeling errors. In [76], a method of statistically describing system harmonic voltages in terms of parameters of the harmonic current sources is presented. It is shown that a large number of sources, a complete probabilistic characterization of the harmonic voltages can be found in terms of the 2^{nd} order moments of each current phasor's rectangular components. Paper [77] reports a superposition-based current and voltage indices to quantify the contribution of harmonic sources. Using these indices, the validity of the power direction method for harmonic source determination is investigated. The main findings of these works are summarized as follows:

- It is the source magnitudes instead of phase angles that are of main interest for the harmonic source detection problem. The direction of active power is mainly affected by the relative phase angle between the two harmonic sources;
- The direction of active power is mainly affected by the source magnitudes and that of the reactive power by the phase angles. The implication of this conclusion is that the characteristic of the circuit impedance (R-X ratio) will affect the reliability of the active or reactive power-direction-based harmonic source detection methods;
- The metering point or the relative size of the source and the customer impedances will also affect the direction of either active or reactive powers. This is another important factor that makes the power-direction-based methods unreliable.

2.5 EFFECTS OF HARMONICS

Harmonics have the effect increasing equipment copper, iron, dielectric losses and thus the thermal stress. A detailed study is provided in [78-84]. In paper [78], the effects of harmonics on converter transformer load losses are discussed. Authors have described a simple method of loss calculation which has the potential for application at design stage. Variation of losses with the converter firing angle, with the transformer reactance and with the load has also been discussed in the paper. Reference [79] reports the state-of-knowledge of the effects of power system harmonics on equipment. The general mechanism presented is thermal overloading, disruption and dielectric stressing. The equipment considered adjustable-speed drives, capacitors, circuit breakers, fuses, conductors, electronic equipment, lightning, metering, protective relays, rotating machines, telephones and transformers. Massey [80] has introduced a method of estimating the composite harmonic current generated by the operation of several nonlinear loads connected to a single power distribution transformer. The author draws upon the information available from industry and proposes an intuitive expansion of the current available 'K-factor' calculation. The proposed expansion provides a useful tool in specifying properly designed dry-type power distribution transformers for operation in a non-sinusoidal load environment. Paper [81] is concerned with the effect of both harmonic voltage and current distortion on power transformer loss of life. The influence of possible dc current components is also taken into account. Using this, a complete frequency domain equivalent circuit has been proposed that includes harmonics, the dc current and the asymmetrical magnetizing current. It has been shown that the influence of typical harmonic voltage is not a matter of great concern as for as temperature increase and loss of life are concerned. However, the influence of harmonic current distortion within the normal range typically produced has shown to be of importance when transformer operating temperature and loss of life are concerned. Author further states that small dc components (up to the RMS magnitude of the magnetizing current at rated voltage) have no significant effect on the thermal conditions and transformer loss of life. In [82], authors have focused attention on the evaluation of harmonic pollution in traction line voltage and current waveforms. Attempt was made to experimental research aimed at determining the dc voltage wave shapes that may statistically occur on any railway line subjected to heavy traffic. Paper [83] presents the degradation mechanism for all film PC, with emphasis on the activities of partial discharges. A methodology for the evaluation of the influence of harmonic in the degradation of PC, based on the applied voltage and its respective waveform, is developed. Based on the above studies, the general expression for the power dissipated in pure resistance, inductance and capacitance are:

The active power dissipated in a pure resistance is

$$P_R = 1 + THD_V^2 = \sum_{n=1} V_n^2, \qquad \text{or}$$

$$P_R = 1 + THD_I^2 = \sum_{n=1} I_n^2 \tag{2.1}$$

The reactive power absorbed by an inductor is given by

$$Q_L = \sum_{n=1} n.I_n^2 = \sum_{n=1} V_n^2 / n \tag{2.2}$$

The reactive power delivered by a capacitor is given by

$$Q_C = \sum_{n=1} I_n^2 / n = \sum_{n=1} nV_n^2 \tag{2.3}$$

Similarly, the iron (core) losses are given by

$$P_h = \sum_{n=1} n.I_n^{1.6} \tag{2.4}$$

$$P_e = \sum_{n=1} n^2.I_n^2 \tag{2.5}$$

$$P_i = P_h + P_e \tag{2.6}$$

where, P_R is the total active power loss (in p.u.) in the resistance, Q_L is the total p.u. reactive power absorbed by the inductor, Q_C is the total p.u. reactive power delivered by the capacitor, P_h is the total p.u. Hysteresis loss, P_e is the total p.u. eddy current loss, V_n is the n^{th} harmonic voltage in p.u. of the rated voltage, I_n is the n^{th} harmonic current in p.u. of the rated current.

Harmonics result in increased losses and equipment loss-of-life. Triplen harmonics result in the neutral carrying a current, which might equal or exceed the phase currents even the loads are balanced leading to derating or oversizing of neutral wires. The noticeable findings are:

- Capacitors are overloaded by harmonic currents, since the fact that their reactance decreases with frequency makes them act as sinks for harmonics. Also, harmonic voltages produce large currents causing capacitor fuses to be blown;

- Capacitors combine with source inductance to form a parallel resonant circuit. In the presence of resonance, harmonics are amplified. The resulting voltages excessively exceed the rated voltage leading to capacitor damage or blown fuses;
- Increased load losses, which comprises copper losses and stray losses (winding eddy current loss) in transformer. The increase in the later is the most significant factor in determining the additional transformer core heating losses due to non-linear loads;
- Increased hysteresis and eddy-current losses in transformer. However, temperature rise in the core due to the increased iron losses is less critical than in the winding;
- Increased possibility of resonance between the power factor correction capacitors and transformer inductance;
- Increased insulation stress in transformer due to the increased peak voltages;
- Increased copper and iron losses in rotating machines resulting in heating and derating of the machine;
- Presence of harmonics in the supply system results in torque pulsations in electrical machine;
- Harmonics affect the interruption capability of circuit breakers;
- Malfunctioning of the metering and instrumentation devices. Harmonics also impair the operation of electronic equipment and control circuits through the shifting of zero crossing;
- Harmonics result in interference with telephone circuits through inductive coupling;
- Harmonics interfere with customer loads. This is of special concern in computer systems;
- Relays whose operation is governed by the voltage /current peak or zero voltage are affected by harmonics. Electromechanical relays time delay characteristics are changed in the presence of harmonics. Ground relays cannot distinguish between zero sequence and third harmonic currents resulting in erroneous tripping.

2.6 HARMONIC ANALYSIS

Harmonic analysis aims at predicting the harmonic distortion at one or more locations in the power network. Such a study can be done to estimate the effect of a new non-linear load or of the installation of a harmonic filter. There are two distinctly different methods of harmonic analysis.

(i) Time Domain Study: The system (i.e. network and load) are modeled in detail after which a time-domain study is done resulting in the actual waveforms. The harmonic components are obtained by applying a Fourier transform to the waveforms;

(ii) Frequency Domain Study: A separate system model is made for each frequency component included in the study. Each single-frequency model is relatively simple as it only needs to be valid for that specific frequency. The resulting models are the same used for fundamental frequency analysis resulting in complex voltages and currents. The main difference, and also the main difficulty, is in the choice of the impedance values. Especially for higher frequency components, different models are needed because the various capacitive currents become significant, but the calculation methods remain the same. More details of frequency domain studies are found in [85].

The term 'harmonic analysis' is normally used for the second method, but the first method will equally result in a harmonic spectrum. The reason that the second method is most commonly used is its simplicity as the same analysis method can be applied to harmonic components as to the fundamental frequency. The basic assumptions behind this method are that nonlinearity is restricted to a limited number of components and that the current waveform of a nonlinear component is not significantly affected by the voltage waveform. References [86-106] embody the detailed study about the power system harmonic analysis.

Paper [86] describes the new iterative procedures using FFT algorithm for the harmonic studies of three-phase transformer banks with various connections under steady state operating conditions. The paper states that the accuracy depends upon the number of linear segments used for the approximation of the magnetization curve. Any higher harmonic of interest can be predicted as long as the sampling frequency is increased accordingly. Also it was observed that if the input voltage is odd (or even) symmetric in case of a grounded wye or ungrounded wye connection, the current waveform will be even (or odd) symmetric. Authors of the paper [87, 88] have presented a multiphase harmonic load flow solution technique for analyzing the harmonic problems in power system caused by the operation of nonlinear devices under unbalanced condition. Control characteristic of the static compensator and the comparison with field test results are also included. Arrillaga and Callaghan [89] have questioned the validity of assuming fundamental frequency load flow conditions of ac-dc to be unaffected by the presence of harmonics, and have presented an algorithm, which is capable of determining the load flow conditions in the presence of harmonics. The algorithm takes root in the standard three-phase ac-dc load flow, and in IHA (iterative harmonic analysis). The integration of the two algorithms has been described in detail with computational efficiency in mind. Authors in paper [90] have presented a new harmonic power flow for unbalanced systems. It allows the analysis of characteristic and non-characteristic harmonics generated by nonlinear loads in their interaction with the utility network. The developed procedure based on the interaction of a fundamental frequency power flow subprogram and an iterative harmonic subprogram, in which conventional and non-conventional loads are treated in terms of power. The ac linear network is represented by a generalized Thevenin's equivalent with respect to the nonlinear loads, obtained from the power flow solution. Paper [91] presents the implementation of a Newton type harmonic steady state calculation method for initializing time domain solutions in the EMTP. It uses a generalized and theoretically supported formulation of the harmonic Norton equivalent modeling of nonlinear branches with simplified harmonic coupling, and states that there is no requirement for analytical formulation of nonlinear branch characteristics or pre-calculated knowledge of fundamental frequency behavior. Another generalized harmonic balance method for EMTP initialization for the steady state analysis of power system models is reported in [92]. In reference [93], a new frame of reference for harmonic analysis of power system has been described. In this structure of harmonic domain, the network bus bars and coupling between phases and between harmonics are explicitly represented.

Vittek et al [94] have reported the time advantages analysis of *m*-phase symmetrical inverter systems in complex plain. Equations of characteristic values of voltage and current waveforms in the complex domain are developed. In [95], an overview of the methods for calculation of ac /dc converter harmonics has been described. Comparison of all the harmonic analysis technology based on practical application has been presented. It has been shown that modulated lapped transform offers the time-dependent higher harmonic propagation following with higher accuracy than using FT (Fourier transform) and WT (Wavelet Transform). Moreno et al [96] have reported a hybrid method in the time and frequency domain for the analysis of the harmonic distortion in power systems. The method integrates a three-phase load flow at fundamental frequency with a hybrid harmonic-interaction analysis algorithm. Authors of the paper [97] present a frequency domain method, which is useful for traction drives design and harmonic generation studies. An iterative solving algorithm is used for load flow and converter operating point calculation. A numerical application is also developed and results are compared with time domain simulation results. Reference [98] gives a substantial review of the different single and three-phase harmonic load flow formulations. It presents the data, unknowns, and equations of these formulations in balanced network considerations. The influence of the main harmonic load flow hypothesis (harmonic interaction and fundamental power consumption consideration) in the final load flow results is also studied. In [99], an arc model for three-phase arc furnace to carry out the harmonic analysis with a single phase circuit is given. The model is based on the V-I characteristic of the arc and takes into account the effect of the arcs unbalance over the zero sequence harmonics. The model is implanted in EMTDC and tuned with field data. Simulations are performed in continuous work using Monte Carlo method to obtain the arc length. The important findings of these works are summarized as follows:

- The non-characteristic harmonic current injections are generally proportional to the degree of unbalance in the compensator bus voltage, TCR reactance, and firing angle etc;
- For the calculation of the non-characteristic harmonic injection, it is advisable to use the double iterative scheme, i.e. adjust the load flow following harmonic domain iteration;
- The harmonic components are more sensitive to unbalanced conditions than the fundamental frequency components;
- In general, it is found that the convergence rate is inversely affected by the degree of saturation and network harmonic voltage resonance;
- A significant improvement of the convergence rate by moving from a current source model to a Norton equivalent model can be achieved;
- The waveform distortions in the network are low in a properly designed static compensator systems. In particular, the harmonic cancellation scheme with a three-winding transformer connection is quite effective in most unbalance cases;

- Linearized model of a non-linear load gives inaccurate results;
- The presence of nonlinear load on a power system causes harmonic currents to flow through the system and other customer load as well;
- Time domain method preserves the nonlinearity of the problem and hence it gives more accurate results;
- Time domain method models the nonlinear load as a circuit and hence allows studying the effect of its individual components on power system harmonics;
- Frequency domain method linearizes the harmonic problem in non-linear load modeling as well as in the method of solution. Thus, it gives pessimistic results. For certain cases of study, the frequency domain method gives incorrect results and hence, this method needs to be used with caution.

2.7 HARMONIC STANDARDS

Most countries have their own regulatory standards (recommendations) to control the levels of harmonic distortion in distribution power systems, according to their local conditions. In this era of globalization, the need for equipments manufactured in one country to comply with standards in another country has prompted efforts in formulating international standards for harmonics and inter-harmonics. More recently a number of countries have collectively started applying similar harmonic control methodologies and recommended limits through the adoption of international standards such as IEC 61000-3-6 [109] and IEEE 519-1992 [28].

The IEC (International Electrotechnical Commission) has defined a series of standards, called Electromagnetic Compatibility (EMC) Standards, to deal with power quality issues. The IEC 61000 series includes harmonics and inter-harmonics as one of the conducted low-frequency electromagnetic phenomena. A widely accepted alternative to the IEC series is the IEEE 519-1992 document, which provides guidelines on harmonics.

In an attempt to control the levels of harmonic voltage distortion within distribution systems, most standards apply limits to harmonic current emissions in the hope that if customers are limited appropriately the net effect of all customer emissions will result in an acceptable level of harmonic voltage distortion. The IEEE 519-1992 limits are applicable only at the point of common coupling (PCC) of the utility and plant interface. IEEE 519-1992 restricts customer's harmonic current emissions to a relative value derived from the short circuit current level at PCC and the size of customer's nonlinear load. According to these limits, as the size of user load decreases with respect to the size of the power system, the percentage of harmonic current that user is allowed to inject into the utility system increases. The limits are recommended to be used as system design values for the 'worst case' for normal operation. Normal operation is the operating condition lasting longer than an hour. For shorter periods, such as during start-ups or unusual conditions, the limits may be exceeded by 50%.

The IEC approach differs slightly from the IEEE standard in that it considers future customers in the harmonic allocation. IEC 61000-3-6 provides formulas to estimate the allowed current emission for each customer such that all customers, including future ones, share the harmonic absorbing capability of the system.

The IEC 61000 Series provides internationally accepted information for the control of power system harmonic (and inter-harmonic) distortion [110]. The IEC 61000 1-4 present the information for limiting power frequency conducted harmonic and inter-harmonic current emissions from equipment in the frequency range up to 9 kHz. IEC 61000 2-1 summarizes the major sources of harmonics in three categories of equipment i.e. power system equipment, industrial loads and residential loads. IEC 61000 2-2 [111] defines the limits for inter-harmonic voltage distortion in public low-voltage power industry systems, in the range 10-90 Hz, corresponding to the compatibility level with respect to the flicker effect. IEC 61000 2- 4 [112] defines the compatibility levels for inter-harmonic voltages in industrial plants. It also describes the main effects of inter-harmonics. IEC 61000 2-12 deals with compatibility levels for low-frequency conducted disturbances, in this case relating to medium voltage power supply systems. It also covers the subject of injected signals such as those used in ripple control. IEC 61000 3-2 and 3-4 include limits for harmonic current emissions by equipment with input currents of 16 Amp per phase and below. It also specifies the measurement circuit, supply source and testing conditions as well as the requirements for the instrumentation. IEC 61000 3-6 specifies the capability levels for harmonic voltages in low-and medium-voltage networks as well as planning levels for MV, HV and EHV power systems. It then makes an assessment of emission limits for distorting loads in MV and HV power systems. IEC 61000 3-12 stipulates limits for the harmonic currents produced by equipment connected to low-voltage systems with input currents equal to and below 75 A per phase and subject to restricted connection. IEC 61000 4-7 has the information about the testing and measurement techniques.

It is a general guide on harmonic and inter-harmonic measurements and instrumentation for power systems. IEC 61000 4-13 is also a document on testing and measurement techniques with reference to harmonics and inter-harmonics, including mains signaling at ac power ports as well as low-frequency immunity tests.

As IEC and IEEE are two principally different approaches, for harmonic current limits, the Table 2.2 gives a comparison between them. It is important to point out that the IEC 1000-3-6 contains a lot of useful information and technical considerations. One of them is the discussion on the supply system impedances which is very important for limit compliance verification. This subject is missing in IEEE 519-1992. While the recommended harmonic voltage levels from the IEC standard are more generous than those of the IEEE standard, the allowable customer harmonic current contributions are usually more restrictive, although this will depend much upon circuit configuration. Although the international standards are used as a basis for global co-ordination, individual countries make their own adjustments to accommodate various national priorities. These are normally motivated by special characteristics of their power system configuration and load management (e.g. the use of ripple control in some countries).

Table 2.2: Comparison of Harmonic Standards

	IEC 61000 Series	IEEE 519-1992
1.	The IEC standards set limits to the amount of emission of individual equipment.	IEEE harmonic standard limits the emission per customer.
2.	The responsibility lies with the manufacturers of polluting equipment.	The responsibility lies with the customer who may decide to install filters instead of buying better equipment.
3.	IEC documents mainly aims at small customers that do not have the means to choose between mitigation options.	IEEE standard aims at regulating the connection of large industrial customers.

2.8 MITIGATION OF HARMONICS

The proliferation of nonlinear loads in industrial systems deviate the voltage and current waveforms from their sinusoidal nature and consequently harmonics are generated. The harmonic distortion influences the power quality and has many detrimental effects on the system equipment and consumers connected to the point of common coupling (PCC), interfere with communication signals and cause erroneous operation of control circuit. To lessen harmonic problems, utilities are increasingly enforcing international harmonic standards for industrial customers. By manufacturer's literature review, it has been found that harmonic mitigation techniques are seldom done because of the extra-cost for the consumer. Hence, a cost effective control strategy is needed to suppress and hopefully eliminate the harmonic effects on the system. Various harmonic mitigation techniques to reduce the effect of magnitude of harmonics have been proposed as listed below [113]:

(i) Phase Multiplication: This technique is quite effective to reduce low-order harmonics as long as there is balanced load on each of the converters;

(ii) Passive Filters: They improve power factor, reduce high frequency harmonics but are large in size. If tuning reactors are not used, instability may occur due to parallel resonance with the source inductance. Performance depends on the source impedance, which is usually not known accurately and can vary with system changes. References [39, 110, 115-119];

(iii) Active Filters: They also improve power factor, allow the output current to be controlled, provide stable operation against ac source impedance variations, and fast response irrespective of the order and magnitude of the harmonic. Initial and running costs are usually higher than for passive filters. The injection currents may flow into other system components. References [17-27, 120-129] provide recent information on active filters;

(iv) Harmonic Injection: This technique takes care of uncharacteristic harmonics. System impedance is no part of the design criteria. May give rise to lower order harmonics;

(v) Harmonic Mitigation Technique with PWM: This technique is capable of obtaining harmonic reductions of less than 1% of the fundamental. Programmable to eliminate specific harmonic.

To avoid undesirable effects of harmonics due to their unduly interference with power system, both passive and active compensation techniques (filters) can be implemented. Passive filters have the drawback of bulky size, component ageing, resonance and fixed compensation performance. These provide either over- or under-compensation of harmonics, whenever a load-change occurs [129]. Hence, active compensation known as active power filter (APF) is preferred over passive compensation. APFs are an up-to-date solution to power quality problems, which allow the compensation of current harmonics and unbalance together with power factor improvement [17-22, 129]. Active filters are developed to alleviate the disadvantages of conventional passive filters, namely [60]:

- The filtering characteristics being dependent on the source impedance;
- Aggravating the impedance below the lowest tuned harmonics;
- Being inadequate for filtering non-characteristic harmonics (different from the filter's tuned frequency), such as those produced by cycloconverters.

2.9 CONCLUDING REMARKS

The presence of harmonics pose many problems to power system engineers, due to the detrimental effect that they have on the power system apparatus, and more importantly due to the adverse manner in which they affect power quality. Industrial standards and recommended practice for power systems have been established as a step towards minimizing the effects of harmonics. In spite of this power systems must be able to withstand harmonic flow, since they can not be eliminated completely. The ever-increasing growth of nonlinear loads on power systems will necessitate the availability of better methods for evaluating the effects that harmonic source have on each other and on the power system. Substantial progress has been made in the area of power system harmonics covering analysis, simulation, and hardware development and testing for identification, classification and mitigation etc. However, many problems and issues, especially those related to development of protective schemes, efficient fault analysis tools, etc. still need to be addressed for appropriate system planning and operation of the power system to supply a good quality and reliable electric power.

ESTIMATION OF HARMONIC CURRENTS FOR SOME COMMON SINGLE-PHASE NONLINEAR LOADS

3.1 INTRODUCTORY REMARK

The application of power electronics converters, as nonlinear loads, results in increased harmonics levels and therewith degradation of the system conditions. These converters are widely-used in all electronics devices, e.g. personal computer (PC), television (TV), video, audio and similar equipments. At one hand, such devices are quite sensitive towards any deterioration in power quality attributes, but on the other hand, they also act as harmonic source.

Although single PC or any other single modern electronic device is nonlinear in nature and it is a significant source of harmonics, but has minor effects on power network in terms of voltage and current distortion, and may not be considered as a threat to power quality due to their low power level. However, if large number of such loads are connected and operated simultaneously, as in commercial or residential buildings, then they produce significant harmonics distortion of network voltage and current.

The similar situation also exists in residential areas, where number of low power home electronics appliances in a home is rapidly rising. The dominant nonlinear loads are TV sets, PC /Laptop, audio /video players, cordless telephones, mobile telephones chargers microwave ovens, variable speed drives in washing machines, dish-wash machines, refrigerators, air-conditioning devices, heat pumps and so on. They all have the same AC /DC converter with smoothing capacitor at the input same as the PC, which certainly contributes in increasing the harmonic distortion produced by a single apartment or house.

The net harmonic currents injected by multiple /large numbers of single-phase power electronic loads are significantly affected by attenuation and diversity factors [130]. Attenuation describes the reduction in harmonic magnitude, and change in phase angle, as a load connected to a switched mode power supplies (SMPS) increases. Attenuation is also observed where multiple identical loads share the same source impedance. Diversity describes a similar effect where a reduction /partial cancellation or even a complete harmonic cancellation is likely to take place due to differing harmonic current phase angles or various loads connected through different system and load impedances. The results shown and conclusion drawn are based upon these two key factors.

In an attempt to quantify the harmonic contents in power system, two different case studies are presented here. In the first case considered here, the impact of multiple units of PCs and in second case various types of modern home appliances and equipments are taken up for their individual and /or grouped harmonic contribution. The harmonic spectrum of each of the common appliances and equipment are presented. These loads include personal computer, printer, fluorescent lights, photocopier, television, VCD player, microwave, fridge and washing machine. The harmonic spectrums of the combined loads are also obtained, and the effects of the load combinations are analyzed and discussed.

The harmonic spectrums of these various nonlinear loads are recorded by the 'Fluke-43 B Power Quality Analyzer', which is a hand held instrument and combines the most useful capabilities of a power quality analyzer, multi-meter and scope. It displays both time- and frequency- domain (up to 51^{st} harmonic order along with phase angle of individual harmonics) waveforms of voltage and current. This instrument has storage and interfacing facilities with PC through an optically isolated interface cable.

3.2 HARMONIC IMPACT OF PERSONAL COMPUTER (PC) ON POWER QUALITY

Computer loads and systems can be found in all of society's industrial, commercial, and residential sectors. Computer laboratories at educational institutes, cyber cafes, industrial computerized processes, and computerized offices are common in today's electrical environment. The nature of these loads is such that they distort the line-current waveforms, and in some cases, can significantly distort the supply voltage waveforms causing disruption in computer system performance.

Personal computing impacts on power quality are due to the commonplace usage of SMPS for converting single phase AC into low voltage DC, for supplying processing electronics. SMPS are by no means restricted to PCs and can be found in a variety of other widely used electrical equipment including low energy lighting, battery chargers, televisions, and their peripherals.

This study is an endeavor to investigate the relation between single and multiple PCs power quality characteristics. In [131], it is shown that line current harmonics from a single PC differ significantly from the harmonics produced cumulatively by a number of PCs of the same type. The influence of processing mode of PC on the generation of line current harmonics has been investigated in [132], but it gives the results only for PC box, i.e. CPU (central processing unit). In present study, the influence of processing mode of PC on the current harmonic distortion and its components is studied. The two processing modes are investigated, i.e. idle mode, and hard disc drive (HDD) processing mode. The measurements taken for these two processing modes are combined with two different conditions of monitor status: with monitor power ON and with monitor power OFF. These two conditions are taken with the concern to make the study-results more general and reliable in present and future scenario, as it is expected that in near future the energy efficient LCD monitors may replace the presently existing CRT monitors. Thus the results discussed here provide harmonic analysis for all four possible combinations, as given following:

i) Case-1: Idle PC with monitor ON

ii) Case-2: HDD processing with monitor ON

iii) Case-3: Idle PC with monitor OFF

iv) Case-4: HDD processing with monitor OFF

The number of PCs is given as N. The harmonic current and voltage measurements are taken for single PC (N=1), two PCs (N=2), five PCs (N=5), and ten PCs (N=10).

3.2.1 CASE-1: Idle PC with monitor ON

3.2.1.1 Without UPS

The measured rms load current with their total harmonic current distortion (THD_I) is shown in Fig. 3.1(a), (b), (c), and (d) respectively for single PC, two PCs, five PCs and ten PCs. Fig. 3.2(a), (b), (c), and (d) display the power consumption for single PC, two PCs, five PCs and ten PCs correspondingly.

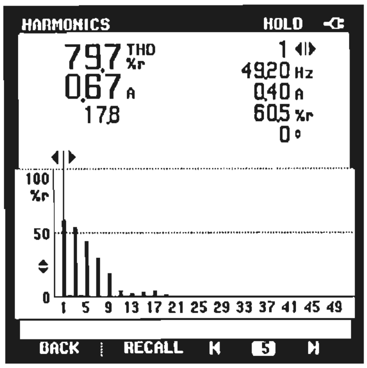

(a) For Single PC (N=1)

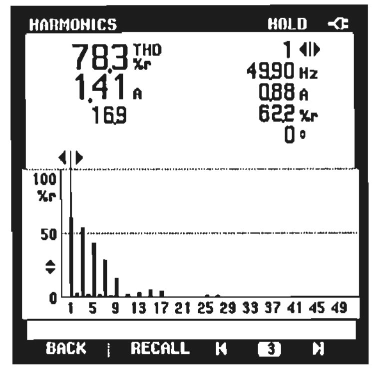

(b) For two PC (N=2)

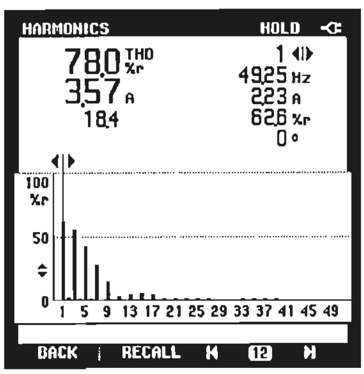

(c) For five PC (N=5)

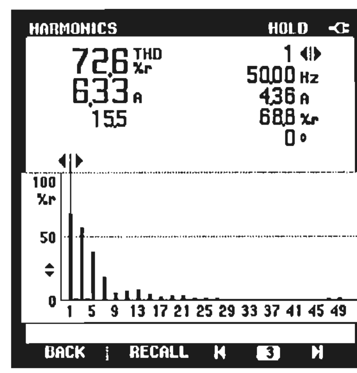

(d) For ten PC (N=10)

Fig. 3.1: Measured rms load current with their total harmonic current distortion under case-1 for without UPS condition

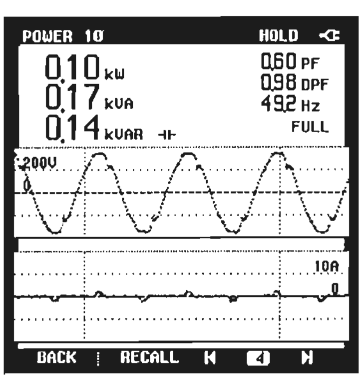

(a) For Single PC (N=1)

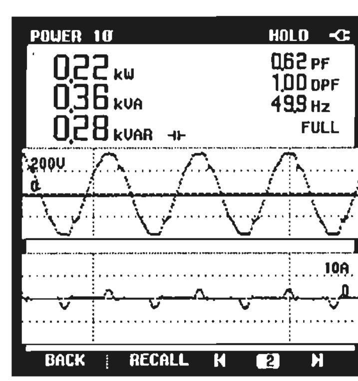

(b) For two PC (N=2)

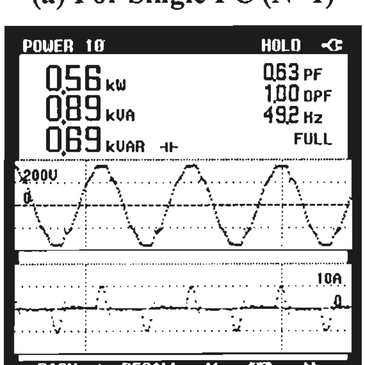

(c) For five PC (N=5)

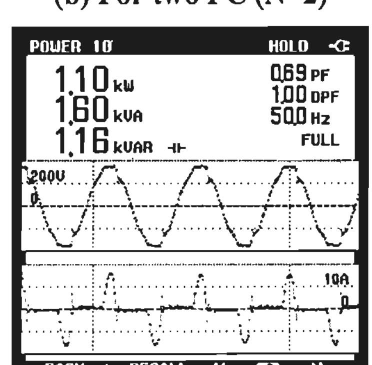

(d) For ten PC (N=10)

Fig. 3.2: Measured power consumption under case-1 for without UPS condition

All of these results are also summarized in Table-3.1 along with their harmonic component's magnitude and respective phase angle. Fig. 3.3 shows the corresponding harmonic spectrum of the current waveform (with their magnitude expressed as a percentage of the fundamental). The variation of magnitude of various current components for multiple (*N* in number) PCs is depicted in Fig. 3.4 which helps in understanding the presence of attenuation factor.

It can be concluded that the magnitude of harmonic currents increases with number (N) of PCs, but not as rapidly as the fundamental current. This figure clearly indicates that as the *N* increases, the magnitude of fundamental current component increases proportionally, but the magnitude of harmonic current components does not vary linearly. This illustrates the harmonic current attenuation. The attenuation factor AF_n for n^{th} harmonic current component is defined as the net current magnitude to load when *N* number of loads are connected, divided by the product of single unit current magnitude and *N* [133].

$$AF_n = \frac{I_n^N}{N.I_n^1} \tag{3.1}$$

where I_n^N = Resultant current for n^{th} harmonic component for *N* units operating in parallel,

and I_n^1 = current for nth harmonic component when N=1.

For example, in Table-3.1, the attenuation factor for the 3rd harmonic with $N = 10$, is $AF_3 = 3.59/(10*0.37) = 0.97$.

Table- 3.2 displays the attenuation factor for $N = 10$.

Table-3.1: Comparison of power, net rms current and magnitude of harmonic current components with their phase angles under case-1 without UPS

No. of PCs (N)	Power (KW)	RMS current	THD_I (%)	Harmonic order															
				1		3		5		7		9		11		13		15	
				Mag.	angle	Mag.	angle	Mag.	angle	Mag.	angle	Mag.	angle	Mag.	angle	Mag.	angle	Mag.	angle
1	0.10	0.67	**79.7**	0.4057	0	0.370	147	0.295	-53	0.206	102	0.122	-100	0.036	72	0.02	-45	0.027	146
2	0.22	1.41	**78.3**	0.8801	0	0.784	152	0.61	-45	0.410	111	0.213	-94	0.042	41	0.053	56	0.08	-143
5	0.56	3.57	**78.0**	2.2325	0	1.982	155	1.519	-40	1.01	118	0.343	-87	0.129	36	0.164	88	0.22	-122
10	1.10	6.33	**72.6**	4.35	0	3.59	158	2.39	-36	1.19	119	0.388	-117	0.298	-46	0.192	92	0.315	-122

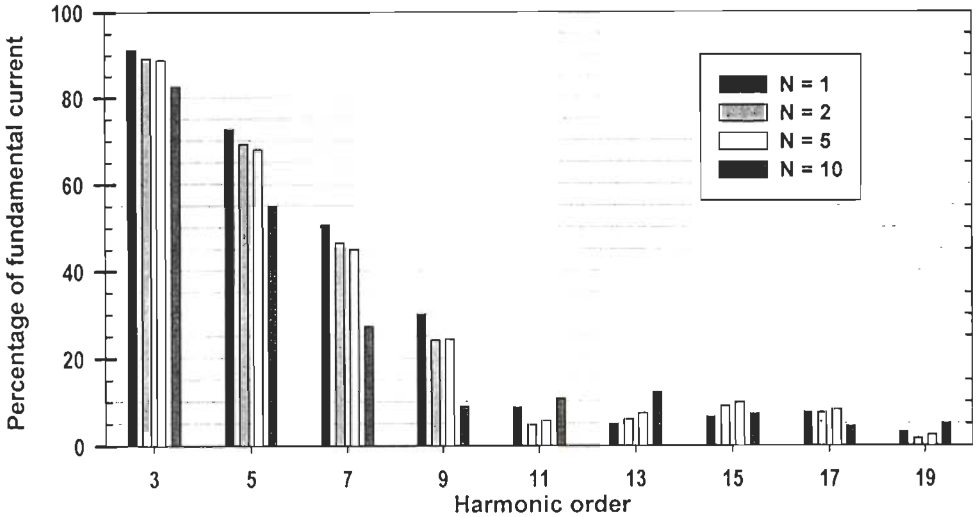

Fig. 3.3: **Harmonic spectrum of load current, measured as percentage of fundamental current, for *N* number of PCs under case-1 without UPS**

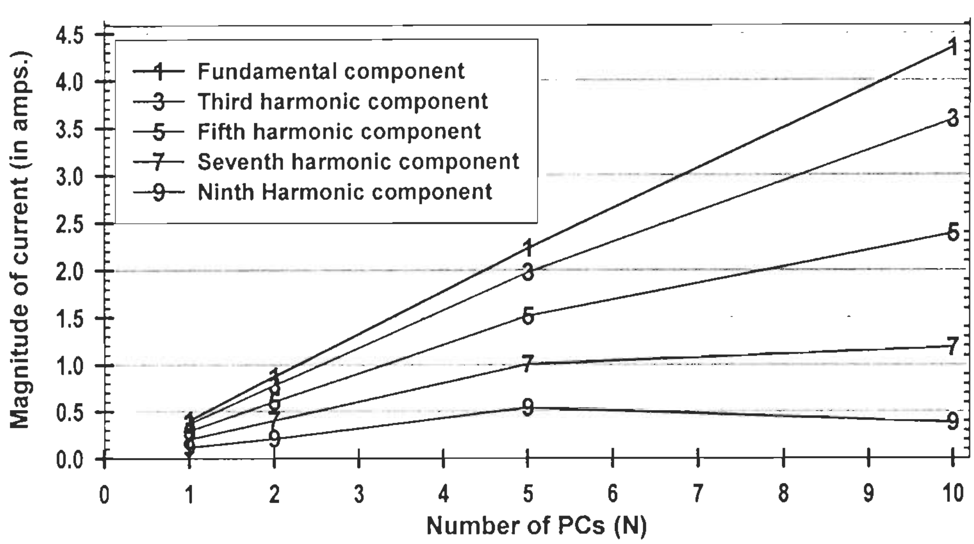

Fig. 3.4: **Variation of magnitude of various current components for multiple PCs under case-1 without UPS**

Table-3.2: Harmonic order with their attenuation factor under case-1 'without UPS'

Harmonic order	3	5	7	9	11	13	15
Attenuation Factor (AF)	0.97	0.81	0.58	0.32	0.83	0.96	1.17

Here, the most affected harmonic component due to attenuation is the 9th harmonic as it has the lowest value of attenuation factor.

3.2.1.2 With UPS

The measured rms load current with their THD_I are shown in Fig. 3.5(a), (b), (c), and (d) respectively for single PC, two PCs, five PCs and ten PCs with UPS. Fig. 3.5(a), (b), (c), and (d) display the power consumption for single PC, two PCs, five PCs and ten PCs correspondingly with UPS. Also, the results are summarized in Table-3.3 along with their harmonic component's magnitude and respective phase angle.

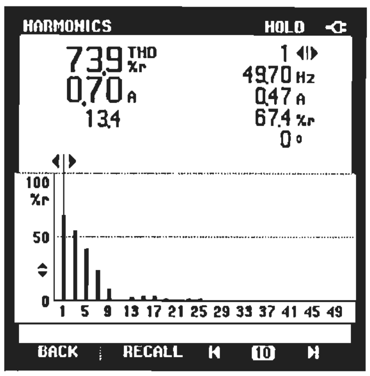

(a) For Single PC (*N*=1)

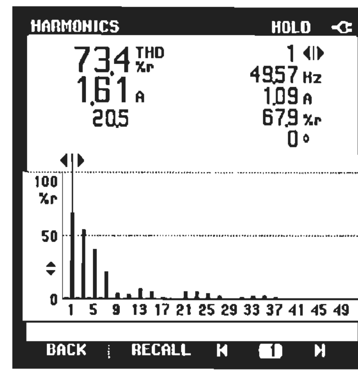

(b) For two PC (*N*=2)

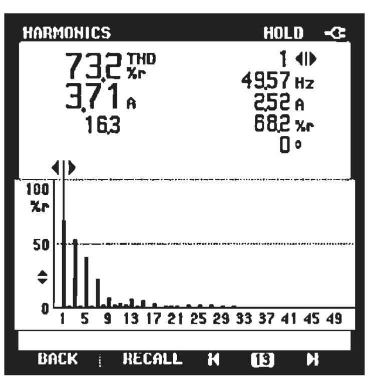

(c) For five PC (*N*=5)

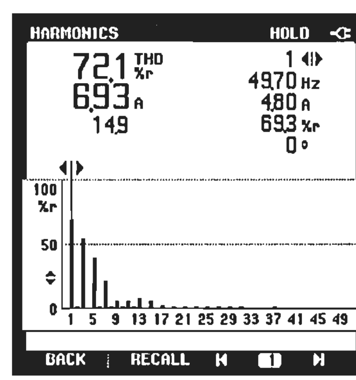

(d) For ten PC (*N*=10)

Fig. 3.5: Measured rms load current with their total harmonic current distortion under case-1 with UPS

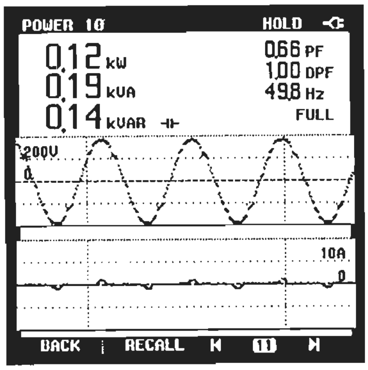

(a) For Single PC (*N*=1)

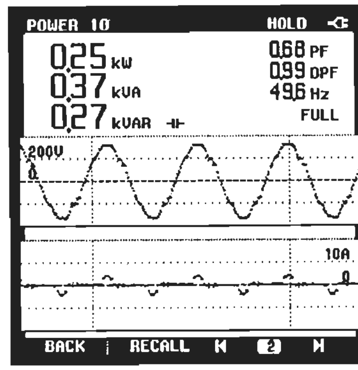

(b) For two PC (*N*=2)

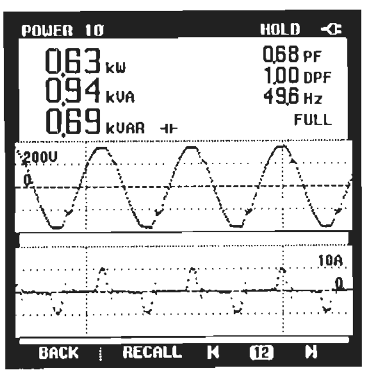

(c) For five PC (*N*=5)

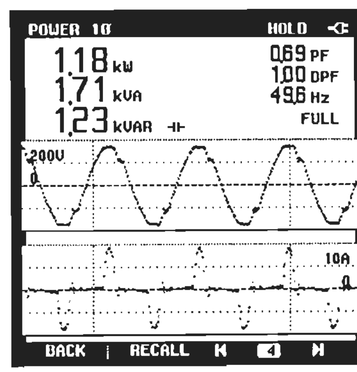

(d) For ten PC (*N*=10)

Fig. 3.6: Measured power consumption under case-1 with UPS

Table-3.3: Comparison of power, net rms current and magnitude of harmonic current components with their phase angles under case-1 with UPS

No. of PCs (N)	Power (KW)	RMS current	THD_I (%)	Harmonic order															
				1		3		5		7		9		11		13		15	
				Mag.	angle	Mag.	angle	Mag.	angle	Mag.	angle	Mag.	angle	Mag.	angle	Mag.	angle	Mag.	angle
1	0.12	0.70	73.9	0.474	0	0.41	-179	0.296	-10	0.171	161	0.0643	-37	0.047	77	0.053	159	0.051	-26
2	0.25	1.61	73.4	1.091	0	0.887	167	0.641	-25	0.344	141	0.0732	-53	0.0599	-85	0.098	85	0.0975	-105
5	0.63	3.71	73.2	2.527	0	2.013	172	1.481	-18	0.862	150	0.299	-57	0.155	-11	0.27	130	0.23	-59
10	1.18	6.93	72.1	4.802	0	3.775	173	2.705	-16	1.519	153	0.459	-60	0.399	-18	0.4742	132	0.4212	-57

The corresponding harmonic spectrum of the current waveform (with their magnitude expressed as a percentage of the fundamental) as given in Fig. 3.7 shows that the dominant harmonic current components are 3^{rd}, 5^{th}, 7^{th}, and 9^{th} harmonics. Comparison of results shown in Table-3.1 and Table-3.3 concludes that with UPS, the power consumption of

PC load increases approximately by 10 % but THD_I level of PC load is almost stabilized and it does not show large variation in THD_I value with increase in number of unit loads as compared to without UPS. In both the conditions (i.e. with and without UPS), the demonstrated harmonic profile is almost identical. This comparison of THD_I for N number of PC loads under 'with and without UPS' is displayed in Fig. 3.8. Table-3.4 displays the attenuation factor for $N = 10$.

From the result it is clear that the most affected harmonic component due to attenuation is the 9th harmonic as it has the lowest value of attenuation factor. Fig. 3.9 demonstrates the comparison of attenuation factor for various harmonic components under with, and without UPS conditions, which explains that attenuation is more effective for 'without UPS' condition for 5th, 7th, and 9th harmonics as they have lower values.

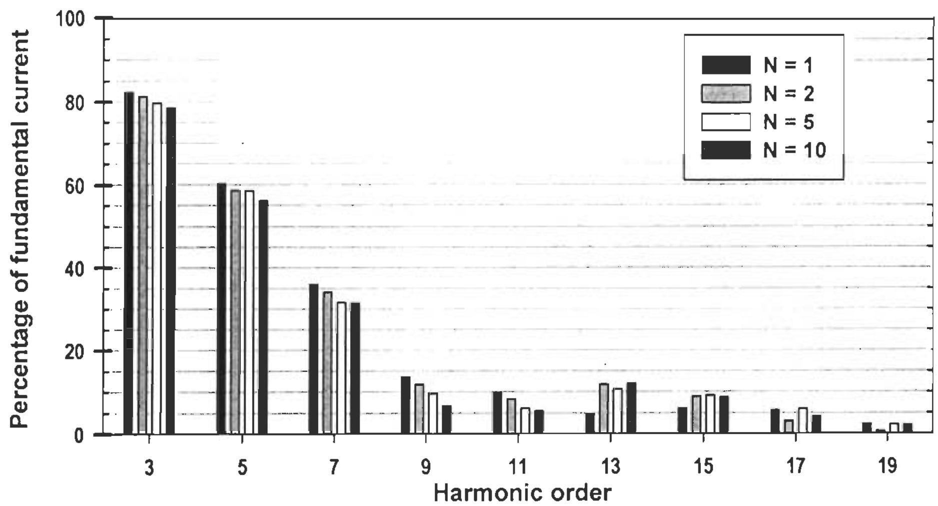

Fig. 3.7: Harmonic spectrum of load current, measured as percentage of fundamental current, for N number of PCs with UPS

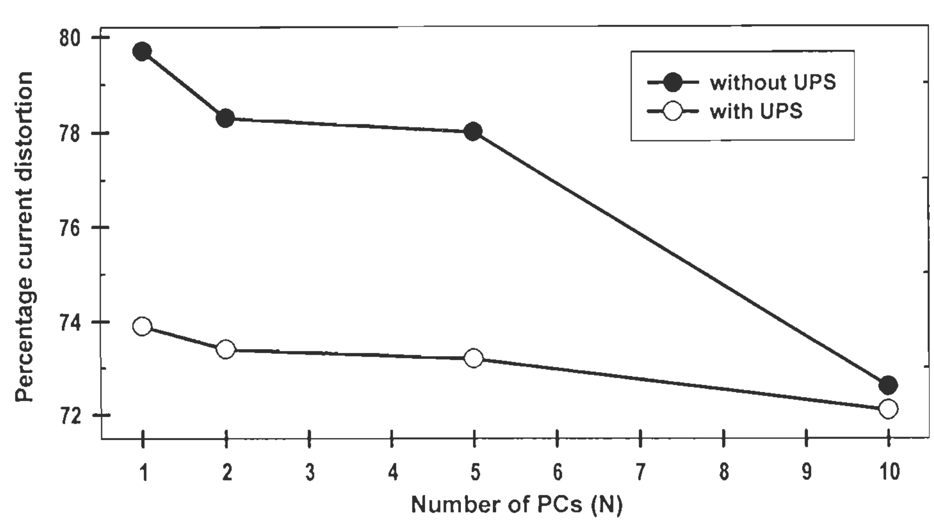

Fig. 3.8: Comparison of percentage current harmonic distortion (THD_I) for N number of PC loads with and without UPS

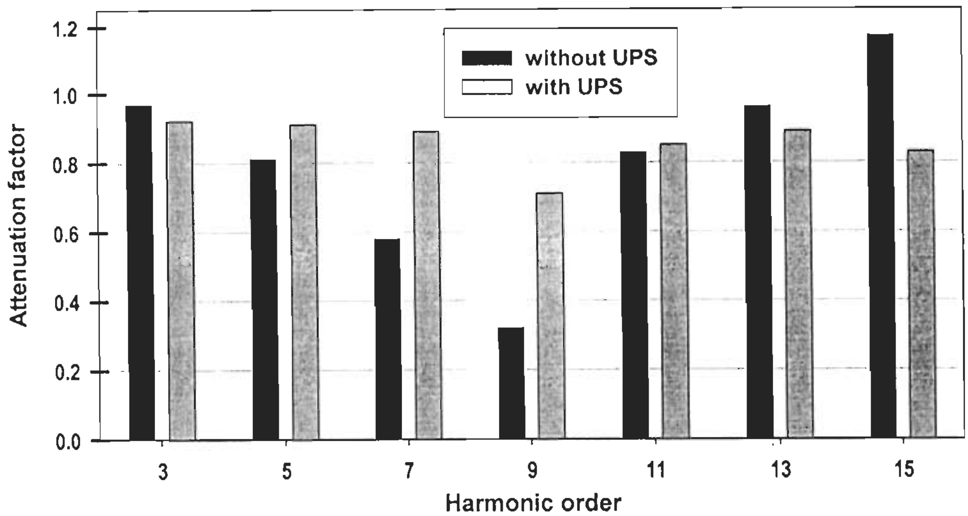

Fig. 3.9: **Comparison of attenuation factor for various harmonic components under case-1 with and without UPS (N=10)**

Table-3.4: Harmonic order with their attenuation factor under case-1 with UPS

Harmonic order	3	5	7	9	11	13	15
Attenuation Factor (AF)	0.92	0.91	0.89	0.71	0.85	0.89	0.83

3.2.2 CASE-2: HDD processing with monitor ON

The measured rms load current with their THD_I are shown in Fig. 3.10(a), (b), (c), and (d) respectively for number of PCs (N) = 1, 2,5, and 10. These measurements are taken with UPS. Fig. 3.11(a), (b), (c), and (d) display the power consumption for single PC, two PCs, five PCs and ten PCs correspondingly. Summary of all of these measurements for case-2 with UPS condition is presented in Table-3.5 with their harmonic component's magnitude and respective phase angle. The corresponding harmonic spectrum of the current waveform (with their magnitude expressed as a percentage of the fundamental) as given in Fig. 3.12 shows that the dominant harmonic current components are 3rd, 5th, 7th, and 9th harmonics.

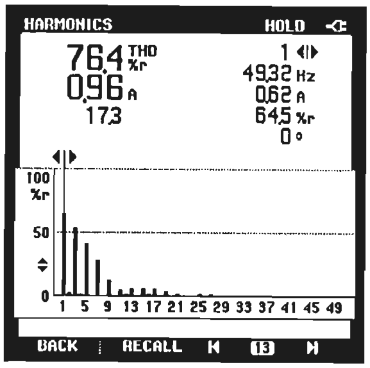

(a) For Single PC (*N*=1)

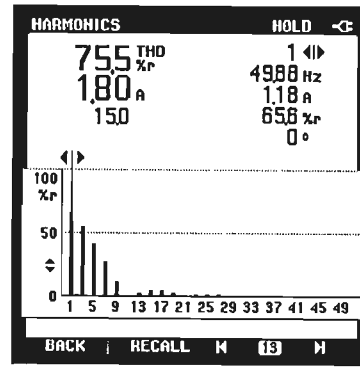

(b) For two PC (*N*=2)

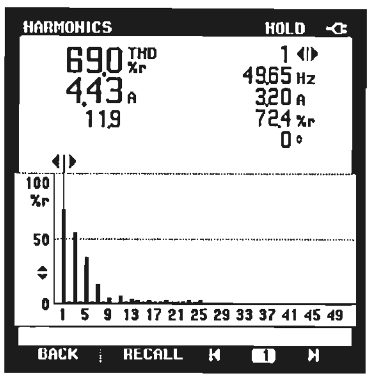

(c) For five PC (*N*=5)

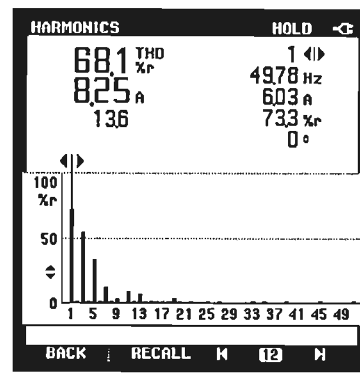

(d) For ten PC (*N*=10)

Fig. 3.10: Measured rms load current with their total harmonic distortion under case-2

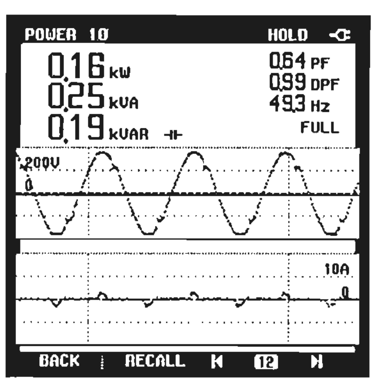

(a) For Single PC (N=1)

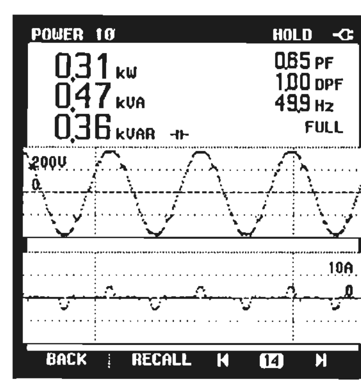

(b) For two PC (N=2)

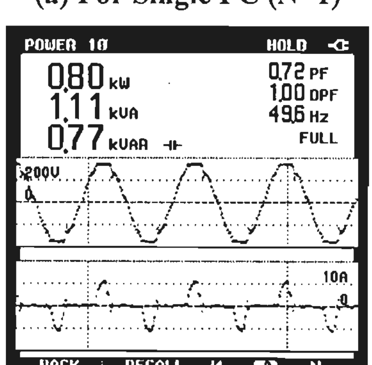

(c) For five PC (N=5)

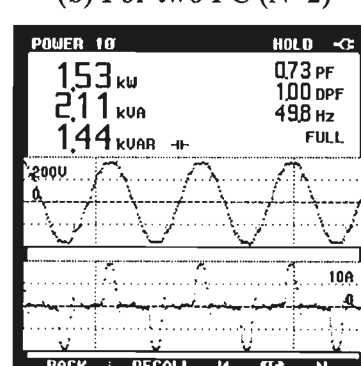

(d) For ten PC (N=10)

Fig. 3.11: Measured power consumption under case-2 with UPS condition

Table-3.5: Comparison of power, net rms current and magnitude of harmonic current components with their phase angles under case-2 with UPS condition

No. of PCs (N)	Power (KW)	RMS current	THD_I (%)	Harmonic order															
				1		3		5		7		9		11		13		15	
				Mag.	angle	Mag.	angle	Mag.	angle	Mag.	angle	Mag.	angle	Mag.	angle	Mag.	angle	Mag.	angle
1	0.16	0.96	**76.4**	0.6163	0	0.5188	168	0.399	-23	0.2705	148	0.126	-36	0.044	178	0.576	43	0.062	-125
2	0.31	1.80	**75.5**	1.182	0	0.9932	175	0.7515	-15	0.4811	157	0.2040	-36	0.0155	158	0.0576	123	0.0842	-57
5	0.80	4.43	**69.0**	3.206	0	2.454	176	1.594	-13	0.687	157	0.2084	-96	0.2771	-4	0.184	160	0.0621	-50
10	1.53	8.25	**68.1**	6.03	0	4.567	178	2.811	-9	1.04	170	0.3281	-168	0.7781	-20	0.55	156	0.1153	-28

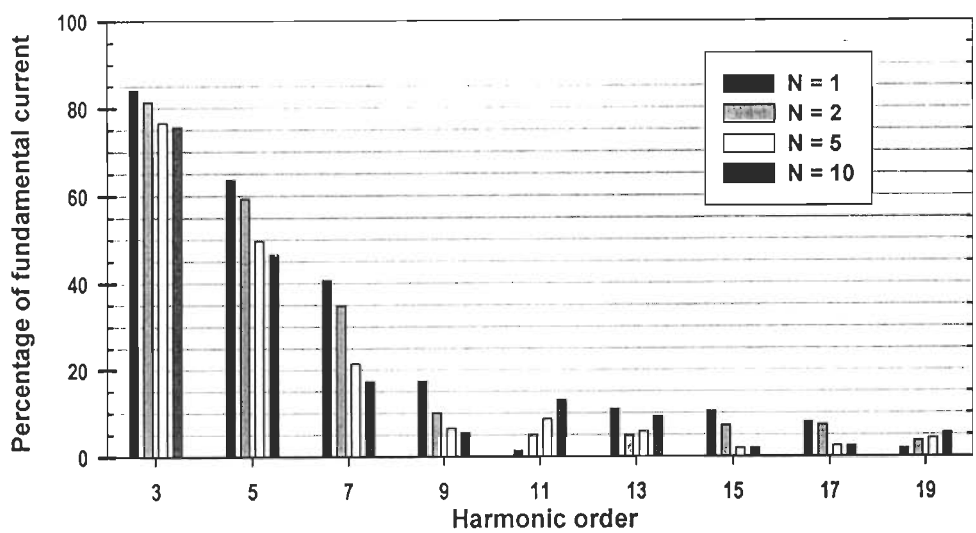

Fig. 3.12: Harmonic spectrum of load current, measured as percentage of fundamental current, for *N* number of PCs under case-2, with UPS

Comparison of results shown in Table-3.3 for case-1, and Table-3.5 for case-2, clearly indicates that under case-2 the power consumption of PC load increases in a range 24 % to 33 %. The numerical value of THD_I is observed comparatively lower under 'case-2' for more numbers (N =5 and 10) of PC loads.

An increase in magnitude (expressed as a percentage of the fundamental component) of dominant (3^{rd}, 5^{th}, 7^{th}, and 9^{th}) harmonic current components can be observed on making comparison of results shown in Fig. 3.5 for case-1, and Fig. 3.9 for case-2, otherwise in both conditions (i.e. case-1 and 2), the demonstrated harmonic profile is almost the same. Table-3.6 displays the attenuation factor for $N = 10$.

Table-3.6: Harmonic order with their attenuation factor under case-2 with UPS

Harmonic order	3	5	7	9	11	13	15
Attenuation Factor (AF)	0.88	0.70	0.38	0.26	1.77	0.10	0.19

Here, again the attenuation factor has the lowest value for the 9th harmonic; hence the most affected harmonic component (among dominant harmonics) due to attenuation is the 9th harmonic. Fig. 3.13 demonstrates the comparison of attenuation factor for various harmonic components between case-1 and case-2 which elucidates that attenuation effect is higher under case-2 for dominant (3rd, 5th, 7th, and 9th) harmonics as they have lower values. It is very high for 11th harmonic but the harmonic contribution of 11th harmonic (in terms of magnitude) is very small.

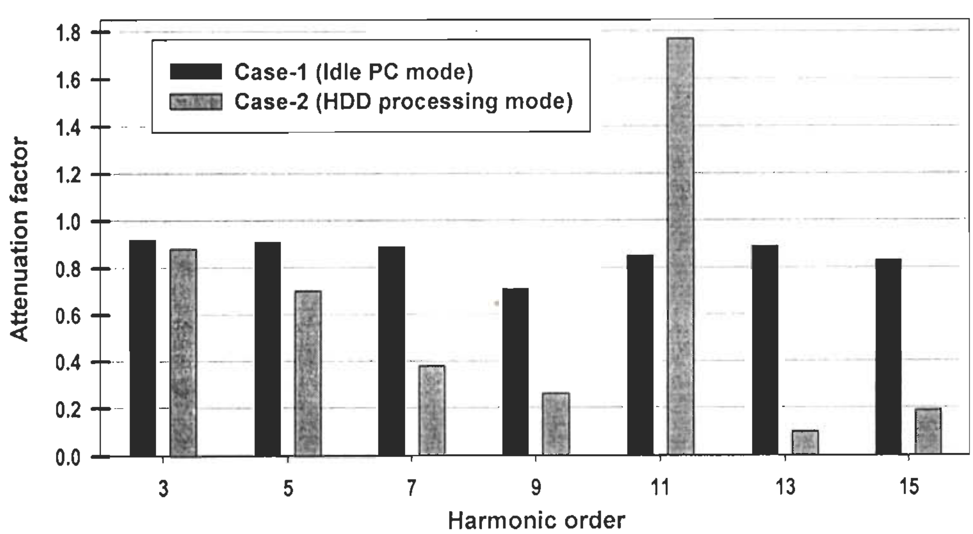

Fig. 3.13: Comparison of attenuation factor for various harmonic components under case-1 and case-2 with UPS condition ($N = 10$)

3.2.3 CASE-3: Idle PC with monitor OFF

The measured rms load current with their THD_I and the power consumption correspondingly for number of PCs (N) = 1, 2, 5, and 10 are summarized in Table-3.7. The magnitude of harmonic current components is shown along with their individual phase angle. These measurements are taken with UPS. The corresponding harmonic spectrum of the current waveform (with their magnitude expressed as a percentage of the fundamental) as given in Fig. 3.14 shows that for $N = 1$ and 2 the dominant harmonic current components are 3^{rd}, 5^{th}, 7^{th}, 9^{th}, 11^{th}, and 13^{th} harmonics, but for higher number of PCs (N = 5 and 10) the dominant harmonic current components are only 3^{rd}, 5^{th}, 7^{th}, and 9^{th}, i.e. same as case-1 and case-2.

Table-3.7: Comparison of power, net rms current and magnitude of harmonic current components with their phase angles under case-3 with UPS condition

No. of PCs (N)	Power (KW)	RMS current	THD_I (%)	Harmonic order															
				1		3		5		7		9		11		13		15	
				Mag.	angle	Mag.	angle	Mag.	angle	Mag.	angle	Mag.	angle	Mag.	angle	Mag.	angle	Mag.	angle
1	0.07	0.46	79.1	0.284	0	0.235	165	0.186	-32	0.142	133	0.095	-50	0.0842	117	0.0687	-72	0.0421	89
2	0.13	0.93	77.8	0.583	0	0.479	167	0.377	-28	0.273	140	0.164	-40	0.1375	141	0.1086	-34	0.0798	130
5	0.34	2.03	74.9	1.343	0	1.042	175	0.840	-19	0.585	149	0.313	-53	0.060	91	0.044	119	0.080	-59
10	0.69	4.27	73.9	2.875	0	2.246	174	1.7314	-18	1.1705	152	0.5431	-48	0.288	62	0.204	113	0.215	-63

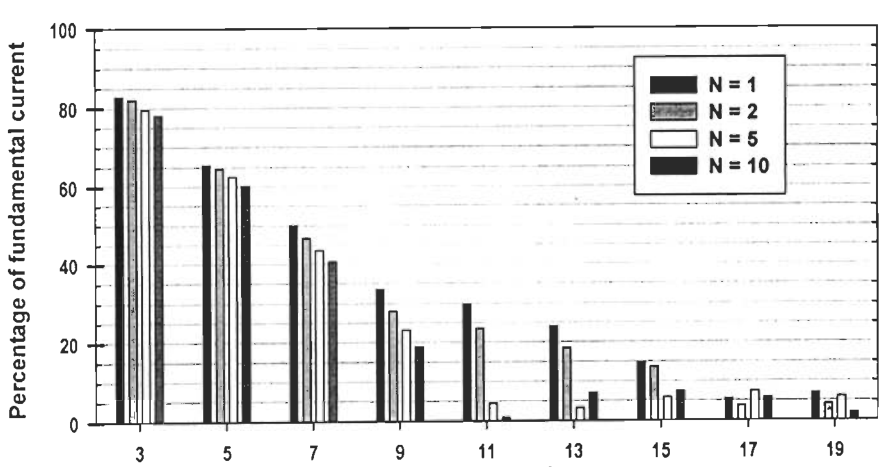

Fig. 3.14: **Harmonic spectrum of load current, measured as percentage of fundamental current, for *N* number of PCs under case-3, with UPS**

From the comparison of results, as shown in Table-3.3 (for case-1) and Table-3.7 (for case-3) together with Fig. 3.7 (for case-1) and Fig. 3.14 (for case-3), it is clearly observable that as the load current decreases with monitor OFF condition, the THD_I slightly increases for respective values of *N*. In addition to this dominant harmonic components 5^{th}, 7^{th}, and 9^{th} harmonic components exhibit a significant increase in their numerical value when expressed as a percentage of the fundamental component. Table-3.8 presents the attenuation factor for *N* = 10, which clearly states that among dominant (3^{rd}, 5^{th}, 7^{th}, and 9^{th}) harmonic current components, the attenuation factor has the lowest value for the 9^{th} harmonic; hence the most affected harmonic component (among dominant harmonics) due to attenuation is the 9^{th} harmonic. Fig. 3.15 demonstrates the comparison of attenuation factor for various harmonic components between case-1 and case-3 (as shown in table-3.4 and Table-3.8, respectively). It is found that the attenuation effect is almost same in both cases for 3^{rd}, 5^{th}, and 7^{th} harmonic, but is more effective under case-3 for 9^{th}, 11^{th}, 13^{th}, and 15^{th} harmonics among which only 9^{th} harmonic is the dominant one.

Table-3.8: Harmonic order with their attenuation factor under case-3 with UPS

Harmonic order	3	5	7	9	11	13	15
Attenuation Factor (AF)	0.96	0.93	0.82	0.57	0.34	0.30	0.51

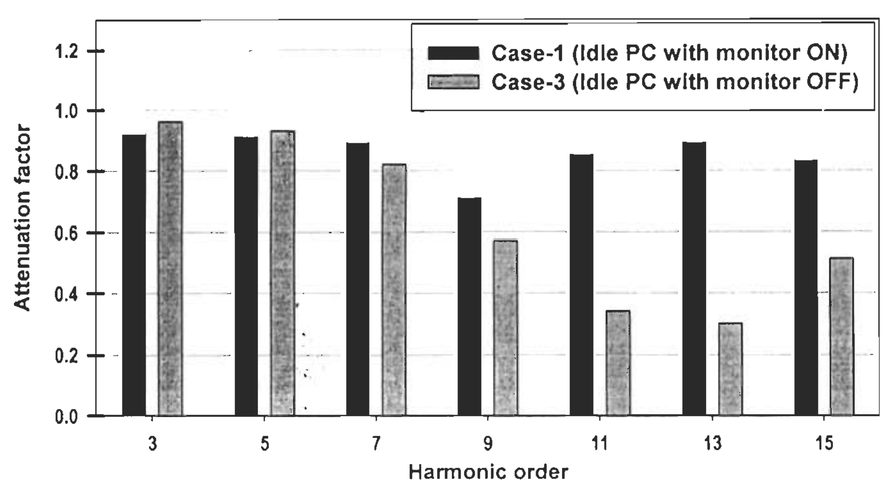

Fig. 3.15: Comparison of attenuation factor for various harmonic components under case-1 and case-3, with UPS condition (*N* = 10)

3.2.4 CASE-4: HDD processing with monitor OFF

The summary of rms load current measurement with their THD_I and the power consumption correspondingly for number of PCs (N) = 1, 2, 5, and 10, under case- 4 is demonstrated in Table-3.9 the magnitude of harmonic current components is shown along with their individual phase angle These measurements are taken with UPS. The corresponding harmonic spectrum of the current waveform (with their magnitude expressed as a percentage of the fundamental) as given in Fig. 3.16 shows that for *N* = 1 and 2 the dominant harmonic current components are 3^{rd}, 5^{th}, 7^{th}, and 9^{th} harmonics, but for higher number of PCs (N = 5 and 10) the dominant harmonic current components are limited only to 3^{rd}, 5^{th}, and 7^{th} while 9^{th} harmonic is almost negligible.

Table-3.9: Comparison of power, net rms current and magnitude of harmonic current components with their phase angles under case-4 with UPS condition

No. of PCs (N)	Power (KW)	RMS current	THD_I (%)	Harmonic order															
				1		3		5		7		9		11		13		15	
				Mag.	angle	Mag.	angle	Mag.	angle	Mag.	angle	Mag.	angle	Mag.	angle	Mag.	angle	Mag.	angle
1	0.09	0.57	77.2	0.361	0	0.304	167	0.242	-29	0.169	136	0.0842	-57	0.0333	139	0.02	-16	0.015	-163
2	0.19	1.14	76.8	0.732	0	0.6096	179	0.4833	-12	0.3414	162	0.1818	-28	0.0665	166	0.0133	41	0.0244	-63
5	0.52	2.95	70.4	2.093	0	1.605	179	1.1195	-12	0.5897	163	0.2106	-60	0.1153	7	0.1175	164	0.0931	-39
10	0.96	5.30	69.8	3.786	0	2.911	-173	1.9	-1	0.944	-178	0.069	-92	0.379	-9	0.3835	178	0.2306	5

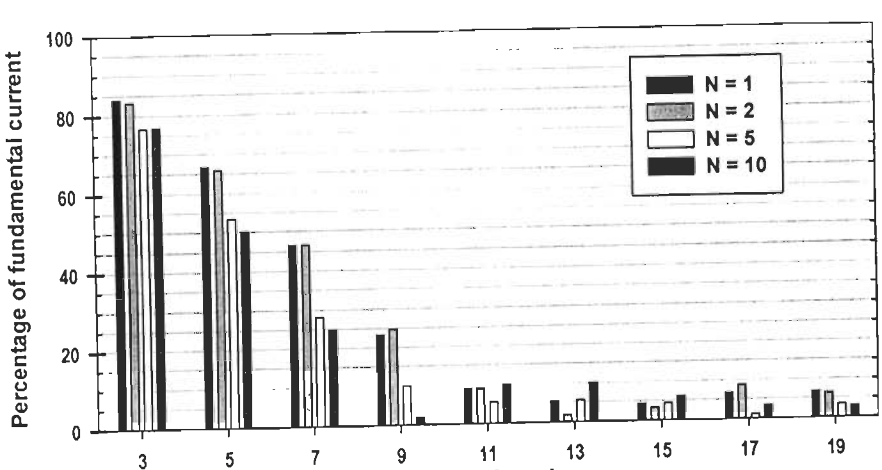

Fig. 3.16: **Harmonic spectrum of load current, measured as percentage of fundamental current, for *N* number of PCs under case-4 with UPS**

From the comparison of results as shown in Table-3.3 (for case-1) and Table-3.9 (for case-4) it is found that as the load current decreases with monitor OFF condition, the THD_I increases for $N = 1$ and 2 but decrease further for $N = 5$ and 10, which is similar to the pattern of dominant harmonic current components. Table-3.10 presents the attenuation factor for $N = 10$.

Among dominant (3rd, 5th, 7th, and 9th) harmonic current components, the attenuation factor has the lowest value for the 9th harmonic; hence the most affected harmonic component (among dominant harmonics) due to attenuation is the 9th harmonic. Fig. 3.17 demonstrates the comparison of attenuation factor for various harmonic components between case-1 and case-4, (as shown in Table-3.4 and Table-3.10, respectively). It reveals that the attenuation effect is almost same in both cases for 3rd, and 5th harmonic, but is more effective under case-4 for 7th, 9th, and 11th harmonics among which only 7th and 9th are dominant harmonic current components.

Table-3.10: Harmonic order with their attenuation factor under case-4 with UPS

Harmonic order	3	5	7	9	11	13	15
Attenuation Factor (AF)	0.97	0.96	0.79	0.56	0.08	1.14	1.92

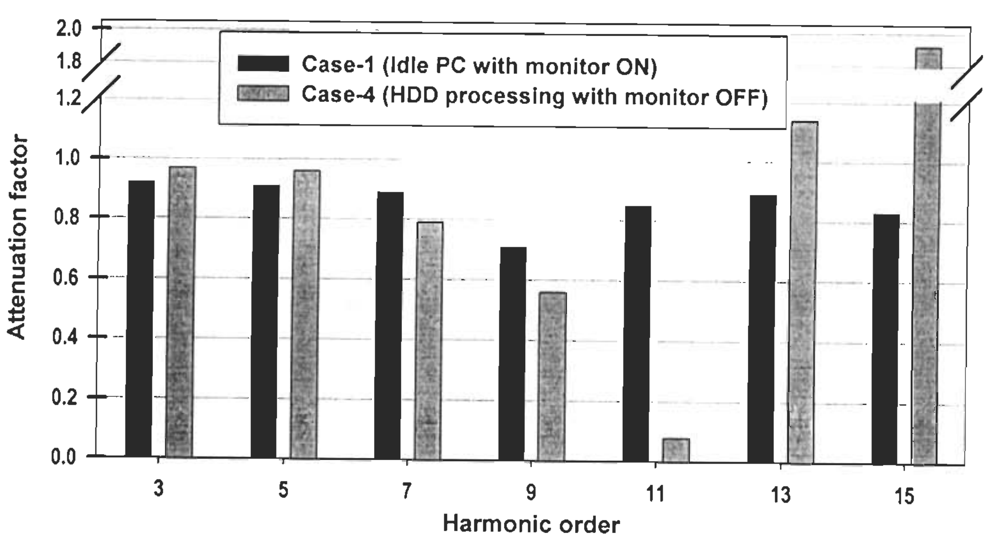

Fig. 3.17: Comparison of attenuation factor for various harmonic components under case-1 and case-4 with UPS condition ($N = 10$)

3.2.5 Comparison of All Four Cases

3.2.5.1 Mode of Operation and Monitor Status

For above mentioned four different cases, the results of line current harmonics are summarized in this section for the harmonic contribution made by a single PC, in Table-3.11, where magnitudes of harmonic components are expressed as a percentage of the fundamental component and their corresponding phase angles are also given relative to phase angle of fundamental.

Table-3.11: Comparison of magnitudes and phase angles of various harmonic current components for four different cases

Mode of Operation	RMS Current (A)	THD_I (%)	Harmonic order															
			1		3		5		7		9		11		13		15	
			Mag.	angle	Mag.	angle	Mag.	angle	Mag.	angle	Mag.	angle	Mag.	angle	Mag.	angle	Mag.	angle
Case-1	0.70	73.9	100	0	82.3	-179	60.3	-10	36.0	161	13.6	-37	0.90	77	4.7	159	6.1	-26
Case-2	0.96	76.4	100	0	84.1	168	63.6	-23	40.7	148	17.3	-36	1.3	178	10.86	43	10.41	-125
Case-3	0.36	73.0	100	0	78.38	165	58.56	-32	36.04	133	17.12	-50	0.90	117	5.41	-72	4.50	89
Case-4	0.57	77.2	100	0	84.04	167	66.86	-29	46.62	136	23.31	-57	9.20	139	5.52	-16	4.29	-163

It is clearly observable from the Table-3.11 that HDD processing mode contributes the more harmonics in comparison to idle PC mode. This statement is valid irrespective of the monitor status, i.e. either monitor ON or OFF. It is also apparent from this table that the net rms current is considerably high for HDD processing mode as compared to idle PC. As compared on the basis of their magnitude, it is found that the dominant harmonics are the 3rd, 5th, 7th, and 9th. Variation in the level of harmonics as compared between two modes of operation is reasonably higher for monitor OFF status than monitor ON status. The major evident deviations in harmonic levels are distinguished in 3rd, 5th, and 7th harmonics, while the difference in higher order harmonics is not as much of prominent.

3.2.5.2 Attenuation Effect

The attenuation effect results in the reduction in magnitude of harmonic component. The reason of attenuation is the connection of multiple similar loads to a particular phase circuit, having the common source impedance. Fig. 3.4 elucidates the basic idea of harmonic current attenuation. In the previous sections of this chapter the attenuation factor is calculated for ten number of PC loads, under every case, individually. An assessment of attenuation factors for all four cases is presented in Table- 3.12.

Table-3.12: Comparison of attenuation factors for all four different cases

Mode of Operation	Attenuation factor (AF_n) for n^{th} harmonic order						
	n = 3	n = 5	n = 7	n = 9	n = 11	n = 13	n = 15
Case-1	0.92	0.91	0.89	0.71	0.85	0.89	0.83
Case-2	0.88	0.70	0.38	0.26	1.77	0.10	0.19
Case-3	0.96	0.93	0.82	0.57	0.34	0.30	0.51
Case-4	0.97	0.96	0.79	0.56	0.08	1.14	1.92

Among all four possible modes of operations, it is found that attenuation is most effective for case-2 (HDD processing mode with monitor ON) in which it is particularly significant for 7^{th} and 9^{th} harmonics as for these two harmonic components they are having the minimum value.

3.3 HARMONIC IMPACT OF MODERN HOME APPLIANCES AND EQUIPMENTS ON POWER QUALITY

In a system with only one harmonic-producing load, the phase angles of the harmonic currents are not a concern since the harmonic distortion in the system is determined completely by the magnitudes of the injected currents. However, if there are multiple harmonic sources in the system, the harmonics from each source will add as per vector addition rule. As a result, the combined harmonic distortion levels are highly dependent on the phase angles of the individual loads.

The work presented in this section is intended to estimate the net harmonic currents injected by some selected combinations of nonlinear loads (modern home appliances and equipments) present within typical domestic premises. Harmonic currents generated by these loads are, individually too small to cause any appreciable distortion feeders. However, as the number of these loads increases with multiplicity of the home units with each unit using the different possible combinations of these loads, the cumulative harmonics may become very significant. That is why the increasing use of these modern home appliances has raised serious concerns. These appliances have the power ratings ranging from less than ten watts to hundreds of watts. Table-3.13 (a), (b), and (c) display the measurement results for various home appliances and equipments. The nonlinear home appliances and equipments considered here are television, VCD player; personal computer, microwave, fridge and washing machine, as these appliances are the most widespread in the modern homes /apartments. Various possible combinations of these loads are investigated to observe the diversity effect, which implies the partial cancellation of harmonic currents among different loads due to dispersion in harmonic current phase angles.

The harmonic spectrums of all these measurements taken are presented in Table-3.14, where magnitudes of harmonic components are expressed as a percentage of the fundamental component and their corresponding phase angles are also given relative to phase angle of fundamental.

Fig. 3.18 shows the phase angle dispersion of individual harmonic currents up to 19^{th} harmonic. Phase angle dispersion of individual harmonic occurs mainly due to variation in following three parameters:

i) Power level

ii) Line impedance magnitude, and

iii) Line impedance X/R ratio.

Table-3.13 (a): Measurement results for various home appliances and equipments

<table>
<tr><th>Appliance / Equipment</th><th>THD_I Measurement</th><th>Power Measurement</th><th>Harmonic Spectrum</th></tr>
<tr><td>Fridge</td><td>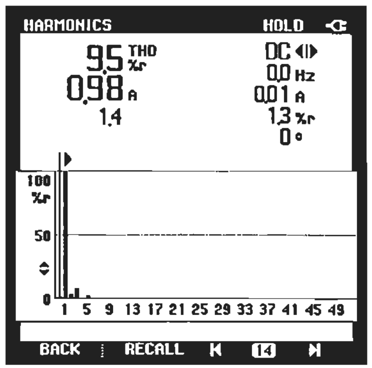

(a)</td><td>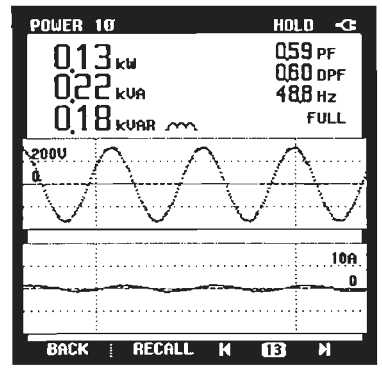

(b)</td><td>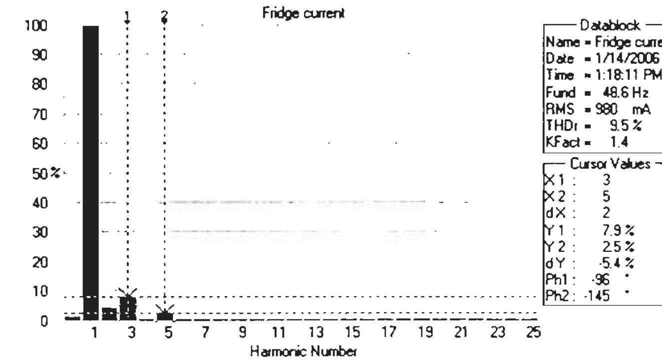

(c)</td></tr>
<tr><td></td><td></td><td></td><td></td></tr>
<tr><td>Microwave Owen</td><td>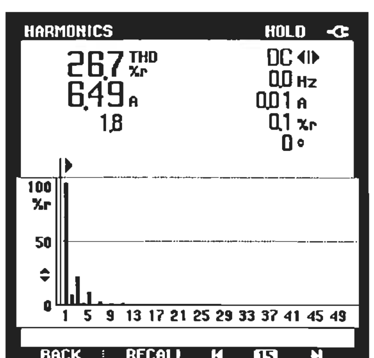

(a)</td><td>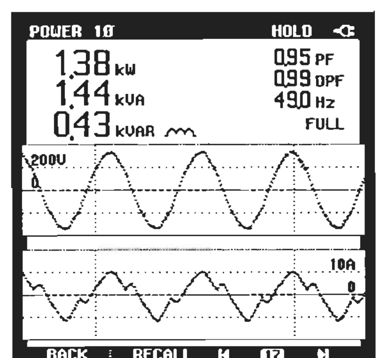

(b)</td><td>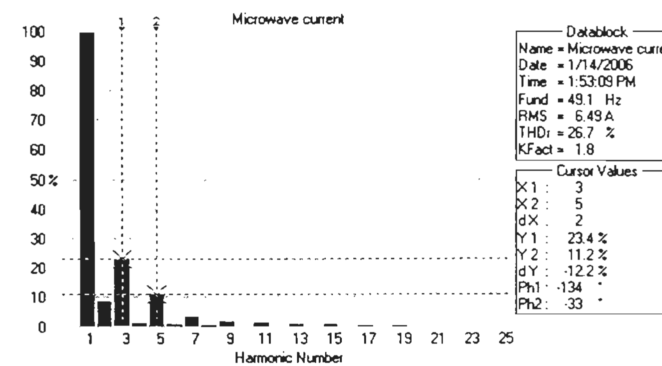

(c)</td></tr>
</table>

Table-3.13 (b): Measurement results for various home appliances and equipments

<table>
<tr><th>Appliance / Equipment</th><th>THD_I Measurement</th><th>Power Measurement</th><th>Harmonic Spectrum</th></tr>
<tr><td>Washing machine</td><td>
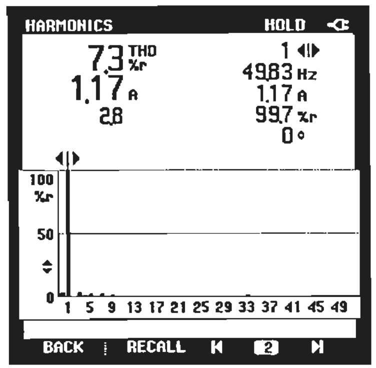

(a)</td><td>
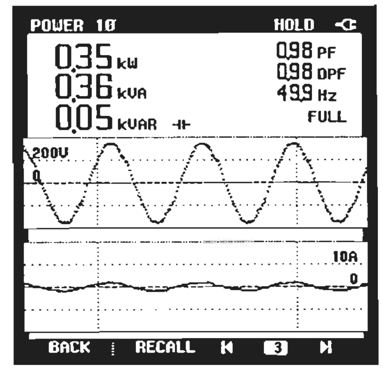

(b)</td><td>
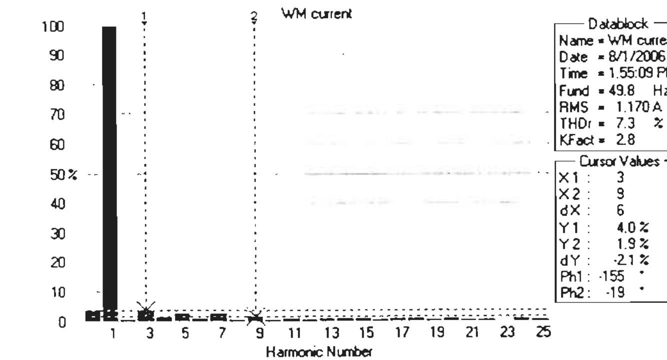

(c)</td></tr>
<tr><td></td><td></td><td></td><td></td></tr>
<tr><td>Television</td><td>
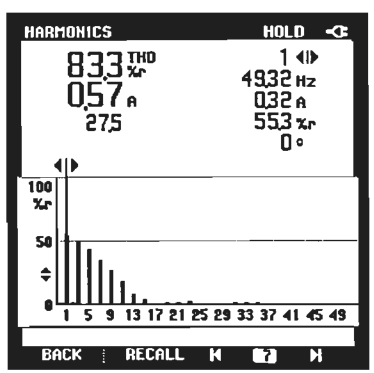

(a)</td><td>
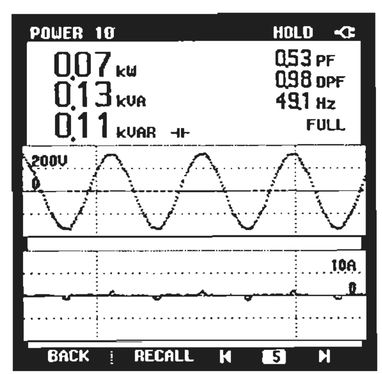

(b)</td><td>
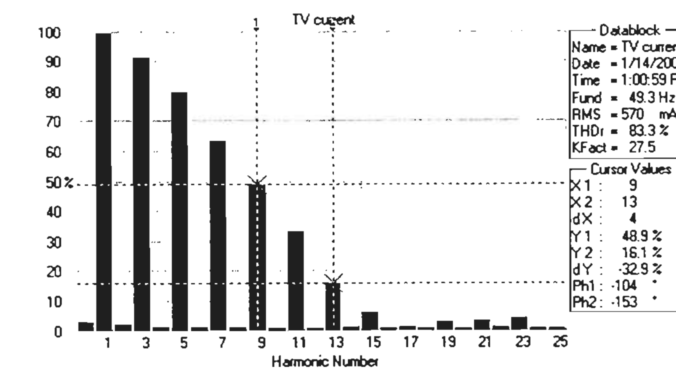

(c)</td></tr>
</table>

Table-3.13 (c): Measurement results for various home appliances and equipments

<table>
<tr><th>Appliance / Equipment</th><th>THD_I Measurement</th><th>Power Measurement</th><th>Harmonic Spectrum</th></tr>
<tr><td>Television + VCD</td><td>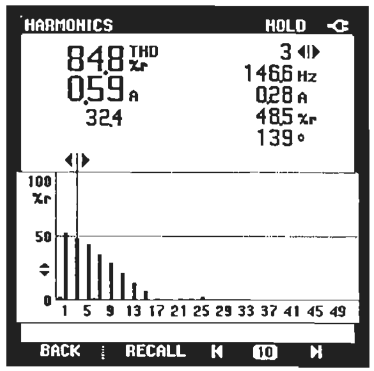
</td><td>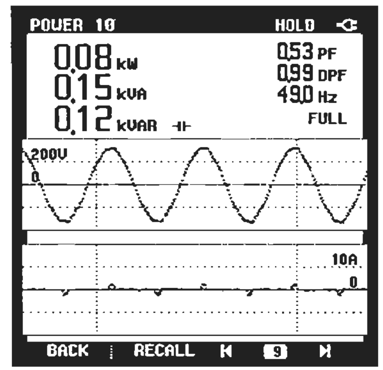
</td><td>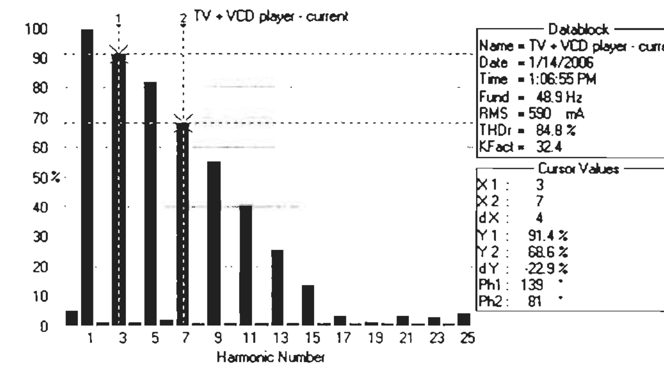
</td></tr>
<tr><td></td><td></td><td></td><td></td></tr>
<tr><td>Personal computer</td><td>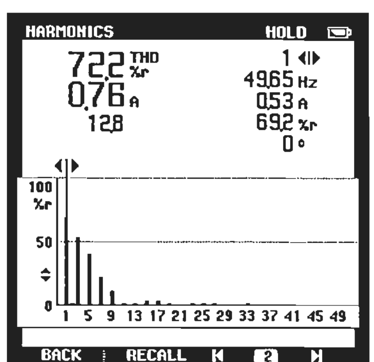
</td><td>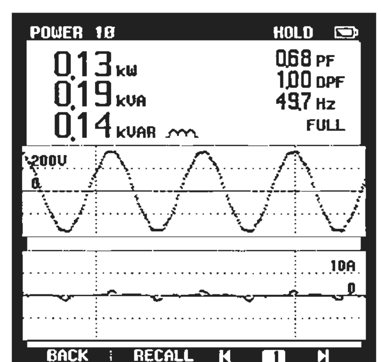
</td><td>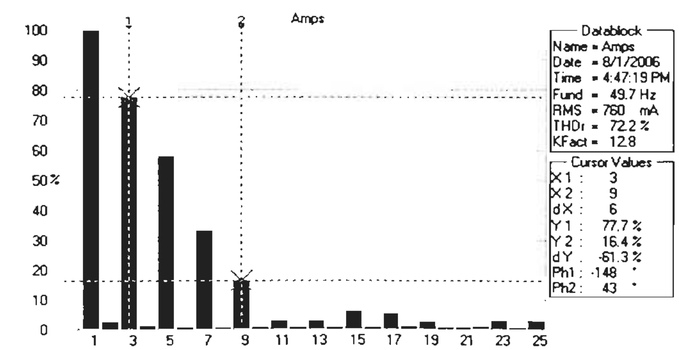
</td></tr>
</table>

Table-3.14: Comparison of measured power, net rms value and THD_I of load current with its harmonic spectrum for various home appliances and equipments

Appliance / Equipment	RMS Current (A)	Power (KW)	THD_I (%)		Harmonic order									
					1	3	5	7	9	11	13	15	17	19
Fridge	0.98	0.13	9.5	Mag. (A)	0.978	0.078	0.024	0.002	0.004	0.002	0.002	0.002	0.002	0.002
				Mag.(%)	100	7.9	2.5	0.2	0.5	0.2	0.2	0.2	0.2	0.2
				angle	0	-96	-145	-3	-160	14	80	-63	73	132
Microwave Owen	6.49	1.38	26.7	Mag. (A)	6.256	1.463	0.698	0.213	0.106	0.073	0.064	0.044	0.020	0.016
				Mag.(%)	100	23.4	11.2	3.4	1.7	1.2	1.0	0.7	0.3	0.2
				angle	0	-134	-33	-23	65	141	-138	-76	19	56
Washing machine	1.17	0.35	7.3	Mag. (A)	1.164	0.047	0.031	0.029	0.022	0.009	0.011	0.009	0.009	0.007
				Mag.(%)	100	4.0	2.7	2.5	1.9	0.8	1.0	0.8	0.8	0.6
				angle	0	-155	-93	-104	-19	-92	19	-85	-19	-114
Television	0.57	0.07	83.3	Mag. (A)	0.317	0.29	0.253	0.202	0.155	0.106	0.051	0.02	0.004	0.009
				Mag.(%)	100	91.6	79.7	63.6	48.9	33.6	16.1	6.3	1.4	2.8
				angle	0	147	-55	99	-104	52	-153	4	175	118
Television + VCD	0.59	0.08	84.8	Mag. (A)	0.310	0.284	0.255	0.213	0.173	0.126	0.08	0.042	0.011	0.004
				Mag.(%)	100	91.4	82.1	68.6	55.7	40.7	25.7	13.6	3.6	1.4
				angle	0	139	-68	81	-126	27	-178	-21	144	50
Personal computer	0.76	0.13	72.2	Mag. (A)	0.528	0.410	0.306	0.175	0.087	0.016	0.016	0.031	0.027	0.013
				Mag.(%)	100	77.7	58.0	33.2	16.4	2.9	2.9	5.9	5.0	2.5
				angle	0	-148	29	-134	43	-149	-79	91	-78	119

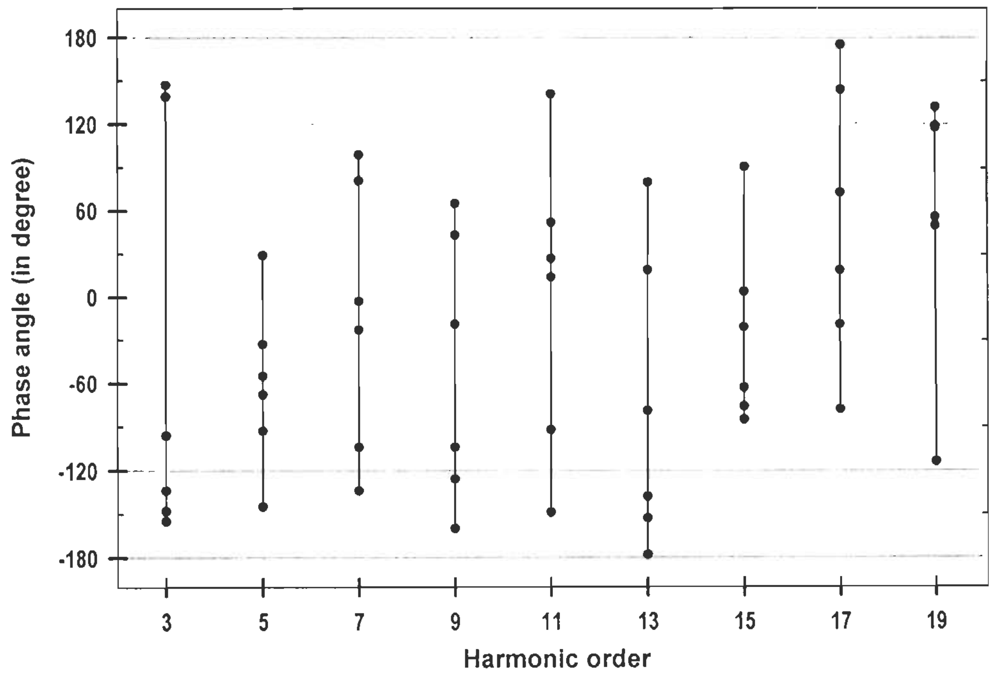

Fig. 3.18: Harmonic component's phase angle dispersion for various home appliances and equipments

Here, the phase angle dispersion makes possible significant cancellation due to the circulation of harmonic currents among multiple loads with different power levels, especially for higher order harmonics. In order to quantify the effect of phase angle dispersion, the current harmonic diversity factor (DFn) for any harmonic order n is defined as the ratio of phasor magnitude of net current to the sum of magnitudes of the individual currents [133].

$$DF_n = \frac{\text{net current for } n^{th} \text{ harmonic}}{\text{sum of individual currents for } n^{th} \text{ harmonic}} \tag{3.2}$$

The diversity factor ranges between 0 and 1. A small value implies a significant amount of cancellation.

For various possible combinations of home appliances and equipments, the comparison of measured power, net rms value and THD_I of load current with its harmonic spectrum is shown in Table-3.15.

On the basis of calculation of diversity factor as demonstrated in Table-3.15 it can be concluded that the cumulative magnitude of 7^{th} and above harmonic current components exhibit noticeable decrease due to phase angle cancellation, which is attributable only to single and /or combined variation in power level, here. The 3^{rd} and 5^{th} harmonics show small diversity effect as having higher values of diversity factor for these harmonic components.

Table-3.15: **Comparison of measured power, net rms value and THD_I of load current with its harmonic spectrum for various possible combinations of home appliances and equipments**

RMS Current (A)	Power (KW)	THD_I (%)		Harmonic order									
				1	3	5	7	9	11	13	15	17	19
Combination-1 (Microwave Owen +Washing machine + Television + VCD + Fridge + Personal computer)													
9.12	1.92	24.1	Mag. (A)	8.846	1.89	0.980	0.390	0.271	0.091	0.036	0.067	0.058	0.031
			Mag.(%)	100	21.4	11.1	4.4	3.1	1.0	0.4	0.8	0.7	0.4
			angle	0	-125	17	-24	122	-169	-54	-73	83	79
Diversity factor for combination-1					*0.828*	*0.746*	*0.617*	*0.691*	*0.403*	*0.208*	*0.5*	*0.841*	*0.74*
Combination-2: (Washing machine + Television + VCD + Fridge + Personal computer)													
2.99	0.70	32.8	Mag. (A)	2.827	0.736	0.561	0.264	0.153	0.029	0.058	0.053	0.036	0.016
			Mag.(%)	100	26	19.8	9.3	5.4	1.0	2.0	1.9	1.3	0.5
			angle	0	-147	64	-72	135	-58	39	-110	111	8
Diversity factor for combination-2					*0.899*	*0.911*	*0.63*	*0.535*	*0.19*	*0.532*	*0.631*	*0.7*	*0.615*
Combination-3: (Television + VCD + Fridge + Personal computer)													
1.89	0.36	49.5	Mag. (A)	1.643	0.683	0.541	0.299	0.140	0.022	0.038	0.055	0.033	0.004
			Mag.(%)	100	41.6	32.9	18.2	8.5	1.3	2.3	3.4	2.0	0.3
			angle	0	-91	148	33	-86	124	-124	110	-2	-97
Diversity factor for combination-3					*0.885*	*0.925*	*0.767*	*0.53*	*0.153*	*0.388*	*0.7*	*0.825*	*0.21*
Combination-4: (Television + VCD + Fridge)													
1.27	0.21	31.2	Mag. (A)	1.204	0.253	0.231	0.135	0.111	0.071	0.033	0.013	0.002	0.007
			Mag.(%)	100	21	19.2	11.2	9.2	5.9	2.8	1.1	0.2	0.6
			angle	0	-69	-150	119	25	-74	-170	85	-131	96
Diversity factor for combination-4					*0.699*	*0.828*	*0.628*	*0.627*	*0.555*	*0.402*	*0.295*	*0.2*	*0.778*

3.4 CONCLUDING REMARKS

These two different case studies are performed to measure the harmonic contents in power system in case of single /multiple PC loads for different operating conditions and processing modes; and a variety of modern home appliances and equipments having different power levels.

It is illustrated here that the parameters, which have an effect on harmonics produced in the line current are multiplicity of PC loads, mode of operation, and status of monitor. It is shown that presence of UPS also affects the harmonic distortion.

In case of identical loads sharing common system impedance, attenuation effect is observed. That is why for multiple PC loads, harmonic distortion is reduced. This reduction due to attenuation increases significantly with increasing number of loads, i.e. system loading and more pronounced results are obtained using simulation for larger number of PC loads, though not presented here. The cancellation of harmonic currents due to phase angle variation is not significant in case of multiple PC loads, as discussed in section 3.2 of this chapter, because they lack the power variation and have very small (negligible) variation in line impedance parameters. Furthermore, the internal series resistance and inductance of the PCs dilute any variation in branch circuit impedance that causes dispersion in harmonic phase angles among individual loads.

The diversity effect due to cancellation of harmonic currents because of phase angle variation is found effective in case of combination of nonlinear loads (modern home appliances and equipments) with different power levels. This reduction due to phase angle diversity is relatively independent of system loading. On the basis these results, it is observed that attenuation and diversity are two important factors while studying the harmonic behavior of single-phase nonlinear loads, in particular for the higher order harmonic components.

CHAPTER IV

EVALUATION OF HARMONIC DISTORTION UNDER UNBALANCED VOLTAGE SUPPLY CONDITIONS

4.1 INTRODUCTORY REMARKS

Voltage unbalance is regarded as a power quality problem of significant concern at the electricity distribution level. In three-phase power systems, the generated voltages are sinusoidal and equal in magnitude, with their individual phases 120° apart from each other. However, the resulting power system voltages at the distribution end and at the point of utilization can be unbalanced for several reasons. Voltage unbalance is a condition in which the three phase voltages differ in amplitude, or are displaced from their standard 120° phase relationship, or both.

Unbalance of three-phase voltages result from asymmetry of line /cable impedances and from inequality of the loads in the three phases [134]. The former is related to the structure of the electric power system in which geometric allocation of lines /cables significantly influences their impedances. Efforts are made to reduce the asymmetry of the transmission line impedances by means of transposition, in general. Additional causes of power system voltage unbalance can be asymmetrical transformer winding impedances, open wye- and open delta- transformer connections, asymmetrical transmission impedances possibly caused by incomplete transposition of transmission lines, and blown fuses on three-phase capacitor banks [135, 136]. This problem is aggravated by the fact that the presence of a small unbalance in the line voltages will cause an unbalance in the line currents that can be disproportionately many times larger.

Another major cause of voltage unbalance is the uneven distribution of single-phase loads in low voltage residential and /or commercial systems, which can be continuously changing across a three-phase power system. Wherever possible, efforts are made to distribute the single-phase loads uniformly over three phases. For example, problem areas can be rural electric power systems with long distribution lines, as well as large urban power systems where heavy single-phase demands, such as lighting loads, are imposed by large commercial facilities [135, 136]. However, from a statistical point of view distributing single-phase loads uniformly over the three phases only ensures that the expected values of the loads in each phase will be approximately equal. But it is unlikely that at a given instant, all single-phase loads will be balanced because they vary in a random manner. In other words, even if the average loads in the three phases are kept the same, the instantaneous power demands in three phases differ from each other, leading to unbalanced voltages at the point of common coupling.

Large single-phase loads such as single-phase induction motors, traction systems, induction heating, etc., are typical examples that cause considerable voltage unbalance on the utility three-phase system unless proper design steps are taken [11]. Industrial and commercial facilities may have well balanced incoming supply voltages, but unbalance can develop within the building from its own single-phase power requirements if the loads are not uniformly spread among the three phases. Unbalanced voltages can also be caused by unbalanced and overloaded equipments, and high impedance connections (i.e. loose contacts).

When a balanced three-phase load is connected to an unbalanced supply system, the currents drawn by the load also become unbalanced. Practically, it is difficult or virtually impossible to provide a perfectly balanced supply system to a customer. However, every attempt has to be taken to minimize the voltage unbalance to reduce its effects on customer loads, i.e. high DC distortion, over-voltages and high currents, excessive losses in other rotating machines, KVAr inductive meter errors, protection relay malfunction, etc. [137].

Many utilities do not keep track of their voltage unbalance in the interest of time /task prioritization, as the undesirable effects are not instantaneously noticeable and unbalance is only paid attention, in case of any complaint. The power quality issues are gaining the attention and concern of various researchers, because of large diffusion of non-linear and time varying single-phase loads and their interactions with the distribution networks in residential, commercial and industrial areas. Therefore, it has become very essential that unbalance phenomena should also be well monitored, detected and corrected. The work presented here is an endeavor in this direction.

4.2 TYPES OF VOLTAGE UNBALANCE AND THEIR CAUSES

There are various possible cases of voltage unbalance. In the present work, following eight different unbalanced cases are discussed [138]:

i) Single-Phase Under-Voltage Unbalance (1Φ-UV)

This type of situation arises, when there is a large single-phase load in the system and it does not have enough compensation. In this situation, the voltage in that particular phase will be lower than the other two phases.

ii) Two-Phase Under-Voltage Unbalance (2Φ-UV)

If two of the three phases have heavy load and do not have enough compensation, then these two phases will have higher voltage drop than the third phase.

iii) Three-Phase Under-Voltage Unbalance (3Φ-UV)

When the loads in all three phases are too heavy and not balanced, in that case three-phase under-voltage unbalance will take place.

iv) Single-Phase Over-Voltage Unbalance (1Φ-OV)

Over-voltage unbalance is defined as unbalance due to the positive sequence voltage component being higher than the balanced rated voltage, a rare situation that usually takes place during off-peak period. Capacitors are normally used to compensate system reactive power. In order to maintain a system voltage at rated value, if any one of the three-phase voltages has been over-compensated, then voltage of this phase goes higher than the rated value and leads to single-phase over-voltage unbalance.

v) Two-Phase Over-Voltage Unbalance (2Φ-OV)

If two of the three phases are over compensated, then the voltages of these two phases will be higher than the rated value. This situation arises in a two phase over-voltage unbalance.

vi) Three-Phase Over-Voltage Unbalance (3Φ-OV)

If the three-phase voltages are over-compensated to different levels, then in all three phases, voltages will be higher than the rated value and not equal. This situation usually occurs at the time when an industry shuts down but capacitors are still connected to the system.

vii) Single Phase Angle Displacement (1Φ-Angle)

If the three-phase voltages are balanced, the angle displacement between them should be equal to 120°. Let phase *A* be the reference, if one of the other two phase angles is deflected, unequal displacement in single-phase angle occurs.

viii) Unequal Two Phase Angles Displacement (2Φ-Angle)

Similarly, if the two phase angles are deflected simultaneously, then unequal angle displacement in two phase angles occurs, and leads to voltage unbalance.

4.3 DEFINITIONS OF VOLTAGE UNBALANCE AND THEIR COMPARISONS

In a three-phase system, voltage unbalance takes place when the magnitudes of phase or line voltages are different and the phase angles differ from the balanced conditions, or both. The five different definitions of voltage unbalance [139-146] developed by various power communities (CIGRE, NEMA, IEEE, and IEC) are stated and analyzed below:

4.3.1 CIGRE (Conseil International des Grands Reseaux Electriques) Definition

As per the method [142] recommended by CIGRE, the voltage unbalance can be determined by equation given as

$$\%\,\text{Unbalance factor} = \sqrt{\frac{1-\sqrt{3-6.\beta}}{1+\sqrt{3-6.\beta}}} \tag{4.1}$$

where, $\beta = \dfrac{|V_{ab}|^4 + |V_{bc}|^4 + |V_{ca}|^4}{\left(|V_{ab}|^2 + |V_{bc}|^2 + |V_{ca}|^2\right)^2}$; and V_{ab}, V_{bc}, and V_{ca} are line voltages.

4.3.2 NEMA (National Equipment Manufacturer's Association) Definition

The NEMA definition [143] of voltage unbalance, also known as the line voltage unbalance rate (%LVUR), is given by

$$\%\text{LVUR} = \frac{\text{maximum voltage deviation from average Line voltage}}{\text{average Line voltage}} * 100$$

$$= \frac{\text{maximum}\left[\,|V_{ab} - V_{L_{av}}|,\ |V_{bc} - V_{L_{av}}|,\ |V_{ca} - V_{L_{av}}|\,\right]}{V_{L_{av}}} * 100 \tag{4.2}$$

where, V_{ab}, V_{bc}, and V_{ca} are line voltages and average line voltage $(V_{L_{av}}) = \dfrac{V_{ab}+V_{bc}+V_{ca}}{3}$.

The NEMA definition assumes that the average voltage is always equal to the rated value and since it works only with magnitudes, phase angles are not included.

4.3.3 IEEE Definition 1

Definition of voltage unbalance according to IEEE 112-1991 [144], also known as the phase voltage unbalance rate (%PVUR), is given by "The maximum deviation from the average phase voltage, referred to the average of the three-phase voltages".

$$\% PVUR = \frac{\text{maximum voltage deviation from average phase voltage}}{\text{average phase voltage}} * 100$$

$$= \frac{\max.\left[\,|V_{an} - V_{Pav.}|,\ |V_{bn} - V_{Pav.}|,\ |V_{cn} - V_{Pav.}|\,\right]}{V_{P_{av}}} * 100 \qquad (4.3)$$

where, average phase voltage($V_{P_{av}}$) $= \frac{V_{an} + V_{bn} + V_{cn}}{3}$, and V_{an}, V_{bn}, and V_{cn} are individual phase voltages.

The IEEE uses the same definition of voltage unbalance as NEMA, the only difference being that the IEEE uses phase voltages rather than line-to-line voltages. Here again, the phase angle information is lost since only magnitudes are considered.

4.3.4 IEEE Definition 2

"IEEE dictionary" [145] gives a slightly different definition of voltage unbalance (referring to IEEE Std. 936-1987). "The difference between the highest and the lowest rms voltage, referred to the average of the three voltages". This inconsistency between different IEEE documents is unfortunately not uncommon [140].

$$\% PVUR\ 1 = \frac{\text{difference between the highest and the lowest rms phase voltage}}{\text{average phase voltage}} * 100$$

$$= \frac{V_{max} - V_{min}}{V_{P_{av}}} * 100 \qquad (4.4)$$

where, $V_{max} = \max.(V_{an}, V_{bn}, V_{cn})$; $V_{min} = \min.(V_{an}, V_{bn}, V_{cn})$; and V_{an}, V_{bn}, and V_{cn} are individual phase voltages.

The IEEE Std.1159-1995 (recently reaffirmed) gives both the IEEE 112 definition and the true definition.

4.3.5 True Definition

The "true definition" [2] of voltage unbalance is defined as the ratio of the negative sequence voltage component (V_2) to the positive sequence voltage component (V_1). The percentage voltage unbalance factor (VUF), or the "true definition", is given by

$$\%\,\text{VUF} = \frac{\text{negative sequence voltage component}\,(V_2)}{\text{positive sequence voltage component}\,(V_1)} * 100 \tag{4.5}$$

These sequence voltage components are obtained by resolving three-phase unbalanced line voltages, V_{ab}, V_{bc}, and V_{ca} (or phase voltages) into two symmetrical components V_1 and V_2, which are given by

$$V_1 = \frac{V_{ab} + a.V_{bc} + a^2.\,V_{ca}}{3}, \quad \text{and} \quad V_2 = \frac{V_{ab} + a^2.V_{bc} + a.\,V_{ca}}{3} \tag{4.6}$$

where, $a = 1\angle 120^\circ$ and $a^2 = 1\angle 240^\circ$

This "true definition" of voltage unbalance is also approved by IEC [146]. However, field engineers, whether familiar or not with symmetrical components, seem to prefer the simpler way of representing the degree of voltage unbalance such as the maximum percentage deviation from the average of three-phase voltages. One of the reasons is that they often have difficulties in evaluating the VUF with voltage phasors that requires measurement of the phase angles and involved manipulations of complex quantities. To avoid the use of complex mathematics involved in calculating the V_1 and V_2, following formula is proposed in [139] that gives a good approximation to the true definition:

$$\%\,\text{Voltage unbalance} = \frac{82.\sqrt{V_{ab*}^2 + V_{bc*}^2 + V_{ca*}^2}}{V_{L_{av}}} \tag{4.7}$$

where, $V_{L_{av}}$ the average line voltage is similar to eqn. (4.2), and $V_{ab*} = V_{ab} \sim V_{L_{av}}$, $V_{bc*} = V_{bc} \sim V_{L_{av}}$ and $V_{ca*} = V_{ca} \sim V_{L_{av}}$.

There are certain limitations with this approximation formula that below 5% unbalance, the difference between the LVUR (NEMA definition) and the VUF (true definition) is very small (0.8 %) but as the LVUR increases this approximation formula deviates more from the true definition.

Recently, it is shown in [147] that the positive, negative and zero sequence components of a three-phase, sinusoidal and unbalanced voltage system can be calculated exactly without the application of the complex mathematics. Here, only the root mean square (RMS) line-to-line voltages are required, and without the knowledge of phase relationships between these voltages. This results in a convenient procedure to assess voltage unbalance in the field.

Jeong [148] has derived an expression of the VUF in terms of the magnitude of line-to-line voltages, which appears to be related to the area of the triangle of unbalanced line voltages and the area of equivalent balanced voltage triangle. Although the formula avoids the measurement of phase angles and complex number manipulations, it still needs the calculation for the area of voltage triangles. The calculation can be completely avoided by using a proposed voltage unbalance chart derived from constant VUF condition applied to the line voltage triangle, which can be used to determine the magnitude of VUF in a straightforward graphical manner with measured line voltage magnitudes.

Although, no simple way of approximation has been found that applies over the whole range of voltage unbalance. These various attempts only facilitate the representation of voltage unbalance for field engineers under usually encountered unbalance conditions.

In [140], with the help of an example, it is concluded that both IEEE definitions (PVUR and PVUR1) deviate significantly from the true value (VUF) and from the NEMA definition (LVUR) of voltage unbalance. More serious fact is that even the results of the two IEEE definitions deviate from each other. It is also observed that in cases where phase angle unbalance is involved, PVUR and PVUR1 are unable to reflect the source voltage unbalance conditions. Hence, the PVUR and PVUR1 are seldom used. To calculate the degree of voltage unbalance industries and utilities prefer to use NEMA definition (LVUR), as measuring line voltages is easier in the industry. But, this particular definition does not offer any hint to operator about the remedial action to be taken to improve the unbalance status and preventive action to avoid their harmful consequences. Also, the NEMA definition (LVUR) of voltage unbalance is not comprehensive, as several conditions of the unbalance in the phase voltages (the voltage amplitude is same but different phase angles) leads to a single value of voltage unbalance. The true definition (VUF) involves both magnitude and angle when calculating the value of positive and negative sequence components where as CIGRE definition uses the magnitude of line voltages only, based on simple measurement. Still it was observed that the value of CIGRE definition is exactly the same as VUF. This shows the versatility of the CIGRE definition, which employs simple arithmetical calculation. Therefore, it can also be concluded that in absence of angle measurement, the method of CIGRE is most suitable and simple to quantify the voltage unbalance.

Considering VUF for degree of voltage unbalance, V_1 and V_2 are also to be obtained, in process of calculating VUF, which helps in evaluating some important characteristics of power system. Comparison of balanced voltages with the V_1 gives a more exact estimation of voltage unbalances. V_1 and V_2 play an important role in describing a more clear view of degree of voltage unbalance. As zero-sequence voltage components are never present in line voltages, for three-phase loads without neutral, the negative sequence voltage component is the primary cause of voltage unbalance. Normally, the positive sequence voltage components are very close to rated (balanced voltage) value. While expressing in per unit (p.u.) quantities, the V_1 will be very close to 1.0 p.u. and the corresponding V_2 will be very close to VUF. Thus, the VUF can definitely be considered as the V_2 in per unit. This clearly explains the advantage of using VUF as an index for analyzing the effects of voltage unbalance.

In present study it is observed that the difference between the NEMA definition (LVUR) and the true definition (VUF) may differ substantially at high level of voltage unbalance. Here, the quantitative evaluation of impacts of degree of unbalance (VUF) on input and output characteristics provides a deep insight about the role of voltage sequence components in harmonic analysis under unbalanced supply conditions. For the purpose of this work, only four definitions (LVUR, PVUR, PVUR1 and VUF) are shown, as the CIGRE definition is concerned, it is observed that at every stage of unbalance, it is precisely equal to VUF. For different compositions of unbalance source voltages there is a variation in the relation among the numerical values of these four definitions. This gives an important conclusion that it is not merely sufficient to know the degree of voltage unbalance of supply system, but it is equally important to know that 'how' they are unbalanced.

4.4 DEFINITION OF PHASE TOTAL HARMONIC DISTORTION UNBALANCE FACTOR (PTHDUF)

For a balanced three-phase system under balanced operating conditions, the phase harmonic currents have equal magnitudes and a known phase sequence. Hence, analysis of only one phase is carried out. But in case of unbalanced system, harmonic content of each phase current differs with other phases and the difference in various phase harmonic component and their distortion levels can be significant. To simplify the harmonic current analysis in three different phases a new term "Phase Total Harmonic Distortion Unbalance Factor" (PTHDUF) is introduced.

The proposed term PTHDUF is defined as "The maximum deviation from the average Total Harmonic Distortion of current (THD_I) in three different phases, referred to the average of THD_I in three different phases."

$$\%PTHDUF = \frac{\text{maximum deviation from average of } THD_I \text{ in 3 phases}}{\text{average of } THD_I \text{ in three phases}} * 100$$

$$= \frac{\max\left[T_A.T_B.T_C\right]}{THD_{I_{Average}}} * 100 \tag{4.8}$$

where,
$$T_A = \left|THD_{I_{phase\,A}} - THD_{I_{Average}}\right|,$$
$$T_B = \left|THD_{I_{phase\,B}} - THD_{I_{Average}}\right|,$$
$$T_C = \left|THD_{I_{phase\,C}} - THD_{I_{Average}}\right|; \text{ and}$$

$$THD_{I_{Average}} = \frac{THD_{I_{phase\,A}} + THD_{I_{phase\,B}} + THD_{I_{phase\,C}}}{3}$$

Here, it is important to mention that T_A, T_B and T_C are absolute values.

4.5 EFFECTS OF VOLTAGE UNBALANCE

Three phase voltage unbalance is a frequently encountered power quality issue in weak power networks and in power systems that supply large single-phase loads. It results in severe effects on both the power systems and equipments, such as induction motors and power electronic converters and drives.

4.5.1 Effects on Induction Motors

Unbalance voltage supply to a three-phase induction motor, which is a critical component of many industrial processes and integrated in various commercially available equipments used in industrial and residential systems, leads to several detrimental effects on its performance [149].

These adverse effects include increased losses and consequently temperature rise, reduced motor efficiency, decreased insulation life resulting in premature motor failure, noisy motor operation due to torque and motor pulsations, excessive tripping of protective relays along with negative impact on power system stability as the power system will be in a better position to respond to emergency load transfers, if the phases are balanced [150]. Several contributions made by different researchers on the performance of induction motors under unbalanced voltage supply are listed in [11, 16].

4.5.2 Effects on Power Electronic Converters

In recent years, the three-phase AC-DC rectifiers are finding great industrial utility. These power electronic converters serve as the interface between the three-phase electric utility and power electronic loads such as adjustable speed AC motor drives, DC motor drives, three-phase uninterruptible power supplies (UPS), induction heating systems etc. The three-phase bridge rectifier is the preferred choice for high power applications over single-phase rectifiers primarily due to its low ripple content in DC output and higher power handling capability [151]. Most of these converters contain a diode rectifier front-end, and DC-link capacitor to convert the incoming AC voltage to a low-ripple DC voltage. These three-phase converters with diode rectifier front-ends are non-linear in nature and draw non-sinusoidal currents rich in odd harmonics.

These harmonic currents cause additional voltage drops across the source inductances, which result in increased distortion of the supply system voltage waveforms. As a result, the power factor of the converters is usually poor and varies with the load. For rectifier systems supplied by balanced utility voltages, the input current characteristic harmonics are determined by:

$$n = k.P \pm 1 \qquad (4.9)$$

where, n = order of the harmonics;

k =1, 2, 3, 4... ; and P = number of pulses of the rectifier system.

Conventional "six-pulse" rectifiers (P = 6), are defined by the fact that the DC bus voltage consists of portions of the line-to-line AC waveform and repeats with a 60° duration, i.e., containing six pulses in 360°. Therefore, the characteristic current harmonics present in the utility input current are 5^{th}, 7^{th}, 11^{th} and 13^{th} etc. But, under the conditions of utility voltage unbalance, the input current harmonics are not restricted to the converter characteristic harmonics, and uncharacteristic triplen harmonics can appear, which may make the power factor and system efficiency very low.

These converters are designed on the basis of balanced three-phase supply at the fundamental frequency having small voltage and current ripple components permitting the reduction of filtering components resulting in decrease of input losses and magnetic noise, in input transformers wherever used. These advantages can be fully realized only when the three-phase input source voltage is balanced, which is not necessarily a true condition in many practical industrial and distribution systems. Under unbalanced input voltage supply conditions, there is deterioration of rectifier input and output characteristics. The behavior of multi phase converters, in which the individual input phase voltage contributes to the DC output, is also affected by the unbalanced supply. This leads to the appearance of non-characteristic harmonics and changes in characteristic harmonics in the input port to the rectifier and undesirable harmonic distortion in the output. Uncontrolled rectifiers are more sensitive to the voltage unbalance due to their non-linear behavior under unbalanced voltage supply. As a result, it is not uncommon to encounter rectifier currents significantly unbalanced, even when the supply voltage unbalance is well below a usually acceptable level. Unbalanced rectifier currents cause detrimental effects viz. i) uneven current distribution over the legs of the rectifier bridge that increases the conduction loss and may cause failure of rectifying devices; ii) increased rms ripple current in the smoothing capacitor; iii) increased total rms line current and harmonics [152]. The situation is more aggravated when the presence of an unbalance load produces the unbalanced load current components. These components cause voltage drop across the source impedance, and hence generate harmonic powers flowing backward from the load to the power supply system [153].

In general, frequency or time-domain methods are used for theoretical investigations. The frequency domain approach is based on the conventional converter theory and gives results which may be somewhat inaccurate due to simplified assumptions usually involved, i.e. perfectly smooth DC current, sinusoidal voltage at input port of converters etc. In frequency domain, the six-pulse converter is modeled as a multiple frequency current source [154, 155]. For each harmonic and fundamental current component, harmonic order and current together with phase angle is specified. This suggests that frequency domain method of analysis is a linear approximation of non-linear problem. In time domain method, the actual voltage and current waveforms are used for circuit simulation, as the six-pulse converter is modeled using actual diodes, thyristors etc. In frequency domain analysis, there is no access to the DC side of converter, while in time-domain simulation, the results show that the change in DC side of load has a large impact on the harmonic currents, injected by the non-linear loads [156]. Hence, time-domain analysis methods, which involve actual circuit simulation, provide more latitude in modeling various circuit components and hence the results are more accurate.

In the present work, the simulation is carried out in time-domain and the harmonic spectra of distorted input and output waveform is obtained using FFT in frequency domain.

4.6 RECTIFIER PERFORMANCE UNDER SOURCE VOLTAGE UNBALANCE WITH VARIABLE VUF

The problem of voltage unbalance has attracted the special attention of many researchers dealing with power quality issues in recent past. This work, therefore, presents a detailed analytical study on the effect of voltage unbalance in the supply system on the harmonics injected by a three-phase AC-DC rectifier. A quantitative evaluation of the impact of positive and negative sequence voltages on the performance of three-phase AC-DC rectifier is done. There may be several possible voltage unbalance conditions in a power system [138]. In this work, following cases of voltage unbalance are studied:

i) Single-phase voltage magnitude unbalance: under-voltage (UV) and over-voltage (OV)

ii) Single-phase unbalance due to phase angle movement: clockwise (CW) and anticlockwise (ACW)

iii) Change in two phase angles with equal change in each phase

   a) Two phasors moving in opposite direction for increasing phase angle between two phases

   b) Two phasors moving in same direction for decreasing phase angle between two phases

iv) Change in two phase angles with unequal change in each phase

   a) Two phasors moving in opposite direction, i.e. increasing phase angle between two phases

   b) Two phasors moving in same direction, i.e. decreasing phase angle between two phases

v) Eight unbalance cases with same degree of unbalance (VUF)

a) Single phase under-voltage unbalance (1Φ-UV)

b) Two phases under-voltage unbalance (2Φ-UV)

c) Three phases under-voltage unbalance (3Φ-UV)

d) Single phase over-voltage unbalance (1Φ-OV)

e) Two phases over-voltage unbalance (2Φ-OV)

f) Three phases over-voltage unbalance (3Φ-OV)

g) Single phase angle displacement (1Φ-Angle)

h) Unequal two phase angles displacement (2Φ-Angle)

These case-studies are performed to find out the importance of V_1 and V_2 in voltage unbalance analysis. The negative sequence voltage component (V_2) also has its own impact on the performance of rectifier. To identify the role and effects of V_2 apart from those of V_1, an exceptional case is taken up for study, in which the increased value of VUF is obtained, only by increasing (regulating) the value of V_2 and keeping V_1 constant. This study, discussed in section 4.8 of this chapter points out the exclusive effect of V_2.

These case studies are categorized on the basis of parameter (i.e. voltage magnitude /phase angle of different phases) regulating the increasing value of VUF, and an attempt has been made to find out the answer of the question- "how the composition of voltage unbalance affects the performance?"

For every case the effect of unbalance on performance is studied on the following factors:

i) Comparison of different definitions of voltage unbalance

ii) Effect of voltage unbalance on magnitude of DC parameters and their distortion

iii) Effect of voltage unbalance on AC parameters and their distortion

iv) Effect of voltage unbalance on PTHDUF and variation of PTHDUF with degree of voltage unbalance (VUF)

The DC parameters under consideration are DC voltage (V_{DC}), DC load current (I_{DC}), and DC power (P_{DC}); while AC parameters are rms line currents (I_A, I_B, and I_C) and their corresponding THD_I.

Also, the variation of different characteristic and non-characteristic harmonics is investigated to verify that how these voltage unbalance conditions affect the pattern of characteristic harmonics and generation of non-characteristic harmonics.

4.7 SINGLE-PHASE VOLTAGE MAGNITUDE UNBALANCE CASES

To study the effect of single-phase voltage magnitude unbalance in source voltage on the performance of AC-DC rectifier, the VUF is gradually increased from 0% (balanced case) to 16% through deviation in magnitude of voltage phasors. This deviation in magnitude of voltage is considered in both directions, i.e. under-voltage (UV) and over-voltage (OV).

4.7.1 Single-Phase Under-Voltage Unbalance Case

For single-phase UV unbalance case the results are shown in Table-4.1, which also includes the three-phase supply voltages, their V_1 and V_2 along with the numerical values of four different definitions of voltage unbalance. Here, the considered single-phase under-voltage unbalance is due to reduction in magnitude of line-neutral voltage of phase *A*. Table-4.2 details the results for single-phase UV unbalance conditions considered independently for other two phases; *B* and *C* (unbalance in one phase of source voltage at a time).

4.7.2 Single-Phase Over-Voltage Unbalance Case

Table-4.3 describes the input and output parameter performance of rectifier under single-phase over-voltage unbalanced condition with VUF gradually varying from 0% (balanced case) to 16 %. Corresponding three-phase supply voltages, their V_1 and V_2 and the values of four different definitions of voltage unbalance, are also shown in Table-4.3. Here, again the unbalance in three-phase source voltage is due to increasing magnitude of line-neutral voltage of phase *A*. Table-4.4 details the results for single-phase over-voltage unbalance conditions considered individually in three different phases.

In both of the cases discussed above, it is found that the effect of single-phase UV /OV unbalance on DC parameters is quite characteristic and for a given value of VUF, it makes no difference on the performance of DC parameters regardless of whether the voltage unbalance is taking place in phase *A*, *B* or *C*. The only difference observed in these three different cases is in the values of AC parameters i.e. rms currents and their distortion. Table-4.5 (a) and Table- 4.5 (b) present the behavior of characteristic and non-characteristic harmonics, respectively for the increasing values of VUF. The percentages of harmonic components are based on considering the magnitude of fundamental frequency current component as 100%. This variation in harmonic pattern behavior is discussed in section 4.13.

Table-4.1: **Comparison of four different definitions of voltage unbalance and rectifier performance for 1-Φ under-voltage unbalance in phase *A* for increasing VUF**

LVUR (%)	PVUR 1 (%)	PVUR (%)	VUF (%)	Unbalanced voltage source						+ve seq. Volt. (V_1)	-ve seq. Volt. (V_2)	AC parameters						Average THD_I	PTHDUF (%)	DC parameters					
				Phase *A*		Phase *B*		Phase *C*				I_A		I_B		I_C				I_{DC}		V_{DC}		P_{DC}	
				Mag.	Angle	Mag.	Angle	Mag.	Angle			RMS	THD_I (%)	Mag.	THD_I (%)	Mag.	THD_I (%)			Mag.	THD_I (%)	Mag.	THD_I (%)	Mag.	THD_I (%)
0.0	0	0	0	1.000	0	1.0	240	1.0	120	1.000	0.000	1.000	27.87	1.000	27.87	1.000	27.87	27.87	0.0	1.00	5.95	1.00	6.72	1.00	12.13
1.0	3	2	1	0.970	0	1.0	240	1.0	120	0.990	0.010	0.980	28.40	0.995	27.64	0.995	27.58	27.87	1.89	0.990	6.03	0.990	6.80	0.980	12.30
1.99	6	4	2	0.941	0	1.0	240	1.0	120	0.980	0.020	0.961	28.94	0.990	27.41	0.991	27.30	27.88	3.79	0.980	6.28	0.980	7.02	0.961	12.79
2.98	9	6	3	0.913	0	1.0	240	1.0	120	0.971	0.029	0.941	29.50	0.985	27.18	0.987	27.02	27.90	5.73	0.971	6.67	0.971	7.38	0.943	13.58
3.96	12	8	4	0.885	0	1.0	240	1.0	120	0.962	0.038	0.922	30.06	0.980	26.95	0.983	26.75	27.92	7.66	0.962	7.18	0.962	7.86	0.926	14.61
4.93	15	10	5	0.857	0	1.0	240	1.0	120	0.952	0.048	0.903	30.64	0.976	26.72	0.979	26.47	27.94	9.65	0.953	7.80	0.953	8.44	0.909	15.85
5.90	18	12	6	0.830	0	1.0	240	1.0	120	0.943	0.057	0.884	31.24	0.972	26.50	0.976	26.21	27.98	11.64	0.944	8.50	0.944	9.10	0.893	17.26
6.86	21	14	7	0.804	0	1.0	240	1.0	120	0.935	0.065	0.866	31.85	0.968	26.27	0.973	25.94	28.02	13.67	0.936	9.25	0.936	9.83	0.878	18.79
7.82	24	16	8	0.778	0	1.0	240	1.0	120	0.926	0.074	0.847	32.47	0.965	26.05	0.970	25.68	28.07	15.69	0.946	10.06	0.927	10.61	0.863	20.42
8.77	27	18	9	0.752	0	1.00	240	1.00	120	0.917	0.083	0.829	33.11	0.961	25.82	0.967	25.42	28.12	17.76	0.919	10.91	0.919	11.43	0.848	22.12
9.71	30	20	10	0.727	0	1.00	240	1.00	120	0.909	0.091	0.811	33.77	0.958	25.59	0.964	25.16	28.17	19.87	0.911	11.78	0.911	12.29	0.835	23.89
10.65	33	22	11	0.703	0	1.00	240	1.00	120	0.901	0.099	0.794	34.44	0.955	25.37	0.961	24.91	28.24	21.95	0.904	12.65	0.904	13.17	0.822	25.70
11.57	36	24	12	0.679	0	1.00	240	1.00	120	0.893	0.107	0.776	35.13	0.952	25.14	0.959	24.65	28.31	24.11	0.896	13.60	0.896	14.08	0.809	27.55
12.49	39	26	13	0.655	0	1.00	240	1.00	120	0.885	0.115	0.759	35.83	0.950	24.91	0.957	24.40	28.38	26.25	0.889	14.54	0.889	15.0	0.797	29.42
13.41	42	28	14	0.632	0	1.00	240	1.00	120	0.877	0.123	0.741	36.55	0.947	24.67	0.954	24.14	28.45	28.46	0.882	15.49	0.882	15.94	0.785	31.31
14.31	45	30	15	0.609	0	1.00	240	1.00	120	0.870	0.130	0.725	37.29	0.945	24.44	0.952	23.89	28.54	30.66	0.875	16.45	0.875	16.90	0.774	33.21
15.20	48	32	16	0.586	0	1.00	240	1.00	120	0.862	0.138	0.708	38.04	0.943	24.20	0.951	23.63	28.62	32.90	0.868	17.41	0.868	17.86	0.763	35.12

Table-4.2: Comparison of AC current parameters (rms value and THD_I) for 1-Φ under-voltage unbalance, considered individually in three different phases for increasing VUF

VUF (%)	+ve seq. Volt. (V_1)	-ve seq. Volt. (V_2)	PTHDUF (%)	Average THD_I	Unbalance only in phase *A*						Unbalance only in phase *B*						Unbalance only in phase *C*					
					I_A		I_B		I_C		I_A		I_B		I_C		I_A		I_B		I_C	
					RMS	THD_I (%)	Mag.	THD_I (%)	Mag.	THD_I (%)	RMS	THD_I (%)	Mag.	THD_I (%)	Mag.	THD_I (%)	RMS	THD_I (%)	Mag.	THD_I (%)	Mag.	THD_I (%)
0	1.000	0.000	0.0	27.87	1.000	27.87	1.000	27.87	1.000	27.87	1.000	27.87	1.000	27.87	1.000	27.87	1.000	27.87	1.000	27.87	1.000	27.87
1	0.990	0.010	1.89	27.87	0.980	28.40	0.995	27.64	0.995	27.58	0.996	27.59	0.980	28.40	0.995	27.64	0.995	27.64	0.995	27.58	0.980	28.40
2	0.980	0.020	3.79	27.88	0.961	28.94	0.990	27.41	0.991	27.30	0.991	27.30	0.960	28.94	0.990	27.41	0.990	27.41	0.996	27.30	0.960	28.94
3	0.971	0.029	5.73	27.90	0.941	29.50	0.985	27.18	0.987	27.02	0.987	27.03	0.941	29.49	0.985	27.18	0.985	27.18	0.987	27.02	0.941	29.49
4	0.962	0.038	7.66	27.92	0.922	30.06	0.980	26.95	0.983	26.75	0.983	26.75	0.922	30.06	0.980	26.95	0.981	26.96	0.983	26.75	0.922	30.06
5	0.952	0.048	9.65	27.94	0.903	30.64	0.976	26.72	0.979	26.47	0.980	26.48	0.903	30.64	0.976	26.72	0.976	26.73	0.979	26.48	0.903	30.64
6	0.943	0.057	11.64	27.98	0.884	31.24	0.972	26.50	0.976	26.21	0.976	26.21	0.884	31.23	0.972	26.50	0.972	26.50	0.976	26.21	0.884	31.23
7	0.935	0.065	13.67	28.02	0.866	31.85	0.968	26.27	0.973	25.94	0.973	25.95	0.866	31.84	0.968	26.27	0.968	26.28	0.973	25.94	0.866	31.84
8	0.926	0.074	15.69	28.07	0.847	32.47	0.965	26.05	0.970	25.68	0.970	25.69	0.847	32.46	0.965	26.05	0.965	26.05	0.970	25.68	0.847	32.46
9	0.917	0.083	17.76	28.12	0.829	33.11	0.961	25.82	0.967	25.42	0.967	25.43	0.829	33.10	0.961	25.82	0.962	25.82	0.967	25.42	0.829	33.10
10	0.909	0.091	19.87	28.17	0.811	33.77	0.958	25.59	0.964	25.16	0.964	25.17	0.811	33.76	0.958	25.59	0.958	25.6	0.964	25.17	0.811	33.76
11	0.901	0.099	21.95	28.24	0.794	34.44	0.955	25.37	0.961	24.91	0.962	24.91	0.793	34.43	0.955	25.37	0.955	25.37	0.961	24.91	0.793	34.43
12	0.893	0.107	24.11	28.31	0.776	35.13	0.952	25.14	0.959	24.65	0.959	24.66	0.776	35.12	0.952	25.14	0.952	25.14	0.959	24.65	0.776	35.12
13	0.885	0.115	26.25	28.38	0.759	35.83	0.950	24.91	0.957	24.40	0.957	24.40	0.759	35.82	0.950	24.91	0.950	24.91	0.957	24.40	0.759	35.82
14	0.877	0.123	28.46	28.45	0.741	36.55	0.947	24.67	0.954	24.14	0.955	24.15	0.742	36.54	0.947	24.68	0.948	24.68	0.954	24.14	0.742	36.54
15	0.870	0.130	30.66	28.54	0.725	37.29	0.945	24.44	0.952	23.89	0.952	23.89	0.725	37.28	0.945	24.44	0.945	24.45	0.952	23.89	0.725	37.28
16	0.862	0.138	32.90	28.62	0.708	38.04	0.943	24.20	0.951	23.63	0.951	23.63	0.708	38.03	0.943	24.21	0.943	24.21	0.951	23.63	0.708	38.03

Table-4.3: **Comparison of four different definitions of voltage unbalance and performance of rectifier for 1-Φ over-voltage unbalance in phase *A* for increasing VUF**

LVUR (%)	PVUR 1 (%)	PVUR (%)	VUF (%)	Unbalanced voltage source: Phase *A* Mag.	Phase *A* Angle	Phase *B* Mag.	Phase *B* Angle	Phase *C* Mag.	Phase *C* Angle	+ve seq. Volt. (V_1)	-ve seq. Volt. (V_2)	AC parameters: I_A RMS	I_A THD_I (%)	I_B Mag.	I_B THD_I (%)	I_C Mag.	I_C THD_I (%)	Average THD_I	PTHDUF (%)	DC parameters: I_{DC} Mag.	I_{DC} THD_I (%)	V_{DC} Mag.	V_{DC} THD_I (%)	P_{DC} Mag.	P_{DC} THD_I (%)
0.0	0	0	0	1.000	0	1.00	240	1.00	120	1.000	0.000	1.00	27.87	1.000	27.87	1.000	27.87	27.87	0.00	1.000	5.95	1.000	6.72	1.000	12.13
1.00	3	2	1	1.030	0	1.00	240	1.00	120	1.010	0.010	1.02	27.35	1.005	28.10	1.005	28.16	27.87	1.87	1.010	6.03	1.010	6.80	1.020	12.30
2.01	6	4	2	1.061	0	1.00	240	1.00	120	1.020	0.020	1.04	26.85	1.011	28.34	1.010	28.46	27.88	3.71	1.021	6.27	1.021	7.02	1.042	12.77
3.02	9	6	3	1.093	0	1.00	240	1.00	120	1.031	0.031	1.06	26.36	1.017	28.58	1.015	28.76	27.90	5.52	1.031	6.65	1.031	7.37	1.064	13.52
4.04	12	8	4	1.125	0	1.00	240	1.00	120	1.042	0.042	1.08	25.88	1.024	28.82	1.020	29.06	27.92	7.31	1.042	7.14	1.042	7.82	1.087	14.48
5.06	15	10	5	1.130	0	1.00	240	1.00	120	1.053	0.053	1.10	25.41	1.030	29.06	1.026	29.38	27.95	9.09	1.053	7.73	1.053	8.37	1.111	15.63
6.08	18	12	6	1.192	0	1.00	240	1.00	120	1.064	0.064	1.13	24.95	1.037	29.31	1.032	29.70	27.99	10.85	1.065	8.38	1.065	9.00	1.136	16.91
7.11	21	14	7	1.226	0	1.00	240	1.00	120	1.075	0.075	1.15	24.50	1.045	29.56	1.038	30.02	28.03	12.58	1.077	9.09	1.077	9.67	1.162	18.27
8.14	24	16	8	1.261	0	1.00	240	1.00	120	1.087	0.087	1.17	24.08	1.052	29.83	1.044	30.37	28.09	14.29	1.089	9.84	1.089	10.39	1.189	19.71
9.17	27	18	9	1.297	0	1.00	240	1.00	120	1.099	0.099	1.19	23.63	1.060	30.07	1.051	30.69	28.13	16.00	1.101	10.61	1.101	11.15	1.218	21.21
10.21	30	20	10	1.333	0	1.00	240	1.00	120	1.111	0.111	1.22	23.21	1.069	30.33	1.058	31.03	28.19	17.67	1.114	11.41	1.114	11.93	1.247	22.73
11.25	33	22	11	1.371	0	1.00	240	1.00	120	1.124	0.124	1.24	22.82	1.077	30.62	1.065	31.40	28.28	19.31	1.127	12.23	1.127	12.73	1.278	24.28
12.30	36	24	12	1.409	0	1.00	240	1.00	120	1.136	0.136	1.26	22.42	1.086	30.88	1.073	31.76	28.35	20.93	1.141	13.06	1.141	13.54	1.310	25.84
13.34	39	26	13	1.448	0	1.00	240	1.00	120	1.149	0.149	1.29	22.03	1.096	31.15	1.081	32.12	28.43	22.52	1.155	13.89	1.155	14.37	1.343	27.41
14.39	42	28	14	1.488	0	1.00	240	1.00	120	1.163	0.163	1.31	21.64	1.106	31.43	1.089	32.49	28.52	24.12	1.169	14.73	1.169	15.20	1.378	28.97
15.44	45	30	15	1.529	0	1.00	240	1.00	120	1.176	0.176	1.34	21.27	1.116	31.71	1.098	32.87	28.62	25.67	1.183	15.58	1.183	16.04	1.415	30.53
16.49	48	32	16	1.571	0	1.00	240	1.00	120	1.190	0.190	1.36	20.88	1.126	31.97	1.106	33.23	28.69	27.23	1.198	16.42	1.198	16.88	1.452	32.08

Table-4.4: **Comparison of AC current parameters (rms value and THD_I) for 1-Φ over-voltage unbalance, considered individually in three different phases for increasing VUF**

VUF (%)	+ve seq. Volt. (V_1)	-ve seq. Volt. (V_2)	PTHDUF (%)	Average THD_I	Unbalance only in phase *A*						Unbalance only in phase B						Unbalance only in phase C					
					I_A		I_B		I_C		I_A		I_B		I_C		I_A		I_B		I_C	
					RMS	THD_I (%)	Mag.	THD_I (%)	Mag.	THD_I (%)	RMS	THD_I (%)	Mag.	THD_I (%)	Mag.	THD_I (%)	RMS	THD_I (%)	Mag.	THD_I (%)	Mag.	THD_I (%)
0	1.000	0.000	0.00	27.87	1.00	27.87	1.000	27.87	1.000	27.87	1.000	27.87	1.00	27.87	1.000	27.87	1.000	27.87	1.000	27.87	1.00	27.87
1	1.010	0.010	1.87	27.87	1.02	27.35	1.005	28.10	1.005	28.16	1.005	28.16	1.02	27.35	1.005	28.10	1.005	28.10	1.005	28.16	1.02	27.35
2	1.020	0.020	3.71	27.88	1.04	26.85	1.011	28.34	1.010	28.46	1.010	28.46	1.04	26.85	1.011	28.34	1.011	28.34	1.010	28.46	1.04	26.85
3	1.031	0.031	5.52	27.90	1.06	26.36	1.017	28.58	1.015	28.76	1.015	28.76	1.06	26.36	1.017	28.58	1.017	28.58	1.015	28.76	1.06	26.36
4	1.042	0.042	7.31	27.92	1.08	25.88	1.024	28.82	1.020	29.06	1.020	29.06	1.08	25.88	1.024	28.82	1.024	28.82	1.020	29.06	1.08	25.88
5	1.053	0.053	9.09	27.95	1.10	25.41	1.030	29.06	1.026	29.38	1.026	29.38	1.10	25.41	1.030	29.06	1.030	29.06	1.026	29.38	1.10	25.41
6	1.064	0.064	10.85	27.99	1.13	24.95	1.037	29.31	1.032	29.70	1.032	29.70	1.13	24.95	1.037	29.31	1.037	29.31	1.032	29.70	1.13	24.95
7	1.075	0.075	12.58	28.03	1.15	24.50	1.045	29.56	1.038	30.02	1.038	30.02	1.15	24.50	1.045	29.56	1.045	29.56	1.038	30.02	1.15	24.50
8	1.087	0.087	14.29	28.09	1.17	24.08	1.052	29.83	1.044	30.37	1.044	30.37	1.17	24.08	1.052	29.83	1.052	29.83	1.044	30.37	1.17	24.08
9	1.099	0.099	16.00	28.13	1.19	23.63	1.060	30.07	1.051	30.69	1.051	30.69	1.19	23.63	1.060	30.07	1.060	30.07	1.051	30.69	1.19	23.63
10	1.111	0.111	17.67	28.19	1.22	23.21	1.069	30.33	1.058	31.03	1.058	31.03	1.22	23.21	1.069	30.33	1.069	30.33	1.058	31.03	1.22	23.21
11	1.124	0.124	19.31	28.28	1.24	22.82	1.077	30.62	1.065	31.40	1.065	31.40	1.24	22.82	1.077	30.62	1.077	30.62	1.065	31.40	1.24	22.82
12	1.136	0.136	20.93	28.35	1.26	22.42	1.086	30.88	1.073	31.76	1.073	31.76	1.26	22.42	1.086	30.88	1.086	30.88	1.073	31.76	1.26	22.42
13	1.149	0.149	22.52	28.43	1.29	22.03	1.096	31.15	1.081	32.12	1.081	32.12	1.29	22.03	1.096	31.15	1.096	31.15	1.081	32.12	1.29	22.03
14	1.163	0.163	24.12	28.52	1.31	21.64	1.106	31.43	1.089	32.49	1.089	32.49	1.31	21.64	1.106	31.43	1.106	31.43	1.089	32.49	1.31	21.64
15	1.176	0.176	25.67	28.62	1.34	21.27	1.116	31.71	1.098	32.87	1.098	32.87	1.34	21.27	1.116	31.71	1.116	31.71	1.098	32.87	1.34	21.27
16	1.190	0.190	27.23	28.69	1.36	20.88	1.126	31.97	1.106	33.23	1.106	33.23	1.36	20.88	1.126	31.97	1.126	31.97	1.106	33.23	1.36	20.88

Table-4.5(a): Characteristic harmonic current components with increasing VUF for 1-Φ under-voltage unbalance, in phase *A*

		VUF = 0.0 %	VUF = 1.0 %	VUF = 2.0 %	VUF = 3.0 %	VUF = 4.0 %	VUF = 5.0 %	VUF = 6.0 %	VUF = 7.0 %	VUF = 8.0 %	VUF = 9.0 %	VUF = 10.0 %	VUF = 11.0 %	VUF = 12.0 %	VUF = 13.0 %	VUF = 14.0 %	VUF = 15.0 %	VUF = 16.0 %
Phase *A*	THD_I	**27.87**	**28.40**	**28.94**	**29.50**	**30.06**	**30.64**	**31.24**	**31.85**	**32.47**	**33.11**	**33.77**	**34.44**	**35.13**	**35.83**	**36.55**	**37.29**	**38.04**
	h 5	22.37	23.03	23.67	24.30	24.91	25.50	26.06	26.60	27.11	27.59	28.03	28.43	28.79	29.11	29.38	29.60	29.76
	h 7	10.86	10.49	10.06	9.58	9.03	8.41	7.73	6.99	6.18	5.31	4.37	3.37	2.30	1.18	0.05	1.23	2.52
	h 11	8.35	8.82	9.22	9.55	9.81	9.99	10.08	10.07	9.96	9.74	9.41	8.98	8.43	7.77	7.00	6.13	5.15
	h 13	5.74	5.34	4.85	4.27	3.60	2.85	2.03	1.15	0.22	0.78	1.80	2.83	3.87	4.89	5.87	6.81	7.67
	h 17	4.62	4.99	5.26	5.43	5.47	5.40	5.19	4.85	4.38	3.79	3.08	2.26	1.37	0.41	0.60	1.62	2.62
	h 19	3.56	3.17	2.68	2.09	1.42	0.68	0.14	0.94	1.77	2.57	3.32	3.99	4.56	5.00	5.28	5.39	5.32
	h 23	2.83	3.11	3.28	3.32	3.22	2.98	2.60	2.10	1.49	0.79	0.03	0.75	1.52	2.23	2.85	3.33	3.65
	h 25	2.3	1.96	1.51	0.98	0.37	0.29	0.94	1.56	2.13	2.60	2.94	3.13	3.14	2.97	2.63	2.11	1.45
	h 29	1.77	1.98	2.07	2.02	1.84	1.53	1.10	0.59	0.02	0.57	1.13	1.61	1.98	2.20	2.25	2.11	1.78
	h 31	1.48	1.20	0.83	0.38	0.14	0.62	1.08	1.47	1.75	1.89	1.87	1.69	1.36	0.90	0.34	0.26	0.85
Phase *B*	THD_I	**27.87**	**27.64**	**27.41**	**27.18**	**26.95**	**26.72**	**26.50**	**26.27**	**26.05**	**25.82**	**25.59**	**25.37**	**25.14**	**24.91**	**24.67**	**24.44**	**24.20**
	h 5	22.36	22.06	21.74	21.40	21.04	20.66	20.26	19.85	19.41	18.96	18.49	18.01	17.51	16.99	16.46	15.93	15.38
	h 7	10.87	11.01	11.15	11.29	11.43	11.58	11.72	11.86	11.99	12.12	12.24	12.36	12.47	12.56	12.65	12.72	12.78
	h 11	8.34	8.11	7.85	7.57	7.27	6.94	6.60	6.24	5.86	5.46	5.06	4.65	4.23	3.82	3.40	3.00	2.61
	h 13	5.75	5.90	6.05	6.19	6.32	6.44	6.55	6.64	6.71	6.76	6.78	6.78	6.75	6.69	6.60	6.48	6.32
	h 17	4.62	4.41	4.19	3.93	3.66	3.37	3.06	2.74	2.41	2.08	1.74	1.41	1.09	0.79	0.53	0.36	0.42
	h 19	3.56	3.71	3.84	3.95	4.04	4.11	4.16	4.18	4.16	4.11	4.03	3.92	3.77	3.59	3.38	3.15	2.89
	h 23	2.82	2.65	2.46	2.24	2.01	1.76	1.51	1.25	0.98	0.71	0.45	0.20	0.11	0.35	0.60	0.86	1.10
	h 25	2.30	2.42	2.53	2.61	2.66	2.68	2.68	2.63	2.56	2.45	2.32	2.15	1.97	1.76	1.55	1.32	1.08
	h 29	1.76	1.63	1.47	1.30	1.12	0.93	0.73	0.53	0.32	0.12	0.11	0.32	0.53	0.75	0.95	1.15	1.32
	h 31	1.49	1.58	1.66	1.71	1.73	1.72	1.68	1.61	1.51	1.39	1.26	1.11	0.94	0.77	0.59	0.41	0.22
Phase *C*	THD_I	**27.87**	**27.58**	**27.30**	**27.02**	**26.75**	**26.47**	**26.21**	**25.94**	**25.68**	**25.42**	**25.16**	**24.91**	**24.65**	**24.40**	**24.14**	**23.89**	**23.63**
	h 5	22.36	21.98	21.57	21.14	20.70	20.23	19.75	19.25	18.73	18.19	17.64	17.08	16.50	15.91	15.31	14.70	14.08
	h 7	10.87	11.06	11.24	11.42	11.59	11.74	11.89	12.02	12.15	12.26	12.36	12.44	12.51	12.56	12.60	12.61	12.61
	h 11	8.34	8.05	7.73	7.38	7.01	6.60	6.17	5.72	5.25	4.77	4.27	3.76	3.25	2.73	2.22	1.72	1.25
	h 13	5.75	5.94	6.11	6.26	6.38	6.48	6.56	6.61	6.63	6.62	6.58	6.51	6.41	6.27	6.10	5.90	5.66
	h 17	4.62	4.37	4.09	3.78	3.43	3.05	2.65	2.23	1.79	1.35	0.90	0.46	0.18	0.49	0.89	1.29	1.66
	h 19	3.56	3.73	3.86	3.96	4.03	4.07	4.06	4.02	3.94	3.83	3.67	3.47	3.24	2.97	2.66	2.33	1.97
	h 23	2.82	2.62	2.38	2.10	1.79	1.45	1.09	0.72	0.34	0.06	0.42	0.78	1.13	1.44	1.72	1.97	2.18
	h 25	2.3	2.44	2.53	2.59	2.61	2.59	2.52	2.42	2.27	2.09	1.87	1.61	1.33	1.02	0.68	0.34	0.04
	h 29	1.76	1.60	1.40	1.17	0.91	0.62	0.32	0.02	0.31	0.60	0.88	1.14	1.35	1.53	1.66	1.75	1.78
	h 31	1.49	1.59	1.65	1.67	1.65	1.59	1.50	1.36	1.19	0.99	0.76	0.51	0.24	0.05	0.32	0.59	0.84

Table-4.5(b): Non-characteristic Harmonic Current Components with increasing VUF for 1-Φ under-voltage unbalance, in phase *A*

		VUF = 0.0 %	VUF = 1.0 %	VUF = 2.0 %	VUF = 3.0 %	VUF = 4.0 %	VUF = 5.0 %	VUF = 6.0 %	VUF = 7.0 %	VUF = 8.0 %	VUF = 9.0 %	VUF = 10.0 %	VUF = 11.0 %	VUF = 12.0 %	VUF = 13.0 %	VUF = 14.0 %	VUF = 15.0 %	VUF = 16.0 %
Phase *A*	THD_I	27.87	28.40	28.94	29.50	30.06	30.64	31.24	31.85	32.47	33.11	33.77	34.44	35.13	35.83	36.55	37.29	38.04
	h 3	0.01	0.71	1.44	2.19	2.97	3.78	4.62	5.49	6.38	7.30	8.25	9.23	10.24	11.27	12.33	13.42	14.54
	h 9	0.01	0.86	1.74	2.64	3.55	4.46	5.38	6.29	7.19	8.06	8.90	9.70	10.46	11.15	11.78	12.34	12.80
	h 15	0.01	0.79	1.58	2.37	3.15	3.88	4.57	5.19	5.72	6.16	6.48	6.67	6.73	6.63	6.38	5.97	5.41
	h 21	0.01	0.68	1.35	1.99	2.58	3.10	3.51	3.80	3.95	3.94	3.78	3.45	2.96	2.33	1.57	0.71	0.23
	h 27	0.01	0.55	1.09	1.57	1.97	2.26	2.43	2.44	2.30	2.00	1.56	1.00	0.35	0.36	1.06	1.71	2.26
	h 33	0.01	0.43	0.82	1.15	1.39	1.51	1.50	1.34	1.06	0.66	0.19	0.32	0.81	1.24	1.55	1.71	1.69
Phase *B*	THD_I	27.87	27.64	27.41	27.18	26.95	26.72	26.50	26.27	26.05	25.82	25.59	25.37	25.14	24.91	24.67	24.44	24.20
	h 3	0.01	0.65	1.28	1.90	2.51	3.10	3.68	4.24	4.78	5.30	5.81	6.30	6.77	7.21	7.64	8.05	8.43
	h 9	0.01	0.39	0.76	1.12	1.46	1.80	2.11	2.42	2.70	2.98	3.24	3.48	3.71	3.94	4.15	4.35	4.54
	h 15	0.0	0.33	0.64	0.94	1.23	1.51	1.78	2.04	2.29	2.53	2.77	3.00	3.22	3.44	3.65	3.86	4.05
	h 21	0.0	0.27	0.53	0.79	1.03	1.27	1.51	1.74	1.96	2.18	2.38	2.58	2.75	2.91	3.04	3.14	3.21
	h 27	0.0	0.21	0.42	0.63	0.84	1.04	1.24	1.43	1.60	1.76	1.90	2.01	2.10	2.14	2.15	2.13	2.07
	h 33	0.0	0.16	0.32	0.48	0.64	0.80	0.95	1.09	1.21	1.30	1.37	1.40	1.40	1.37	1.31	1.23	1.13
Phase *C*	THD_I	27.87	27.58	27.30	27.02	26.75	26.47	26.21	25.94	25.68	25.42	25.16	24.91	24.65	24.40	24.14	23.89	23.63
	h 3	0.01	0.71	1.39	2.06	2.72	3.35	3.97	4.56	5.14	5.70	6.23	6.75	7.24	7.71	8.16	8.58	8.98
	h 9	0.01	0.51	1.01	1.48	1.94	2.39	2.81	3.21	3.59	3.95	4.29	4.61	4.90	5.17	5.42	5.65	5.86
	h 15	0.01	0.46	0.90	1.33	1.73	2.12	2.48	2.82	3.14	3.42	3.68	3.91	4.12	4.30	4.45	4.57	4.67
	h 21	0.0	0.40	0.78	1.15	1.50	1.82	2.11	2.37	2.60	2.79	2.95	3.07	3.15	3.20	3.21	3.19	3.12
	h 27	0.0	0.33	0.65	0.95	1.23	1.48	1.69	1.86	2.00	2.09	2.14	2.14	2.10	2.03	1.91	1.76	1.57
	h 33	0.0	0.27	0.52	0.75	0.96	1.13	1.26	1.35	1.40	1.40	1.36	1.28	1.17	1.02	0.85	0.65	0.43

4.7.3 Comparison of Four Different Definitions of Voltage Unbalance

The magnitudes of PVUR1, PVUR, LVUR and VUF are seen to be in the ratio of 3:2:1:1. As the VUF goes very high (beyond 10 % in this case), then LVUR happens to be little lower than VUF as displayed in Fig. 4.1, for the single-phase under-voltage unbalance. For the single-phase over-voltage unbalance, the relation among various definitions of voltage unbalance remains same except for the fact that as the VUF increases, the LVUR happens to be little higher than VUF.

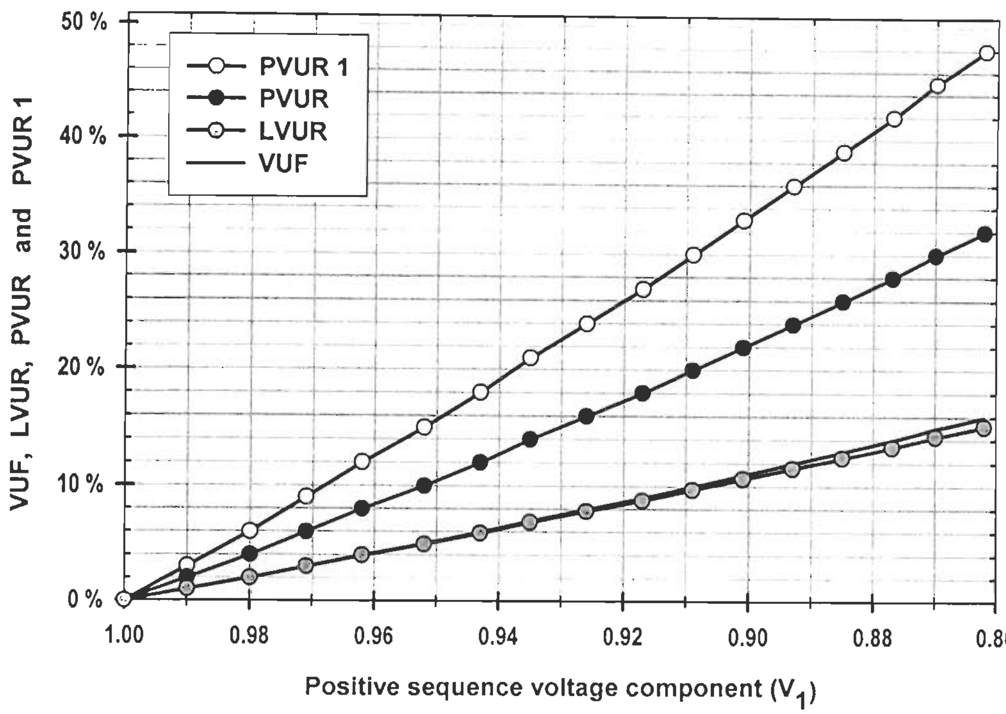

Fig. 4.1: Comparison of four different definitions of voltage unbalance for single-phase under-voltage unbalances case

4.7.4 Effect of Voltage Magnitude Unbalance on DC Parameters

The positive and negative sequence voltage components play an important role in describing a more clear view of degree of voltage unbalance. For both cases of voltage unbalance (under-voltage and over-voltage), it is observed that V_2 increases with the increase in VUF. The change in value of V_1 depends on the type of unbalance as the V_1 increases for over-voltage unbalance case and decreases for under-voltage unbalance case with the rising VUF. The variation of V_1 and V_2 as a function of VUF is displayed in Fig. 4.2(a) and Fig. 4.2(b) for under-voltage and over-voltage unbalance cases respectively.

In addition to this, it is also observed from the results depicted in Table-4.1 and Table-4.3 for single-phase under-voltage and over-voltage unbalances, that for a given value of VUF, the numerical value of V_2 is almost equal to the change in the numerical value of V_1 as compared to its value for balanced case, i.e. 1.0 p.u. Also, for a specified value of VUF, the difference in values of V_1 and V_2 from their corresponding values under balanced conditions (V_1 = 1.0 p.u. and V_2 = 0.0 p.u.) is found to be higher for single-phase over-voltage unbalance as compared to the values for under-voltage unbalance case, e.g. for VUF equal to 16% from Table-4.1 (for under-voltage case), V_1 is 0.862 p.u. and V_2 is 0.138 p.u. i.e. (=1.00~0.862) p.u., while for the same VUF from Table-4.3 (for over-voltage case), V_1 is 1.190 p.u. and V_2 is 0.190 p.u. i.e. (=1.00~1.190) p.u. This example justifies the conclusions made above.

Decrease in the V_1 due to increasing VUF causes decrease in magnitudes of DC output parameters (P_{DC}, V_{DC}, and I_{DC}) in case of single-phase under-voltage unbalance case, as shown in Fig. 4.3(a). Similarly, for single-phase over-voltage unbalance case, as the V_1 increases with increasing degree of unbalance. The magnitudes of DC output parameters are seen to be increasing as given in Fig. 4.3(b). It can be concluded that the V_1 plays an important role in the voltage unbalance analysis and the magnitudes of DC output parameters are found to be proportional to it.

For both the single-phase (under-voltage and over-voltage unbalance cases studied here, it is observed that the V_2 increases with increasing VUF. This increasing V_2 has its own impact on rectifier performance which is reflected on the distortion of DC output parameters. The distortion is found to be proportional to degree of unbalance. The change in distortion of DC output parameters with increasing VUF is shown in Fig. 4.4(a) and Fig. 4.4(b) for under-voltage and over-voltage unbalance cases respectively.

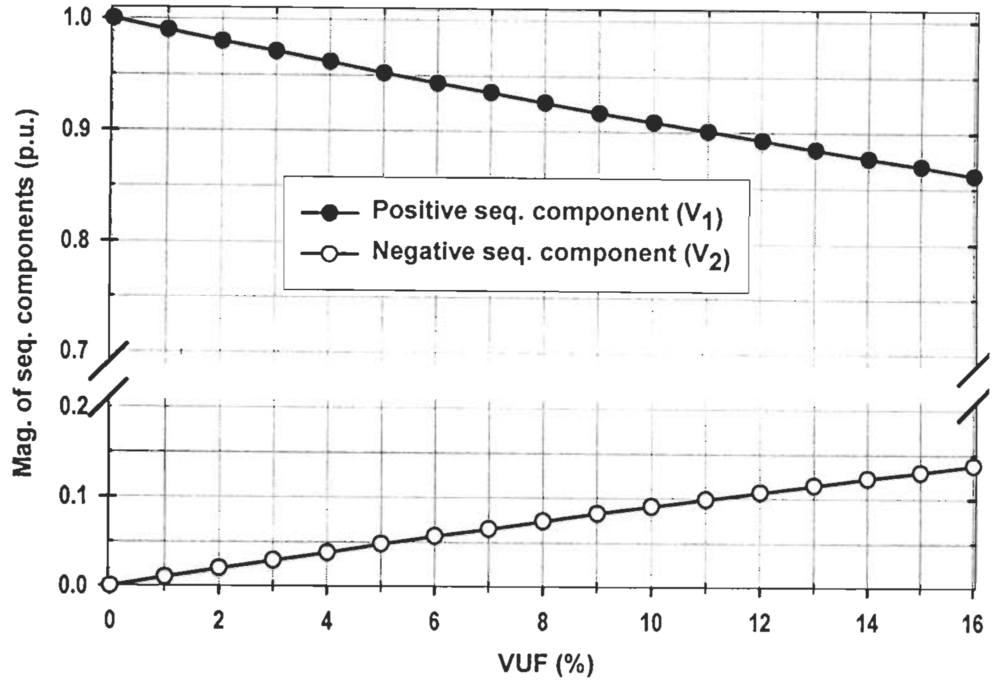

Fig. 4.2(a): **Variation of magnitude of V_1 and V_2 as a function of VUF for single-phase under-voltage unbalance**

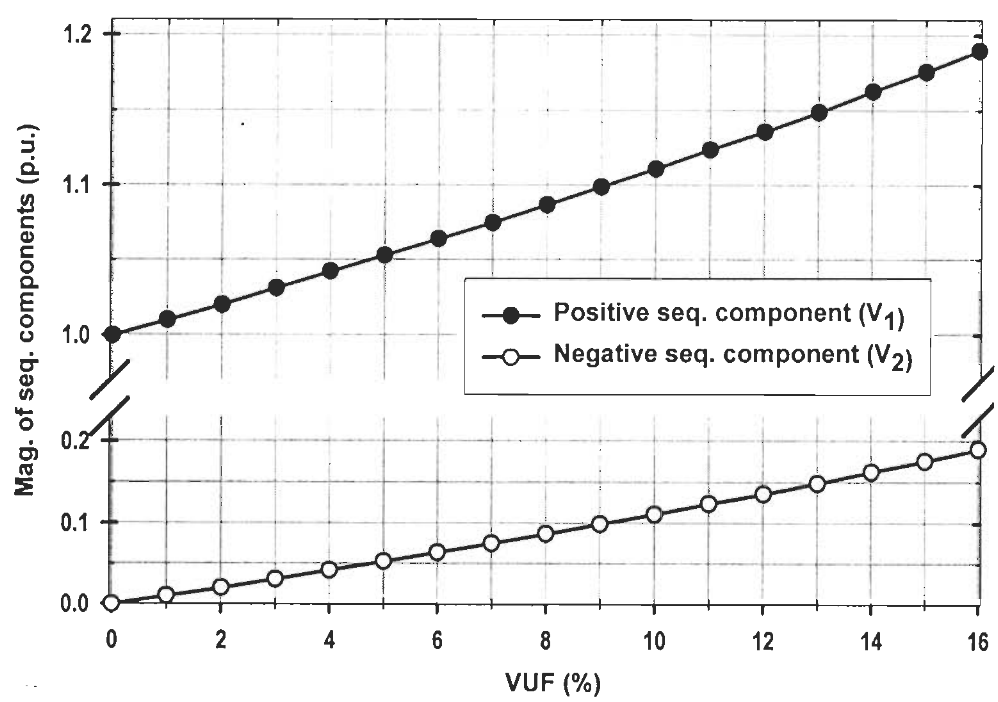

Fig. 4.2(b): **Variation of magnitude of V_1 and V_2 as a function of VUF for single-phase over-voltage unbalance**

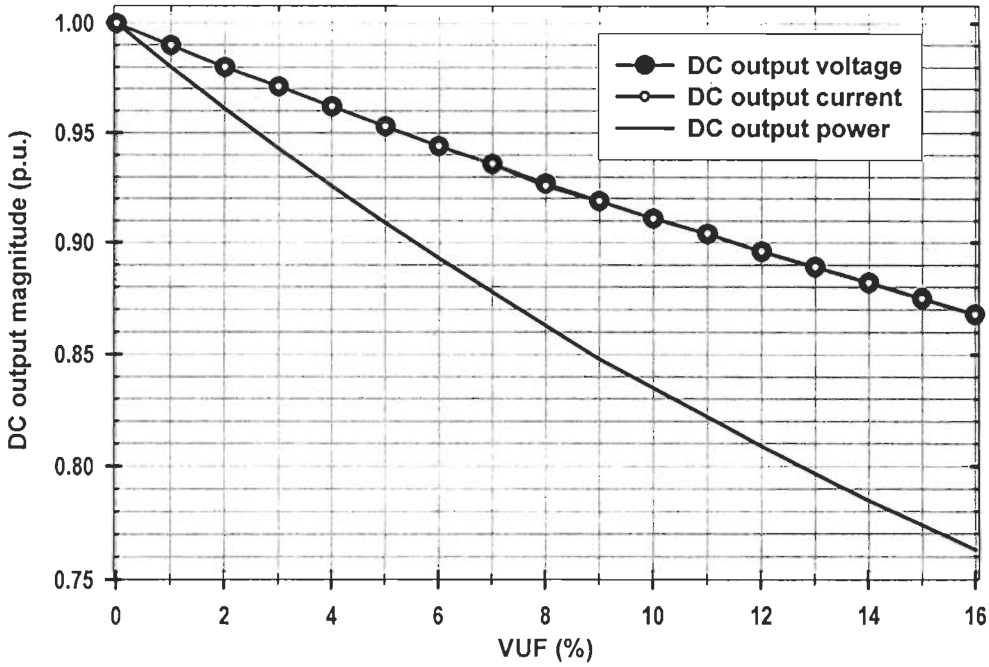

Fig. 4.3(a): Variation of magnitude of DC output parameters as a function of VUF for single-phase under-voltage unbalance

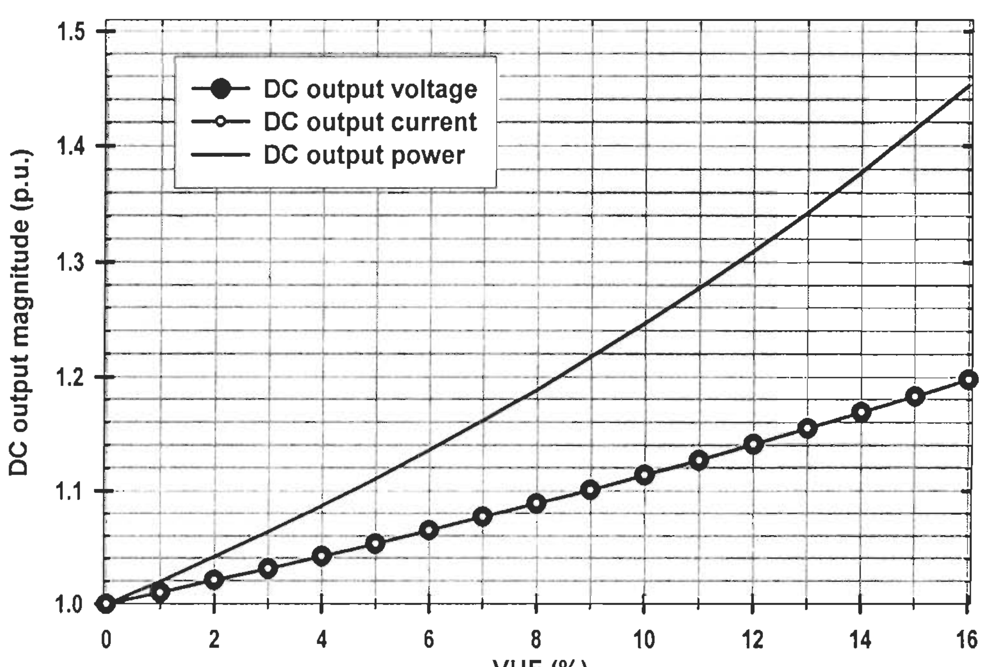

Fig. 4.3(b): Variation of magnitude of DC output parameters as a function of VUF for single-phase over-voltage unbalance

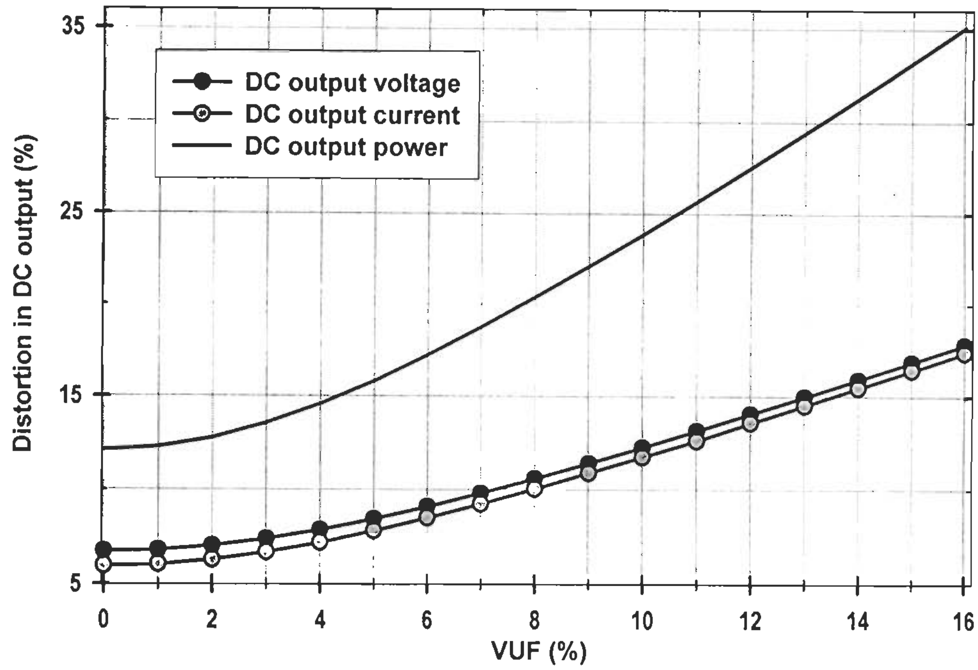

Fig. 4.4(a): **Effect of variation in VUF on distortion of DC output parameters as a function of VUF for single-phase under-voltage unbalance**

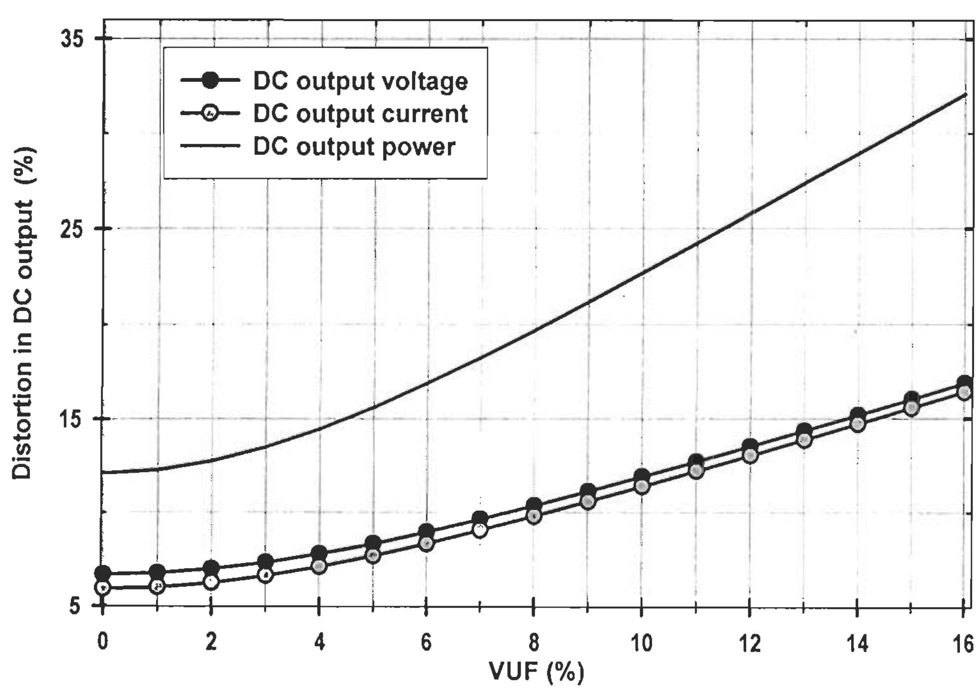

Fig. 4.4(b): **Effect of variation in VUF on distortion of DC output parameters, as a function of VUF for single-phase over-voltage unbalance**

4.7.5 Effect of Voltage Unbalance on AC Parameters

It is clear from Table-4.1 through Table-4.4 that even for a single-phase voltage unbalance, the current waveforms of all three phases (I_A, I_B, and I_C) are affected. For single-phase under-voltage (UV) unbalance (Table-4.1), phase voltage and, therefore, load current in phase *A* is decreasing very rapidly, while for single-phase over-voltage (OV) unbalance (Table-4.3), phase voltage, and therefore, load current in phase *A* is increasing. The change in rms values of phase currents in remaining two phases is very nominal. This change in rms currents is presented in Fig. 4.5(a) and Fig. 4.5(b) for UV and OV unbalance cases respectively. It is observed that phase in which the unbalance is taking place (*A* here) is the most affected as compared to remaining two phases. It is also observed from Table-4.1 that THD_I is highest for the phase *A*, which has minimum voltage value and, therefore, minimum current. This observation is also verified from Table-4.2, where the single-phase UV unbalance is considered individually in phase *B* and phase *C*, turn by turn.

The same sample of results can also be extended for the case of single-phase OV unbalance. It can be observed from Table-4.3 that THD_I is having minimum numerical value for the phase having maximum voltage value i.e. the maximum current. This variation in THD_I of three different phases as a function of VUF is presented in Fig. 4.6(a) and Fig. 4.6(b) for UV and OV unbalance considered in phase *A* respectively. As depicted in Table-4.2 and Table-4.4, single-phase voltage magnitude (UV and OV) unbalance conditions when considered independently in three different phases, the variation in their AC current parameters (rms value and THD_I) follows the same pattern as displayed in Fig. 4.5 and Fig. 4.6 relative to phase in which the unbalance is taking place. The variation in THD_I of three different phases as a function of VUF is presented in Fig. 4.7(a) and Fig. 4.7(b) for UV and OV unbalance considered in phase *B* and in Fig. 4.8(a) and Fig. 4.8(b) when UV and OV unbalance is considered in phase *C*, respectively.

On the basis of these observations, a general remark can be made that even a single-phase supply voltage unbalance has its qualitative influence on AC current waveforms and its parameters (rms value and THD_I) of all three phases (I_A, I_B, and I_C). The change in voltage magnitude 'most affects' the phase in which the voltage unbalance is taking place.

From the above study it is found that as the VUF increases, THD_I of three different phases also vary depending on the nature of unbalance. But during the analysis it was observed that the average THD_I of all three different phases remains almost constant (very small variation) irrespective of type of voltage unbalance (UV and OV) and phase (*A*, *B* or *C*). It was also observed that VUF has no effect on this average THD_I.

Phase Total Harmonic Distortion Unbalance Factor (PTHDUF) has been proposed as a very effective measure of voltage source unbalance in presence of harmonic distortion. For a given value of VUF, it remains unchanged regardless of the phase being affected by voltage unbalance. Furthermore, the values of PTHDUF are found to be quite distinctive for both (under-voltage and over-voltage unbalance cases for a given VUF. Plots of average THD_I and PTHDUF with variation of VUF are given in Fig. 4.9(a) and Fig. 4.9(b) for single-phase UV and OV unbalance cases respectively.

It is evident from these two Figures that for a given value of VUF, the PTHDUF has its value somewhat higher for the case of single-phase UV unbalance case as compared to single-phase OV unbalance case. Hence, it is concluded that PTHDUF is reasonably idiosyncratic for the type (UV or OV) and degree (VUF) of voltage unbalance.

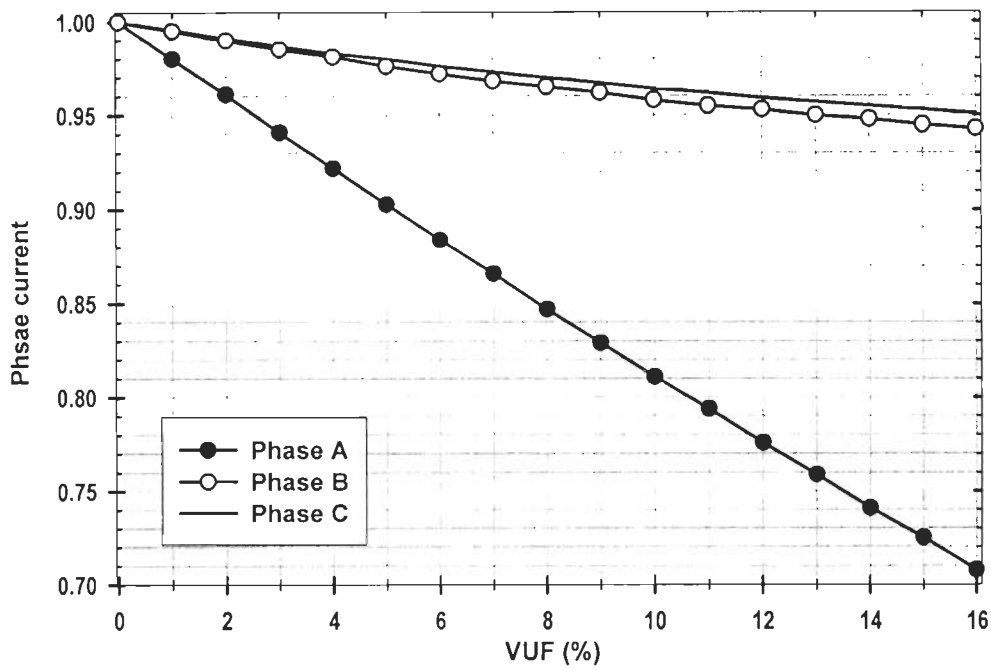

Fig. 4.5(a): **Variation in rms phase currents in three different phases as a function of VUF for single-phase under-voltage unbalance considered in phase *A***

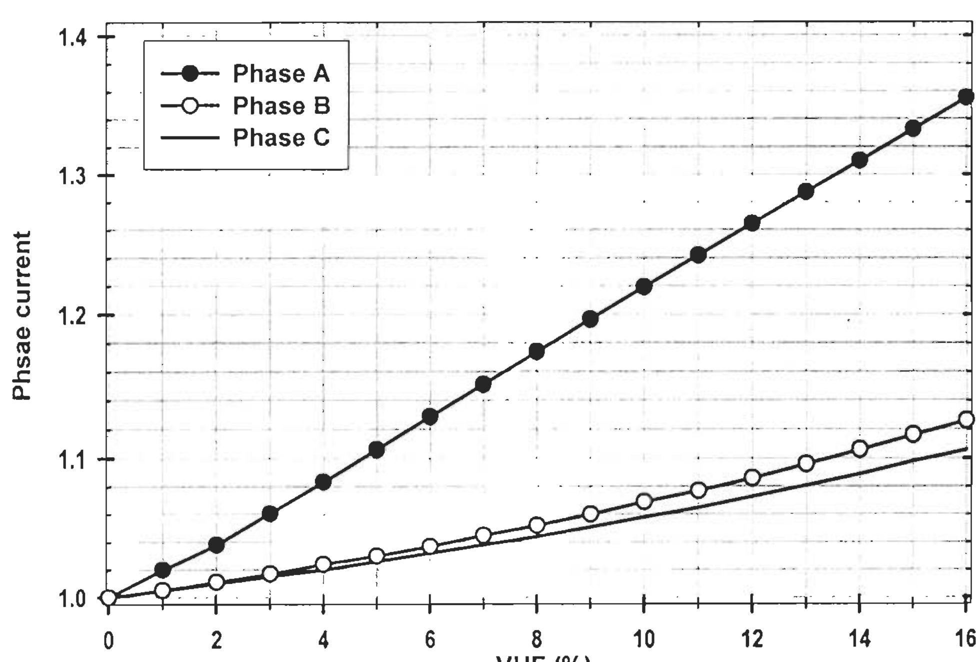

Fig. 4.5(b): **Variation in rms phase currents in three different phases as a function of VUF for single-phase over-voltage unbalance considered in phase *A***

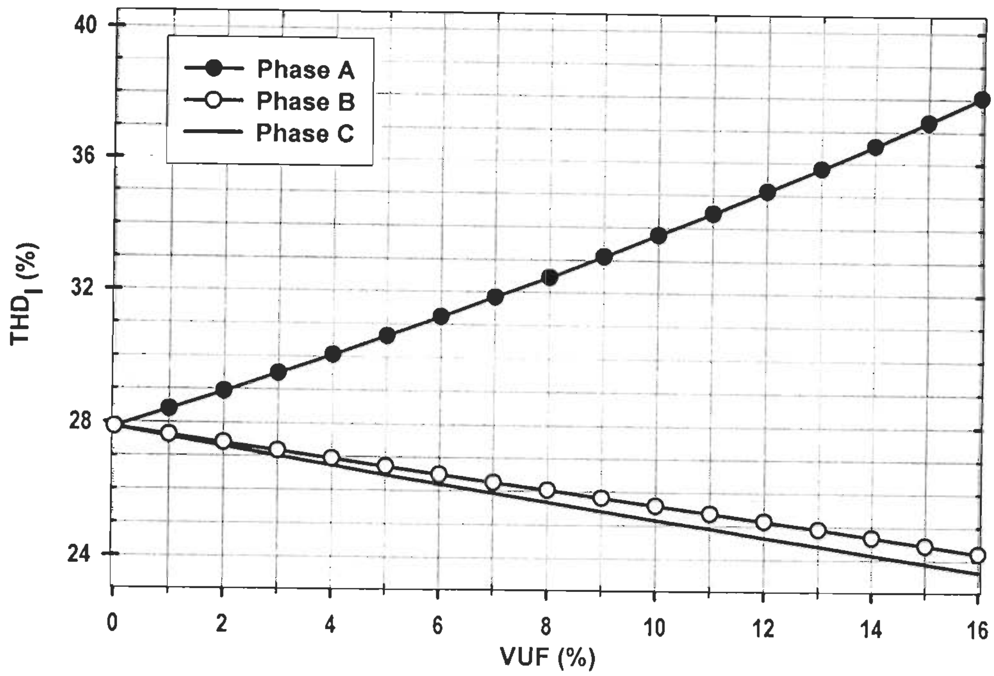

Fig. 4.6(a): Variation in THD_I of currents in three different phases as a function of VUF for single-phase under-voltage unbalance considered in phase *A*

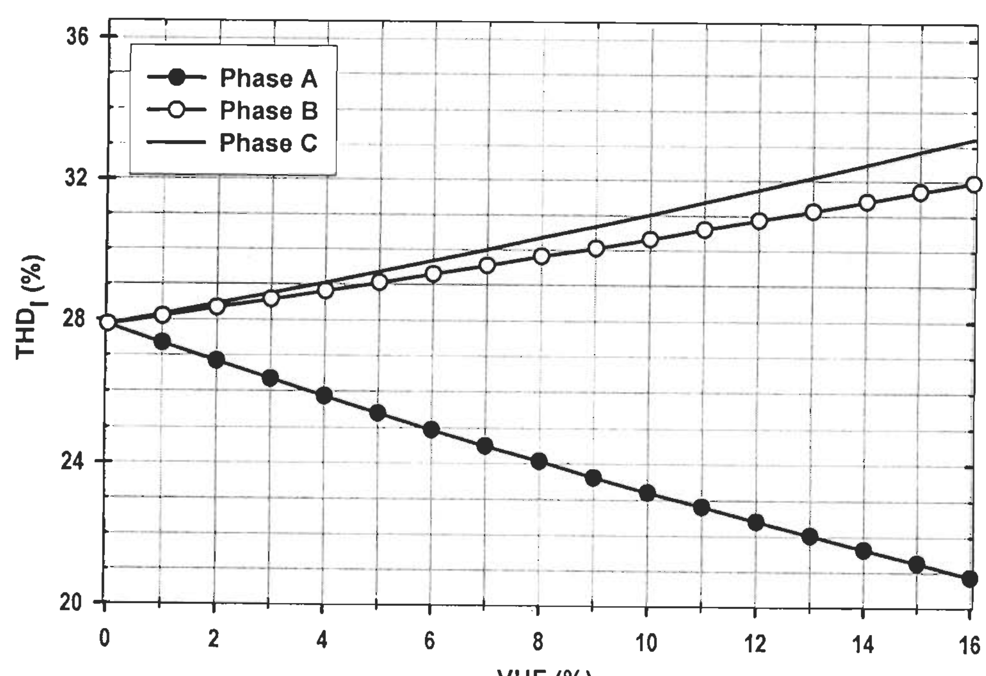

Fig. 4.6(b): Variation in THD_I of currents in three different phases as a function of VUF for single-phase over-voltage unbalance considered in phase *A*

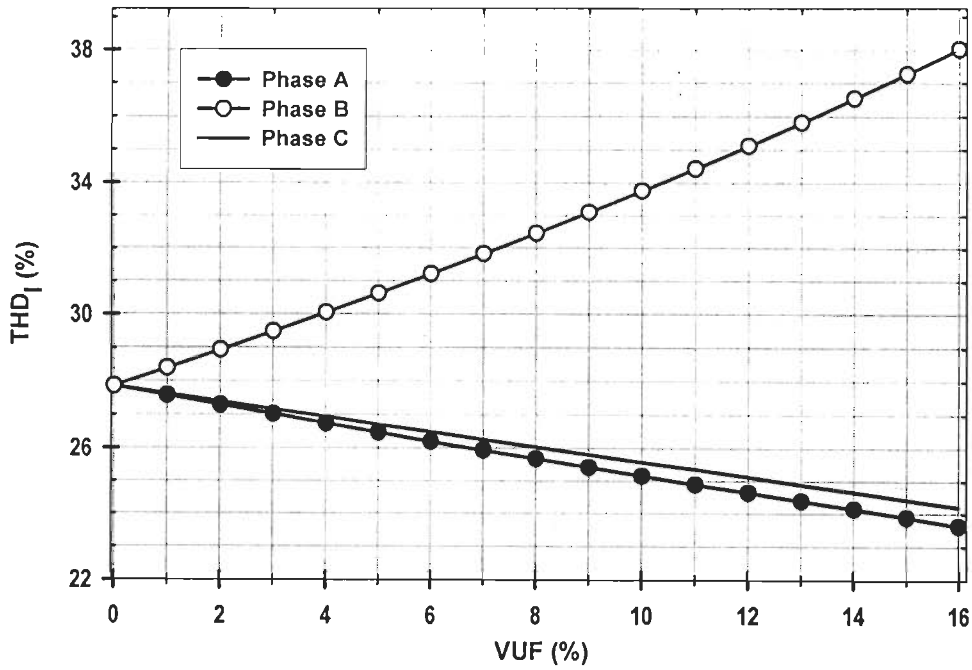

Fig. 4.7(a): Variation in THD$_I$ of currents in three different phases as a function of VUF for single-phase under-voltage unbalance considered in phase *B*

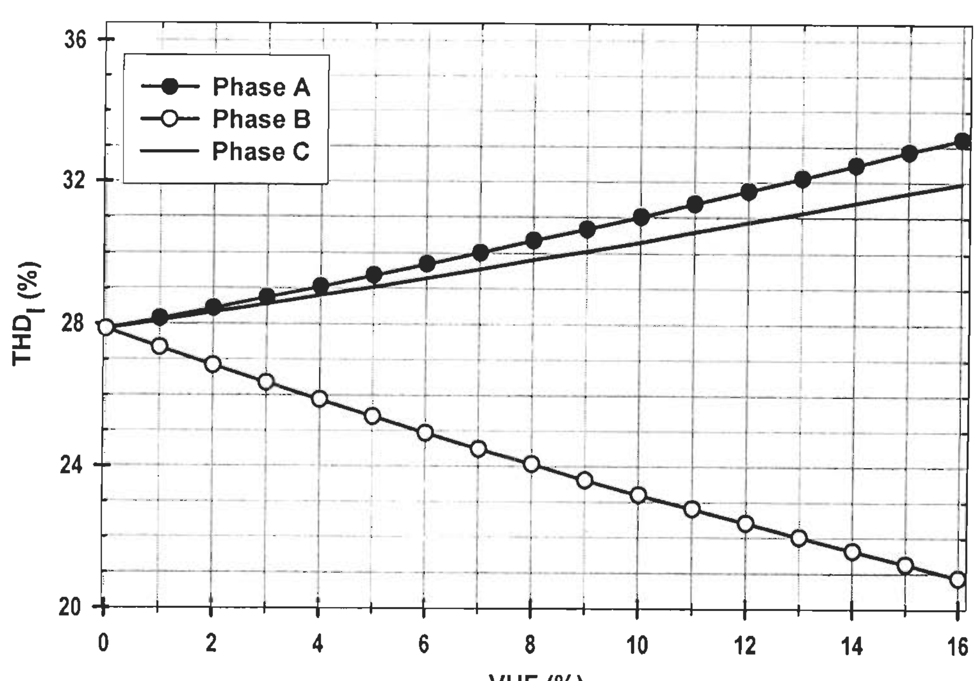

Fig. 4.7(b): Variation in THD$_I$ of currents in three different phases as a function of VUF for single-phase over-voltage unbalance considered in phase *B*

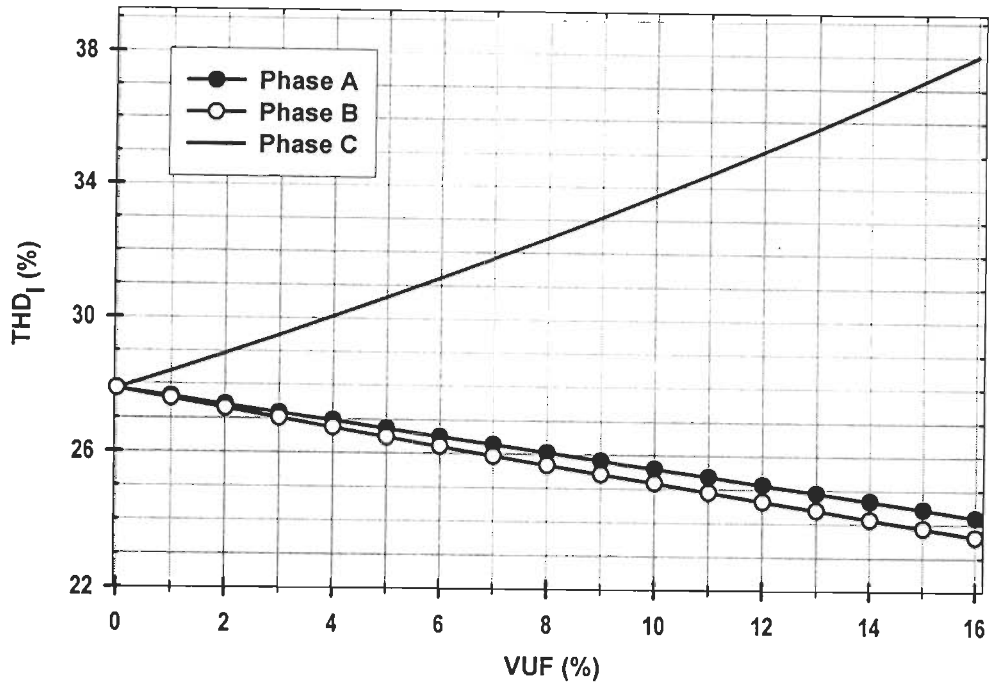

Fig. 4.8(a): Variation in THD_I of currents in three different phases as a function of VUF for single-phase under-voltage unbalance considered in phase *C*

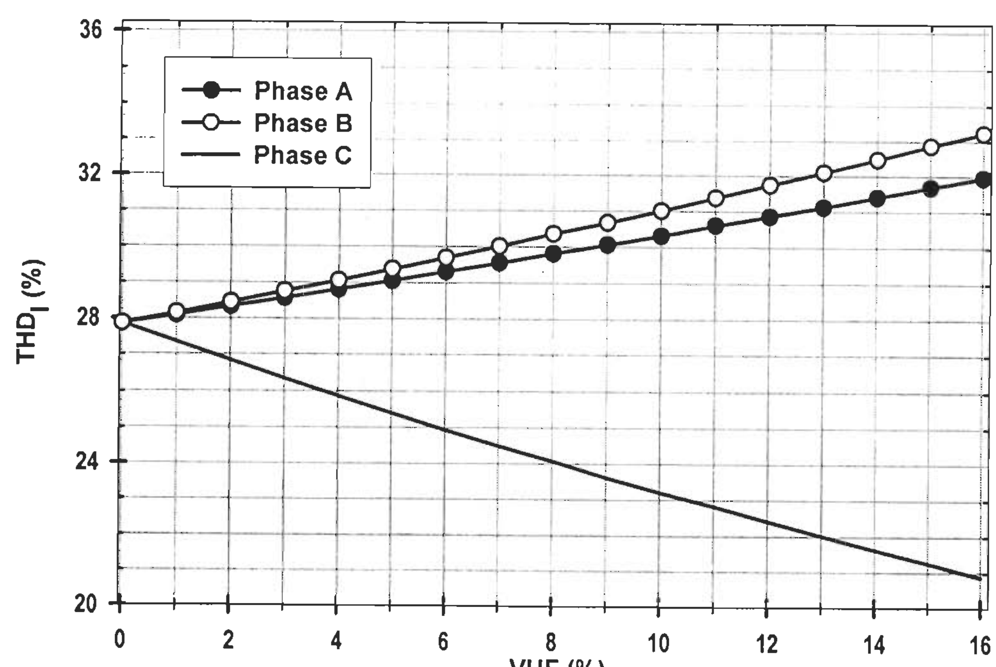

Fig. 4.8(b): Variation in THD_I of currents in three different phases as a function of VUF for single-phase over-voltage unbalance considered in phase *C*

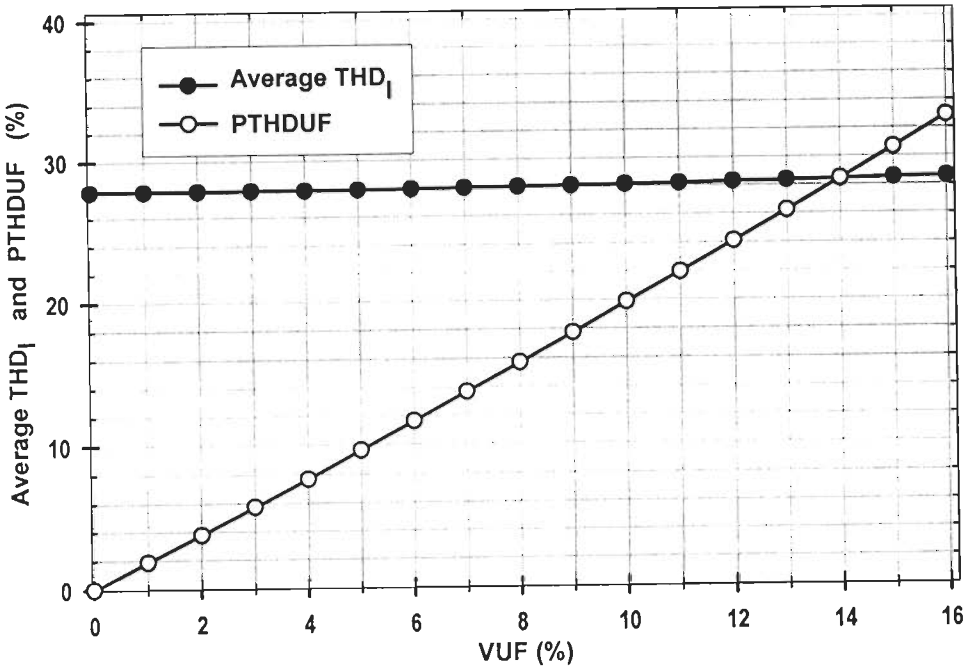

Fig. 4.9(a): Variation in average THD$_I$ and PTHDUF with increasing VUF for single-phase under-voltage unbalance

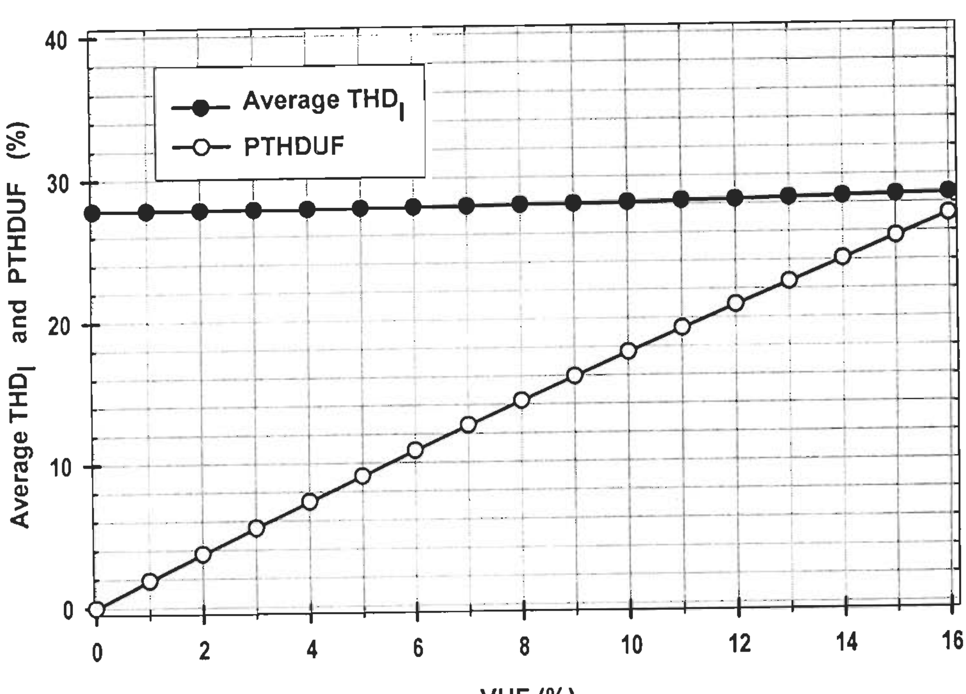

Fig. 4.9(b): Variation in average THD$_I$ and PTHDUF with increasing VUF for single-phase over-voltage unbalance

4.8 THE EFFECTS OF NEGATIVE SEQUENCE VOLTAGE COMPONENT

The negative sequence voltage component (V_2) also has its own impact on the performance of AC-DC rectifier. To identify the effects of V_2 apart from those of V_1, the increased value of VUF is obtained by increasing (regulating) the value of V_2 and keeping V_1 constant. Table-4.6 shows the three-phase supply voltages, their corresponding V_1, V_2 and VUF for this case where the changes in magnitude of voltage of phase *A* and phase *C* are made in such a manner that the V_1 is fixed at 1.0 p.u.. The V_2 is the only parameter being regulated for variation in VUF from 1% to 16%. The variation of V_1 and V_2 is graphically presented in Fig. 4.10.

When unbalanced three-phase voltages are supplied, the net effects of the unbalanced voltages are equivalent to the superposition of the V_2 on the V_1. Table-4.6 presents the apparent effects of the negative sequence voltage on the AC-DC rectifier performance, in terms of increased distortion in DC output parameters. The rectifier output performance is also presented in Fig. 4.11(a) and Fig. 4.11(b). In Fig. 4.11(a) the magnitude of DC output parameters are seem to be constant with variable VUF as the magnitude of the V_1 remains constant throughout the variation of VUF. Here plots of all three parameters V_{DC}, I_DC, and P_{DC} are almost overlapped as they remain at their rated value, for this case. The distortion of DC parameters is found to be increasing proportional to V_2 with increasing VUF, as shown in Fig. 4.14(b).

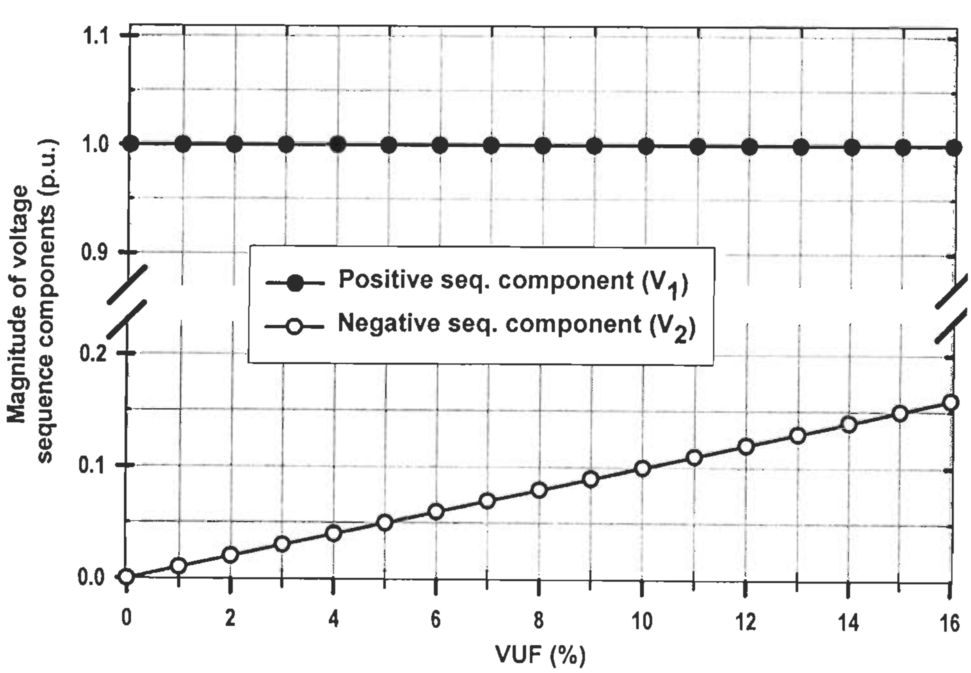

Fig. 4.10: Variation of magnitude of V_1 and V_2 as a function of VUF, when only V_2 is regulating the VUF

Table-4.6: Rectifier performance under constant V_1 and variable V_2 for increasing VUF

VUF (%)	Unbalanced source voltage						+ve seq. Volt. (V_1)	-ve seq. Volt. (V_2)	DC parameters					
	Phase A		Phase B		Phase C				I_{DC}		V_{DC}		P_{DC}	
	Mag.	Angle	Mag.	Angle	Mag.	Angle			Mag.	THD_I (%)	Mag.	THD_I (%)	Mag.	THD_I (%)
0.00	1.000	0	1.00	240	1.000	120	1.00	0.00	1.00	5.95	1.00	6.72	1.00	12.13
1.0	1.017	0	1.00	240	0.983	120	1.00	0.01	1.00	6.03	1.00	6.80	1.00	12.30
2.0	1.035	0	1.00	240	0.965	120	1.00	0.02	1.00	6.27	1.00	7.02	1.00	12.78
3.0	1.052	0	1.00	240	0.948	120	1.00	0.03	1.00	6.66	1.00	7.37	1.00	13.55
4.0	1.069	0	1.00	240	0.931	120	1.00	0.04	1.00	7.16	1.00	7.84	1.00	14.55
5.0	1.087	0	1.00	240	0.913	120	1.00	0.05	1.00	7.76	1.00	8.41	1.00	15.74
6.0	1.104	0	1.00	240	0.896	120	1.00	0.06	1.00	8.44	1.00	9.05	1.00	17.08
7.0	1.121	0	1.00	240	0.879	120	1.00	0.07	1.00	9.17	1.00	9.75	1.00	18.54
8.0	1.139	0	1.00	240	0.861	120	1.00	0.08	1.00	9.95	1.00	10.50	1.01	20.08
9.0	1.156	0	1.00	240	0.844	120	1.00	0.09	1.00	10.76	1.00	11.30	1.01	21.68
10.0	1.173	0	1.00	240	0.827	120	1.00	0.10	1.00	11.60	1.00	12.11	1.01	23.33
11.0	1.191	0	1.00	240	0.809	120	1.00	0.11	1.00	12.46	1.00	12.95	1.01	25.01
12.0	1.208	0	1.00	240	0.792	120	1.00	0.12	1.00	13.34	1.00	13.82	1.01	26.72
13.0	1.225	0	1.00	240	0.775	120	1.00	0.13	1.00	14.22	1.00	14.69	1.02	28.45
14.0	1.243	0	1.00	240	0.757	120	1.00	0.14	1.00	15.12	1.00	15.6	1.02	30.19
15.0	1.260	0	1.00	240	0.740	120	1.00	0.15	1.00	16.02	1.01	16.48	1.02	31.93
16.0	1.277	0	1.00	240	0.723	120	1.00	0.16	1.00	16.93	1.01	17.39	1.03	33.67

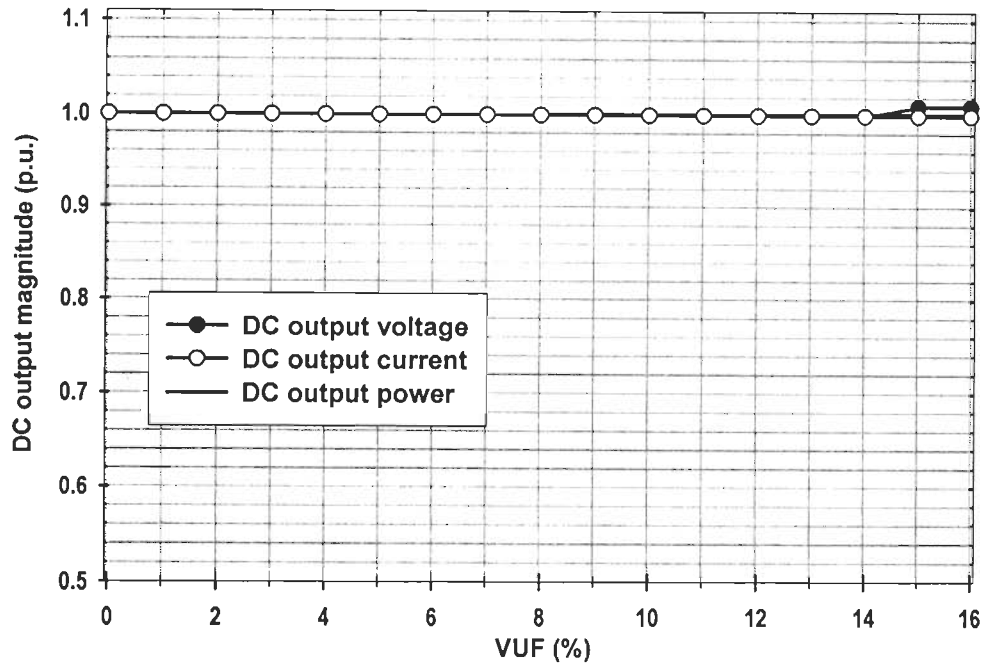

Fig. 4.11(a): Effect of variation in VUF on DC output parameters, when only V_2 is regulating the VUF

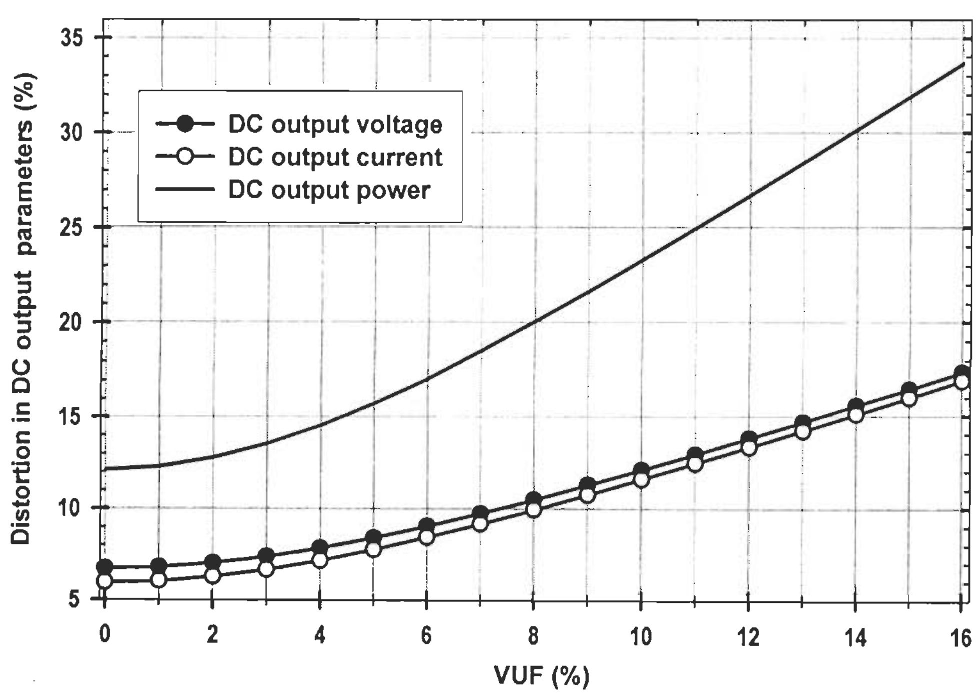

Fig. 4.11 (b): Effect of variation in VUF on distortion of DC output parameters, when only V_2 is regulating the VUF

4.9 SINGLE-PHASE ANGLE UNBALANCE CASES

For a three-phase balanced source voltage system, the angle displacement between any two phases must be equal to 120°. Considering any particular phase as reference phasor, if one of the other two phases is deflected, unequal displacement in single-phase occurs.

4.9.1 Single-Phase Unbalance due to Phase Angle Clockwise (CW) Movement

To study the effect of single-phase unbalance due to phase angle CW movement on the performance of AC-DC rectifier, the VUF is gradually increased from 0% (balanced case) to 16% by considering the deflection in any individual phase, in CW direction. Here, the variation in VUF is adjusted by CW movement in phase angle of voltage phasor *A* of a balanced source voltage supply, as shown in Fig. 4.12.

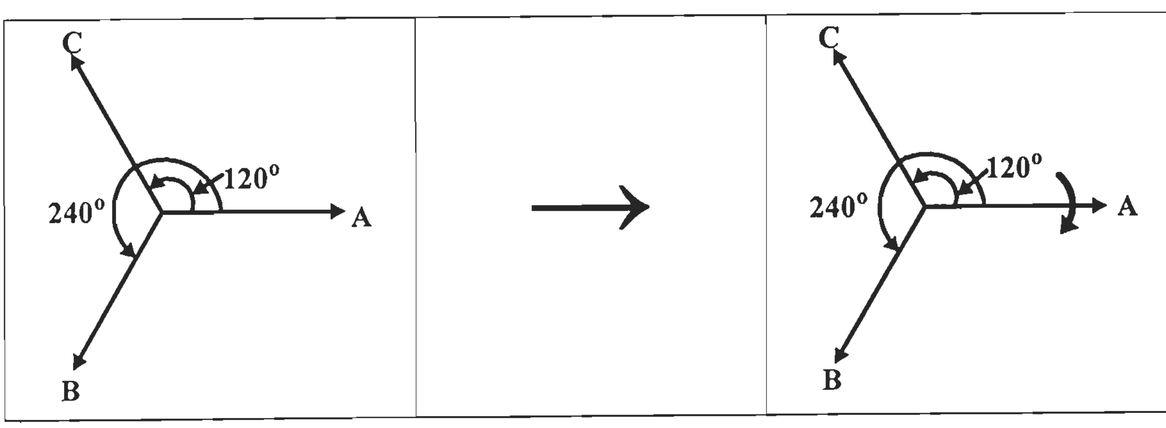

Fig. 4.12: An unbalance in three-phase voltage source due to CW movement in angle position of voltage phasor *A*

This movement causes the unbalance in voltage source. The comparison of input and output parameters is given in Table-4.7, which includes the three-phase supply voltages, their V_1 and V_2 along with the numerical values of four different definitions of voltage unbalance. Table-4.8 gives the .results for phase angle unbalance due to phase angle CW movement conditions considered independently in other two phases; *B* and *C* (unbalance in only one phase of source voltage, at a time).

4.9.2 Single-Phase Unbalance due to Phase Angle Anticlockwise (ACW) Movement

Here, the VUF is regulated only by moving the voltage phasor *A* in ACW direction, as shown in Fig. 4.13. Table-4.9 shows the three-phase supply voltages, their V_1 and V_2, the numerical values of four different definitions of voltage unbalance along with the output performance parameters of rectifier.

Table-4.10 contains the results for single-phase voltage unbalance due to ACW movement of voltage phasor considered individually in three different phases.

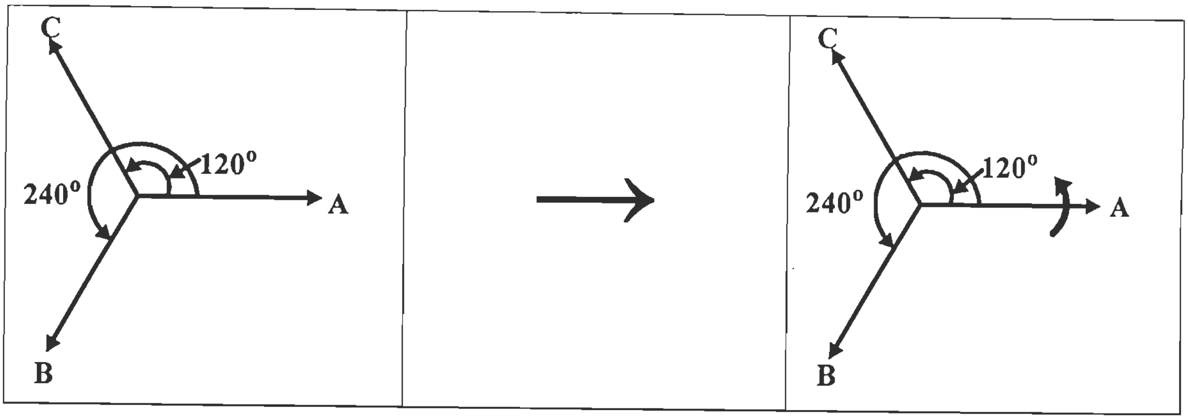

Fig. 4.13: An unbalance in three-phase voltage source due to ACW movement in angle position of voltage phasor *A*

The effect of this type of voltage unbalance on DC parameters is found typical and it makes no difference on the DC parameters of the rectifier. The only variation observed in these three different cases of single-phase voltage unbalance due to ACW movement of voltage phasor is in the values of AC side performance parameters (rms currents and their distortion).

It was observed that the impact of phase angle unbalance due to phase angle movement (CW or ACW) on DC parameters is very distinctive and for a given value of VUF it does not show any divergence on DC parameters regardless of whether the unbalance is taking place in phase A, B or C. The only difference observed in these three different cases is in the values of AC parameters i.e. rms currents and their distortion. This variation in AC parameters is found dependent on two parameters:

(i) direction of movement of voltage phasor, i.e. CW /ACW;

(ii) phase in which the unbalance is taking place viz. *A*, *B*, or *C*.

With increasing VUF, the behavior of characteristic and non-characteristic harmonics is shown in Table-4.11(a) and Table-4.11(b) for CW movement and in Table-4.12(a) and Table-4.12(b) for ACW movement, respectively. This variation in harmonic pattern behavior is discussed in section 4.13.

Table-4.7: Comparison of four different definitions of voltage unbalance and performance of rectifier for 1-Φ Angle unbalance case due to CW movement of phase *A* for increasing VUF

LVUR (%)	PVUR 1 (%)	PVUR (%)	VUF (%)	Unbalanced voltage source						+ve seq. Volt. (V_1)	-ve seq. Volt. (V_2)	AC parameters						Average THD_I	PTHDUF (%)	DC parameters					
				Phase *A*		Phase *B*		Phase *C*				I_A		I_B		I_C				I_{DC}		V_{DC}		P_{DC}	
				Mag.	Angle	Mag.	Angle	Mag.	Angle			RMS	THD_I (%)	Mag.	THD_I (%)	Mag.	THD_I (%)			Mag.	THD_I (%)	Mag.	THD_I (%)	Mag.	THD_I (%)
0.00	0	0	0	1.0	0	1.0	240	1.0	120	1.000	0.00	1.000	27.87	1.000	27.87	1.000	27.87	27.87	0.00	1.000	5.95	1.000	6.72	1.000	12.13
0.87	0	0	1	1.0	-1.72	1.0	240	1.0	120	1.000	0.010	1.000	27.84	0.991	28.34	1.008	27.43	27.87	1.69	1.000	6.03	1.000	6.80	1.000	12.30
1.75	0	0	2	1.0	-3.44	1.0	240	1.0	120	1.000	0.020	1.001	27.82	0.982	28.82	1.016	27.01	27.88	3.36	1.000	6.27	1.000	7.02	1.000	12.78
2.63	0	0	3	1.0	-5.16	1.0	240	1.0	120	0.999	0.030	1.001	27.80	0.972	29.31	1.024	26.58	27.90	5.07	0.999	6.66	0.999	7.38	0.999	13.55
3.52	0	0	4	1.0	-6.87	1.0	240	1.0	120	0.998	0.040	1.001	27.79	0.963	29.81	1.032	26.16	27.92	6.77	0.999	7.16	0.999	7.84	0.998	14.55
4.43	0	0	5	1.0	-8.59	1.0	240	1.0	120	0.998	0.050	1.002	27.78	0.953	30.32	1.040	25.75	27.95	8.48	0.998	7.76	0.998	8.41	0.998	15.74
5.33	0	0	6	1.0	-10.3	1.0	240	1.0	120	0.996	0.060	1.002	27.78	0.943	30.84	1.047	25.34	27.99	10.20	0.997	8.44	0.997	9.05	0.996	17.07
6.24	0	0	7	1.0	-12	1.0	240	1.0	120	0.995	0.070	1.002	27.78	0.933	31.36	1.054	24.93	28.02	11.91	0.996	9.16	0.996	9.74	0.995	18.51
7.16	0	0	8	1.0	-13.7	1.0	240	1.0	120	0.994	0.080	1.002	27.79	0.923	31.90	1.061	24.53	28.07	13.63	0.995	9.94	0.995	10.49	0.994	20.03
8.08	0	0	9	1.0	-15.4	1.0	240	1.0	120	0.992	0.089	1.002	27.80	0.912	32.44	1.068	24.14	28.13	15.34	0.994	10.74	0.994	11.27	0.992	21.61
9.02	0	0	10	1.0	-17.09	1.0	240	1.0	120	0.990	0.099	1.001	27.81	0.902	33.00	1.074	23.75	28.19	17.08	0.993	11.57	0.993	12.08	0.990	23.23
9.95	0	0	11	1.0	-18.77	1.0	240	1.0	120	0.988	0.109	1.001	27.83	0.891	33.56	1.081	23.36	28.25	18.80	0.991	12.42	0.991	12.92	0.988	24.88
10.89	0	0	12	1.0	-20.45	1.0	240	1.0	120	0.986	0.118	1.001	27.86	0.880	34.14	1.086	22.97	28.32	20.54	0.989	13.28	0.989	13.77	0.986	26.55
11.84	0	0	13	1.0	-22.12	1.0	240	1.0	120	0.984	0.128	1.001	27.89	0.870	34.73	1.092	22.59	28.40	22.27	0.988	14.16	0.988	14.63	0.984	28.23
12.80	0	0	14	1.0	-23.79	1.0	240	1.0	120	0.981	0.137	1.000	27.92	0.859	35.33	1.098	22.21	28.49	24.02	0.986	15.04	0.986	15.51	0.981	29.92
13.76	0	0	15	1.0	-25.44	1.0	240	1.0	120	0.978	0.147	1.000	27.95	0.848	35.93	1.103	21.84	28.57	25.75	0.984	15.92	0.984	16.38	0.978	31.60
14.72	0	0	16	1.0	-27.08	1.0	240	1.0	120	0.975	0.156	1.000	27.99	0.837	36.55	1.108	21.47	28.67	27.49	0.982	16.81	0.982	17.26	0.975	33.27

Table-4.8: Comparison of AC current parameters for 1-Φ Angle unbalance case due to CW movement considered individually in three different phases for increasing VUF

VUF (%)	+ve seq. Volt. (V_1)	-ve seq. Volt. (V_2)	PTHDUF (%)	Average THD_I	CW Movement only in phase *A*						CW Movement only in phase *B*						CW Movement only in phase *C*					
					I_A		I_B		I_C		I_A		I_B		I_C		I_A		I_B		I_C	
					RMS	THD_I (%)	Mag.	THD_I (%)	Mag.	THD_I (%)	RMS	THD_I (%)	Mag.	THD_I (%)	Mag.	THD_I (%)	RMS	THD_I (%)	Mag.	THD_I (%)	Mag.	THD_I (%)
0	1.000	0.00	0.00	27.87	1.000	27.87	1.000	27.87	1.000	27.87	1.000	27.87	1.000	27.87	1.000	27.87	1.000	27.87	1.000	27.87	1.000	27.87
1	1.000	0.010	1.69	27.87	1.000	27.84	0.991	28.34	1.008	27.43	1.009	27.44	1.000	27.84	0.991	28.34	0.991	28.35	1.008	27.43	1.000	27.84
2	1.000	0.020	3.36	27.88	1.001	27.82	0.982	28.82	1.016	27.01	1.017	27.01	1.001	27.81	0.982	28.82	0.982	28.83	1.017	27.01	1.001	27.81
3	0.999	0.030	5.07	27.90	1.001	27.80	0.972	29.31	1.024	26.58	1.025	26.59	1.001	27.80	0.972	29.31	0.972	29.32	1.024	26.58	1.001	27.80
4	0.998	0.040	6.77	27.92	1.001	27.79	0.963	29.81	1.032	26.16	1.033	26.17	1.001	27.78	0.963	29.81	0.963	29.81	1.008	26.16	1.001	27.78
5	0.998	0.050	8.48	27.95	1.002	27.78	0.953	30.32	1.040	25.75	1.040	25.75	1.001	27.78	0.953	30.32	0.953	30.32	1.040	25.75	1.001	27.77
6	0.996	0.060	10.20	27.99	1.002	27.78	0.943	30.84	1.047	25.34	1.048	25.34	1.001	27.77	0.943	30.84	0.943	30.84	1.047	25.34	1.002	27.77
7	0.995	0.070	11.91	28.02	1.002	27.78	0.933	31.36	1.054	24.93	1.055	24.94	1.002	27.78	0.933	31.36	0.933	31.37	1.054	24.93	1.002	27.77
8	0.994	0.080	13.63	28.07	1.002	27.79	0.923	31.90	1.061	24.53	1.062	24.54	1.002	27.78	0.923	31.90	0.923	31.90	1.061	24.53	1.002	27.78
9	0.992	0.089	15.34	28.13	1.002	27.80	0.912	32.44	1.068	24.14	1.068	24.14	1.001	27.79	0.912	32.44	0.912	32.45	1.068	24.14	1.001	27.79
10	0.990	0.099	17.08	28.19	1.001	27.81	0.902	33.00	1.074	23.75	1.075	23.75	1.001	27.81	0.902	33.00	0.902	33.01	1.074	23.75	1.001	27.81
11	0.988	0.109	18.80	28.25	1.001	27.83	0.891	33.56	1.081	23.36	1.081	23.36	1.001	27.83	0.891	33.56	0.891	33.57	1.081	23.36	1.001	27.83
12	0.986	0.118	20.54	28.32	1.001	27.86	0.880	34.14	1.086	22.97	1.087	22.98	1.001	27.85	0.880	34.14	0.881	34.15	1.086	22.97	1.001	27.85
13	0.984	0.128	22.27	28.40	1.001	27.89	0.870	34.73	1.092	22.59	1.092	22.59	1.001	27.88	0.870	34.73	0.870	34.74	1.092	22.59	1.001	27.88
14	0.981	0.137	24.02	28.49	1.000	27.92	0.859	35.33	1.098	22.21	1.098	22.21	1.000	27.91	0.859	35.33	0.859	35.34	1.098	22.21	1.000	27.91
15	0.978	0.147	25.75	28.57	1.000	27.95	0.848	35.93	1.103	21.84	1.103	21.84	1.000	27.95	0.848	35.93	0.848	35.94	1.103	21.84	1.000	27.95
16	0.975	0.156	27.49	28.67	1.000	27.99	0.837	36.55	1.108	21.47	1.108	21.48	1.000	27.98	0.837	36.55	0.837	36.56	1.108	21.47	1.000	27.98

Table-4.9: Comparison of four different definitions of voltage unbalance and performance of rectifier for 1-Φ Angle unbalance case due to ACW movement of phase *A* for increasing VUF

LVUR (%)	PVUR 1 (%)	PVUR (%)	VUF (%)	Unbalanced voltage source						+ve seq. Volt. (V_1)	-ve seq. Volt. (V_2)	AC parameters						Average THD_I	PTHDUF (%)	DC parameters					
				Phase *A*		Phase *B*		Phase *C*				I_A		I_B		I_C				I_{DC}		V_{DC}		P_{DC}	
				Mag.	Angle	Mag.	Angle	Mag.	Angle			RMS	THD_I (%)	Mag.	THD_I (%)	Mag.	THD_I (%)			Mag.	THD_I (%)	Mag.	THD_I (%)	Mag.	THD_I (%)
0.00	0	0	0	1.0	0	1.0	240	1.0	120	1.000	0.00	1.000	27.87	1.000	27.87	1.000	27.87	27.87	0.00	1.000	5.95	1.000	6.72	1.000	12.13
0.87	0	0	1	1.0	1.72	1.0	240	1.0	120	1.000	0.010	1.000	27.91	1.009	27.40	0.991	28.31	27.87	1.70	1.000	6.03	1.000	6.80	1.000	12.30
1.75	0	0	2	1.0	3.44	1.0	240	1.0	120	1.000	0.020	0.999	27.95	1.017	26.95	0.983	28.75	27.88	3.35	1.000	6.27	1.000	7.02	1.000	12.78
2.63	0	0	3	1.0	5.16	1.0	240	1.0	120	0.999	0.030	0.999	28.00	1.026	26.50	0.974	29.20	27.90	5.02	0.999	6.66	0.999	7.38	0.999	13.55
3.52	0	0	4	1.0	6.87	1.0	240	1.0	120	0.998	0.040	0.998	28.05	1.034	26.06	0.965	29.65	27.92	6.66	0.999	7.16	0.999	7.84	0.998	14.55
4.43	0	0	5	1.0	8.59	1.0	240	1.0	120	0.998	0.050	0.997	28.11	1.042	25.62	0.956	30.11	27.95	8.33	0.998	7.76	0.998	8.41	0.998	15.74
5.33	0	0	6	1.0	10.3	1.0	240	1.0	120	0.996	0.060	0.996	28.17	1.049	25.20	0.946	30.58	27.98	9.95	0.997	8.44	0.997	9.05	0.996	17.07
6.24	0	0	7	1.0	12	1.0	240	1.0	120	0.995	0.070	0.995	28.24	1.057	24.78	0.937	31.05	28.02	11.57	0.996	9.16	0.996	9.74	0.995	18.51
7.16	0	0	8	1.0	13.7	1.0	240	1.0	120	0.994	0.080	0.994	28.31	1.064	24.38	0.927	31.53	28.07	13.16	0.995	9.94	0.995	10.49	0.994	20.03
8.08	0	0	9	1.0	15.4	1.0	240	1.0	120	0.992	0.089	0.993	28.40	1.071	23.97	0.918	32.01	28.13	14.78	0.994	10.74	0.994	11.27	0.992	21.61
9.02	0	0	10	1.0	17.09	1.0	240	1.0	120	0.990	0.099	0.992	28.48	1.077	23.57	0.908	32.50	28.18	16.37	0.993	11.57	0.993	12.08	0.990	23.23
9.95	0	0	11	1.0	18.77	1.0	240	1.0	120	0.988	0.109	0.991	28.57	1.084	23.18	0.899	33.00	28.25	17.95	0.991	12.42	0.991	12.92	0.988	24.88
10.89	0	0	12	1.0	20.45	1.0	240	1.0	120	0.986	0.118	0.990	28.67	1.089	22.80	0.889	33.50	28.32	19.50	0.989	13.28	0.989	13.77	0.986	26.55
11.84	0	0	13	1.0	22.12	1.0	240	1.0	120	0.984	0.128	0.989	28.77	1.095	22.42	0.879	34.01	28.40	21.06	0.988	14.16	0.988	14.63	0.984	28.23
12.80	0	0	14	1.0	23.79	1.0	240	1.0	120	0.981	0.137	0.988	28.88	1.101	22.05	0.869	34.52	28.48	22.59	0.986	15.04	0.986	15.51	0.981	29.92
13.76	0	0	15	1.0	25.44	1.0	240	1.0	120	0.978	0.147	0.986	28.99	1.106	21.68	0.860	35.04	28.57	24.12	0.984	15.92	0.984	16.38	0.978	31.60
14.72	0	0	16	1.0	27.08	1.0	240	1.0	120	0.975	0.156	0.985	29.10	1.110	21.32	0.850	35.57	28.66	25.62	0.982	16.81	0.982	17.26	0.975	33.27

Table-4.10: Comparison of AC current parameters (rms value and THD_I) for 1-Φ Angle unbalance case due to ACW movement considered individually in three different phases for increasing VUF

VUF (%)	+ve seq. Volt. (V_1)	-ve seq. Volt. (V_2)	PTHDUF (%)	Average THD_I	ACW Movement only in phase A						ACW Movement only in phase B						ACW Movement only in phase C					
					I_A		I_B		I_C		I_A		I_B		I_C		I_A		I_B		I_C	
					RMS	THD_I (%)	Mag.	THD_I (%)	Mag.	THD_I (%)	RMS	THD_I (%)	Mag.	THD_I (%)	Mag.	THD_I (%)	RMS	THD_I (%)	Mag.	THD_I (%)	Mag.	THD_I (%)
0	1.000	0.00	0.00	27.87	1.000	27.87	1.000	27.87	1.000	27.87	1.000	27.87	1.000	27.87	1.000	27.87	1.000	27.87	1.000	27.87	1.000	27.87
1	1.000	0.010	1.70	27.87	1.000	27.91	1.009	27.40	0.991	28.31	0.992	28.31	1.000	27.90	1.009	27.40	1.009	27.41	0.991	28.31	1.000	27.90
2	1.000	0.020	3.35	27.88	0.999	27.95	1.017	26.95	0.983	28.75	0.983	28.76	0.999	27.94	1.017	26.95	1.018	26.95	0.983	28.75	0.999	27.94
3	0.999	0.030	5.02	27.90	0.999	28.00	1.026	26.50	0.974	29.20	0.974	29.20	0.998	27.99	1.026	26.50	1.026	26.50	0.974	29.20	0.998	27.99
4	0.998	0.040	6.66	27.92	0.998	28.05	1.034	26.06	0.965	29.65	0.965	29.66	0.998	28.04	1.034	26.06	1.034	26.06	0.965	29.65	0.998	28.04
5	0.998	0.050	8.33	27.95	0.997	28.11	1.042	25.62	0.956	30.11	0.956	30.12	0.997	28.10	1.042	25.62	1.042	25.63	0.956	30.11	0.997	28.10
6	0.996	0.060	9.95	27.98	0.996	28.17	1.049	25.20	0.946	30.58	0.947	30.59	0.996	28.16	1.049	25.20	1.049	25.20	0.946	30.58	0.996	28.17
7	0.995	0.070	11.57	28.02	0.995	28.24	1.057	24.78	0.937	31.05	0.937	31.06	0.995	28.23	1.057	24.78	1.057	24.79	0.937	31.05	0.995	28.23
8	0.994	0.080	13.16	28.07	0.994	28.31	1.064	24.38	0.927	31.53	0.928	31.54	0.994	28.31	1.064	24.37	1.064	24.38	0.927	31.53	0.994	28.31
9	0.992	0.089	14.78	28.13	0.993	28.40	1.071	23.97	0.918	32.01	0.918	32.02	0.993	28.39	1.071	23.97	1.071	23.97	0.918	32.01	0.996	28.39
10	0.990	0.099	16.37	28.18	0.992	28.48	1.077	23.57	0.908	32.50	0.909	32.51	0.992	28.47	1.077	23.57	1.077	23.58	0.908	32.50	0.992	28.48
11	0.988	0.109	17.95	28.25	0.991	28.57	1.084	23.18	0.899	33.00	0.899	33.00	0.991	28.57	1.084	23.18	1.084	23.19	0.899	33.00	0.991	28.57
12	0.986	0.118	19.50	28.32	0.990	28.67	1.089	22.80	0.889	33.50	0.889	33.51	0.990	28.66	1.089	22.80	1.090	22.80	0.889	33.50	0.990	28.66
13	0.984	0.128	21.06	28.40	0.989	28.77	1.095	22.42	0.879	34.01	0.904	34.02	0.989	28.76	1.095	22.42	1.095	22.42	0.879	34.01	0.989	28.76
14	0.981	0.137	22.59	28.48	0.988	28.88	1.101	22.05	0.869	34.52	0.869	34.53	0.987	28.87	1.101	22.05	1.101	22.05	0.869	34.52	0.987	28.87
15	0.978	0.147	24.12	28.57	0.986	28.99	1.106	21.68	0.860	35.04	0.860	35.05	0.986	28.98	1.106	21.68	1.106	21.68	0.859	35.05	0.986	28.98
16	0.975	0.156	25.62	28.66	0.985	29.10	1.110	21.32	0.850	35.57	0.850	35.58	0.985	29.09	1.110	21.32	1.111	21.33	0.850	35.57	0.985	29.10

Table-4.11 (a): Characteristic harmonic current components with increasing VUF for 1-ϕ Angle unbalance in phase *A* due to CW movement

		VUF = 0.0 %	VUF = 1.0 %	VUF = 2.0 %	VUF = 3.0 %	VUF = 4.0 %	VUF = 5.0 %	VUF = 6.0 %	VUF = 7.0 %	VUF = 8.0 %	VUF = 9.0 %	VUF = 10.0 %	VUF = 11.0 %	VUF = 12.0 %	VUF = 13.0 %	VUF = 14.0 %	VUF = 15.0 %	VUF = 16.0 %
Phase *A*	**THD_I**	27.87	27.84	27.82	27.80	27.79	27.78	27.78	27.78	27.79	27.80	27.81	27.83	27.86	27.89	27.92	27.95	27.99
	h 5	22.37	22.31	22.24	22.15	22.04	21.91	21.77	21.61	21.44	21.25	21.05	20.83	20.61	20.37	20.12	19.86	19.59
	h 7	10.86	10.90	10.95	11.01	11.08	11.17	11.26	11.36	11.47	11.59	11.71	11.83	11.96	12.09	12.21	12.34	12.46
	h 11	8.35	8.31	8.26	8.19	8.11	8.01	7.91	7.79	7.66	7.53	7.39	7.26	7.12	6.99	6.86	6.74	6.62
	h 13	5.74	5.77	5.81	5.87	5.93	6.00	6.07	6.15	6.23	6.31	6.39	6.46	6.53	6.58	6.63	6.66	6.68
	h 17	4.62	4.60	4.56	4.50	4.44	4.37	4.28	4.20	4.11	4.02	3.93	3.85	3.78	3.72	3.67	3.63	3.59
	h 19	3.56	3.58	3.61	3.65	3.69	3.74	3.80	3.85	3.90	3.95	3.99	4.01	4.03	4.04	4.03	4.01	3.99
	h 23	2.83	2.81	2.78	2.74	2.69	2.64	2.57	2.51	2.44	2.38	2.33	2.28	2.23	2.20	2.17	2.14	2.11
	h 25	2.3	2.31	2.33	2.36	2.39	2.43	2.46	2.50	2.53	2.56	2.57	2.58	2.58	2.57	2.55	2.53	2.50
	h 29	1.77	1.76	1.74	1.71	1.67	1.63	1.58	1.52	1.47	1.42	1.38	1.34	1.31	1.28	1.25	1.22	1.18
	h 31	1.48	1.49	1.50	1.52	1.54	1.57	1.60	1.63	1.65	1.67	1.67	1.67	1.66	1.64	1.62	1.61	1.60
Phase *B*	**THD_I**	**27.87**	**28.34**	**28.82**	**29.31**	**29.81**	**30.32**	**30.84**	**31.16**	**31.90**	**32.44**	**33.00**	**33.56**	**34.04**	**34.73**	**35.33**	**35.93**	**36.55**
	h 5	22.36	22.95	23.52	24.07	24.60	25.10	25.58	26.02	26.44	26.83	27.18	27.50	27.79	28.04	28.26	28.43	28.57
	h 7	10.87	10.54	10.16	9.74	9.29	8.78	8.24	7.66	7.04	6.38	5.68	4.95	4.19	3.40	2.58	1.75	0.92
	h 11	8.34	8.76	9.12	9.42	9.66	9.83	9.93	9.96	9.91	9.78	9.58	9.30	8.95	8.53	8.03	7.47	6.86
	h 13	5.75	5.39	4.97	4.48	3.93	3.32	2.66	1.96	1.22	0.45	0.36	1.16	1.96	2.77	3.56	4.33	5.06
	h 17	4.62	4.95	5.19	5.35	5.42	5.39	5.25	5.02	4.69	4.27	3.76	3.18	2.53	1.83	1.10	0.47	0.71
	h 19	3.56	3.23	2.81	2.31	1.76	1.14	0.50	0.22	0.88	1.56	2.22	2.83	3.39	3.88	4.30	4.61	4.83
	h 23	2.82	3.08	3.24	3.29	3.23	3.06	2.79	2.42	1.95	1.41	0.82	0.19	0.47	1.12	1.74	2.31	2.81
	h 25	2.30	2.01	1.63	1.17	0.67	0.15	0.46	1.00	1.52	1.99	2.38	2.68	2.88	2.96	2.93	2.78	2.51
	h 29	1.76	1.95	2.04	2.02	1.89	1.65	1.32	0.92	0.46	0.07	0.55	1.02	1.46	1.81	2.08	2.23	2.27
	h 31	1.49	1.24	0.92	0.54	0.14	0.34	0.75	1.13	1.44	1.66	1.79	1.80	1.69	1.48	1.18	0.80	0.39
Phase *C*	**THD_I**	**27.87**	**27.43**	**27.01**	**26.58**	**26.16**	**25.75**	**25.34**	**24.93**	**24.53**	**24.14**	**23.75**	**23.36**	**22.97**	**22.59**	**22.21**	**21.84**	**21.47**
	h 5	22.36	21.80	21.23	20.64	20.03	19.42	18.79	18.16	17.52	16.87	16.22	15.57	14.92	14.26	13.61	12.96	12.32
	h 7	10.87	11.12	11.35	11.54	11.70	11.83	11.92	11.99	12.02	12.02	11.99	11.94	11.85	11.74	11.61	11.45	11.27
	h 11	8.34	7.91	7.43	6.92	6.38	5.81	5.22	4.61	3.99	3.35	2.72	2.09	1.46	0.84	0.27	0.39	0.94
	h 13	5.75	6.02	6.23	6.38	6.48	6.52	6.50	6.43	6.30	6.13	5.90	5.63	5.33	4.98	4.60	4.20	3.77
	h 17	4.62	4.24	3.81	3.32	2.81	2.25	1.68	1.10	0.52	0.12	0.64	1.17	1.67	2.14	2.56	2.93	3.25
	h 19	3.56	3.80	3.97	4.06	4.07	4.01	3.88	3.68	3.41	3.09	2.72	2.31	1.87	1.40	0.91	0.43	0.07
	h 23	2.82	2.50	2.12	1.68	1.21	0.72	0.23	0.30	0.77	1.22	1.62	1.97	2.26	2.48	2.63	2.70	2.71
	h 25	2.30	2.50	2.62	2.65	2.60	2.46	2.25	1.97	1.63	1.25	0.83	0.40	0.07	0.47	0.88	1.25	1.57
	h 29	1.76	1.50	1.18	0.81	0.42	0.07	0.40	0.77	1.10	1.39	1.60	1.75	1.82	1.81	1.72	1.57	1.35
	h 31	1.49	1.64	1.71	1.70	1.61	1.43	1.19	0.90	0.57	0.22	0.19	0.52	0.84	1.11	1.33	1.48	1.56

Table-4.11 (b): Non-characteristic harmonic current components with increasing VUF for 1-ϕ Angle unbalance in phase A due to CW movement

		VUF = 0.0 %	VUF = 1.0 %	VUF = 2.0 %	VUF = 3.0 %	VUF = 4.0 %	VUF = 5.0 %	VUF = 6.0 %	VUF = 7.0 %	VUF = 8.0 %	VUF = 9.0 %	VUF = 10.0 %	VUF = 11.0 %	VUF = 12.0 %	VUF = 13.0 %	VUF = 14.0 %	VUF = 15.0 %	VUF = 16.0 %
Phase A	THD_I	27.87	27.84	27.82	27.80	27.79	27.78	27.78	27.78	27.79	27.80	27.81	27.83	27.86	27.89	27.92	27.95	27.99
	h 3	0.01	0.68	1.36	2.03	2.70	3.36	4.02	4.67	5.32	5.96	6.58	7.20	7.82	8.42	9.01	9.59	10.16
	h 9	0.01	0.20	0.39	0.57	0.75	0.91	1.08	1.22	1.36	1.48	1.59	1.69	1.77	1.84	1.89	1.94	1.97
	h 15	0.01	0.11	0.21	0.31	0.40	0.47	0.54	0.59	0.63	0.66	0.68	0.69	0.71	0.72	0.74	0.76	0.80
	h 21	0.01	0.07	0.15	0.21	0.27	0.32	0.36	0.39	0.42	0.45	0.48	0.52	0.57	0.63	0.70	0.77	0.85
	h 27	0.01	0.06	0.12	0.18	0.23	0.27	0.30	0.33	0.37	0.41	0.45	0.50	0.56	0.63	0.69	0.76	0.81
	h 33	0.01	0.06	0.11	0.16	0.21	0.24	0.27	0.30	0.33	0.37	0.42	0.47	0.53	0.58	0.63	0.68	0.71
Phase B	THD_I	27.87	28.34	28.82	29.31	29.81	30.32	30.84	31.16	31.90	32.44	33.00	33.56	34.04	34.73	35.33	35.93	36.55
	h 3	0.01	0.72	1.47	2.25	3.04	3.87	4.72	5.58	6.47	7.39	8.32	9.27	10.25	11.24	12.26	13.28	14.32
	h 9	0.01	0.78	1.58	2.39	3.21	4.03	4.85	5.67	6.47	7.26	8.03	8.76	9.48	10.15	10.79	11.38	11.93
	h 15	0.0	0.71	1.44	2.16	2.86	3.54	4.18	4.78	5.32	5.79	6.19	6.51	6.74	6.88	6.93	6.88	6.73
	h 21	0.0	0.62	1.23	1.83	2.38	2.88	3.31	3.65	3.89	4.03	4.06	3.97	3.78	3.47	3.06	2.57	2.00
	h 27	0.0	0.51	1.00	1.46	1.85	2.17	2.39	2.50	2.49	2.37	2.14	1.81	1.38	0.89	0.36	0.22	0.76
	h 33	0.0	1.39	0.77	1.09	1.34	1.50	1.56	1.51	1.35	1.09	0.76	0.38	0.10	0.48	0.87	1.19	1.44
Phase C	THD_I	27.87	27.43	27.01	26.58	26.16	25.75	25.34	24.93	24.53	24.14	23.75	23.36	22.97	22.59	22.21	21.84	21.47
	h 3	0.01	0.65	1.27	1.87	2.45	3.00	3.53	4.04	4.53	4.99	5.43	5.84	6.24	6.61	6.96	7.29	7.59
	h 9	0.01	0.69	1.36	2.00	2.62	3.21	3.77	4.30	4.79	5.25	5.67	6.06	6.41	6.72	6.99	7.22	7.42
	h 15	0.01	0.63	1.23	1.80	2.34	2.83	3.29	3.69	4.04	4.33	4.57	4.74	4.86	4.92	4.93	4.87	4.77
	h 21	0.0	0.54	1.05	1.53	1.96	2.34	2.66	2.91	3.09	3.20	3.24	3.20	3.10	2.93	2.70	2.42	2.10
	h 27	0.0	0.44	0.85	1.22	1.54	1.80	1.99	2.11	2.14	2.10	1.98	1.79	1.55	1.25	0.91	0.55	0.17
	h 33	0.0	0.33	0.64	0.91	1.13	1.29	1.38	1.39	1.32	1.19	0.99	0.74	0.46	0.16	0.17	0.46	0.73

Table-4.12 (a): Characteristic harmonic current components with increasing VUF for 1-ϕ Angle unbalance in phase *A* due to ACW movement

		VUF = 0.0 %	VUF = 1.0 %	VUF = 2.0 %	VUF = 3.0 %	VUF = 4.0 %	VUF = 5.0 %	VUF = 6.0 %	VUF = 7.0 %	VUF = 8.0 %	VUF = 9.0 %	VUF = 10.0 %	VUF = 11.0 %	VUF = 12.0 %	VUF = 13.0 %	VUF = 14.0 %	VUF = 15.0 %	VUF = 16.0 %
Phase *A*	**THD_I**	27.87	27.91	27.95	28.00	28.05	28.11	28.17	28.24	28.31	28.40	28.48	28.57	28.67	28.77	28.88	28.99	29.10
	h 5	22.37	22.41	22.43	22.44	22.43	22.40	22.36	22.30	22.23	22.14	22.03	21.92	21.79	21.65	21.50	21.34	21.17
	h 7	10.86	10.83	10.81	10.81	10.81	10.83	10.86	10.89	10.93	10.98	11.03	11.08	11.14	11.20	11.25	11.31	11.36
	h 11	8.35	8.37	8.38	8.38	8.36	8.33	8.29	8.24	8.19	8.13	8.07	8.01	7.94	7.89	7.84	7.79	7.76
	h 13	5.74	5.72	5.71	5.71	5.72	5.73	5.74	5.75	5.77	5.77	5.78	5.77	5.76	5.74	5.71	5.67	5.62
	h 17	4.62	4.64	4.64	4.64	4.62	4.61	4.59	4.57	4.55	4.54	4.53	4.53	4.55	4.56	4.59	4.62	4.66
	h 19	3.56	3.54	3.53	3.53	3.52	3.52	3.50	3.49	3.46	3.42	3.38	3.32	3.26	3.18	3.10	3.01	2.92
	h 23	2.83	2.84	2.84	2.84	2.84	2.84	2.84	2.85	2.87	2.89	2.92	2.94	2.97	3.00	3.02	3.03	3.04
	h 25	2.3	2.29	2.28	2.26	2.24	2.22	2.19	2.14	2.09	2.03	1.97	1.90	1.84	1.77	1.71	1.65	1.60
	h 29	1.77	1.78	1.78	1.79	1.80	1.81	1.84	1.86	1.89	1.91	1.93	1.94	1.95	1.95	1.93	1.92	1.89
	h 31	1.48	1.47	1.46	1.44	1.41	1.37	1.33	1.28	1.22	1.17	1.12	1.08	1.04	1.01	0.98	0.95	0.92
Phase *B*	**THD_I**	27.87	27.40	26.95	26.50	26.06	25.62	25.20	24.78	24.38	23.97	23.57	23.18	22.80	22.42	22.05	21.68	21.32
	h 5	22.36	21.75	21.13	20.49	19.84	19.18	18.51	17.84	17.17	16.48	15.80	15.12	14.44	13.77	13.10	12.44	11.78
	h 7	10.87	11.15	11.40	11.60	11.76	11.88	11.96	12.00	12.00	11.97	11.90	11.80	11.68	11.52	11.34	11.13	10.90
	h 11	8.34	7.87	7.36	6.81	6.23	5.61	4.98	4.33	3.67	3.00	2.34	1.69	1.04	0.41	0.21	0.79	1.35
	h 13	5.75	6.03	6.25	6.39	6.46	6.46	6.40	6.27	6.09	5.84	5.55	5.22	4.84	4.43	3.99	3.54	3.06
	h 17	4.62	4.21	3.74	3.22	2.66	2.07	1.46	0.84	0.23	0.38	0.95	1.49	1.99	2.44	2.83	3.17	3.45
	h 19	3.56	3.81	3.97	4.03	4.00	3.89	3.69	3.42	3.08	2.69	2.25	1.78	1.29	0.79	0.33	0.34	0.76
	h 23	2.82	2.48	2.06	1.59	1.08	0.55	0.06	0.52	1.01	1.46	1.85	2.17	2.42	2.59	2.68	2.69	2.62
	h 25	2.30	2.50	2.60	2.60	2.49	2.29	2.01	1.66	1.26	0.82	0.36	0.14	0.56	0.98	1.35	1.67	1.92
	h 29	1.76	1.48	1.13	0.73	0.30	0.15	0.57	0.95	1.27	1.53	1.71	1.80	1.80	1.71	1.55	1.32	1.04
	h 31	1.49	1.64	1.69	1.63	1.48	1.25	0.94	0.59	0.21	0.18	0.55	0.89	1.17	1.38	1.51	1.57	1.54
Phase *C*	**THD_I**	27.87	28.31	28.75	29.20	29.65	30.11	30.58	31.05	31.53	32.01	32.50	33.00	33.50	34.01	34.52	35.04	35.57
	h 5	22.36	22.90	23.43	23.93	24.41	24.87	25.30	25.71	26.09	26.45	26.78	27.08	27.35	27.60	27.82	28.00	28.16
	h 7	10.87	10.57	10.25	9.89	9.51	9.09	8.65	8.18	7.68	7.15	6.60	6.03	5.44	4.83	4.20	3.56	2.91
	h 11	8.34	8.73	9.07	9.37	9.60	9.79	9.91	9.98	9.99	9.94	9.83	9.66	9.44	9.16	8.82	8.44	8.02
	h 13	5.75	5.43	5.05	4.63	4.16	3.64	3.09	2.51	1.89	1.25	0.60	0.08	0.75	1.42	2.09	2.75	3.40
	h 17	4.62	4.93	5.18	5.35	5.45	5.47	5.41	5.27	5.05	4.76	4.40	3.98	3.50	2.97	2.39	1.80	1.20
	h 19	3.56	3.25	2.88	2.45	1.97	1.44	0.89	0.31	0.28	0.87	1.45	2.01	2.55	3.04	3.49	3.89	4.23
	h 23	2.82	3.07	3.24	3.33	3.32	3.23	3.05	2.79	2.46	2.06	1.60	1.11	0.58	0.15	0.56	1.09	1.60
	h 25	2.3	2.03	1.69	1.29	0.85	0.38	0.11	0.59	1.06	1.51	1.91	2.26	2.55	2.77	2.91	2.98	2.97
	h 29	1.76	1.95	2.06	2.09	2.02	1.87	1.64	1.35	0.99	0.60	0.18	0.25	0.68	1.07	1.43	1.74	1.98
	h 31	1.49	1.26	0.97	0.64	0.27	0.11	0.49	0.84	1.16	1.43	1.63	1.77	1.83	1.81	1.73	1.57	1.36

Table-4.12 (b): Non-characteristic harmonic current components with increasing VUF for 1-ϕ Angle unbalance in phase *A* due to ACW movement

		VUF = 0.0 %	VUF = 1.0 %	VUF = 2.0 %	VUF = 3.0 %	VUF = 4.0 %	VUF = 5.0 %	VUF = 6.0 %	VUF = 7.0 %	VUF = 8.0 %	VUF = 9.0 %	VUF = 10.0 %	VUF = 11.0 %	VUF = 12.0 %	VUF = 13.0 %	VUF = 14.0 %	VUF = 15.0 %	VUF = 16.0 %
Phase *A*	**THD_I**	**27.87**	**27.91**	**27.95**	**28.00**	**28.05**	**28.11**	**28.17**	**28.24**	**28.31**	**28.40**	**28.48**	**28.57**	**28.67**	**28.77**	**28.88**	**28.99**	**29.10**
	h 3	0.01	0.68	1.37	2.05	2.74	3.42	4.11	4.79	5.46	6.14	6.81	7.48	8.14	8.79	9.45	10.09	10.72
	h 9	0.01	0.21	0.42	0.63	0.84	1.05	1.26	1.46	1.66	1.86	2.05	2.24	2.41	2.58	2.74	2.89	3.03
	h 15	0.01	0.13	0.25	0.38	0.50	0.63	0.75	0.87	0.98	1.08	1.18	1.26	1.34	1.40	1.46	1.50	1.54
	h 21	0.01	0.09	0.18	0.27	0.36	0.45	0.53	0.60	0.67	0.73	0.78	0.82	0.85	0.88	0.91	0.94	0.97
	h 27	0.01	0.08	0.15	0.22	0.29	0.35	0.40	0.45	0.49	0.52	0.55	0.59	0.62	0.66	0.71	0.76	0.81
	h 33	0.01	0.07	0.13	0.19	0.24	0.28	0.31	0.34	0.37	0.40	0.44	0.48	0.53	0.58	0.64	0.69	0.74
Phase *B*	**THD_I**	**27.87**	**27.40**	**26.95**	**26.50**	**26.06**	**25.62**	**25.20**	**24.78**	**24.38**	**23.97**	**23.57**	**23.18**	**22.80**	**22.42**	**22.05**	**21.68**	**21.32**
	h 3	0.01	0.71	1.38	2.03	2.65	3.25	3.83	4.37	4.89	5.39	5.86	6.30	6.73	7.12	7.50	7.85	8.17
	h 9	0.01	0.77	1.50	2.21	2.89	3.54	4.14	4.71	5.24	5.73	6.17	6.57	6.93	7.24	7.51	7.74	7.92
	h 15	0.0	0.70	1.38	2.01	2.60	3.15	3.63	4.05	4.41	4.70	4.92	5.07	5.15	5.17	5.12	5.01	4.84
	h 21	0.0	0.61	1.19	1.72	2.19	2.60	2.92	3.17	3.32	3.39	3.37	3.26	3.08	2.83	2.51	2.15	1.75
	h 27	0.0	0.50	0.97	1.39	1.73	1.99	2.16	2.24	2.22	2.10	1.90	1.62	1.29	0.91	0.50	0.09	0.32
	h 33	0.0	0.39	0.75	1.05	1.28	1.42	1.46	1.41	1.27	1.05	0.77	0.45	0.10	0.24	0.56	0.84	1.07
Phase *C*	**THD_I**	**27.87**	**28.31**	**28.75**	**29.20**	**29.65**	**30.11**	**30.58**	**31.05**	**31.53**	**32.01**	**32.50**	**33.00**	**33.50**	**34.01**	**34.52**	**35.04**	**35.57**
	h 3	0.01	0.66	1.35	2.06	2.78	3.53	4.30	5.08	5.89	6.71	7.55	8.40	9.27	10.15	11.05	11.96	12.88
	h 9	0.01	0.70	1.42	2.14	2.88	3.62	4.35	5.09	5.81	6.53	7.24	7.92	8.59	9.24	9.86	10.44	11.00
	h 15	0.01	0.63	1.27	1.92	2.55	3.17	3.76	4.32	4.84	5.32	5.75	6.12	6.44	6.69	6.88	7.00	7.05
	h 21	0.0	0.54	1.08	1.61	2.11	2.58	2.99	3.35	3.64	3.86	4.00	4.06	4.04	3.94	3.76	3.51	3.19
	h 27	0.0	0.43	0.86	1.27	1.63	1.94	2.19	2.36	2.46	2.47	2.40	2.24	2.02	1.72	1.37	0.98	0.56
	h 33	0.0	0.33	0.65	0.93	1.17	1.36	1.47	1.51	1.48	1.37	1.20	0.97	0.69	0.39	0.10	0.30	0.61

4.9.3 Comparison of Four Different Definitions of Voltage Unbalance

For both the cases of single-phase voltage unbalance caused by phase angle variation (either CW or ACW), the magnitudes of PVUR1 and PVUR are zero. The VUF happens to be always little higher than LVUR, throughout the unbalance. With increasing VUF, the difference between VUF and LVUR also increases as displayed in Fig. 4.14.

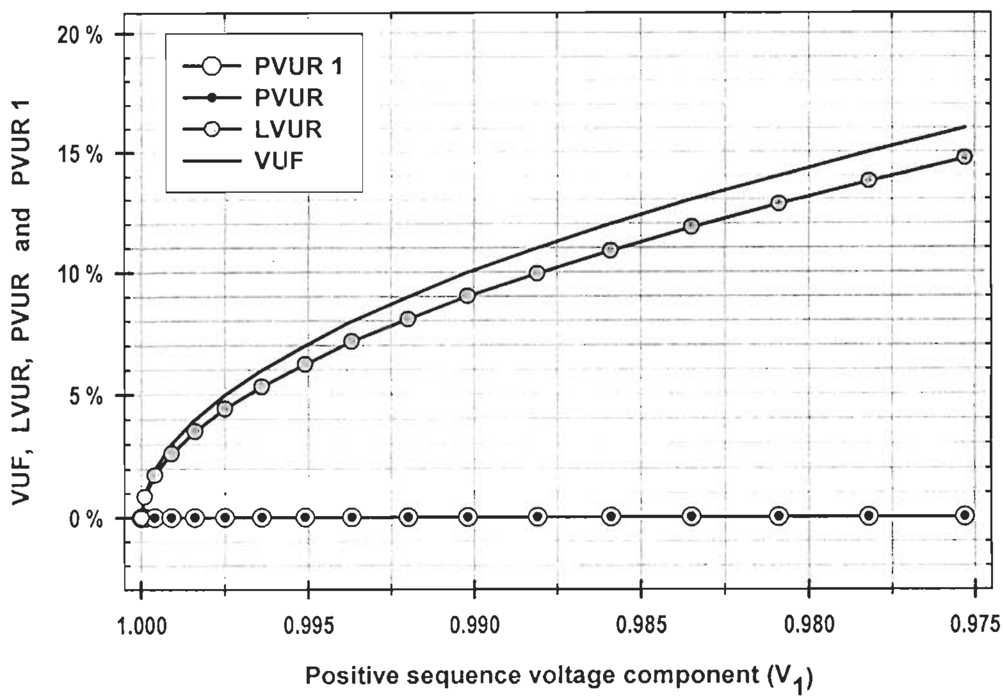

Fig. 4.14: Comparison of four different definitions of voltage unbalance for single-phase voltage unbalance due to phase angle (CW or ACW) movement

4.9.4 Effect of Voltage Unbalance on DC Parameters

For both the cases of voltage unbalance due to phase angle (CW or ACW) movement taken up for study, it is observed that V_2 increases in proportion to the increasing VUF. There is a very small decrease in the value of V_1 with increasing VUF. Also, the corresponding values of V_1 and V_2 are identical for both the cases of single-phase voltage unbalance due to movement of voltage phasors, either CW or ACW. Fig. 4.15 presents the variation of V_1 and V_2 as a function of VUF for single-phase voltage unbalance cases due to movement (CW /ACW) of voltage phasors. It is observed that due to voltage unbalance, the change in value of V_1 is very small. For the total variation of VUF from zero percent to 16 %, the change in p.u. value of V_1 is from 1.00 p.u. to 0.975 p.u.. However, the corresponding value of V_2 is almost equal to p.u. value of VUF, which clearly describes the advantage of using VUF as an effective measure of voltage unbalance.

For both the cases of single-phase voltage unbalance due to CW and ACW movement of voltage phasors, it is found that

i) As the VUF increases, the decrease in V_1 causes decrease in magnitudes of DC output parameters as shown in Fig. 4.16, which concludes that the magnitudes of DC output parameters are proportional to the V_1. Thus V_1 has an important role in the voltage unbalance study.

ii) The impact of increasing V_2 on rectifier performance is reflected on the distortion of DC output parameters and the distortion is found to be proportional to VUF. The change in distortion of DC output parameters with increasing VUF is shown in Fig. 4.17.

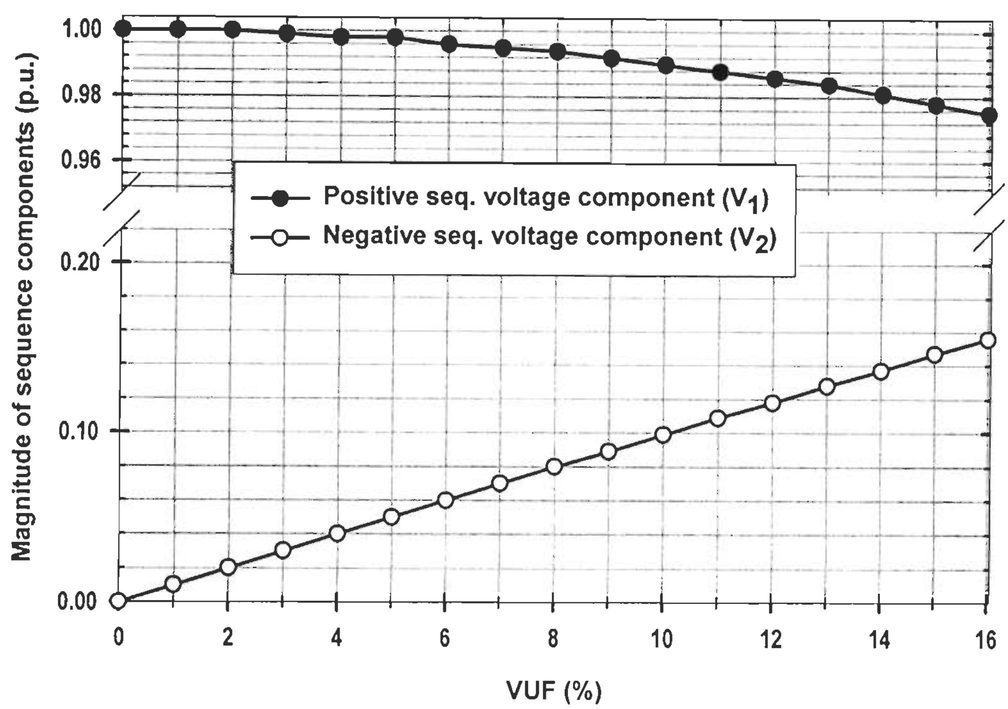

Fig. 4.15: Variation of magnitude of V_1 and V_2 as a function of VUF for single-phase voltage unbalance due to phase angle (CW or ACW) movement

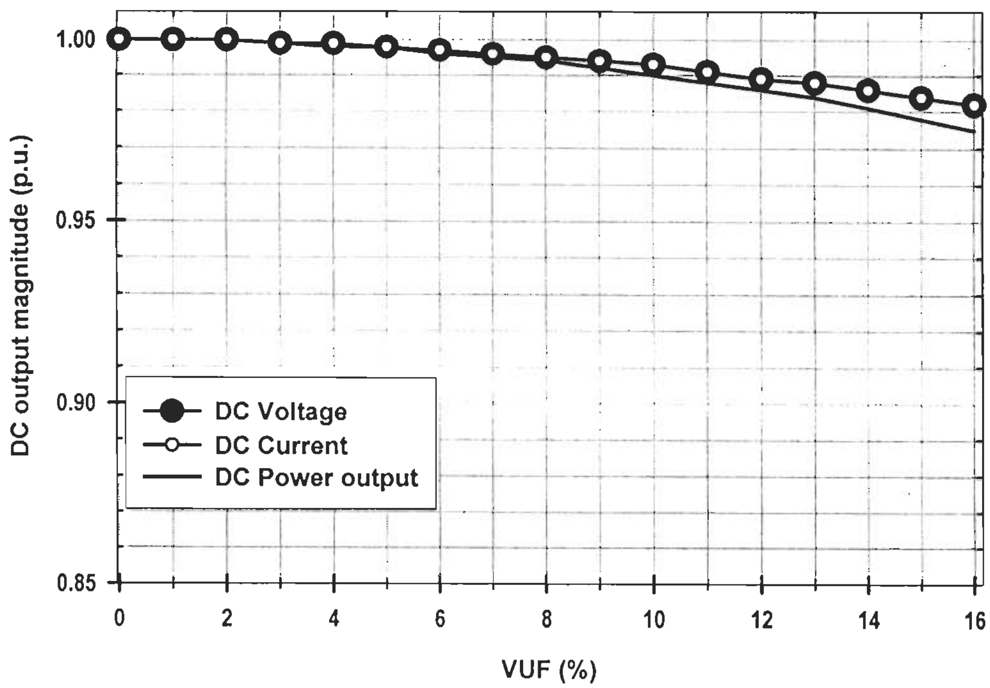

Fig. 4.16: Variation of magnitude of DC output parameters, as a function of VUF for single-phase voltage unbalance due to phase angle (CW or ACW) movement

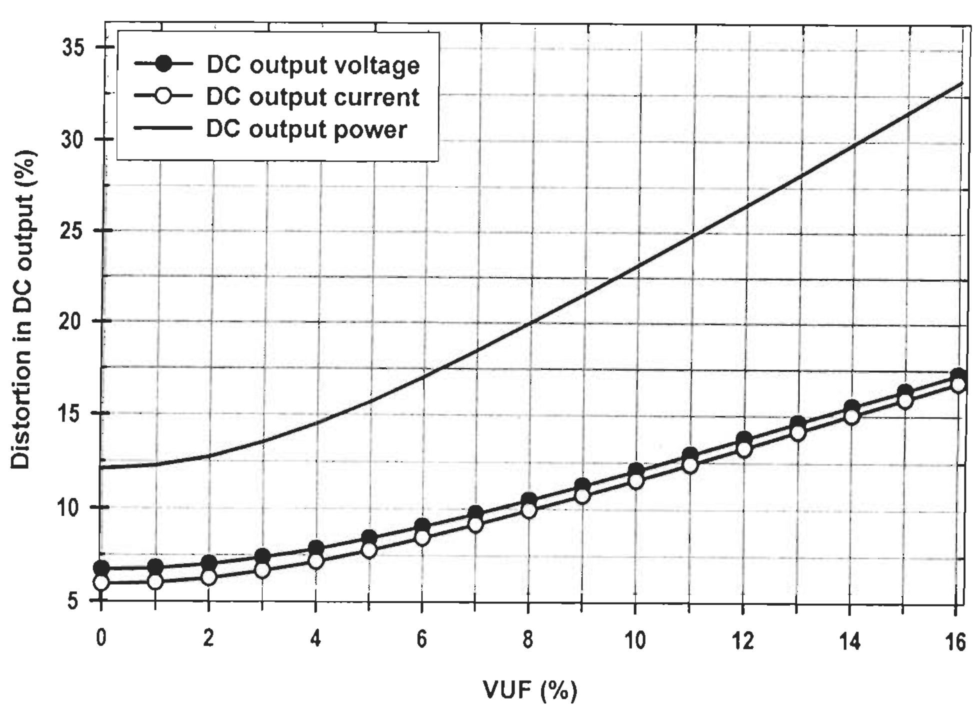

Fig. 4.17: Variation in distortion of DC output parameters, as a function of VUF for single-phase voltage unbalance due to phase angle (CW or ACW) movement

4.9.5 Effect of Voltage Unbalance on AC Parameters

The current waveforms of all three phases (I_A, I_B, and I_C) are affected by that even for a single-phase voltage unbalance, as shown in Table-4.7 to Table-4.10.

For single-phase voltage unbalance due to movement of voltage phasor *A* from its reference position, the load current in phase *A* is least affected in comparison of other two phases, in which phase angles are unaffected. For the case of single-phase voltage unbalance due to CW movement of voltage phasor *A*, as shown in Table-4.7 , there is no change in rms values of phase current in phase *A*, while for single-phase voltage unbalance due to ACW movement of voltage phasor *A* as in Table-4.9, the decrease in load current in phase *A* is very small. However, the change in rms values of phase currents in remaining two phases is observed relatively noticeable. In case of CW movement of voltage phasor *A*, the p.u. change in decreasing rms load current of phase *B* is found almost equal to p.u. value of VUF, while for ACW movement of voltage phasor *A*, the rms load current of phase *B* increases but the change in numerical value is found lesser in comparison to CW movement of voltage phasor *A*.

For this observation the generalized statement can be given as:

i) The load current is least affected for the phase in which the voltage phasor movement is taking place (i.e. phase *A* here);

ii) The load current increases for the phase from which the moving phasor is going away (i.e. phase *C* in case of CW movement and phase *B* in case of ACW movement); and

iii) The load current decreases for the phase towards which it is moving (i.e. phase *B* in case of CW movement and phase *C* in case of ACW movement).

The amount of change in numerical values of load currents is same as discussed above. This change in rms values of load currents is displayed in Fig. 4.18(a) and Fig. 4.18(b) for single-phase voltage unbalance due to CW and ACW movement of voltage phasor *A*, respectively. Fig. 4.19(a) and Fig. 4.19(b) present the load current variation for CW and ACW movement of voltage phasor *B*, whereas Fig. 4.20(a) and Fig. 4.20(b) present the load variation for CW and ACW movement of voltage phasor *C*, in that order.

It is also observed from Table-4.7 that for CW movement of phasor *A*, there is no change in the THD_I for the phase *A*, which is having the unaffected load current throughout the variation in VUF. THD_I is found increasing for the phase towards which the voltage phasor *A* is moving (i.e. phase *B*) and decreasing for the phase from which the voltage phasor *A* is moving away (i.e. phase *C*). This observation is also verified from Table-4.8, where the single-phase voltage unbalance due to CW movement of voltage phasor *B* and *C*, is considered individually, only one at a time.

The same illustration of results can also be extended for the case of single-phase voltage unbalance due to ACW movement of voltage phasor. It can be viewed from Table-4.9 that for increasing VUF caused by ACW movement of phasor *A*, THD_I for phase *A* is slightly increasing, with its little decreasing load current. Again, the THD_I is found increasing for the phase towards which the voltage phasor *A* is moving (i.e. phase *C* here) and decreasing for the phase from which the voltage phasor *A* is moving away (i.e. phase *B*). It is also clear from Table-4.9 that THD_I is having minimum numerical value for the phase having the maximum load current.

This variation in THD_I of three different phases as a function of VUF is presented in Fig. 4.21(a) and Fig. 4.21(b) for CW and ACW movement in phase *A*, respectively. For single-phase voltage unbalance conditions considered independently in three different phases is presented in Table-4.8 and Table-4.10. The variation in AC current parameters follows the same pattern as displayed in Fig. 4.18 and Fig. 4.21 (for rms current value and THD_I, in that order), relative to the phase in which the unbalance is taking place. For three different phases, this variation in THD_I w.r.t. variable VUF is presented in Fig. 4.22(a) and Fig. 4.22(b) for the CW and ACW movement considered in phase *B*; and in Fig. 4.23(a) and Fig. 4.23(b) for CW and ACW movement considered in phase *C*, respectively. On the basis of these observations, a general remark can be made that:

- Even a single-phase supply voltage unbalance has its specific influence on AC current waveforms and its parameters (rms value and THD_I) of all three phases (I_A, I_B, and I_C), and

- The change in voltage phase angle 'least affects' the phase in which the phase angle movement is taking place, and 'most affects' the phase towards which it is moving.

It was found that the average THD_I of all three different phases remains almost constant (very small variation) irrespective of the direction of movement (CW or ACW) of voltage phasor, and phase (*A*, *B* or *C*) under movement. It was also observed that VUF has no effect on this average THD_I.

PTHDUF has been recommended as a proficient index of voltage source unbalance in presence of harmonic distortion. For a given value of VUF, it does not change for the phases (*A*, *B* or *C*) regardless of the reason of voltage unbalance. Furthermore, for the given VUF, the values of PTHDUF are found to be quite unique for both cases of single-phase voltage unbalance due to phase angle movement (CW or ACW). Plots of average THD_I and PTHDUF with variable VUF are shown in Fig. 4.24(a) for the case of CW movement and in Fig. 4.24(b) for ACW movement of voltage phasors.

It is evident from these two Figures that for a given value of VUF, the PTHDUF has its value somewhat higher for the case of single-phase voltage unbalance due to ACW movement of voltage phasors, as compared to case of single-phase voltage unbalance due to CW movement of voltage phasors. Hence, it can be concluded that PTHDUF is reasonably characteristic for the reason of unbalance and VUF.

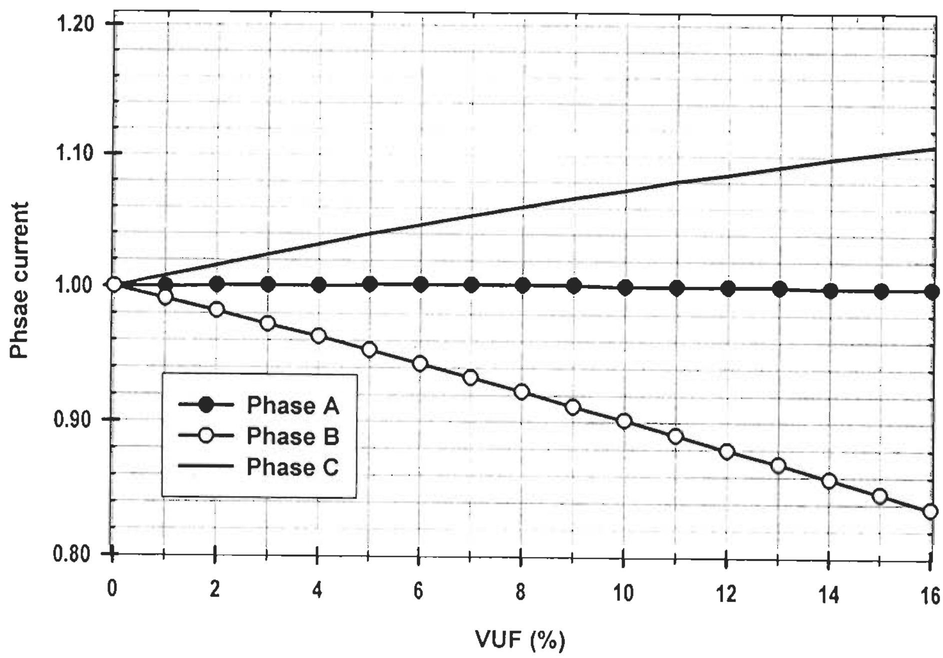

Fig. 4.18 (a): Variation of rms currents in three different phases as a function of VUF for single-phase voltage unbalance due to CW movement of voltage phasor *A*

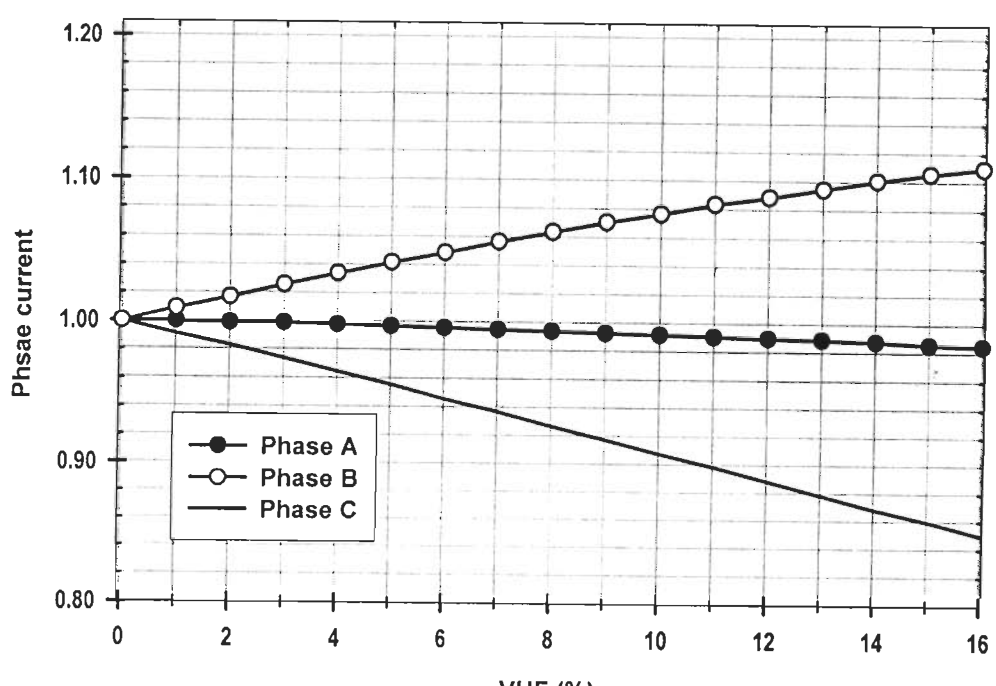

Fig. 4.18 (b): Variation of rms currents in three different phases as a function of VUF for single-phase voltage unbalance due to ACW movement of voltage phasor *A*

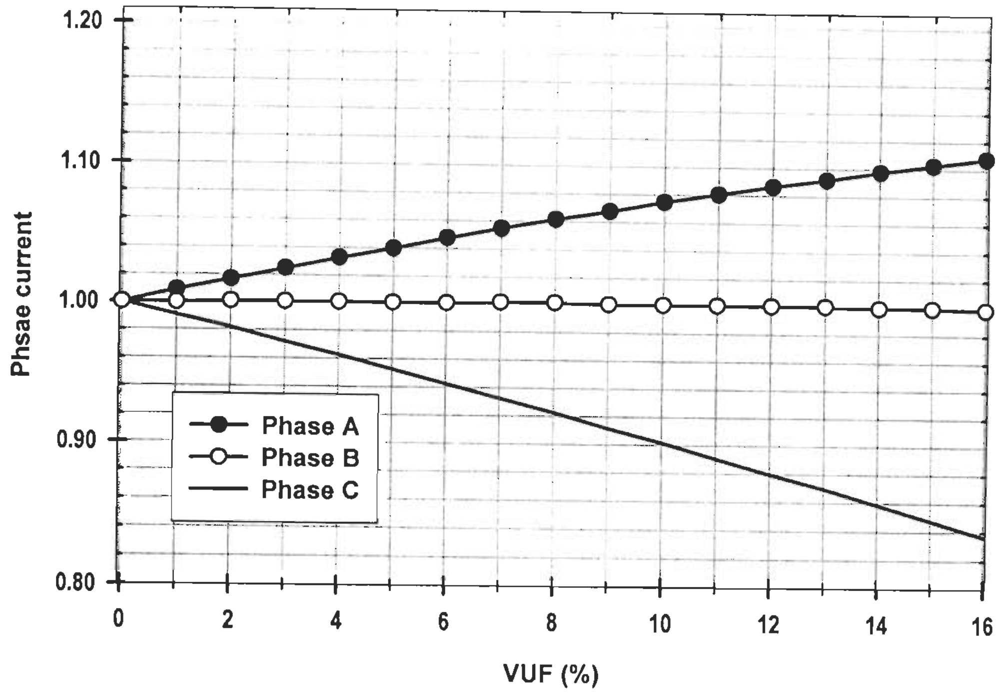

Fig. 4.19 (a): Variation of rms currents in three different phases as a function of VUF for single-phase voltage unbalance due to CW movement of voltage phasor *B*

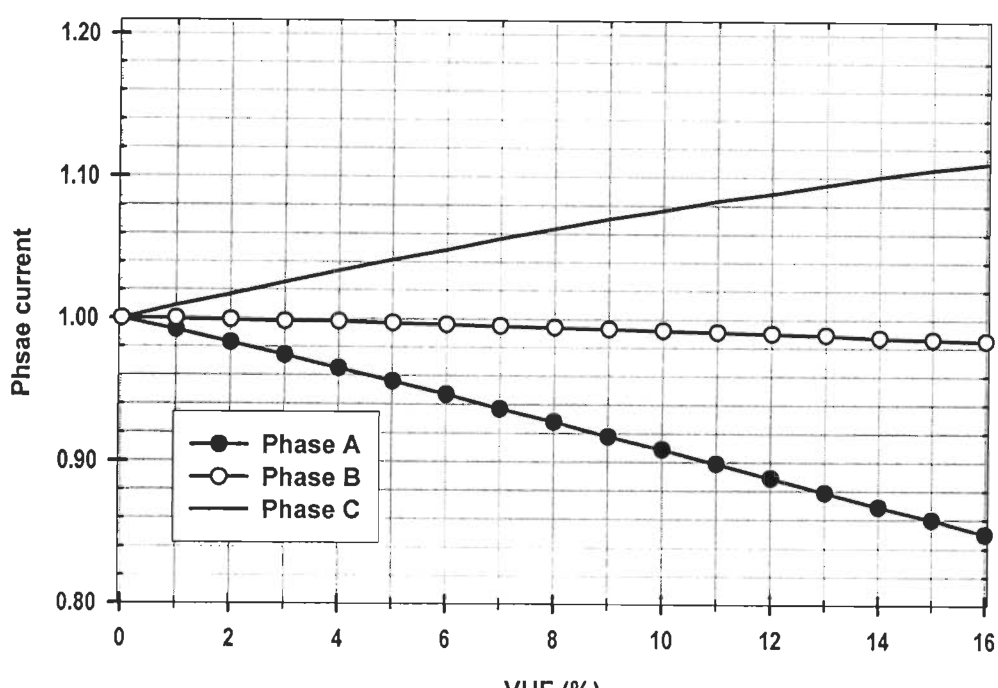

Fig. 4.19 (b): Variation of rms currents in three different phases as a function of VUF for single-phase voltage unbalance due to ACW movement of voltage phasor *B*

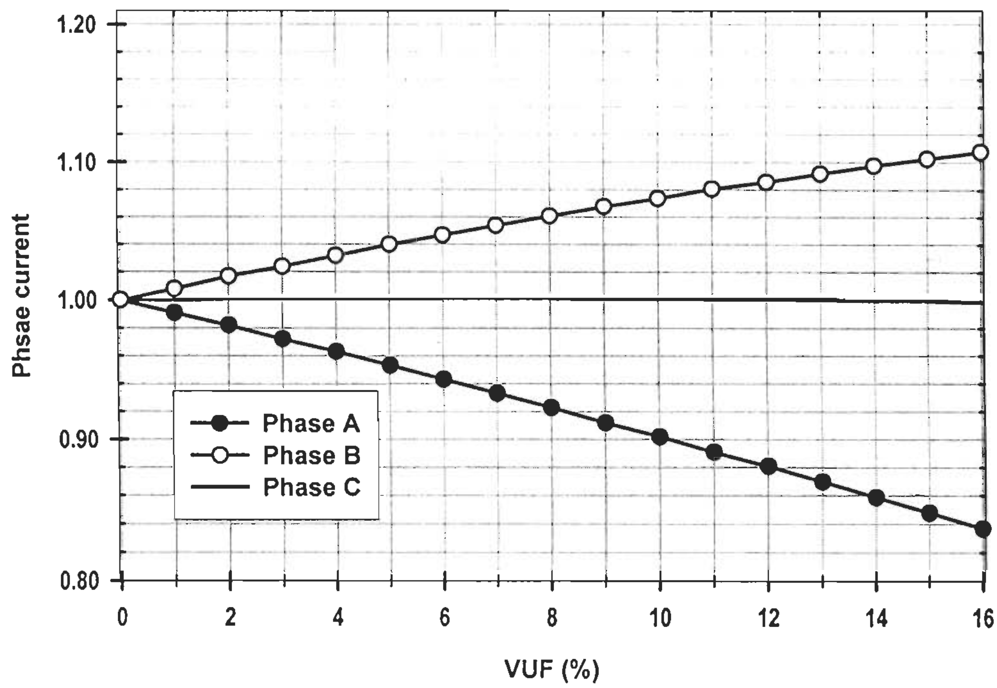

Fig. 4.20 (a): Variation of rms currents in three different phases as a function of VUF for single-phase voltage unbalance due to CW movement of voltage phasor *C*

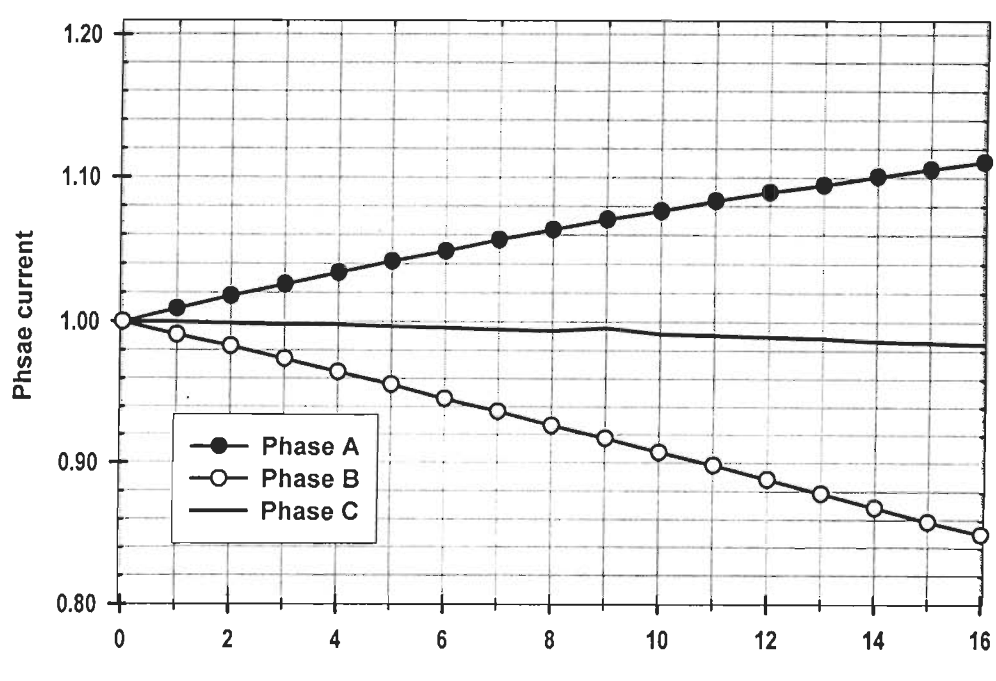

Fig. 4.20 (b): Variation of rms currents in three different phases as a function of VUF for single-phase voltage unbalance due to ACW movement of voltage phasor *C*

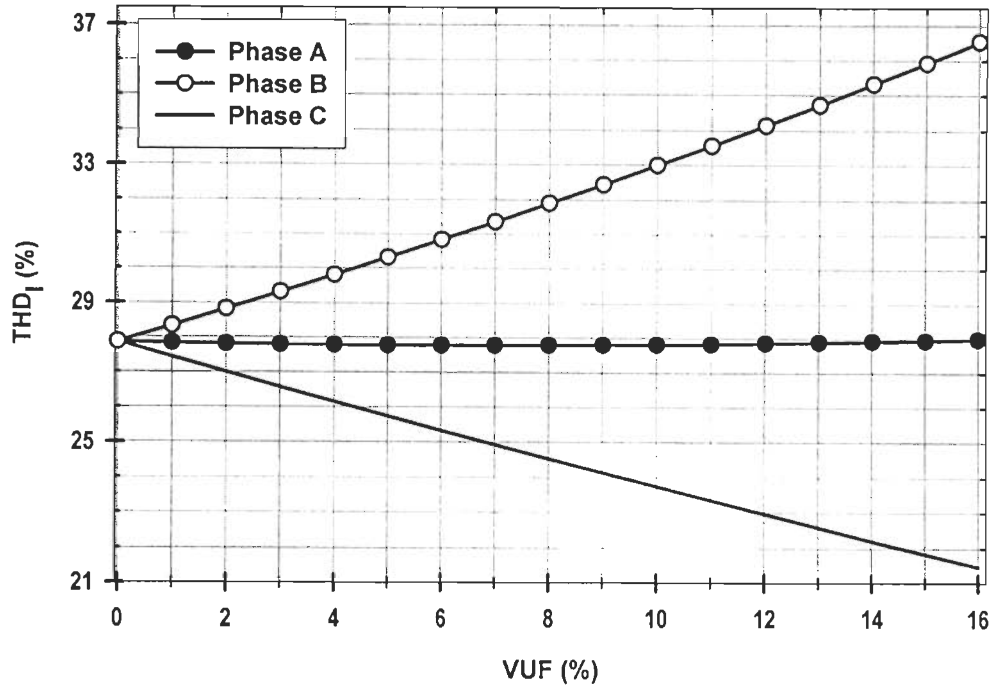

Fig. 4.21 (a): Variation of THD$_I$ of currents in three different phases as a function of VUF for single-phase voltage unbalance due to CW movement of voltage phasor *A*

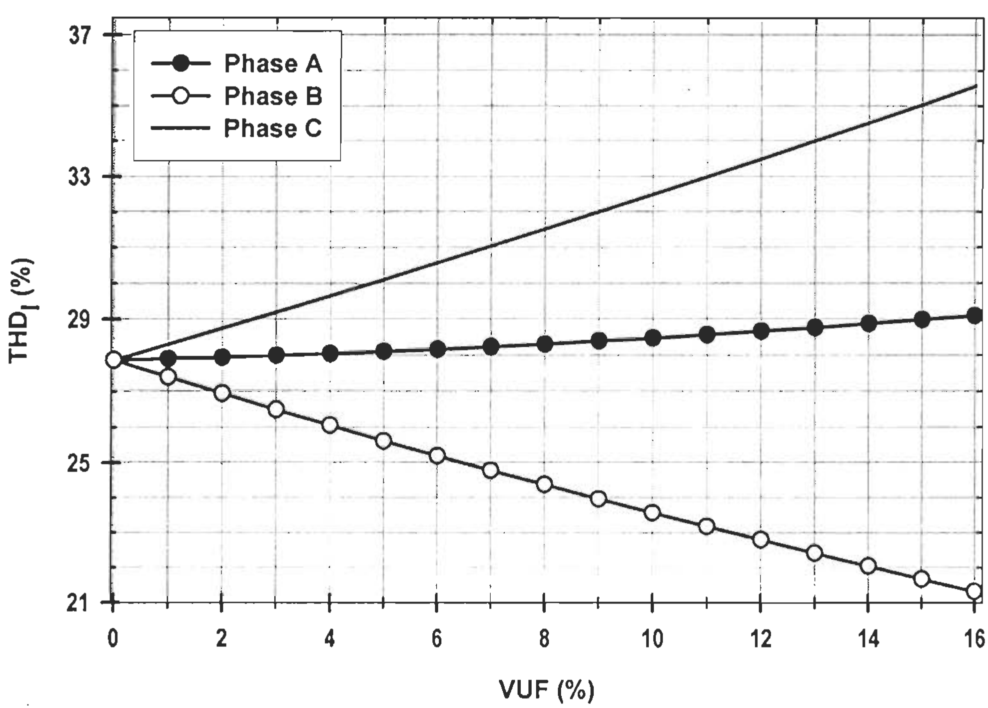

Fig. 4.21 (b): Variation of THD$_I$ of currents in three different phases as a function of VUF for single-phase voltage unbalance due to ACW movement of voltage phasor *A*

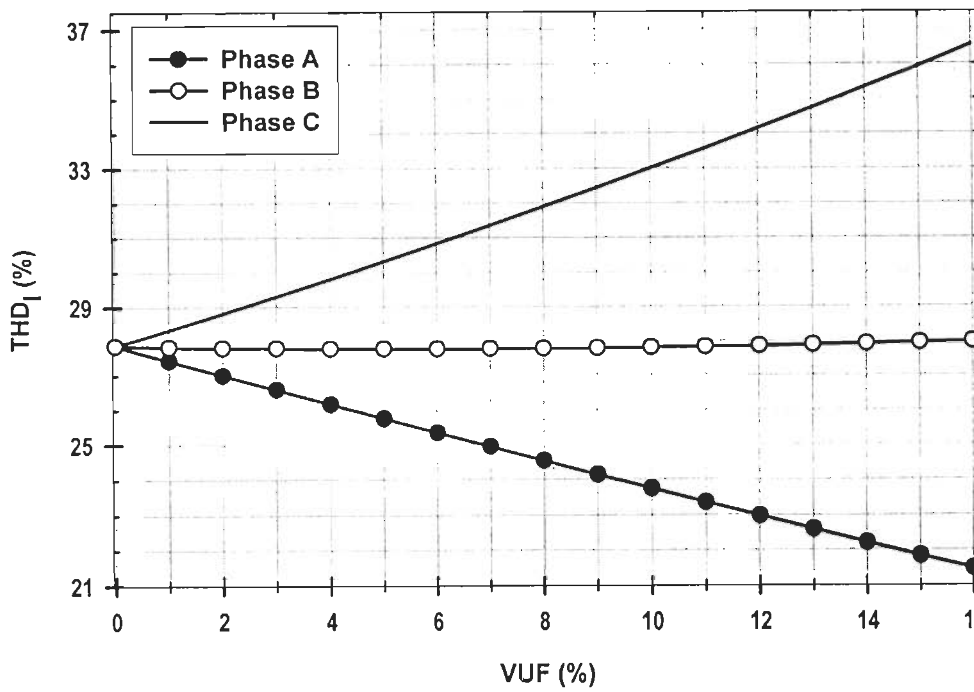

Fig. 4.22 (a): Variation of THD_I of currents in three different phases as a function of VUF for single-phase voltage unbalance due to CW movement of voltage phasor *B*

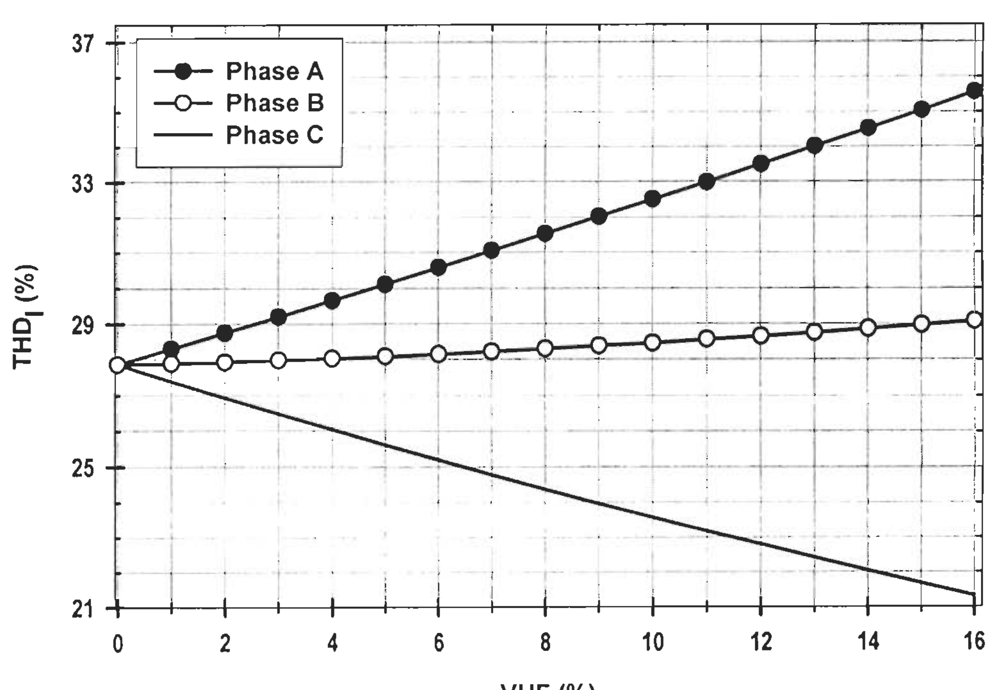

Fig. 4.22 (b): Variation of THD_I of currents in three different phases as a function of VUF for single-phase voltage unbalance due to ACW movement of voltage phasor *B*

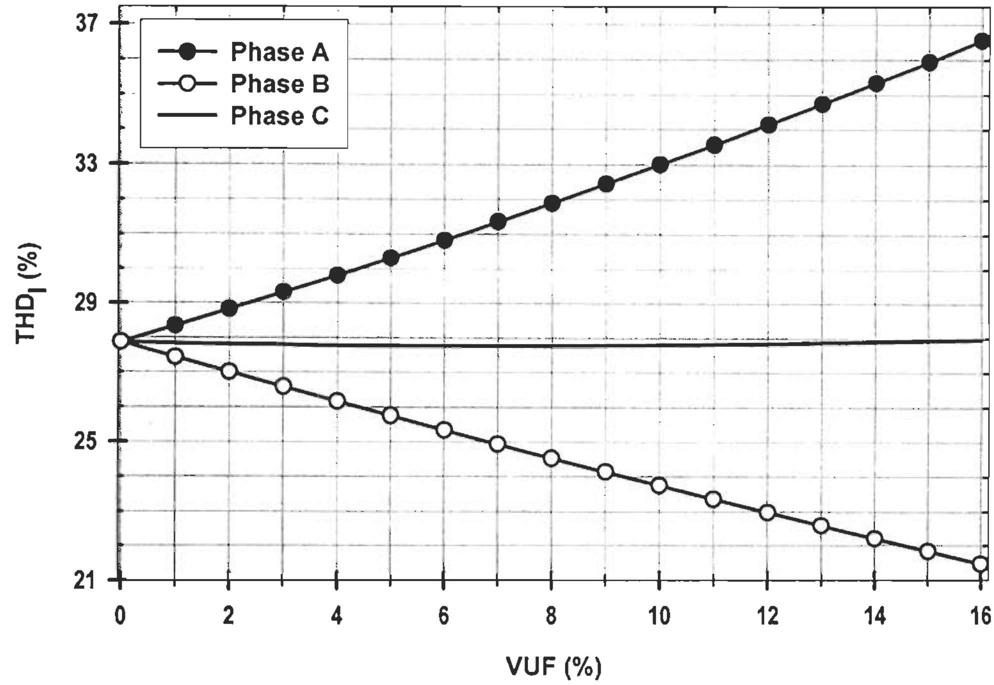

Fig. 4.23 (a): Variation of THD_I of currents in three different phases as a function of VUF for single-phase voltage unbalance due to CW movement of voltage phasor *C*

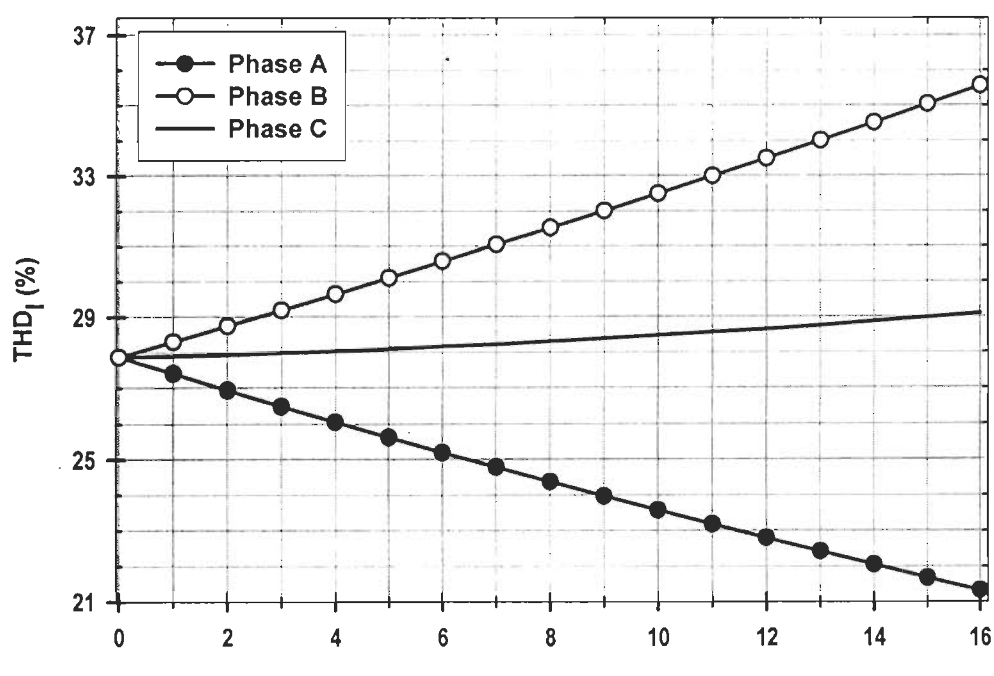

Fig. 4.23 (b): Variation of THD_I of currents in three different phases as a function of VUF for single-phase voltage unbalance due to ACW movement of voltage phasor *C*

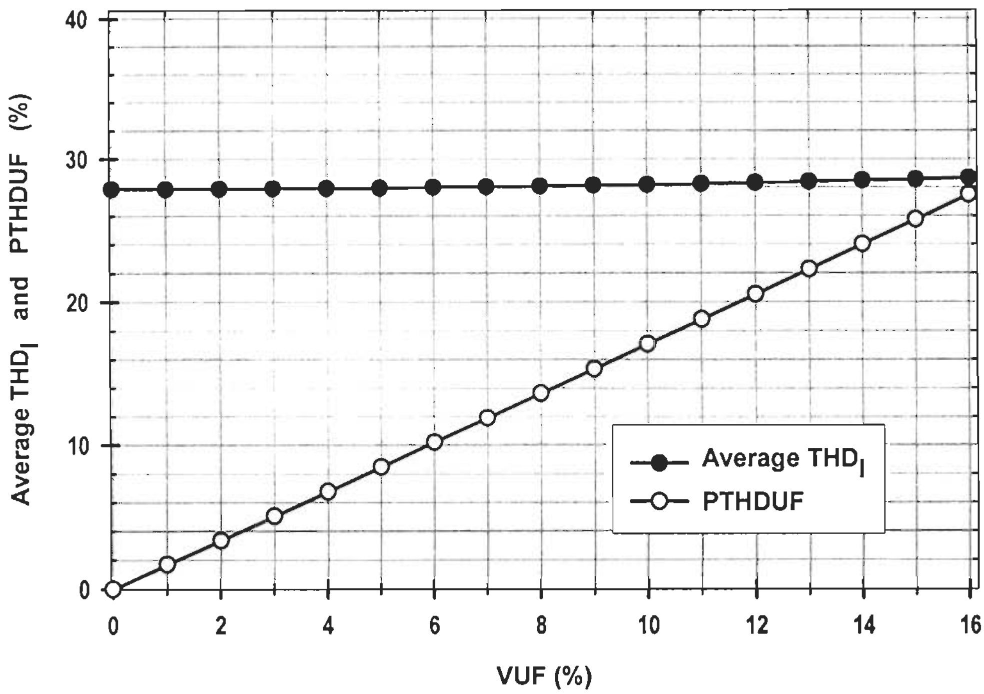

Fig. 4.24 (a): Variation of average THD$_I$ and PTHDUF with increasing VUF for single-phase voltage unbalance due to CW movement of voltage phasors

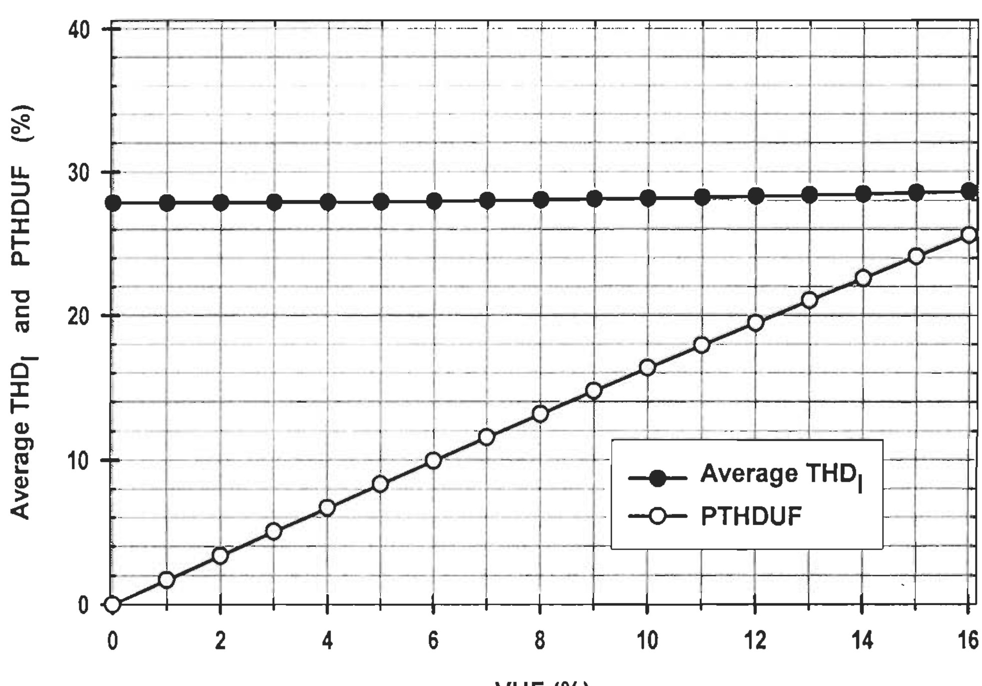

Fig. 4.24(b): Variation of average THD$_I$ and PTHDUF with increasing VUF for single-phase voltage unbalance due to ACW movement of voltage phasors

4.10 CHANGES IN TWO PHASE ANGLES WITH EQUAL CHANGE IN EACH PHASE

For a three-phase balanced source voltage system, the displacement of voltage phasors between any two phases must be equal to 120°. Considering any specific phase as a reference phasor, if remaining two phases are deflected, in opposite directions i.e., one in CW and another in ACW, which leads to two different cases. In one case the angle between the remaining two phases is increased and in another case the angle between the remaining two phases is decreased. Both the cases are considered for analysis. To make the results more reliable, two different sets of voltage phasors are considered under movement i.e. phase B with phase C and phase A with phase C. The most important point to mention here is that the contribution of each phase angle deflection towards voltage unbalance is half of the total amount of VUF.

4.10.1 Two-Phase Angle Unbalance due to 'Increasing Angle' between Two Phases

4.10.1.1 Increasing Angle between Phase *B* and Phase *C*

Here, phase *A* is considered as reference phasor and remaining two phases, i.e. *B* and *C*, shift in opposite directions. In this particular case, the variation in VUF is adjusted by ACW movement of voltage phasor *B* and CW movement of voltage phasor *C* of a balanced voltage supply, as shown in Fig. 4.25. This movement increases the angle between voltage phasors *B* and *C* and causes the unbalance in voltage source.

The input supply parameters, voltage sequence components V_1 and V_2, and numerical values of four definitions of voltage unbalance for single-phase angle unbalance case due to CW movement of voltage phasor *C* are shown in Table-4.13(a), while Table-4.13(b) presents the same parameters for the ACW movement of voltage phasor *B*. Here, the change in phase angle position of a particular phase regulates the variable VUF.

A combination of cases given in Table-4.13(a) and Table-4.13(b) is considered in Table-4.14, to analyze the combined effect of change in position of phasor *C* together with phasor *B*, with equal change in each phase. The contribution of each phase angle deflection towards voltage unbalance is considered half of the total value of VUF, but it is observed that net VUF is smaller than the sum of the individual contributions e.g. angle (Φ_C =119.14°) gives 0.50 % VUF, and angle (Φ_B =240.86°) gives 0.50 % VUF, but combination of both provides just 0.86 % VUF.

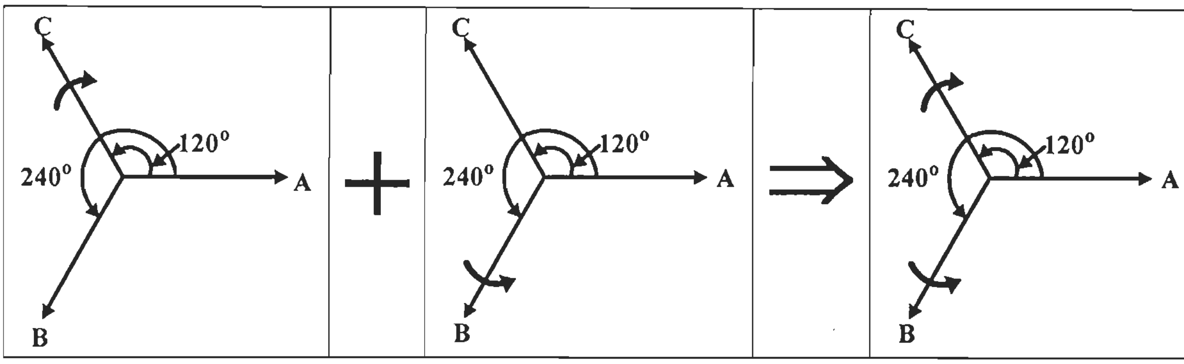

Fig. 4.25: An unbalance in three-phase voltage source due to 2-Φ equal angle unbalance for increasing angle between phase *B* and Phase *C*

4.10.1.2 Increasing Angle between Phase *A* and Phase *C*

At this point, phase *B* is considered as reference phasor and remaining two phases specifically, phase *C* and phase *A* are modified in opposite directions. In this case, the direction of movement for phase *A* is CW and ACW for phase *C*, as shown in Fig. 4.26. This condition leads towards increasing angle between voltage phasors *A* and *C*, and thus, unbalanced voltage source.

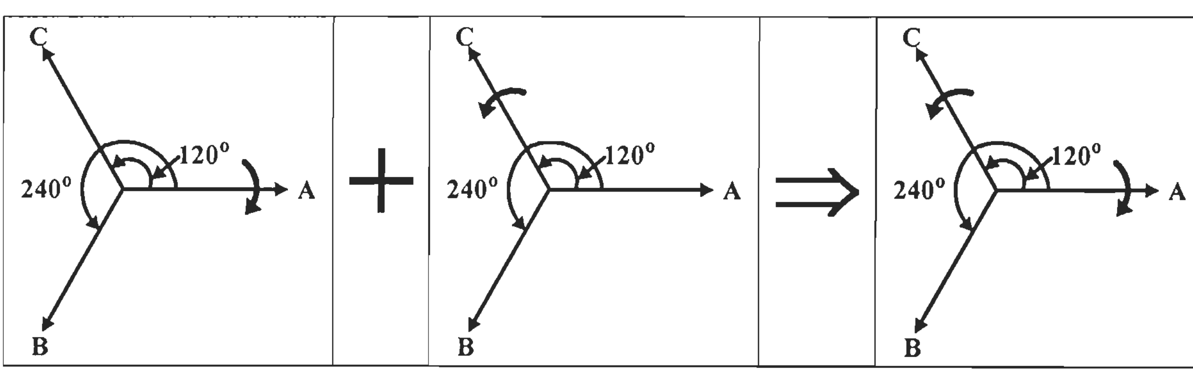

Fig. 4.26: An unbalance in three-phase voltage source due to 2-Φ equal angle unbalance by phase *A* and *C* for increasing angle between phase *A* and Phase *C*

The movement of phasors *A* and *B*, in equal steps, is shown in Table-4.15(a) and Table-4.15(b), respectively. These two tables also include the details of three-phase voltage supply, their V_1 and V_2, and the numerical values of four definitions of voltage unbalance. To analyze the effect of change in position of phasor *C* along with phasor *A* with equal change in each phase, a combination of these two cases (of Table-4.15) is considered in Table-4.16. The each phase angle deflection contributes half of the total amount of VUF considered, but it is observed that net VUF is smaller than the sum of the individual contributions e.g. angle (Φ_C =120.86°) gives 0.50 % VUF, and angle (Φ_A = - 0.86°) gives 0.50 % VUF, but combination of both provides just 0.87 % VUF.

4.10.2 Two-Phase Angle Unbalance due to 'Decreasing Angle' between Two Phases

4.10.2.1 Decreasing Angle between Phase *B* and Phase *C*

In this case, phase A is considered as reference phasor and other two phases (*B* and *C*) are shifted in opposite direction. The variation in VUF is adjusted by CW movement of voltage phasor *B* and ACW movement of voltage phasor *C*, of a balanced source voltage supply, as shown in Fig. 4.27. This movement decreases the angle between voltage phasors *B* and *C* and results in unbalanced voltage source.

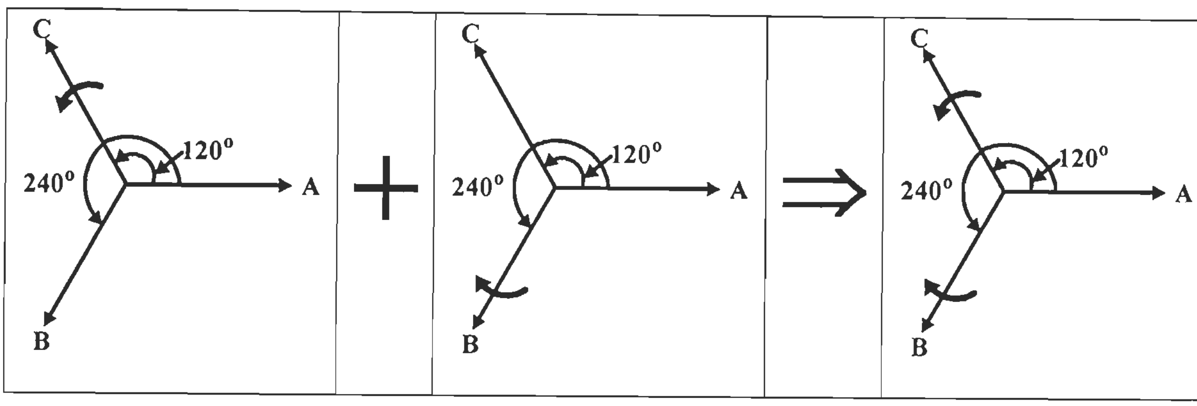

Fig. 4.27: An unbalance in three-phase voltage source, due to 2-Φ equal angle unbalance for decreasing angle between phase *B* and Phase *C*

The movements of phasors *B* and *C*, in equal steps, are shown in Table-4.17(a) and Table-4.17(b), respectively. These tables also contain the corresponding three-phase supply voltages, their V_1 and V_2, with the numerical values of four definitions of voltage unbalance.

A combination of these two single-phase angle unbalance cases is considered in Table-4.18, to analyze the collective effect of change in position of phasor *C* along with phasor *B*, with equal change in each phase. Table-4.18 also contains the numerical values of four definitions of voltage unbalance, their three-phase supply voltages with corresponding V_1 and V_2, and DC output parameters. The contribution of both of the moving voltage phasors towards voltage unbalance is considered half of the net VUF, but it is observed that net VUF is smaller than the sum of the individual contributions e.g. angle (Φ_C =120.86°) gives 0.50 % VUF, and angle (Φ_b=239.14°) gives 0.50 % VUF, but combination of both provides just 0.86 % VUF.

4.10.2.2 Decreasing Angle between Phase A and Phase C

Here, phase *B* is considered as reference phasor and angle positions of remaining two phases (*C* and *A*) are modified in opposite direction. In this case, the movement in phase *A* is ACW and in phase *C* it is CW, as shown in Fig. 4.28. Thus the angle between voltage phasors *A* and *C* decreases and causes unbalance in balanced voltage supply.

The movements of phasors *A* and *C*, in equal steps, are shown in Table-4.19(a) and Table-4.19(b), respectively. The contribution of each phase angle deflection towards voltage unbalance is considered half of the total value of VUF, but it is observed that net VUF is smaller than the sum of the individual contributions e.g. angle (Φ_C =119.14°) gives 0.50 % VUF, and angle (Φ_A=0.86°) gives 0.50 % VUF, but combination of both cases provides just 0.87 % VUF. The corresponding three-phase supply voltages, their V_1 and V_2 along with the numerical values (in percentage) of four definitions of voltage unbalance are also given.

Table-4.20 includes the combination of cases given in Table-4.19(a) and Table-4.19(b), to analyze the collective effect of change in position of phasor *C* along with phasor *A*, with equal change in each phase. This table also presents the values of four definitions of voltage unbalance, their three-phase supply voltages, their corresponding V_1 and V_2, and DC output parameters.

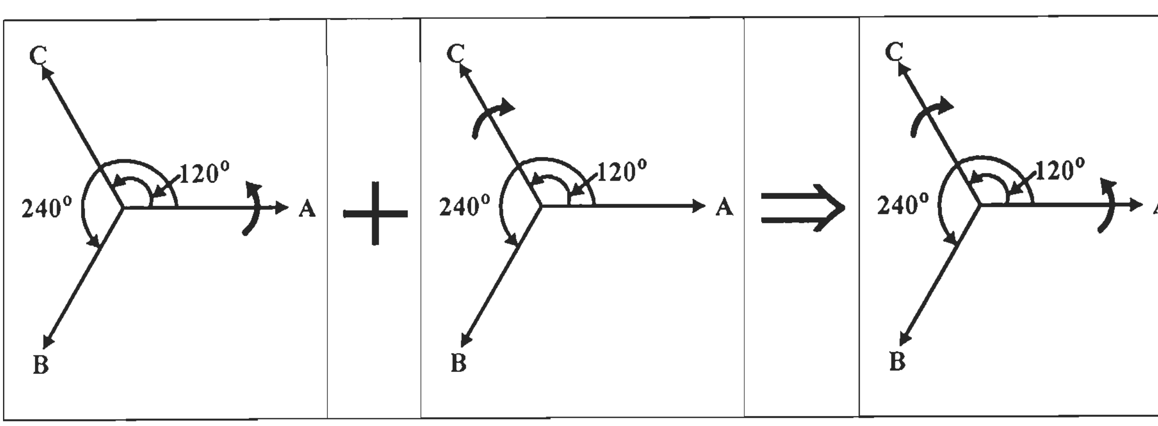

Fig. 4.28: An unbalance in three-phase voltage source due to 2-Φ equal angle unbalance for decreasing angle between phase *A* and Phase *C*

For the increasing VUF, the behavior of characteristic and non-characteristic harmonics is presented in Table-4.21 (a) and Table-4.21 (b) for the case of increasing angle between phasors *B* and *C*, while for the case of decreasing angle between them, this harmonic behavior is shown in Table-4.22 (a) and Table-4.22 (b), respectively. This variation in harmonic pattern behavior is discussed in section 4.13.

Table-4.13 (a): Comparison of four different definitions of voltage unbalance for 1-Φ angle unbalance in phase *C* (moving CW) for increasing VUF.

LVUR (%)	PVUR 1 (%)	PVUR (%)	VUF (%)	Unbalanced voltage source						+ve seq. Volt. (V_1)	-ve seq. Volt. (V_2)
				Phase *A*		Phase *B*		Phase *C*			
				Mag.	Angle	Mag.	Angle	Mag.	Angle		
0.00	0	0	0.00	1.0	0	1.0	240	1.0	120	1.000	0.00
0.43	0	0	0.50	1.0	0	1.0	240	1.0	119.14	1.000	0.005
0.87	0	0	1.00	1.0	0	1.0	240	1.0	118.28	1.000	0.010
1.31	0	0	1.50	1.0	0	1.0	240	1.0	117.42	1.000	0.015
1.75	0	0	2.00	1.0	0	1.0	240	1.0	116.56	1.000	0.020
2.19	0	0	2.50	1.0	0	1.0	240	1.0	115.7	0.999	0.025
2.63	0	0	3.00	1.0	0	1.0	240	1.0	114.84	0.999	0.030
3.08	0	0	3.50	1.0	0	1.0	240	1.0	113.98	0.999	0.035
3.52	0	0	4.00	1.0	0	1.0	240	1.0	113.13	0.998	0.040
3.97	0	0	4.50	1.0	0	1.0	240	1.0	112.27	0.998	0.045
4.43	0	0	5.00	1.0	0	1.0	240	1.0	111.41	0.998	0.050
4.88	0	0	5.50	1.0	0	1.0	240	1.0	110.55	0.997	0.055
5.33	0	0	6.00	1.0	0	1.0	240	1.0	109.7	0.996	0.060
5.78	0	0	6.50	1.0	0	1.0	240	1.0	108.85	0.996	0.065
6.24	0	0	7.00	1.0	0	1.0	240	1.0	108	0.995	0.070
6.70	0	0	7.50	1.0	0	1.0	240	1.0	107.15	0.994	0.075
7.16	0	0	8.00	1.0	0	1.0	240	1.0	106.3	0.994	0.080

Table-4.13 (b): Comparison of four different definitions of voltage unbalance for 1-Φ angle unbalance in phase *B* (moving ACW) for increasing VUF.

LVUR (%)	PVUR 1 (%)	PVUR (%)	VUF (%)	Unbalanced voltage source						+ve seq. Volt. (V_1)	-ve seq. Volt. (V_2)
				Phase *A*		Phase *B*		Phase *C*			
				Mag.	Angle	Mag.	Angle	Mag.	Angle		
0.00	0	0	0.00	1.0	0	1.0	240	1.0	120	1.000	0.00
0.43	0	0	0.50	1.0	0	1.0	240.86	1.0	120	1.000	0.005
0.87	0	0	1.00	1.0	0	1.0	241.72	1.0	120	1.000	0.010
1.31	0	0	1.50	1.0	0	1.0	242.58	1.0	120	1.000	0.015
1.75	0	0	2.00	1.0	0	1.0	243.44	1.0	120	1.000	0.020
2.19	0	0	2.50	1.0	0	1.0	244.3	1.0	120	0.999	0.025
2.63	0	0	3.00	1.0	0	1.0	245.16	1.0	120	0.999	0.030
3.08	0	0	3.50	1.0	0	1.0	246.02	1.0	120	0.999	0.035
3.52	0	0	4.00	1.0	0	1.0	246.87	1.0	120	0.998	0.040
3.97	0	0	4.50	1.0	0	1.0	247.73	1.0	120	0.998	0.045
4.43	0	0	5.00	1.0	0	1.0	248.59	1.0	120	0.998	0.050
4.88	0	0	5.50	1.0	0	1.0	249.45	1.0	120	0.997	0.055
5.33	0	0	6.00	1.0	0	1.0	250.3	1.0	120	0.996	0.060
5.78	0	0	6.50	1.0	0	1.0	251.15	1.0	120	0.996	0.065
6.24	0	0	7.00	1.0	0	1.0	252	1.0	120	0.995	0.070
6.70	0	0	7.50	1.0	0	1.0	252.85	1.0	120	0.994	0.075
7.16	0	0	8.00	1.0	0	1.0	253.7	1.0	120	0.994	0.080

Table-4.14: **Comparison of four definitions of voltage unbalance and rectifier performance for 2-Φ equal angle unbalance for increasing angle between phase *B* and *C* - two phasors moving in opposite direction for increasing VUF**

LVUR (%)	PVUR 1 (%) and PVUR (%)	VUF (%)	Unbalanced voltage source						+ve seq. Volt. (V_1)	-ve seq. Volt. (V_2)	AC parameters						Average THD_I	PTHDUF (%)	DC parameters					
			Phase *A*		Phase *B*		Phase *C*				I_A		I_B		I_C				I_{DC}		V_{DC}		P_{DC}	
			Mag.	Angle	Mag.	Angle	Mag.	Angle			RMS	THD_I (%)	Mag.	THD_I (%)	Mag.	THD_I (%)			Mag.	THD_I (%)	Mag.	THD_I (%)	Mag.	THD_I (%)
0.00	0	0.00	1.0	0	1.0	240	1.0	120	1.0000	0.00	1.000	27.87	1.000	27.87	1.000	27.87	27.87	0.00	1.000	5.95	1.000	6.72	1.000	12.13
0.86	0	0.86	1.0	0	1.0	240.86	1.0	119.14	0.9999	0.0086	0.991	28.33	1.004	27.67	1.005	27.62	27.87	1.64	1.000	6.01	1.000	6.78	1.000	12.26
1.71	0	1.72	1.0	0	1.0	241.72	1.0	118.28	0.9997	0.0172	0.982	28.79	1.008	27.47	1.009	27.38	27.88	3.26	1.000	6.19	1.000	6.95	1.000	12.62
2.55	0	2.57	1.0	0	1.0	242.58	1.0	117.42	0.9993	0.0257	0.973	29.25	1.012	27.28	1.014	27.14	27.89	4.88	0.999	6.48	0.999	7.21	0.999	13.20
3.38	0	3.41	1.0	0	1.0	243.44	1.0	116.56	0.9988	0.0340	0.964	29.72	1.015	27.08	1.018	26.91	27.90	6.51	0.999	6.86	0.999	7.56	0.999	13.97
4.20	0	4.24	1.0	0	1.0	244.3	1.0	115.7	0.9981	0.0423	0.954	30.20	1.019	26.89	1.022	26.68	27.92	8.15	0.999	7.32	0.999	7.99	0.998	14.89
5.00	0	5.07	1.0	0	1.0	245.16	1.0	114.84	0.9973	0.0506	0.945	30.69	1.023	26.71	1.026	26.46	27.95	9.79	0.998	7.85	0.998	8.48	0.997	15.95
5.80	0	5.89	1.0	0	1.0	246.02	1.0	113.98	0.9963	0.0587	0.935	31.18	1.026	26.52	1.030	26.24	27.98	11.44	0.997	8.42	0.997	9.02	0.996	17.10
6.58	0	6.70	1.0	0	1.0	246.87	1.0	113.13	0.9952	0.0667	0.925	31.66	1.030	26.34	1.034	26.02	28.01	13.04	0.996	9.02	0.996	9.60	0.995	18.31
7.35	0	7.51	1.0	0	1.0	247.73	1.0	112.27	0.9939	0.0746	0.915	32.16	1.033	26.16	1.038	25.81	28.04	14.68	0.995	9.66	0.995	10.22	0.994	19.60
8.12	0	8.31	1.0	0	1.0	248.59	1.0	111.41	0.9925	0.0825	0.905	32.67	1.036	25.97	1.042	25.60	28.08	16.35	0.994	10.32	0.994	10.86	0.992	20.94
8.87	0	9.11	1.0	0	1.0	249.45	1.0	110.55	0.9910	0.0903	0.895	33.18	1.039	25.79	1.045	25.39	28.12	17.99	0.993	11.00	0.993	11.52	0.991	22.31
9.61	0	9.90	1.0	0	1.0	250.3	1.0	109.7	0.9893	0.0978	0.884	33.69	1.042	25.62	1.049	25.19	28.17	19.61	0.992	11.68	0.992	12.19	0.989	23.69
10.34	0	10.67	1.0	0	1.0	251.15	1.0	108.85	0.9874	0.1054	0.874	34.21	1.045	25.44	1.052	24.99	28.21	21.25	0.990	12.38	0.990	12.87	0.987	25.09
11.06	0	11.44	1.0	0	1.0	252	1.0	108	0.9854	0.1127	0.863	34.74	1.048	25.26	1.055	24.79	28.26	22.92	0.989	13.08	0.989	13.56	0.985	26.50
11.77	0	12.21	1.0	0	1.0	252.85	1.0	107.15	0.9833	0.1201	0.852	35.27	1.050	25.09	1.058	24.60	28.32	24.54	0.987	13.79	0.987	14.27	0.982	27.93
12.47	0	12.97	1.0	0	1.0	253.7	1.0	106.3	0.9810	0.1273	0.842	35.81	1.053	24.91	1.061	24.40	28.37	26.21	0.985	14.51	0.986	14.97	0.980	29.35

Table-4.15 (a): Comparison of four different definitions of voltage unbalance for 1-Φ angle unbalance in phase *C* (moving ACW) for increasing VUF.

LVUR (%)	PVUR 1 (%)	PVUR (%)	VUF (%)	Unbalanced voltage source						+ve seq. Volt. (V_1)	-ve seq. Volt. (V_2)
				Phase *A*		Phase *B*		Phase *C*			
				Mag.	Angle	Mag.	Angle	Mag.	Angle		
0.00	0	0	0.00	1.0	0	1.0	240	1.0	120	1.000	0.00
0.43	0	0	0.50	1.0	0	1.0	240	1.0	120.86	1.000	0.005
0.87	0	0	1.00	1.0	0	1.0	240	1.0	121.72	1.000	0.010
1.31	0	0	1.50	1.0	0	1.0	240	1.0	122.58	1.000	0.015
1.75	0	0	2.00	1.0	0	1.0	240	1.0	123.44	1.000	0.020
2.19	0	0	2.50	1.0	0	1.0	240	1.0	124.3	0.999	0.025
2.63	0	0	3.00	1.0	0	1.0	240	1.0	125.16	0.999	0.030
3.08	0	0	3.50	1.0	0	1.0	240	1.0	126.02	0.999	0.035
3.52	0	0	4.00	1.0	0	1.0	240	1.0	126.87	0.998	0.040
3.97	0	0	4.50	1.0	0	1.0	240	1.0	127.73	0.998	0.045
4.43	0	0	5.00	1.0	0	1.0	240	1.0	128.59	0.998	0.050
4.88	0	0	5.50	1.0	0	1.0	240	1.0	129.45	0.997	0.055
5.33	0	0	6.00	1.0	0	1.0	240	1.0	130.3	0.996	0.060
5.78	0	0	6.50	1.0	0	1.0	240	1.0	131.15	0.996	0.065
6.24	0	0	7.00	1.0	0	1.0	240	1.0	132	0.995	0.070
6.70	0	0	7.50	1.0	0	1.0	240	1.0	132.85	0.994	0.075
7.16	0	0	8.00	1.0	0	1.0	240	1.0	133.7	0.994	0.080

Table-4.15 (b): Comparison of four different definitions of voltage unbalance for 1-Φ angle unbalance in phase *A* (moving CW) for increasing VUF.

LVUR (%)	PVUR 1 (%)	PVUR (%)	VUF (%)	Unbalanced voltage source						+ve seq. Volt. (V_1)	-ve seq. Volt. (V_2)
				Phase *A*		Phase *B*		Phase *C*			
				Mag.	Angle	Mag.	Angle	Mag.	Angle		
0.00	0	0	0.00	1.0	0	1.0	240	1.0	120	1.000	0.00
0.43	0	0	0.50	1.0	-0.86	1.0	240	1.0	120	1.000	0.005
0.87	0	0	1.00	1.0	-1.72	1.0	240	1.0	120	1.000	0.010
1.31	0	0	1.50	1.0	-2.58	1.0	240	1.0	120	1.000	0.015
1.75	0	0	2.00	1.0	-3.44	1.0	240	1.0	120	1.000	0.020
2.19	0	0	2.50	1.0	-4.3	1.0	240	1.0	120	0.999	0.025
2.63	0	0	3.00	1.0	-5.16	1.0	240	1.0	120	0.999	0.030
3.08	0	0	3.50	1.0	-6.02	1.0	240	1.0	120	0.999	0.035
3.52	0	0	4.00	1.0	-6.87	1.0	240	1.0	120	0.998	0.040
3.97	0	0	4.50	1.0	-7.73	1.0	240	1.0	120	0.998	0.045
4.43	0	0	5.00	1.0	-8.59	1.0	240	1.0	120	0.998	0.050
4.88	0	0	5.50	1.0	-9.45	1.0	240	1.0	120	0.997	0.055
5.33	0	0	6.00	1.0	-10.3	1.0	240	1.0	120	0.996	0.060
5.78	0	0	6.50	1.0	-11.15	1.0	240	1.0	120	0.996	0.065
6.24	0	0	7.00	1.0	-12	1.0	240	1.0	120	0.995	0.070
6.70	0	0	7.50	1.0	-12.85	1.0	240	1.0	120	0.994	0.075
7.16	0	0	8.00	1.0	-13.7	1.0	240	1.0	120	0.994	0.080

Table-4.16: Comparison of four definitions of voltage unbalance and rectifier performance for 2-Φ equal angle unbalance for increasing angle between phase *A* and *C* - two phasors moving in opposite direction for increasing VUF

LVUR (%)	PVUR 1 (%) and PVUR (%)	VUF (%)	Unbalanced voltage source: Phase *A* Mag.	Phase *A* Angle	Phase *B* Mag.	Phase *B* Angle	Phase *C* Mag.	Phase *C* Angle	+ve seq. Volt. (V_1)	-ve seq. Volt. (V_2)	AC parameters: I_A RMS	I_A THD_I (%)	I_B Mag.	I_B THD_I (%)	I_C Mag.	I_C THD_I (%)	Average THDI	PTHDUF (%)	DC parameters: I_{DC} Mag.	I_{DC} THD_I (%)	V_{DC} Mag.	V_{DC} THD_I (%)	P_{DC} Mag.	P_{DC} THD_I (%)
0.00	0	0.00	1.0	0	1.0	240	1.0	120	1.0000	0.00	1.000	27.87	1.000	27.87	1.000	27.87	27.87	0.00	1.000	5.95	1.000	6.72	1.000	12.13
0.86	0	0.86	1.0	-0.86	1.0	240	1.0	120.86	0.9999	0.0086	1.005	27.63	0.991	28.32	1.004	27.67	27.87	1.60	1.000	6.01	1.000	6.78	1.000	12.26
1.71	0	1.72	1.0	-1.72	1.0	240	1.0	121.72	0.9997	0.0172	1.009	27.38	0.982	28.78	1.008	27.47	27.88	3.24	1.000	6.19	1.000	6.95	1.000	12.62
2.55	0	2.57	1.0	-2.58	1.0	240	1.0	122.58	0.9993	0.0257	1.014	27.15	0.973	29.25	1.012	27.28	27.89	4.86	0.999	6.48	1.000	7.21	0.999	13.20
3.38	0	3.41	1.0	-3.44	1.0	240	1.0	123.44	0.9988	0.0340	1.018	26.91	0.964	29.72	1.015	27.08	27.90	6.51	0.999	6.86	0.999	7.56	0.999	13.97
4.20	0	4.24	1.0	-4.3	1.0	240	1.0	124.3	0.9981	0.0423	1.022	26.68	0.954	30.20	1.019	26.90	27.93	8.14	0.999	7.32	0.999	7.99	0.998	14.89
5.00	0	5.07	1.0	-5.16	1.0	240	1.0	125.16	0.9973	0.0506	1.026	26.46	0.945	30.68	1.023	26.71	27.95	9.77	0.998	7.84	0.998	8.48	0.997	15.94
5.80	0	5.89	1.0	-6.02	1.0	240	1.0	126.02	0.9963	0.0587	1.030	26.24	0.935	31.17	1.026	26.52	27.98	11.41	0.997	8.41	0.997	9.02	0.996	17.09
6.58	0	6.70	1.0	-6.87	1.0	240	1.0	126.87	0.9952	0.0667	1.034	26.03	0.925	31.66	1.030	26.34	28.01	13.03	0.996	9.02	0.996	9.60	0.995	18.31
7.35	0	7.51	1.0	-7.73	1.0	240	1.0	127.73	0.9939	0.0746	1.038	25.81	0.915	32.16	1.033	26.16	28.04	14.68	0.995	9.65	0.995	10.21	0.994	19.60
8.12	0	8.31	1.0	-8.59	1.0	240	1.0	128.59	0.9925	0.0825	1.042	25.60	0.905	32.66	1.036	25.98	28.08	16.31	0.994	10.32	0.994	10.86	0.992	20.93
8.87	0	9.11	1.0	-9.45	1.0	240	1.0	129.45	0.9910	0.0903	1.045	25.40	0.895	33.17	1.039	25.80	28.12	17.94	0.993	11.00	0.993	11.52	0.990	22.30
9.61	0	9.90	1.0	-10.3	1.0	240	1.0	130.3	0.9893	0.0978	1.049	25.20	0.884	33.68	1.042	25.62	28.17	19.57	0.992	11.68	0.992	12.19	0.989	23.69
10.34	0	10.67	1.0	-11.15	1.0	240	1.0	131.15	0.9874	0.1054	1.052	25.00	0.874	34.20	1.045	25.44	28.21	21.22	0.990	12.38	0.990	12.87	0.987	25.09
11.06	0	11.44	1.0	-12	1.0	240	1.0	132	0.9854	0.1127	1.055	24.80	0.863	34.73	1.048	25.27	28.27	22.87	0.989	13.08	0.989	13.56	0.984	26.50
11.77	0	12.21	1.0	-12.85	1.0	240	1.0	132.85	0.9833	0.1201	1.058	24.60	0.853	35.26	1.050	25.09	28.32	24.52	0.987	13.79	0.987	14.26	0.982	27.92
12.47	0	12.97	1.0	-13.7	1.0	240	1.0	133.7	0.9810	0.1273	1.061	24.41	0.842	35.80	1.053	24.91	28.37	26.17	0.985	14.50	0.985	14.97	0.980	29.35

Table-4.17 (a): Comparison of four different definitions of voltage unbalance for 1-Φ angle unbalance in phase *C* (moving ACW) for increasing VUF

LVUR (%)	PVUR 1 (%)	PVUR (%)	VUF (%)	Unbalanced voltage source						+ve seq. Volt. (V_1)	-ve seq. Volt. (V_2)
				Phase *A*		Phase *B*		Phase *C*			
				Mag.	Angle	Mag.	Angle	Mag.	Angle		
0.00	0	0	0.00	1.0	0	1.0	240	1.0	120	325.00	0.00
0.43	0	0	0.50	1.0	0	1.0	240	1.0	120.86	324.99	1.63
0.87	0	0	1.00	1.0	0	1.0	240	1.0	121.72	324.97	3.25
1.31	0	0	1.50	1.0	0	1.0	240	1.0	122.58	324.93	4.88
1.75	0	0	2.00	1.0	0	1.0	240	1.0	123.44	324.87	6.50
2.19	0	0	2.50	1.0	0	1.0	240	1.0	124.3	324.80	8.13
2.63	0	0	3.00	1.0	0	1.0	240	1.0	125.16	324.71	9.75
3.08	0	0	3.50	1.0	0	1.0	240	1.0	126.02	324.60	11.38
3.52	0	0	4.00	1.0	0	1.0	240	1.0	126.87	324.48	12.98
3.97	0	0	4.50	1.0	0	1.0	240	1.0	127.73	324.34	14.60
4.43	0	0	5.00	1.0	0	1.0	240	1.0	128.59	324.19	16.23
4.88	0	0	5.50	1.0	0	1.0	240	1.0	129.45	324.02	17.85
5.33	0	0	6.00	1.0	0	1.0	240	1.0	130.3	323.83	19.45
5.78	0	0	6.50	1.0	0	1.0	240	1.0	131.15	323.63	21.05
6.24	0	0	7.00	1.0	0	1.0	240	1.0	132	323.42	22.65
6.70	0	0	7.50	1.0	0	1.0	240	1.0	132.85	323.19	24.25
7.16	0	0	8.00	1.0	0	1.0	240	1.0	133.7	322.94	25.84

Table-4.17 (b): Comparison of four different definitions of voltage unbalance for 1-Φ angle unbalance in phase *B* (moving CW) for increasing VUF

LVUR (%)	PVUR 1 (%)	PVUR (%)	VUF (%)	Unbalanced voltage source						+ve seq. Volt. (V_1)	-ve seq. Volt. (V_2)
				Phase *A*		Phase *B*		Phase *C*			
				Mag.	Angle	Mag.	Angle	Mag.	Angle		
0.00	0	0	0.00	1.0	0	1.0	240	1.0	120	325.00	0.00
0.43	0	0	0.50	1.0	0	1.0	239.14	1.0	120	324.99	1.63
0.87	0	0	1.00	1.0	0	1.0	238.28	1.0	120	324.97	3.25
1.31	0	0	1.50	1.0	0	1.0	237.42	1.0	120	324.93	4.88
1.75	0	0	2.00	1.0	0	1.0	236.56	1.0	120	324.87	6.50
2.19	0	0	2.50	1.0	0	1.0	235.7	1.0	120	324.80	8.13
2.63	0	0	3.00	1.0	0	1.0	234.84	1.0	120	324.71	9.75
3.08	0	0	3.50	1.0	0	1.0	233.98	1.0	120	324.60	11.38
3.52	0	0	4.00	1.0	0	1.0	233.13	1.0	120	324.48	12.98
3.97	0	0	4.50	1.0	0	1.0	232.27	1.0	120	324.34	14.60
4.43	0	0	5.00	1.0	0	1.0	231.41	1.0	120	324.19	16.23
4.88	0	0	5.50	1.0	0	1.0	230.55	1.0	120	324.02	17.85
5.33	0	0	6.00	1.0	0	1.0	229.7	1.0	120	323.83	19.45
5.78	0	0	6.50	1.0	0	1.0	228.85	1.0	120	323.63	21.05
6.24	0	0	7.00	1.0	0	1.0	228	1.0	120	323.42	22.65
6.70	0	0	7.50	1.0	0	1.0	227.15	1.0	120	323.19	24.25
7.16	0	0	8.00	1.0	0	1.0	226.3	1.0	120	322.94	25.84

Table-4.18: Comparison of four definitions of voltage unbalance and rectifier performance for 2-Φ equal angle unbalance for decreasing angle between phase *B* and *C* - two phasors moving in opposite direction for increasing VUF

LVUR (%)	PVUR 1 (%) and PVUR (%)	VUF (%)	Unbalanced voltage source						+ve seq. Volt. (V_1)	-ve seq. Volt. (V_2)	AC parameters						Average THD_I	PTHDUF (%)	DC parameters					
			Phase *A*		Phase *B*		Phase *C*				I_A		I_B		I_C				I_{DC}		V_{DC}		P_{DC}	
			Mag.	Angle	Mag.	Angle	Mag.	Angle			RMS	THD_I (%)	Mag.	THD_I (%)	Mag.	THD_I (%)			Mag.	THD_I (%)	Mag.	THD_I (%)	Mag.	THD_I (%)
0.00	0	0.00	1.0	0	1.0	240	1.0	120	1.0000	0.000	1.000	27.87	1.000	27.87	1.000	27.87	27.87	0.00	1.000	5.95	1.000	6.72	1.000	12.13
0.87	0	0.87	1.0	0	1.0	239.14	1.0	120.86	0.9999	0.0087	1.009	27.42	0.996	28.07	0.995	28.12	27.87	1.61	1.000	6.01	1.000	6.78	1.000	12.26
1.76	0	1.75	1.0	0	1.0	238.28	1.0	121.72	0.9997	0.0175	1.017	26.98	0.992	28.28	0.990	28.38	27.88	3.23	1.000	6.19	1.000	6.95	1.000	12.62
2.65	0	2.63	1.0	0	1.0	237.42	1.0	122.58	0.9993	0.0263	1.025	26.54	0.988	28.49	0.986	28.65	27.89	4.85	0.999	6.50	1.000	7.22	0.999	13.22
3.56	0	3.53	1.0	0	1.0	236.56	1.0	123.44	0.9988	0.0352	1.033	26.10	0.983	28.70	0.980	28.92	27.91	6.47	0.999	6.90	0.999	7.60	0.999	14.01
4.48	0	4.43	1.0	0	1.0	235.7	1.0	124.3	0.9981	0.0442	1.041	25.67	0.979	28.92	0.975	29.20	27.93	8.09	0.999	7.39	0.999	8.05	0.998	14.96
5.41	0	5.34	1.0	0	1.0	234.84	1.0	125.16	0.9973	0.0533	1.049	25.25	0.975	29.15	0.970	29.48	27.96	9.69	0.998	7.95	0.998	8.58	0.997	16.05
6.35	0	6.26	1.0	0	1.0	233.98	1.0	126.02	0.9963	0.0624	1.056	24.83	0.971	29.37	0.965	29.78	27.99	11.30	0.997	8.57	0.997	9.17	0.996	17.26
7.30	0	7.18	1.0	0	1.0	233.13	1.0	126.87	0.9952	0.0714	1.064	24.42	0.966	29.60	0.960	30.08	28.03	12.89	0.997	9.22	0.996	9.80	0.995	18.53
8.26	0	8.12	1.0	0	1.0	232.27	1.0	127.73	0.9939	0.0807	1.071	24.01	0.962	29.84	0.954	30.39	28.08	14.49	0.996	9.93	0.996	10.48	0.994	19.90
9.24	0	9.06	1.0	0	1.0	231.41	1.0	128.59	0.9925	0.0900	1.077	23.61	0.957	30.09	0.949	30.71	28.14	16.09	0.994	10.67	0.994	11.20	0.993	21.31
10.24	0	10.02	1.0	0	1.0	230.55	1.0	129.45	0.9910	0.0993	1.084	23.21	0.953	30.34	0.943	31.04	28.2	17.69	0.993	11.44	0.993	11.95	0.991	22.78
11.23	0	10.98	1.0	0	1.0	229.7	1.0	130.3	0.9893	0.1086	1.091	22.81	0.948	30.59	0.938	31.38	28.26	19.29	0.992	12.22	0.992	12.71	0.990	24.26
12.24	0	11.94	1.0	0	1.0	228.85	1.0	131.15	0.9874	0.1179	1.097	22.42	0.944	30.85	0.932	31.72	28.33	20.86	0.991	13.01	0.991	13.50	0.988	25.76
13.26	0	12.92	1.0	0	1.0	228	1.0	132	0.9854	0.1273	1.103	22.04	0.939	31.11	0.927	32.07	28.41	22.41	0.989	13.83	0.989	14.31	0.986	27.29
14.29	0	13.91	1.0	0	1.0	227.15	1.0	132.85	0.9833	0.1367	1.108	21.66	0.935	31.38	0.921	32.44	28.49	23.98	0.988	14.66	0.988	15.13	0.984	28.84
15.34	0	14.90	1.0	0	1.0	226.3	1.0	133.7	0.9810	0.1462	1.114	21.28	0.930	31.66	0.915	32.81	28.58	25.55	0.986	15.50	0.986	15.97	0.982	30.40

Table-4.19 (a): Comparison of four different definitions of voltage unbalance for 1-Φ angle unbalance in phase *A* (moving ACW) for increasing VUF

LVUR (%)	PVUR 1 (%)	PVUR (%)	VUF (%)	Unbalanced voltage source						+ve seq. Volt. (V_1)	-ve seq. Volt. (V_2)
				Phase *A*		Phase *B*		Phase *C*			
				Mag.	Angle	Mag.	Angle	Mag.	Angle		
0.00	0	0	0.0	1.0	0	1.0	240	1.0	120	1.000	0.00
0.43	0	0	0.5	1.0	0.86	1.0	240	1.0	120	1.000	0.005
0.87	0	0	1.0	1.0	1.72	1.0	240	1.0	120	1.000	0.010
1.31	0	0	1.5	1.0	2.58	1.0	240	1.0	120	1.000	0.015
1.75	0	0	2.0	1.0	3.44	1.0	240	1.0	120	1.000	0.020
2.19	0	0	2.5	1.0	4.3	1.0	240	1.0	120	0.999	0.025
2.63	0	0	3.0	1.0	5.16	1.0	240	1.0	120	0.999	0.030
3.08	0	0	3.5	1.0	6.02	1.0	240	1.0	120	0.999	0.035
3.52	0	0	4.0	1.0	6.87	1.0	240	1.0	120	0.998	0.040
3.97	0	0	4.5	1.0	7.73	1.0	240	1.0	120	0.998	0.045
4.43	0	0	5.0	1.0	8.59	1.0	240	1.0	120	0.998	0.050
4.88	0	0	5.5	1.0	9.45	1.0	240	1.0	120	0.997	0.055
5.33	0	0	6.0	1.0	10.3	1.0	240	1.0	120	0.996	0.060
5.78	0	0	6.5	1.0	11.15	1.0	240	1.0	120	0.996	0.065
6.24	0	0	7.0	1.0	12	1.0	240	1.0	120	0.995	0.070
6.70	0	0	7.5	1.0	12.85	1.0	240	1.0	120	0.994	0.075
7.16	0	0	8.0	1.0	13.7	1.0	240	1.0	120	0.994	0.080

Table-4.19 (b): Comparison of four different definitions of voltage unbalance for 1-Φ angle unbalance in phase *C* (moving CW) for increasing VUF.

LVUR (%)	PVUR 1 (%)	PVUR (%)	VUF (%)	Unbalanced voltage source						+ve seq. Volt. (V_1)	-ve seq. Volt. (V_2)
				Phase *A*		Phase *B*		Phase *C*			
				Mag.	Angle	Mag.	Angle	Mag.	Angle		
0.00	0	0	0.0	1.0	0	1.0	240	1.0	120	1.000	0.00
0.43	0	0	0 .5	1.0	0	1.0	240	1.0	119.14	1.000	0.005
0.87	0	0	1.0	1.0	0	1.0	240	1.0	118.28	1.000	0.010
1.31	0	0	1.5	1.0	0	1.0	240	1.0	117.42	1.000	0.015
1.75	0	0	2.0	1.0	0	1.0	240	1.0	116.56	1.000	0.020
2.19	0	0	2.5	1.0	0	1.0	240	1.0	115.7	0.999	0.025
2.63	0	0	3.0	1.0	0	1.0	240	1.0	114.84	0.999	0.030
3.08	0	0	3.5	1.0	0	1.0	240	1.0	113.98	0.999	0.035
3.52	0	0	4.0	1.0	0	1.0	240	1.0	113.13	0.998	0.040
3.97	0	0	4.5	1.0	0	1.0	240	1.0	112.27	0.998	0.045
4.43	0	0	5.0	1.0	0	1.0	240	1.0	111.41	0.998	0.050
4.88	0	0	5.5	1.0	0	1.0	240	1.0	110.55	0.997	0.055
5.33	0	0	6.0	1.0	0	1.0	240	1.0	109.7	0.996	0.060
5.78	0	0	6.5	1.0	0	1.0	240	1.0	108.85	0.996	0.065
6.24	0	0	7.0	1.0	0	1.0	240	1.0	108	0.995	0.070
6.70	0	0	7.5	1.0	0	1.0	240	1.0	107.15	0.994	0.075
7.16	0	0	8.0	1.0	0	1.0	240	1.0	106.3	0.994	0.080

Table-4.20: Comparison of four definitions of voltage unbalance and rectifier performance for 2-Φ equal angle unbalance for decreasing angle between phase *A* and *C* - two phasors moving in opposite direction for increasing VUF

LVUR (%)	PVUR 1 (%) and PVUR (%)	VUF (%)	Unbalanced voltage source: Phase *A* Mag.	Phase *A* Angle	Phase *B* Mag.	Phase *B* Angle	Phase *C* Mag.	Phase *C* Angle	+ve seq. Volt. (V_1)	-ve seq. Volt. (V_2)	AC parameters: I_A RMS	I_A THD_I (%)	I_B Mag.	I_B THD_I (%)	I_C Mag.	I_C THD_I (%)	Average THD_I	PTHDUF (%)	DC parameters: I_{DC} Mag.	I_{DC} THD_I (%)	V_{DC} Mag.	V_{DC} THD_I (%)	P_{DC} Mag.	P_{DC} THD_I (%)
0.00	0	0.00	1.0	0	1.0	240	1.0	120	1.0000	0.000	1.000	27.87	1.000	27.87	1.000	27.87	27.87	0.00	1.000	5.95	1.000	6.72	1.000	12.13
0.87	0	0.87	1.0	0.86	1.0	240	1.0	119.14	0.9999	0.0087	0.995	28.13	1.009	27.42	0.996	28.07	27.87	1.63	1.000	6.01	1.000	6.78	1.000	12.26
1.76	0	1.75	1.0	1.72	1.0	240	1.0	118.28	0.9997	0.0175	0.990	28.39	1.017	26.97	0.992	28.28	27.88	3.26	1.000	6.20	1.000	6.95	1.000	12.62
2.65	0	2.63	1.0	2.58	1.0	240	1.0	117.42	0.9993	0.0263	0.986	28.65	1.025	26.53	0.988	28.49	27.89	4.88	1.000	6.50	1.000	7.23	0.999	13.22
3.56	0	3.53	1.0	3.44	1.0	240	1.0	116.56	0.9988	0.0352	0.981	28.92	1.033	26.10	0.984	28.70	27.91	6.47	0.999	6.90	0.999	7.60	0.999	14.01
4.48	0	4.43	1.0	4.3	1.0	240	1.0	115.7	0.9981	0.0442	0.975	29.20	1.041	25.67	0.979	28.92	27.93	8.09	0.999	7.39	0.999	8.05	0.998	14.96
5.41	0	5.34	1.0	5.16	1.0	240	1.0	114.84	0.9973	0.0533	0.970	29.49	1.049	25.25	0.975	29.14	27.96	9.69	0.998	7.95	0.998	8.58	0.997	16.06
6.35	0	6.26	1.0	6.02	1.0	240	1.0	113.98	0.9963	0.0624	0.965	29.79	1.056	24.83	0.971	29.37	28.00	11.31	0.997	8.57	0.997	9.17	0.996	17.26
7.30	0	7.18	1.0	6.87	1.0	240	1.0	113.13	0.9952	0.0714	0.960	30.09	1.063	24.42	0.966	29.60	28.04	12.90	0.997	9.22	0.997	9.80	0.995	18.54
8.26	0	8.12	1.0	7.73	1.0	240	1.0	112.27	0.9939	0.0807	0.954	30.40	1.071	24.01	0.962	29.84	28.08	14.50	0.996	9.93	0.996	10.48	0.994	19.90
9.24	0	9.06	1.0	8.59	1.0	240	1.0	111.41	0.9925	0.0900	0.949	30.72	1.077	23.60	0.957	30.09	28.14	16.12	0.994	10.67	0.995	11.20	0.993	21.31
10.24	0	10.02	1.0	9.45	1.0	240	1.0	110.55	0.9910	0.0993	0.943	31.05	1.084	23.20	0.953	30.34	28.20	17.72	0.993	11.44	0.993	11.95	0.991	22.78
11.23	0	10.98	1.0	10.3	1.0	240	1.0	109.7	0.9893	0.1086	0.938	31.38	1.090	22.81	0.948	30.59	28.26	19.29	0.992	12.22	0.992	12.71	0.990	24.26
12.24	0	11.94	1.0	11.15	1.0	240	1.0	108.85	0.9874	0.1179	0.932	31.73	1.097	22.42	0.944	30.85	28.33	20.87	0.991	13.01	0.991	13.50	0.988	25.76
13.26	0	12.92	1.0	12	1.0	240	1.0	108	0.9854	0.1273	0.927	32.08	1.102	22.04	0.939	31.11	28.41	22.42	0.989	13.83	0.989	14.31	0.986	27.29
14.29	0	13.91	1.0	12.85	1.0	240	1.0	107.15	0.9833	0.1367	0.921	32.44	1.108	21.66	0.935	31.38	28.49	23.98	0.988	14.66	0.988	15.31	0.984	28.84
15.34	0	14.90	1.0	13.7	1.0	240	1.0	106.3	0.9810	0.1462	0.915	32.82	1.114	21.28	0.930	31.66	28.59	25.56	0.986	15.50	0.986	15.97	0.982	30.39

Table-4.21 (a): Characteristic harmonic current components with increasing VUF for 2-Φ equal angle unbalance for increasing angle between phase *B* and *C* - two phasors moving in opposite direction for increasing VUF

		VUF = 0.0 %	VUF = 1.0 %	VUF = 2.0 %	VUF = 3.0 %	VUF = 4.0 %	VUF = 5.0 %	VUF = 6.0 %	VUF = 7.0 %	VUF = 8.0 %	VUF = 9.0 %	VUF = 10.0 %	VUF = 11.0 %	VUF = 12.0 %	VUF = 13.0 %	VUF = 14.0 %	VUF = 15.0 %	VUF = 16.0 %
Phase *A*	THD_I	27.87	28.33	28.79	29.25	29.72	30.20	30.69	31.18	31.66	32.16	32.67	33.18	33.69	34.21	34.74	35.27	35.81
	h 5	22.37	22.94	23.49	24.03	24.55	25.06	25.54	26.00	26.44	26.86	27.26	27.64	27.98	28.30	28.60	28.86	29.10
	h 7	10.86	10.54	10.19	9.79	9.36	8.88	8.37	7.81	7.22	6.59	5.92	5.21	4.47	3.71	2.91	2.08	1.22
	h 11	8.35	8.75	9.11	9.42	9.67	9.86	10.00	10.07	10.08	10.02	9.90	9.71	9.45	9.13	8.75	8.30	7.79
	h 13	5.74	5.40	5.00	4.53	4.01	3.43	2.80	2.13	1.42	0.68	0.12	0.89	1.69	2.49	3.29	4.08	4.86
	h 17	4.62	4.95	5.20	5.37	5.46	5.47	5.39	5.22	4.97	4.63	4.21	3.71	3.16	2.54	1.88	1.17	0.43
	h 19	3.56	3.23	2.83	2.36	1.83	1.25	0.63	0.08	0.69	1.36	2.02	2.65	3.24	3.78	4.26	4.66	4.99
	h 23	2.83	3.08	3.25	3.32	3.30	3.18	2.96	2.65	2.26	1.80	1.28	0.70	0.11	0.50	1.10	1.67	2.21
	h 25	2.3	2.01	1.65	1.22	0.74	0.23	0.33	0.87	1.38	1.86	2.29	2.64	2.91	3.08	3.15	3.12	2.98
	h 29	1.77	1.96	2.06	2.06	1.97	1.78	1.50	1.15	0.75	0.30	0.17	0.63	1.07	1.46	1.79	2.04	2.20
	h 31	1.48	1.25	0.94	0.58	0.19	0.25	0.65	1.03	1.36	1.62	1.81	1.89	1.88	1.77	1.56	1.27	0.91
Phase *B*	THD_I	27.87	27.67	27.47	27.28	27.08	26.89	26.71	26.52	26.34	26.16	25.97	25.79	25.62	25.44	25.26	25.09	24.91
	h 5	22.36	22.10	21.83	21.55	21.26	20.95	20.64	20.31	19.98	19.63	19.27	18.91	18.54	18.17	17.79	17.40	17.01
	h 7	10.87	10.99	11.11	11.23	11.35	11.47	11.59	11.70	11.81	11.93	12.03	12.14	12.23	12.32	12.41	12.49	12.56
	h 11	8.34	8.14	7.93	7.70	7.45	7.19	6.92	6.64	6.35	6.04	5.73	5.42	5.10	4.79	4.47	4.15	3.83
	h 13	5.75	5.88	6.01	6.13	6.25	6.35	6.45	6.54	6.61	6.68	6.72	6.76	6.78	6.78	6.77	6.74	6.69
	h 17	4.62	4.44	4.25	4.05	3.83	3.59	3.35	3.09	2.84	2.57	2.31	2.04	1.78	1.52	1.27	1.03	0.80
	h 19	3.56	3.69	3.80	3.90	3.99	4.06	4.12	4.16	4.17	4.17	4.15	4.11	4.04	3.96	3.86	3.74	3.60
	h 23	2.82	2.68	2.51	2.34	2.15	1.95	1.75	1.54	1.33	1.11	0.90	0.69	0.48	0.28	0.10	0.16	0.34
	h 25	2.30	2.41	2.50	2.58	2.63	2.67	2.68	2.68	2.65	2.60	2.53	2.44	2.33	2.21	2.07	1.93	1.77
	h 29	1.76	1.65	1.52	1.38	1.23	1.07	0.91	0.75	0.59	0.42	0.26	0.10	0.09	0.25	0.41	0.58	0.74
	h 31	1.49	1.57	1.64	1.69	1.72	1.73	1.71	1.68	1.63	1.56	1.47	1.38	1.27	1.16	1.04	0.91	0.78
Phase *C*	THD_I	27.87	27.62	27.38	27.14	26.91	26.68	26.46	26.24	26.02	25.81	25.60	25.39	25.19	24.99	24.79	24.60	24.40
	h 5	22.36	22.03	21.69	21.33	20.96	20.59	20.20	29.80	19.40	18.99	18.56	18.13	17.70	17.27	16.82	16.38	15.93
	h 7	10.87	11.03	11.19	11.34	11.49	11.63	11.75	11.87	11.99	12.09	12.19	12.27	12.35	12.42	12.47	12.52	12.56
	h 11	8.34	8.09	7.83	7.54	7.23	6.91	6.57	6.22	5.86	5.49	5.10	4.71	4.32	3.93	3.53	3.14	2.75
	h 13	5.75	5.91	6.06	6.19	6.31	6.41	6.49	6.55	6.59	6.62	6.63	6.62	6.59	6.54	6.47	6.38	6.28
	h 17	4.62	4.41	4.17	3.92	3.64	3.34	3.02	2.69	2.36	2.01	1.65	1.30	0.95	0.60	0.29	0.21	0.48
	h 19	3.56	3.71	3.83	3.92	4.00	4.04	4.07	4.07	4.04	3.99	3.91	3.81	3.69	3.54	3.37	3.18	2.98
	h 23	2.82	2.65	2.45	2.22	1.98	1.71	1.43	1.13	0.83	0.53	0.22	0.09	0.38	0.67	0.94	1.19	1.43
	h 25	2.3	2.42	2.51	2.57	2.60	2.61	2.58	2.53	2.45	2.35	2.22	2.07	1.90	1.70	1.49	1.26	1.02
	h 29	1.76	1.63	1.46	1.27	1.06	0.84	0.60	0.35	0.10	0.15	0.40	0.64	0.86	1.06	1.24	1.39	1.53
	h 31	1.49	1.58	1.63	1.66	1.67	1.64	1.59	1.51	1.41	1.28	1.14	0.97	0.79	0.60	0.39	0.18	0.05

Table-4.21 (b): non-characteristic harmonic current components with increasing VUF for 2-Φ equal angle unbalance for increasing angle between phase *B* and *C* - two phasors moving in opposite direction for increasing VUF

		VUF = 0.0 %	VUF = 1.0 %	VUF = 2.0 %	VUF = 3.0 %	VUF = 4.0 %	VUF = 5.0 %	VUF = 6.0 %	VUF = 7.0 %	VUF = 8.0 %	VUF = 9.0 %	VUF = 10.0 %	VUF = 11.0 %	VUF = 12.0 %	VUF = 13.0 %	VUF = 14.0 %	VUF = 15.0 %	VUF = 16.0 %
Phase *A*	THD_I	27.87	28.33	28.79	29.25	29.72	30.20	30.69	31.18	31.66	32.16	32.67	33.18	33.69	34.21	34.74	35.27	35.81
	h 3	0.01	0.61	1.23	1.86	2.51	3.17	3.84	4.53	5.22	5.94	6.66	7.40	8.15	8.90	9.67	10.45	11.24
	h 9	0.01	0.75	1.49	2.25	3.01	3.77	4.53	5.28	6.02	6.75	7.46	8.15	8.81	9.44	10.04	10.61	11.13
	h 15	0.01	0.68	1.36	2.03	2.69	3.33	3.93	4.50	5.01	5.47	5.87	6.20	6.45	6.62	6.71	6.72	6.63
	h 21	0.01	0.59	1.16	1.72	2.24	2.72	3.13	3.47	3.72	3.89	3.96	3.93	3.80	3.58	3.25	2.84	2.35
	h 27	0.01	0.48	0.94	1.37	1.74	2.05	2.28	2.42	2.45	2.39	2.22	1.96	1.62	1.20	0.72	0.21	0.34
	h 33	0.01	0.37	0.71	1.02	1.26	1.43	1.52	1.51	1.40	1.21	0.94	0.61	0.24	0.16	0.55	0.91	1.23
Phase *B*	THD_I	27.87	27.67	27.47	27.28	27.08	26.89	26.71	26.52	26.34	26.16	25.97	25.79	25.62	25.44	25.26	25.09	24.91
	h 3	0.01	0.56	1.11	1.64	2.15	2.65	3.14	3.62	4.07	4.51	4.94	5.36	5.75	6.14	6.50	6.86	7.20
	h 9	0.01	0.34	0.66	0.96	1.26	1.55	1.82	2.08	2.33	2.56	2.79	3.01	3.21	3.40	3.59	3.76	3.93
	h 15	0.0	0.28	0.55	0.81	1.06	1.30	1.53	1.75	1.96	2.16	2.36	2.56	2.74	2.92	3.10	3.27	3.44
	h 21	0.0	0.23	0.46	0.68	0.89	1.09	1.29	1.49	1.67	1.85	2.03	2.20	2.36	2.52	2.66	2.79	3.90
	h 27	0.0	0.19	0.37	0.54	0.72	0.89	1.05	1.22	1.37	1.52	1.66	1.78	1.89	1.98	2.05	2.11	2.14
	h 33	0.0	0.14	0.27	0.41	0.55	0.68	0.81	0.94	1.05	1.15	1.24	1.31	1.36	1.39	1.40	1.40	1.37
Phase *C*	THD_I	27.87	27.62	27.38	27.14	26.91	26.68	26.46	26.24	26.02	25.81	25.60	25.39	25.19	24.99	24.79	24.60	24.40
	h 3	0.01	0.61	1.20	1.78	2.33	2.87	3.40	3.90	4.39	4.86	5.32	5.76	6.18	6.58	6.97	7.34	7.69
	h 9	0.01	0.44	0.87	1.28	1.67	2.05	2.42	2.76	3.09	3.41	3.71	3.99	4.25	4.50	4.74	4.96	5.16
	h 15	0.01	0.40	0.78	1.15	1.50	1.83	2.15	2.45	2.72	2.98	3.23	3.45	3.65	3.84	4.01	4.16	4.29
	h 21	0.0	0.35	0.68	0.99	1.30	1.58	1.84	2.08	2.30	2.49	2.66	2.81	2.93	3.03	3.11	3.17	3.20
	h 27	0.0	0.29	0.56	0.83	1.07	1.29	1.49	1.67	1.82	1.94	2.03	2.09	2.13	2.14	2.13	2.09	2.03
	h 33	0.0	0.23	0.45	0.65	0.84	1.00	1.14	1.25	1.33	1.38	1.40	1.40	1.37	1.31	1.24	1.14	1.03

Table-4.22 (a): Characteristic harmonic current components with increasing VUF for 2-Φ equal angle unbalance for decreasing angle between phase *B* and *C* - two phasors moving in opposite direction for increasing VUF

		VUF = 0.0 %	VUF = 1.0 %	VUF = 2.0 %	VUF = 3.0 %	VUF = 4.0 %	VUF = 5.0 %	VUF = 6.0 %	VUF = 7.0 %	VUF = 8.0 %	VUF = 9.0 %	VUF = 10.0 %	VUF = 11.0 %	VUF = 12.0 %	VUF = 13.0 %	VUF = 14.0 %	VUF = 15.0 %	VUF = 16.0 %
Phase *A*	THD_I	27.87	27.42	26.98	26.54	26.10	25.67	25.25	24.83	24.42	24.01	23.61	23.21	22.81	22.42	22.04	21.66	21.28
	h 5	22.37	21.79	21.20	20.59	19.98	19.35	18.72	18.09	17.45	16.81	16.16	15.51	14.87	14.22	13.58	12.94	12.31
	h 7	10.86	11.13	11.36	11.55	11.70	11.81	11.89	11.92	11.92	11.89	11.82	11.71	11.58	11.41	11.21	10.99	10.74
	h 11	8.35	7.90	7.41	6.89	6.34	5.76	5.16	4.54	3.92	3.28	2.64	2.01	1.38	0.78	0.23	0.45	1.00
	h 13	5.74	6.02	6.23	6.37	6.45	6.46	6.41	6.29	6.12	5.89	5.61	5.28	4.91	4.51	4.07	3.60	3.11
	h 17	4.62	4.23	3.79	3.30	2.76	2.20	1.61	1.02	0.44	0.20	0.74	1.28	1.77	2.23	2.64	3.00	3.29
	h 19	3.56	3.80	3.86	4.04	4.03	3.93	3.76	3.52	3.21	2.84	2.41	1.95	1.47	0.96	0.45	0.06	0.56
	h 23	2.83	2.50	2.10	1.65	1.17	0.66	0.16	0.39	0.87	1.33	1.73	2.07	2.35	2.55	2.67	2.71	2.67
	h 25	2.3	2.50	2.61	2.62	2.54	2.38	2.13	1.81	1.44	1.02	0.57	0.11	0.34	0.77	1.16	1.51	1.80
	h 29	1.77	1.50	1.17	0.78	0.37	0.10	0.48	0.87	1.20	1.48	1.69	1.82	1.85	1.81	1.68	1.47	1.21
	h 31	1.48	1.64	1.70	1.67	1.55	1.35	1.08	0.76	0.40	0.03	0.35	0.69	1.00	1.24	1.41	1.51	1.52
Phase *B*	THD_I	27.87	28.07	28.28	28.49	28.70	28.92	29.15	29.37	29.60	29.84	30.09	30.34	30.59	30.85	31.11	31.38	31.66
	h 5	22.36	22.61	22.84	23.05	23.26	23.44	23.62	23.78	23.92	24.05	24.16	24.26	24.34	24.41	24.46	24.50	24.52
	h 7	10.87	10.74	10.62	10.51	10.39	10.27	10.15	10.04	9.92	9.81	9.70	9.58	9.47	9.36	9.25	9.14	9.03
	h 11	8.34	8.52	8.69	8.84	8.96	9.08	9.17	9.24	9.30	9.34	9.36	9.37	9.36	9.34	9.31	9.27	9.21
	h 13	5.75	5.61	5.47	5.33	5.18	5.03	4.87	4.71	4.55	4.38	4.21	4.04	3.85	3.67	3.48	3.28	3.08
	h 17	4.62	4.77	4.90	5.02	5.11	5.18	5.23	5.26	5.27	5.27	5.25	5.21	5.16	5.10	5.03	4.96	4.87
	h 19	3.56	3.43	3.29	3.14	2.99	2.83	2.66	2.49	2.31	2.13	1.93	1.73	1.53	1.31	1.09	0.88	0.66
	h 23	2.82	2.95	3.06	3.14	3.20	3.25	3.27	3.27	3.25	3.22	3.17	3.10	3.03	2.94	2.85	2.75	2.65
	h 25	2.30	2.19	2.06	1.92	1.78	1.63	1.47	1.31	1.14	0.97	0.79	0.60	0.41	0.21	0.05	0.22	0.42
	h 29	1.76	1.86	1.95	2.01	2.05	2.07	2.07	2.05	2.02	1.96	1.90	1.82	1.74	1.65	1.56	1.46	1.35
	h 31	1.49	1.39	1.28	1.17	1.04	0.92	0.79	0.66	0.53	0.39	0.25	0.10	0.08	0.22	0.38	0.53	0.68
Phase *C*	THD_I	27.87	28.12	28.38	28.65	28.92	29.20	29.48	29.78	30.08	30.39	30.71	31.04	31.38	31.72	32.07	32.44	32.81
	h 5	22.36	22.68	22.98	23.27	23.55	23.81	24.06	24.29	24.50	24.69	24.87	25.04	25.18	25.31	25.41	25.51	25.58
	h 7	10.87	10.69	10.51	10.32	10.12	9.91	9.70	9.48	9.25	9.01	8.77	8.51	8.25	7.98	7.71	7.42	7.13
	h 11	8.34	8.57	8.77	8.95	9.11	9.24	9.35	9.43	9.48	9.51	9.51	9.49	9.44	9.37	9.27	9.15	9.00
	h 13	5.75	5.57	5.37	5.16	4.93	4.68	4.42	4.14	3.85	3.54	3.22	2.88	2.53	2.17	1.80	1.42	1.05
	h 17	4.62	4.80	4.95	5.07	5.16	5.23	5.25	5.25	5.22	5.16	5.06	4.94	4.79	4.61	4.41	4.18	3.93
	h 19	3.56	3.40	3.21	2.99	2.76	2.50	2.23	1.93	1.62	1.29	0.94	0.58	0.22	0.20	0.57	0.96	1.35
	h 23	2.82	2.96	3.08	3.16	3.20	3.21	3.19	3.14	3.05	2.94	2.79	2.61	2.41	2.18	1.93	1.66	1.37
	h 25	2.3	2.16	1.99	1.79	1.57	1.32	1.06	0.77	0.48	0.17	0.16	0.48	0.80	1.11	1.41	1.70	1.96
	h 29	1.76	1.87	1.95	2.00	2.01	1.99	1.94	1.86	1.75	1.60	1.44	1.24	1.03	0.80	0.55	0.31	0.15
	h 31	1.49	1.37	1.22	1.05	0.86	0.64	0.41	0.16	0.12	0.36	0.61	0.85	1.08	1.28	1.45	1.59	1.69

Table-4.22 (b): Non-Characteristic harmonic current components with increasing VUF for 2-Φ equal angle unbalance for decreasing angle between phase *B* and *C* - two phasors moving in opposite direction for increasing VUF

		VUF = 0.0 %	VUF = 1.0 %	VUF = 2.0 %	VUF = 3.0 %	VUF = 4.0 %	VUF = 5.0 %	VUF = 6.0 %	VUF = 7.0 %	VUF = 8.0 %	VUF = 9.0 %	VUF = 10.0 %	VUF = 11.0 %	VUF = 12.0 %	VUF = 13.0 %	VUF = 14.0 %	VUF = 15.0 %	VUF = 16.0 %
Phase *A*	THD_I	27.87	27.42	26.98	26.54	26.10	25.67	25.25	24.83	24.42	24.01	23.61	23.21	22.81	22.42	22.04	21.66	21.28
	h 3	0.01	0.57	1.14	1.70	2.24	2.76	3.27	3.76	4.23	4.68	5.12	5.55	5.95	6.33	6.70	7.05	7.38
	h 9	0.01	0.71	1.41	2.09	2.75	3.38	3.98	4.55	5.08	5.58	6.05	6.48	6.86	7.20	7.51	7.77	8.00
	h 15	0.01	0.65	1.29	1.90	2.48	3.01	3.50	3.93	4.30	4.61	4.86	5.04	5.16	5.21	5.20	5.12	4.99
	h 21	0.01	0.56	1.11	1.62	2.08	2.48	2.82	3.08	3.25	3.35	3.36	3.29	3.15	2.93	2.65	2.31	1.92
	h 27	0.01	0.46	0.90	1.30	1.64	1.90	2.09	2.19	2.19	2.11	1.95	1.70	1.40	1.04	0.66	0.25	0.19
	h 33	0.01	0.35	0.69	0.98	1.20	1.35	1.42	1.39	1.29	1.10	0.85	0.55	0.23	0.14	0.45	0.75	1.01
Phase *B*	THD_I	27.87	28.07	28.28	28.49	28.70	28.92	29.15	29.37	29.60	29.84	30.09	30.34	30.59	30.85	31.11	31.38	31.66
	h 3	0.01	0.57	1.15	1.75	2.36	2.99	3.63	4.28	4.93	5.60	6.29	6.99	7.68	8.39	9.11	9.84	10.57
	h 9	0.01	0.34	0.69	1.04	1.41	1.79	2.17	2.55	2.94	3.33	3.73	4.12	4.51	4.90	5.29	5.67	6.04
	h 15	0.0	0.28	0.58	0.88	1.18	1.50	1.81	2.12	2.43	2.75	3.05	3.35	3.64	3.91	4.18	4.43	4.66
	h 21	0.0	0.23	0.47	0.72	0.97	1.22	1.47	1.72	1.96	2.19	2.42	2.63	2.82	2.99	3.15	3.29	3.41
	h 27	0.0	0.18	0.37	0.56	0.75	0.94	1.13	1.32	1.49	1.65	1.80	1.94	2.05	2.15	2.23	2.28	2.32
	h 33	0.0	0.13	0.27	0.41	0.55	0.68	0.82	0.95	1.07	1.18	1.27	1.35	1.41	1.45	1.47	1.48	1.48
Phase *C*	THD_I	27.87	28.12	28.38	28.65	28.92	29.20	29.48	29.78	30.08	30.39	30.71	31.04	31.38	31.72	32.07	32.44	32.81
	h 3	0.01	0.62	1.26	1.92	2.59	3.28	3.99	4.71	5.44	6.19	6.96	7.75	8.54	9.35	10.16	11.00	11.85
	h 9	0.01	0.45	0.91	1.38	1.87	2.36	2.86	3.37	3.88	4.39	4.91	5.43	5.94	6.45	6.96	7.46	7.95
	h 15	0.01	0.40	0.81	1.23	1.65	2.08	2.50	2.92	3.32	3.73	4.11	4.49	4.83	5.16	5.47	5.74	5.99
	h 21	0.0	0.35	0.70	1.06	1.41	1.75	2.08	2.40	2.69	2.97	3.21	3.43	3.61	3.75	3.86	3.93	3.96
	h 27	0.0	0.29	0.58	0.86	1.14	1.39	1.63	1.85	2.03	2.18	2.30	2.38	2.42	2.42	2.39	2.31	2.20
	h 33	0.0	0.23	0.45	0.67	0.87	1.05	1.20	1.33	1.42	1.47	1.49	1.48	1.43	1.35	1.24	1.10	0.94

4.10.3 Comparison of Four Different Definitions of Voltage Unbalance

The numerical values of two IEEE definitions of voltage unbalance, PVUR1 and PVUR are always zero for the cases of voltage unbalance only because of phase angle movement (either CW or ACW). For the case of increasing angle between two voltage phasors caused by their movement in opposite directions, the VUF happens to be always little higher than LVUR, since the inception of unbalance. With increasing VUF, the difference between VUF and LVUR also increases as displayed in Fig. 4.29(a).

The movement of two voltage phasors in opposite directions (towards each other), for the case of decreasing angle between them, leads towards a phasor arrangement, where the phase angle of voltage phasors under movement relative to their reference phasor, increases beyond 120°. Such as, for the case of decreasing angle between phasors *B* and *C*, (where, phasor *A* is the reference) the angle between voltage phasors *B* and *A*, along with the angle between voltage phasors *C* and *A* increases beyond 120°, as shown in Fig. 4.27.

This specific condition makes this case unique in comparison of other cases of voltage unbalance. It is shown in Fig. 4.29(b) that for this specific case of voltage unbalance the VUF happens to be always little lower than LVUR (i.e. VUF < LVUR), for each value of V_1, similar to the case of OV unbalance. As the VUF increases, the difference between VUF and LVUR also increases, as displayed in Fig. 4.29(b). It is found in present study that for all voltage unbalance cases other than these two types, VUF > LVUR.

It is also apparent in Fig. 4.29(a) and Fig. 4.29(b) with Table-4.14, Table-4.16, Table-4.18, and Table-4.20 that for the same value of V_1, the VUF and LVUR have higher values, for the case of decreasing angle as compared to the case of increasing angle between two phasors. For the same values of 'change in phase angles' (which are individually changing in equal steps of 0.86° to provide the 0.5 % change in VUF for each step of change), as considered for the case of voltage unbalance due to equal change in phase angles of two voltage phasors, the value of V_1 is same at different steps irrespective of the case of 'increasing or decreasing angle' but at those corresponding steps the V_2 is more in case of 'decreasing angle' as compared with the case of 'increasing angle' between two phasors. This discussion explains the reason of higher VUF for the case of 'decreasing angle' between two phasors.

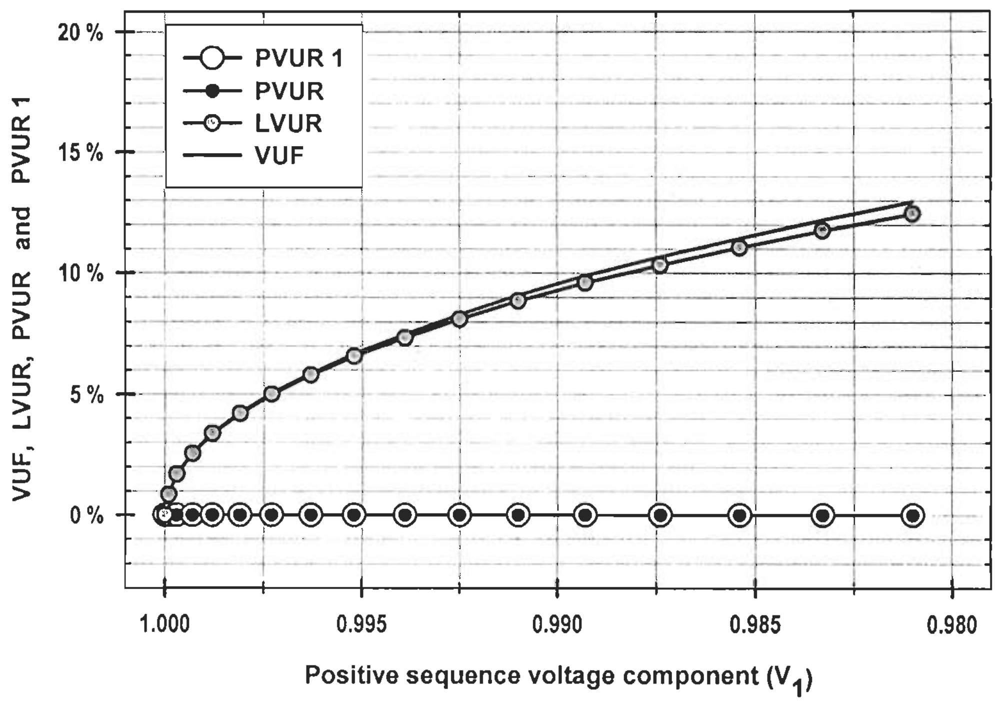

Fig. 4.29(a): Comparison of four different definitions of voltage unbalance for the case of voltage unbalance due to two-phase angle movement in opposite direction, for increasing angle between these two phasors

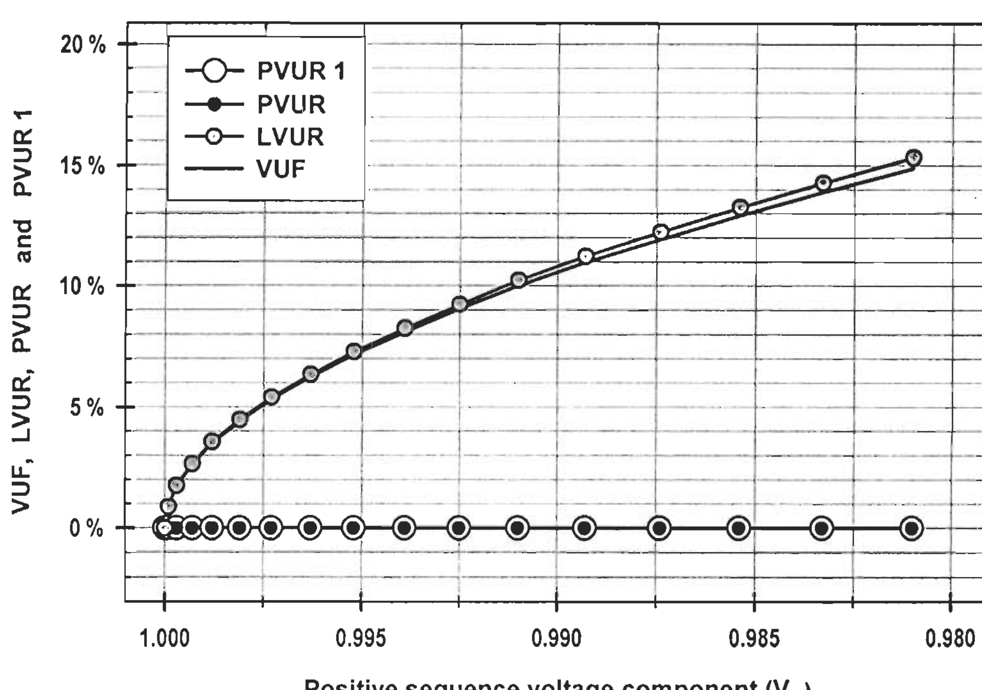

Fig. 4.29 (b): Comparison of four different definitions of voltage unbalance for the case of voltage unbalance due to two-phase angle movement in opposite direction, for decreasing angle between these two phasors

4.10.4 Effect of Voltage Unbalance on DC Parameters

As the VUF increases, the V_1 decreases and V_2 increases. This variation of V_1 and V_2 as a function of VUF is shown in Fig. 4.30(a) for the case of increasing angle between two phasors; and in Fig. 4.30(b) for the case of decreasing angle between two phasors. The existence of V_2 in power system indicates the presence of unbalance. With the increasing VUF, change in V_1 is very small (i.e., almost negligible). The similar variation reflects on the change in magnitude of DC output parameters, is clear from Fig. 4.31(a) along with Table-4.14 and Table-4.16, for the case of increasing angle. For the case of decreasing angle between two phasors is is shown in Fig. 4.31(b) with Table-4.18, and Table-4.20. The change in magnitude of DC output parameters magnitude is observed to be in ratio of variation in V_1.

The distortion of DC output parameters is affected by V_2 and it is observed to be increasing in proportional to increasing VUF and hence, V_2. This variation in distortion of DC output parameters with increasing VUF is shown in Fig. 4.32(a) for the case of increasing angle and Fig. 4.32(b) for the case of decreasing angle between two phasors for two-phase voltage unbalance condition.

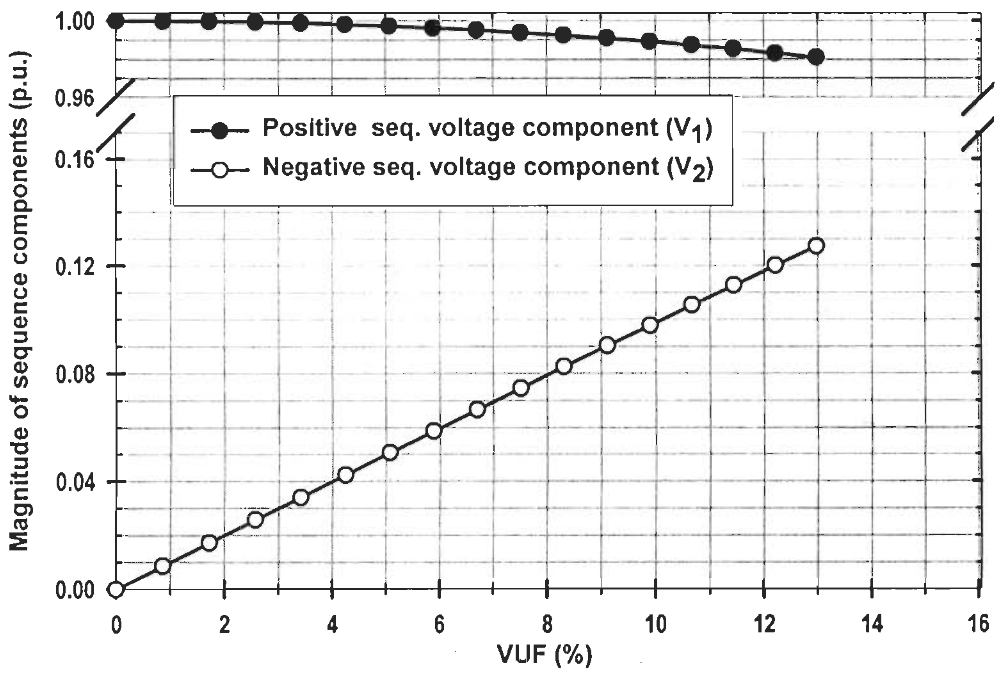

Fig. 4.30(a): Variation of V_1 and V_2 as a function of VUF for two-phase voltage unbalance condition due to increasing angle between two voltage phasors

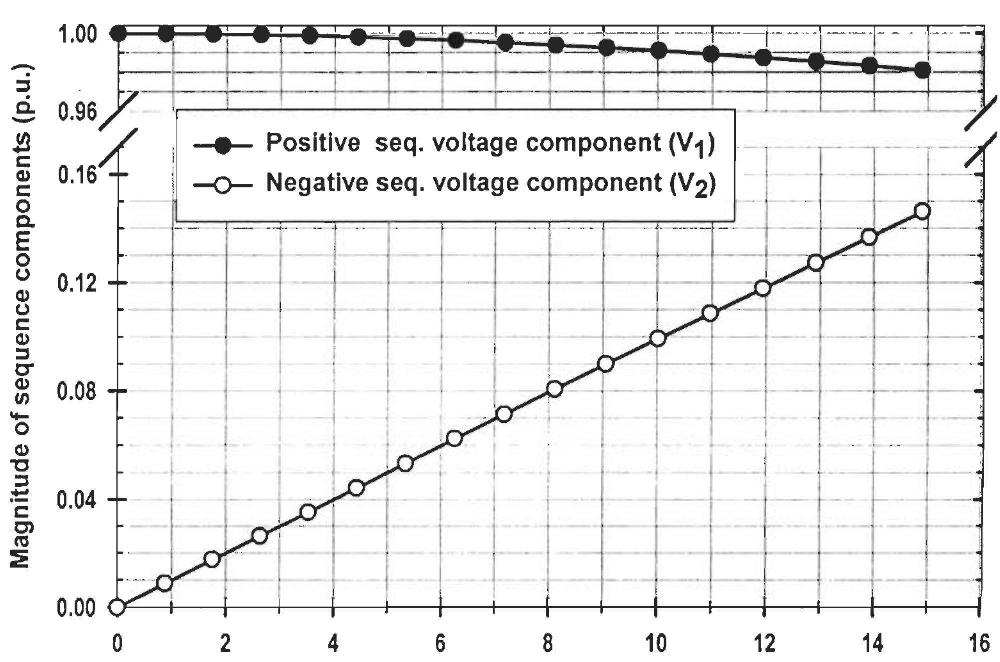

Fig. 4.30(b): Variation of V_1 and V_2 as a function of VUF for two-phase voltage unbalance condition due to decreasing angle between two voltage phasors

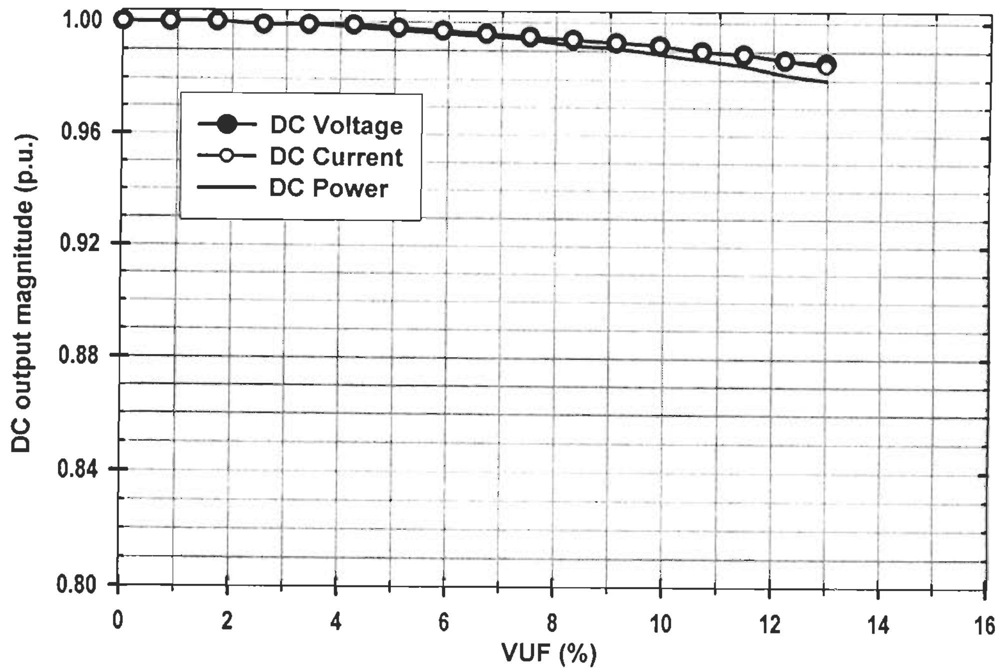

Fig. 4.31(a): Variation of magnitude of DC output parameters as a function of VUF for two-phase voltage unbalance condition due to increasing angle between two voltage phasors

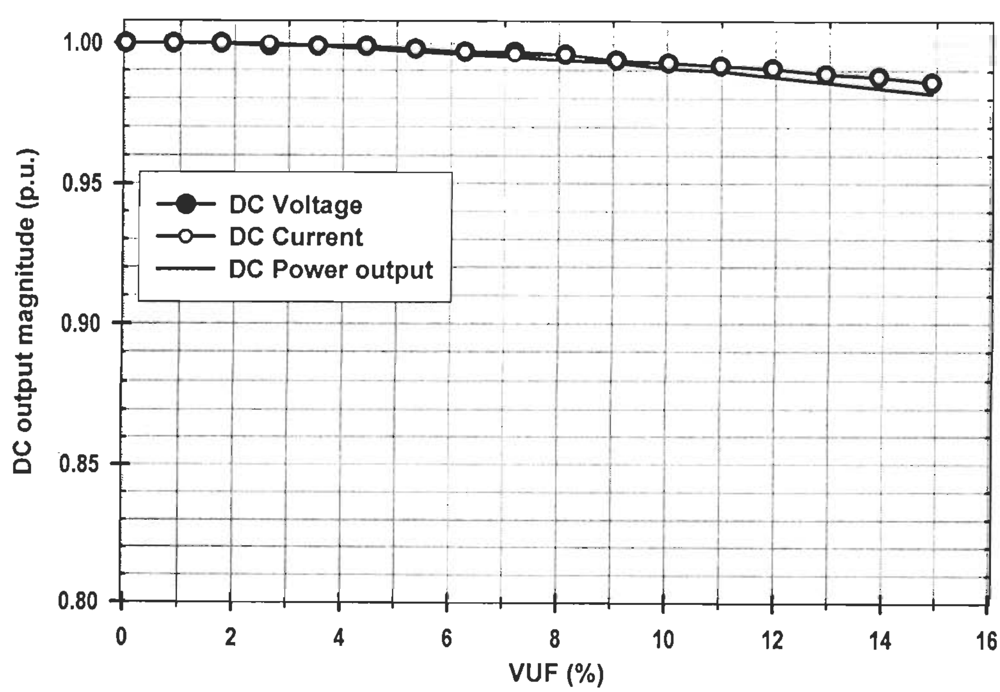

Fig. 4.31(b): Variation of magnitude of DC output parameters as a function of VUF for two-phase voltage unbalance condition due to decreasing angle between two voltage phasors

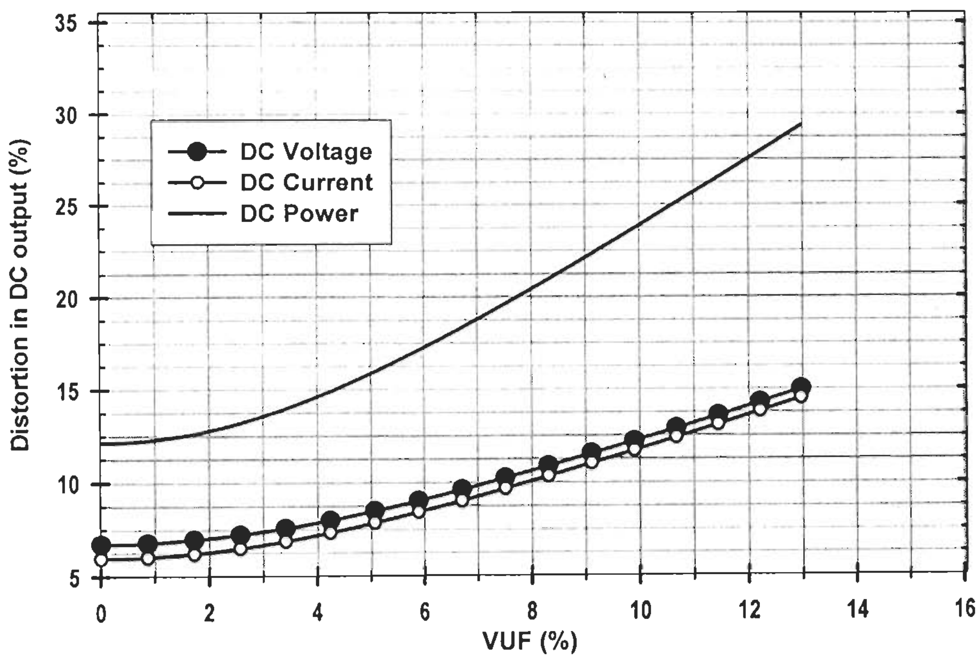

Fig. 4.32(a): Variation in distortion of DC output parameters, as a function of VUF for two-phase voltage unbalance condition due to increasing angle between two voltage phasors

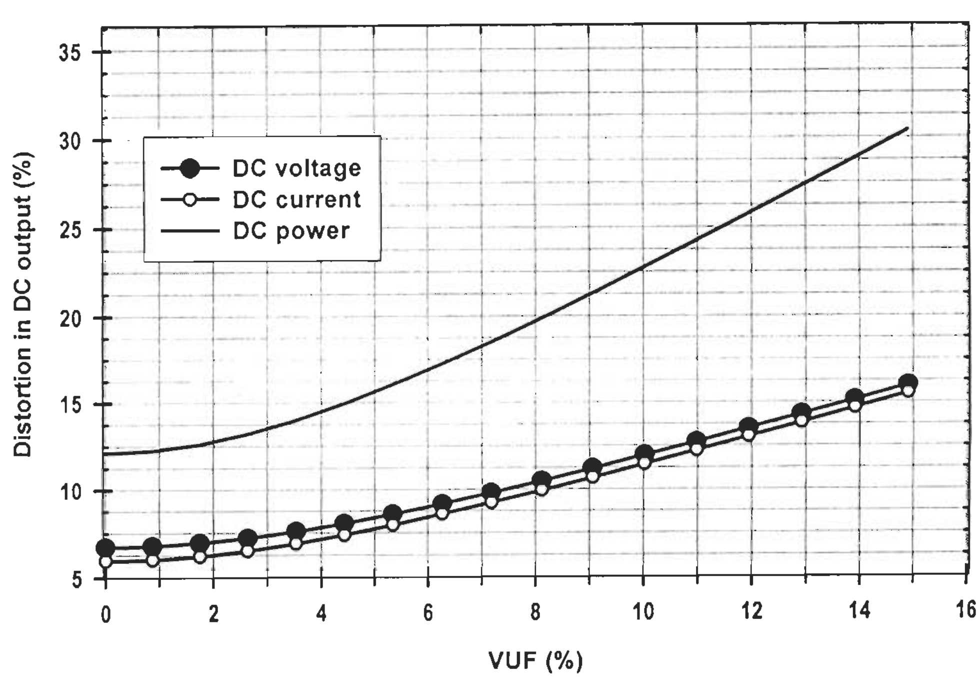

Fig. 4.32(b): Variation in distortion of DC output parameters, as a function of VUF for two-phase voltage unbalance condition due to decreasing angle between two voltage phasors

4.10.5 Effect of Voltage Unbalance on AC Parameters

It is observed from Table-4.14, Table-4.16, Table-4.18, and Table-4.20 that current waveforms of all three phases (I_A, I_B, and I_C) are affected (may be less or more) under two-phase voltage unbalance condition owing to either increasing or decreasing angle between two voltage phasors.

It has already been discussed in previous sections in accordance with single-phase angle (CW or ACW) movement that the change in voltage phase angle 'least affects' the phase in which the phase angle movement is taking place, and 'most affects' the phase towards which it is moving. As shown in Table-4.7 and Table-4.8, in earlier section that in case of CW movement of voltage phasor, the AC performance parameters (i.e. rms load current and THD_I) are almost constant for 'phasor under movement', THD_I increases (and rms load current decreases) for phase towards which it is moving, whereas THD_I decreases (and rms load current increases) for the phase from which it is moving away. For ACW movement of voltage phasor, as presented in Table-4.9 and Table-4.10, it is apparent that for 'phasor under movement', THD_I slightly increases whilst rms load current decreases a bit (not constant as in case CW phasor movement). For other two phases the change in AC performance parameters, are found same as discussed for the case of CW movement of voltage phasor. This very inference is also applicable here in both cases of two-phase voltage unbalance condition due to 'increasing angle' between two voltage phasors, i.e. either between phase *B* and *C* or between *A* and *C*.

It is observed from Table-4.8 and Table-4.10 that the rms load current decreases and THD_I increases in the phase towards which, both the phasors under movement are approaching whereas the phasors under movement do not experience much change in their values of AC performance parameters (i.e. rms load current and THD_I).

In the case of 'increasing angle' between phase *B* and *C* (phasor *B* moving ACW and *C* moving CW) as considered in Table-4.14 , phasors *B* and *C* both are moving towards phasor *A*. Consequently, in phase *A* the load current is decreasing and THD_I increasing due to the combined contribution of 'phasors under movement' (*B* and *C*). In phases *B* and *C* (phasors under movement) the changes in AC performance parameters are rather less significant. As a result of CW movement of phasor *C*, THD_I and rms load current of phase *C* are almost constant and THD_I of phase *B* decreases (as *C* is moving away from *B*). In consequence of ACW movement of phasor *B*, THD_I of phase *B* increases slightly and THD_I of phase C decreases (as B is moving away from C). It explains that both phasors under movement (*B* and *C*) are reducing the THD_I of each other, but the phasor under ACW movement (*B*) is having a higher value of THD_I (and lower value of load current) in comparison to phasor under CW movement (*C*). This change in rms values of load currents in three different phases with variable VUF is displayed in Fig. 4.33(a) whereas variation in THD_I of three different phases as a function of VUF is presented in Fig. 4.33(b).

Similarly, for the case of 'increasing angle' between phase *A* and *C* (phasor *A* moving CW and *C* moving ACW) as taken up in Table-4.16. Here, phasor *A* and *C* are moving towards phasor *B*, therefore the AC performance parameters phase *B* are most affected, where the load current is decreasing and THD_I increasing due to the combined contribution of 'phasors under movement' (*A* and *C*). The changes in AC performance parameters of phase *A* and *C* are relatively smaller. Here also the both phasors under movement (*A* and *C*) are reducing the THD_I of each other, but the phasor under ACW movement (*C*) is having a higher value of THD_I (and lower value of load current) in comparison to phasor under CW movement (*A*). For the case of 'increasing angle' between phase *A* and *C*, this change in rms values of load currents in three different phases with variable VUF is displayed in Fig. 4.34(a) whereas variation in THD_I of three different phases as a function of VUF is presented in Fig. 4.34 (b).

The analogous justification is also valid for the case of 'decreasing angle' between two moving voltage phasors. For the case of 'decreasing angle' between phase *B* and *C* (phasor *B* moving CW and *C* moving ACW) as considered in Table-4.18, phasors *B* and *C* both are moving away from reference phasor *A*. Thus THD_I is decreasing (rms load current increasing) in phase *A* due to the combined contribution of 'phasors under movement' (*B* and *C*). Also the both phasors under movement (*B* and *C*) are causing an increase in THD_I of each other, but the phasor under ACW movement (*C*) is having a higher value of THD_I (and lower value of load current) in comparison to phasor under CW movement (*A*). This change in rms values of load currents in three different phases with variable VUF is displayed in Fig. 4.35(a) whereas variation in THD_I of three different phases as a function of VUF is presented in Fig. 4.35(b).

Correspondingly, for the case of 'decreasing angle' between phase *A* and *C* (phasor *A* moving ACW and *C* moving CW) as taken up in Table-4.20, phasors *A* and *C* both are moving away from reference phasor *B*. This condition results in the reduction in THD_I (and subsequent increase in rms load current) in phase *B* due to the combined contribution of 'phasors under movement' (*A* and *C*). Besides this, both phasors under movement (*A* and *C*) are reducing the THD_I of each other, but the phasor under ACW movement (*A*) is having a higher value of THD_I (and lower value of load current) in comparison to phasor under CW movement (*C*). Fig. 4.36(a) shows the variation in rms currents in three different phases with variable VUF while Fig. 4.36(b) exhibits the variation in THD_I of three different phases as a function of VUF, for this case of 'decreasing angle' between phase *A* and *C*.

As in case of unbalanced system, the THD_I of every phase differs with other phases significantly. PTHDUF has been introduced to simplify the harmonic current analysis and to quantify the voltage source unbalance in presence of harmonic distortion. For a particular type of voltage unbalance, the value of VUF remains unchanged regardless of the phase being affected by voltage unbalance. Furthermore, the values of PTHDUF are found to be quite unique for both (increasing or decreasing angle) types of cases of voltage unbalance caused by of movement of two voltage phasors, for a given value VUF, as presented in Table-4.14, Table-4.16, Table-4.18, and Table-4.20. Plots of average THD_I and PTHDUF with variation of VUF are given in Fig. 4.37(a) for the case of 'increasing angle' between two voltage phasors, and in Fig. 4.37(b) for the case of 'decreasing angle' between two voltage phasors, caused by their movement in opposite directions. These two Figures clearly illustrate that for the same value of VUF, the PTHDUF has its value somewhat higher for the case of 'increasing angle' between two voltage phasors as compared to the case of 'decreasing angle' between two voltage phasors.

Hence, PTHDUF is found convincingly characteristic for the type (increasing /decreasing angle between two voltage phasors under movement) and degree (VUF) of voltage unbalance.

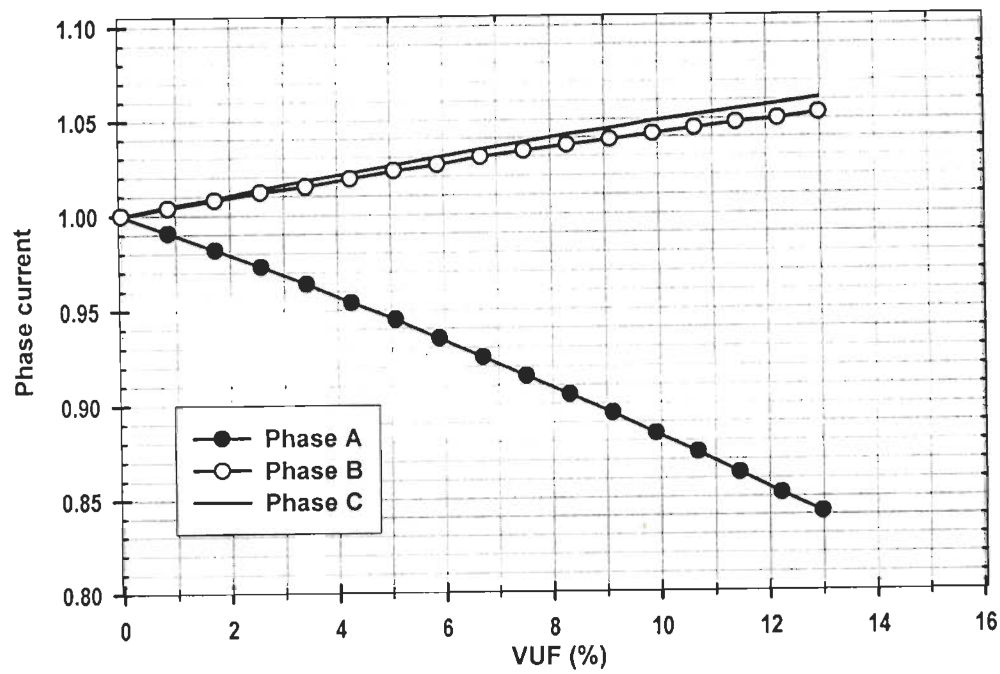

Fig. 4.33(a): **Variation in rms phase currents in three different phases as a function of VUF for two-phase voltage unbalance condition due to increasing angle between voltage phasors *B* and *C***

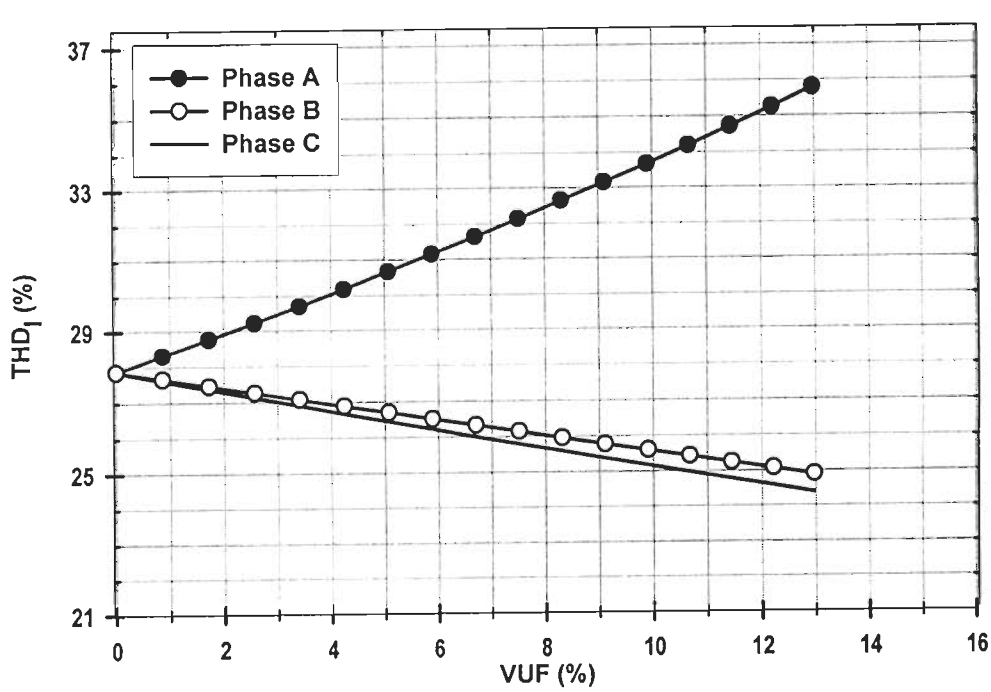

Fig. 4.33(b): **Variation in THD$_I$ of currents in three different phases as a function of VUF for two-phase voltage unbalance condition due to increasing angle between voltage phasors *B* and *C***

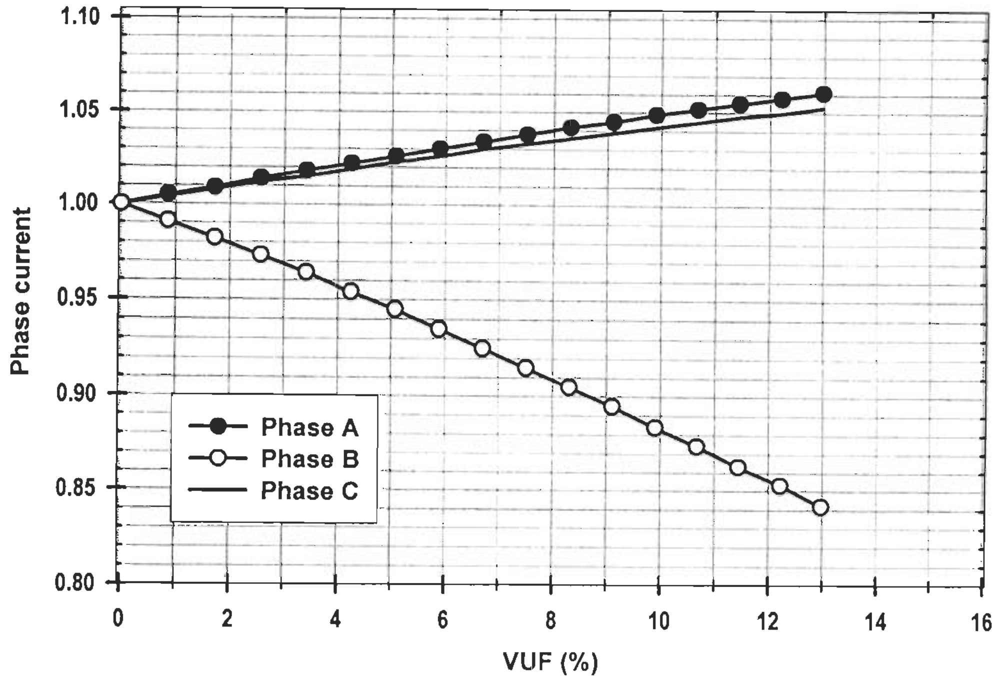

Fig. 4.34(a): **Variation in rms phase currents in three different phases as a function of VUF for two-phase voltage unbalance condition due to increasing angle between voltage phasors *A* and *C***

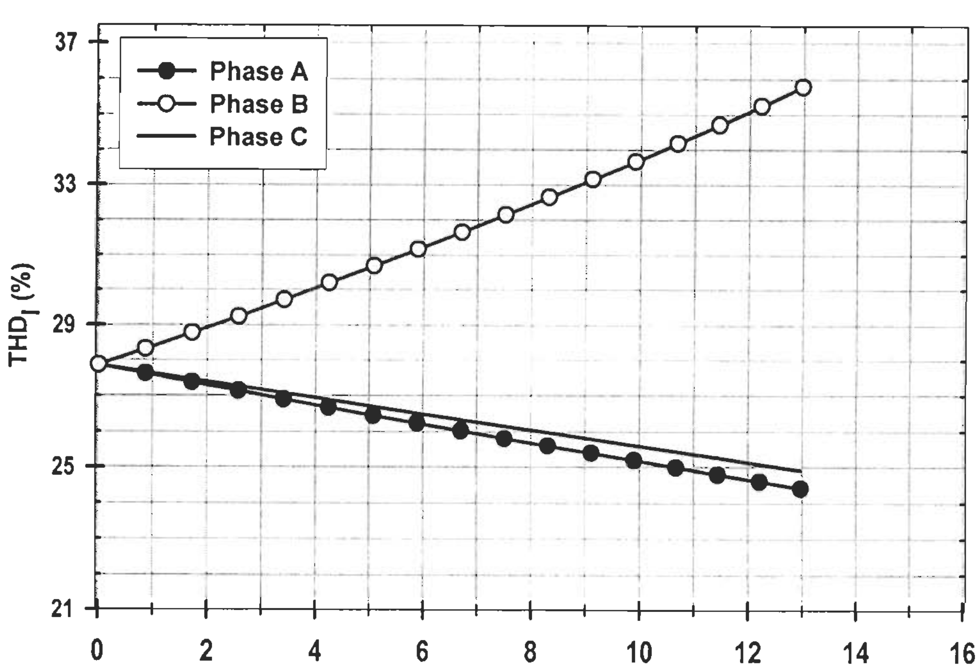

Fig. 4.34(b): **Variation in THD_I of currents in three different phases as a function of VUF for two-phase voltage unbalance condition due to increasing angle between voltage phasors *A* and *C***

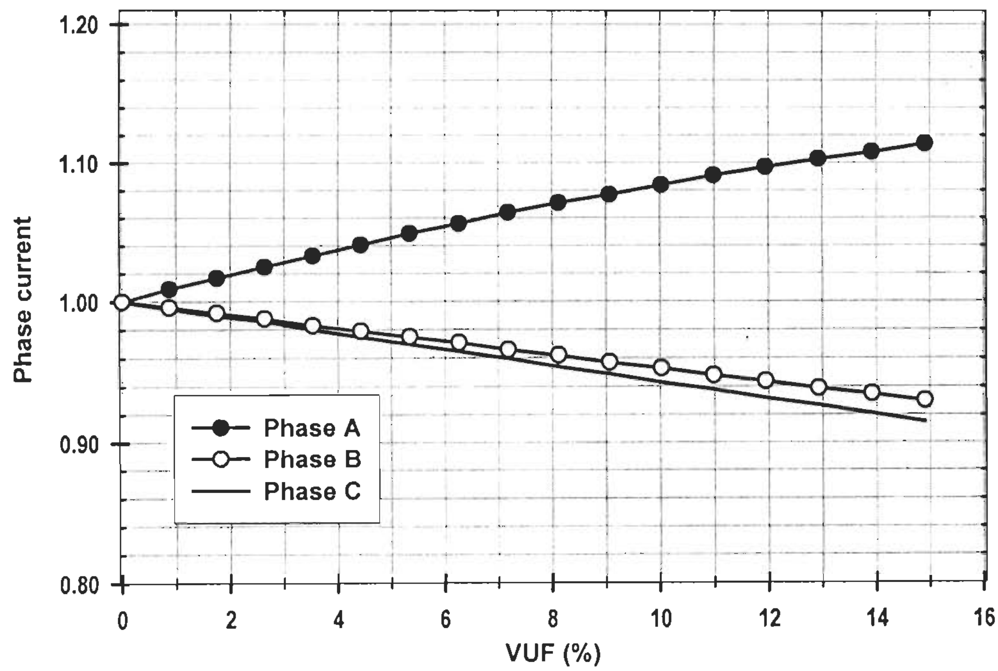

Fig. 4.35(a): Variation in rms phase currents in three different phases as a function of VUF for two-phase voltage unbalance condition due to decreasing angle between voltage phasors *B* and *C*

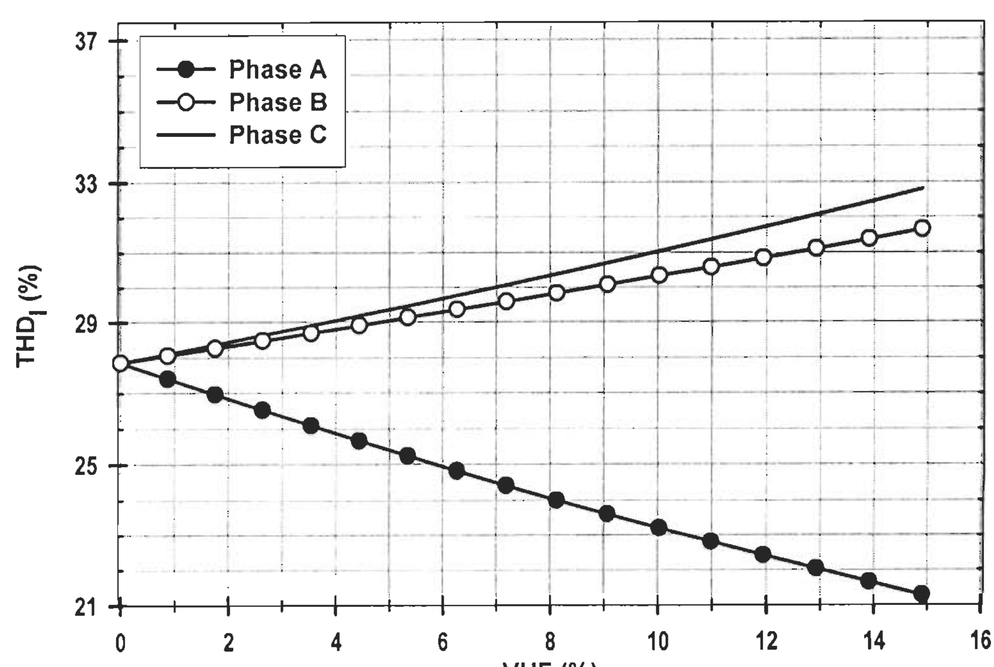

Fig. 4.35(b): Variation in THD_I of currents in three different phases as a function of VUF for two-phase voltage unbalance condition due to decreasing angle between voltage phasors *B* and *C*

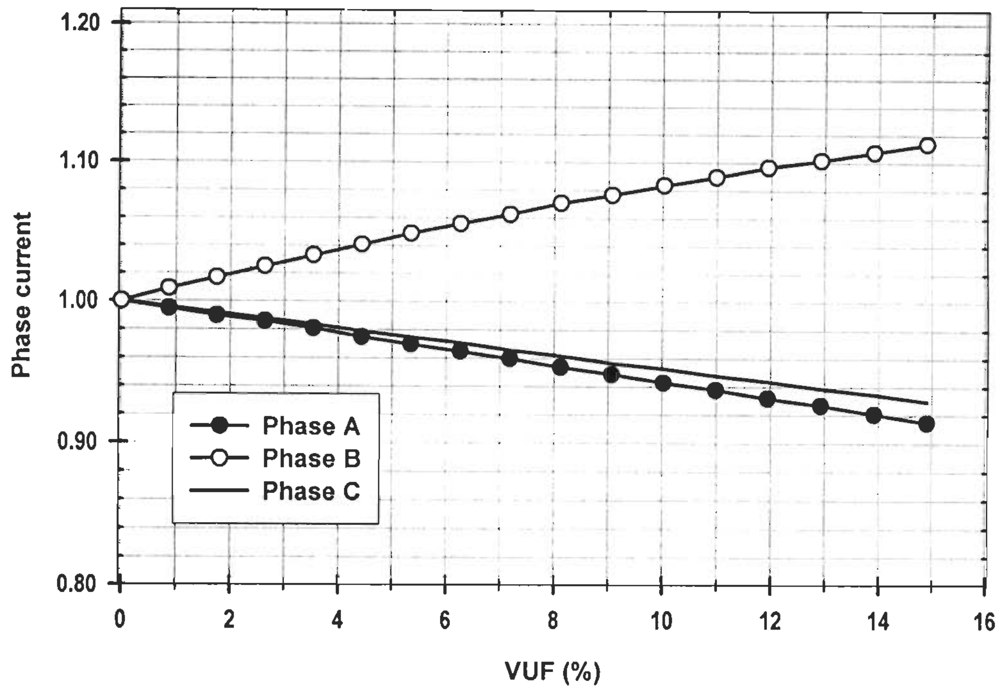

Fig. 4.36(a): Variation in rms phase currents in three different phases as a function of VUF for two-phase voltage unbalance condition due to decreasing angle between voltage phasors *A* and *C*

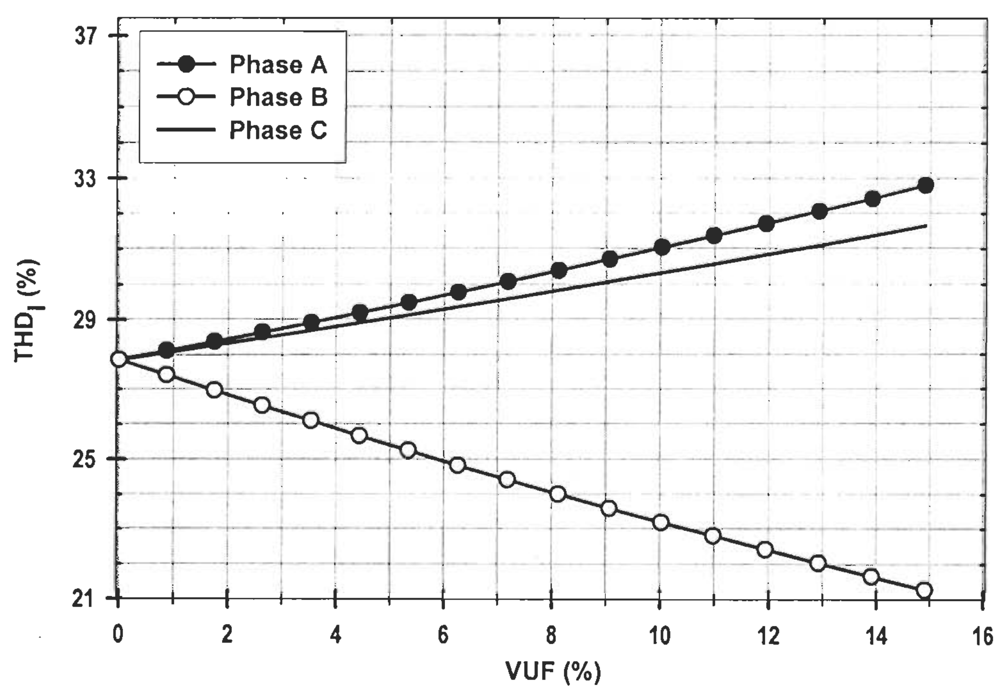

Fig. 4.36(b): Variation in THD_I of currents in three different phases as a function of VUF for two-phase voltage unbalance condition due to decreasing angle between voltage phasors *A* and *C*

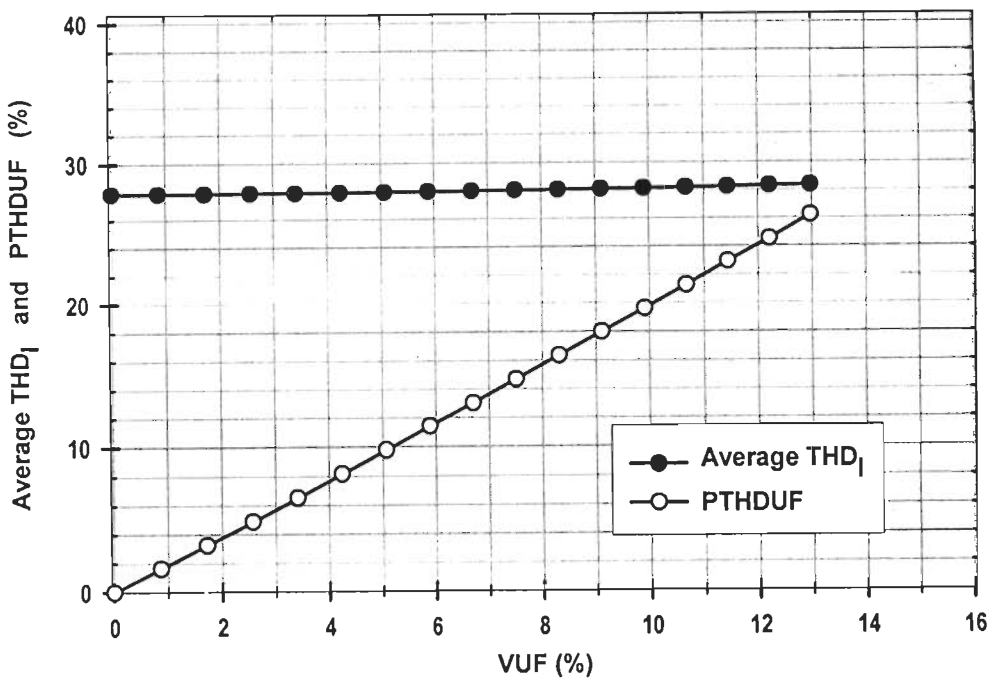

Fig. 4.37(a): Variation in average THD_I and PTHDUF with increasing VUF for two-phase voltage unbalance condition due to increasing angle between two voltage phasors under movement

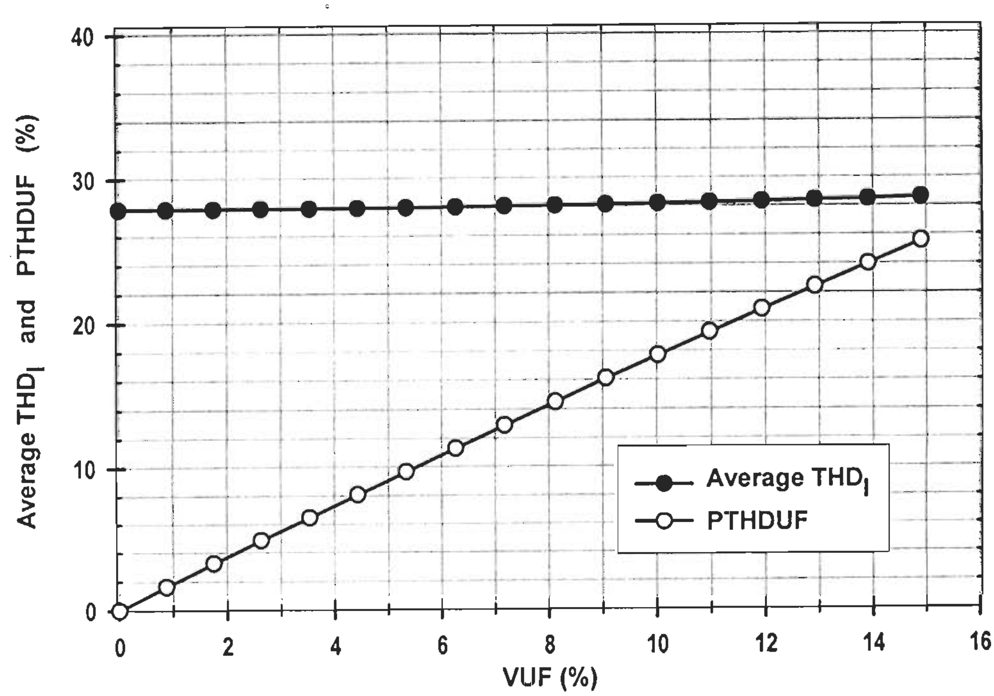

Fig. 4.37(b): Variation in average THD_I and PTHDUF with increasing VUF for two-phase voltage unbalance condition due to decreasing angle between two voltage phasors under movement

4.11 CHANGES IN TWO PHASE ANGLES WITH UNEQUAL CHANGE IN EACH PHASE

In the earlier case, it is considered that the contribution of each phase angle deflection towards voltage unbalance is half of the total value of VUF, but it is observed that net VUF is smaller than the sum of the individual contributions, e.g. as considered in Table-4.14, where angle (Φ_C = 119.14°) gives 0.50 % VUF, and angle (Φ_B = 240.86°) gives 0.50 % VUF, but combination of both provides just 0.86 % VUF. Hence, to make the VUF equal to the total of two individual contributions (i.e. 1% in the example taken) any one of the two angles is deflected further to increase its contribution.

Here, two dissimilar cases are taken up; in one case both the phasors are moving in opposite direction and in another case, phasors are moving in same direction. In case of phasors moving in opposite direction, the net VUF is the more than the individual contribution of each phase, i.e. they reflect partial addition effect, while for the case of phasors moving in same direction, the unbalance contribution of each phasor movement is partially cancelled by the other phasor.

4.11.1 Two Phasors Moving in Opposite Direction

In this case, phase *A* is considered as reference phasor and remaining two phases specifically, phase *B* and phase *C* are shifted in opposite direction. In this particular case, the variation in VUF is adjusted by ACW movement in phase angle of voltage phasor *B* and CW movement in phase angle of voltage phasor *C* of a balanced source voltage supply, as shown in Fig. 4.25, which increases the angle between voltage phasors *B* and *C* and this movement of two voltage phasors becomes the reason of unbalance in voltage source.

It can be explained more clearly with the example taken for VUF equal to 1%. Here, phase angle of voltage phasor *C* (Φ_C = 119.14°) gives 0.50 % VUF, and phase angle of phasor *B* (Φ_B = 240.86°) gives 0.50 % VUF, but combination of both provides 0.86 % VUF. Hence, phase angle of phasor *B* (Φ_B) is further increased to 241.13° to make VUF = 1%. In the same approach, other changes are made in the positions of phasor *B* and *C*, to regulate the VUF from 1% to 16%.

In other words in can be said that in this case, the angle between one set of specific phasors is increasing beyond 120° and for other two sets of voltage phasors their in between angle is decreasing within 120°. Between these two decreasing angle, for every step the change in angle position is more in one case than other, which is a more practical condition to be happen in real system.

The input parameters, voltage sequence components (V_1 and V_2), and percentage values of four definitions of voltage unbalance for single-phase angle unbalance case due to CW movement of voltage phasor *C* are shown in Table-4.23(a). Table-4.23(b) presents the same parameters for the ACW movement of voltage phasor *B*. Here, the change in phase angle position of a particular phase regulates the variable VUF. The contribution of each phase angle deflection towards voltage unbalance is unequal. A combination of cases given in Table-4.23(a) and Table-4.23(b) is considered in Table-4.24, to analyze the combined effect of change in position of phasor *C* together with phasor *B*, with their unequal contribution towards voltage unbalance.

4.11.2 Two Phasors Moving in Same Direction

Phase *A* is considered as reference phasor in this case also and the remaining two phasors *B* and *C*, both are moving in same direction, i.e. phase *B* is moving CW together with phase *C*, as shown in Fig. 4.38. It can be explained more clearly with the example taken for VUF equal to 1%. Here, phase angle *C* (Φ_C = 119.14°) gives 0. 50 % VUF, and phase angle *B* (Φ_B = 239.14°) gives 0.50 % VUF, but combination of both provides but combination of both also provides VUF = 0.50 % and LVUR = 0.43 %. Here, the net VUF and LVUR value are reduced to half than the earlier case of opposite direction with equal change in each phase, which only due to their movement in same direction. Hence, phase angle *B* (Φ_B) is further increased to 238° to make VUF = 1%. In the similar approach, other changes are made in the positions of phasor *B* and phasor *C*, to regulate the VUF. The angle between one set of specific phasors (*A* and *B*) is increasing beyond 120° and for other two sets of voltage phasors (*B* and *C*, *C* and *A*) the angle between them is decreasing within 120°. Between these two decreasing angle, for every step the change in angle position is more in one case than other, to be exact the change in angle between *B* and *C* is more than the change in angle between *C* and *A*, which is a more practical condition to take place in a real system.

The input parameters and voltage sequence components (V_1 and V_2) along with the percentage values of four definitions of voltage unbalance for single-phase angle unbalance case due to CW movement of voltage phasor *B* and *C* are shown in Table-4.25(a), and Table-4.25(b) respectively. Here, the change in phase angle position of a particular phase regulates the variable VUF. The contribution of each phase angle deflection towards voltage unbalance is unequal. A combination of cases given in Table-4.25(a) and Table-4.25(b) is considered in Table-4.26, to analyze the combined effect of change in position of phasor C together with phasor B, with their unequal contribution towards voltage unbalance.

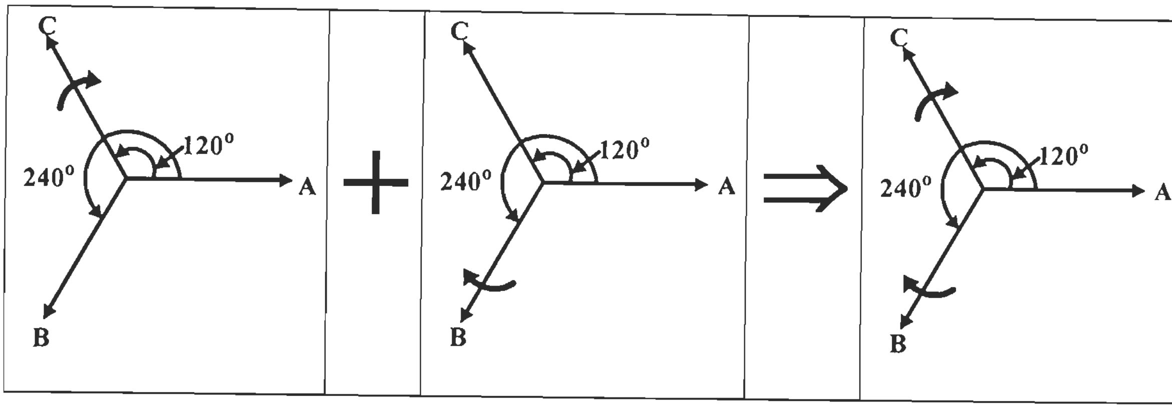

Fig. 4.38: An unbalance in three-phase voltage source due to 2-Φ unequal angle unbalance by phase *B* and *C* as two phasors moving in same direction

With increasing VUF, the behavior of characteristic and non-characteristic harmonics is presented in Table-4.27(a) and Table-4.27(b) for the movement of phasors B and C in opposite direction, while Table-4.28(a) and Table-4.28(b) show this harmonic behavior for their movement in same direction. This variation in harmonic pattern behavior is discussed in section 4.13.

Table-4.23 (a): Comparison of four different definitions of voltage unbalance for 1-Φ angle unbalance in phase *B* (moving ACW) for increasing VUF

LVUR (%)	PVUR 1 (%)	PVUR (%)	VUF (%)	Unbalanced voltage source						+ve seq. Volt. (V_1)	-ve seq. Volt. (V_2)
				Phase *A*		Phase *B*		Phase *C*			
				Mag.	Angle	Mag.	Angle	Mag.	Angle		
0.00	0	0	0.00	1.0	0	1.0	240	1.0	120	1.0000	0.000
0.57	0	0	0.66	1.0	0	1.0	241.13	1.0	120	1.0000	0.0066
1.16	0	0	1.33	1.0	0	1.0	242.28	1.0	120	0.9998	0.0133
1.75	0	0	2.00	1.0	0	1.0	243.44	1.0	120	0.9996	0.0200
2.36	0	0	2.69	1.0	0	1.0	244.63	1.0	120	0.9993	0.0269
2.98	0	0	3.39	1.0	0	1.0	245.83	1.0	120	0.9989	0.0339
3.62	0	0	4.11	1.0	0	1.0	247.05	1.0	120	0.9983	0.0410
4.27	0	0	4.83	1.0	0	1.0	248.29	1.0	120	0.9977	0.0482
4.93	0	0	5.56	1.0	0	1.0	249.54	1.0	120	0.9969	0.0554
5.61	0	0	6.31	1.0	0	1.0	250.82	1.0	120	0.9960	0.0629
6.29	0	0	7.06	1.0	0	1.0	252.1	1.0	120	0.9950	0.0703
7.00	0	0	7.83	1.0	0	1.0	253.4	1.0	120	0.9939	0.0778
7.71	0	0	8.60	1.0	0	1.0	254.72	1.0	120	0.9927	0.0854
8.36	0	0	9.30	1.0	0	1.0	255.9	1.0	120	0.9915	0.0922
9.19	0	0	10.19	1.0	0	1.0	257.41	1.0	120	0.9898	0.1009
9.96	0	0	11.01	1.0	0	1.0	258.78	1.0	120	0.9881	0.1088
10.73	0	0	11.83	1.0	0	1.0	260.16	1.0	120	0.9863	0.1167

Table-4.23 (b): Comparison of four different definitions of voltage unbalance for 1-Φ angle unbalance in phase *C* (moving CW) for increasing VUF

LVUR (%)	PVUR 1 (%)	PVUR (%)	VUF (%)	Unbalanced voltage source						+ve seq. Volt. (V_1)	-ve seq. Volt. (V_2)
				Phase *A*		Phase *B*		Phase *C*			
				Mag.	Angle	Mag.	Angle	Mag.	Angle		
0.00	0	0	0.00	1.0	0	1.0	240	1.0	120	1.000	0.00
0.43	0	0	0.50	1.0	0	1.0	240	1.0	119.14	1.000	0.005
0.87	0	0	1.00	1.0	0	1.0	240	1.0	118.28	1.000	0.010
1.31	0	0	1.50	1.0	0	1.0	240	1.0	117.42	1.000	0.015
1.75	0	0	2.00	1.0	0	1.0	240	1.0	116.56	1.000	0.020
2.19	0	0	2.50	1.0	0	1.0	240	1.0	115.7	0.999	0.025
2.63	0	0	3.00	1.0	0	1.0	240	1.0	114.84	0.999	0.030
3.08	0	0	3.50	1.0	0	1.0	240	1.0	113.98	0.999	0.035
3.52	0	0	4.00	1.0	0	1.0	240	1.0	113.13	0.998	0.040
3.97	0	0	4.50	1.0	0	1.0	240	1.0	112.27	0.998	0.045
4.43	0	0	5.00	1.0	0	1.0	240	1.0	111.41	0.998	0.050
4.88	0	0	5.50	1.0	0	1.0	240	1.0	110.55	0.997	0.055
5.33	0	0	6.00	1.0	0	1.0	240	1.0	109.7	0.996	0.060
5.78	0	0	6.50	1.0	0	1.0	240	1.0	108.85	0.996	0.065
6.24	0	0	7.00	1.0	0	1.0	240	1.0	108	0.995	0.070
6.70	0	0	7.50	1.0	0	1.0	240	1.0	107.15	0.994	0.075
7.16	0	0	8.00	1.0	0	1.0	240	1.0	106.3	0.994	0.080

Table-4.24: Comparison of four different definitions of voltage unbalance and performance of rectifier for 2-Φ unequal angle unbalance in phase *B* and *C* - Two phasors moving in opposite direction for increasing VUF from 1% to 16%.

LVUR (%)	PVUR 1 (%)	PVUR (%)	VUF (%)	Unbalanced voltage source						+ve seq. Volt. (V_1)	-ve seq. Volt. (V_2)	AC parameters						Average THD_I	PTHDUF (%)	DC parameters					
				Phase *A*		Phase *B*		Phase *C*				I_A		I_B		I_C				I_{DC}		V_{DC}		P_{DC}	
				Mag.	Angle	Mag.	Angle	Mag.	Angle			RMS	THD_I (%)	Mag.	THD_I (%)	Mag.	THD_I (%)			Mag.	THD_I (%)	Mag.	THD_I (%)	Mag.	THD_I (%)
0.00	0	0	0.0	1.0	0	1.0	240	1.0	120	1.0000	0.00	1.000	27.87	1.000	27.87	1.000	27.87	27.87	0.00	1.000	5.95	1.000	6.72	1.000	12.13
1.00	0	0	1.0	1.0	0	1.0	241.13	1.0	119.14	0.9999	0.010	0.990	28.40	1.004	27.67	1.006	27.55	27.87	1.85	1.000	6.03	1.000	6.80	1.000	12.30
1.99	0	0	2.0	1.0	0	1.0	242.28	1.0	118.28	0.9996	0.020	0.979	28.93	1.008	27.48	1.012	27.23	27.88	3.70	1.000	6.28	1.000	7.02	1.000	12.79
2.97	0	0	3.0	1.0	0	1.0	243.44	1.0	117.42	0.9991	0.030	0.969	29.48	1.011	27.30	1.018	26.92	27.90	5.55	0.999	6.67	0.999	7.38	0.999	13.57
3.95	0	0	4.0	1.0	0	1.0	244.63	1.0	116.56	0.9983	0.040	0.958	30.04	1.015	27.12	1.024	26.60	27.92	7.46	0.999	7.18	0.999	7.86	0.998	14.61
4.91	0	0	5.0	1.0	0	1.0	245.83	1.0	115.7	0.9974	0.050	0.946	30.61	1.018	26.94	1.029	26.29	27.95	9.40	0.998	7.80	0.998	8.44	0.997	15.85
5.88	0	0	6.0	1.0	0	1.0	247.05	1.0	114.84	0.9962	0.060	0.934	31.20	1.022	26.76	1.035	25.98	27.98	11.37	0.997	8.49	0.997	9.10	0.996	17.25
6.84	0	0	7.0	1.0	0	1.0	248.29	1.0	113.98	0.9948	0.070	0.922	31.80	1.025	26.59	1.040	25.67	28.02	13.34	0.996	9.25	0.996	9.83	0.995	18.78
7.78	0	0	8.0	1.0	0	1.0	249.54	1.0	113.13	0.9931	0.079	0.910	32.41	1.028	26.43	1.046	25.36	28.07	15.29	0.995	10.05	0.995	10.60	0.993	20.40
8.72	0	0	9.0	1.0	0	1.0	250.82	1.0	112.27	0.9912	0.089	0.897	33.03	1.031	26.26	1.051	25.06	28.12	17.38	0.993	10.90	0.993	11.42	0.991	22.10
9.66	0	0	10.0	1.0	0	1.0	252.1	1.0	111.41	0.9890	0.099	0.885	33.67	1.034	26.10	1.056	24.75	28.17	19.37	0.992	11.77	0.992	12.28	0.989	23.85
10.58	0	0	11.0	1.0	0	1.0	253.4	1.0	110.55	0.9866	0.109	0.871	34.32	1.037	25.94	1.061	24.45	28.24	21.46	0.990	12.67	0.990	13.16	0.986	25.65
11.50	0	0	12.0	1.0	0	1.0	254.72	1.0	109.7	0.9840	0.118	0.858	34.99	1.039	25.78	1.066	24.14	28.30	23.19	0.988	13.58	0.988	14.06	0.983	27.48
12.42	0	0	13.0	1.0	0	1.0	255.9	1.0	108.85	0.9811	0.128	0.844	35.69	1.042	25.57	1.070	23.87	28.38	25.14	0.985	14.52	0.986	14.98	0.980	29.35
13.30	0	0	14.0	1.0	0	1.0	257.41	1.0	108	0.9779	0.137	0.830	36.37	1.043	25.47	1.074	23.52	28.45	27.09	0.983	15.45	0.983	15.91	0.976	31.21
14.19	0	0	15.0	1.0	0	1.0	258.78	1.0	107.15	0.9745	0.146	0.816	37.08	1.045	25.32	1.079	23.21	28.54	29.04	0.980	16.41	0.980	16.86	0.972	33.09
15.08	0	0	16.0	1.0	0	1.0	260.16	1.0	106.3	0.9708	0.155	0.802	37.80	1.047	25.17	1.082	22.91	28.63	30.99	0.978	17.37	0.978	17.81	0.968	34.98

Table-4.25 (a): Comparison of four different definitions of voltage unbalance for 1-Φ angle unbalance in phase *B* (moving CW) for increasing VUF.

LVUR (%)	PVUR 1 (%)	PVUR (%)	VUF (%)	Unbalanced voltage source						+ve seq. Volt. (V_1)	-ve seq. Volt. (V_2)
				Phase *A*		Phase *B*		Phase *C*			
				Mag.	Angle	Mag.	Angle	Mag.	Angle		
0.00	0	0	0.00	1.0	0	1.0	240	1.0	120	1.000	0.00
1.01	0	0	1.16	1.0	0	1.0	238	1.0	120	1.000	1.000
2.04	0	0	2.33	1.0	0	1.0	236	1.0	120	0.999	0.012
3.08	0	0	3.50	1.0	0	1.0	233.98	1.0	120	0.999	0.023
4.14	0	0	4.69	1.0	0	1.0	231.95	1.0	120	0.998	0.035
5.24	0	0	5.90	1.0	0	1.0	229.88	1.0	120	0.997	0.047
6.35	0	0	7.12	1.0	0	1.0	227.80	1.0	120	0.995	0.059
7.48	0	0	8.36	1.0	0	1.0	225.7	1.0	120	0.993	0.071
8.63	0	0	9.60	1.0	0	1.0	223.6	1.0	120	0.991	0.083
9.82	0	0	10.87	1.0	0	1.0	221.46	1.0	120	0.988	0.095
11.02	0	0	12.14	1.0	0	1.0	219.32	1.0	120	0.986	0.107
12.26	0	0	13.44	1.0	0	1.0	217.15	1.0	120	0.982	0.120
13.51	0	0	14.75	1.0	0	1.0	214.98	1.0	120	0.979	0.132
14.81	0	0	16.10	1.0	0	1.0	212.76	1.0	120	0.975	0.144
16.10	0	0	17.43	1.0	0	1.0	210.59	1.0	120	0.971	0.157
17.43	0	0	18.79	1.0	0	1.0	208.38	1.0	120	0.966	0.169
18.79	0	0	20.18	1.0	0	1.0	206.15	1.0	120	0.962	0.182

Table-4.25 (b): Comparison of four different definitions of voltage unbalance for 1-Φ angle unbalance in phase *C* (moving CW) for increasing VUF.

LVUR (%)	PVUR 1 (%)	PVUR (%)	VUF (%)	Unbalanced voltage source						+ve seq. Volt. (V_1)	-ve seq. Volt. (V_2)
				Phase *A*		Phase *B*		Phase *C*			
				Mag.	Angle	Mag.	Angle	Mag.	Angle		
0.00	0	0	0.00	1.0	0	1.0	240	1.0	120	1.000	0.00
0.43	0	0	0.50	1.0	0	1.0	240	1.0	119.14	1.000	0.005
0.87	0	0	1.00	1.0	0	1.0	240	1.0	118.28	1.000	0.010
1.31	0	0	1.50	1.0	0	1.0	240	1.0	117.42	1.000	0.015
1.75	0	0	2.00	1.0	0	1.0	240	1.0	116.56	1.000	0.020
2.19	0	0	2.50	1.0	0	1.0	240	1.0	115.7	0.999	0.025
2.63	0	0	3.00	1.0	0	1.0	240	1.0	114.84	0.999	0.030
3.08	0	0	3.50	1.0	0	1.0	240	1.0	113.98	0.999	0.035
3.52	0	0	4.00	1.0	0	1.0	240	1.0	113.13	0.998	0.040
3.97	0	0	4.50	1.0	0	1.0	240	1.0	112.27	0.998	0.045
4.43	0	0	5.00	1.0	0	1.0	240	1.0	111.41	0.998	0.050
4.88	0	0	5.50	1.0	0	1.0	240	1.0	110.55	0.997	0.055
5.33	0	0	6.00	1.0	0	1.0	240	1.0	109.7	0.996	0.060
5.78	0	0	6.50	1.0	0	1.0	240	1.0	108.85	0.996	0.065
6.24	0	0	7.00	1.0	0	1.0	240	1.0	108	0.995	0.070
6.70	0	0	7.50	1.0	0	1.0	240	1.0	107.15	0.994	0.075
7.16	0	0	8.00	1.0	0	1.0	240	1.0	106.3	0.994	0.080

Table-4.26: Comparison of four different definitions of voltage unbalance and performance of rectifier for 2-Φ unequal angle unbalance in phase *B* and *C* - two phasors moving in same direction for increasing VUF.

LVUR (%)	PVUR 1 (%)	PVUR (%)	VUF (%)	Unbalanced voltage source						+ve seq. Volt. (V_1)	-ve seq. Volt. (V_2)	AC parameters						Average THD_I	PTHDUF (%)	DC parameters					
				Phase *A*		Phase *B*		Phase *C*				I_A		I_B		I_C				I_{DC}		V_{DC}		P_{DC}	
				Mag.	Angle	Mag.	Angle	Mag.	Angle			RMS	THD_I (%)	Mag.	THD_I (%)	Mag.	THD_I (%)			Mag.	THD_I (%)	Mag.	THD_I (%)	Mag.	THD_I (%)
0.00	0	0	0.0	1.0	0	1.0	240	1.0	120	1.0000	0.000	1.000	27.87	1.000	27.87	1.000	27.87	27.87	0.00	1.000	5.95	1.000	6.72	1.000	12.13
1.00	0	0	1.0	1.0	0	1.0	238	1.0	119.14	0.9999	0.010	1.005	27.60	1.005	27.62	0.990	28.40	27.87	1.89	1.000	6.03	1.000	6.80	1.000	12.30
1.99	0	0	2.0	1.0	0	1.0	236	1.0	118.28	0.9996	0.020	1.011	27.34	1.009	27.37	0.979	28.94	27.88	3.79	1.000	6.28	1.000	7.02	1.000	12.79
2.97	0	0	3.0	1.0	0	1.0	233.98	1.0	117.42	0.9991	0.030	1.016	27.07	1.014	27.13	0.968	29.49	27.90	5.71	0.999	6.67	0.999	7.38	0.999	13.57
3.94	0	0	4.0	1.0	0	1.0	231.95	1.0	116.56	0.9983	0.040	1.021	26.80	1.018	26.90	0.957	30.06	27.92	7.66	0.999	7.18	0.999	7.85	0.998	14.60
4.91	0	0	5.0	1.0	0	1.0	229.88	1.0	115.7	0.9974	0.050	1.026	26.53	1.022	26.67	0.946	30.64	27.95	9.64	0.998	7.79	0.998	8.43	0.997	15.84
5.87	0	0	6.0	1.0	0	1.0	227.80	1.0	114.84	0.9962	0.060	1.031	26.25	1.026	26.45	0.934	31.24	27.98	11.65	0.997	8.49	0.997	9.09	0.996	17.24
6.83	0	0	7.0	1.0	0	1.0	225.7	1.0	113.98	0.9948	0.070	1.036	25.98	1.030	26.23	0.921	31.85	28.02	13.67	0.996	9.25	0.996	9.82	0.995	18.77
7.78	0	0	8.0	1.0	0	1.0	223.6	1.0	113.13	0.9931	0.079	1.041	25.70	1.034	26.03	0.909	32.47	28.07	15.69	0.995	10.05	0.995	10.60	0.993	20.39
8.72	0	0	9.0	1.0	0	1.0	221.46	1.0	112.27	0.9912	0.089	1.046	25.42	1.037	25.82	0.896	33.12	28.12	17.78	0.993	10.90	0.993	11.42	0.991	22.10
9.66	0	0	10.0	1.0	0	1.0	219.32	1.0	111.41	0.9891	0.099	1.051	25.13	1.041	25.62	0.883	33.77	28.17	19.87	0.992	11.77	0.992	12.27	0.988	23.85
10.58	0	0	11.0	1.0	0	1.0	217.15	1.0	110.55	0.9866	0.109	1.055	24.85	1.044	25.42	0.869	34.44	28.24	21.97	0.990	12.67	0.990	13.16	0.986	25.66
11.50	0	0	12.0	1.0	0	1.0	214.98	1.0	109.7	0.9840	0.118	1.060	24.56	1.047	25.22	0.856	35.13	28.30	24.12	0.988	13.58	0.988	14.06	0.983	27.49
12.42	0	0	13.0	1.0	0	1.0	212.76	1.0	108.65	0.9811	0.128	1.063	24.31	1.051	24.98	0.841	35.84	28.38	26.30	0.982	14.51	0.985	14.98	0.980	29.35
13.30	0	0	14.0	1.0	0	1.0	210.59	1.0	108	0.9779	0.137	1.068	23.97	1.052	24.84	0.827	36.56	28.46	28.48	0.983	15.46	0.983	15.91	0.976	31.22
14.19	0	0	15.0	1.0	0	1.0	208.38	1.0	107.15	0.9745	0.146	1.072	23.67	1.055	24.66	0.813	37.29	28.54	30.66	0.980	16.41	0.980	16.86	0.972	33.10
15.07	0	0	16.0	1.0	0	1.0	206.15	1.0	106.3	0.9708	0.155	1.075	23.36	1.057	24.47	0.798	38.05	28.63	32.92	0.977	17.37	0.978	17.81	0.968	34.98

Table-4.27(a): **Characteristic harmonic current components with increasing VUF for 2-ϕ unequal angle unbalance in phase *B* and *C* - two phasors moving in opposite direction**

		VUF= 0.0 %	VUF = 1.0 %	VUF = 2.0 %	VUF = 3.0 %	VUF = 4.0 %	VUF = 5.0 %	VUF = 6.0 %	VUF = 7.0 %	VUF = 8.0 %	VUF = 9.0 %	VUF = 10.0 %	VUF = 11.0 %	VUF = 12.0 %	VUF = 13.0 %	VUF = 14.0 %	VUF = 15.0 %	VUF = 16.0 %
Phase *A*	THD_I	27.87	28.40	28.93	29.48	30.04	30.61	31.20	31.80	32.41	33.03	33.67	34.32	34.99	35.69	36.37	37.08	37.80
	h 5	22.37	23.02	23.66	24.28	24.88	25.46	26.02	26.55	27.05	27.52	27.95	28.35	28.70	29.03	29.28	29.50	29.67
	h 7	10.86	10.49	10.07	9.60	9.05	8.46	7.79	7.07	6.30	5.45	4.55	3.59	2.58	1.48	0.40	0.76	1.97
	h 11	8.35	8.81	9.21	9.55	9.81	9.98	10.07	10.07	9.98	9.78	9.47	9.07	8.56	7.93	7.23	6.42	5.52
	h 13	5.74	5.34	4.86	4.29	3.63	2.90	2.10	1.24	0.33	0.63	1.62	2.62	3.62	4.63	5.56	6.46	7.31
	h 17	4.62	4.99	5.26	5.43	5.48	5.41	5.21	4.89	4.45	3.88	3.21	2.43	1.58	0.65	0.37	1.31	2.28
	h 19	3.56	3.18	2.69	2.11	1.45	0.73	0.09	0.86	1.66	2.45	3.19	3.86	4.43	4.90	5.20	5.36	5.35
	h 23	2.83	3.11	3.28	3.32	3.23	3.01	2.65	2.16	1.58	0.90	0.18	0.59	1.34	2.07	2.67	3.19	3.56
	h 25	2.3	1.96	1.52	0.99	0.40	0.25	0.89	1.51	2.06	2.54	2.89	3.10	3.16	3.03	2.75	2.31	1.72
	h 29	1.77	1.98	2.07	2.03	1.86	1.56	1.15	0.65	0.11	0.47	1.02	1.51	1.90	2.16	2.25	2.18	1.94
	h 31	1.48	1.20	0.83	0.39	0.11	0.59	1.05	1.44	1.72	1.88	1.90	1.76	1.47	1.04	0.55	0.02	0.60
Phase *B*	THD_I	27.87	27.67	27.48	27.30	27.12	26.94	26.76	26.59	26.43	26.26	26.10	25.94	25.78	25.57	25.47	25.32	25.17
	h 5	22.36	22.11	21.84	21.56	21.25	20.93	20.60	20.25	19.89	19.51	19.11	18.71	18.29	17.79	17.42	16.98	16.52
	h 7	10.87	10.98	11.10	11.23	11.36	11.49	11.62	11.76	11.89	12.03	12.16	12.29	12.42	12.55	12.66	12.76	12.86
	h 11	8.34	8.15	7.93	7.70	7.45	7.18	6.89	6.60	6.30	5.98	5.66	5.34	5.03	4.65	4.41	4.12	3.84
	h 13	5.75	5.88	6.01	6.14	6.26	6.38	6.49	6.58	6.67	6.74	6.80	6.84	6.85	6.84	6.82	6.77	6.69
	h 17	4.62	4.45	4.26	4.05	3.83	3.59	3.35	3.10	2.85	2.60	2.36	2.12	1.90	1.62	1.49	1.30	1.12
	h 19	3.56	3.69	3.80	3.91	4.00	4.07	4.13	4.17	4.19	4.18	4.15	4.10	4.02	3.90	3.80	3.67	3.52
	h 23	2.82	2.68	2.52	2.34	2.16	1.97	1.78	1.58	1.39	1.20	1.02	0.83	0.65	0.41	0.28	0.10	0.12
	h 25	2.30	2.41	2.50	2.58	2.63	2.67	2.68	2.67	2.64	2.58	2.51	2.42	2.31	2.18	2.09	1.97	1.85
	h 29	1.76	1.65	1.52	1.39	1.25	1.10	0.96	0.82	0.68	0.53	0.38	0.22	0.10	0.20	0.32	0.48	0.64
	h 31	1.49	1.57	1.64	1.69	1.71	1.72	1.70	1.66	1.61	1.55	1.48	1.40	1.32	1.21	1.15	1.05	0.94
Phase *C*	THD_I	27.87	27.55	27.23	26.92	26.60	26.29	25.98	25.67	25.36	25.06	24.75	24.45	24.14	23.87	23.52	23.21	22.91
	h 5	22.36	21.93	21.48	21.01	20.51	20.00	19.46	18.91	18.34	17.74	17.14	16.52	15.89	15.29	14.59	13.93	13.26
	h 7	10.87	11.08	11.28	11.46	11.63	11.79	11.93	12.05	12.15	12.24	12.31	12.35	12.37	12.39	12.35	12.31	12.24
	h 11	8.34	8.02	7.66	7.27	6.84	6.39	5.90	5.39	4.87	4.31	3.75	3.18	2.60	2.06	1.44	0.88	0.41
	h 13	5.75	5.96	6.14	6.29	6.41	6.50	6.55	6.57	6.55	6.49	6.40	6.26	6.08	5.90	5.61	5.32	4.99
	h 17	4.62	4.34	4.02	3.67	3.27	2.84	2.38	1.90	1.41	0.90	0.39	0.17	0.64	1.08	1.58	2.01	2.40
	h 19	3.56	3.74	3.89	3.99	4.04	4.05	4.01	3.93	3.79	3.61	3.38	3.10	2.78	2.46	2.04	1.62	1.19
	h 23	2.82	2.59	2.32	2.00	1.64	1.26	0.85	0.42	0.02	0.44	0.85	1.24	1.60	1.89	2.19	2.41	2.57
	h 25	2.3	2.45	2.55	2.60	2.60	2.55	2.44	2.28	2.07	1.82	1.53	1.20	0.84	0.50	0.10	0.32	0.70
	h 29	1.76	1.58	1.35	1.08	0.78	0.45	0.11	0.24	0.57	0.90	1.18	1.43	1.62	1.75	1.83	1.84	1.78
	h 31	1.49	1.60	1.66	1.67	1.63	1.54	1.40	1.21	0.98	0.72	0.43	0.13	0.18	0.45	0.77	1.02	1.24

Table-4.27 (b): Non-characteristic harmonic current components with increasing VUF for 2-ϕ unequal angle unbalance in phase *B* and *C* - two phasors moving in opposite direction

		VUF= 0.0 %	VUF = 1.0 %	VUF = 2.0 %	VUF = 3.0 %	VUF = 4.0 %	VUF = 5.0 %	VUF = 6.0 %	VUF = 7.0 %	VUF = 8.0 %	VUF = 9.0 %	VUF = 10.0 %	VUF = 11.0 %	VUF = 12.0 %	VUF = 13.0 %	VUF = 14.0 %	VUF = 15.0 %	VUF = 16.0 %
Phase *A*	**THD_I**	**27.87**	**28.40**	**28.93**	**29.48**	**30.04**	**30.61**	**31.20**	**31.80**	**32.41**	**33.03**	**33.67**	**34.32**	**34.99**	**35.69**	**36.37**	**37.08**	**37.80**
	h 3	0.01	0.71	1.43	2.17	2.95	3.75	4.57	5.43	6.31	7.22	8.15	9.11	10.09	11.12	12.13	13.19	14.28
	h 9	0.01	0.86	1.73	2.61	3.51	4.41	5.31	6.21	7.09	7.95	8.78	9.57	10.32	11.03	11.64	12.21	12.69
	h 15	0.01	0.78	1.57	2.35	3.11	3.84	4.52	5.13	5.67	6.11	6.44	6.66	6.74	6.68	6.50	6.16	5.68
	h 21	0.01	0.67	1.34	1.97	2.55	3.06	3.48	3.77	3.94	3.95	3.82	3.53	3.10	2.50	1.83	1.03	0.17
	h 27	0.01	0.55	1.07	1.55	1.95	2.24	2.41	2.44	2.32	2.05	1.65	1.12	0.51	0.17	0.83	1.47	2.04
	h 33	0.01	0.42	0.81	1.14	1.38	1.50	1.50	1.36	1.10	0.72	0.28	0.21	0.69	1.14	1.46	1.67	1.72
Phase *B*	**THD_I**	**27.87**	**27.67**	**27.48**	**27.30**	**27.12**	**26.94**	**26.76**	**26.59**	**26.43**	**26.26**	**26.10**	**25.94**	**25.78**	**25.57**	**25.47**	**25.32**	**25.17**
	h 3	0.01	0.65	1.29	1.92	2.54	3.14	3.74	4.32	4.88	5.43	5.97	6.49	6.99	7.46	7.95	8.41	8.85
	h 9	0.01	0.34	0.65	0.96	1.24	1.51	1.77	2.00	2.22	2.42	2.61	2.79	2.94	3.15	3.23	3.36	3.48
	h 15	0.0	0.27	0.53	0.77	1.00	1.21	1.42	1.61	1.80	1.99	2.17	2.36	2.54	2.78	2.91	3.10	3.29
	h 21	0.0	0.22	0.43	0.63	0.83	1.02	1.21	1.39	1.58	1.76	1.95	2.13	2.30	2.50	2.61	2.74	2.85
	h 27	0.0	0.17	0.34	0.51	0.67	0.84	1.01	1.17	1.33	1.48	1.62	1.74	1.84	1.94	1.98	2.02	2.03
	h 33	0.0	0.13	0.26	0.39	0.52	0.66	0.79	0.91	1.02	1.12	1.20	1.25	1.29	1.32	1.32	1.32	1.31
Phase *C*	**THD_I**	**27.87**	**27.55**	**27.23**	**26.92**	**26.60**	**26.29**	**25.98**	**25.67**	**25.36**	**25.06**	**24.75**	**24.45**	**24.14**	**23.87**	**23.52**	**23.21**	**22.91**
	h 3	0.01	0.71	1.40	2.06	2.71	3.34	3.95	4.54	5.10	5.65	6.16	6.66	7.13	7.59	8.00	8.40	8.77
	h 9	0.01	0.56	1.10	1.63	2.15	2.64	3.12	3.57	4.00	4.41	4.80	5.15	5.49	5.75	6.07	6.32	6.55
	h 15	0.01	0.51	1.00	1.47	1.93	2.36	2.76	3.14	3.48	3.79	4.06	4.29	4.48	4.62	4.75	4.82	4.85
	h 21	0.0	0.44	0.87	1.27	1.66	2.01	2.32	2.60	2.83	3.01	3.14	3.22	3.25	3.22	3.14	3.00	2.82
	h 27	0.0	0.37	0.72	1.05	1.35	1.61	1.83	2.00	2.11	2.17	2.16	2.10	1.98	1.83	1.59	1.32	1.03
	h 33	0.0	0.29	0.57	0.82	1.04	1.22	1.34	1.41	1.43	1.38	1.28	1.12	0.92	0.72	0.43	0.16	0.12

Table-4.28 (a): Characteristic harmonic current components with increasing VUF for 2-ϕ unequal angle unbalance in phase *B* and *C* - two phasors moving in same direction

		VUF = 0.0 %	VUF = 1.0 %	VUF = 2.0 %	VUF = 3.0 %	VUF = 4.0 %	VUF = 5.0 %	VUF = 6.0 %	VUF = 7.0 %	VUF = 8.0 %	VUF = 9.0 %	VUF = 10.0 %	VUF = 11.0 %	VUF = 12.0 %	VUF = 13.0 %	VUF = 14.0 %	VUF = 15.0 %	VUF = 16.0 %
Phase *A*	THD_I	27.87	27.60	27.34	27.07	26.80	26.53	26.25	25.98	25.70	25.42	25.13	24.85	24.56	24.31	23.97	23.67	23.36
	h 5	22.37	22.02	21.66	21.27	20.86	20.42	19.96	19.48	18.99	18.47	17.93	17.38	16.81	16.29	15.63	15.03	14.41
	h 7	10.86	11.02	11.18	11.34	11.49	11.64	11.78	11.92	12.04	12.16	12.26	12.35	12.43	12.49	12.52	12.54	12.54
	h 11	8.35	8.08	7.79	7.46	7.11	6.73	6.32	5.90	5.45	4.98	4.50	4.00	3.50	3.06	2.49	1.99	1.50
	h 13	5.74	5.92	6.08	6.23	6.37	6.49	6.58	6.65	6.69	6.71	6.69	6.63	6.54	6.44	6.24	6.04	5.80
	h 17	4.62	4.39	4.13	3.83	3.51	3.16	2.79	2.40	2.00	1.58	1.17	0.75	0.37	0.21	0.54	0.91	1.27
	h 19	3.56	3.72	3.86	3.98	4.07	4.13	4.15	4.14	4.08	3.98	3.84	3.65	3.42	3.19	2.85	2.51	2.14
	h 23	2.83	2.63	2.40	2.15	1.87	1.57	1.25	0.93	0.59	0.25	0.09	0.41	0.73	0.99	1.32	1.59	1.84
	h 25	2.3	2.44	2.55	2.63	2.67	2.68	2.64	2.56	2.44	2.27	2.06	1.82	1.54	1.28	0.92	0.60	0.26
	h 29	1.77	1.61	1.43	1.22	1.00	0.76	0.51	0.25	0.03	0.27	0.52	0.77	1.00	1.18	1.41	1.56	1.68
	h 31	1.48	1.59	1.67	1.72	1.73	1.70	1.63	1.51	1.37	1.18	0.98	0.75	0.51	0.30	0.06	0.25	0.49
Phase *B*	THD_I	27.87	27.62	27.37	27.13	26.90	26.67	26.45	26.23	26.03	25.82	25.62	25.42	25.22	24.98	24.84	24.66	24.47
	h 5	22.36	22.02	21.66	21.29	20.89	20.48	20.06	19.62	19.17	18.69	18.21	17.71	17.21	16.63	16.16	15.63	15.09
	h 7	10.87	11.04	11.21	11.37	11.53	11.68	11.83	11.98	12.11	12.24	12.37	12.48	12.59	12.67	12.76	12.83	12.89
	h 11	8.34	8.09	7.81	7.50	7.18	6.83	6.46	6.07	5.68	5.26	4.84	4.41	3.98	3.49	3.14	2.73	2.34
	h 13	5.75	5.92	6.07	6.21	6.34	6.45	6.54	6.62	6.67	6.71	6.72	6.71	6.67	6.59	6.52	6.41	6.26
	h 17	4.62	4.40	4.16	3.89	3.59	3.27	2.93	2.58	2.21	1.84	1.47	1.10	0.75	0.40	0.32	0.49	0.75
	h 19	3.56	3.71	3.83	3.93	4.01	4.06	4.09	4.09	4.07	4.01	3.92	3.80	3.66	3.44	3.27	3.04	2.78
	h 23	2.82	2.64	2.44	2.20	1.94	1.65	1.35	1.04	0.72	0.40	0.10	0.25	0.54	0.86	1.07	1.30	1.52
	h 25	2.30	2.42	2.51	2.57	2.61	2.61	2.59	2.53	2.45	2.33	2.19	2.01	1.81	1.54	1.34	1.07	0.80
	h 29	1.76	1.62	1.45	1.26	1.03	0.79	0.53	0.27	0.03	0.26	0.51	0.74	0.95	1.17	1.29	1.42	1.53
	h 31	1.49	1.58	1.63	1.66	1.67	1.64	1.58	1.50	1.39	1.25	1.09	0.90	0.69	0.43	0.24	0.06	0.24
Phase *C*	THD_I	27.87	28.40	28.94	29.49	30.06	30.64	31.24	31.85	32.47	33.12	33.77	34.44	35.13	35.84	36.56	37.29	38.05
	h 5	22.36	23.02	23.67	24.30	24.90	25.50	26.06	26.60	27.11	27.58	28.02	28.42	28.78	29.09	29.35	29.56	29.71
	h 7	10.87	10.50	10.07	9.58	9.03	8.41	7.73	6.98	6.18	5.29	4.36	3.35	2.29	1.16	0.08	1.24	2.52
	h 11	8.34	8.81	9.22	9.55	9.81	9.99	10.07	10.06	9.95	9.72	9.40	8.95	8.40	7.74	6.97	6.10	5.12
	h 13	5.75	5.34	4.85	4.27	3.61	2.86	2.04	1.15	0.22	0.79	1.81	2.85	3.88	4.90	5.87	6.79	7.64
	h 17	4.62	4.99	5.26	5.42	5.47	5.39	5.18	4.80	4.37	3.76	3.05	2.23	1.33	0.37	0.65	1.66	2.66
	h 19	3.56	3.18	2.69	2.10	1.43	0.69	0.15	0.94	1.77	2.57	3.32	3.99	4.56	4.99	5.26	5.36	5.28
	h 23	2.82	3.11	3.28	3.32	3.22	2.97	2.59	2.08	1.47	0.76	0.02	0.79	1.56	2.26	2.88	3.36	3.67
	h 25	2.3	1.96	1.52	0.98	0.38	0.29	0.93	1.56	2.12	2.59	2.93	3.11	3.12	2.94	2.59	2.06	1.40
	h 29	1.76	1.98	2.07	2.02	1.84	1.52	1.09	0.57	0.01	0.60	1.16	1.64	2.01	2.22	2.26	2.11	1.78
	h 31	1.49	1.21	0.83	0.38	0.13	0.62	1.08	1.46	1.74	1.87	1.85	1.66	1.32	0.85	0.29	0.32	0.91

Table-4.28(b): Non-characteristic harmonic current components with increasing VUF or 2-ϕ unequal angle unbalance in phase *B* and *C* - two phasors moving in same direction

		VUF = 0.0 %	VUF = 1.0 %	VUF = 2.0 %	VUF = 3.0 %	VUF = 4.0 %	VUF = 5.0 %	VUF = 6.0 %	VUF = 7.0 %	VUF = 8.0 %	VUF = 9.0 %	VUF = 10.0 %	VUF = 11.0 %	VUF = 12.0 %	VUF = 13.0 %	VUF = 14.0 %	VUF = 15.0 %	VUF = 16.0 %
Phase *A*	THD_I	27.87	27.60	27.34	27.07	26.80	26.53	26.25	25.98	25.70	25.42	25.13	24.85	24.56	24.31	23.97	23.67	23.36
	h 3	0.01	0.64	1.27	1.88	2.47	3.05	3.62	4.16	4.68	5.19	5.67	6.13	6.57	7.00	7.38	7.75	8.09
	h 9	0.01	0.43	0.85	1.26	1.66	2.06	2.44	2.81	3.16	3.50	3.82	4.13	4.42	4.64	4.96	5.20	5.44
	h 15	0.01	0.37	0.73	1.09	1.43	1.77	2.10	2.41	2.71	3.00	3.26	3.52	3.76	3.94	4.18	4.35	4.50
	h 21	0.01	0.31	0.62	0.92	1.21	1.50	1.77	2.03	2.28	2.51	2.71	2.89	3.03	3.13	3.21	3.24	3.22
	h 27	0.01	0.25	0.49	0.74	0.98	1.21	1.43	1.63	1.81	1.96	2.07	2.15	2.17	2.16	2.08	1.95	1.78
	h 33	0.01	0.18	0.37	0.56	0.74	0.92	1.08	1.22	1.33	1.40	1.43	1.41	1.35	1.25	1.09	0.90	0.69
Phase *B*	THD_I	27.87	27.62	27.37	27.13	26.90	26.67	26.45	26.23	26.03	25.82	25.62	25.42	25.22	24.98	24.84	24.66	24.47
	h 3	0.01	0.71	1.39	2.06	2.71	3.36	3.98	4.59	5.17	5.75	6.30	6.84	7.35	7.84	8.32	8.78	9.21
	h 9	0.01	0.46	0.90	1.33	1.73	2.12	2.48	2.83	3.15	3.45	3.73	3.99	4.23	4.51	4.65	4.84	5.02
	h 15	0.0	0.41	0.80	1.18	1.53	1.86	2.18	2.47	2.74	2.99	3.22	3.43	3.63	3.85	3.98	4.14	4.28
	h 21	0.0	0.36	0.70	1.02	1.33	1.61	1.87	2.10	2.31	2.50	2.67	2.81	2.94	3.06	3.12	3.18	3.22
	h 27	0.0	0.30	0.58	0.85	1.10	1.32	1.52	1.69	1.83	1.94	2.02	2.08	2.12	2.13	2.11	2.07	2.00
	h 33	0.0	0.24	0.47	0.68	0.86	1.02	1.15	1.25	1.32	1.37	1.38	1.37	1.34	1.27	1.20	1.10	0.96
Phase *C*	THD_I	27.87	28.40	28.94	29.49	30.06	30.64	31.24	31.85	32.47	33.12	33.77	34.44	35.13	35.84	36.56	37.29	38.05
	h 3	0.01	0.70	1.43	2.19	2.97	3.79	4.64	5.52	6.42	7.35	8.31	9.31	10.32	11.36	12.45	13.54	14.67
	h 9	0.01	0.86	1.74	2.63	3.54	4.47	5.39	6.30	7.20	8.08	8.92	9.72	10.47	11.17	11.79	12.34	12.81
	h 15	0.01	0.79	1.58	2.37	3.14	3.89	4.58	5.20	5.73	6.17	6.49	6.68	6.73	6.63	6.38	5.97	5.41
	h 21	0.0	0.68	1.35	1.99	2.58	3.10	3.52	3.81	3.96	3.95	3.78	3.45	2.96	2.32	1.56	0.71	0.24
	h 27	0.0	0.55	1.08	1.57	1.97	2.27	2.44	2.45	2.31	2.00	1.56	0.99	0.35	0.38	1.06	1.71	2.25
	h 33	0.0	0.42	0.82	1.16	1.40	1.52	1.50	1.35	1.06	0.66	0.19	0.34	0.82	1.24	1.54	1.68	1.65

4.11.3 Comparison of Four Different Definitions of Voltage Unbalance

The numerical values of two IEEE definitions of voltage unbalance, PVUR1 and PVUR are always zero for the cases of voltage unbalance caused by phase angle movement (either CW or ACW). For the case of increasing angle between two voltage phasors caused by their movement in opposite directions, the VUF happens to be always little higher than LVUR, since the beginning of unbalance in voltage source. Similarly for the case of unbalance due to movement of two voltage phasors in same direction the same set of values of VUF and LVUR is observed. The plot of these values of VUF and LVUR with respect to their corresponding values of V_1 is displayed in Fig. 4.39. As the degree of unbalance increases, the difference between VUF and LVUR also increases.

In both cases there is one angle between two specific phasors (between *A* and *B*, for the case of movement in opposite direction, and between *B* and *C*, in case of movement in same direction) which is going beyond 120° and in both the cases it has the equal numerical value, as given in Table-4.24 and Table-4.26. Correspondingly, the angle between phasors *A* and *B* along with the angle between phasors A and C, for the case of movement in opposite direction are equivalent to angle between phasors *B* and *C*, together with angle between phasors *A* and *C*. This identical phase angle orientation leads to the equal values of definitions of voltage unbalance.

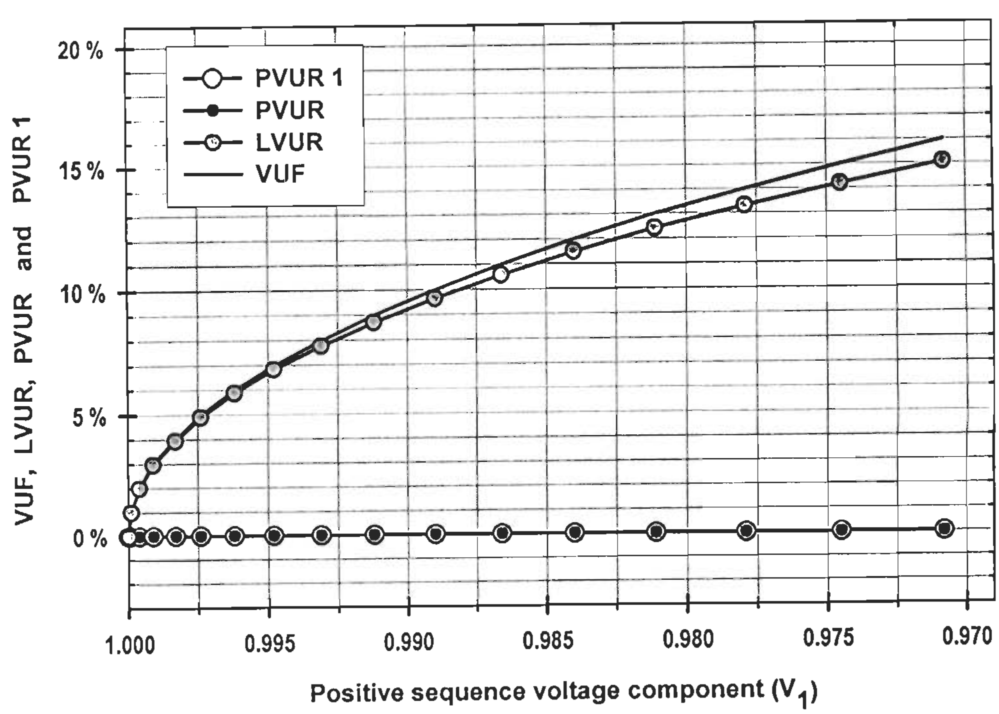

Fig. 4.39: **Comparison of four different definitions of voltage unbalance for the case of unbalance due to two-phase angle movement for unequal change in angles**

4.11.4 Effect of Voltage Unbalance on DC Parameters

Despite the fact that both cases have different phase angle position of phasors, due to identical phase angle orientation (as discussed in section 4.11.3), V_1 and V_2 are found typically same for a given VUF. This variation of V_1 and V_2 is presented in Table-4.24 and Table-4.26, and also depicted in Fig. 4.40 as a function of VUF. Due to this equal value of V_1 and V_2 for both the cases for a given value of VUF, the DC output parameters (magnitude and distortion) are also found identical, as shown in Table-4.24 and Table-4.26. With the increasing VUF, change in V_1 is very small (i.e., almost negligible) and the same reflects on the change in magnitude of DC output parameters as apparent in Fig. 4.41. The change in DC output magnitude is observed to be in ratio of variation in V_1.

The increase in V_2 is found to be proportional to increasing VUF. The distortion of DC output parameters is affected by this increasing V_2 and consequently the distortion is observed to be increasing proportionally to the increasing VUF. This variation in distortion of DC output parameters with increasing VUF is shown in Fig. 4.42.

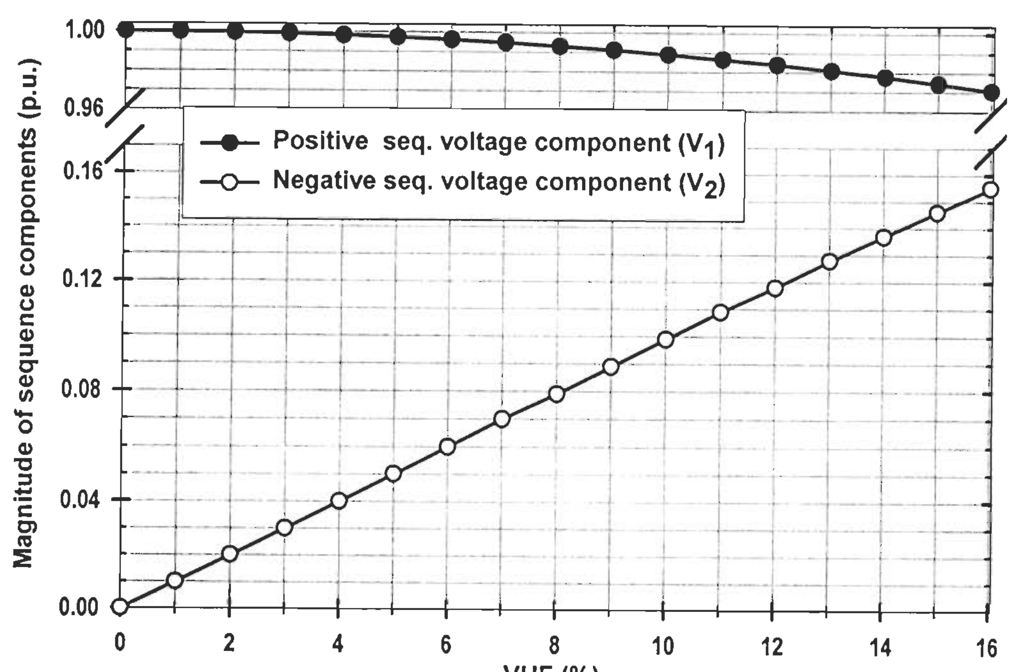

Fig. 4.40: Variation of V_1 and V_2 as a function of VUF for the case of unbalance due to two-phase angle movement for unequal change in angles

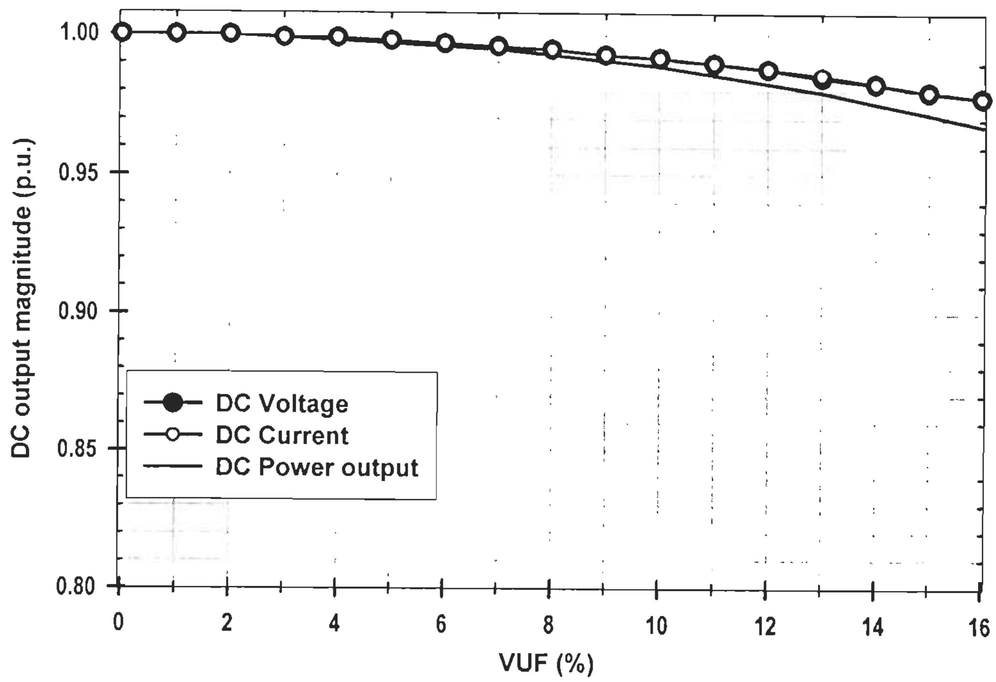

Fig. 4.41: Variation of magnitude of DC output parameters as a function of VUF, for the case of unbalance due to two-phase angle movement for unequal change in angles

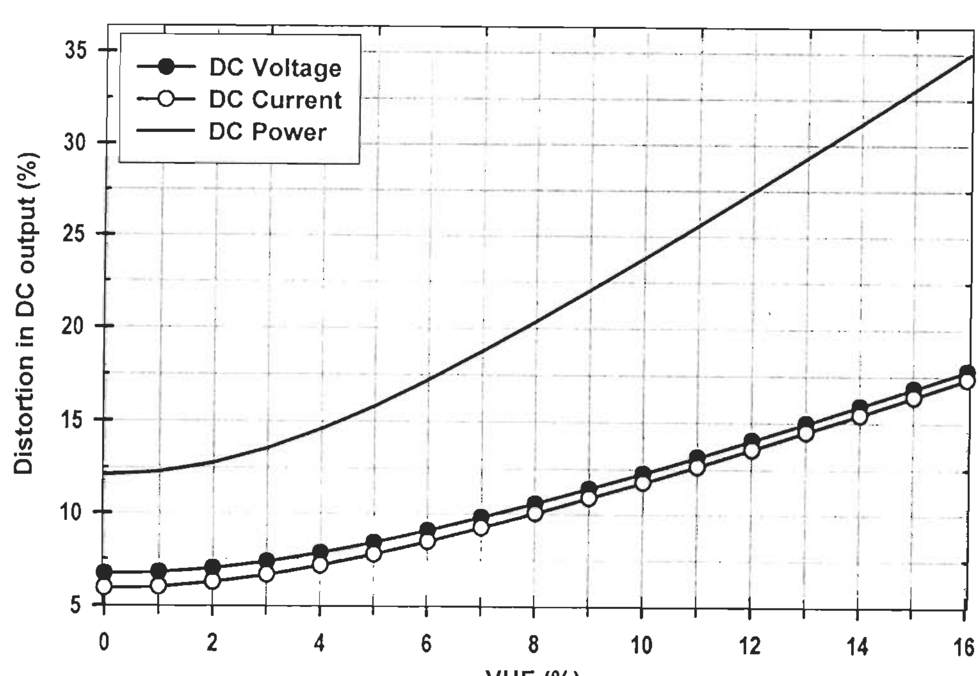

Fig. 4.42: Variation in distortion of DC output parameters, as a function of VUF for the case of unbalance due to two-phase angle movement for unequal change in angles

4.11.5 Effect of Voltage Unbalance on AC Parameters

It can be seen from Table-4.24, and Table-4.26 that current waveforms of all three phases (I_A, I_B, and I_C) are affected under two-phase voltage unbalance condition because of unequal change in their phase angle positions irrespective of direction of movement. Despite the fact that the both cases show the identical phasor orientation, which results in similar V_1 and V_2 and, therefore, equal magnitude and distortion of DC output parameters, still they affect the AC parameters in different manner.

Analysis of these two cases is presented here using the results of single-phase angle movement, as discussed in section 4.7.5. In case of CW movement of voltage phasor, as shown in Table-4.7 and Table-4.8, AC parameters (i.e. rms load current and THD_I) are almost constant for phasor under movement, THD_I increases (and rms load current decreases) for phase towards which it is moving, whereas THD_I decreases (and rms load current increases) for the phase from which it is moving away. For ACW movement of voltage phasor, as presented in Table-4.9 and Table-4.10, it is apparent that for phasor under movement, THD_I slightly increases whilst rms load current decreases a bit (not constant as in case CW phasor movement). For other two phases the change in AC performance parameters, are found same as discussed for the case of CW movement of voltage phasor. These conclusions are also applicable here in both cases, where the voltage phasor *A* is considered as reference phasor.

In case of voltage phasors *B* and *C* moving in opposite direction with unequal change in their angle positions as considered in Table-4.24, it is shown that the rms load current decreases and THD_I increases in the phase (*A*) towards which, both the phasors under movement are approaching whereas the phasors under movement (*B* and *C*) experience very small change in their values of AC performance parameters (i.e. rms load current and THD_I). The changes in THD_I and load current are due to the collective contribution of phasors under movement.

In consequence of CW movement of phasor *C*, THD_I and rms load current of phase *C* are almost constant and THD_I of phase *B* decreases (as *C* is moving away from *B*). Due to ACW movement of phasor *B*, THD_I of phase *B* increases slightly and THD_I of phase C decreases (as *B* is moving away from *C*). It explains that both phasors under movement (*B* and *C*) are reducing the THD_I of each other, but the phasor under ACW movement (*B*) is having a higher value of THD_I (and lower value of load current) in comparison to phasor under CW movement (*C*). This change in rms values of load currents in three different phases with variable VUF is displayed in Fig. 4.43(a) whereas variation in THD_I of three different phases as a function of VUF is presented in Fig. 4.43(b).

The comparable rationalization of results is also applicable for the case movement of voltage phasors *B* and *C* in 'same direction' (both CW) with unequal change in their angle positions as considered in Table-4.26. Here, phasor *C* is moving towards reference phasor *A* while phasor *C* is moving away from reference phasor *A*. Here it is important to mention that the contribution of phasor *B* is more for unbalance condition in comparison to phasor *C*, thus in analysis of this specific condition (unequal change in phase angle) it is also important to recognize the dominant role of phasor *B*. The CW movement of Phasor *C* does not affect its own AC performance parameters (rms load current and THD_I) while it increases the THD_I (decreases the load current) in phase *A* and decreases the THD_I (increases the load current) in phase *B*. Likewise the CW movement of Phasor *B* does not affect its own AC performance parameters, increases the THD_I (decreases the load current) in phase *C* and decreases the THD_I (increases the load current) in phase A. In conclusion, THD_I increases (load current decreases) for phase *C*, as for phase *A* THD_I decreases (load current increases) due to the dominant contribution of movement of phase *B*; and for phase *B* THD_I decreases (load current increases) by a comparatively lesser amount of 'change in initial values' due to minor contribution of movement of phase C. This change in rms values of load currents in three different phases with variable VUF is displayed in Fig. 4.44(a) whereas variation in THD_I of three different phases as a function of VUF is presented in Fig. 4.44(b). The more clear view of individual and net impact of changes in position of phasor *B* and phasor *C*, on the THD_I of phases *A*, *B* and *C*, are given respectively in Table-4.29(a), Table-4.29(b), and Table-4.29(c), in which the actual THD_I value comes from Table-4.261 and estimated THD_I value is calculated using the results presented in Table-4.25(a) and Table-4.25(b).

PTHDUF simplifies the harmonic current analysis and quantization of voltage source unbalance in presence of harmonic distortion. For a particular type of voltage unbalance, the value of VUF remains unchanged regardless of the phase being affected by voltage unbalance. Furthermore, the values of PTHDUF are found to be quite distinctive for both cases (i.e., the two phasors movement in opposite direction and in same direction with unequal change in the position of both phasors) for a given value of VUF, as presented in Table-4.24, and Table-4.26. Variation of average THD_I and PTHDUF as a function of VUF is depicted and compared in Fig. 4.45 for the cases of unequal movement of two voltage phasors in opposite direction, and in same direction, where it is also observed that for the same value of VUF, the PTHDUF has its value somewhat higher for the case of movement in 'same direction' between two voltage phasors than the case of movement in 'opposite direction' between two voltage phasors, which makes the PTHDUF a reasonably effective index for the type (opposite /same direction) and degree (VUF) of voltage unbalance.

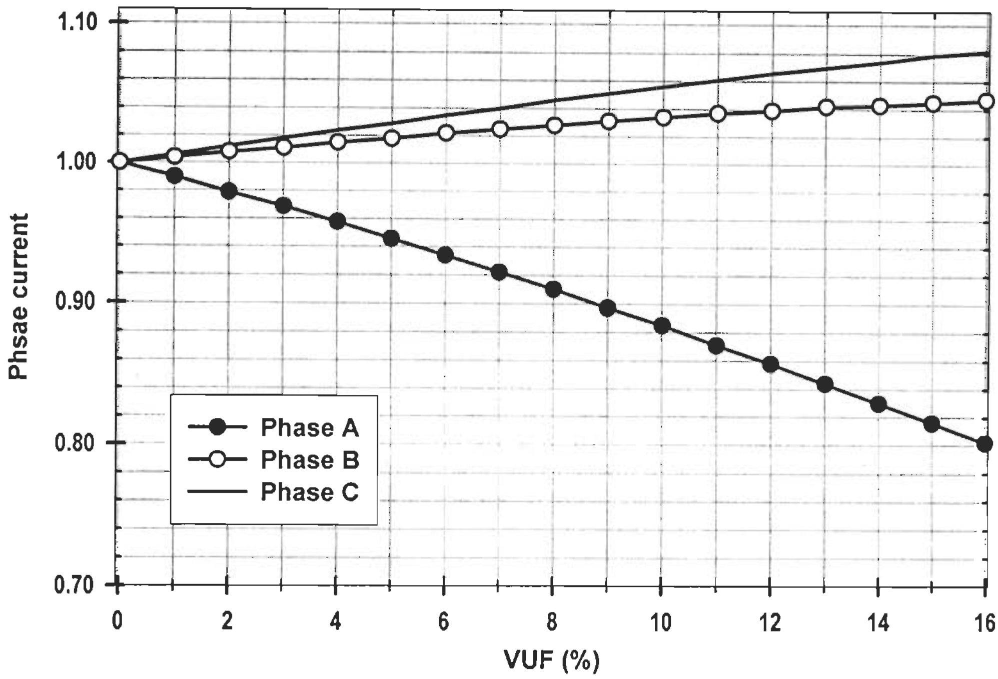

Fig. 4.43(a): **Variation in rms phase currents in three different phases as a function of VUF for the case of unequal movement of voltage phasors *B* and *C* in opposite direction**

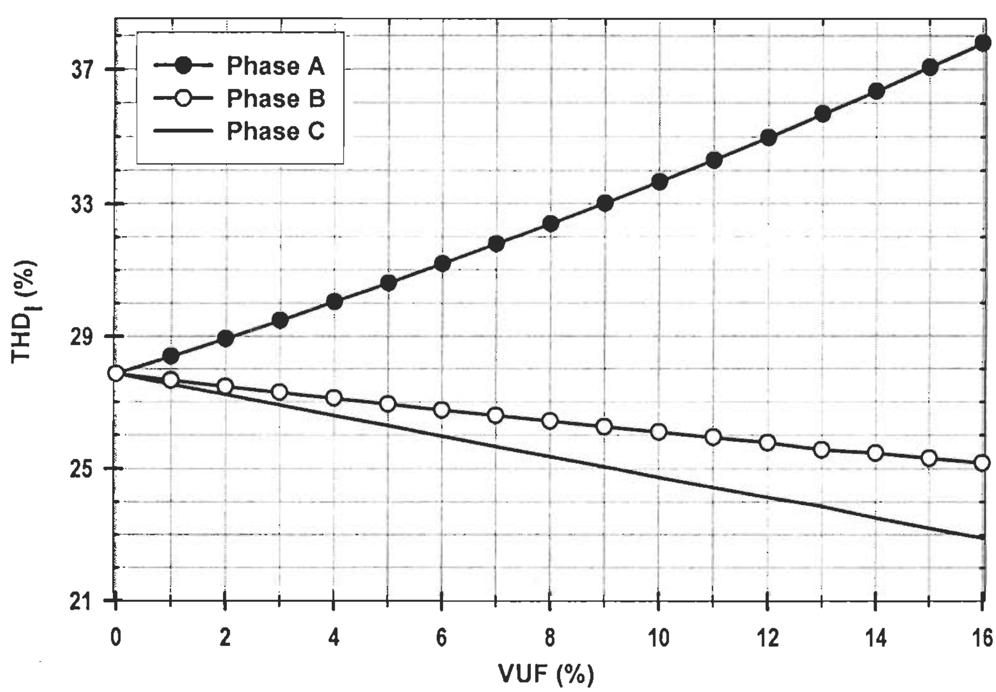

Fig. 4.43(b): **Variation in THD$_I$ of currents in three different phases as a function of VUF for the case of unequal movement of voltage phasors *B* and *C* in opposite direction**

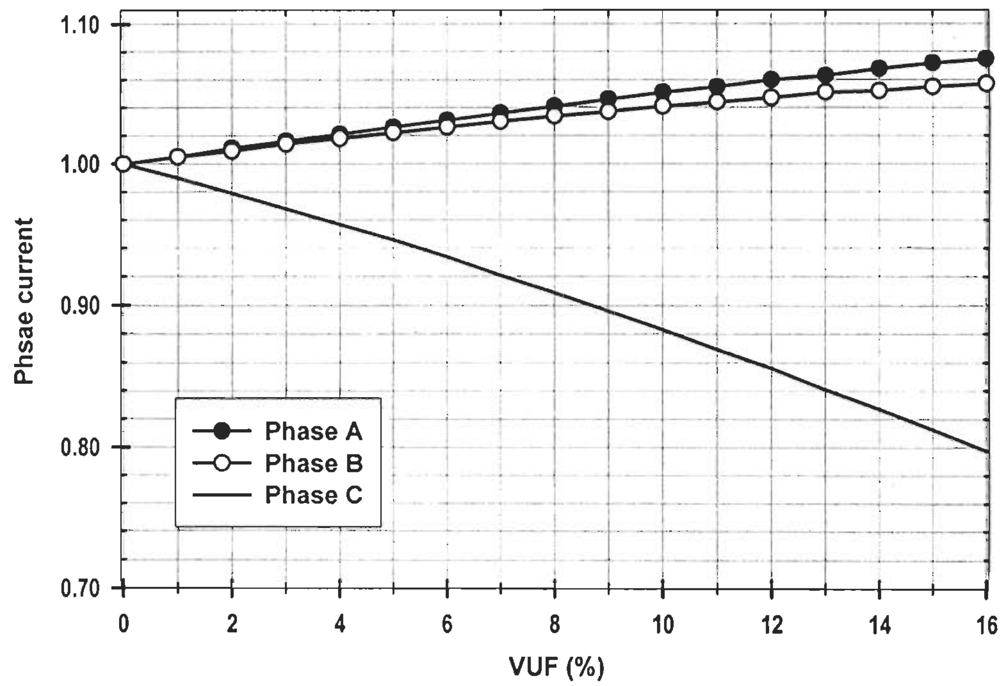

Fig. 4.44(a): Variation in rms phase currents in three different phases as a function of VUF for the case of unequal movement of voltage phasors *B* and *C* in same direction

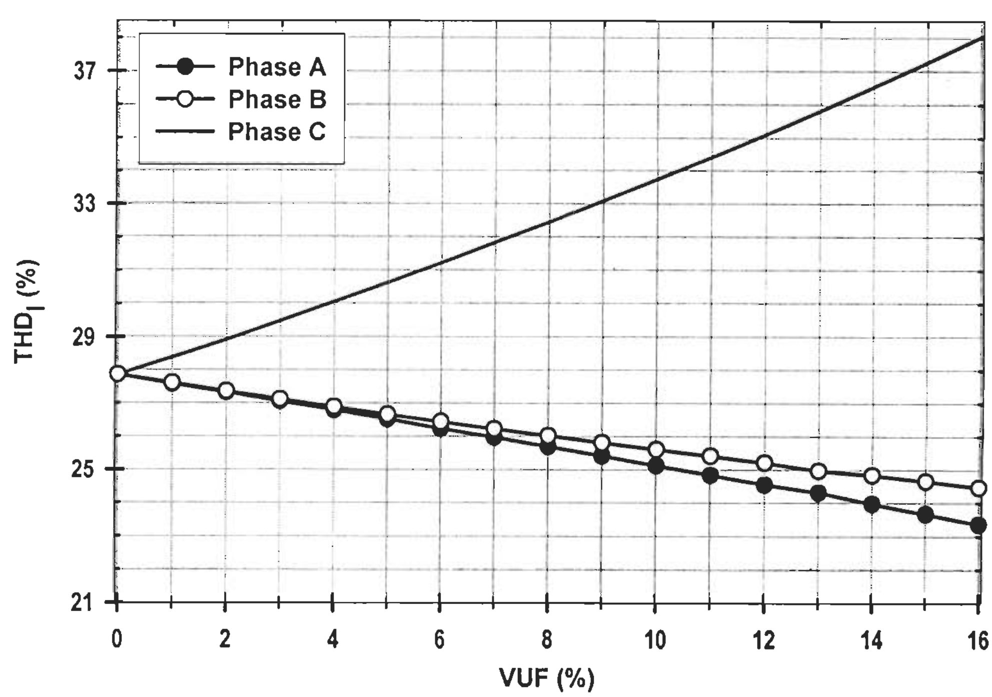

Fig. 4.44(b): Variation in THD_I of currents in three different phases as a function of VUF for the case of unequal movement of voltage phasors *B* and *C* in same direction

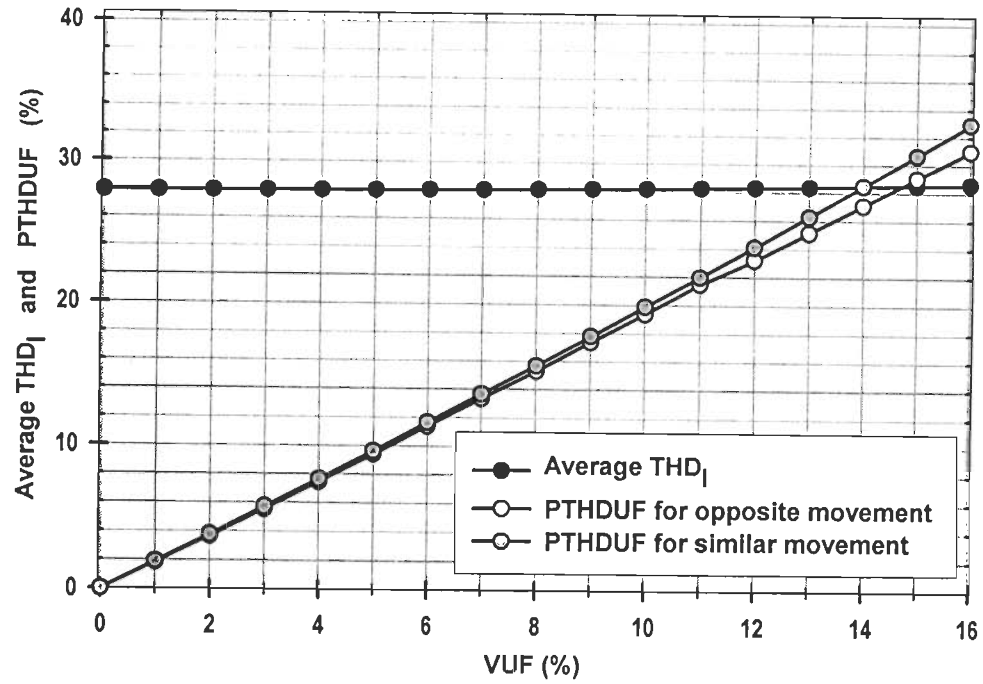

Fig. 4.45: **Comparison of variation in average THD$_I$ and PTHDUF with increasing VUF for the case of unbalance due to two-phase angle unequal movement in opposite and similar direction**

Table-4.29 (a): Effect of movement of phasors *B* and *C* on THD$_I$ of phase *A*

Effect of CW movement of Phase *B*	Effect of CW movement of Phase *C*	Actual Effect	Estimated Effect	Actual THD$_I$ Value	Estimated THD$_I$ Value
0.00	0.00	-0.00	-0.00	27.87	27.87
-0.48	0.25	-0.27	-0.23	27.60	27.64
-0.98	0.49	-0.53	-0.49	27.34	27.38
-1.48	0.73	-0.80	-0.75	27.07	27.12
-1.97	0.97	-1.07	-1.00	26.80	26.87
-2.47	1.22	-1.34	-1.25	26.53	26.62
-2.96	1.46	-1.62	-1.50	26.25	26.37
-3.46	1.71	-1.89	-1.75	25.98	26.12
-3.95	1.96	-2.17	-1.99	25.70	25.88
-4.44	2.21	-2.45	-2.23	25.42	25.64
-4.93	2.47	-2.74	-2.46	25.13	25.41
-5.42	2.73	-3.02	-2.69	24.85	25.18
-5.91	2.99	-3.31	-2.92	24.56	24.95
-6.41	3.25	-3.56	-3.16	24.31	24.71
-6.90	3.51	-3.90	-3.39	23.97	24.48
-7.39	3.78	-4.20	-3.61	23.67	24.26
-7.88	4.05	-4.51	-3.83	23.36	24.04

Table-4.29 (b): Effect of movement of phasors *B* and *C* on THD_I of phase *B*

Effect of CW movement of Phase *B*	Effect of CW movement of Phase *C*	Actual Effect	Estimated Effect	Actual THD_I Value	Estimated THD_I Value
-0.00	0.00	0.00	0.00	27.87	27.87
-0.02	-0.20	-0.25	-0.22	27.62	27.65
-0.04	-0.41	-0.50	-0.45	27.37	27.42
-0.06	-0.63	-0.74	-0.69	27.13	27.18
-0.07	-0.84	-0.97	-0.91	26.90	26.96
-0.08	-1.06	-1.20	-1.14	26.67	26.73
-0.07	-1.27	-1.42	-1.34	26.45	26.53
-0.06	-1.48	-1.64	-1.54	26.23	26.33
-0.05	-1.69	-1.84	-1.74	26.03	26.13
-0.02	-1.89	-2.05	-1.91	25.82	25.96
0.01	-2.10	-2.25	-2.09	25.62	25.78
0.04	-2.31	-2.45	-2.27	25.42	25.60
0.09	-2.51	-2.65	-2.42	25.22	25.45
0.14	-2.71	-2.89	-2.57	24.98	25.30
0.19	-2.91	-3.03	-2.72	24.84	25.15
0.25	-3.12	-3.21	-2.87	24.66	25.00
0.32	-3.32	-3.40	-3.00	24.47	24.87

Table-4.29 (c): Effect of movement of phasors *B* and *C* on THD_I of phase *C*

Effect of CW movement of Phase *B*	Effect of CW movement of Phase *C*	Actual Effect	Estimated Effect	Actual THD_I Value	Estimated THD_I Value
0.00	0.00	0.00	0.00	27.87	27.87
0.57	0.00	0.53	0.57	28.40	28.44
1.13	-0.01	1.07	1.12	28.94	29.00
1.71	-0.02	1.62	1.69	29.49	29.58
2.31	-0.03	2.19	2.28	30.06	30.18
2.93	-0.04	2.77	2.89	30.64	30.80
3.58	-0.05	3.37	3.53	31.24	31.45
4.24	-0.06	3.98	4.18	31.85	32.11
4.92	-0.07	4.60	4.85	32.47	32.79
5.64	-0.07	5.25	5.57	33.12	33.51
6.37	-0.07	5.90	6.30	33.77	34.24
7.14	-0.08	6.57	7.06	34.44	35.01
7.93	-0.08	7.26	7.85	35.13	35.80
8.76	-0.08	7.97	8.68	35.84	36.63
9.60	-0.07	8.69	9.53	36.56	37.47
10.48	-0.07	9.42	10.41	37.29	38.35
11.40	-0.07	10.18	11.33	38.05	39.27

4.12 EIGHT DIFFERENT UNBALANCE CASES WITH SAME DEGREE OF UNBALANCE

There are many possible voltage unbalance conditions in a power system. In this study, the eight cases of source voltage unbalance have been considered. These cases are 3-phase under-voltage unbalance (3-Φ UV), 2-phase under-voltage unbalance (2-Φ UV), 1-phase under-voltage unbalance (1-Φ UV), 2-phase unequal angle Unbalance (2-Φ A), 1-phase angle Unbalance (1-Φ A), 1-phase over-voltage unbalance (1-Φ OV), 2-phase over-voltage unbalance (2-Φ OV), and 3-phase over-voltage unbalance(3-Φ OV). The variation of different harmonic components and total harmonic distortion are analyzed for all the eight cases of voltage unbalances listed above with varying VUF of 4 %, 8 %, 12 % and 16 %. These different thirty two cases have been studied to find out the importance of sequence voltage components in voltage unbalance analysis, and how these voltage unbalance conditions affect the pattern of characteristic harmonics and generation of non- characteristic harmonics.

Table-4.30 shows the comparison of performance of rectifier for the eight different voltage unbalance cases with VUF of 4 %, 8%, 12 % and 16 %, along with three-phase supply voltages, their positive and negative sequence components and comparison of values of four different definitions of voltage unbalance.

The conclusions obtained from this study are discussed in next sections.

Table-4.30: Comparison of four different definitions of voltage unbalance and performance of rectifier for eight different unbalance cases with VUF of 4%, 8%, 12% and 16 %

Type of Voltage Source	VUF	LVUR	PVUR 1	PVUR	V_A Mag.	V_A Angle	V_B Mag.	V_B Angle	V_C Mag.	V_C Angle	V_1 Positive seq. voltage	V_2 Negative seq. voltage	I_{DC} Mag.	I_{DC} Distortion (%)	V_{DC} Mag.	V_{DC} Distortion (%)	P_{DC} Mag.	P_{DC} Distortion (%)	THD_I (%) Phase A	THD_I (%) Phase B	THD_I (%) Phase C	Average THD_I (%)	PTHDUF (%)
Balanced	0.00	0.00	0.00	0.00	1.00	0	1.00	240	1.00	120	1.000	0.000	1.000	5.95	1.000	6.72	1.000	12.13	27.87	27.87	27.87	27.87	0.00
3-ϕ UV	3.98	3.96	12.94	7.85	***0.87***	0	***0.89***	240	***0.98***	120	0.913	0.036	0.913	7.14	0.913	7.82	0.834	14.48	29.13	28.73	25.89	27.92	7.26
2-ϕ UV	4.00	3.99	12.92	7.90	***0.88***	0	***0.90***	240	1.00	120	0.927	0.037	0.927	7.15	0.927	7.83	0.860	14.50	29.11	28.77	25.88	27.92	7.31
1-ϕ UV	3.98	3.94	11.95	7.97	***0.89***	0	1.00	240	1.00	120	0.962	0.038	0.962	7.17	0.962	7.85	0.926	14.59	30.05	26.95	26.75	27.92	7.64
2-ϕ Ang.	4.00	3.96	0.00	0.00	1.00	0	1.00	***231.9***	1.00	***116***	0.998	0.040	0.999	7.18	0.999	7.86	0.998	14.61	26.94	26.76	30.06	27.92	7.66
1-ϕ Ang.	4.02	3.54	0.00	0.00	1.00	0	1.00	240	1.00	***113.1***	0.998	0.040	0.999	7.17	0.999	7.85	0.998	14.57	29.82	26.16	27.78	27.92	6.81
1-ϕ OV	4.00	4.04	12.02	8.01	***1.13***	0	1.00	240	1.00	120	1.042	0.042	1.042	7.15	1.042	7.83	1.087	14.49	25.88	28.82	29.06	27.92	7.31
2-ϕ OV	4.00	3.64	13.79	7.35	***1.15***	0	***1.09***	240	1.00	120	1.079	0.043	1.080	7.17	1.080	7.85	1.167	14.57	26.32	27.51	29.93	27.92	7.20
3-ϕ OV	4.00	3.56	13.82	7.17	***1.17***	0	***1.10***	240	***1.02***	120	1.094	0.044	1.095	7.16	1.095	7.84	1.200	14.55	26.26	27.61	29.89	27.92	7.06
3-ϕ UV	8.00	7.75	25.68	15.85	***0.74***	0	***0.93***	240	***0.96***	120	0.877	0.070	0.878	10.05	0.878	10.60	0.773	20.39	32.38	26.55	25.28	28.07	15.35
2-ϕ UV	8.00	7.65	26.44	15.62	***0.76***	0	***0.95***	240	1.00	120	0.902	0.072	0.903	10.04	0.904	10.59	0.819	20.35	32.28	26.87	25.06	28.07	15.00
1-ϕ UV	8.00	7.82	24.00	16.00	***0.78***	0	1.00	240	1.00	120	0.926	0.074	0.927	10.06	0.927	10.61	0.863	20.42	32.47	26.05	25.68	28.07	15.69
2-ϕ Ang.	8.00	7.80	0.00	0.00	1.00	0	1.00	***223.54***	1.00	***112.7***	0.993	0.079	0.995	10.05	0.995	10.60	0.993	20.40	25.80	25.92	32.48	28.07	15.72
1-ϕ Ang.	8.00	7.16	0.00	0.00	1.00	0	1.00	240	1.00	***106.3***	0.994	0.080	0.995	9.94	0.995	10.49	0.994	20.04	31.90	24.53	27.78	28.07	13.64
1-ϕ OV	8.00	8.14	24.00	16.00	***1.26***	0	1.00	240	1.00	120	1.087	0.087	1.089	9.84	1.089	10.39	1.189	19.72	24.06	29.81	30.35	28.07	14.30
2-ϕ OV	8.00	8.09	25.38	15.90	***1.28***	0	***1.03***	240	1.00	120	1.105	0.088	1.107	9.84	1.107	10.40	1.228	19.74	24.10	29.36	30.77	28.08	14.16
3-ϕ OV	8.00	7.95	26.38	15.64	***1.31***	0	***1.08***	240	***1.01***	120	1.136	0.091	1.138	9.86	1.138	10.41	1.299	19.79	24.17	28.93	31.12	28.07	13.90
3-ϕ UV	12.00	11.23	40.13	23.21	***0.64***	0	***0.89***	240	***0.98***	120	0.839	0.101	0.841	13.53	0.842	14.01	0.715	27.32	34.71	26.57	23.65	28.31	22.61
2-ϕ UV	12.00	11.56	37.06	23.97	***0.67***	0	***0.98***	240	1.00	120	0.884	0.106	0.887	13.60	0.887	14.08	0.793	27.54	35.08	25.41	24.42	28.3	23.94
1-ϕ UV	12.00	11.58	36.01	24.01	***0.68***	0	1.00	240	1.00	120	0.893	0.107	0.896	13.61	0.896	14.08	0.812	27.55	35.13	25.14	24.65	28.31	24.11
2-ϕ Ang.	12.00	11.49	0.00	0.00	1.00	0	1.00	***215***	1.00	***109.8***	0.984	0.118	0.989	13.58	0.988	14.06	0.983	27.48	24.54	25.25	35.13	28.31	24.11
1-ϕ Ang.	12.00	10.89	0.00	0.00	1.00	0	1.00	240	1.00	***99.55***	0.986	0.118	0.989	13.29	0.989	13.77	0.986	26.58	34.15	22.97	27.85	28.32	20.57
1-ϕ OV	12.00	12.30	36.01	24.01	***1.41***	0	1.00	240	1.00	120	1.136	0.136	1.141	13.06	1.141	13.55	1.310	25.85	22.40	30.86	31.74	28.33	20.94
2-ϕ OV	12.00	12.28	37.16	23.97	***1.43***	0	***1.03***	240	1.00	120	1.152	0.138	1.157	13.06	1.156	13.55	1.346	25.86	22.42	30.5	32.1	28.34	20.89
3-ϕ OV	12.00	12.21	38.04	23.86	***1.48***	0	***1.08***	240	***1.02***	120	1.192	0.143	1.197	13.07	1.197	13.56	1.443	25.89	22.45	30.16	32.4	28.34	20.77
3-ϕ UV	16.00	15.97	53.18	31.1	***0.58***	0	***0.68***	240	***0.98***	120	0.746	0.119	0.750	16.57	0.750	17.02	0.570	32.50	34.00	31.00	21.00	28.67	26.74
2-ϕ UV	16.00	16.00	53.11	31.15	***0.60***	0	***0.69***	240	1.00	120	0.762	0.122	0.767	16.56	0.766	17.02	0.594	32.49	34.00	31.1	20.98	28.69	26.87
1-ϕ UV	16.00	15.21	48.01	32.00	***0.59***	0	1.00	240	1.00	120	0.862	0.138	0.868	17.42	0.868	17.86	0.763	35.12	38.04	24.20	23.63	28.62	32.90
2-ϕ Ang.	16.00	15.12	0.00	0.00	1.00	0	1.00	***206***	1.00	***105.6***	0.971	0.155	0.977	17.38	0.977	17.83	0.968	35.03	23.52	24.3	38.06	28.63	32.95
1-ϕ Ang.	16.02	14.73	0.00	0.00	1.00	0	1.00	240	1.00	***92.9***	0.975	0.156	0.981	16.83	0.981	17.28	0.975	33.33	36.57	21.47	28.00	28.68	27.51
1-ϕ OV	16.00	16.50	48.02	32.01	***1.57***	0	1.00	240	1.00	120	1.191	0.191	1.198	16.43	1.198	16.89	1.453	32.09	20.88	31.97	33.23	28.69	27.23
2-ϕ OV	16.00	16.46	49.68	31.94	***1.60***	0	***1.04***	240	1.00	120	1.216	0.195	1.224	16.43	1.224	16.89	1.515	32.12	20.90	31.4	33.8	28.70	27.18
3-ϕ OV	16.00	16.38	50.77	31.81	***1.66***	0	***1.10***	240	***1.02***	120	1.261	0.202	1.269	16.45	1.269	16.91	1.629	32.18	20.93	30.97	34.18	28.69	27.06

4.12.1 Comparison of Four Different Definitions of Voltage Unbalance

It is evident from the Table-4.30 that for a given value of VUF, LVUR has lowest value for 1-ϕ angle unbalance and highest value for 1-ϕ over-voltage unbalance. As for as 1-ϕ voltage unbalance (either under-voltage or over-voltage) is concerned, the magnitudes of PVUR1, PVUR, LVUR and VUF are seem to be in the ratio of 3:2:1:1.

For phase angle movement unbalance cases, for the same VUF, the LVUR is always higher for 2-ϕ phase angle movement unbalance case in comparison to 1-ϕ phase angle movement unbalance case. Comparison between the 1-ϕ angle unbalance cases and 1-ϕ under voltage (magnitude) unbalance cases, also concludes that LVUR is always little lower than VUF.

4.12.2 Effect of Voltage Unbalance on DC Parameters

As the VUF increases, the V_l decreases and V_2 increases, as shown in Fig. 4.46(a) for V_l and Fig. 4.46(b) for V_2. So far as the magnitude of V_l and V_2 is concerned, for the same VUF, these can be ranked in the order in which they are considered, from lower to higher magnitude (i.e. lowest for 3-ϕ UV and highest for 3-ϕ OV).

The effect of the voltage unbalance on rectifier output performance can be estimated by the V_l. Considering for all thirty two different cases, the rectifier output performance (DC voltage, V_{DC}, DC current, I_{DC}, and DC power, P_{DC}) is proportional to the magnitude of the V_l, as depicted in Fig. 4.47. For eight different unbalance cases, the variation of V_l with increasing VUF is shown in Fig. 4.48(a), whereas the variation of DC output voltage V_{DC}, and DC current, I_{DC} is depicted in Fig. 4.48(b), along with variation of DC output power P_{DC} in Fig. 4.48(c). It is apparent in Fig. 4.48(a) that the V_l decreases for phase-angle and under-voltage magnitude unbalance cases whereas, increases for over-voltage magnitude unbalance cases with rising VUF.

It is also evident from Table-4.30 that for a given value of VUF, the distortion in DC output parameters is almost constant and its difference from the distortion for the balanced voltage source case increases with increasing VUF as shown in Fig. 4.49(a) through Fig. 4.49(c), respectively. Also, the distortion in DC output parameters, as presented in Fig. 4.49 is found to be proportional to V_2 (Fig. 4.46(b)).

4.12.3 Effect of Voltage Unbalance on AC Parameters

It is clear from Table-4.30 that irrespective of nature and type of unbalance (either voltage magnitude or phase angle, single-phase or multi-phase), the current waveforms of all three phases (I_A, I_B, and I_C) and their total harmonic distortion (THD_I) are affected. For magnitude unbalance case, THD_I decreases for the phase in which voltage value is increased and vice-versa.

For a constant VUF, average value of THD_I is almost constant for all the eight cases of unbalance, as reflected from Table-4.30. Also, for a given value of VUF, the value of PTHDUF is approximately constant and is almost in direct proportion to the value of VUF for all the eight cases of voltage unbalance as shown in Fig. 4.50.

4.12.4 Analysis of Harmonic Pattern under Unbalanced Voltage Supply

The presence of voltage source unbalance has a strong effect on harmonic current components. Further analysis is carried out in order to study how VUF affects the harmonic pattern. The frequency spectra of the distorted waveforms are obtained using Fast Fourier Transform (FFT).

Table-4.31 presents the behavior of characteristic (5, 7, 11 and 13) and non-characteristic harmonics ("triplens" or 3, 9, 15), for all the three phases and for the different values of VUF (4 %, 8 %, 12 %, 16%). The percentages of harmonic components are based on considering the fundamental frequency current component as 100%.

It is clearly visible from Table-4.31 that, "triplens" magnitudes are zero at 0 % VUF (i.e., balanced voltage source). It indicates that unbalance in source voltage produces non-characteristic harmonics and their magnitude increases with increase in VUF. This increase in VUF also affects the characteristic harmonics, and the harmonic current components do not follow the same sequence arrangement as the balanced one. Fifth and eleventh harmonics are changing according the pattern of change in THD_I but changes in the seventh and thirteenth harmonic are opposite to it.

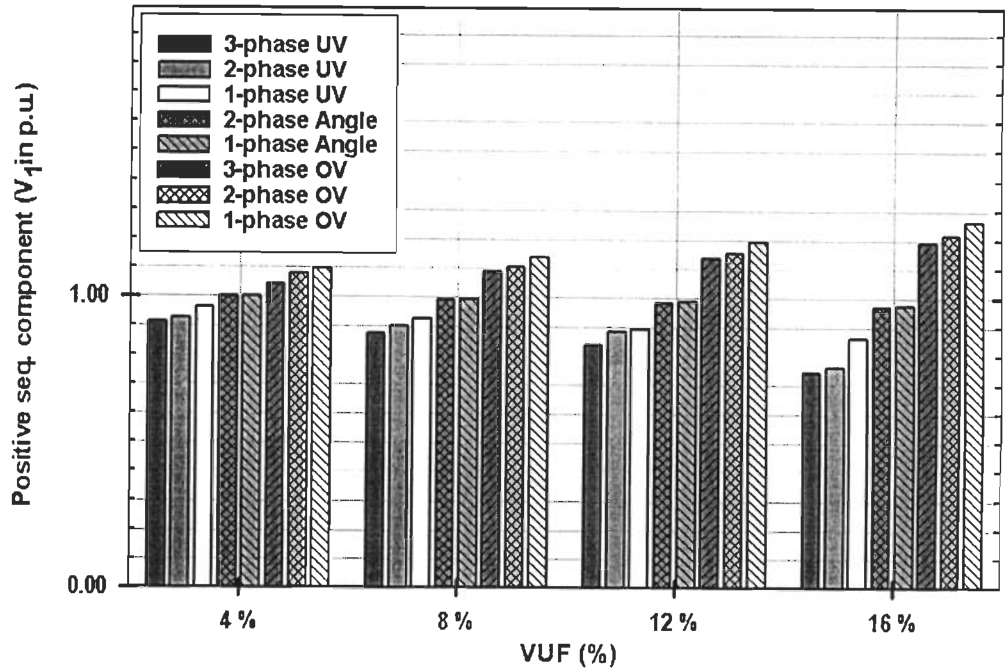

Fig. 4.46(a): Variation of positive sequence component with increasing VUF for eight different unbalance cases

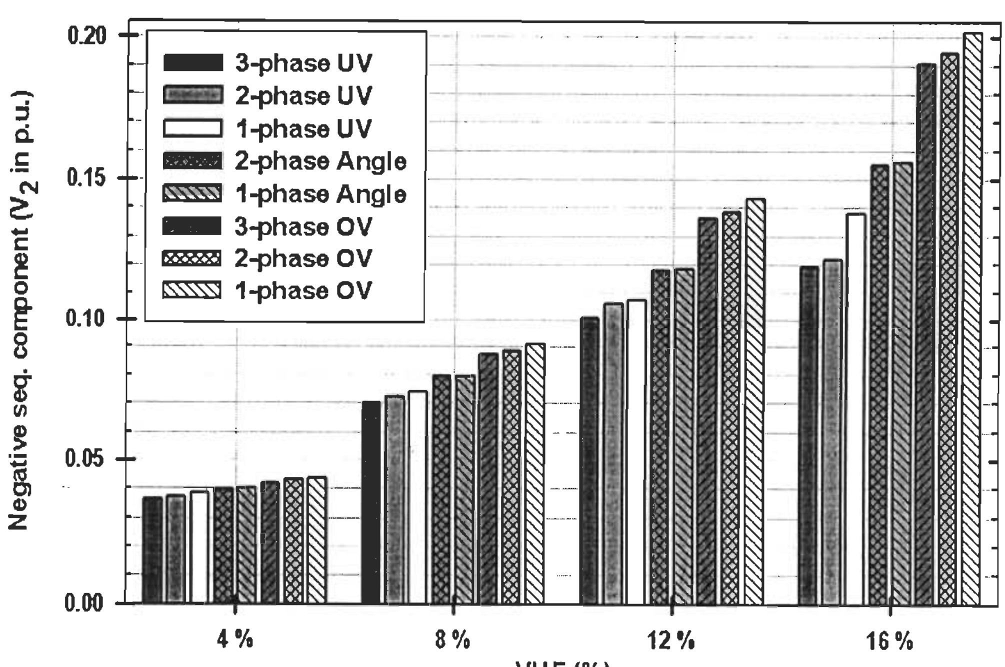

Fig. 4.46(b): Variation of negative sequence component with increasing VUF for eight different unbalance cases

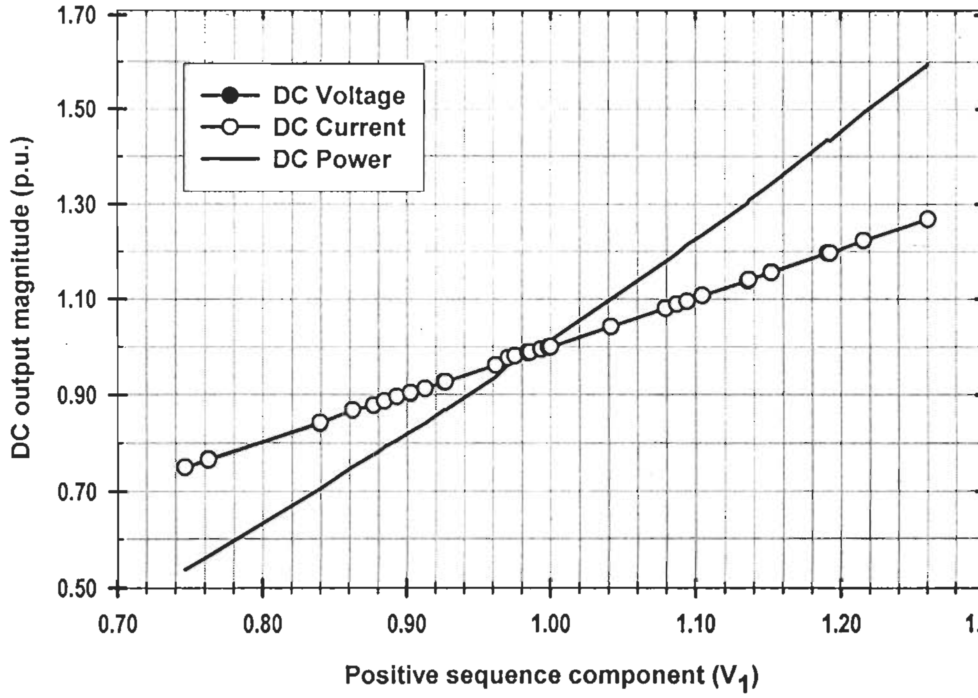

Fig. 4.47: Variation of magnitudes of DC output parameters relative to V_1. Plots for DC current and voltage are overlapped.

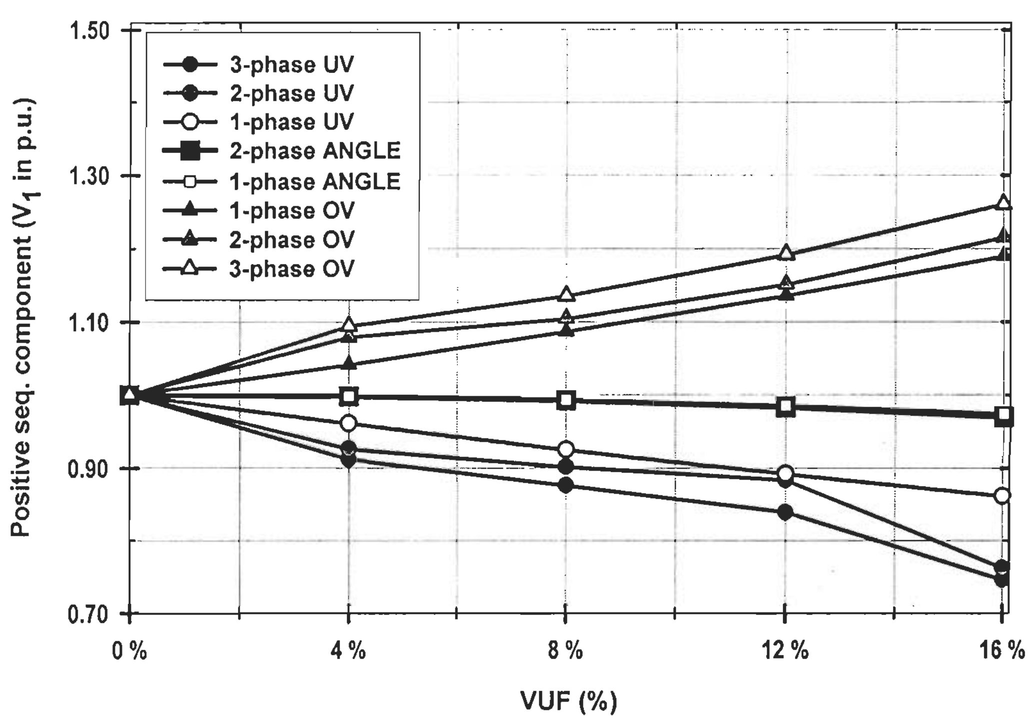

Fig. 4.48(a): Variation of V_1 with increasing VUF for eight different unbalance cases

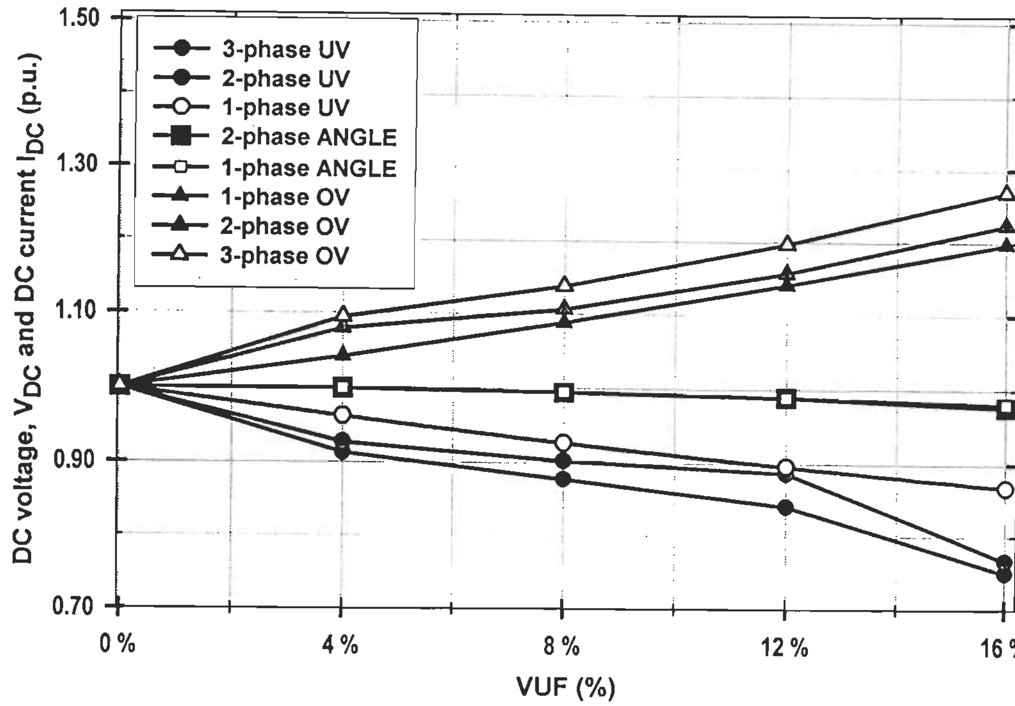

Fig. 4.48(b): **Variation of magnitude of DC current with increasing VUF for eight different unbalance cases**

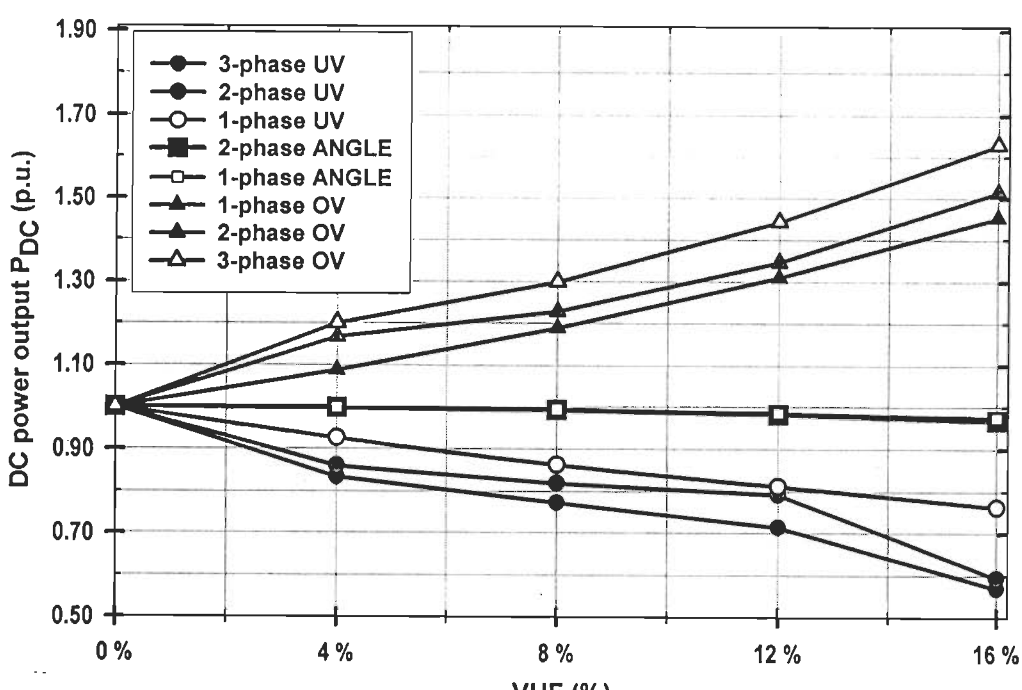

Fig.4.48(c): **Variation of magnitude of DC power output with increasing VUF for eight different unbalance cases**

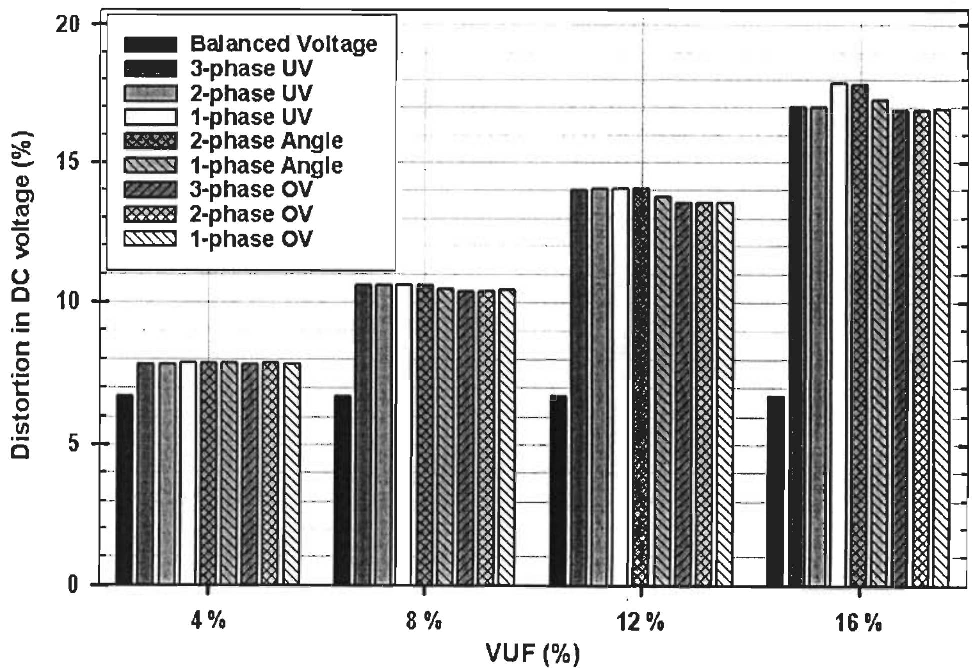

Fig. 4.49(a): Variation of distortion in DC voltage with increasing VUF for eight different unbalance cases

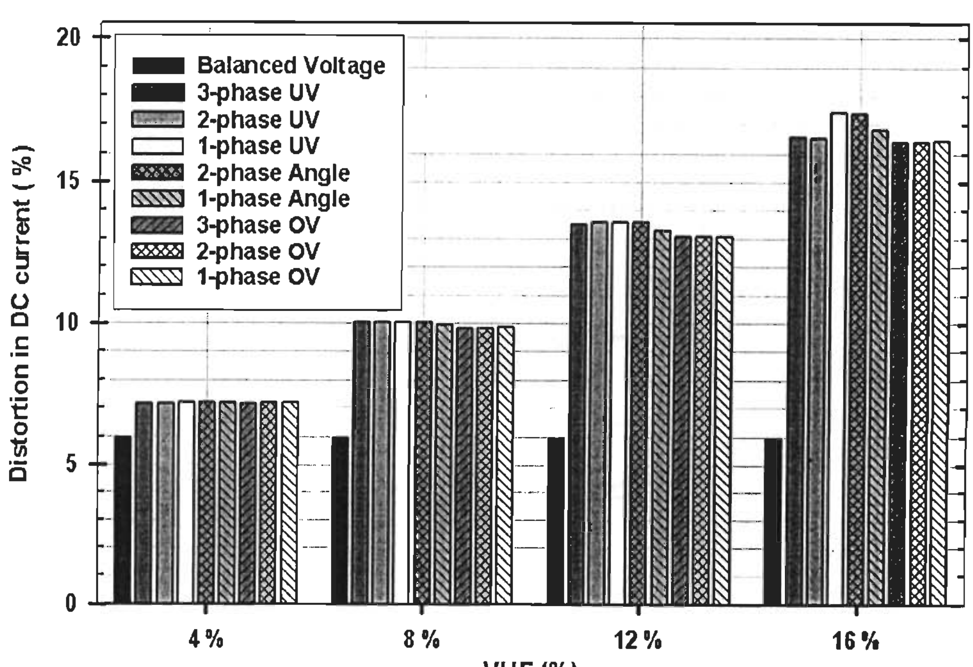

Fig. 4.49(b): Variation of distortion in DC current with increasing VUF for eight different unbalance cases

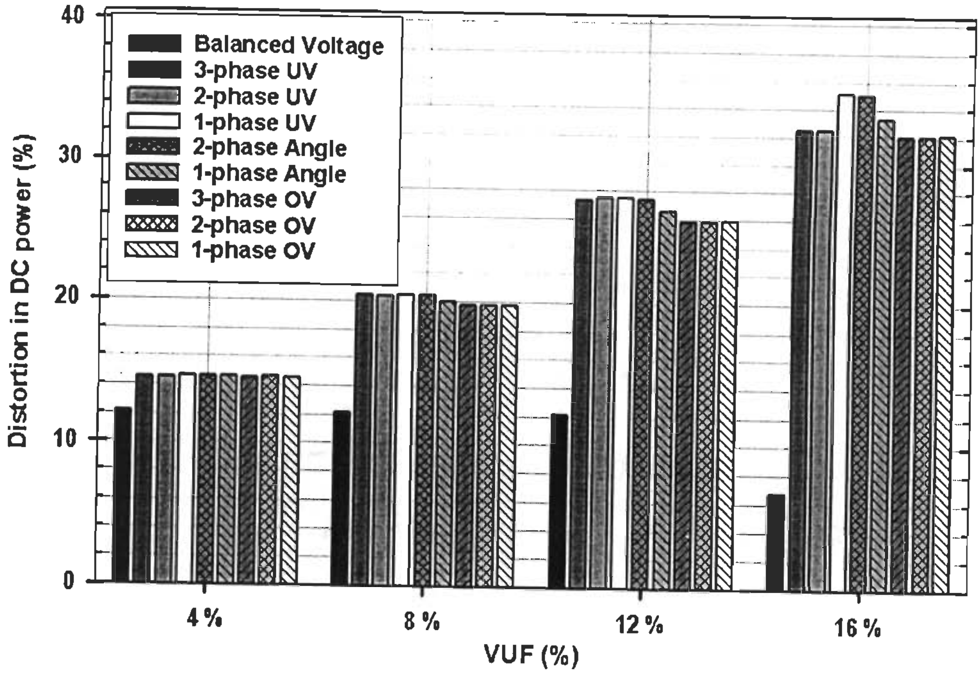

Fig. 4.49(c): Variation of distortion in DC power with increasing VUF for eight different unbalance cases

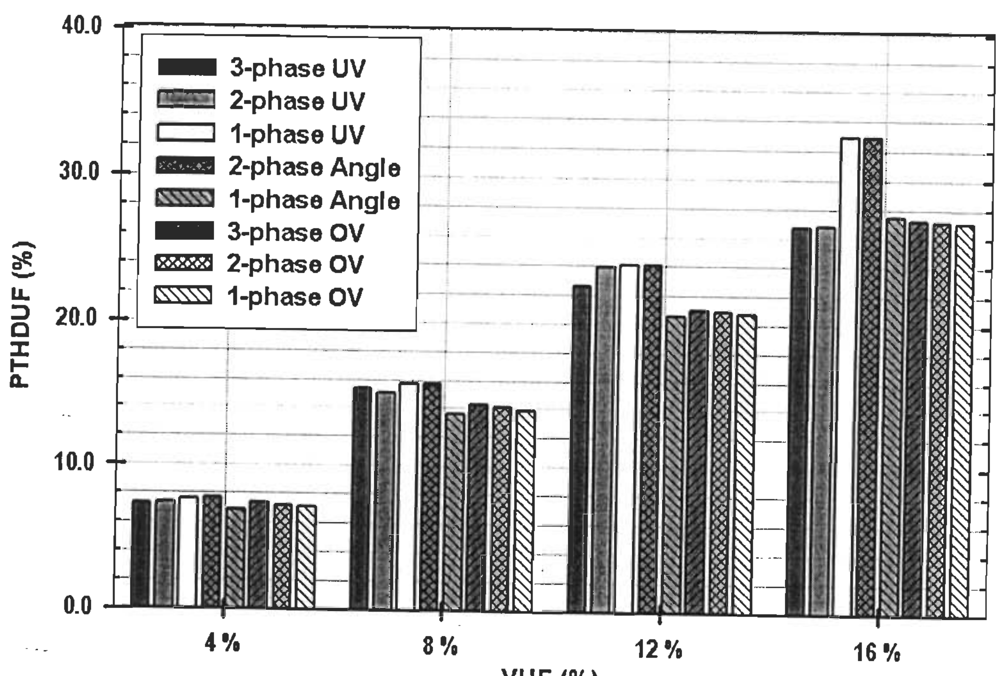

Fig. 4.50: Variation in the value of PTHDUF with increasing VUF for eight different unbalance cases

Table-4.31: Comparison of variation of THD_I and harmonic current components with increasing VUF

	→ VUF	Phase *A*					Phase *B*					Phase *C*				
		0 %	*4 %*	*8 %*	*12 %*	*16 %*	*0 %*	*4 %*	*8 %*	*12 %*	*16 %*	*0 %*	*4 %*	*8 %*	*12 %*	*16 %*
Case 1: 3- Φ UV	THD_I	27.87	29.13	32.38	34.71	34.04	27.87	28.73	26.55	26.57	31.04	27.87	25.89	25.28	23.65	20.99
	h 3	0.01	2.71	6.28	9.88	12.19	0.01	2.88	4.92	7.29	11.69	0.01	2.56	5.09	7.01	7.94
	h 5	22.37	23.76	27.02	28.48	26.74	22.36	23.28	20.04	19.25	23.34	22.36	19.66	18.23	15.32	11.59
	h 7	10.86	10.03	6.35	3.16	5.78	10.87	10.3	11.86	12.24	9.61	10.87	11.77	12.15	12.17	10.52
	h 9	0.01	2.08	7.04	10.02	9.25	0.01	1.66	2.07	2.11	5.56	0.01	3.09	4.12	6.04	8.18
	h 11	8.35	9.27	9.98	8.78	8.93	8.34	8.94	6.43	5.94	8.71	8.34	6.04	4.76	1.99	1.55
	h 13	5.74	4.76	0.39	3.07	0.68	5.75	5.14	6.65	6.80	3.68	5.75	6.46	6.52	5.69	2.60
	h 15	0.01	1.81	5.64	6.76	6.70	0.0	1.42	1.65	1.61	4.04	0.01	2.78	3.57	4.78	4.81
Case 2: 2- Φ UV	THD_I	27.87	29.11	32.28	35.08	37.82	27.87	27.35	26.87	25.41	25.12	27.87	25.88	25.06	24.42	22.94
	h 3	0.01	2.72	6.21	10.18	14.29	0.01	2.89	5.01	6.86	8.82	0.01	2.57	5.05	7.19	8.78
	h 5	22.37	23.73	26.92	28.77	29.68	22.36	21.92	20.43	17.83	16.46	22.36	19.64	17.96	16.22	13.30
	h 7	10.86	10.05	6.51	2.39	2.01	10.87	11.12	11.74	12.46	12.86	10.87	11.77	12.13	12.46	12.26
	h 9	0.01	2.05	6.90	10.41	12.70	0.01	1.71	1.73	3.39	3.54	0.01	3.11	4.39	5.16	6.51
	h 11	8.35	9.25	10.00	8.47	5.49	8.34	7.96	6.78	4.57	3.78	8.34	6.03	4.49	2.95	0.44
	h 13	5.74	4.79	0.57	3.79	7.34	5.75	6.14	6.57	6.81	6.68	5.75	6.46	6.44	6.27	5.03
	h 15	0.01	1.78	5.56	6.73	5.66	0.0	0.67	1.24	2.95	3.34	0.01	2.79	3.79	4.29	4.84
Case 3: 1- Φ UV	THD_I	27.87	30.05	32.47	35.13	38.04	27.87	26.95	26.05	25.14	24.20	27.87	26.75	25.68	24.65	23.63
	h 3	0.01	2.96	6.38	10.24	14.54	0.01	2.50	4.78	6.77	8.43	0.01	2.71	5.14	7.24	8.98
	h 5	22.37	24.90	27.11	28.79	29.76	22.36	21.05	19.41	17.50	15.38	22.36	20.71	18.73	16.50	14.08
	h 7	10.86	9.03	6.18	2.30	2.52	10.87	11.43	11.99	12.47	12.78	10.87	11.58	12.15	12.51	12.61
	h 9	0.01	3.53	7.19	10.46	12.80	0.01	1.46	2.70	3.72	4.54	0.01	1.94	3.59	4.90	5.86
	h 11	8.35	9.81	9.96	8.43	5.15	8.34	7.27	5.86	4.23	2.61	8.34	7.01	5.25	3.24	1.25
	h 13	5.74	3.61	0.22	3.87	7.67	5.75	6.32	6.71	6.75	6.32	5.75	6.38	6.63	6.41	5.66
	h 15	0.01	3.13	5.72	6.73	5.40	0.0	1.22	2.29	3.22	4.05	0.01	1.73	3.14	4.12	4.67
Case 4: 2- Φ Angle	THD_I	27.87	26.94	25.80	24.54	23.52	27.87	26.76	25.92	25.25	24.30	27.87	30.06	32.48	35.13	38.06
	h 3	0.01	2.5	4.71	6.56	8.15	0.01	2.72	5.17	7.36	9.17	0.01	2.96	6.40	10.33	14.66
	h 5	22.37	21.04	19.11	16.79	14.59	22.36	20.71	19.03	17.24	14.88	22.36	24.9	27.11	28.77	29.73
	h 7	10.86	11.43	12.03	12.42	12.59	10.87	11.58	12.13	12.59	12.85	10.87	9.04	6.17	2.29	2.56
	h 9	0.01	1.47	3.03	4.45	5.27	0.01	1.93	3.28	4.20	5.20	0.01	3.54	7.20	10.47	12.81
	h 11	8.35	7.26	5.56	3.47	1.71	8.34	7.02	5.55	4.01	2.11	8.34	9.81	9.95	8.40	5.10
	h 13	5.74	6.32	6.70	6.53	5.91	5.75	6.38	6.66	6.68	6.15	5.75	3.61	0.21	3.87	7.67
	h 15	0.01	1.23	2.59	3.78	4.43	0.0	1.72	2.86	3.61	4.38	0.01	3.14	5.73	6.73	5.39
Case 5: 1-Φ Angle	THD_I	27.87	29.82	31.90	34.15	36.57	27.87	26.16	24.53	22.97	21.47	27.87	27.78	27.78	27.85	27.98
	h 3	0.01	3.07	6.49	10.26	14.35	0.01	2.46	4.53	6.24	7.60	0.01	2.71	5.32	7.81	10.16
	h 5	22.37	24.62	26.45	27.80	28.58	22.36	20.02	17.52	14.91	12.31	22.36	22.02	21.43	20.60	19.58
	h 7	10.86	9.27	7.02	4.17	0.89	10.87	11.71	12.02	11.85	11.27	10.87	11.09	11.48	11.97	12.47
	h 9	0.01	3.24	6.48	9.49	11.94	0.01	2.63	4.79	6.41	7.42	0.01	0.76	1.36	1.77	1.97
	h 11	8.35	9.67	9.91	8.94	6.84	8.34	6.37	3.99	1.46	0.95	8.34	8.1	7.65	7.11	6.61
	h 13	5.74	3.91	1.20	1.98	5.08	5.75	6.48	6.30	5.33	3.77	5.75	5.93	6.24	6.53	6.69
	h 15	0.01	2.88	5.33	6.74	6.72	0.0	2.34	4.04	4.86	4.77	0.01	0.41	0.64	0.71	0.82
Case 6: 1- Φ OV	THD_I	27.87	25.88	24.06	22.40	20.88	27.87	28.82	29.81	30.86	31.97	27.87	29.06	30.35	31.74	33.23
	h 3	0.01	2.52	4.63	6.36	7.72	0.01	2.69	5.52	8.43	11.38	0.01	2.95	6.10	9.39	12.78
	h 5	22.37	19.65	16.89	14.18	11.62	22.36	23.36	24.03	24.41	24.52	22.36	23.69	24.67	25.31	25.63
	h 7	10.86	11.77	11.89	11.40	10.45	10.87	10.32	9.82	9.36	8.91	10.87	10.01	9.05	7.97	6.80
	h 9	0.01	3.09	5.52	7.22	8.19	0.01	1.61	3.28	4.93	6.44	0.01	2.13	4.33	6.48	8.47
	h 11	8.35	6.03	3.36	0.74	1.57	8.34	9.03	9.33	9.34	9.14	8.34	9.18	9.51	9.36	8.82
	h 13	5.74	6.46	5.93	4.48	2.56	5.75	5.1	4.41	3.66	2.85	5.75	4.8	3.58	2.15	0.70
	h 15	0.01	2.77	4.57	5.21	4.78	0.0	1.35	2.71	3.93	4.89	0.01	1.88	3.68	5.18	6.23
Case 7: 2- Φ OV	THD_I	27.87	26.32	24.06	22.42	20.90	27.87	27.15	29.81	30.49	31.39	27.87	29.93	30.35	32.09	33.79
	h 3	0.01	2.43	4.63	6.32	7.68	0.01	2.71	5.52	8.34	11.18	0.01	3.04	6.10	9.53	13.05
	h 5	22.37	20.24	16.89	14.22	11.67	22.36	21.68	24.03	23.96	23.85	22.36	24.75	24.67	25.7	26.18
	h 7	10.86	11.66	11.89	11.42	10.50	10.87	11.25	9.82	9.79	9.63	10.87	9.16	9.05	7.48	5.95
	h 9	0.01	2.38	5.52	7.18	8.14	0.01	0.96	3.28	4.39	5.62	0.01	3.38	4.33	6.96	9.15
	h 11	8.35	6.57	3.36	0.77	1.55	8.34	7.83	9.33	9.18	9.00	8.34	9.73	9.51	9.39	8.67
	h 13	5.74	6.47	5.93	4.53	2.65	5.75	6.09	4.41	4.15	3.66	5.75	3.77	3.58	1.59	0.54
	h 15	0.01	2.11	4.57	5.19	4.77	0.0	0.71	2.71	3.44	4.19	0.01	3.01	3.68	5.52	6.58
Case 8: 3- Φ OV	THD_I	27.87	26.26	24.17	22.45	20.93	27.87	27.61	28.93	30.16	30.97	27.87	29.89	31.12	32.39	34.18
	h 3	0.01	2.43	4.55	6.30	7.65	0.01	2.7	5.41	8.27	11.04	0.01	3.04	6.31	9.64	13.24
	h 5	22.37	20.17	17.06	14.27	11.71	22.36	21.8	22.91	23.55	23.34	22.36	24.7	25.56	26.01	26.55
	h 7	10.86	11.67	11.93	11.45	10.55	10.87	11.2	10.67	10.14	10.11	10.87	9.2	8.10	7.06	5.31
	h 9	0.01	2.46	5.32	7.13	8.10	0.01	0.87	2.08	3.93	5.02	0.01	3.32	5.41	7.35	9.62
	h 11	8.35	6.51	3.52	0.82	1.52	8.34	7.92	8.71	9.00	8.84	8.34	9.71	9.78	9.39	8.52
	h 13	5.74	6.47	6.04	4.59	2.73	5.75	6.04	5.37	4.56	4.20	5.75	3.83	2.47	1.12	1.06
	h 15	0.01	2.19	4.43	5.16	4.76	0.00	0.59	1.48	3.00	3.64	0.01	2.96	4.57	5.79	6.78

4.12.5 Analysis of Voltage Unbalance in Two-Phase and Three-Phase

Analysis for eight different possible cases of voltage unbalance with four distinctive values of VUF is presented here.

4.12.5.1 Three-phase Under-voltage (3-Φ UV) Unbalance Case

Three-phase UV unbalance case is the combination of three single-phase UV cases. Results presented in Table-4.32 reflect the impact of three-phase under-voltage on the AC parameters, whereas impact of individual phase unbalance in a three-phase unbalanced case is depicted in Table-4.33(a) through Table-4.33(c).

Correspondingly, Table-4.34(a) through Table-4.34(c) present the individual and net impact of three single-phase unbalance conditions on variation of THD_I of phases *A*, *B* and *C*; in which the actual THD_I value comes from Table-4.32 and estimated THD_I value is calculated using the results presented in Table-4.33(a), Table-4.33(b), and Table-4.33(c).

Table-4.32: Impact of three-phase under-voltage cases on AC performance parameters

LVUR (%)	PVUR 1 (%)	PVUR (%)	VUF (%)	Unbalance voltage source						+ve seq. Volt. (V_1)	-ve seq. Volt. (V_2)	AC performance parameters					
				Phase *A*		Phase *B*		Phase *C*				I_A		I_B		I_C	
				Mag.	Angle	Mag.	Angle	Mag.	Angle			RMS	THD_I (%)	Mag.	THD_I (%)	Mag.	THD_I (%)
0.00	0.00	0.00	0.00	1.000	0	1.000	240	1.000	120	1.00	0.00	1.000	27.87	1.000	27.87	1.000	27.87
3.96	12.94	7.85	4.00	**0.866**	0	**0.887**	240	**0.984**	120	0.9126	0.0363	0.891	29.13	0.899	28.73	0.948	25.89
7.75	25.68	15.85	8.00	**0.738**	0	**0.930**	240	**0.963**	120	0.8767	0.0702	0.804	32.38	0.905	26.55	0.924	25.28
11.23	40.13	23.21	12.01	**0.645**	0	**0.892**	240	**0.982**	120	0.8395	0.1008	0.736	34.71	0.875	26.57	0.916	23.65
15.97	53.18	31.1	16.0	**0.582**	0	**0.679**	240	**0.978**	120	0.7464	0.1194	0.674	34.00	0.725	31.00	0.853	21.00

Table-4.33(a): AC performance parameters under impact of single-phase under-voltage in phase *A*

LVUR (%)	PVUR1 (%)	PVUR (%)	VUF (%)	Unbalance voltage source						+ve seq. Volt. (V_1)	-ve seq. Volt. (V_2)	AC performance parameters					
				Phase *A*		Phase *B*		Phase *C*				I_A		I_B		I_C	
				Mag.	Angle	Mag	Angle	Mag	Angle			RMS	THD_I (%)	Mag.	THD_I (%)	Mag.	THD_I (%)
4.61	14.01	9.34	4.67	**0.866**	0	1.000	240	1.000	120	0.955	0.045	0.909	30.47	0.978	26.82	0.981	26.59
9.31	28.73	19.16	9.58	**0.738**	0	1.000	240	1.000	120	0.913	0.087	0.819	33.50	0.960	25.71	0.965	25.29
12.89	40.31	26.88	13.44	**0.645**	0	1.000	240	1.000	120	0.882	0.118	0.751	36.16	0.949	24.83	0.956	24.31
15.39	48.63	32 42	16.21	**0.582**	0	1.000	240	1.000	120	0.861	0.139	0.704	38.22	0.943	24.17	0.950	23.60

Table-4.33(b): AC performance parameters under impact of single-phase under-voltage in phase *B*

LVUR (%)	PVUR1 (%)	PVUR (%)	VUF (%)	Unbalance voltage source						+ve seq. Volt. (V_1)	-ve seq. Volt. (V_2)	AC performance parameters					
				Phase *A*		Phase *B*		Phase *C*				I_A		I_B		I_C	
				Mag.	Angle	Mag.	Angle	Mag	Angle			RMS	THD_I (%)	Mag.	THD_I (%)	Mag.	THD_I (%)
3.86	11.70	7.80	3.90	1.000	0	**0.887**	240	1.000	120	0.962	0.038	0.984	26.80	0.924	30.02	0.981	26.99
2.39	7.22	4.81	2.41	1.000	0	**0.930**	240	1.000	120	0.977	0.023	0.990	27.21	0.952	29.18	0.988	27.33
3.69	11.17	7.45	3.72	1.000	0	**0.892**	240	1.000	120	0.964	0.036	0.984	26.84	0.927	29.92	0.982	27.03
11.55	35.94	23.96	11.98	1.000	0	**0.679**	240	1.000	120	0.893	0.107	0.959	24.68	0.777	35.13	0.952	25.16

Table-4.33(c): AC performance parameters under impact of single-phase under-voltage in phase *C*

LVUR (%)	PVUR1 (%)	PVUR (%)	VUF (%)	Unbalance voltage source						+ve seq. Volt. (V_1)	-ve seq. Volt. (V_2)	AC performance parameters					
				Phase *A*		Phase *B*		Phase *C*				I_A		I_B		I_C	
				Mag	Angle	Mag	Angle	Mag	Angle			RMS	THD_I (%)	Mag.	THD_I (%)	Mag.	THD_I (%)
0.53	1.58	1.06	0.53	1.000	0	1.000	240	**0.984**	120	0.995	0.005	0.997	27.77	0.998	27.74	0.989	28.17
1.25	3.75	2.50	1.25	1.000	0	1.000	240	**0.963**	120	0.988	0.012	0.993	27.60	0.994	27.53	0.975	28.55
0.62	1.86	1.24	0.62	1.000	0	1.000	240	**0.982**	120	0.994	0.006	0.997	27.75	0.997	27.71	0.988	28.21
0.72	2.17	1.45	0.72	1.000	0	1.000	240	**0.978**	120	0.993	0.007	0.996	27.72	0.997	27.68	0.986	28.27

Table-4.34(a): **Effect of three-phase under-voltage unbalance source on THD_I of Phase *A***

Effect of unbalance in Phase *A* (α)	Effect of unbalance in Phase *B* (β)	Effect of unbalance in Phase *C* (γ)	Estimated Effect (δ) $=(\alpha)+(\beta)+(\gamma)$	Estimated THD_I Value $= (\delta) + 27.87$*	Actual Effect	Actual THD_I Value
2.58	-1.09	-0.12	*1.37*	29.24	*1.26*	29.13
5.61	-0.68	-0.29	*4.64*	32.51	*4.51*	32.38
8.27	-1.05	-0.14	*7.08*	34.95	*6.84*	34.71
10.33	-3.21	-0.17	*6.95*	34.82	*6.13*	34.00

* 27.87 % is value of THD_I for phase current under balanced voltage source

Table-4.34(b): **Effect of three-phase under-voltage unbalance source on THD_I of Phase *B***

Effect of unbalance in Phase *A* (α)	Effect of unbalance in Phase *B* (β)	Effect of unbalance in Phase *C* (γ)	Estimated Effect (δ) $=(\alpha)+(\beta)+(\gamma)$	Estimated THD_I Value $= (\delta) + 27.87$	Actual Effect	Actual THD_I Value
-1.07	2.13	-0.15	*0.91*	28.78	*0.86*	28.73
-2.18	1.29	-0.36	*-1.25*	26.62	*-1.32*	26.55
-3.06	2.03	-0.18	*-1.21*	26.66	*-1.30*	26.57
-3.72	7.24	-0.21	*3.31*	31.18	*3.13*	31.00

Table-4.34(c): **Effect of three-phase under-voltage unbalance source on THD_I of Phase *C***

Effect of unbalance in Phase *A* (α)	Effect of unbalance in Phase *B* (β)	Effect of unbalance in Phase *C* (γ)	Estimated Effect (δ) $=(\alpha)+(\beta)+(\gamma)$	Estimated THD_I Value (%) $= (\delta) + 27.87$	Actual Effect	Actual THD_I Value (%)
-1.3	-0.9	0.28	-1.92	25.95	-1.98	25.89
-2.6	-0.56	0.66	-2.5	25.37	-2.59	25.28
-3.58	-0.86	0.32	-4.12	23.75	-4.22	23.65
-4.29	-2.73	0.38	-6.64	21.23	-6.87	21.00

4.12.5.2 Two-phase Under-voltage (2-Φ UV) Unbalance Case

Two-phase UV unbalance case is the combination of two single-phase UV cases. Results presented in Table-4.35 reveal the impact of two-phase under-voltage on the AC parameters, whereas impact of individual phase unbalance in a two-phase unbalanced case is depicted in Table-4.36(a) and Table-4.36(b). In the same way, Table-4.37(a), Table-4.37(b), and Table-4.37(c) present the individual and net impact of two single-phase UV unbalance conditions on variation of THD_I of phases *A*, *B* and *C*; in which the actual THD_I value is considered as in Table-4.35 and estimated THD_I value is calculated using the results presented in Table-4.36(a), and Table-4.36(b).

Table-4.35: Impact of two-phase under-voltage cases on AC performance parameters

LVUR (%)	PVUR I (%)	PVUR (%)	VUF (%)	Unbalance voltage source						+ve seq. Volt. (V_1)	-ve seq. Volt. (V_2)	AC performance parameters					
				Phase *A*		Phase *B*		Phase *C*				I_A		I_B		I_C	
				Mag.	Angle	Mag.	Angle	Mag.	Angle			RMS	THD_I (%)	Mag.	THD_I (%)	Mag.	THD_I (%)
0.00	0.00	0.00	0.0	**1.000**	0	**1.000**	240	1.000	120	1.00	0 00	1 000	27.87	1.000	27.87	1 000	27.87
3 99	12.92	7.90	4.0	**0.880**	0	**0.900**	240	1.000	120	0 9268	0.0370	0.905	29.11	0 913	28.77	0.963	25.88
7.65	26.44	15.62	8.0	**0.761**	0	**0.946**	240	1.000	120	0.9023	0.0722	0.829	32.28	0.927	26.87	0.955	25.06
11.56	37 06	23 97	12 0	**0.672**	0	**0.981**	240	1.000	120	0.8843	0.1062	0.769	35.08	0.939	25.41	0.953	24.42
16.00	53.11	31 15	16.0	**0.595**	0	**0.692**	240	1.000	120	0.7625	0.1220	0.689	34.00	0.740	31.10	0.872	20.98

Table-4.36(a): AC performance parameters under impact of single-phase under-voltage in phase *A*

LVUR (%)	PVUR I (%)	PVUR (%)	VUF (%)	Unbalance voltage source						+ve seq. Volt. (V_1)	-ve seq. Volt. (V_2)	AC performance parameters					
				Phase *A*		Phase *B*		Phase *C*				I_A		I_B		I_C	
				Mag.	Angle	Mag	Angle	Mag.	Angle			RMS	THD_I (%)	Mag.	THD (%)	Mag.	THD (%)
4.11	12.47	8.31	4.16	**0.880**	0	1.000	240	1.000	120	0.960	0.040	0.919	30.17	0.980	26.94	40.11	26.73
8.43	25.92	17.28	8.64	**0.761**	0	1.000	240	1.000	120	0.920	0.080	0.836	32.90	0.963	25.92	39.50	25.54
11.82	36.79	24.53	12.26	**0.672**	0	1.000	240	1.000	120	0.891	0.109	0.771	35.32	0.952	25.10	39.11	24.60
14.85	46.81	31.21	15.60	**0.595**	0	1.000	240	1.000	120	0.865	0.135	0.715	37.76	0.944	24.32	38.83	23.75

Table-4.36(b): AC performance parameters under impact of single-phase under-voltage in phase *B*

LVUR (%)	PVUR I (%)	PVUR (%)	VUF (%)	Unbalance voltage source						+ve seq. Volt. (V_1)	-ve seq. Volt. (V_2)	AC performance parameters					
				Phase *A*		Phase *B*		Phase *C*				I_A		I_B		I_C	
				Mag.	Angle	Mag.	Angle	Mag	Angle			RMS	THD_I (%)	Mag.	THD_I (%)	Mag.	THD_I (%)
3.42	10.34	6.90	3.45	1.00	0	**0.900**	240	1.00	120	0.967	0.033	0.986	26.92	0.932	29.76	0.983	27.10
1.84	5.54	3.69	1.85	1.00	0	**0.946**	240	1.00	120	0.982	0.018	0.992	27.36	0.963	28.87	0.990	27.46
0.65	1.95	1.30	0.65	1.00	0	**0.981**	240	1.00	120	0.994	0.006	0.997	27.70	0.987	28.23	0.997	27.74
11.05	34.29	22.86	11.43	1.00	0	**0.692**	240	1.00	120	0.897	0.103	0.960	24.82	0.786	34.75	0.954	25.29

Table-4.37(a): Effect of two-phase under-voltage unbalance source on THD_I of Phase *A*

Effect of unbalance in Phase *A* (α)	Effect of unbalance in Phase *B* (β)	Effect of unbalance in Phase *C* (γ)	Estimated Effect (δ) $=(\alpha)+(\beta)+(\gamma)$	Estimated THD_I Value $=(\delta)+27.87$*	Actual Effect	Actual THD_I Value
2.28	-0.97	0.00	1.31	29.18	1.24	29.11
5.01	-0.53	0.00	4.48	32.35	4.41	32.28
7.43	-0.19	0.00	7.24	35.11	7.21	35.08
9.87	-3.07	0.00	6.8	34.67	6.13	34.00

* 27.87 % is value of THD_I for phase current under balanced voltage source

Table-4.37(b): Effect of two-phase under-voltage unbalance source on THD_I of Phase *B*

Effect of unbalance in Phase *A* (α)	Effect of unbalance in Phase *B* (β)	Effect of unbalance in Phase *C* (γ)	Estimated Effect (δ) $=(\alpha)+(\beta)+(\gamma)$	Estimated THD_I Value $=(\delta)+27.87$	Actual Effect	Actual THD_I Value
-0.95	1.87	0.00	0.92	28.79	0.90	28.77
-1.97	0.98	0.00	-0.99	26.88	-1.00	26.87
-2.79	0.34	0.00	-2.45	25.42	-2.46	25.41
-3.57	6.86	0.00	3.29	31.16	3.23	31.10

Table-4.37(c): Effect of two-phase under-voltage unbalance source on THD_I of Phase *C*

Effect of unbalance in Phase *A* (α)	Effect of unbalance in Phase *B* (β)	Effect of unbalance in Phase *C* (γ)	Estimated Effect (δ) $=(\alpha)+(\beta)+(\gamma)$	Estimated THD_I Value (%) $=(\delta)+27.87$	Actual Effect	Actual THD_I Value (%)
-1.16	-0.79	0.00	-1.95	25.92	-1.99	25.88
-2.35	-0.43	0.00	-2.78	25.09	-2.81	25.06
-3.29	-0.15	0.00	-3.44	24.43	-3.45	24.42
-4.14	-2.60	0.00	-6.74	21.13	-6.89	20.98

4.12.5.3 Two-phase Angle (2-Φ A) Unbalance Case

The two-phase angle unbalance case is combination of two single-phase angle unbalance cases. To understand the individual contribution of these two single-phase angle unbalance cases towards the net impact of two-phase angle unbalance case on AC performance parameters, results of 2-phase angle unbalance case on AC parameters are shown in Table-4.38. Table-4.39(a), and Table-4.39(b) present the AC performance parameters for the single-phase angle unbalance cases considered in phase *B*, and phase *C*, in that order.

Correspondingly, Table-4.40(a), Table-4.40(b), and Table-4.40(c) present the individual and net impact of two single-phase angle unbalance conditions unbalance on variation of THD_I of phases *A*, *B* and *C*; in which the actual THD_I value comes from Table-4.38 and estimated THD_I value is calculated using the results presented in Table-4.39(a), and Table-4.39(b).

Table-4.38: Impact of two-phase under-voltage cases on AC performance parameters

LVUR (%)	PVUR 1 (%)	PVUR (%)	VUF (%)	Unbalance voltage source						+ve seq. Volt. (V_1)	-ve seq. Volt. (V_2)	AC performance parameters					
				Phase *A*		Phase *B*		Phase *C*				I_A		I_B		I_C	
				Mag.	Angle	Mag.	Angle	Mag.	Angle			RMS	THD_I (%)	Mag.	THD_I (%)	Mag.	THD_I (%)
0.00	0.00	0.00	0.00	1.00	0	1.00	240	1.000	120	1.00	0.00	1.000	27.87	1.000	27.87	1.000	27.87
3.96	0.00	0.00	4.00	1.000	0	1.00	231.9	1.00	116	0.9983	0.0399	1.018	26.94	1.021	26.76	0.957	30.06
7.80	0.00	0.00	8.00	1.000	0	1.00	223.5	1.00	112.7	0.9931	0.0794	1.039	25.80	1.036	25.92	0.909	32.48
11.49	0.00	0.00	12.0	1.000	0	1.00	215	1.00	109.8	0.9840	0.1181	1.060	24.54	1.047	25.25	0.856	35.13
15.12	0.00	0.00	16.0	1.000	0	1.00	206	1.00	105.6	0.9706	0.1553	1.073	23.52	1.060	24.3	0.798	38.06

Table-4.39(a): AC performance parameters under impact of single-phase angle unbalance in phase *B*

LVUR (%)	PVUR 1 (%)	PVUR (%)	VUF (%)	Unbalance voltage source						+ve seq. Volt. (V_1)	-ve seq. Volt. (V_2)	AC performance parameters					
				Phase *A*		Phase *B*		Phase *C*				I_A		I_B		I_C	
				Mag.	Angle	Mag.	Angle	Mag.	Angle			RMS	THD_I (%)	Mag.	THD_I (%)	Mag.	THD_I (%)
4.17	0.00	0.00	4.72	1.00	0	1.00	**231.9**	1.00	120	1.000	0.047	1.038	25.89	1.001	27.80	0.956	30.19
8.69	0.00	0.00	9.65	1.00	0	1.00	**223.5**	1.00	120	0.991	0.096	1.072	23.90	1.001	27.82	0.905	32.83
13.50	0.00	0.00	14.74	1.00	0	1.00	**215**	1.00	120	0.979	0.144	1.101	21.96	1.000	27.96	0.851	35.79
18.89	0.00	0.00	20.28	1.00	0	1.00	**206**	1.00	120	0.961	0.195	1.125	19.95	0.997	28.19	0.790	39.33

Table-4.39(b): AC performance parameters under impact of single-phase angle unbalance in phase *C*

LVUR (%)	PVUR I (%) & PVUR (%)	VUF (%)	Unbalance voltage source						+ve seq. Volt. (V_1)	-ve seq. Volt. (V_2)	AC performance parameters					
			Phase *A*		Phase *B*		Phase *C*				I_A		I_B		I_C	
			Mag.	Angle	Mag.	Angle	Mag.	Angle			RMS	THD_I (%)	Mag.	THD_I (%)	Mag.	THD_I (%)
2 04	0 00	2 33	1 000	0	1.000	240	1 000	**116**	0.999	0 023	0.979	29.00	1.019	26.89	1 001	27.83
3 75	0 00	4.25	1.000	0	1.000	240	1 000	**112.7**	0 997	0 042	0 960	29.96	1.034	26.08	1.001	27 80
5.28	0.00	5.95	1.000	0	1.000	240	1.000	**109.8**	0.996	0.059	0.944	30.83	1.047	25.38	1.002	27.79
7 54	0.00	8.41	1.000	0	1.000	240	1 000	**105.6**	0 993	0.084	0.918	32.14	1.064	24.39	1.002	27.81

Table-4.40(a): Effect of two-phase angle unbalance voltage source on THD_I of Phase *A*

Effect of unbalance in Phase *A* (α)	Effect of unbalance in Phase *B* (β)	Effect of unbalance in Phase *C* (γ)	Estimated Effect (δ) $=(\alpha)+(\beta)+(\gamma)$	Estimated THD_I Value $= (\delta) + 27.87$*	Actual Effect	Actual THD_I Value
0.00	-2.00	1.11	-0.89	26.98	-0.93	26.94
0.00	-3.99	2.07	-1.92	25.95	-2.07	25.80
0.00	-5.93	2.94	-2.99	24.88	-3.33	24.54
0.00	-7.94	4.25	-3.69	24.18	-4.35	23.52

* 27.87 % is value of THD_I for phase current under balanced voltage source

Table-4.40(b): Effect of two-phase angle unbalance voltage source on THD_I of Phase *B*

Effect of unbalance in Phase *A* (α)	Effect of unbalance in Phase *B* (β)	Effect of unbalance in Phase *C* (γ)	Estimated Effect (δ) $=(\alpha)+(\beta)+(\gamma)$	Estimated THD_I Value $= (\delta) + 27.87$	Actual Effect	Actual THD_I Value
0.00	-0.09	-1.00	-1.09	26.78	-1.11	26.76
0.00	-0.07	-1.81	-1.88	25.99	-1.95	25.92
0.00	0.07	-2.51	-2.44	25.43	-2.62	25.25
0.00	0.30	-3.50	-3.20	24.67	-3.57	24.30

Table-4.40(c): Effect of two-phase angle unbalance voltage source on THD_I of Phase *C*

Effect of unbalance in Phase *A* (α)	Effect of unbalance in Phase *B* (β)	Effect of unbalance in Phase *C* (γ)	Estimated Effect (δ) $=(\alpha)+(\beta)+(\gamma)$	Estimated THD_I Value (%) $= (\delta) + 27.87$	Actual Effect	Actual THD_I Value (%)
0.00	2.30	-0.06	2.24	*30.11*	2.19	*30.06*
0.00	4.94	-0.09	4.85	*32.72*	4.61	*32.48*
0.00	7.90	-0.10	7.80	*35.67*	7.26	*35.13*
0.00	11.44	-0.08	11.36	*39.23*	10.19	*38.06*

4.12.5.4 Two-phase Over-voltage (2-Φ OV) Unbalance Case

The two-phase OV unbalance case is the combination of two single-phase OV cases. To understand the individual contribution of these two single-phase OV unbalance cases towards the net impact of two-phase OV unbalance case in terms of AC parameters, the results are shown in Table-4.41, while Table-4.42(a), and Table-4.42(b) present the AC performance parameters for the single-phase OV cases considered in phase *A*, and phase *B*, in that order. Correspondingly, Table-4.43(a), Table-4.43(b), and Table-4.43(c) present the individual and net impact of two single-phase OV unbalance conditions on variation of THD_I of phases *A*, *B* and *C*; in which the actual THD_I value comes from Table-4.41 and estimated THD_I value is calculated using the results presented in Table-4.42(a), and Table-4.42(b).

Table-4.41: Impact of two-phase over-voltage cases on AC performance parameters

LVUR (%)	PVUR 1 (%)	PVUR (%)	VUF (%)	Unbalance voltage source						+ve seq. Volt. (V_1)	-ve seq. Volt. (V_2)	AC performance parameters					
				Phase *A*		Phase *B*		Phase *C*				I_A		I_B		I_C	
				Mag.	Angle	Mag.	Angle	Mag.	Angle			RMS	THDI (%)	Mag.	THDI (%	Mag.	THDI (%
0.00	0.00	0.00	0.00	1.000	0	1.000	240	1.000	120	1.00	0.00	1.000	**27.87**	1.000	**27.87**	1.000	**27.87**
3.64	13.79	7.35	4 00	**1.149**	0	**1.089**	240	1.000	120	1.0793	0.0432	1.113	**26.32**	1.088	**27.51**	1.038	**29.93**
8.09	25.38	15 90	8.00	**1.280**	0	**1.034**	240	1.000	120	1.1046	0.0884	1.188	**24.10**	1 080	**29.36**	1 052	**30.77**
12 28	37.16	23 97	12.0	**1.428**	0	**1.028**	240	1 000	120	1.1519	0.1383	1.280	**22.42**	1 110	**30.5**	1.078	**32.10**
16 46	49.68	31.94	16 0	**1.604**	0	**1.043**	240	1.000	120	1.2157	0.1946	1.392	**20.90**	1.165	**31.4**	1.117	**33.80**

Table-4.42(a): AC performance parameters under impact of single-phase over-voltage in phase *A*

LVUR (%)	PVUR 1 (%)	PVUR (%)	VUF (%)	Unbalance voltage source						+ve seq. Volt. (V_1)	-ve seq. Volt. (V_2)	AC performance parameters					
				Phase *A*		Phase *B*		Phase *C*				I_A		I_B		I_C	
				Mag.	Angle	Mag.	Angle	Mag.	Angl e			RMS	THD_I (%)	Mag.	THD_I (%)	Mag.	THD_I (%)
4.78	14.18	9.45	4.73	**1.149**	0	1.000	240	1.000	120	1.050	0.395	1.098	25.55	1.029	29.02	1.025	29.31
8.70	25.64	17.09	8.55	**1.280**	0	1.000	240	1.000	120	1.093	0.744	1.182	23.84	1.057	29.97	1.048	30.56
12.80	37.46	24.97	12.49	**1.428**	0	1.000	240	1.000	120	1.143	1.136	1.275	22.23	1.091	31.02	1.077	31.93
17.29	50.28	33.52	16.76	**1.604**	0	1.000	240	1.000	120	1.201	1.603	1.383	20.62	1.135	32.20	1.113	33.54

Table-4.42(b): AC performance parameters under impact of single-phase over-voltage in phase *B*

LVUR (%)	PVUR 1 (%)	PVUR (%)	VUF (%)	Unbalance voltage source						+ve seq. Volt. (V_1)	-ve seq. Volt. (V_2)	AC performance parameters					
				Phase *A*		Phase *B*		Phase *C*				I_A		I_B		I_C	
				Mag.	Angle	Mag.	Angle	Mag.	Angle			RMS	THD_I (%)	Mag.	THD_I (%)	Mag.	THD_I (%)
2.90	8.64	5.76	2.88	1.00	0	**1.089**	240	1.00	120	1.030	0.030	1.014	28.74	1.059	26.43	1.017	28.57
1.11	3.32	2.21	1.11	1.00	0	**1.034**	240	1.00	120	1.011	0.011	1.005	28.21	1.023	27.32	1.006	28.15
0.92	2.74	1.83	0.91	1.00	0	**1.028**	240	1.00	120	1.009	0.009	1.004	28.16	1.019	27.42	1.005	28.10
1.42	4.25	2.83	1.42	1.00	0	**1.043**	240	1.00	120	1.014	0.014	1.007	28.30	1.029	27.16	1.008	28.22

Table-4.43(a): Effect of two-phase over-voltage unbalance source on THD_I of Phase *A*

Effect of unbalance in Phase *A* (α)	Effect of unbalance in Phase *B* (β)	Effect of unbalance in Phase *C* (γ)	Estimated Effect (δ) $=(\alpha)+(\beta)+(\gamma)$	Estimated THD_I Value $=(\delta)+27.87$*	Actual Effect	Actual THD_I Value
-2.34	0.85	0.00	-1.49	26.38	-1.55	26.32
-4.05	0.32	0.00	-3.73	24.14	-3.77	24.10
-5.66	0.27	0.00	-5.39	22.48	-5.45	22.42
-7.27	0.41	0.00	-6.86	21.01	-6.97	20.90

* 27.87 % is value of THD_I for phase current under balanced voltage source

Table-4.43(b): Effect of two-phase over-voltage unbalance source on THD_I of Phase *B*

Effect of unbalance in Phase *A* (α)	Effect of unbalance in Phase *B* (β)	Effect of unbalance in Phase *C* (γ)	Estimated Effect (δ) $=(\alpha)+(\beta)+(\gamma)$	Estimated THD_I Value $=(\delta)+27.87$	Actual Effect	Actual THD_I Value
1.13	-1.46	0.00	-0.33	27.54	-0.36	27.51
2.08	-0.57	0.00	1.51	29.38	1.49	29.36
3.13	-0.47	0.00	2.66	30.53	2.63	30.5
4.31	-0.73	0.00	3.58	31.45	3.53	31.4

Table-4.43(c): Effect of two-phase over-voltage unbalance source on THD_I of Phase *C*

Effect of unbalance in Phase *A* (α)	Effect of unbalance in Phase *B* (β)	Effect of unbalance in Phase *C* (γ)	Estimated Effect (δ) $=(\alpha)+(\beta)+(\gamma)$	Estimated THD_I Value (%) $=(\delta)+27.87$	Actual Effect	Actual THD_I Value (%)
1.42	0.68	0.00	*2.10*	29.97	*2.06*	29.93
2.67	0.26	0.00	*2.93*	30.80	*2.9*	30.77
4.04	0.21	0.00	*4.25*	32.12	*4.23*	32.10
5.65	0.33	0.00	*5.98*	33.85	*5.93*	33.80

4.12.5.5 Three-phase Over-voltage (3-Φ OV) Unbalance Case

The three-phase OV unbalance case is the combination of three single-phase OV cases. To understand that how any one of these of three single-phase OV cases contributes individually, towards the net impact of three-phase OV unbalance case on AC performance parameters, the results are shown in Table-4.44, while Table-4.45(a), Table-4.45(b), and Table-4.45(c) present the AC parameters for the single-phase OV cases considered in phase *A*, phase *B*, and phase *C*, respectively. Correspondingly, Table-4.46(a), Table-4.46(b), and Table-4.46(c) present the individual and net impact of three single-phase over-voltage unbalance conditions on variation of THD_I of phases *A*, *B* and *C*; in which the actual THD_I value comes from Table-4.44 and estimated THD_I value is calculated using the results presented in Table-4.45(a) through Table-4.45(c).

Table-4.44: Impact of three-phase over-voltage cases on AC performance parameters

LVUR (%)	PVUR 1 (%)	PVUR (%)	VUF (%)	Unbalance voltage source						+ve seq. Volt. (V_1)	-ve seq. Volt. (V_2)	AC performance parameters					
				Phase *A*		Phase *B*		Phase *C*				I_A		I_B		I_C	
				Mag.	Angle	Mag.	Angle	Mag.	Angle			RMS	THD_I (%)	Mag.	THD_I (%)	Mag.	THD_I (%)
0.00	0.00	0.00	0.00	1.000	0	1.000	240	1.000	120	1.00	0.00	1.000	27.87	1.000	27.87	1.000	27.87
3.56	13.82	7.17	4.00	**1.167**	0	**1.100**	240	**1.016**	120	.094	0.043	1.130	26.26	1.102	27.61	1.054	29.89
7.95	26.38	15.64	8.00	**1.313**	0	**1.080**	240	**1.014**	120	.135	0.090	1.221	24.17	1.120	28.93	1.074	31.12
12.21	38.04	23.86	12.0	**1.477**	0	**1.077**	240	**1.023**	120	.192	0.143	1.326	22.45	1.157	30.16	1.110	32.4
16.38	50.77	31.81	16.0	**1.662**	0	**1.098**	240	**1.022**	120	.260	0.201	1.443	20.93	1.219	30.97	1.147	34.18

Table-4.45(a): AC performance parameters under impact of single-phase over-voltage in phase *A*

LVUR (%)	PVUR 1 (%)	PVUR (%)	VUF (%)	Unbalance voltage source						+ve seq. Volt. (V_1)	-ve seq. Volt. (V_2)	AC performance parameters					
				Phase *A*		Phase *B*		Phase *C*				I_A		I_B		I_C	
				Mag.	Angle	Mag	Angle	Mag.	Angle			RMS	THD_I (%)	Mag.	THD_I (%)	Mag.	THD_I (%)
5.33	15.81	10.54	5.27	**1.167**	0	1.000	240	1.000	120	1.056	0.056	1.110	25.30	1.033	29.15	1.028	29.48
9.65	28.37	18.91	9.46	**1.313**	0	1.000	240	1.000	120	1.104	0.104	1.203	23.46	1.064	30.21	1.054	30.87
14.09	41.15	27.43	13.72	**1.477**	0	1.000	240	1.000	120	1.159	0.159	1.305	21.75	1.103	31.35	1.087	32.39
18.67	54.20	36.13	18.07	**1.662**	0	1.000	240	1.000	120	1.221	0.221	1.418	20.16	1.150	32.58	1.126	34.06

Table-4.45(b): AC performance parameters under impact of single-phase over-voltage in phase *B*

LVUR (%)	PVUR I (%)	PVUR (%)	VUF (%)	Unbalance voltage source						+ve seq. Volt. (V_1)	-ve seq. Volt. (V_2)	AC performance parameters					
				Phase *A*		Phase *B*		Phase *C*				I_A		I_B		I_C	
				Mag.	Angle	Mag.	Angle	Mag.	Angle			RMS	THD_I (%)	Mag.	THD_I (%)	Mag.	THD_I (%)
3.25	9.68	6.45	3.23	1.000	0	**1.100**	240	1.000	120	1.033	0.033	1.016	28.85	1.066	26.27	1.019	28.65
2.61	7.79	5.19	2.60	1.000	0	**1.080**	240	1.000	120	1.027	0.027	1.013	28.66	1.053	26.57	1.015	28.50
2.52	7.50	5.00	2.50	1.000	0	**1.077**	240	1.000	120	1.026	0.026	1.012	28.63	1.051	26.62	1.014	28.48
3.20	9.53	6.36	3.18	1.000	0	**1.098**	240	1.000	120	1.033	0.033	1.016	28.83	1.065	26.29	1.019	28.64

Table-4.45(c): AC performance parameters under impact of single-phase over-voltage in phase *C*

LVUR (%)	PVUR I (%)	PVUR (%)	VUF (%)	Unbalance voltage source						+ve seq. Volt. (V_1)	-ve seq. Volt. (V_2)	AC performance parameters					
				Phase *A*		Phase *B*		Phase *C*				I_A		I_B		I_C	
				Mag.	Angle	Mag	Angle	Mag.	Angle			RMS	THD_I (%)	Mag.	THD_I (%)	Mag.	THD_I (%)
0.52	1.57	1.04	0.52	1.000	0	1.000	240	**1.016**	120	1.005	0.005	1.003	28.01	1.002	28.04	1.011	27.62
0.45	1.36	0.91	0.45	1.000	0	1.000	240	**1.014**	120	1.005	0.005	1.002	27.99	1.002	28.02	1.009	27.65
0.77	2.32	1.55	0.77	1.000	0	1.000	240	**1.023**	120	1.008	0.008	1.004	28.07	1.004	28.11	1.016	27.49
0.71	2.14	1.43	0.71	1.000	0	1.000	240	**1.022**	120	1.007	0.007	1.004	28.06	1.003	28.10	1.014	27.52

Table-4.46(a): Effect of three-phase over-voltage unbalance source on THD_I of Phase A

Effect of unbalance in Phase *A* (α)	Effect of unbalance in Phase *B* (β)	Effect of unbalance in Phase *C* (γ)	Estimated Effect (δ) $= (\alpha)+(\beta)+(\gamma)$	Estimated THD_I Value $= (\delta) + 27.87$*	Actual Effect	Actual THD_I Value
-2.59	0.96	0.12	-1.51	26.36	-1.61	26.26
-4.43	0.77	0.1	-3.56	24.31	-3.70	24.17
-6.14	0.74	0.18	-5.22	22.65	-5.42	22.45
-7.73	0.94	0.17	-6.62	21.25	-6.94	20.93

* 27.87 % is value of THD_I for phase current under balanced voltage source

Table-4.46(b): **Effect of three-phase over-voltage unbalance source on THD_I of Phase *B***

Effect of unbalance in Phase *A* (α)	Effect of unbalance in Phase *B* (β)	Effect of unbalance in Phase *C* (γ)	Estimated Effect (δ) $= (\alpha)+(\beta)+(\gamma)$	Estimated THD_I Value $= (\delta) + 27.87$	Actual Effect	Actual THD_I Value
1.26	-1.62	0.15	-0.21	27.66	-0.26	27.61
2.32	-1.32	0.13	1.13	29.00	1.06	28.93
3.46	-1.27	0.22	2.41	30.28	2.29	30.16
4.69	-1.60	0.21	3.30	31.17	3.10	30.97

Table-4.46(c): Effect of three-phase over-voltage unbalance source on THD_I of Phase *C*

Effect of unbalance in Phase *A* (α)	Effect of unbalance in Phase *B* (β)	Effect of unbalance in Phase *C* (γ)	Estimated Effect (δ) $= (\alpha)+(\beta)+(\gamma)$	Estimated THD_I Value (%) $= (\delta) + 27.87$	Actual Effect	Actual THD_I Value (%)
1.59	0.76	-0.27	2.08	29.95	2.02	29.89
2.98	0.61	-0.24	3.35	31.22	3.25	31.12
4.50	0.59	-0.40	4.69	32.56	4.53	32.40
6.17	0.75	-0.37	6.55	34.42	6.31	34.18

On the basis of detailed analysis carried out in section 4.12.5 it is found that effect of unbalance in individual phases is very high (as in phase *A* and phase *B*, here), but the net effect of unbalance in three phases is very much reduced. Hence, this gives a conclusion that if voltage unbalance is present in more than one phase, then the combination of unbalance voltages may nullify the detrimental effect of different individual voltage unbalances and the net effect is very much reduced.

4.13 EFFECTS OF VOLTAGE UNBALANCE ON HARMONIC CURRENT COMPONENTS

Any type of voltage source unbalance introduces the non-characteristic harmonics in load current, even if a single-phase supply voltage (magnitude or phase angle) takes place; it affects the harmonic pattern in all the three phases. A sufficient change in the value of THD_I is observed with the increase in the value of VUF.

A basic difference in single-phase magnitude unbalance and single-phase phase angle unbalance is observed as "THD_I is most affected in the phase, in which the magnitude unbalance is present, while THD_I is least affected (rather almost constant) in that particular phase, in which single-phase angle unbalance is present".

But it is important to mention here that even in the single-phase angle unbalance case where, THD_I is almost constant throughout (with increasing VUF) harmonic current components differ with variation in VUF.

For a six-pulse converter, the harmonic order (n) and the magnitude of harmonic currents (I_n) are given by following equations:

$$n = 6.k \pm 1, \qquad k = 1, 2, 3 \ldots\ldots\ldots \tag{4. 9}$$

$$\frac{I_n}{I_1} = \frac{1}{n} \tag{4. 10}$$

where, I_1 is the magnitude of fundamental current component.

Equation (4.9) gives the harmonic (multiples of fundamental frequency) orders of the 5, 7, 11, 13, 17 ....etc. and assuming a 50 Hertz fundamental frequency corresponds to 250, 350, 550, 650, 850, ... hertz respectively. These harmonic orders are referred as 'characteristic harmonics'.

The magnitudes of actual harmonic current components have been found to often be at variance from the relationship described in equation (4.10). The 1/h values have often been illustrated as theoretical maximum and that in actual fact all harmonic components have magnitude a little lower [154].

An investigation is performed to detect the impact of voltage source unbalance on harmonic generation of rectifier. An attempt has also been made to find out the change in magnitude of different harmonic orders (characteristic and non-characteristic) under the influence of variable VUF.

The characteristic harmonics (as given by $6.k \pm 1$) can be divided into two groups i.e. (6.k+1) and (6.k-1), for a more clear view of results.

In every case, where THD_I is changing with the VUF, it is found that change in magnitude of $(6.k\text{-}1)^{th}$ order harmonics follow the pattern of change in THD_I value, and for $(6.k+1)^{th}$ order harmonics, the pattern is reversed.

- To be more specific, it can be stated that magnitude of $(6.k\text{-}1)^{th}$ order (5^{th}, 11^{th}, - - - - -) harmonics increases with the increase in value of THD_I and vice-versa.

- For $(6.k+1)^{th}$ order (7^{th}, 13^{th}, - - - - -) harmonics, magnitude of harmonics decreases with increase in value of THD_I and vice-versa.

For higher order characteristics harmonics, the direction of change in magnitude is initially increasing but after attaining some specific maximum value it starts decreasing or initially decreasing and after attaining some minimum (possibly zero) value it starts increasing and again after reaching some maximum value (limited by 1/h harmonic component magnitude rule) again starts decreasing. In earlier literature [137], it has been referred as "independent nature of harmonics variation". This discussion about the change in harmonic component magnitude also holds well about non-characteristics harmonics (triplens), in contrary of an earlier conclusion [156] that "non-characteristics harmonics always increase" with the increase in the value of VUF. It is observed that higher order non-characteristic harmonic components are also showing this increasing-decreasing magnitude pattern with increasing VUF.

But an important observation to be mentioned here is that whatever is the behavior of the pattern of change in harmonic component magnitude at higher values of VUF, initially they follow the pattern of change in magnitude of harmonic component, according to classification presented here as (6n-1) and (6n+1) order harmonics.

For example- if it is (6n-1) order harmonics, it will increase initially, if the THD_I is increasing but after attaining some specific (maximum) value it will start decreasing. This observation about the initial change in percentage magnitude in harmonic components holds valid for all the cases of voltage source unbalance considered in this study.

4.14 CONCLUDING REMARKS

Based on a detailed and rigorous simulation study it is found that the harmonic pattern is decided by the degree of voltage unbalance (VUF). Positive sequence voltage component (V_1) regulates the magnitude of output voltage (V_{DC}), and output power (P_{DC}), while distortion in DC quantities (P_{DC}, V_{DC} and I_{DC}) is found to be proportional to negative sequence voltage component (V_2). A new term "Phase Total Harmonic Distortion Unbalance Factor" (PTHDUF) has been introduced to simplify the harmonic current analysis in three different phases. The variation of different characteristic and non-characteristic harmonics is investigated to assess the sensitivity of current harmonic components to different unbalance voltage operating conditions.

CHAPTER V

HARMONIC MITIGATION AND DEVELOPMENT OF FUZZY LOGIC BASED ACTIVE POWER FILTER FOR RANDOM LOAD VARIATION

5.1 INTRODUCTORY REMARKS

The increased use of power electronic controlled equipments and non-linear electronic devices in power systems has given rise to a type of voltage and current waveform distortion, called as "harmonics" or "power system harmonics". Various examples of such loads are rectifiers, DC motor drives, battery chargers, electronic lighting ballasts, variable frequency AC drives, static VAR generators, static motor starters and uninterruptible switching mode power supplies etc. These nonlinear loads draw harmonic and reactive power components of currents from AC mains. Due to tremendous advantages in efficiency and controllability, these power electronic loads are proliferating, and can be found at all power levels from low voltage appliances to high voltage converters. Hence, power system harmonics are an important problem [42].

In electrical power systems, the harmful effects of harmonics are very real. As discussed in literature, harmonics causes various problems in power systems and in consumer products such as distorted voltage waveforms, equipment overheating, blown capacitor fuses, transformer overheating, excessive neutral currents, low power factor etc. [79, 83, 157]. The research has been underway for last three decades to have a control over the harmonics and to supply the consumers with reliable and clean fundamental frequency, sinusoidal electric power that does not represents a damaging threat to their equipments.

To control harmonics and their effects on utility distribution system along with the methods to keep harmonic distortion under control are potential power quality concerns. Harmonic mitigation is the reduction or elimination of power system harmonics. To reduce harmonic distortion, both passive and active compensation techniques (filters) can be implemented. Conventionally, passive LC tuned filters and capacitors (passive harmonic compensation) have been used for harmonic current mitigation and reactive power compensation, by increasing the power factor. These filters have the drawback of bulky size, component ageing, resonance and fixed compensation performance. These provide either over- or under-compensation of harmonics, whenever a load-change occurs [120]. Hence, active compensation, known as active power filter (APF) is preferred over passive compensation. APF's are an up-to-date solution to power quality problems, which allow the compensation of current harmonics and unbalance, together with power factor improvement, and can be a much better solution than conventional passive filters. Before taking any corrective action, it is necessary to evaluate the distortion introduced by the installation into the distribution network and the expected reduction when the active filter is in use. At this stage, simulation has been proved to be a useful tool, when a corrective action is introduced, simulation shows the reduction in the distortion. Also, simulation can be used as a tool for the design of the active filter. Through simulation, it is shown here that the application of an active power filter to a power distribution system with undesirable harmonics can result in a reasonably clean current waveform.

Artificial intelligence is one of the major fields developed since past four decades, and is popular due to its ability to handle complex problem at difficult situations. These tools of artificial intelligence (Fuzzy Logic, Artificial Neural Network, Genetic Algorithms, Wavelet theory, Optimization methods) are used for improving the power quality effectively since 80's and produce good performances. A survey of various techniques is available in [23].

Fuzzy logic is one of the alternatives to artificial intelligence originated by Zadeh [26]. Use of fuzzy logic for minimization of harmonics and improvement of power quality is not a new issue rather various authors have introduced some innovative methodologies using these tools. A survey of various works using fuzzy logic is available in [27]. A brief review of important findings reported by various authors using fuzzy logic is given below:

In [158], Dell'Aquila et al. have developed shunt active filter with fuzzy logic estimation of the power devices duty cycle via current control of PWM inverter. This scheme was tested for compensating the real line current drawn by an AC induction motor drive using virtual instrumentation and found that the scheme is able to compensate the harmonics pollution. In [159], Shaosheng and Yaonan have proposed a Takagi-Sugeno fuzzy model to predict the future harmonics compensating current. The model is derived from input-output data by means of product space fuzzy clustering. The developed control model is applied to compensate the harmonics produced by the variable nonlinear load. An important point of the work is the use of optimization method to minimize the computational steps, which makes the overall scheme complex. In [160], a comparative analysis is given for voltage source active filter compensating current harmonics using conventional PI and fuzzy PI controlled scheme, and it is shown that the fuzzy PI scheme gives better performance. However, the scheme was not tested for variable load conditions. In [161], the authors have introduced a decaying factor with the conventional PI controller of APF keeping the proportional and integral gain constant. This decaying factor is regulated via fuzzy logic and it is shown that the scheme gives better performance in comparison to conventional PI controller. In [162], the authors have focused to minimize the harmonics for unbalanced and voltage sag compensation via fuzzy logic for series APF.

The most important observation from the work reported by various authors for power quality improvement is the design of active power filter under "fixed load" conditions, however in practical life the load are not fixed. Hence, there is the need to design an active power filter, which is capable of maintaining the THD according to the specifications decided by universally accepted IEEE norms [28], under variable load conditions.

This chapter, therefore, presents a simple, robust fuzzy logic based active power filter to control the harmonics under variable load conditions.

5.2 THE SHUNT ACTIVE POWER FILTER

5.2.1 Overview

Active power filters are considered as a feasible alternative over the classical methods to compensate harmonics as well as reactive power requirements of the non-linear loads. These are also referred as active filters (AF), active power line compensators (APLC), instantaneous reactive power compensators etc.

With the significant development and advances in switching speed and capacity of the power semiconductor devices, various topologies of the APF are developed for the compensation of voltage and current harmonics, reactive power, neutral current, voltage unbalance, terminal voltage regulation ,voltage flicker etc.

APFs are generally built around a Pulse Width Modulation (PWM) converter with a capacitor /inductor on its DC side. The PWM converter switches are controlled to draw /supply a compensating current from /to the utility. So that it cancels current harmonics on the AC side, by generating nonlinearities opposite to the load nonlinearities, and make the source current almost sinusoidal, which may be in phase or in phase displacement by some phase angle with mains voltage, based on both harmonic and reactive power compensation simultaneously or only harmonic compensation capability.

The basic principle of shunt active filter was originally presented by Sasaki and Machida [129] in 1971. They controlled the shunt active filter in such a way as to shape the source current into sinusoid by injecting the compensating current in phase opposition. Since a linear amplifier was used to generate the compensating current, its realization was unreasonable due to low efficiency. In 1976, Gyugyi and Strycula [163] presented a family of shunt and series filters, and established the concept of active filters consisting of PWM inverters using power transistors, but it was lacking on the part of control scheme for practical implementation. In the beginning, shunt active power filters were proposed to suppress the harmonics generated by large rated thyristor converters and inverters used in HVDC transmission systems. However, they could not be realized in real power systems due to non-availability of high power, high speed switching devices in 1970's. With remarkable improvement in switching speed and capacity of the power semiconductor devices in the 1980's, shunt active power filters using PWM inverters have been studied, with an attention to their practical implementation in real power systems. However, their practical uses were delayed due to the lack of better control strategies, high losses in the main circuit of active filter, higher initial cost and inferior efficiency [164]. Today, significant advancement in the capacity and switching speed of GTO's and IGBT's, in conjunction with microcomputers and digital signal processors (DSPs) have made it possible to realize APF's with complex control.

Various types of active power filters have been proposed [127] and are classified based on the type of converter, different configurations used, control methodologies, the economic and technical considerations and selection for specific applications. Several types of APF have been usefully categorized and discussed in [20] using ideas of duality to explore the similarity between different approaches. Chen and Xie [128] have presented a review of control strategies (current reference generation techniques as well as current control techniques) applied to APF.

Among the various topologies of APF developed so far, shunt APF based on the current controlled voltage source type PWM converter has been proved to be very effective even when the load is highly nonlinear. The current source inverter as an APF acts as non-sinusoidal current source. It is reliable, but has higher losses and requires higher parallel AC power capacitance. Also, it can not be used in multilevel configuration to improve the performance at higher voltage ratings. The voltage-source inverter as an APF has a self-supporting DC voltage bus with large DC capacitance. It is lighter, cheaper and expandable to multilevel configurations [121].

In [122], an APF scheme was presented, in which the compensating current was determined using a simple synthetic sinusoid generation technique by sensing the load current. This scheme is further modified, by sensing line currents only [123, 124, 165], in which the reference compensating currents are obtained by regulating the DC link voltage, which is simple and easy to implement. A low pass filter is generally used to filter the ripples introduced in the DC link voltage, due to injection of real /reactive power [124]. Use of this low pass filter also introduces a finite delay. To avoid the use of this low pass filter, the DC link voltage is sampled at the zero crossing (positive going) of the source voltages [123, 165].

In [123], it is proposed to sample this voltage at the zero crossing of one of the phase voltages, to make this compensation instantaneous. It makes the compensation instantaneous in single phase systems, but not in three phase systems. Also, sampling only once in a cycle as compared to six times in a cycle has a higher rise /fall in the DC link voltage during transients. Therefore, they have preferred to sample this voltage at the zero crossings on the source voltages (i.e. six times in a cycle). The complete design criterion for selection of power and control circuit parameters is given in [123, 125].

Investigations reported in this chapter are performed on a three phase shunt active filter to compensate harmonics and reactive power requirement of the nonlinear loads. The control scheme is based on sensing line currents only, an approach different from the conventional methods. DC link voltage is regulated to estimate the reference current template. Role of DC link capacitor is described to estimate the reference current. Results presented here are based on exhaustive simulation study to investigate the performance of the APF during transients as well as in steady state for different loading conditions, and important parameters (THD, power factor, etc.) are studied before and after compensation.

5.2.2 APF: Basic Compensation Principle

Fig. 5.1(a) shows the basic compensation principle of the shunt APF. A current controlled voltage source PWM converter with necessary passive components is used as an APF. It is controlled to draw /supply a compensated current from /to the utility, such that it cancels reactive and harmonic currents of the non-linear load. Thus, the resulting total current drawn from the a.c. mains is sinusoidal. Ideally, the APF needs to generate just enough reactive and harmonic current to compensate the non-linear loads in the line. Fig. 5.1(b) illustrates the waveform of load current (curve A), source current, after the harmonic compensation (curve B), and compensating current injected by the APF (curve C), to make the source current sinusoidal.

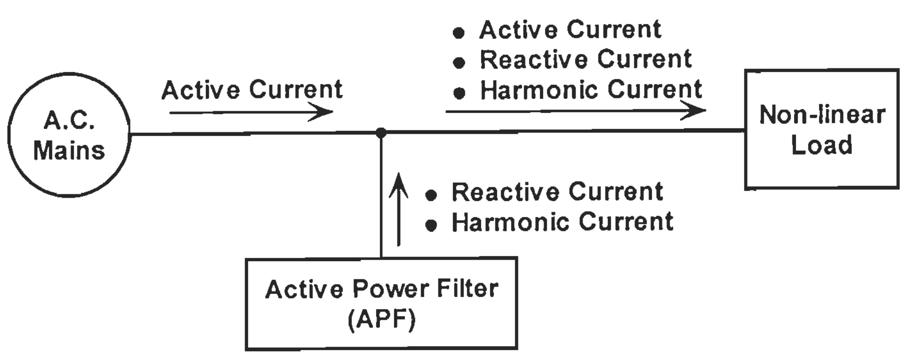

Fig. 5.1(a): Basic compensation principle of the shunt APF

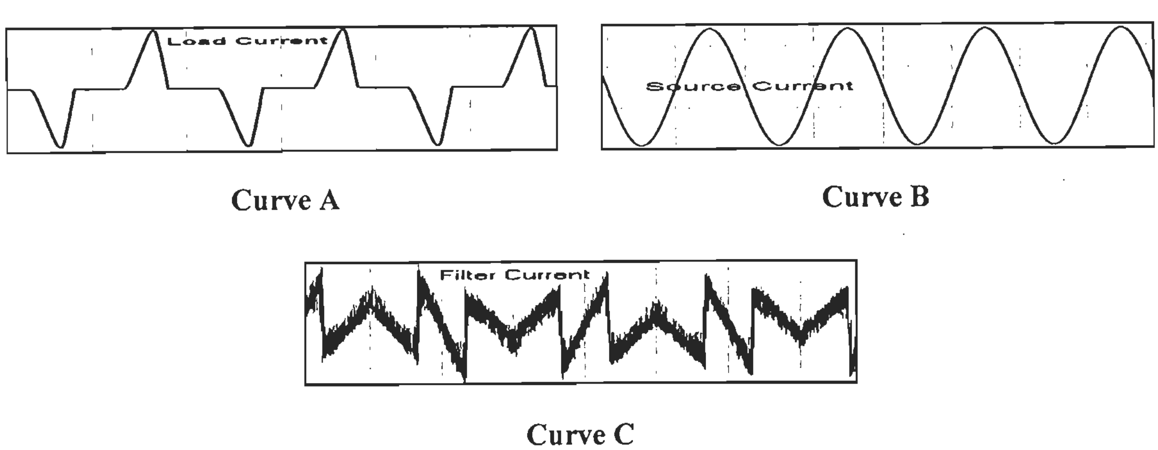

Fig. 5.1(b): Waveform of load current (curve A), desired source current (curve B), and compensating current injected by the APF (curve C)

5.2.3 APF: Working Principle and Configuration

A current controlled voltage source PWM converter with an inductor on its AC side and a capacitor on its DC side is used as an APF. The complete diagrammatic representation of current controlled voltage source type PWM converter based shunt active power filter is shown in Fig. 5.2(a) and Fig. 5.2(b).

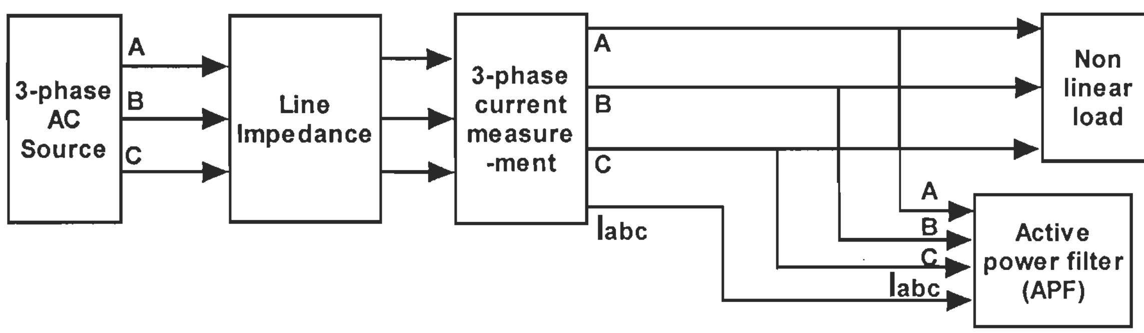

Fig. 5.2 (a): Connection diagram of shunt APF

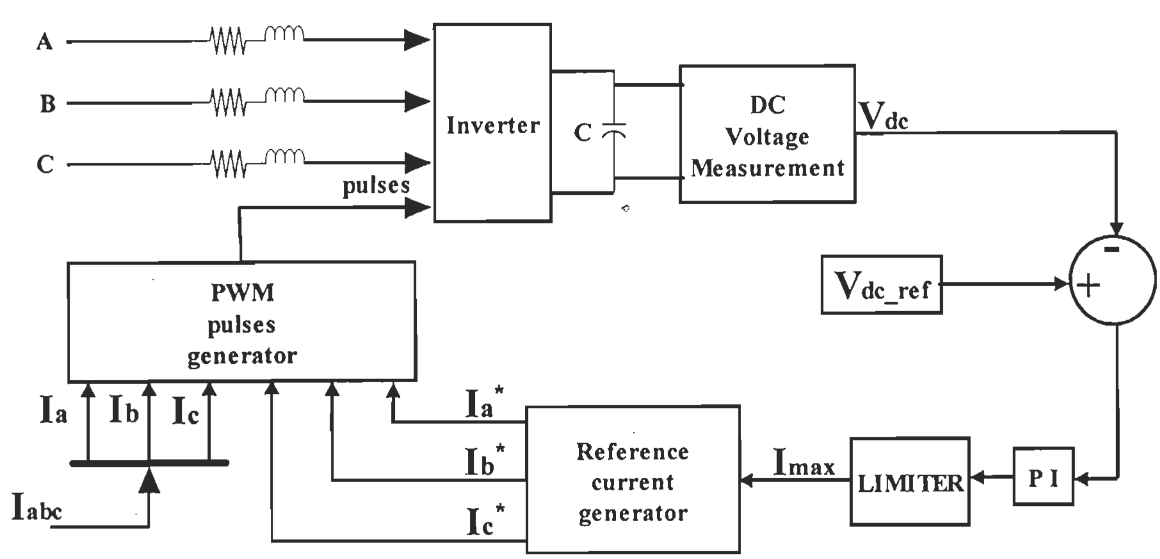

Fig. 5.2 (b): Schematic diagram of shunt APF

5.2.3.1 Control Scheme of APF

The Control scheme consists:

- A PI controller,
- Limiter,
- 3-phase sine wave generator for reference current generation, and
- Generation of switching signal.

The peak value of reference currents is estimated by regulating the DC link voltage. The actual capacitor voltage is compared with a set reference value. The error signal is then processed in a PI controller, which contributes to zero steady error, in tracking the reference current signal. The output of the PI controller is considered as peak value of the supply current (I_{max}), which is composed of two components: (a) fundamental active power component of load current, and (b) loss component of APF; to maintain the average capacitor voltage to a constant value.

Peak value of the current (I_{max}) so obtained, is multiplied by the unit sine vectors in phase with the respective source voltages to obtain the reference compensating currents. These estimated reference currents (I_{sa}*, I_{sb}*, I_{sc}*) and sensed actual currents (I_{sa}, I_{sb}, I_{sc}) are compared at a hysteresis band, which gives the error signal for the modulation technique. This error signal decides the operation of switches of converter. In this current control circuit configuration, the source /supply currents I_{sabc} are made to follow the sinusoidal reference current I_{sabc}*, within a fixed hysteresis band. The width of hysteresis window determines the source current pattern, its harmonic spectrum and switching frequency of the devices.

The dc-link capacitor voltage is kept constant throughout the operating range of the converter. In this scheme, each phase of the converter is controlled independently. To increase the current of a particular phase, the lower switch of the converter associated with that particular phase is turned on while to decrease the current the upper switch of the respective converter phase is turned on.

5.2.3.2 Power Circuit of APF

The APF shown in Fig. 5.3 uses the three-arm current controlled voltage source PWM converter. Here, P_{Load}, P_L, and P_L^H are the total active power, fundamental active power and harmonic active power consumption of the load. Q_{Load}, Q_L, and Q_L^H are total, fundamental, and harmonic reactive power consumption of the load. P_{INV} is the total active power supplied by the APF and P_{Loss} is power losses of inverter which is used to maintain the DC side capacitor voltage. P_S and Q_S are active and reactive power supplied by the source.

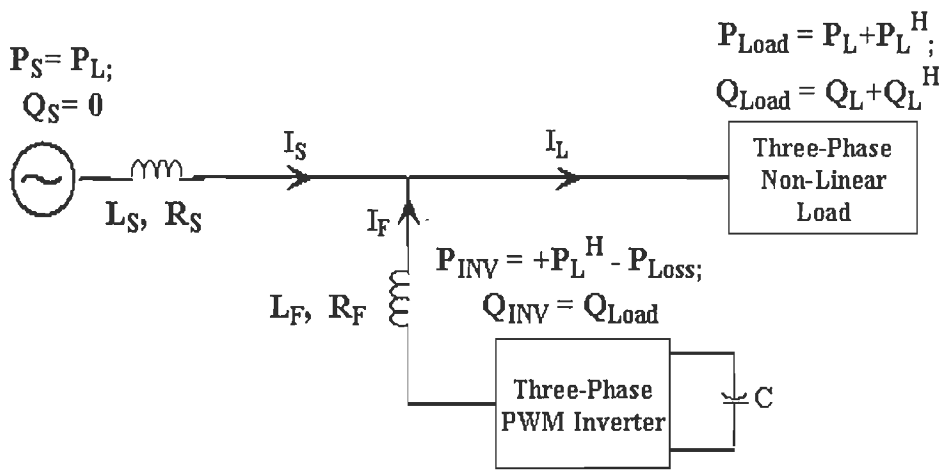

Fig. 5.3: Power circuit diagram of the shunt APF

The reactive power capacity of the APF is set by the level of limiter [125]. With constant limiter level, whenever the load current increases, load reactive power demand also increases, hence, $Q_{INV} < Q_{Load}$; also, $P_L^H > P_{INV}$ as harmonic real power demand of load increases. This unbalance in power equation affects the performance of APF, and it needs an additional supplement of reactive power equal to $Q_{Load} - Q_{INV}$ and harmonic real power equal to $P_L^H - P_{INV}$, to maintain the performance of APF. In order to achieve unity power factor operation, and for drawing sinusoidal currents from the utility, APF must supply all the reactive and harmonic power demand of the non-linear load. Thus, to bring the APF back in proper /normal operation mode, level of limiter has to be increased or decreased with the change in the nonlinear load current. At the same time, APF will draw real component of power (P_{Loss}) from the utility, to supply switching losses and to maintain DC link voltage.

For accurate and instantaneous compensation of reactive and harmonic power, it is necessary to calculate the actual value of the instantaneous current supplied by the source, i.e. $i_S(t) = I_{max} Sin(\omega t)$

5.2.4 Design of Power Circuit Parameters

5.2.4.1 Selection of reference value of DC link voltage $V_{DC_{ref}}$ and Filter Inductor L_F :

For satisfactory operation, the magnitude $V_{DC_{ref}}$ should be higher than the magnitude of source voltage V_S. By suitable operation of switches, voltage V_F, having fundamental component V_{F_1} is generated at AC side of PWM converter of the APF. This results in flow of fundamental current component I_{F_1}, to compensate the reactive power of the load.

In order to maintain the source fundamental current I_{S_1}, in phase with the V_S, APF should compensate all the fundamental reactive power of the load. The vector diagram, shown in Fig. 5.4, represents the reactive power flow, in which, I_{S_1} should be in phase with the source voltage V_S and fundamental filter current I_{F_1} should be orthogonal to V_S, to fulfill the reactive power requirement.

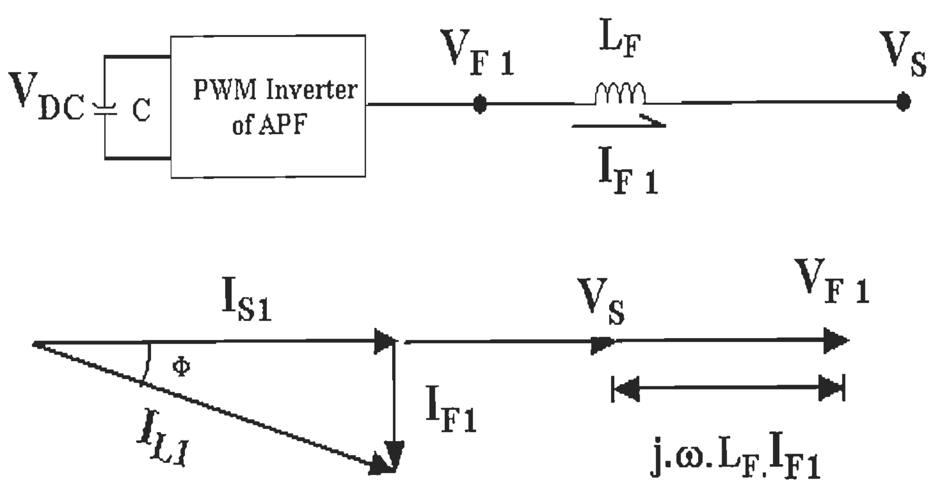

Fig. 5.4: **Single line diagram of APF**

From the Fig. 5.4,

$$V_{F_1} = V_S + j.\omega.L_F.I_{F_1} \tag{5.1}$$

$$I_{F_1} = \left(\left(V_{F_1} - V_S\right)/\omega.L_F\right) = \left(V_{F_1}/\omega.L_F\right)\left(1-\left(V_S/V_{F_1}\right)\right) \tag{5.2}$$

and three-phase reactive power delivered by the APF can be calculated as

$$Q_{F_1} = Q_{L_{F_1}} = 3V_S.I_{F_1} \tag{5.3}$$

from eqn. (5.2) and (5.3)

$$Q_{F_1} = 3V_S\left(V_{F_1}/\omega.L_F\right)\left(1-\left(V_S/V_{F_1}\right)\right) \tag{5.4}$$

From above eqn., it is evident that the APF can compensate the lagging reactive power only when $V_{F_1} > V_S$ as for this value Q_{F_1} is positive. For the case $V_{F_1} < V_S$, Q_{F_1} is negative and APF will draw the reactive power from the utility. The upper limit of V_{F_1} is calculated on the basis of maximum capacity of the APF, determined as below:

To obtain maximum capacity of APF

$$\left(dQ_{F_1}/dV_S\right) = 0; \qquad \frac{d}{dV_S}\left(\frac{3V_S.V_{F_1}}{\omega.L_F} - \frac{3V_S^2}{\omega.L_F}\right) = 0; \qquad \Rightarrow \quad V_{F_1} = 2V_S$$

Maximum capacity of APF is

$$Q_{F_{1\,max}} = \left(3V_S^2/\omega.L_F\right) \tag{5.5}$$

Hence, V_{F_1} must be set according to the capacity requirement of the system. From above discussion the range of V_{F_1} can be given as

$$V_S < V_{F_1} \leq 2V_S \tag{5.6}$$

If it is assumed that the PWM converter operates in the linear modulation mode (i.e. $0 \leq m_a \leq 1$) [166], then amplitude modulation factor $m_a = \left(\left(2\sqrt{2}\right)V_{F_1}/V_{DC}\right)$.

For $m_a = 1$,

$$V_{DC} = \left(2\sqrt{2}\right) V_{F_1} \tag{5.7}$$

The filtering inductor (L_F) is used to attenuate the ripples of converter /filter current, due to the switching of converter. Hence, the design of L_F is based on the principle of harmonic current reduction. For the sinusoidal PWM converter that operates in the linear modulation mode $0 \le m_a \le 1$, the maximum harmonic voltage occurs at the frequency $\omega.m_f$, where m_f is the frequency modulation ratio of the PWM converter [167].

Considering only this harmonic content, the ripple current of the converter current can be given as

$$I_{F_h} \cong I_{F_h}(\omega.m_f) = \left(V_{F_h}(\omega.m_f) / \omega.m_f.L_F\right) \tag{5.8}$$

where, subscript 'h' denotes the harmonic component. For the qualitative representation, ratio of I_{F_h} and $I_{F_{1rated}}$ is defined as Ripple Attenuation Factor (RAF);

$$RAF = \left(I_{F_h} / I_{F_{1rated}}\right) \tag{5.9}$$

where, $I_{F_{1rated}}$ is the rated value of the fundamental component of filter current I_{F_1}, which can be determined from eqn. (5.4)

$$Q_{L_{F_1}} = Q_{F_1} = 3V_S.I_{F_1} = 3V_S \frac{V_{F_1}}{\omega.L_F}\left(1 - \frac{V_S}{V_{F_1}}\right)$$

$$I_{F_{1rated}} = \left(Q_{F_1} / 3V_{S_{rated}}\right) \tag{5.10}$$

$V_{DC_{ref}}$ and L_F can be selected by solving eqn. (5.4) and (5.8) simultaneously.

5.2.4.2 Design of DC Link Capacitor

The role of DC link capacitor is to absorb /supply real power demand of the load during transient. The design of DC link capacitor is either based on the principle of instantaneous power flow or is based on maximum real power rating of load. It is found that the value of C_{DC} depends on the maximum possible variation in load and not on the steady state value of the load current. Hence, a proper forecasting in the load variation reduces the value of C_{DC}.

On the basis of above discussion, for 5 KVA compensation capacity, three-phase, 230 volt, 50 Hz system, with 5% RAF, $m_f = 200$, $m_a = 1$, following parameters are selected for simulation study:

$L_F = 3.35$ mH, $V_{DC_{ref}} = 600$ V, $C_{DC} = 2200$ μF.

5.2.5 Role of Limiter in Active Power Filter

The complete diagrammatic representation of current controlled voltage source type PWM converter based shunt active power filter is shown in Fig. 5.2, which contains a PWM converter, a control unit and a power circuit. As discussed in section 5.2.3, APF must supply all the reactive and harmonic power demand of the non-linear load, level of limiter has to be changed with the increase or decrease into the nonlinear load current, to keep the THD within the acceptable limits.

By increasing the value of load current, a specific value of limiter was obtained corresponding to a particular load current, for minimum possible value of THD_I. On the basis of this rigorous analysis, a look-up table (Table-5.1) is formed between load current and corresponding LIMITER value. Using this look-up table, limiter block changes its value, corresponding to variable load current, to bring the THD_I to lowest possible value. For this purpose, limiter model was reconfigured as two-input and one-output device, earlier which was considered as one-input and one-output device. Second input will now be used to take the saturation (limiter) value from look-up table, on basis of load current. The conventional limiter model used in shunt APF, which has a constant value and the limiter model are shown in Fig.

5.5(a) and Fig. 5.5(b) respectively. The two inputs needed for the proposed (variable) limiter model are (i) PI controller output i.e. I_{max} and (ii) FLC output i.e. limiter value.

The curve, shown in Fig. 5.6 (a), gives a comparison between constant and variable Limiter, in terms of its performance (THD_I vs. non-linear load current). With constant limiter, load current range of operation (for which the value of THD_I is below 5%) of APF is 1.8 A to 9.6 A. With variable limiter, the range of operation is 1.6 A to 80 A.

For ready reference, results are also shown in Fig. 5.6 (b), in form of a characteristic curve, which forms the basis of selection of limiter value for various load currents. It seems necessary to mention here that the "value of 'R' on DC side of non-linear load" is a measure of load current, i.e. higher value of 'R' indicates the lower load current, as it is evident from Table- 5.1. A fuzzy logic controller (FLC) is designed to take over the work of variable limiter based on look-up table.

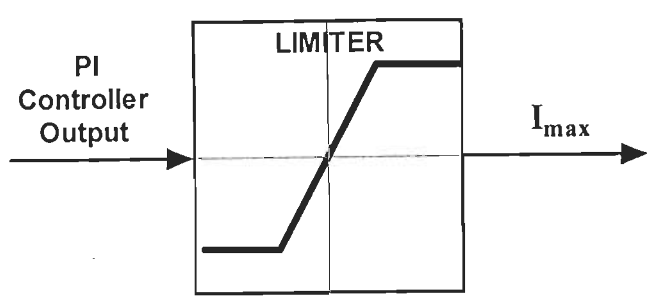

Fig. 5.5(a): Conventional (constant) limiter model

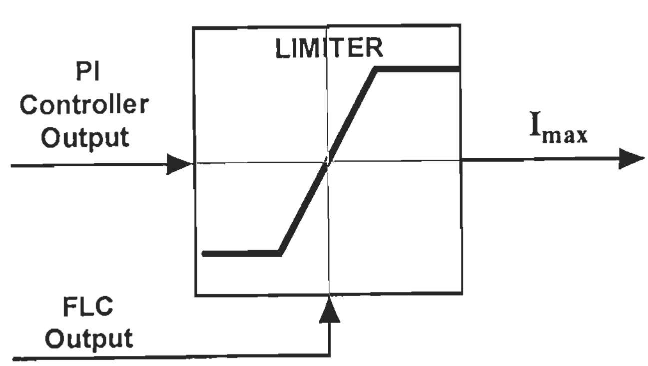

Fig. 5.5(b): Proposed (variable) limiter model

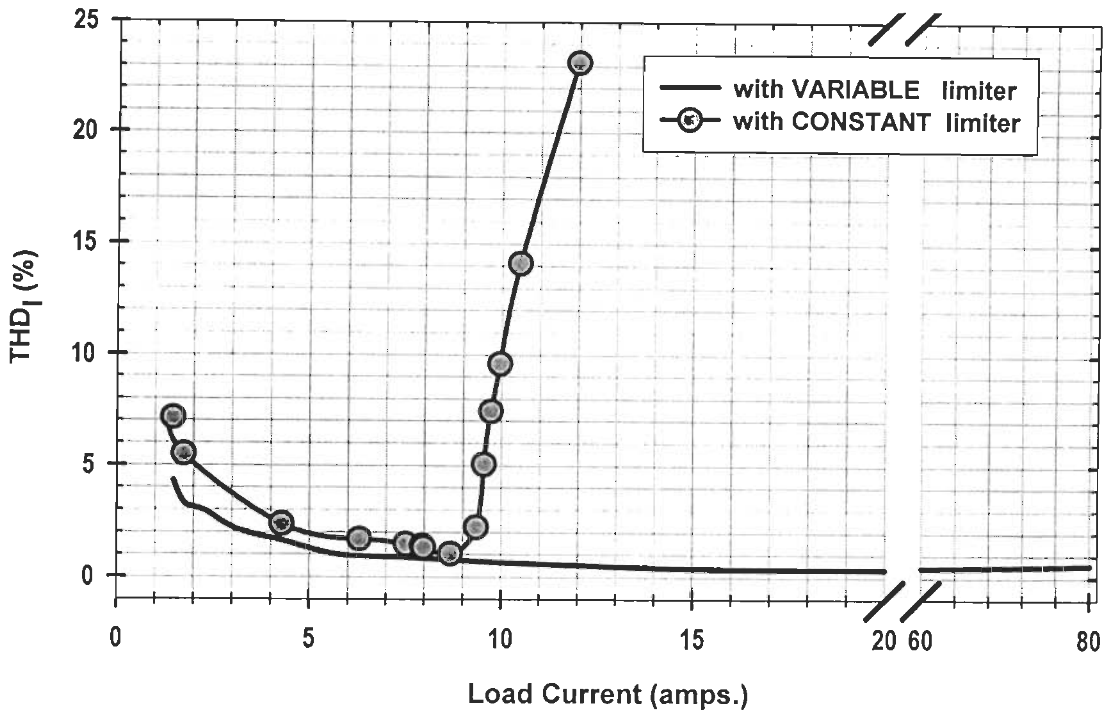

Fig. 5.6(a): Comparison between constant and variable Limiter

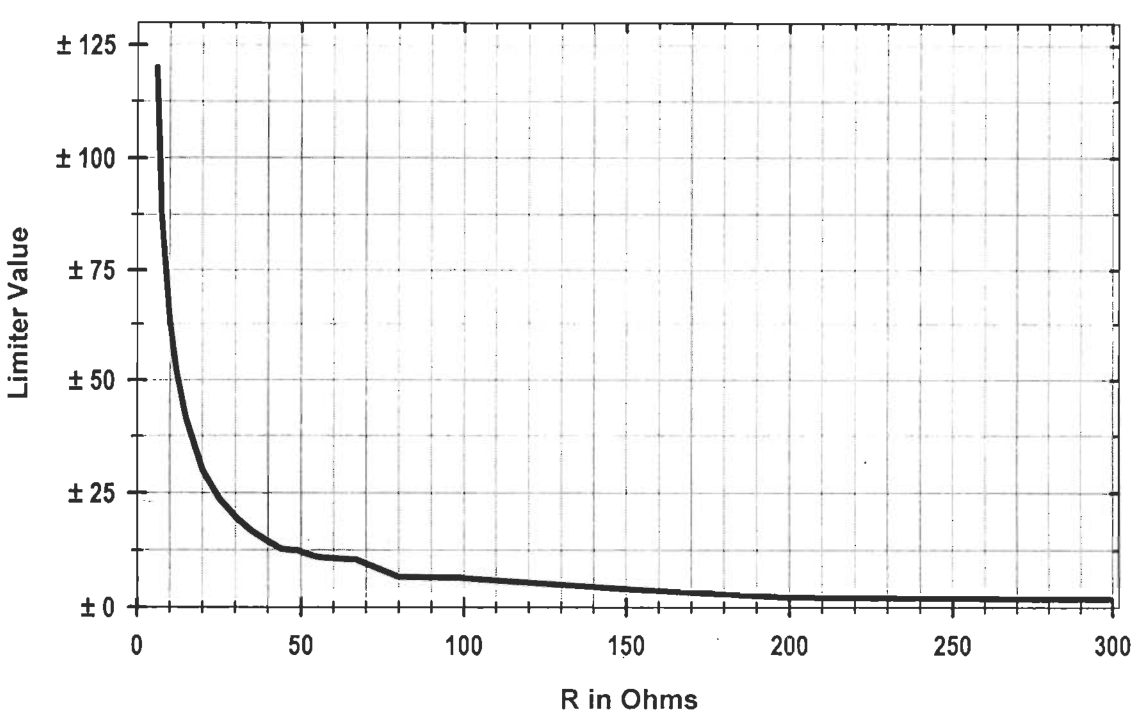

Fig. 5.6 (b): Plot between "value of 'R' on DC side of non-linear load" and Limiter value

Table-5.1: Look-Up table between Load Current and Corresponding Limiter Value

R (in Ohms)	I_{as} (rms) (in amps.)	THD_I (%)	LIMITER Value
299	1.470	4.30	± 1.75
250	1.762	3.29	± 2.00
199	2.267	2.99	± 2.25
150	3.078	2.17	± 4.00
99	4.307	1.63	± 6.50
80	5.428	1.10	± 6.75
67	6.380	0.93	± 10.50
56	7.608	0.86	± 11.00
53	8.048	0.78	± 11.50
49	8.700	0.76	± 12.50
45	9.640	0.68	± 12.75
44	9.860	0.68	± 13.00
43	10.01	0.70	± 13.25
42	10.37	0.63	± 13.75
40	10.89	0.59	± 14.50
35	12.47	0.50	± 16.75
30	14.58	0.39	± 19.75
25	17.42	0.34	± 23.75
20	21.83	0.35	± 30.00
15	29.52	0.32	± 41.00
12	37.44	0.33	± 52.25
10	45.21	0.38	± 63.25
7.5	62.12	0.44	± 87.25
6	80.13	0.57	± 120.0

5.3 FUZZY LOGIC

Power systems are large, complex, broadly distributed systems, influenced by unexpected events. The mathematical formulations of power systems and related events are derived under restrictive assumptions and allow many uncertainties. The system model is not often available, and its operations are based on many vague constraints and multiple conflicting objectives. Computational burden for solving such system using conventional techniques becomes significant. The experience of human experts can be represented as functional knowledge in terms of heuristic rules. Much of human knowledge is imprecise and vague. Fuzzy logic and fuzzy set theory is a convenient framework for dealing with such vague, linguistic articulated knowledge. Additional benefits of fuzzy logic include its simplicity and its flexibility. Fuzzy logic can handle problems with imprecise and incomplete data, and it can model nonlinear functions of arbitrary complexity.

Research on the theory and application of fuzzy logic has been growing since the idea of fuzzy set theory was introduced in 1965 by Zadeh as a new approach to represent vague and inexact nature of real world [26]. Among its many applications, it has been shown to be a powerful tool in dealing with uncertainties and nonlinearities in control systems. In the past decade, fuzzy control has been used in many industrial applications, such as control of the PWM inverter for an AC drive [168], Load Frequency Controller [169], Industrial welding [170], temperature control [171], Modeling of basic electrical machines [172], speed control of an induction motor [173], switch control in DC /DC converters [174], and Voltage Stability Analysis [175], to name just a few. In this section, we give a brief description of fuzzy sets and their application to fuzzy logic control.

Consequently, fuzzy logic is a technique, which can successfully handle imprecise, vague or "fuzzy" information present in power systems. The term fuzzy logic has been used in two different senses. In a narrow sense, fuzzy logic is a logical system that generalizes classical two-valued logic, which is an extension of multi-valued logic for reasoning under uncertainty. In a broad sense, fuzzy logic is the theory of fuzzy sets as a generalization of conventional set theory, by introducing graded membership and relates to sets with soft boundaries [176].

Fuzzy set theory derives from the fact that almost all natural classes and concepts are fuzzy rather than crisp in nature. Fuzzy logic systems provide an excellent framework to model uncertainty and imprecision in human reasoning with the use of linguistic variables with membership functions.

The fuzzy theory is an appropriate tool for dealing with the heuristics of linguistically described algorithms. These linguistic algorithms are simply intuitive natural language statements representing expert knowledge derived out of long experience of human experts /operators. These statements are simple and easy to understand. Additionally, only few of these statements are required for describing complex processes satisfactorily [177]. These natural language statements can be classified as:

i) Deterministic linguistic term (Singleton)

ii) Crisp linguistic term (Crisp sets)

iii) Fuzzy linguistic term (Fuzzy sets)

A natural language statement that is used to represent an element /variable that has one and only one meaning attached to it is called as deterministic linguistic term or singleton. Sometimes, natural language statements refer to a range of values instead of a single value. The set of all values in that interval (range) constitutes a crisp linguistic term or crisp set. The use of natural language statements that are intuitive and include some kind of uncertainty is quite common in daily life. For example statements like 'room temperature is comfortable' or a person is tall (no exact numerical value of temperature or height at that moment) or 'beautiful girl' (for beautiful, no metric exists) etc. Here, comfortable, tall and beautiful are fuzzy sets. These statements are uncertain from the point of view of exact numerical values, but still they are precise enough from the understanding point of view. So, fuzzy concepts are one of the important channels by which we mediate and exchange information, ideas and understanding among ourselves. Such statements are characterized through membership functions whose membership value lies in the interval [0, 1]. These statements are called as fuzzy linguistic terms or fuzzy sets.

In fuzzy theory, a fuzzy set is defined as a set with movable boundaries. The elements of this set are expressed using membership value that lies in the interval [0, 1]. Unlike the elements of conventional sets, elements of fuzzy sets need not satisfy all the properties of this set for becoming a member. In the limiting case, the fuzzy set approaches the conventional set. The membership value 'zero' for an element denotes the complete absence of this element from the fuzzy set where as the value 'one' denotes the full membership of this element in the fuzzy set. A fuzzy set introduces vagueness by eliminating the sharp boundary that divides members from nonmembers in the group. Thus, the transition between full membership and non-membership is gradual rather than abrupt. Hence, fuzzy sets may be viewed as an extension and generalization of the basic concepts of crisp sets; however, some theories are unique to the fuzzy framework.

5.3.1 Definition of Crisp and Fuzzy Sets

A universal set X is defined as a set in a universe of discourse. If a crisp set A is included in the universal set X, the relationship is expressed as

$$A \subseteq X \quad (5.11)$$

An element x is called a member of the set A if it is included in the set A. This is expressed as

$$x \in A \quad (5.12)$$

If elements a_1, a_2 ....a_n are the members of set A, it is represented as

$$A = \{a_1, a_2 \ldots. a_n\} \quad (5.13)$$

Membership functions (characteristic function) are used to represent whether or not an element x is contained in a set A. Thus, the membership function μ_A is defined as

$$\mu_A(x) = 1 \text{ if and only if } x \in A \text{ , and} \quad (5.14)$$

$$\mu_A(x) = 0 \text{ if and only if } x \notin A \quad (5.15)$$

The membership function of a crisp set assigns a value of either 0 or 1 to each member in the universal set. In other words, the membership function μ_A maps elements in the universal set X to the set $\{0, 1\}$. It can be written as

$$\mu_A : X \to \{0,1\}, \ \forall x \in X \tag{5.16}$$

When there is a vague boundary involved, the theory of fuzzy sets is applicable. With fuzzy sets, each element is mapped to a real number between 0 and 1 by the membership function

$$\mu_A : X \to [0,1], \ \forall x \in X. \tag{5.17}$$

The value assigned to each element indicates a probability that the element belongs to the set A.

5.3.2 Membership Function

All the Membership Degrees associated to a fuzzy set generate a shape called Membership functions (MF). A membership function (MF) is a curve that defines how each point in the input space is mapped to a membership value (or degree of membership) between 0 and 1. The distribution of membership does not always vary linearly with universe of discourse. Hence, we have many types of membership distribution generally referred as membership functions. Various types of membership functions (MFs) are triangular, trapezoidal, sigmoidal, exponential, bell membership function (MF) etc. These MF can be expressed either in graphical or in functional form. For the purpose of simulation using fuzzy logic tools, the functional representation of MF is more suitable as it allows itself to be manipulated through fuzzy arithmetic. The simplest membership functions are formed using straight lines. Of these, the simplest is the triangular membership function. it is nothing more than a collection of three points forming a triangle. The trapezoidal membership function has a flat top and really is just a truncated triangle curve, i.e. a special case of a triangular membership function. These straight line membership functions have the advantage of simplicity. That is why these two are the most commonly used membership functions. The functional description of these functions can be given as:

i) **T (triangular) function**

$$T(x;a,b,c)=\begin{cases} 0 & \text{for } x<a \\ (x-a)/(b-a) & \text{for } a\le x\le b \\ (c-x)/(c-b) & \text{for } b\le x\le c \\ 0 & \text{for } x>c \end{cases} \tag{5.18}$$

Graphical presentation of triangular function is given in Fig. 5.7(a).

ii) **Trapezoidal function**

$$T(x;a,b,c,d)=\begin{cases} 0 & \text{for } x\le 0 \\ (x-a)/(b-a) & \text{for } a\le x\le b \\ 1 & \text{for } b\le x\le c \\ (d-x)/(d-c) & \text{for } c\le x\le d \\ 0 & \text{for } x\ge d \end{cases} \tag{5.19}$$

Graphical presentation of trapezoidal function is given in Fig. 5.7(b).

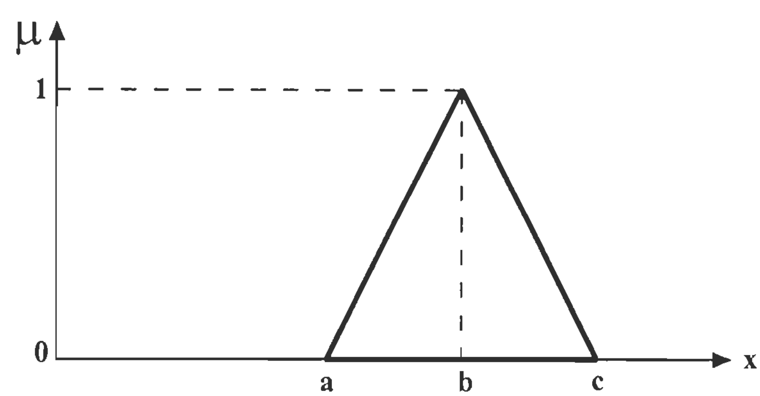

Fig. 5.7 (a): Graphical presentation of triangular function

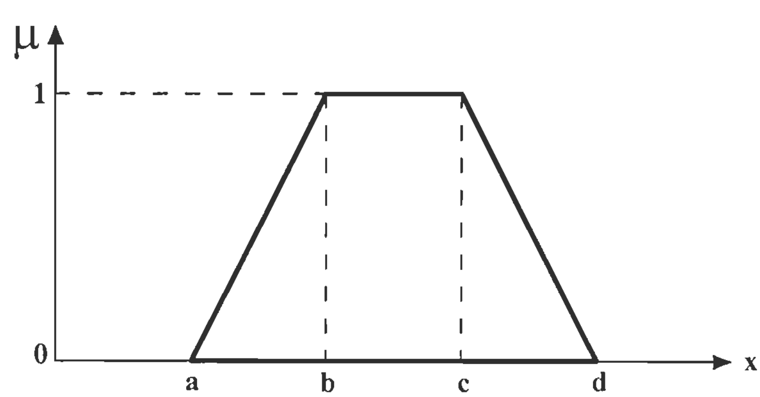

Fig. 5.7 (b): Graphical presentation of trapezoidal function

5.3.3 Basic Structure of Fuzzy Logic Controller

The basic configuration of fuzzy logic controller (FLC) is shown in Fig. 5.8. In general, a fuzzy logic system maps crisp input into crisp output and in such case contains four major components:

i) Fuzzification,

ii) Knowledge Base,

iii) Inference engine and

iv) Defuzzification

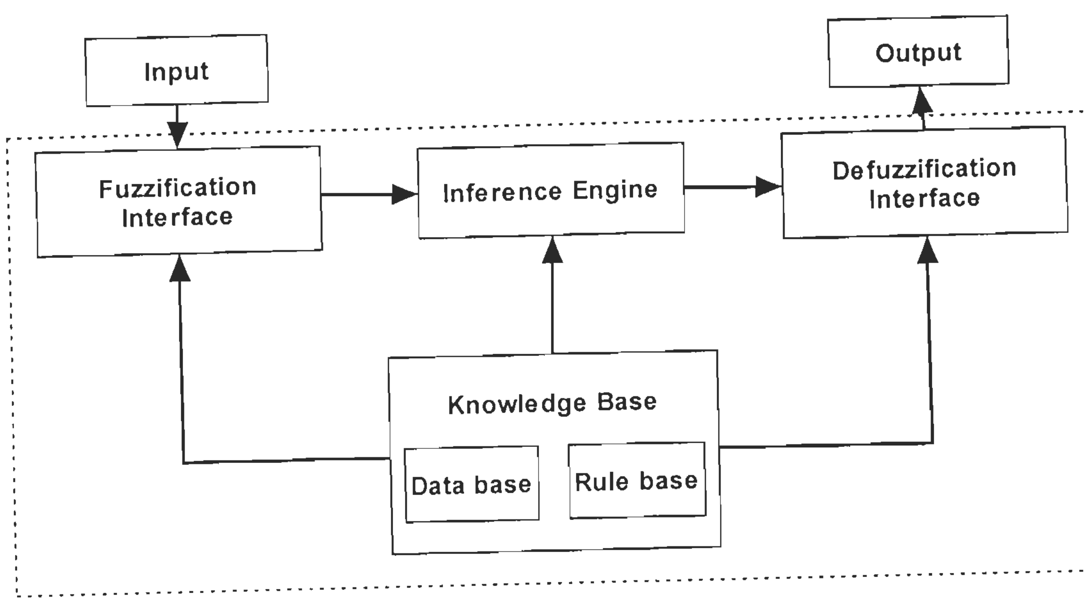

Fig. 5.8: Basic configuration of fuzzy logic controller

Fuzzification converts input data into suitable linguistic values which may be viewed as labels of fuzzy sets. Data base and rule base are the two components of knowledge base of an FLC. Database provides necessary definitions used for linguistic control rules and fuzzy data. If-then rule statements are used to formulate the conditional statements that comprise fuzzy logic. A rule base is the collection of all these statements. The rules are a set of linguistic statements based on expert knowledge, including experience and heuristics, instead of detailed mathematical model. In the fuzzy inference engine, fuzzy logic principles are used to combine fuzzy rules into a mapping from fuzzy input sets to fuzzy output sets. The process of fuzzy inference involves: membership functions, fuzzy logic operators, and if-then rules. Mathematically, fuzzy rule-based inference can be viewed as an interpolation scheme because it enables the fusion of multiple fuzzy rules when their conditions are all satisfied to a degree. Defuzzification produces a crisp output from the fuzzy set that is the output of the inference engine.

5.4 THE PROPOSED FUZZY CONTROLLER

A fuzzy logic controller (FLC) is designed to take over the work of variable limiter based on look-up table. The input-output block diagram of FLC is depicted in Fig. 5.9 to explain its function.

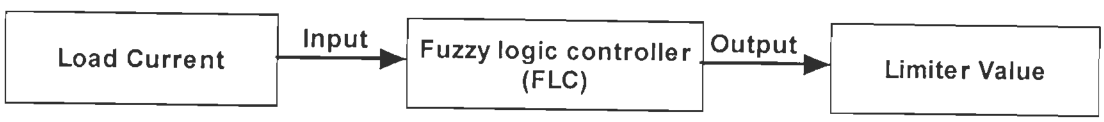

Fig. 5.9: Input-output block diagram of fuzzy logic controller (FLC)

The numerical value of load current works as the input for FLC. For the purpose of load current sensing, two different techniques have been applied. In *technique-1* total DC load current has been taken as input for FLC while in *technique-2* rms value of AC load current is used for this purpose. These two techniques are classified and detailed here as 'DC load current sensing method' and 'AC load current sensing method'.

It has been discussed in section 5.2.5 that the limiter value varies with change in load current. However, the nature of variation is highly nonlinear, and it is difficult to relate it by mathematical expression. Also in practice, the nature of input power to load is not pure sinusoidal rather stochastic in nature. Hence, mathematical modeling of variable saturation value may not be able to fully compensate the effect of harmonics.

Fuzzy logic is an alternative approach to handle this type of problem, which has become more popular during past four decades due to its advantages of robustness against parameter variation, popularity, customization etc. When system is too complex or too poorly understood to be described in precise mathematical terms, fuzzy modeling provides the ability to linguistically specify approximate relationships between the input and desired output. The relationships are represented by a set of fuzzy If-then rules in which the antecedent is an approximate representation of the state of the system and the consequent provides a range of potential responses. In the work presented here, FLC is used to regulate the limiter value according to load current. The range of operating current and particular band of operating current is one of the important design factors of fuzzy controller. The proposed FLC compensates the harmonic current for any load current variation between 1.5-80A.

The block diagram representation of fuzzy logic controller is given in Fig. 5.10, which contains the following design parameters: number and type of membership functions for input and output variables, rule base, defuzzification method.

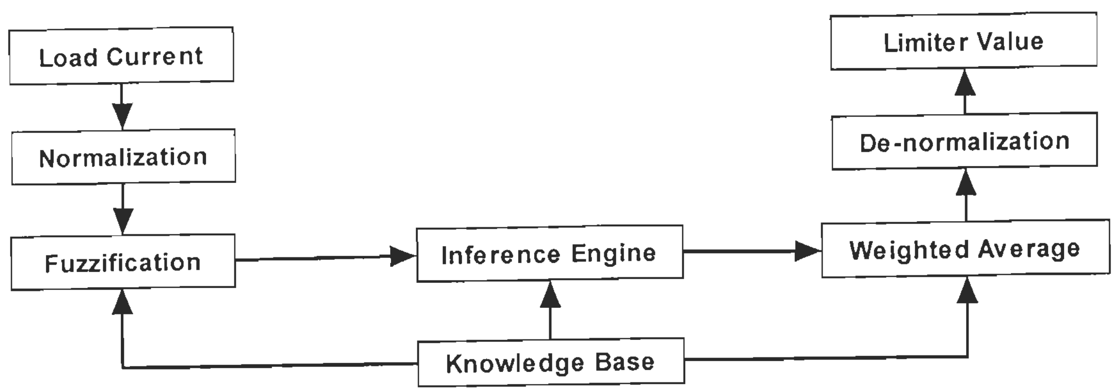

Fig. 5.10: Block Diagram representation of Sugeno fuzzy Controller

5.4.1 Membership Functions for Input Variable:

Computational efficiency, memory requirement and computational time are the few important aspects of evolutionary computational methods. The number and type of membership function (MF) decides the computational efficiency of a FLC. The shape of fuzzy set affects how well a fuzzy system of If-then rules approximate a function.

It is found that the triangular and trapezoidal membership functions are most economical [178]. This is consistent with [179] who found that triangular and trapezoidal membership functions produce the best estimation of the possibility distribution when modeling an 'expert' based system. Triangles have been the most popular If-part set shape for approximating non-linear function. Studies reported in [180] have shown that triangular membership function is most economical in the sense of above said parameters. The triangular membership functions (MFs) have been frequently used in many applications of fuzzy sets including fuzzy controllers, fuzzy models and classification [181]. Triangular membership functions are preferred because of their striking simplicity, solid theoretical basis and ease of computation, since they are symmetrical and have zero value at some point away from their center. Pedrycz [179] has carried out a detailed study legitimizing the use of the triangular membership function.

There has been a recent interest in using trapezoidal membership functions in fuzzy set theory mainly because their special structure yields more efficient computations. By definition, triangular membership functions are special cases of trapezoidal membership functions [182]. For Takagi-Sugeno (TS) fuzzy models, trapezoidal membership functions are better since membership functions with wide core areas are preferable for TS models [183]. In [184], a comparative study between triangular and trapezoidal MFs has concluded that degree of fulfillment for trapezoidal MF is always higher than triangular MF. High sensitivity to small changes in the crisp input near the center of a member is mentioned as a disadvantage of triangular MF [185], however, the parametric functional description of triangular MF is most economic one.

As in the present case, the choice of MF does not much affect the performance of system. Hence, to reduce the complexity and to involve minimum computational memory, the triangular and trapezoidal MFs, both are chosen and applied in FLC for two distinct simulations. In technique-1 (DC load current sensing method) the triangular MFs are chosen, while in technique-2 (AC load current sensing method) the trapezoidal MFs are used. For these two cases different load patterns are considered and it is found that in both cases FLC is controlling the APF very effectively.

5.4.4.1 Triangular Membership Function for Input Variable

For this work, nine unequally spaced triangular membership functions have been chosen (as shown in Fig. 5.11) for representing each linguistic variables viz., Z, VS, S, SS, SM, M, MD, H, VH. The reason for unequal spacing is to cover a band of load current with high accuracy. The number of linguistic variables is directly related to the accuracy of approximating function and plays an important role for approximating the nonlinear input-output mapping. It is shown in [180] that as the number of linguistic variable increases the output of fuzzy controller becomes a linear function of the input. In the present case, a nonlinear mapping of input-output is performed via fuzzy logic.

In order to trade-off between accuracy and complexity, through rigorous simulation studies it has been found that nine MFs are sufficient to produce desired results in required band. Reducing the number of MFs will produce improper results at some band, while increasing the number of MFs will produce a delay due to more computational steps required.

The linguistic variables are defined by $\tilde{M} = (a, b, c)$ where a, b, c are starting, middle point with unity membership grade, and end points respectively. Again, each fuzzy set is 50% overlapped with neighbor. The linguistic names of each fuzzy set with their definition are given in Table-5.2.

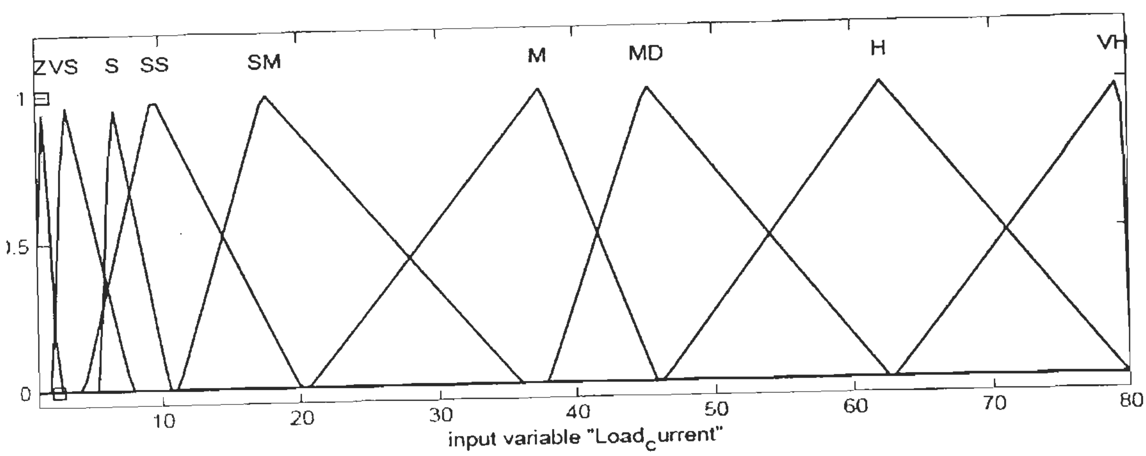

Fig. 5.11: Membership functions for input variable for triangular mf

Table-5.2: Description of membership function considered for input variable with triangular membership function

Linguistic name	Left end point	Modal value	Right end point
Zero	0.5	1.5	2.5
Very Small	2	3	7.85
Small	5.5	6.5	10.6
Slightly Small	4.31	9.5	20
Slightly Medium	11.2	17.5	36
Medium	20.6	37.5	45.8
Moderate	37.9	45.5	62.5
High	46.3	62	79.9
Very High	62.9	79.9	81.5

5.4.1.2 Trapezoidal Membership Function for Input Variable

For this work, nine unequally spaced trapezoidal membership functions have been chosen (as shown in Fig. 5.12) for representing each linguistic variables viz., ZE, VS, SM, SS, SMD, MD, MOD, HG, VHG. The reason for unequal spacing is to cover a band of load current with high accuracy, which is varying nonlinearly. Further, these are defined by $\tilde{M} = (a,b,c,d)$, where a,b,c,d are (a) starting point, (b) starting point with unity membership grade (c) end point with unity membership grade, and (d) end point respectively. Again, each fuzzy set is 50% overlapped with neighbor, which provides significant approximate value between two linguistic variables. The linguistic names of each fuzzy set with their definition are given in following Table-5.3.

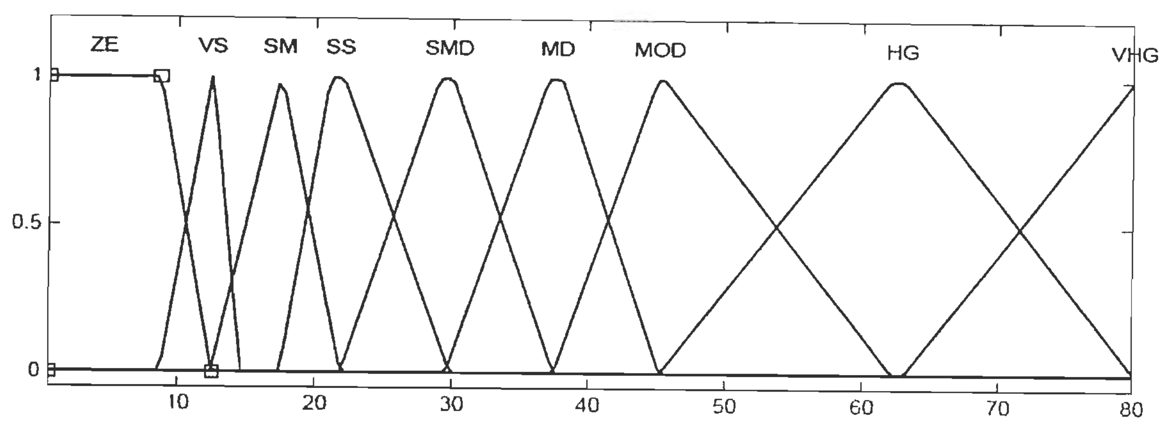

Fig. 5.12: Membership functions for input variable for trapezoidal mf

Table-5.3: Description of membership function considered for input variable with trapezoidal membership function

Linguistic name	(a)	(b)	(c)	(d)
Zero (ZE)	0.5	0.5	8.7	12.47
Very Small (VS)	8.7	12.4	12.5	14.58
Small (SM)	12.4	17.4	17.5	21.83
Slightly Small (SS)	17.42	21	22	29.83
Slightly Medium (SMD)	21.83	29	30	37.44
Medium (MD)	29.52	37	38	45.21
Moderate (MOD)	37.44	45	45.5	62.12
High (HG)	45.21	62	63	80.13
Very High (VHG)	63	80	81	81

5.4.2 Membership Functions for Output Variable

In the case of Sugeno type FLC [186], no membership functions are used for representing output variable, rather these are mapped as mathematical expression of consequent part of rule base. In present case, the function of fuzzy logic is to map a nonlinear input-output function. Thus, the number of rules is directly related with number of MF for input and output. Hence, in the present case nine rules are made.

The weighted factor of Sugeno FLC is an important factor for producing accurate output. Since, the antecedent part of rules are chosen as linear combination of input, the weighted factors are also linear and of zero order.

5.4.3 Design of Rule Base

In general, the rule-base of Sugeno type fuzzy controller is given by

$$\underbrace{(R_i): IF\ load\ current\ is\ I(K)}_{antecedent}\ \underbrace{THEN\ Limiter\ Value\ =\ a_f^M\ I_i(k)}_{consequent}\ , \tag{5.20}$$

for i =1, 2,...9; and f =1, 2,..9; where, antecedent part maps the membership grade of input variable, this membership grade is utilize to find the crisp consequent part which is generally represented by a polynomial of input variables. In this work, the order of consequent variable is zero, $M = 0$. Finally the crisp output is calculated by weighted average, which is given by:

$$\text{Limiter value} = \frac{a_1.I_1(k) + a_2.I_2(k)}{2} \tag{5.21}$$

The universe of discourse of both input and output variables are considered as the actual physical value, hence, normalization and denormalization factors are considered as unity.

5.5 DC LOAD CURRENT SENSING METHOD

The new topology of APF with FLC based limiter is shown in Figs. 5.13(a) and 5.13(b). The total DC load current I_L is sensed from load connected to the utility which acts as the input for FLC. Then on the basis of lookup table (Table 5.1) FLC gives its output as limiter value.

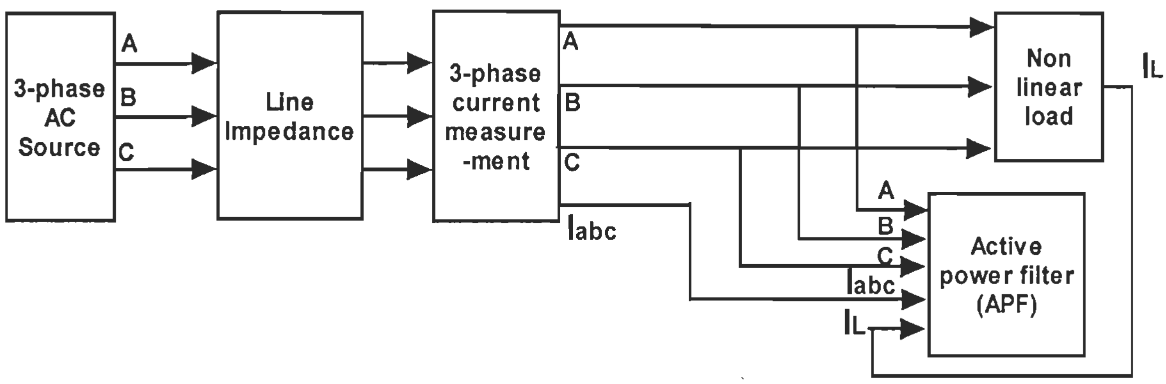

Fig. 5.13 (a): Connection diagram of proposed active power filter

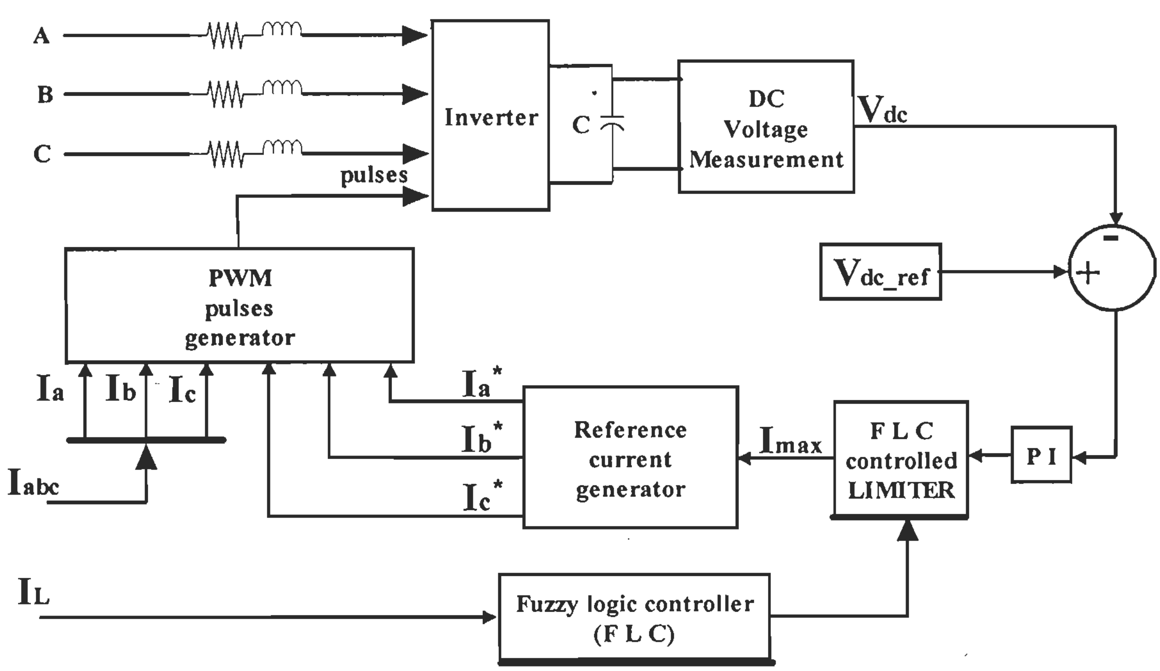

Fig. 5.13 (b): Proposed active power filter topology with fuzzy logic controller

5.5.1 Simulation Results

The performance of the proposed APF is studied on a typical variable load. Variable load is a 7-step increasing load (with four stages), connected through circuit breakers (CB). Initial load is $(R + j\omega L)$, R = 52 ohm, L= 2.5 mH. The load is varied in random steps, (in four stages) to test the effectiveness of the proposed APF. The APF starts working at 0.1 seconds. In stage-1 'another similar load' is connected in 6 steps. Loads are increasing at 0.3, 0.5, 0.7, 0.9, 1.1, 1.3 seconds and decreasing at 1.5, 1.7, 1.9, 2.1, 2.3 and 2.5 seconds. In stage-2, the 'double of the basic load' is connected at 2.5, 2.7 and 2.9 seconds and disconnected at 3.1, 3.3 and 3.5 seconds. In stage-3, the 'three times of the basic load' is connected at 3.5 and 3.7 seconds and disconnected at 3.9 and 4.1 seconds. Finally, in stage-4, the 'four times of the basic load' is connected at 4.1 sec. and disconnected at 4.3 sec.

Every individual load is connected for 10 cycles (0.2 sec.) and the FFT analysis is done for "every cycle" (0.02 sec.) of the entire time. The results are depicted in Fig. 5.9 (a) to Fig. 5.9 (g). Fig. 5.14 shows the random loading and unloading of non-linear loads, in terms of load current on DC side of nonlinear load. It is evident from the Figure that in different stages, the loading pattern is changing continuously. Fig. 5.15 gives the random loading and unloading of non-linear loads, in terms of current drawn from the utility. Two curves in this Figure give the comparison of current drawn from the utility in both cases, with and without APF. It is evident from this figure that, in any condition APF does not become a burden on utility, and losses in APF are insignificant. Fig. 5.16 shows the random loading and unloading pattern of non-linear loads, in terms of source voltage. The curves showing the value of THD_I, for every cycle of utility current waveform are given in Fig. 5.17, Fig. 5.18 and Fig. 5.19. These three different Figures show the APF performance for various stages of loading. Each of these Figures gives the performance comparison between the conditions 'with APF' and 'without APF'. The total harmonic distortion of the current generated by the load is observed to be approximately 28.19 % to 31.5 %, whereas 'compensated supply current' has a total harmonic distortion, well within the limit of 5% (IEEE 519-1992), except at the "instants of non-linear load-change" and APF brings back the THD_I within the acceptable limit immediately, depending on the amount of load change. As reflected in the Fig. 5.18 and Fig. 5.19, the number of cycles (time-period) required by APF to bring back the THD_I within the acceptable limit increases (2 or 3 cycles) when variation in the step-change of load is twice, thrice or four times of the basic load considered. The variation of that much load in one step is a rare event and time taken by the APF is not so high still, this may be taken as limitation of the proposed APF. In Fig. 5.20, THD_V is plotted for all 4-stages of loading, for both cases, 'with APF' and 'without APF'. This very clearly illustrates the effectiveness of the proposed APF. As it is evident from Fig. 5.20, THD_V has reduced to a very small value (well below the required norms) with the aid of APF as compared to the case without APF. Also, the response of the APF to the change in load is very fast.

It is important to mention here that in stage-2, stage-3 and stage-4, loads are changing dynamically at the rate of 200 %, 300 % and 400 % of the basic load. Even the APF is capable of compensating for all these loads, in addition of loads of stage-1 as evident from Fig. 5.18 and Fig. 5.19. This clearly shows that the proposed APF is robust under random load variation.

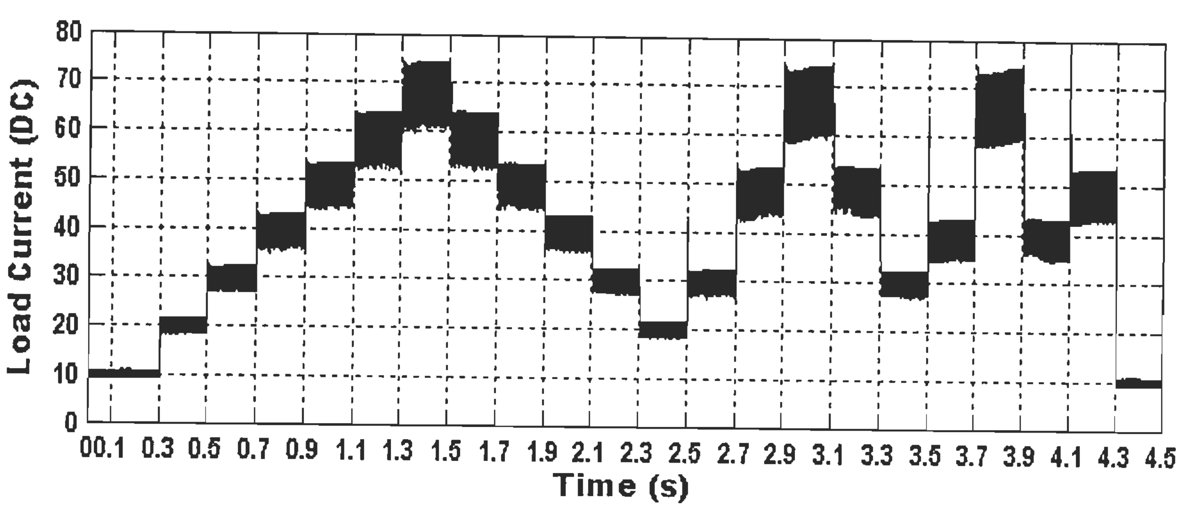

Fig. 5.14: Random loading and unloading (4-stages and multi steps) of non-linear loads, in terms of load current on DC side of nonlinear load.

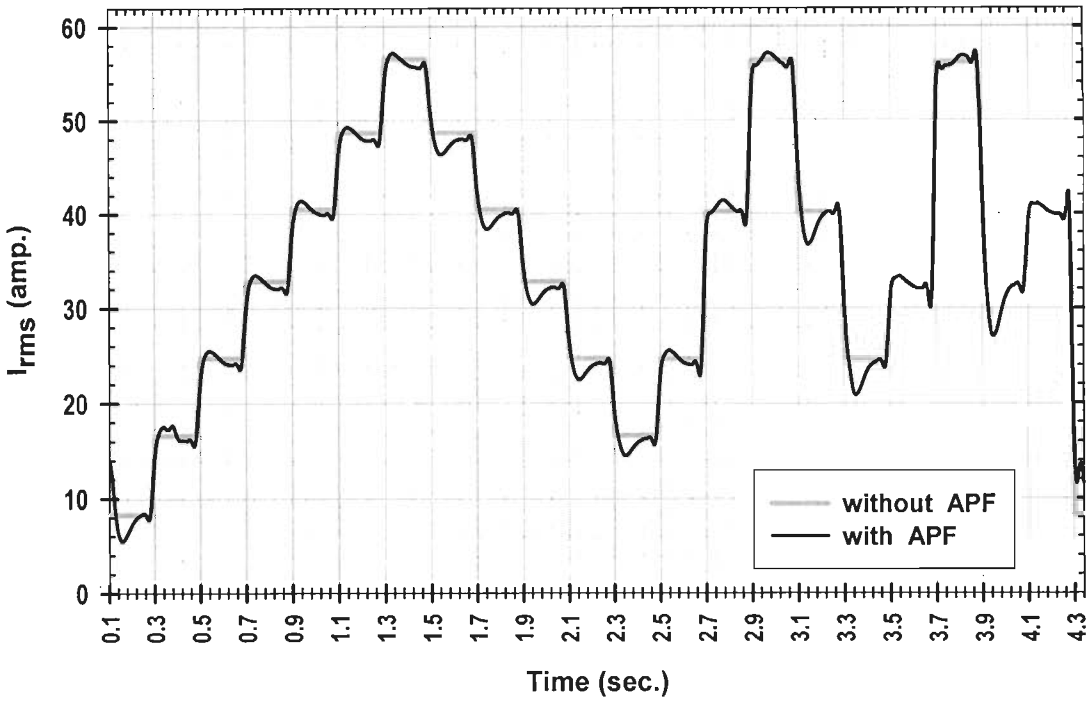

Fig. 5.15: **Random loading and unloading (4-stages and multi steps) of non-linear loads, in terms of current (rms) drawn from the utility**

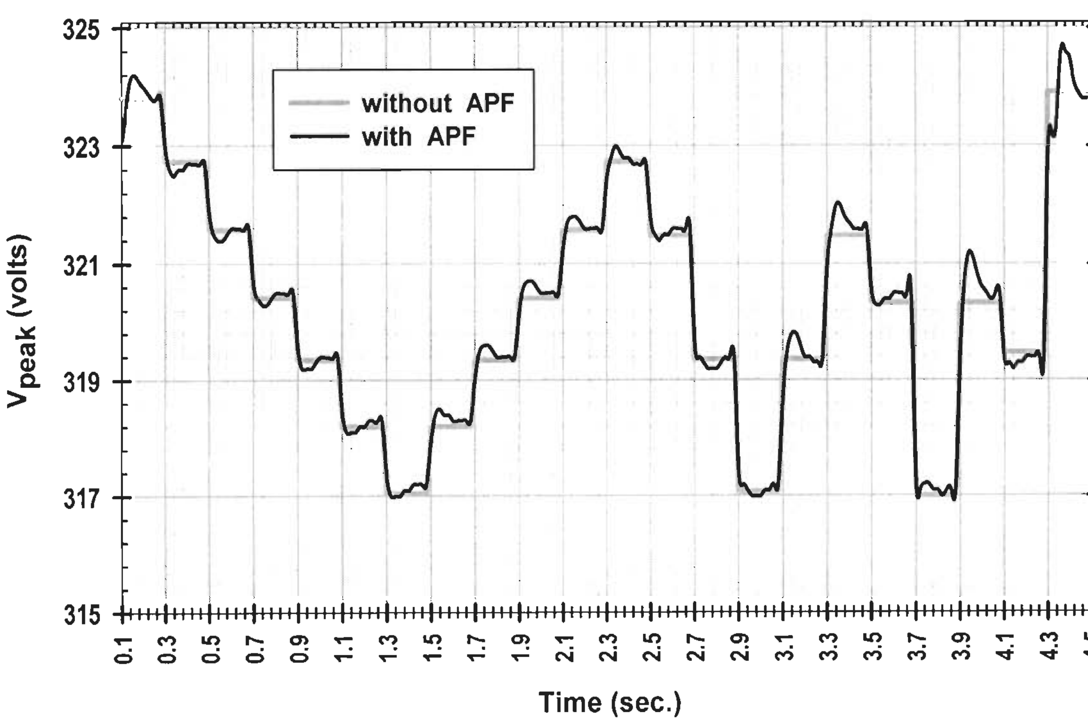

Fig. 5.16: **Random loading and unloading (4-stages and multi steps) of non-linear loads, in terms of source voltage**

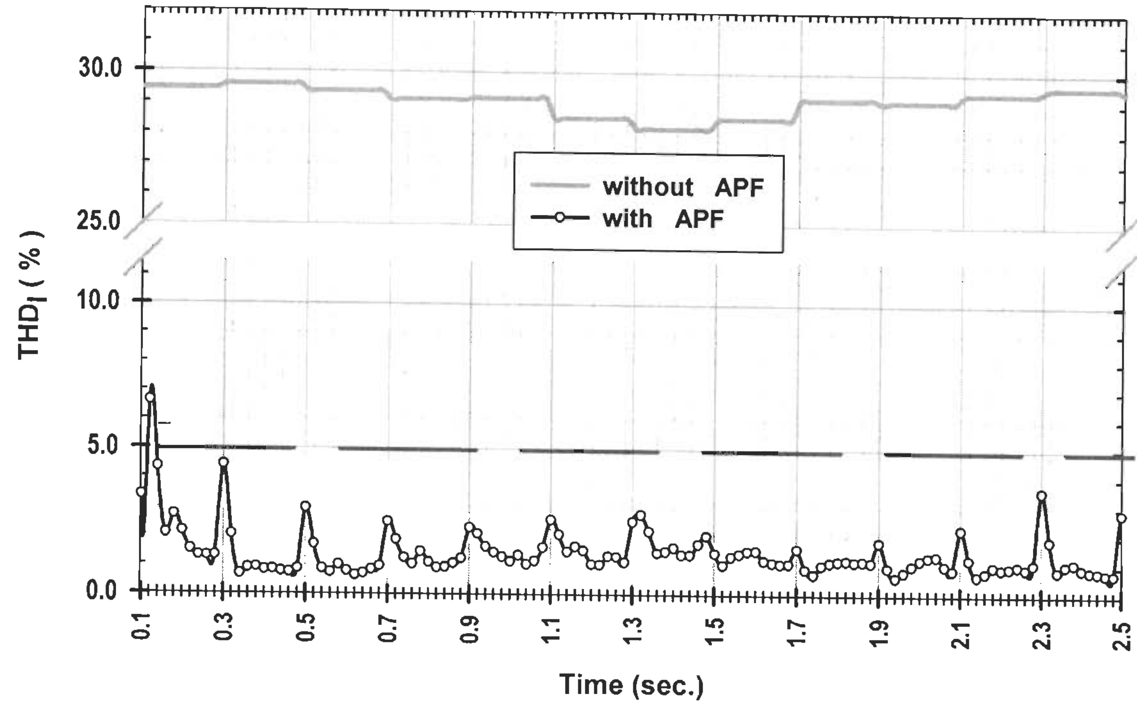

Fig. 5.17: THD_I vs. time for stage-1 of variation of non-linear loads, where single-step change of load is considered

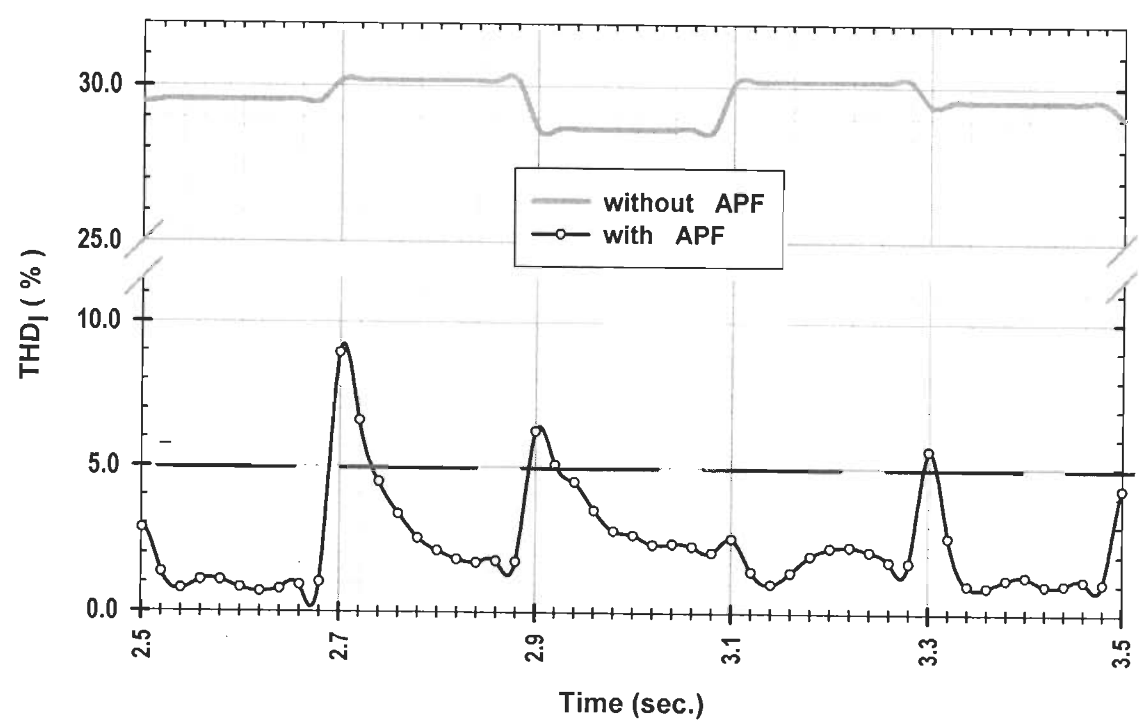

Fig. 5.18: THD_I vs. Time for stage-2 of variation of non-linear loads, where two-step change of load is considered

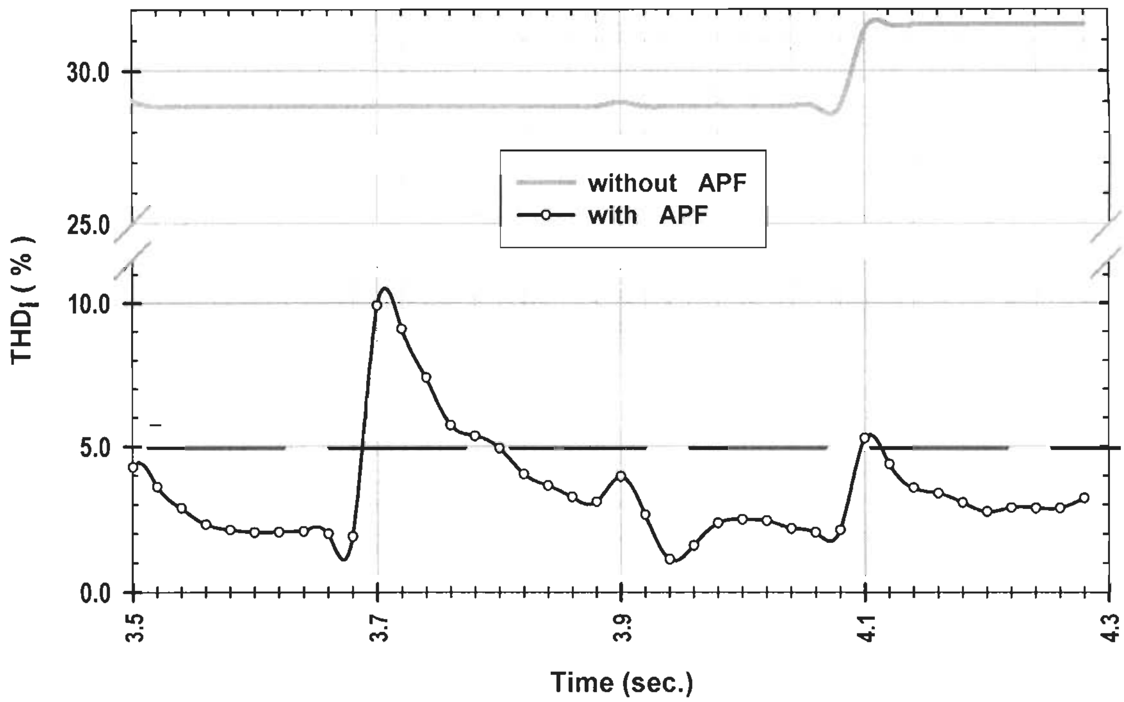

Fig. 5.19: THD_I vs. Time for stage-3 and 4 of variation of non-linear loads, where three and four-step change of load is considered

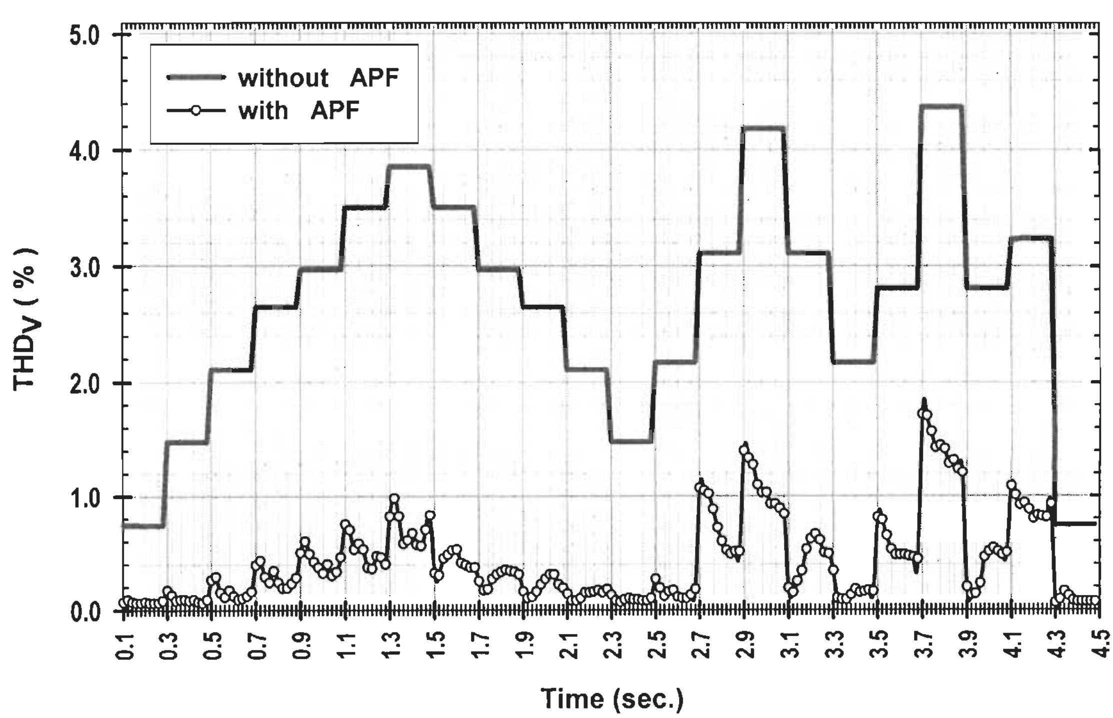

Fig. 5.20: THD_V vs. time for complete (4-stages and multi steps) variation of non-linear loads

5.6 AC LOAD CURRENT SENSING METHOD

The proposed topology of APF with FLC based limiter using AC load current sensing technique is shown in Fig. 5.21. In this method, no additional current sensing is required as the AC load current sensing is already being done to be used at PWM pulse generator block. The same AC load current I_{abc} works as the input to FLC, passing through the load current conditioning block, which performs only in case of load current unbalance by selecting the highest rms value of load current. Then on the basis of lookup table (Table 5.1) FLC gives its output as limiter value.

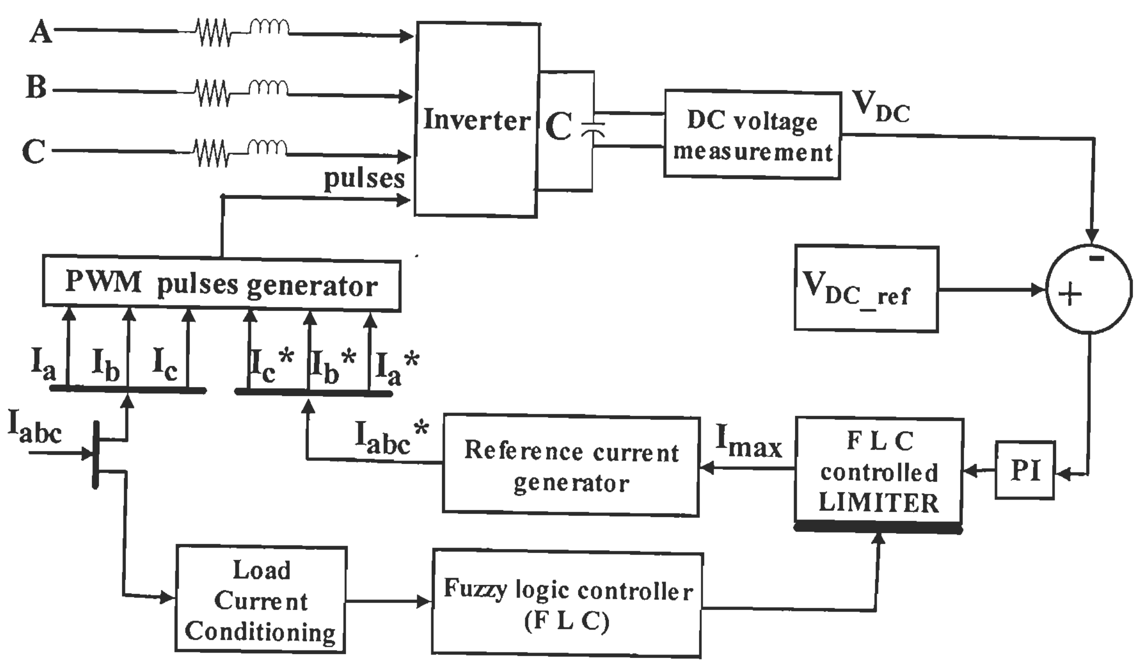

Fig. 5.21: Proposed APF topology with modified control circuit of shunt APF

5.6.1 SIMULATION RESULTS

5.6.1.1 Compensation for Harmonic Distortion:

The performance of the proposed APF is studied on a typical variable load, which has the same loading steps$(R+j\omega L)$ as earlier. The only difference is that now the variable load is a 10-step increasing load connected through circuit breakers (CB). Initial load is$(R+j\omega L)$, R = 52 ohm, L= 2.5 mH. The load is varied in random steps to test the effectiveness of proposed APF. The APF starts working at 0.1 seconds. In single-step load variation 'another similar load' is connected in 10 steps. Loads are increasing at 0.3, 0.5, 0.7, 0.9, 1.1, 1.3, 1.5, 1.7, 1.9 seconds and decreasing at 2.1, 2.3, 2.5, 2.7, 2.9, 3.1, 3.3, 3.5, 3.7 seconds. Variation in DC load current for single-step load variation case is shown in Fig. 5.22.

In multi-step load variation, two-, three-, and four-step load variation is performed, to test the performance of proposed APF for random and dynamic load change. In two-step load variation study, the 'double of the basic load' is connected at 0.3, 0.5, 0.7 and 0.9 seconds and disconnected at 1.1, 1.3, 1.5 and 1.7 seconds. In three-step load variation study, the 'three times of the basic load' is connected at 1.9 and 2.1 seconds and disconnected at 2.3 and 2.5 seconds. The four-step loading is done at 2.1 second by connecting the 'four times of the basic load' and unloading is done at 2.9 second. For the durations 0.1 to 0.3 seconds, 1.7 to 1.9 seconds, 2.5 to 2.7 seconds, and 2.9 to 3.7 seconds, the single-step initial is connected. Fig. 5.23 presents the DC load current variation for multi-step load.

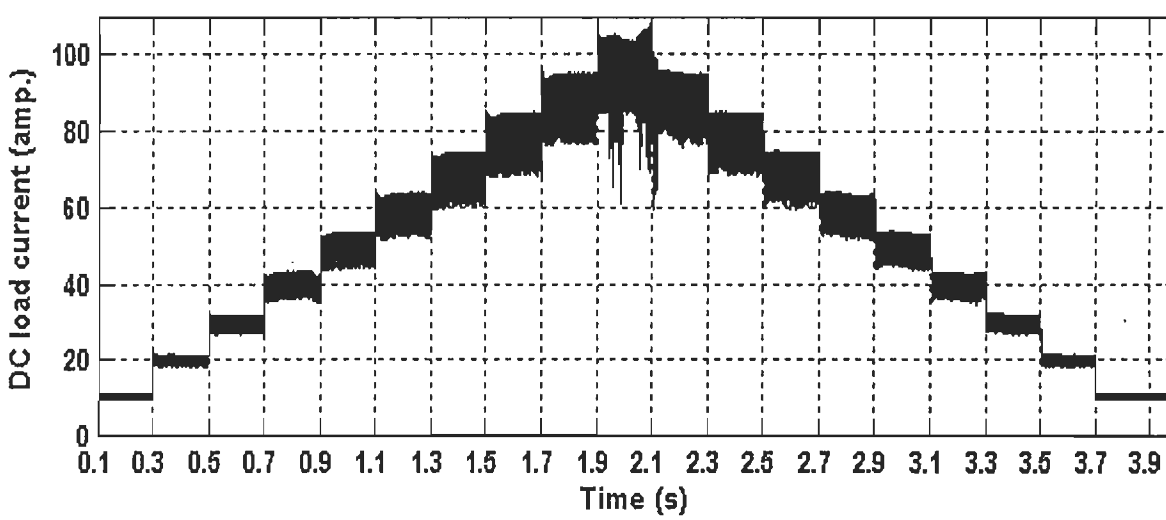

Fig. 5.22: Single-step (up to 10 steps) loading and unloading of non-linear loads, in terms of DC side load current of nonlinear load

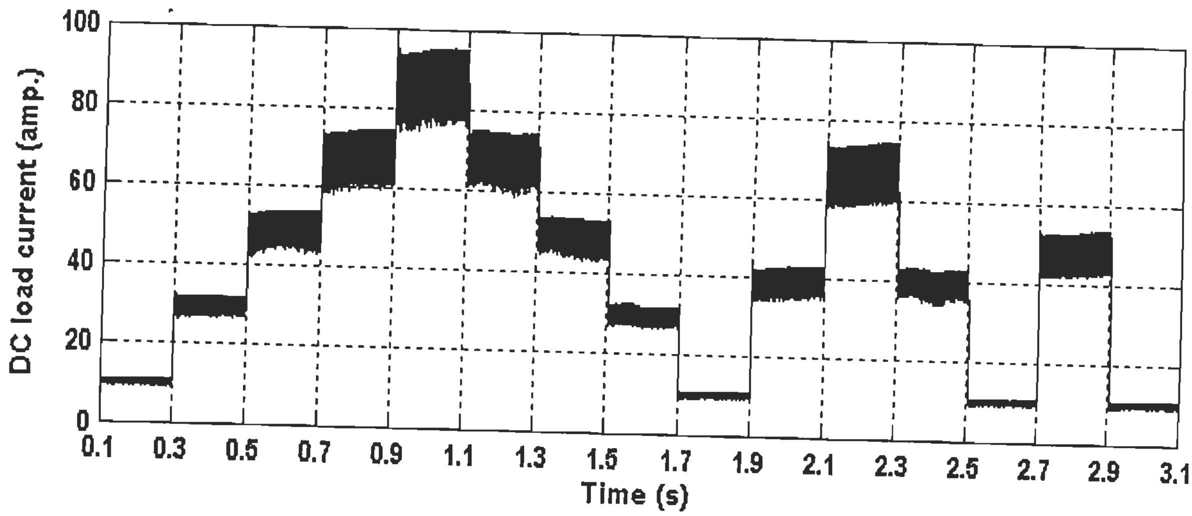

Fig. 5.23: **Multi-step (2, 3, and 4-steps) loading and unloading of non-linear loads, in terms of DC side load current of nonlinear load**

All the steps of non-linear load are connected for 10 cycles (0.2 sec.) and every cycle (0.02 sec. time period for 50 Hz frequency) is analyzed by carrying out FFT of voltage and current waveform, for the complete length of time. The results of this analysis are shown here independently for single-step and multi-step load variation.

Fig. 5.24 displays the pattern of single-step dynamic loading and unloading of non-linear loads in terms of rms utility current, for the cases without and with APF, while the Fig. 5.25 depicts the same pattern for multi-step dynamic loading and unloading of non-linear loads. In both the figures, comparison of these two curves concludes that in any state the APF does not become a burden on utility, and losses in APF are more or less negligible.

The utility voltage variation characterizing the pattern of dynamic loading and unloading of non-linear loads is shown in Fig. 5.26 and Fig. 5.27 for single- and multi-steps, respectively. The addition /removal of non-linear loads are indicated by a decrease /increase in voltage.

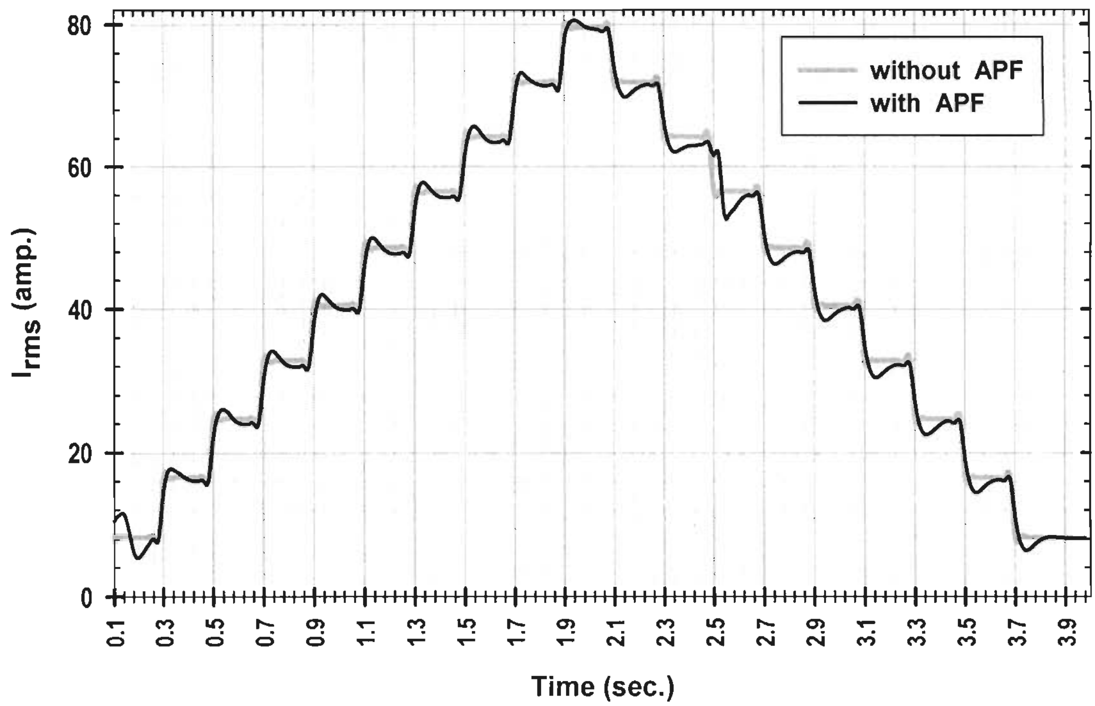

Fig. 5.24: **Single-step (up to 10 steps) loading and unloading of non-linear loads in terms of rms current drawn from the utility**

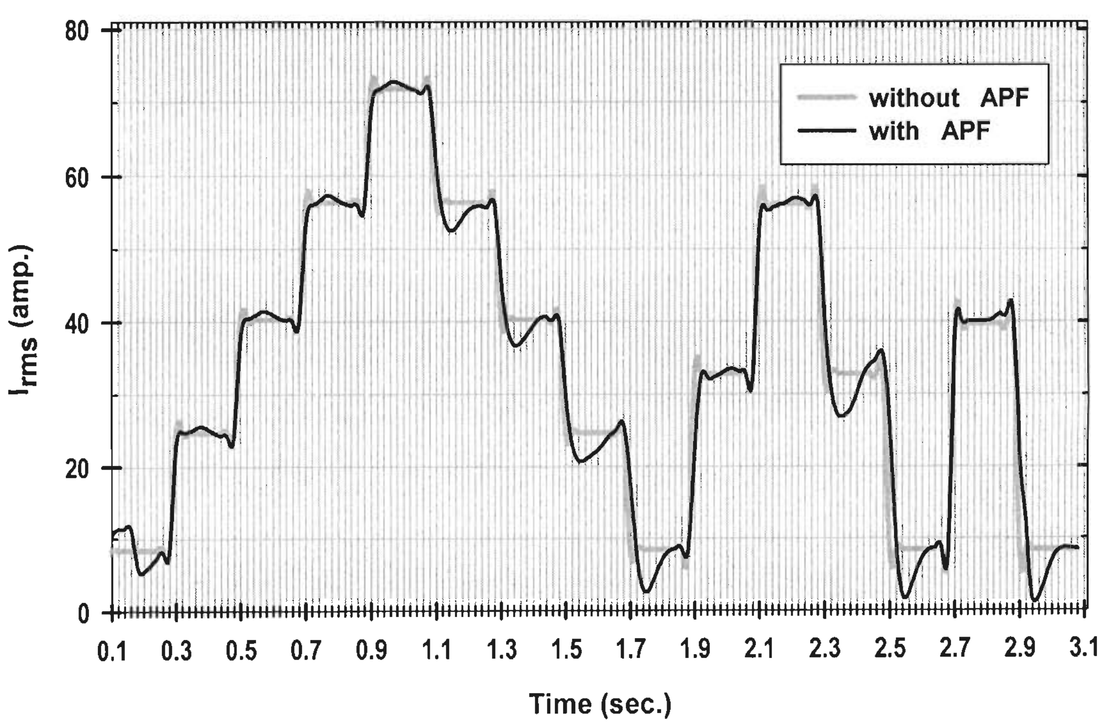

Fig. 5.25: **Multi-step (2, 3, and 4-steps) loading and unloading of non-linear loads in terms of rms current drawn from the utility**

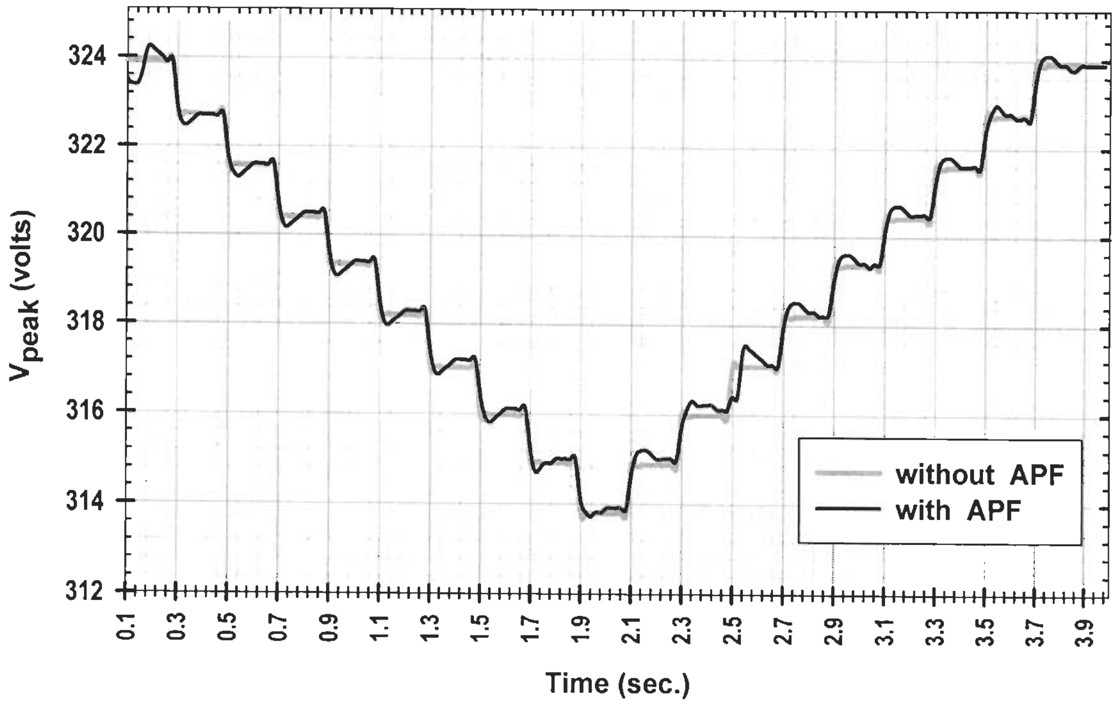

Fig. 5.26: Single-step (up to 10 steps) loading and unloading of non-linear loads, in terms of source voltage

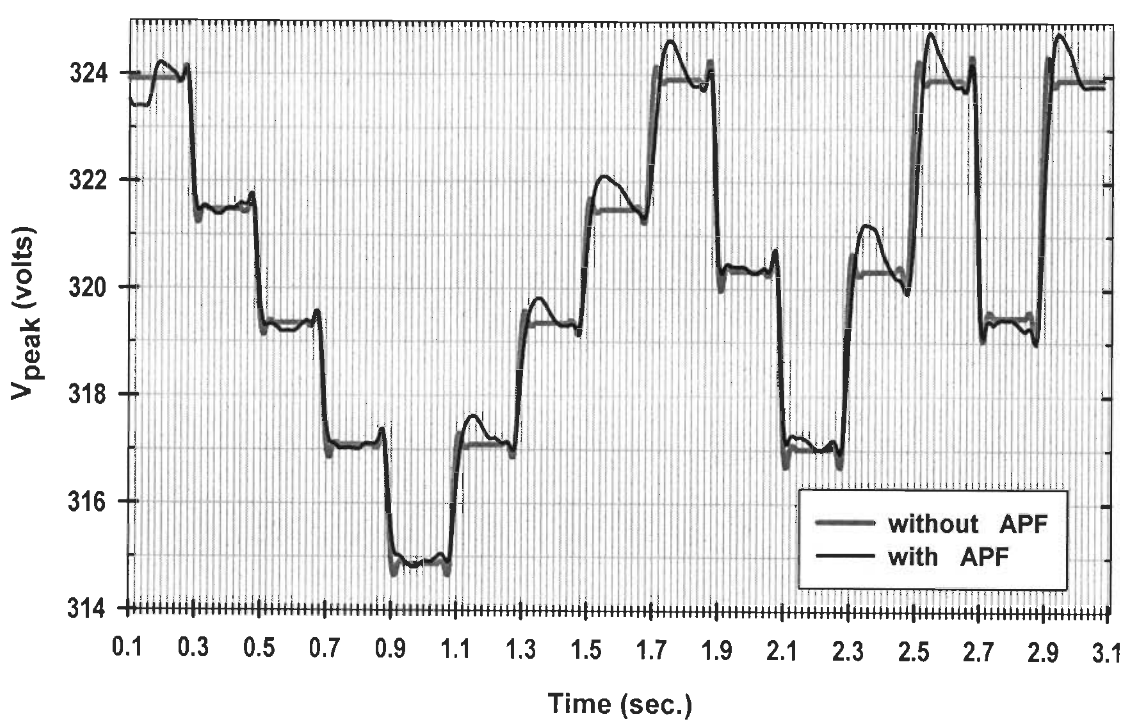

Fig. 5.27: Multi-step (2, 3, and 4-steps) loading and unloading of non-linear loads, in terms of source voltage

The plots showing the variation of THD_I value, for each and every cycle of utility current waveform are given in Fig. 5.28 for single-step loading, Fig. 5.29 for two-step loading and Fig. 5.30 for three- and four-step loading. These figures display the performance comparison between the cases 'without APF' and 'with APF'. The total harmonic current distortion for the 'without APF' case is between 27.5 % to 30.0 % for single-step loading, 28.0 % to 30.4 % for two-step loading and 29.2% to 32.0 % for three- and four-step loading. After compensation 'with APF' it can be observed that the total harmonic current distortion is well within the limit of 5% as per [15], except at the 'instants of load- change', where also it is compensated immediately, depending on the amount of load change. As reflected in the Fig. 5.29 and Fig. 5.30 the maximum number of cycles (time-period) required by APF to bring back the THD_I within the acceptable limit increases to 2 cycles for two-step loading, 3 cycles for three-step loading, and 5 cycles for four-step loading. The variation of that much load in one step is an exceptional experience and time taken by the APF is not so high, albeit, this may be taken as limitation of the proposed APF. It is important to reveal here that wherever it is stated that the THD_I is within the acceptable limits, it is also checked for every cycle of waveform that harmonic current components are also restricted to their individual specified limits, as detailed in [15].

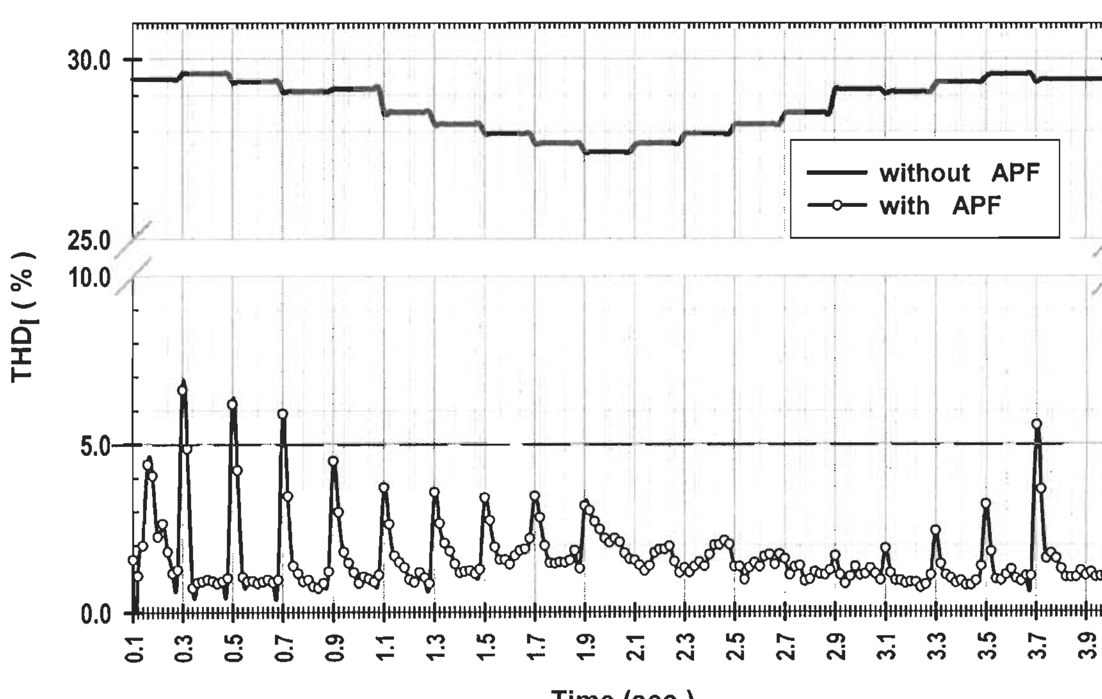

Fig. 5.28: **Variation of THD_I with time for 'single-step' (up to 10 steps) loading and unloading of non-linear loads, for the cases with and without APF.**

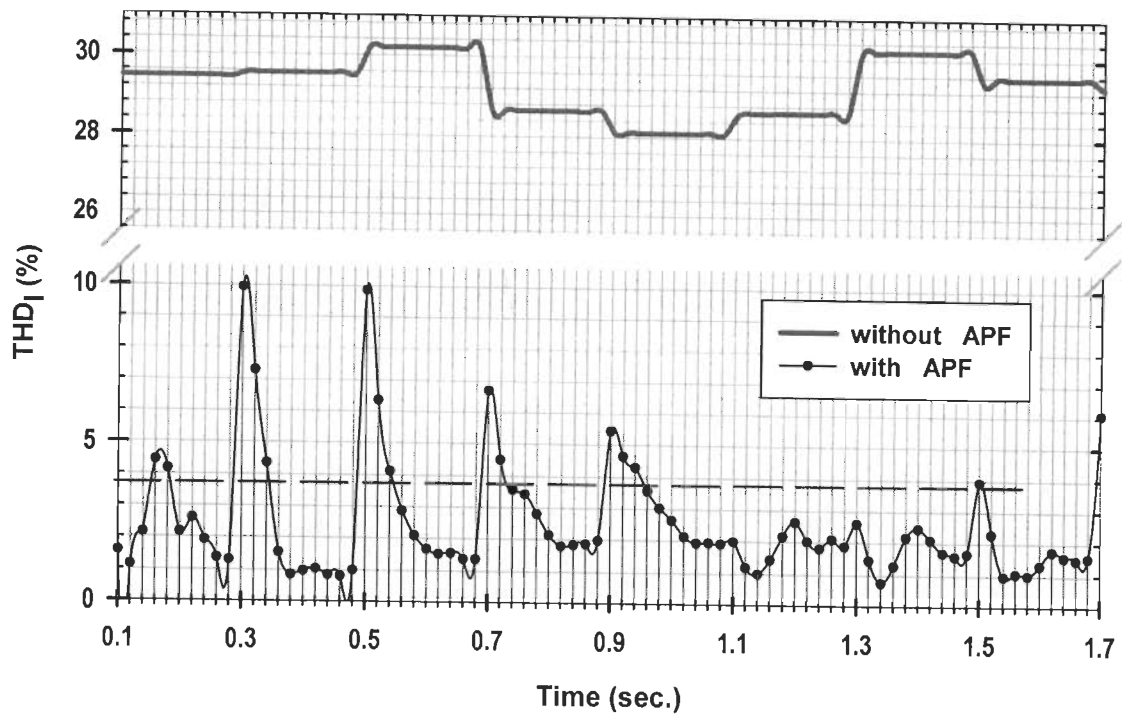

Fig. 5.29: Variation of THD_I with time for 'two-step' loading and unloading of non-linear loads, for the cases with and without APF.

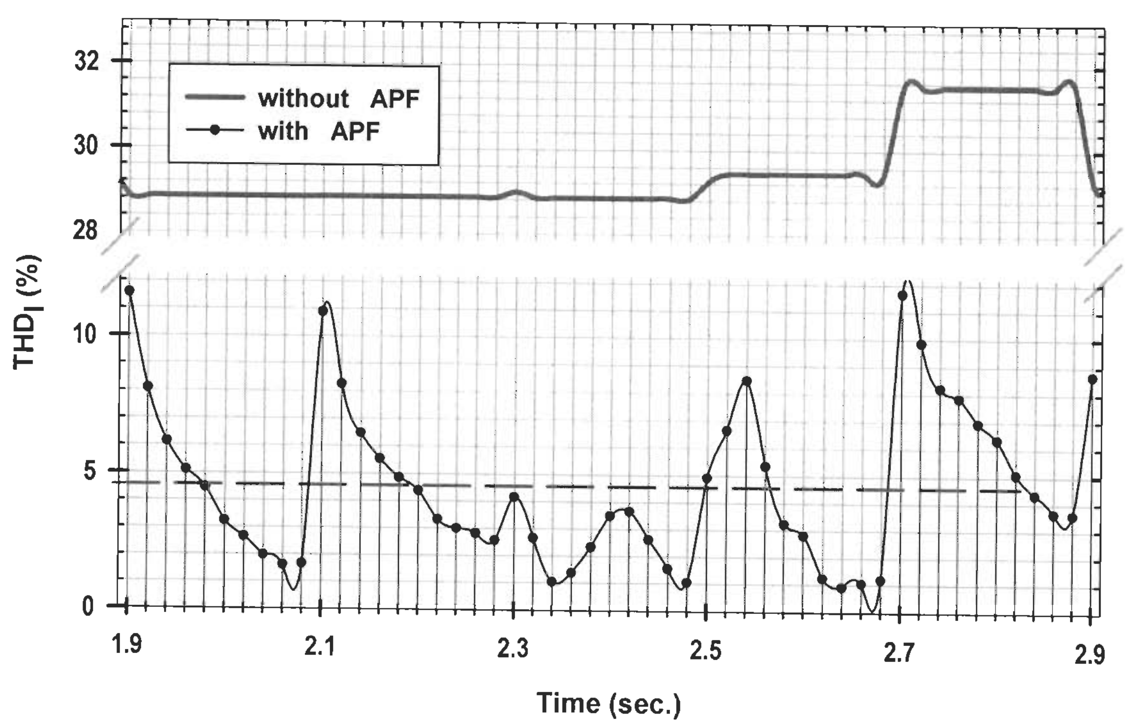

Fig. 5.30: Variation of THD_I with time for 'three-step' and 'four-step' loading and unloading of non-linear loads, for the cases with and without APF.

For both, 'with APF' and 'without APF' cases the curve between THD_V and time is plotted here. The variation of harmonic voltage distortion (THD_V) for every cycle of utility voltage waveform is shown in Fig. 5.31 for single-step loading, Fig. 5.32 for two-step loading, and Fig. 5.33 for three- and four- step loading. This demonstrates the effectiveness of the proposed APF very noticeably. It is apparent from Fig. 5.31 to Fig. 5.33 that THD_V has reduced to 0.07% to 1.6 % (for maximum loading), for different-step loadings after harmonic compensation using the proposed APF. For different-step loadings, their THD_V for the case without APF are also shown in their relevant figures. At the 'instants of load change' the THD_V gives the more clear view than THD_I about the effectiveness of the proposed APF, as THD_I is having higher values at these instants due to presence of high DC current components in load current during initial cycles of loading and unloading. It is also observed that the response of the APF to the load variation is very quick.

It is significant to refer here that in multi-step loading, the loads are changing dynamically at the rate of 200 %, 300 % and 400 % of the basic load. Even that the APF is found capable of providing the compensation for all these loads, as well as the single-step increasing loads. Results shown in Fig. 5.28 to Fig. 5.33 clearly elucidate that the proposed APF is robust under random load variation /conditions.

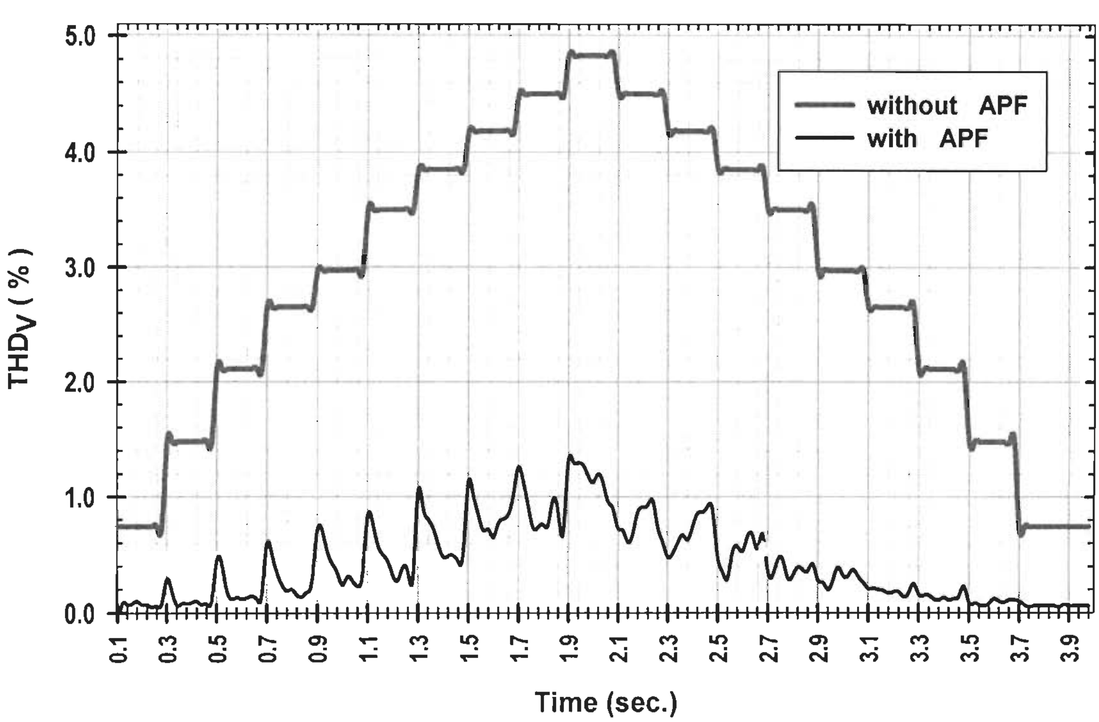

Fig. 5.31: Variation of THD_V with time for Single-step (up to 10 steps) loading and unloading of non-linear loads, for the cases with and without APF

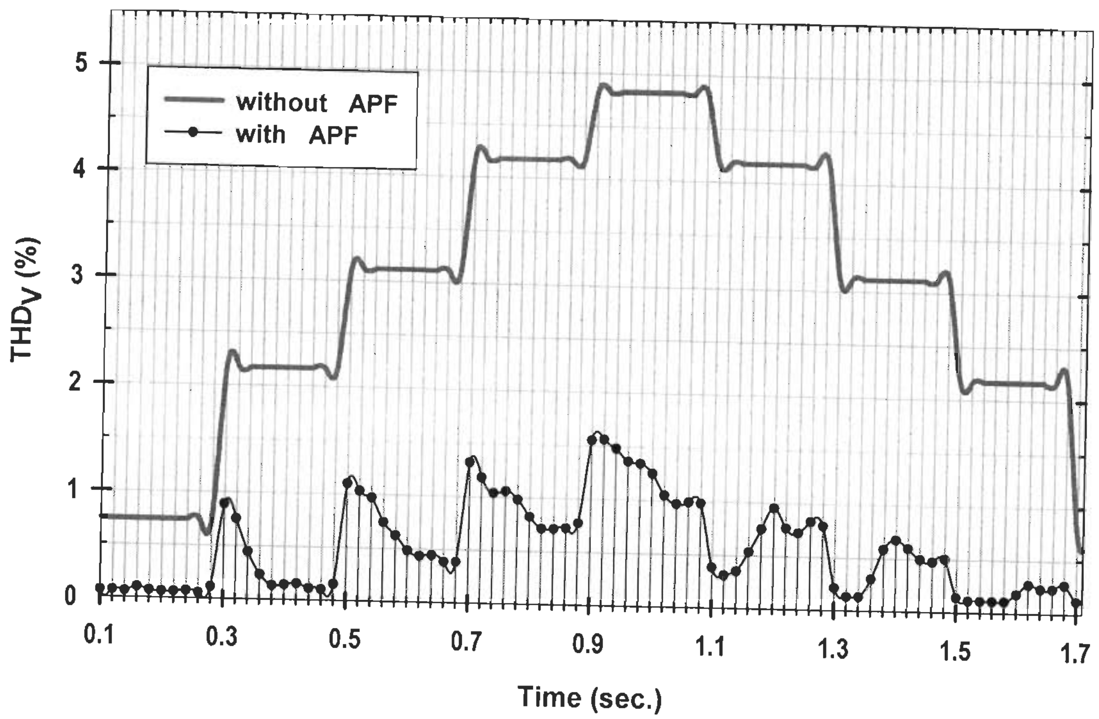

Fig. 5.32: Variation of THD_V with time for two-step loading and unloading of non-linear loads, for the cases with and without APF

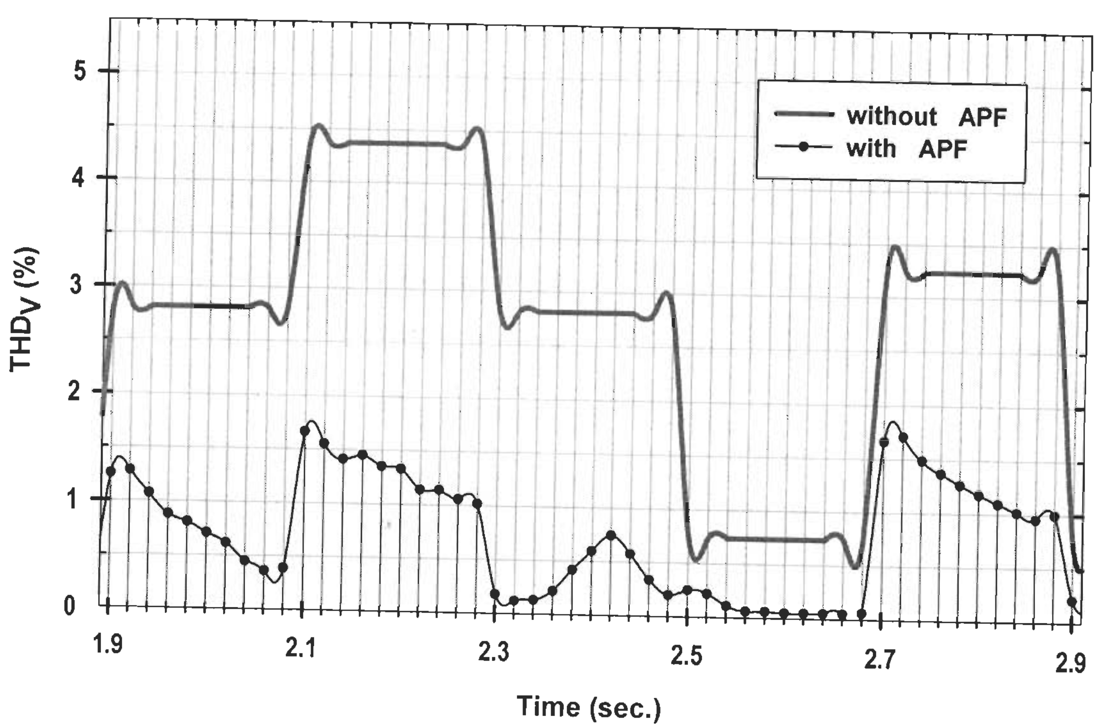

Fig. 5.33: Variation of THD_V with time for three-step and four-step loading and unloading of non-linear loads, for the cases with and without APF

5.6.1.2 Power Factor Improvement

The concept of power factor originated from the need to quantify how efficiently a load utilizes the current it draws from an AC power source. For sinusoidal voltages and currents, the apparent power (S) is given by:

$$S=\sqrt{P^2+Q^2} \tag{5.22}$$

and the power factor is defined as ratio P/S and the power factor angle φ is

$$\phi = \cos^{-1}\frac{P}{S} = \tan^{-1}\frac{Q}{P} \tag{5.23}$$

where S is the total volt-ampere power input from the utility, P is the active power consumption and Q is the reactive power requirement of load. φ, power factor angle can also be expressed as the phase angle between the fundamental components of voltage and current. If ∂_{V_F} and ∂_{I_F} are the phase angles of the fundamental components of voltage and current, respectively, then

$$\cos\varphi = \cos\left(\partial_{V_F} - \partial_{I_F}\right) \tag{5.24}$$

For non-linear loads, φ is still defined as mentioned above, but it is called the displacement angle and the apparent power (S) can be defined as

$$S=\sqrt{P^2+Q^2+D^2} \tag{5.25}$$

where, D is the distortion (harmonic) power requirement of non-linear loads.

An expression for distortion power factor can be arrived from THD_I and THD_V values, as

$$\text{Distortion P.F.} = \frac{1}{\left\{\sqrt{1+\left(THD_V/100\right)^2}\right\}.\left\{\sqrt{1+\left(THD_I/100\right)^2}\right\}} \tag{5.26}$$

By incorporating certain assumptions, the approximate form for true (total) power factor is obtained as

$$\text{True Power Factor} = \left(\cos\varphi\right).\frac{1}{\left\{\sqrt{1+\left(THD_V/100\right)^2}\right\}.\left\{\sqrt{1+\left(THD_I/100\right)^2}\right\}} \tag{5.27}$$

Thus, True Power Factor = (Displacement Power Factor) x (Distortion Power Factor) (5.28)

The true power factor is the product of displacement power factor (which is the same as fundamental power factor) and the distortion power factor as defined above.

Apart from harmonic mitigation, FLC based APF is also providing the reactive power compensation very effectively and improving the total power factor to unity. After compensation, source currents are in phase with their respective source voltages, as the difference in phase angles between the fundamental components of voltage and current is reduced to almost zero. This reduction in the value of angle φ, due to compensation provided by the APF is also presented in Fig. 5.34 and Fig. 5.35, for single- and multi-step loading correspondingly, which concludes that after compensation the utility currents are in phase with the respective source voltages, as the angle φ becomes almost negligible after compensation. The effect of compensation provided by the APF in terms of improvement of true power factor is clearly observable as the Fig. 5.36 displays the true power factor at different loads before (without APF) and after (with APF) compensation, for single-step load variation, while Fig. 5.37 depicts the same for multi-step load variation.

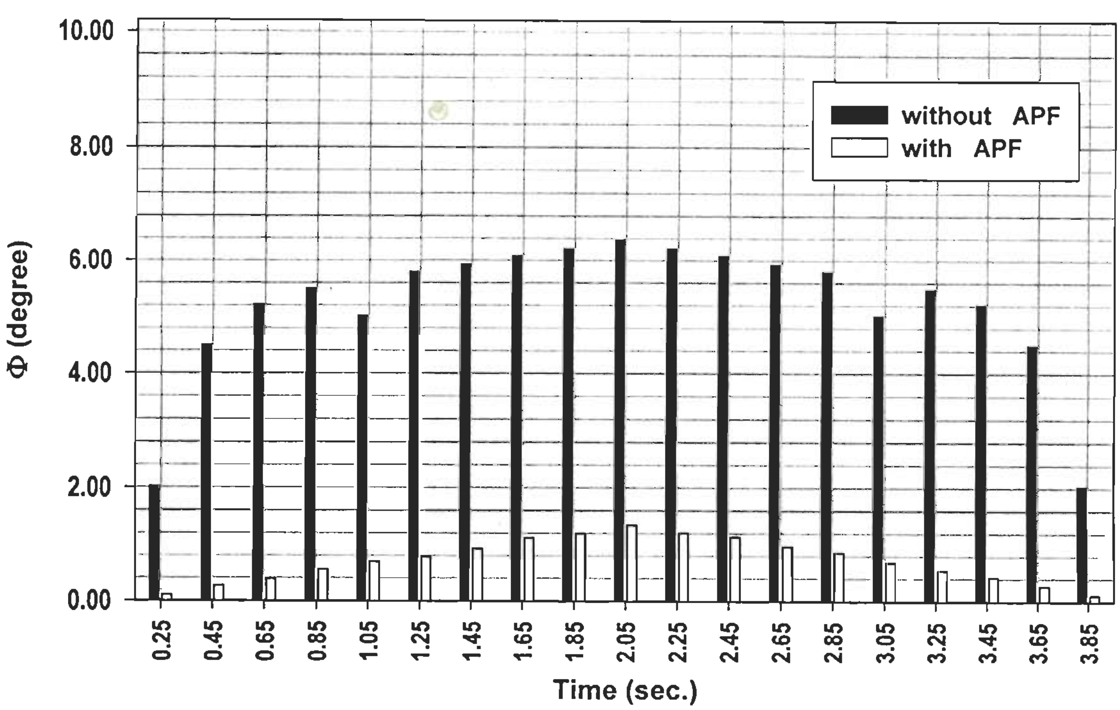

Fig. 5.34: Φ the phase angle between the fundamental components of voltage and current, before and after compensation, at different loads, for single-step load variation

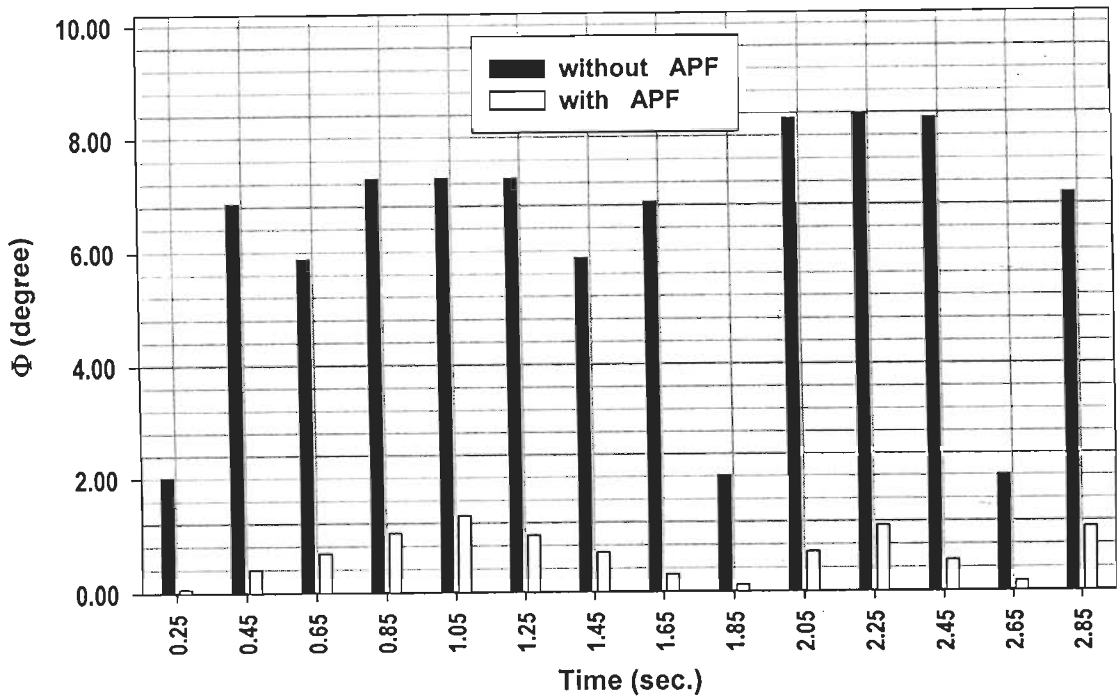

Fig. 5.35: **Φ the phase angle between the fundamental components of voltage and current before (without APF) and after (with APF) compensation, at different loads, for multi-step load variation**

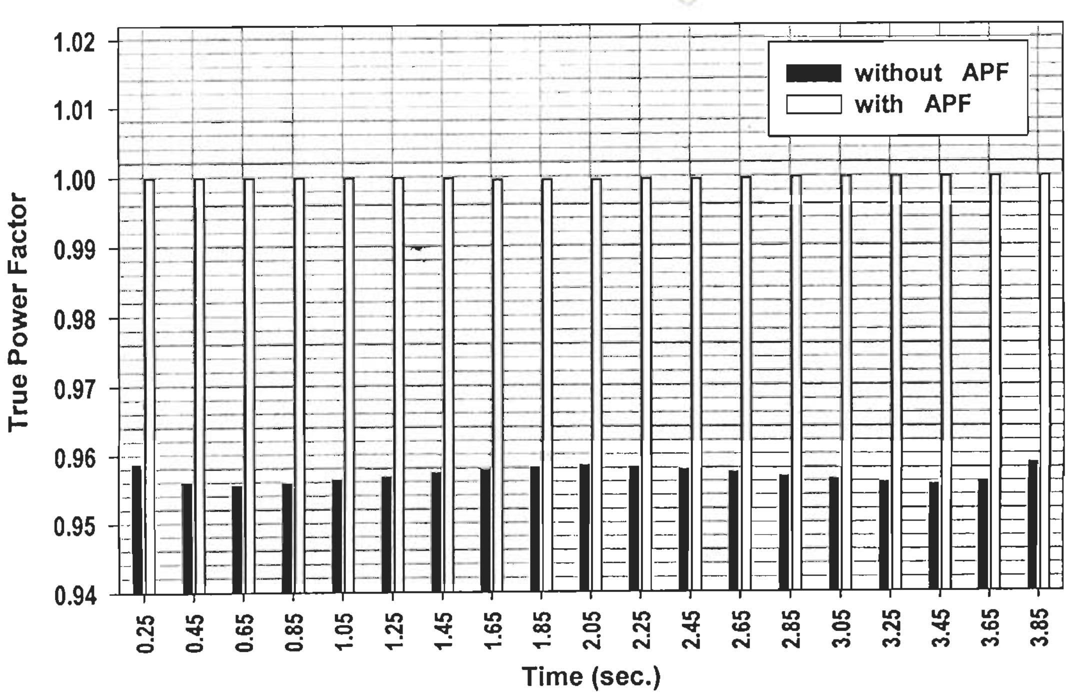

Fig. 5.36: **True power factor at different loads before (without APF) and after (with APF) compensation, for single-step load variation**

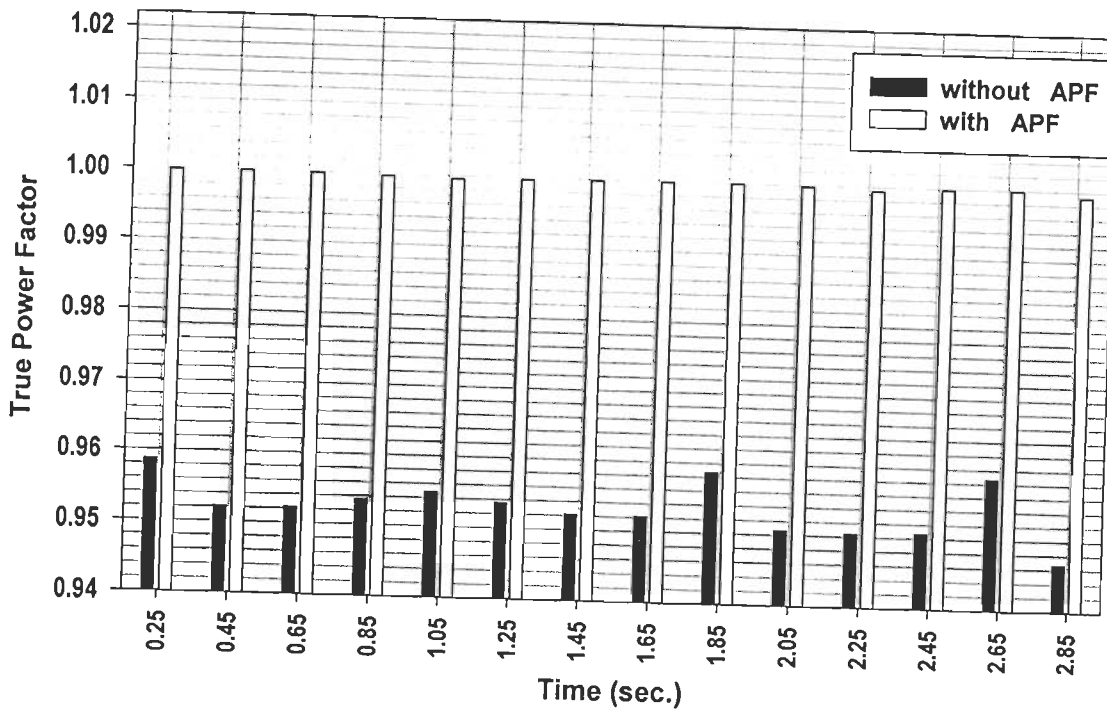

Fig. 5.37: True power factor at different loads, before (without APF) and after (with APF) compensation, for multi-step load variation

5.6.1.3 Compensation of Load Current Unbalance

An unbalance in load currents is considered in two different cases. In case-1, load current unbalance is realized by adding impedance in series of phase 'B' circuit, and results are shown in Fig. 5.38 to Fig. 5.41 along with Table-5.4. The comparison of load currents in three different phases is presented in Fig. 5.38 for the 'without APF' condition while in Fig. 5.39 for the 'with APF' condition. At the same time the evaluation of total harmonic distortion for load currents in three different phases has been shown in Fig. 5.40 for 'without APF' condition and in Fig. 5.41 for the 'with APF' condition.

In case-2, load current unbalance is considered by inserting two different impedances in series of phase 'A' and phase 'C' circuits, and results are depicted in Fig. 5.42 to Fig. 5.45 together with Table-5.5. The comparison of load currents in three different phases is presented in Fig. 5.42 for the 'without APF' condition while in Fig. 5.43 for the 'with APF' condition. At the same time the evaluation of total harmonic distortion for load currents in three different phases has been shown for 'without APF' condition in Fig. 5.44 and for the 'with APF' condition in Fig. 5.45.

It was found that APF with FLC based LIMITER is working properly for this unbalance in load. A detailed simulation analysis for unbalanced load current condition concludes that before compensation, phase load currents are unbalanced. After compensation, currents are almost balanced. it is also observed that before compensation, current distortion (THD_I) for each phase current are very high, and after compensation, current distortion (THD_I) for each phase current is very well within the acceptable limit of 5% .

Table-5.4: Results for "case-1" of load current unbalance

R (ohms)	Utility Current (without APF)						Utility Current (with APF)					
	Phase A		Phase B		Phase C		Phase A		Phase B		Phase C	
	RMS	THD_I (%)	RMS	THD_I (%)	RMS	THD_I (%)	RMS	THD_I (%)	RMS	THD_I (%)	RMS	THD_I (%)
6	60.5	12.9	19.75	34.87	61.11	11.00	45.45	2.41	46.53	2.10	47.22	2.38
7	52.2	13.9	19.01	34.32	52.24	12.58	39.78	2.26	40.61	1.96	41.23	2.26
8	45.9	14.9	18.32	33.84	46.07	13.95	35.5	2.11	36.16	1.80	36.7	2.12
10	37.0	16.4	17.03	33.04	36.97	16.19	29.41	1.91	29.87	1.58	30.29	1.90
12	31.0	17.7	15.89	32.42	30.9	17.93	25.25	1.70	25.59	1.37	25.92	1.76
15	25.0	19.2	14.39	31.73	24.84	19.89	20.98	1.48	21.21	1.16	21.45	1.52
20	19.0	20.9	12.39	30.99	18.78	22.10	16.49	1.24	16.63	0.95	16.79	1.31
25	15.3	22.2	10.85	30.55	15.15	23.57	13.66	1.06	13.76	0.85	13.86	1.15
30	12.9	23.1	9.64	30.26	12.72	24.60	11.7	1.12	11.77	0.87	11.83	1.24
35	11.1	23.7	8.664	30.08	10.97	25.36	10.23	1.13	10.28	0.97	10.33	1.17
40	9.83	24.3	7.864	29.95	9.659	25.95	9.097	1.15	9.14	1.08	9.186	1.23
42	9.38	24.5	7.583	29.91	9.218	26.15	8.715	1.09	8.751	0.98	8.798	1.20
43	9.17	24.6	7.45	29.89	9.013	26.24	8.542	1.20	8.575	1.10	8.618	1.31
44	8.97	24.7	7.321	29.87	8.817	26.33	8.365	1.30	8.405	1.24	8.448	1.31
45	8.78	24.9	7.197	29.86	8.629	26.42	8.211	1.20	8.226	1.06	8.278	1.33
49	8.09	25.1	6.739	29.81	7.954	26.73	7.6	1.15	7.63	1.07	7.665	1.31
53	7.51	25.7	6.334	29.77	7.378	27	7.085	1.32	7.112	1.38	7.151	1.56
56	7.12	25.5	6.062	29.74	6.998	27.17	6.731	1.42	6.744	1.31	6.777	1.56
67	5.99	26.0	5.233	29.69	5.891	27.68	5.731	1.58	5.748	1.61	5.767	1.71
99	4.11	27.0	3.742	29.66	4.042	28.55	4.002	2.30	4.017	2.22	4.009	2.27

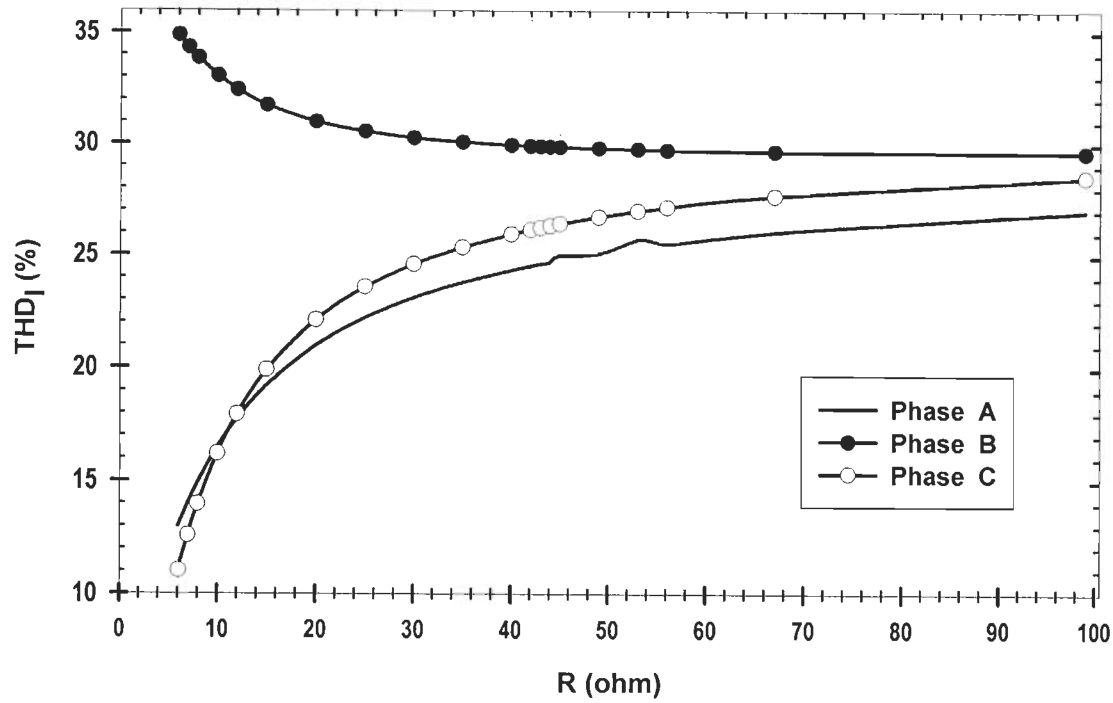

Fig. 5.38: Variation of load current with "value of 'R' on DC side of non-linear load" before compensation (without APF), for case-1 of load current unbalance

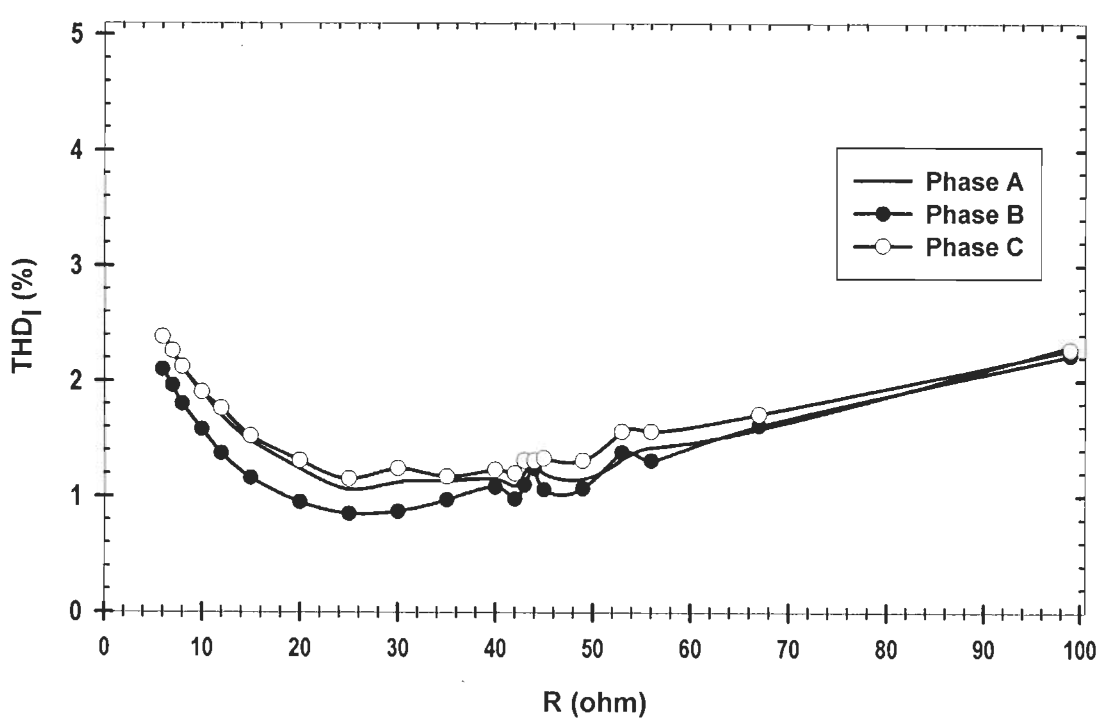

Fig. 5.39: Variation of load current with "value of 'R' on DC side of non-linear load" after compensation (with APF), for case-1 of load current unbalance.

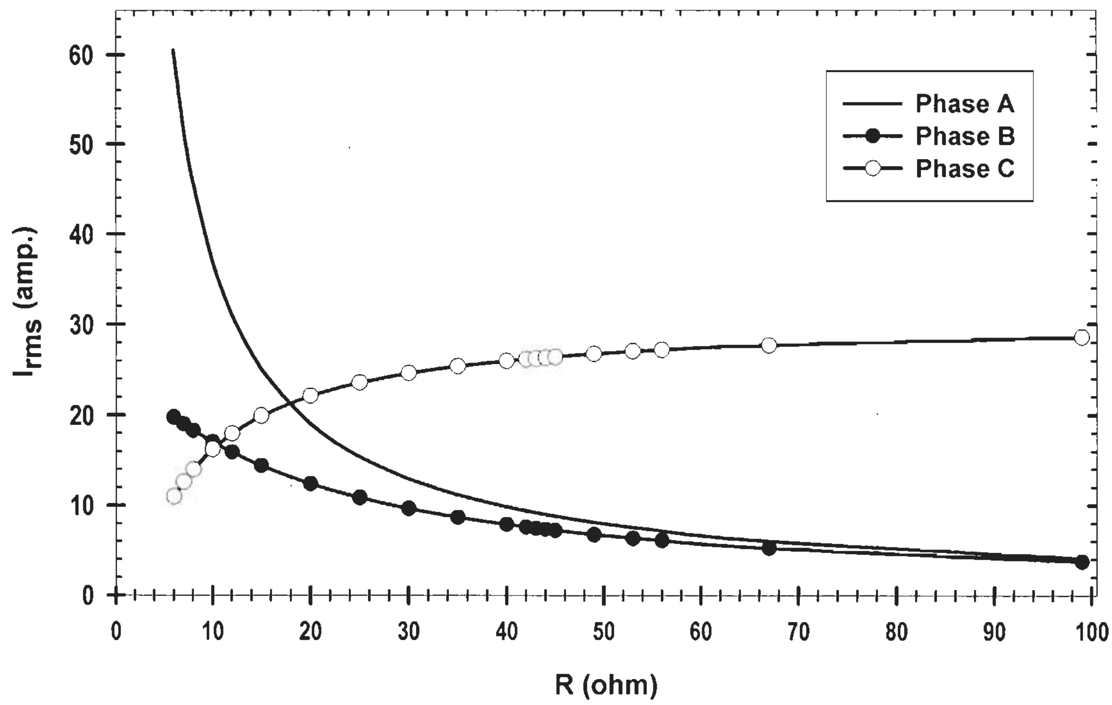

Fig. 5.40: Variation of THD_I with "value of 'R' on DC side of non-linear load" before compensation (without APF), for case-1 of load current unbalance.

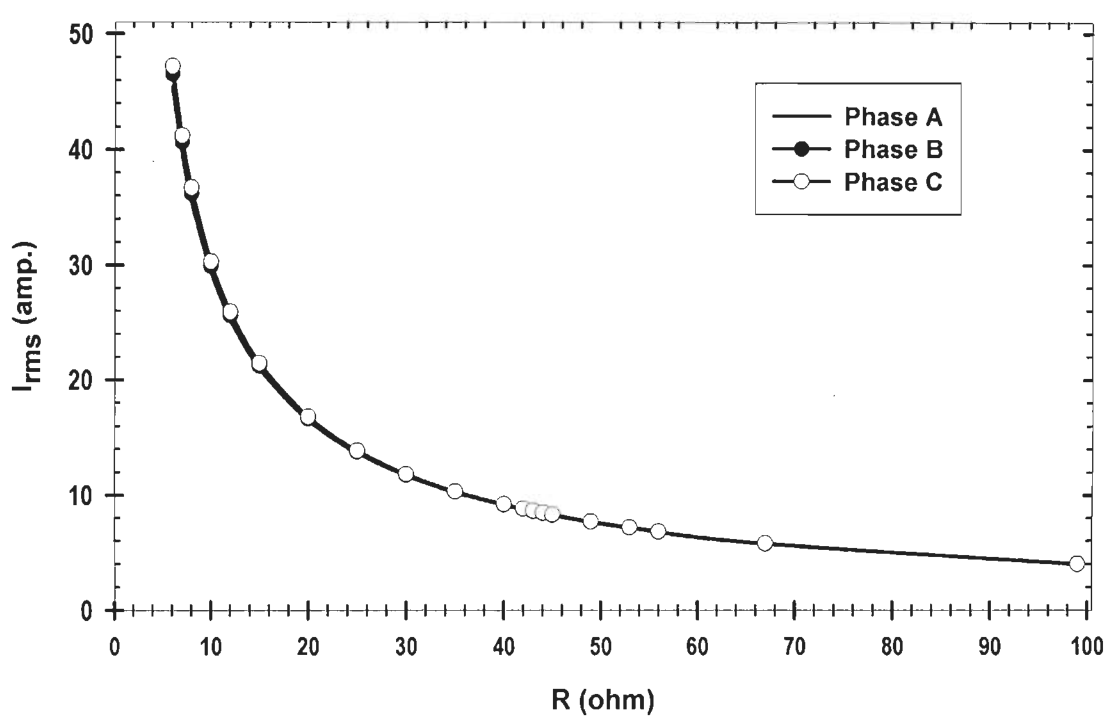

Fig. 5.41: Variation of THD_I with "value of 'R' on DC side of non-linear load" after compensation (with APF), for case-1 of load current unbalance.

Table-5.5: **Results for "case-2" of load current unbalance**

R (ohms)	Utility Current (without APF)						Utility Current (with APF)					
	Phase A		Phase B		Phase C		Phase A		Phase B		Phase C	
	RMS	THD_I (%)	RMS	THD_I (%)	RMS	THD_I (%)	RMS	THD_I (%)	RMS	THD_I (%)	RMS	THD_I (%)
6	32.99	8.11	36.03	9.84	15.88	18.36	28	1.86	27.17	1.72	27.53	1.69
7	30.22	9.17	32.93	10.76	15.22	19.58	25.88	1.78	25.16	1.65	25.45	1.56
8	27.89	10.17	30.32	11.62	14.64	20.57	24.07	1.78	23.43	1.58	23.7	1.53
10	24.19	11.98	26.2	13.16	13.63	22.07	21.19	1.61	20.68	1.45	20.88	1.36
12	21.38	13.56	23.08	14.49	12.77	23.13	18.98	1.52	18.56	1.36	18.71	1.25
15	18.23	15.52	19.61	16.14	11.69	24.22	16.46	1.47	16.14	1.24	16.26	1.14
20	14.68	17.99	15.71	18.24	10.27	25.34	13.55	1.26	13.32	1.16	13.4	1.06
25	12.33	19.78	13.13	19.79	9.163	26.01	11.56	1.32	11.4	1.07	11.46	0.99
30	10.64	21.12	11.29	20.98	8.271	26.46	10.09	1.29	9.973	1.02	10	0.98
35	9.376	22.16	9.911	21.91	7.536	26.79	8.974	1.18	8.877	1.01	8.896	0.98
40	8.386	22.98	8.837	22.67	6.921	27.04	8.079	1.31	7.99	1.21	8.012	1.09
42	8.048	23.27	8.471	22.93	6.702	27.12	7.767	1.23	7.694	1.07	7.712	1.08
43	7.889	23.40	8.299	23.06	6.597	27.16	7.629	1.22	7.563	1.04	7.58	1.17
44	7.737	23.53	8.134	23.18	6.496	27.20	7.49	1.33	7.418	1.25	7.431	1.28
45	7.59	23.65	7.976	23.29	6.398	27.24	7.353	1.24	7.294	1.11	7.305	1.11
49	7.058	24.10	7.4	23.72	6.033	27.37	6.863	1.42	6.805	1.30	6.819	1.37
53	6.596	24.50	6.904	24.10	5.707	27.49	6.43	1.41	6.377	1.23	6.399	1.34
56	6.289	24.76	6.573	24.35	5.484	27.57	6.146	1.49	6.108	1.38	6.119	1.40
67	5.375	25.54	5.594	25.11	4.798	27.81	5.287	1.66	5.248	1.57	5.259	1.67
99	3.788	26.91	3.908	26.48	3.516	28.26	3.77	2.10	3.75	1.99	3.748	2.26

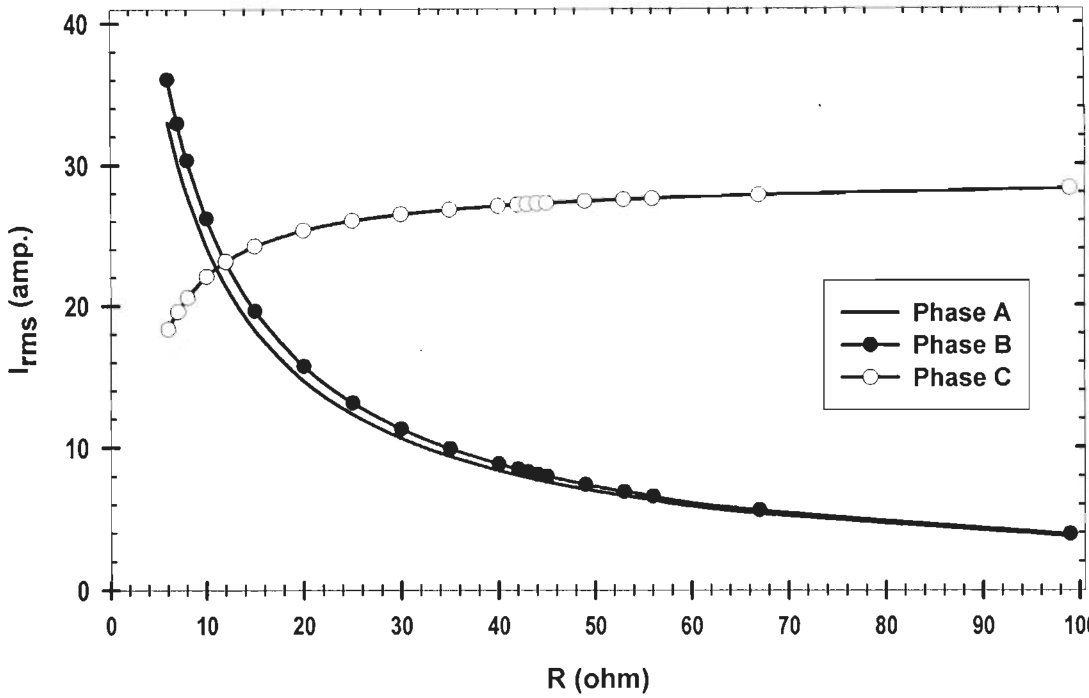

Fig. 5.42: Variation of load current with "value of 'R' on DC side of non-linear load" before compensation (without APF), for case-2 of load current unbalance.

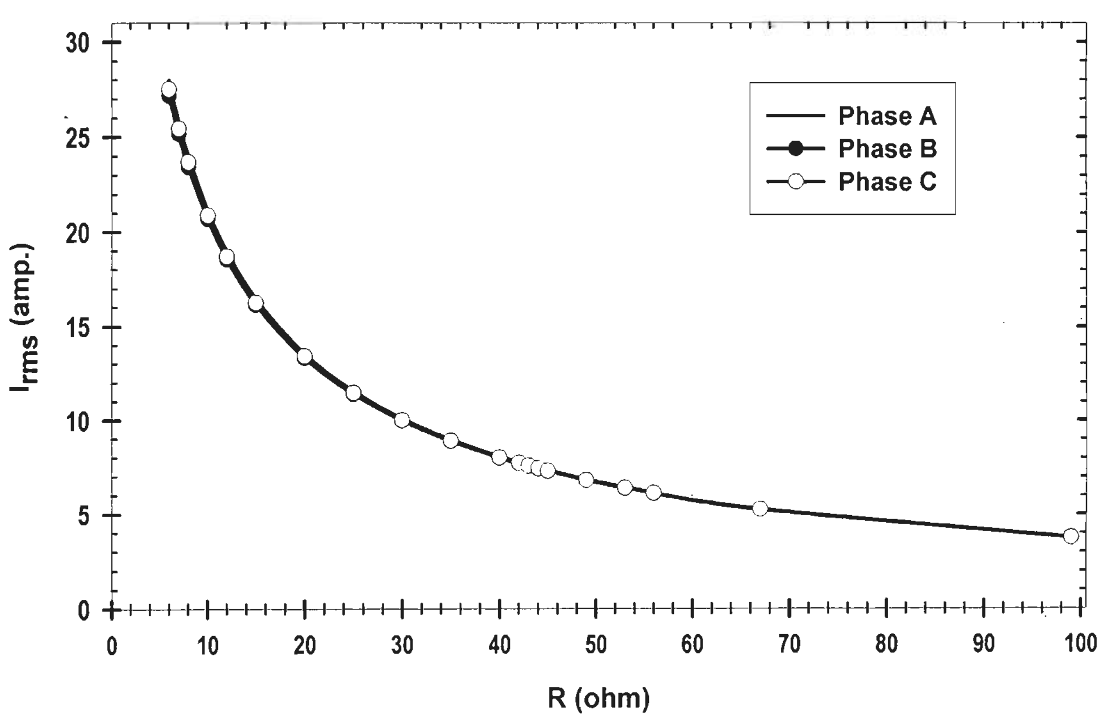

Fig. 5.43: Variation of load current with "value of 'R' on DC side of non-linear load" after compensation (with APF), for case-2 of load current unbalance.

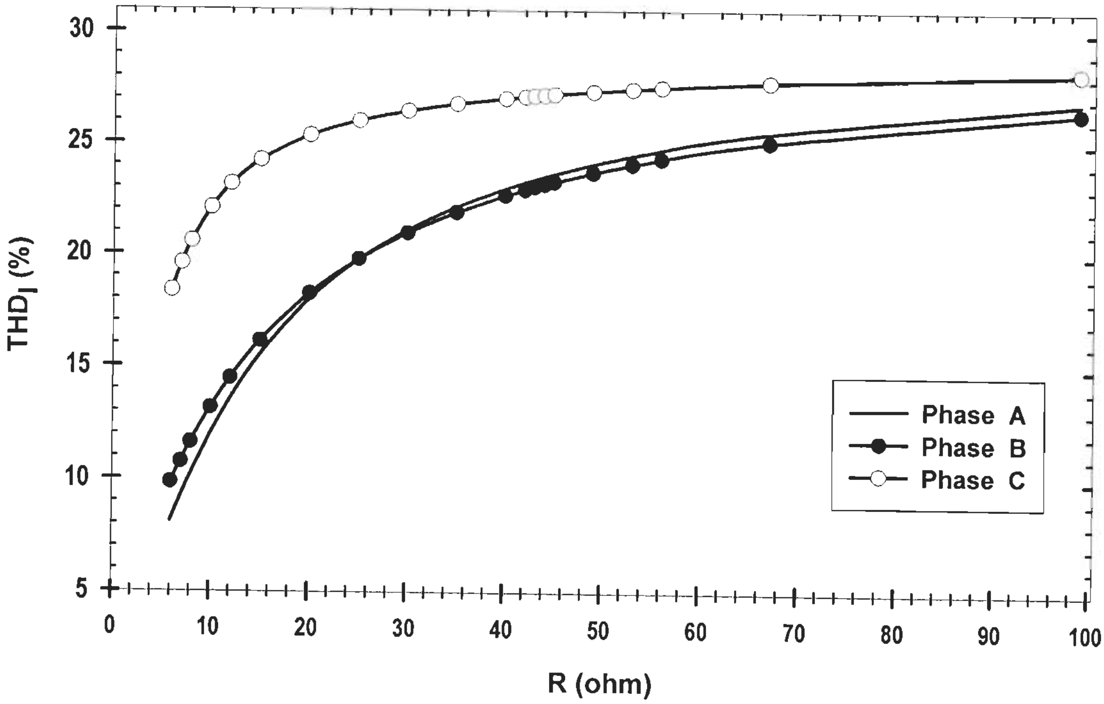

Fig. 5.44: Variation of THD$_I$ with "value of 'R' on DC side of non-linear load" before compensation (without APF), for case-2 of load current unbalance.

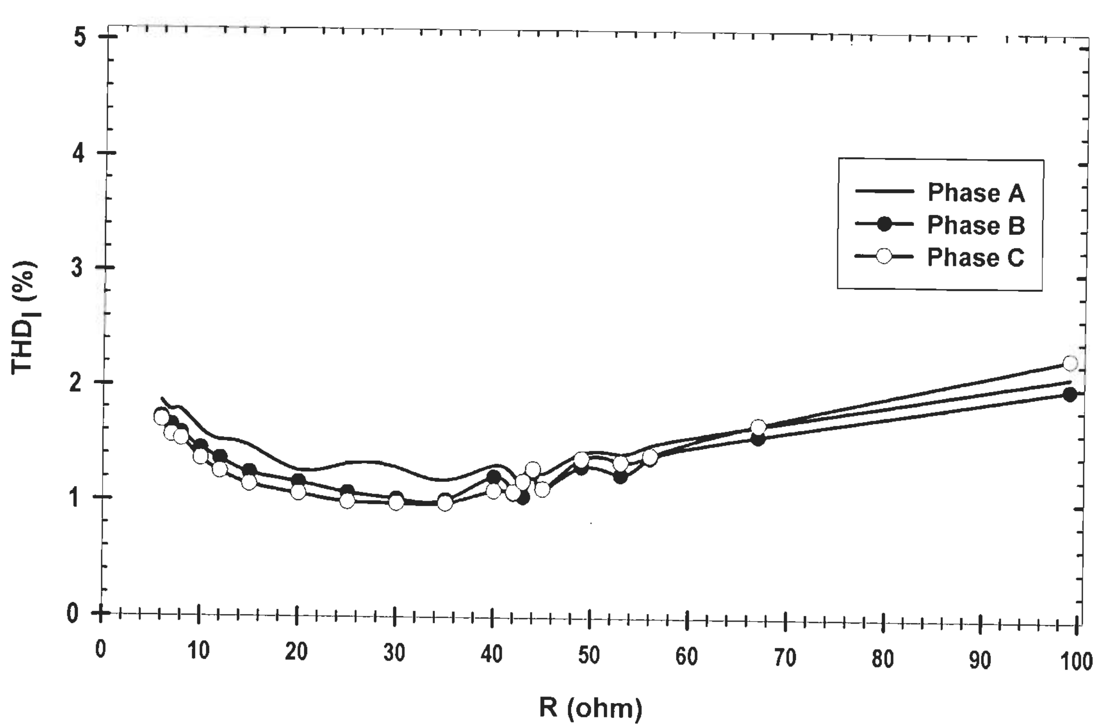

Fig. 5.45: Variation of THD$_I$ with "value of 'R' on DC side of non-linear load" after compensation (with APF), for case-2 of load current unbalance.

5.6.1.4 Compensation of Source Voltage Unbalance:

Voltage unbalance is regarded as an increasing power quality problem of significant concerns at the distribution level. Voltage unbalance in a three-phase electric system is a condition in which the phases have different voltage magnitude or an angular displacement among the phases different from 120 electrical degrees, or even both conditions simultaneously. In practical systems, the supply is usually unbalanced to a certain extent. The unbalance in the supply system causes unbalanced load currents that may lead to further distortion.

Here, an unbalance in source voltage is considered in three different cases. These three cases of source voltage unbalance represent all three conditions discussed earlier, i.e. (i) three-phase source voltage magnitude unbalance, (ii) two-phase angle unbalance, and (iii) combination of 'three-phase source voltage magnitude unbalance' and 'two-phase angle unbalance'.

5.6.1.4.1 Case-1: Three-phase source voltage magnitude unbalance

In case-1, the three-phase unbalanced mains voltages are considered as:

$$\begin{aligned} V_a &= 281.50 \angle 0^{\circ} \\ V_b &= 288.41 \angle 240^{\circ} \\ V_c &= 319.88 \angle 120^{\circ} \end{aligned} \tag{5.29}$$

For this set of three-phase mains voltages, the value of voltage unbalance factor (VUF) is calculated as 4 % and the results are shown in Fig. 5.46 to Fig. 5.49 along with Table-5.6. The comparison of load currents in three different phases is presented in Fig. 5.46 for the 'without APF' condition while in Fig. 5.47 for the 'with APF' condition. At the same time the evaluation of total harmonic distortion for load currents in three different phases has been shown in Fig. 5.48 for 'without APF' condition and in Fig. 5.49 for the 'with APF' condition.

5.6.1.4.2 Case-2: Two-phase angle unbalance

In case-2, the three-phase unbalanced mains voltages are considered as:

$$
\begin{aligned}
V_a &= 325 \angle 0^{\circ} \\
V_b &= 325 \angle 231.9^{\circ} \\
V_c &= 325 \angle 116^{\circ}
\end{aligned}
\tag{5.30}
$$

For this set of three-phase mains voltages, the value of voltage unbalance factor (VUF) is calculated as 4 % and the results are shown in Fig. 5.50 to Fig. 5.53 along with Table-5.7. The comparison of load currents in three different phases is presented in Fig. 5.50 for the 'without APF' condition while in Fig. 5.51 for the 'with APF' condition. At the same time the evaluation of total harmonic distortion for load currents in three different phases has been shown in Fig. 5.52 for 'without APF' condition and in Fig. 5.53 for the 'with APF' condition.

5.6.1.4.3 Case-3: Combination of three-phase source voltage magnitude unbalance (case-1) and two-phase angle unbalance (case-2)

In case-3, the combination of three-phase source voltage magnitude unbalance (case-1) and two-phase angle unbalance (case-2) is taken up for study the three-phase unbalanced mains voltages are considered as:

$$
\begin{aligned}
V_a &= 281.50 \angle 0^{\circ} \\
V_b &= 288.41 \angle 231.9^{\circ} \\
V_c &= 319.88 \angle 116^{\circ}
\end{aligned}
\tag{5.31}
$$

For this arrangement of three-phase mains voltages, results are depicted in Fig. 5.54 to Fig. 5.57, together with Table-5.8. The comparison of load currents in three different phases is presented in Fig. 5.54 for the 'without APF' condition while in Fig. 5.55 for the 'with APF' condition. At the same time the evaluation of total harmonic distortion for load currents in three different phases has been shown for 'without APF' condition in Fig. 5.56 and for the 'with APF' condition in Fig. 5.57.

From these test results it has been demonstrated that APF with FLC based LIMITER is working pertinently under three different possible cases of unbalanced source voltages. This unbalance in the supply system causes unbalanced load currents and consecutively higher values of phase current distortion. It is lucidly observable that after compensation, currents are almost balanced. The APF is found capable to compensate the current distortion (THD_I) for each phase current, very well within the acceptable limit of 5% which was very high before compensation.

Table-5.6: Results for "case-1" of source voltage unbalance (3-phase voltage magnitude unbalance)

R (ohms)	Utility Current (without APF)						Utility Current (with APF)					
	Phase A		Phase B		Phase C		Phase A		Phase B		Phase C	
	RMS	THD_I (%)	RMS	THD_I (%)	RMS	THD_I (%)	RMS	THD_I (%)	RMS	THD_I (%)	RMS	THD_I (%)
6	59.59	28.15	60.23	27.67	63.39	25.00	62.64	0.79	62.83	1.07	62.75	1.05
6.5	55.19	28.33	55.76	27.86	58.7	25.16	57.92	0.76	58.07	0.83	57.99	0.67
7	51.39	28.48	51.91	28.03	54.66	25.3	53.84	0.67	53.96	0.76	53.93	0.82
8	45.17	28.74	45.62	28.31	48.05	25.54	47.23	0.65	47.35	0.76	47.3	0.68
9	40.29	28.96	40.68	28.54	42.86	25.73	42.05	0.62	42.15	0.75	42.11	0.74
10	36.37	29.13	36.71	28.73	38.68	25.89	37.9	0.71	37.99	0.71	37.97	0.72
11	33.14	29.29	33.45	28.89	35.25	26.03	34.46	0.55	34.56	0.68	34.54	0.57
12	30.44	29.42	30.72	29.03	32.37	26.15	31.62	0.44	31.72	0.65	31.62	0.65
13	28.14	29.53	28.4	29.15	29.93	26.25	29.23	0.60	29.32	0.55	29.29	0.49
14	26.17	29.63	26.41	29.25	27.83	26.34	27.17	0.56	27.23	0.61	27.24	0.58
15	24.45	29.72	24.68	29.34	26.01	26.42	25.37	0.55	25.43	0.60	25.44	0.53
16	22.95	29.80	23.16	29.42	24.41	26.49	23.8	0.63	23.86	0.59	23.87	0.67
18	20.44	29.94	20.62	29.56	21.73	26.61	21.18	0.60	21.22	0.59	21.25	0.60
20	18.42	30.05	18.59	29.68	19.59	26.71	19.07	0.64	19.14	0.62	19.15	0.61
22	16.76	30.15	16.92	29.77	17.83	26.80	17.35	0.67	17.41	0.64	17.43	0.72
24	15.38	30.23	15.52	29.85	16.36	26.87	15.93	0.73	15.99	0.84	15.99	0.80
26	14.21	30.30	14.34	29.92	15.11	26.93	14.7	0.76	14.75	0.71	14.77	0.65
28	13.2	30.36	13.33	29.98	14.04	26.99	13.68	0.93	19.41	1.02	13.73	0.99
30	12.33	30.42	12.44	30.03	13.11	27.03	12.77	0.97	12.8	0.84	12.83	0.88
34	10.89	30.51	10.99	30.11	11.58	27.11	11.27	0.80	11.31	1.00	11.33	0.95
38	9.75	30.58	9.843	30.18	10.37	27.18	10.09	1.17	10.13	1.16	10.17	1.18
42	8.827	30.65	8.912	30.24	9.388	27.23	9.154	1.39	9.187	1.39	9.206	1.20
46	8.063	30.70	8.141	30.29	8.576	27.27	8.346	1.30	8.383	1.29	8.409	1.24
50	7.421	30.74	7.494	30.32	7.894	27.31	7.692	1.51	7.737	1.54	7.769	1.43
55	6.75	30.79	6.816	30.36	7.18	27.35	6.987	1.83	7.021	1.74	7.048	1.55
68	5.464	30.88	5.518	30.44	5.812	27.42	5.687	2.04	5.706	2.10	5.728	2.10
80	4.646	30.94	4.694	30.49	4.943	27.47	4.84	2.53	4.859	2.39	4.902	2.16
99	3.757	31.00	3.795	30.55	3.997	27.52	3.929	3.03	3.945	2.76	3.973	2.43

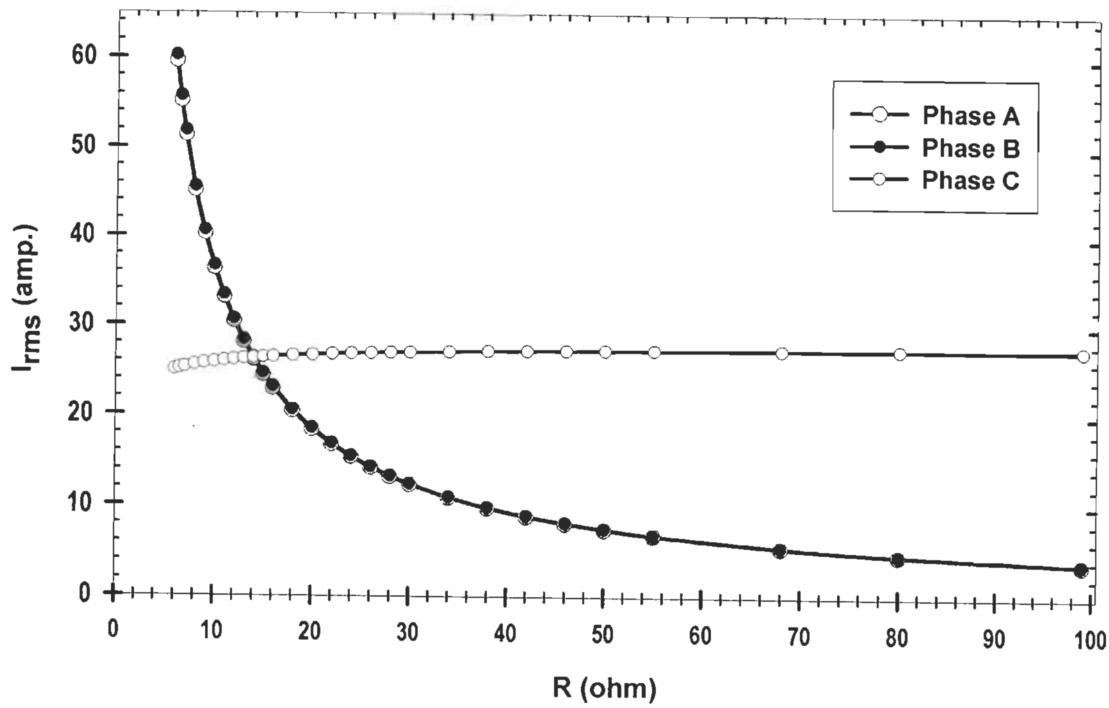

Fig. 5.46: Variation of load current with "value of 'R' on DC side of non-linear load" before compensation (without APF), for case-1 of source voltage unbalance

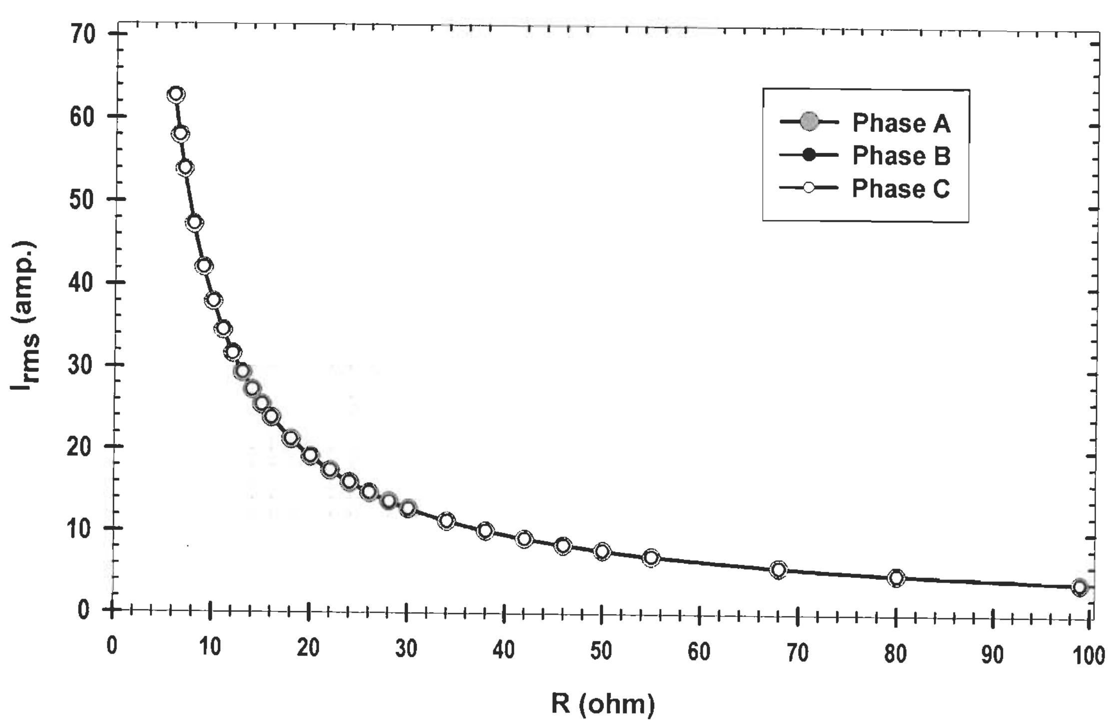

Fig. 5.47: Variation of load current with "value of 'R' on DC side of non-linear load" after compensation (with APF), for case-1 of source voltage unbalance.

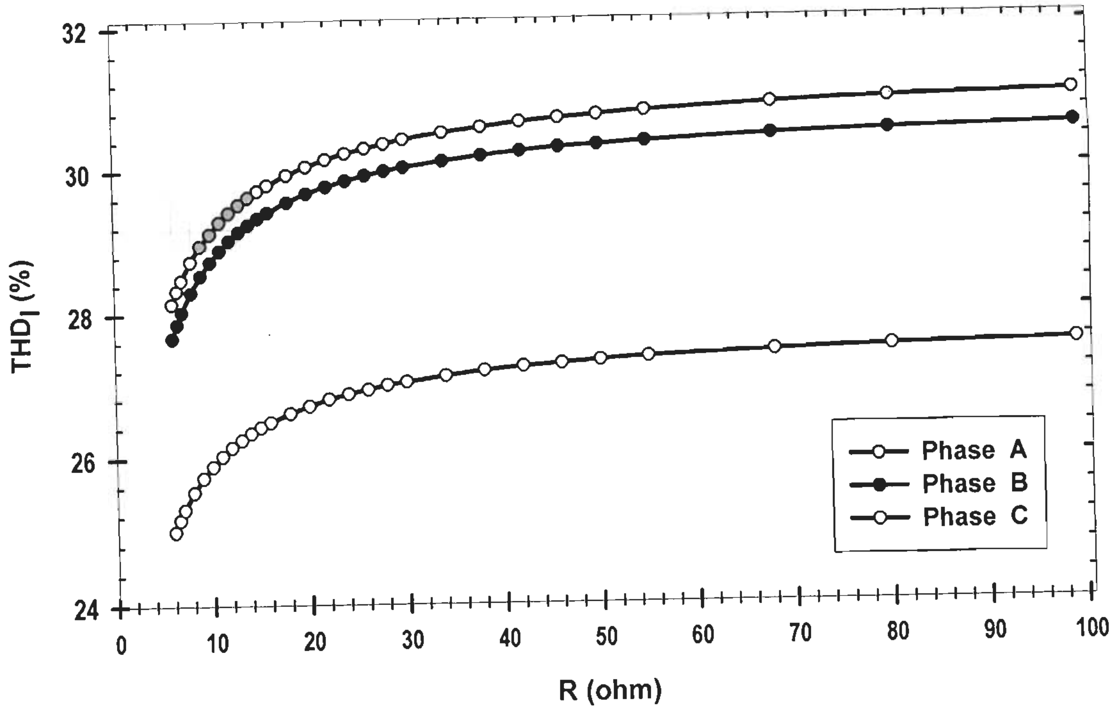

Fig. 5.48: Variation of THD_I with "value of 'R' on DC side of non-linear load" before compensation (without APF), for case-1 of source voltage unbalance

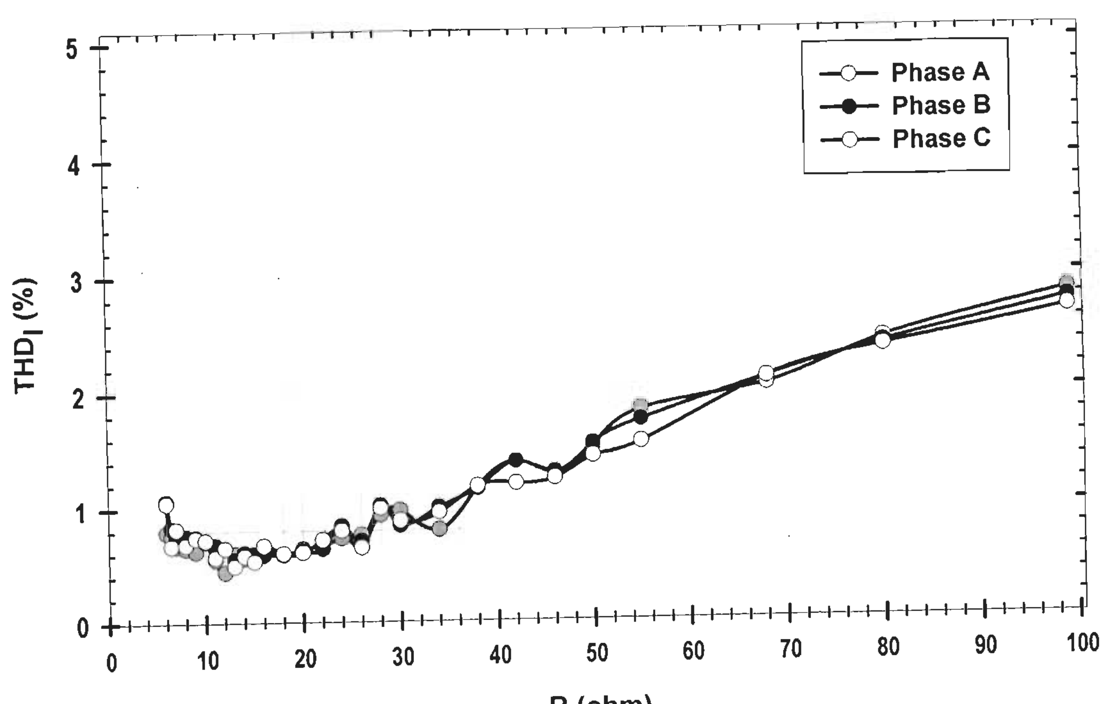

Fig. 5.49: Variation of THD_I with "value of 'R' on DC side of non-linear load" after compensation (with APF), for case-1 of source voltage unbalance.

Table-5.7: Results for "case-2" of source voltage unbalance (2-phase angle unbalance)

R (ohms)	Utility Current (without APF)						Utility Current (with APF)					
	Phase A		Phase B		Phase C		Phase A		Phase B		Phase C	
	RMS	THD_I (%)	RMS	THD_I (%)	RMS	THD_I (%)	RMS	THD_I (%)	RMS	THD_I (%)	RMS	THD_I (%)
6	68.16	25.93	68.26	25.88	64.05	29.00	69 22	1.62	69	1.32	69.11	1.49
6.5	63.11	26.11	63.21	26.04	59.31	29.19	63.99	1.66	63.77	1.29	63.86	1.45
7	58.76	26.27	58.87	26.17	55.22	29.36	59.48	1.56	59.28	1.19	59.34	1.28
8	51.64	26.54	51.75	26.41	48.53	29.64	52.13	1.33	51.97	1.07	52 02	1.27
9	46.06	26.76	46.16	26.60	43.29	29.87	46.38	1.36	46.24	1.09	46.23	0.97
10	41.56	26.94	41.67	26.76	39.07	30.06	41.79	1.31	41.7	1.22	41.66	0.85
11	37 87	27.09	37.97	26.9	35 6	30.22	38.02	1.04	37.89	0.78	37.89	0.86
12	34.78	27.22	34.87	27.01	32.69	30.36	34.89	1.04	34 77	0.84	34.78	0.89
13	32 15	27.34	32.24	27.12	30.23	30.48	32.22	0.79	32.12	0.66	32.11	0.65
14	29 9	27.44	29.98	27.21	28.11	30.58	29.94	0.76	29.85	0.67	29.82	0 69
15	27 94	27.52	28 02	27.29	26 26	30.67	27.96	0.88	27 88	0.64	27.86	0.81
16	26.22	27.60	26.29	27.36	24.65	30 76	26.23	0.89	26 16	0.83	26 13	0.72
18	23.35	27.73	23 41	27.49	21.95	30.90	23 34	0.90	23.26	0.70	23.23	0.83
20	21 4	27.84	21 1	27.59	19.78	31.02	21 00	0.62	20.96	0.76	20.93	0.75
22	19.15	27.93	19.2	27.68	18	31.11	19.12	0.69	19.07	0.78	19.04	0.61
24	17 57	28.00	17 62	27.75	16.52	31.20	17.54	0.79	17.49	0.77	17.46	0.57
26	16 23	28.07	16.28	27.82	15.26	31.27	16.2	0.80	16.15	0.71	16.12	0.78
28	15 08	28.12	15.13	27.88	14 18	31.33	15 04	0.74	15.01	0.72	14 97	0.77
30	14.09	28.17	14.13	27.93	13.24	31.39	14.06	0.82	14.03	0.93	13.98	0.82
34	12.44	28.26	12.48	28.01	11.7	31.48	12.41	1.00	12.38	0.99	12.33	0.94
38	11.14	28.32	11.17	28.08	10.47	31.56	11.13	0.98	11.09	0.88	11 03	0.94
42	10 09	28.37	10.11	28.14	9.483	31.62	10 08	1.05	10.06	1.06	10	1.03
46	9.215	28.42	9.238	28.19	8.663	31.67	9.199	1.01	9.184	1.06	9.12	1.09
50	8.482	28.46	8.502	28.23	7 974	31.71	8.473	1.27	8.458	1.30	8.395	1.28
55	7.715	28.49	7.73	28.27	7.252	31.76	7.714	1.32	7.681	1.31	7.626	1.28
68	6.246	28.57	6.26	28.36	5.871	31.85	6.251	1.70	6.249	1.85	6.19	1.84
80	5.312	28.61	5.323	28.41	4.993	31.9	5.33	1.84	5.312	2.08	5.257	1.88
99	4.296	28.61	4.304	28.47	4.037	31.97	4.33	2.08	4.305	2.22	4 239	2.39

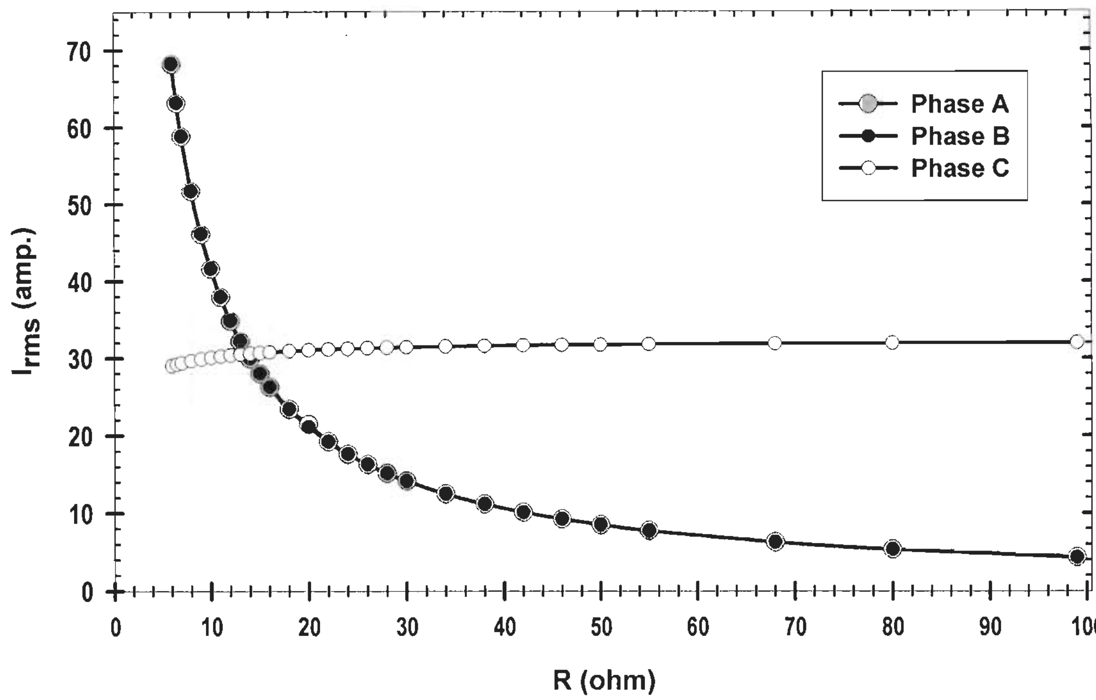

Fig. 5.50: Variation of load current with "value of 'R' on DC side of non-linear load" before compensation (without APF), for case-2 of source voltage unbalance

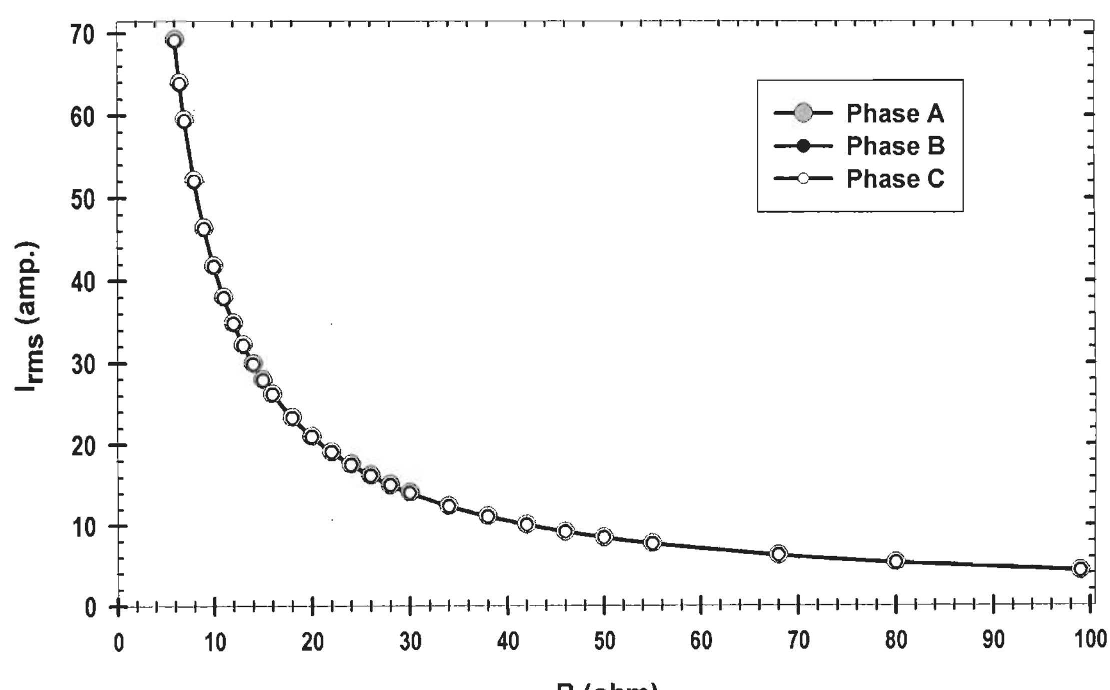

Fig. 5.51: Variation of load current with "value of 'R' on DC side of non-linear load" after compensation (with APF), for case-2 of source voltage unbalance.

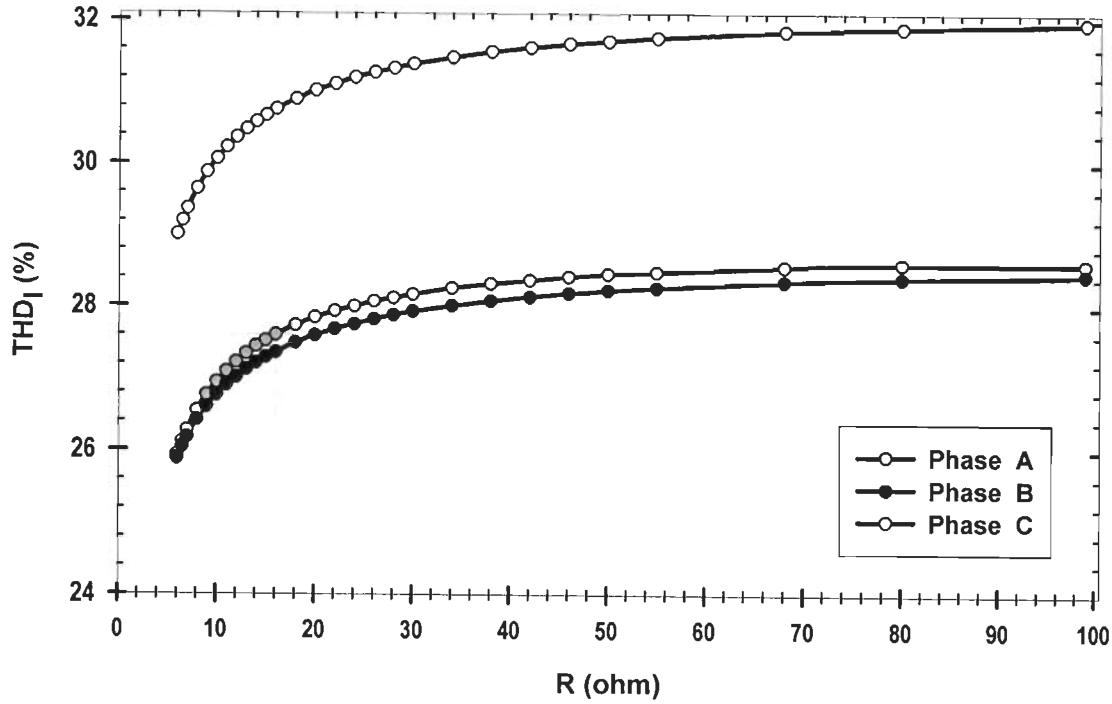

Fig. 5.52: Variation of THD_I with "value of 'R' on DC side of non-linear load" before compensation (without APF), for case-2 of source voltage unbalance

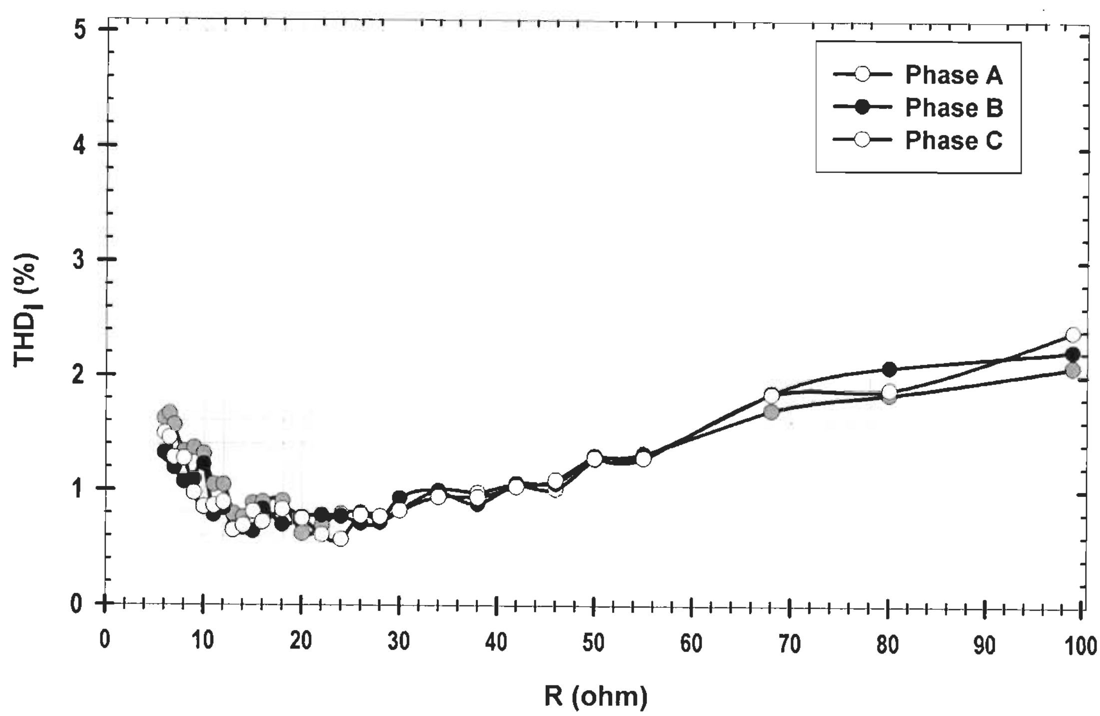

Fig. 5.53: Variation of THD_I with "value of 'R' on DC side of non-linear load" after compensation (with APF), for case-2 of source voltage unbalance.

Table-5.8: Results for "case-3" of source voltage unbalance (combination of 3-phase voltage magnitude and 2-phase-angle unbalance)

R (ohms)	Utility Current (without APF)						Utility Current (with APF)					
	Phase A		Phase B		Phase C		Phase A		Phase B		Phase C	
	RMS	THD_I (%)	RMS	THD_I (%)	RMS	THD_I (%)	RMS	THD_I (%)	RMS	THD_I (%)	RMS	THD_I (%)
6	60.59	27.19	61.24	26.65	61.02	26.83	62.97	0.82	63.00	0.94	62.96	0.75
6.5	56.1	27.37	56.71	26.82	56.5	27.01	58.21	0.82	58.21	0.85	58.19	0.85
7	52.24	27.52	52.8	26.98	52.61	27.16	54.1	0.76	54.11	0.79	54.11	0.89
8	45.91	27.79	46.4	27.24	46.24	27.42	47.39	0.54	47.4	0.55	47.38	0.61
9	40.95	28	41.39	27.45	41.25	27.63	42.17	0.60	42.2	0.54	42.17	0.49
10	36.96	28.18	37.36	27.63	37.23	27.8	38.01	0.52	38.01	0.41	38.0	0.52
11	33.67	28.34	34.04	27.78	33.92	27.95	34.59	0.58	34.6	0.53	34.56	0.53
12	30.93	28.47	31.26	27.91	31.15	28.08	31.74	0.60	31.73	0.53	31.72	0.62
13	28.59	28.58	28.9	28.02	28.8	28.19	29.3	0.63	29.33	0.60	29.29	0.54
14	26.59	28.68	26.87	28.12	26.78	28.29	27.23	0.50	27.24	0.53	27.23	0.48
15	24.85	28.77	25.11	28.20	25.03	28.38	25.42	0.53	25.45	0.52	25.43	0.50
16	23.32	28.85	23.57	28.28	23.49	28.45	23.87	0.59	23.87	0.62	23.87	0.58
18	20.76	28.98	20.99	28.41	20.91	28.59	21.22	0.62	21.23	0.67	21.22	0.68
20	18.71	29.09	18.91	28.52	18.85	28.7	19.13	0.67	19.12	0.63	19.13	0.70
22	17.03	29.19	17.21	28.61	17.16	28.79	17.39	0.73	17.4	0.63	17.39	0.7
24	15.63	29.27	15.8	28.69	15.74	28.87	15.97	0.74	15.97	0.7	15.95	0.7
26	14.44	29.33	14.59	28.76	14.54	28.94	14.75	0.89	14.74	0.74	14.74	0.89
28	13.41	29.39	13.56	28.82	13.51	28.99	13.7	0.8	13.7	0.86	13.7	0.84
30	12.53	29.45	12.66	28.87	12.62	29.05	12.81	0.95	12.8	0.96	12.8	0.8
34	11.07	29.53	11.18	28.96	11.15	29.13	11.31	1.07	11.32	0.94	11.31	1.08
38	9.908	29.6	10.01	29.03	9.98	29.20	10.13	1.19	10.13	1.12	10.12	1.24
42	8.97	29.66	9.067	29.08	9.035	29.26	9.184	1.4	9.176	1.32	9.185	1.34
46	8.195	29.71	8.283	29.13	8.254	29.31	8.377	1.28	8.396	1.25	8.402	1.29
50	7.542	29.75	7.624	29.17	7.597	29.35	7.715	1.32	7.733	1.47	7.729	1.46
55	6.86	29.79	6.934	29.21	6.909	29.4	7.021	1.59	7.027	1.81	7.025	1.62
68	5.553	29.88	5.613	29.3	5.593	29.48	5.703	1.99	5.724	2.10	5.709	1.94
80	4.723	29.93	4.774	29.35	4.757	29.54	4.868	2.41	4.887	2.51	4.865	2.30
99	3.819	29.99	3.86	29.41	3.846	29.60	3.945	2.81	3.956	2.76	3.939	2.87

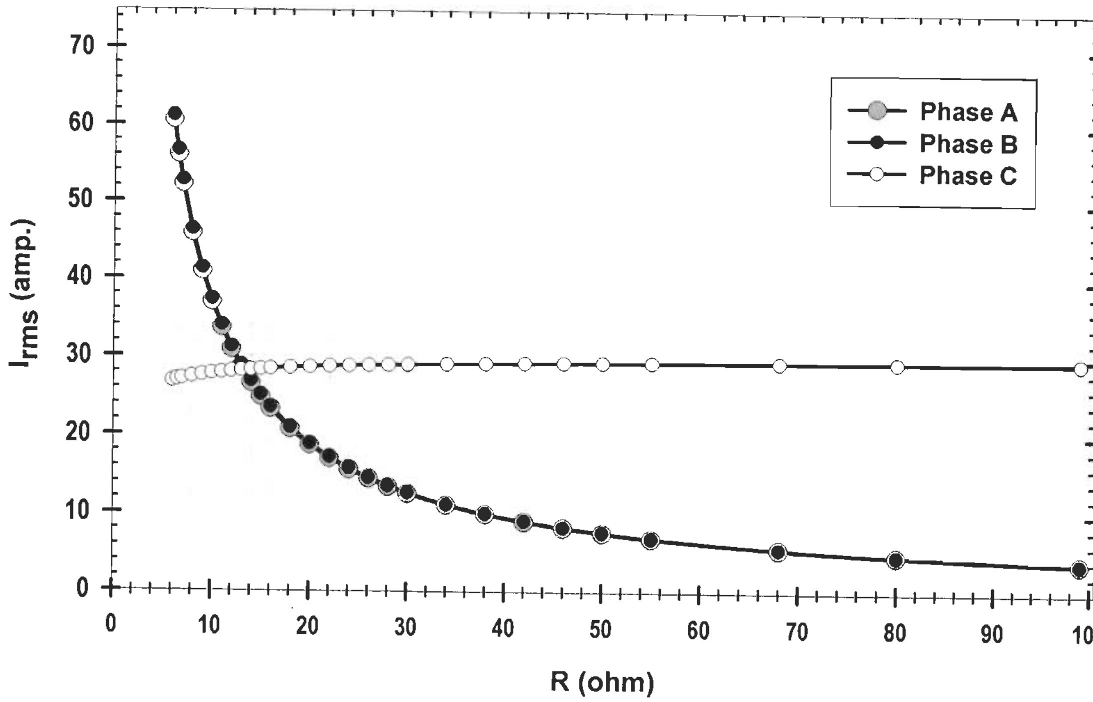

Fig. 5.54: Variation of load current with "value of 'R' on DC side of non-linear load" before compensation (without APF), for case-3 of source voltage unbalance

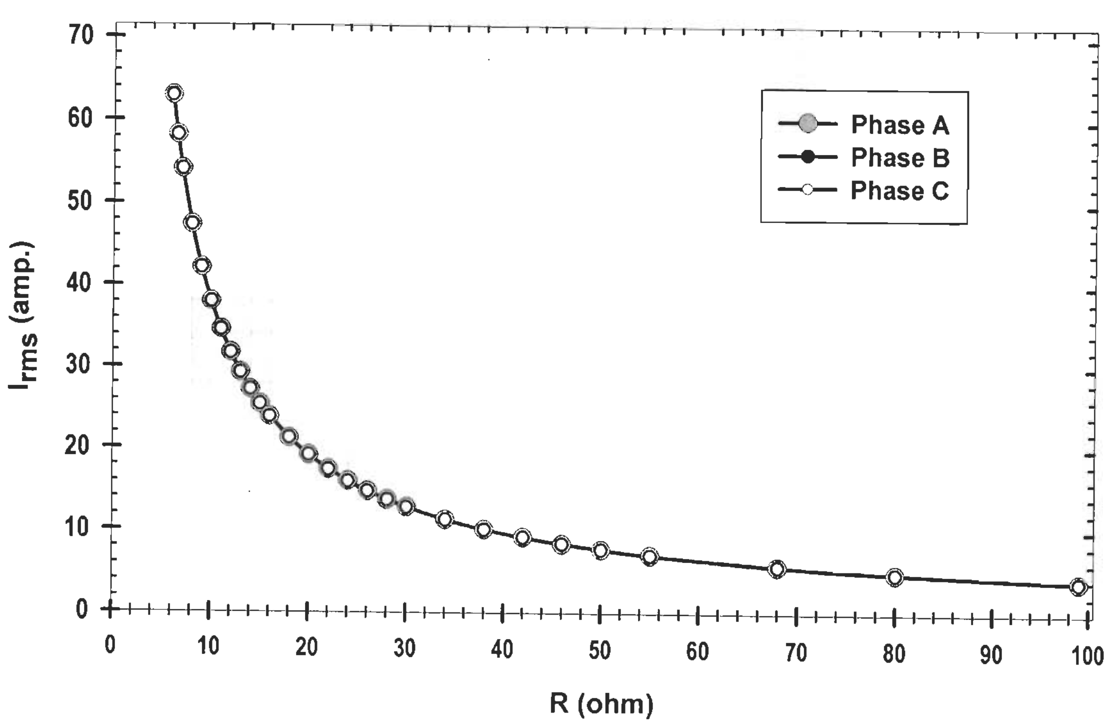

Fig. 5.55: Variation of load current with "value of 'R' on DC side of non-linear load" after compensation (with APF), for case-3 of source voltage unbalance.

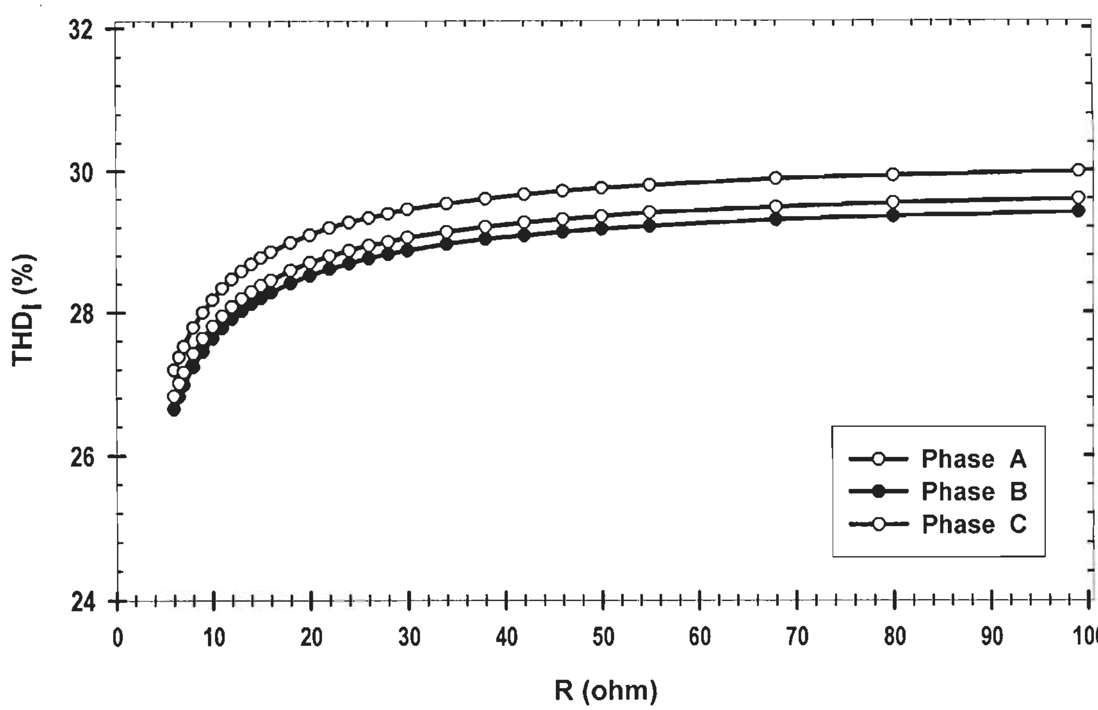

Fig. 5.56: Variation of THD$_I$ with "value of 'R' on DC side of non-linear load" before compensation (without APF), for case-3 of source voltage unbalance

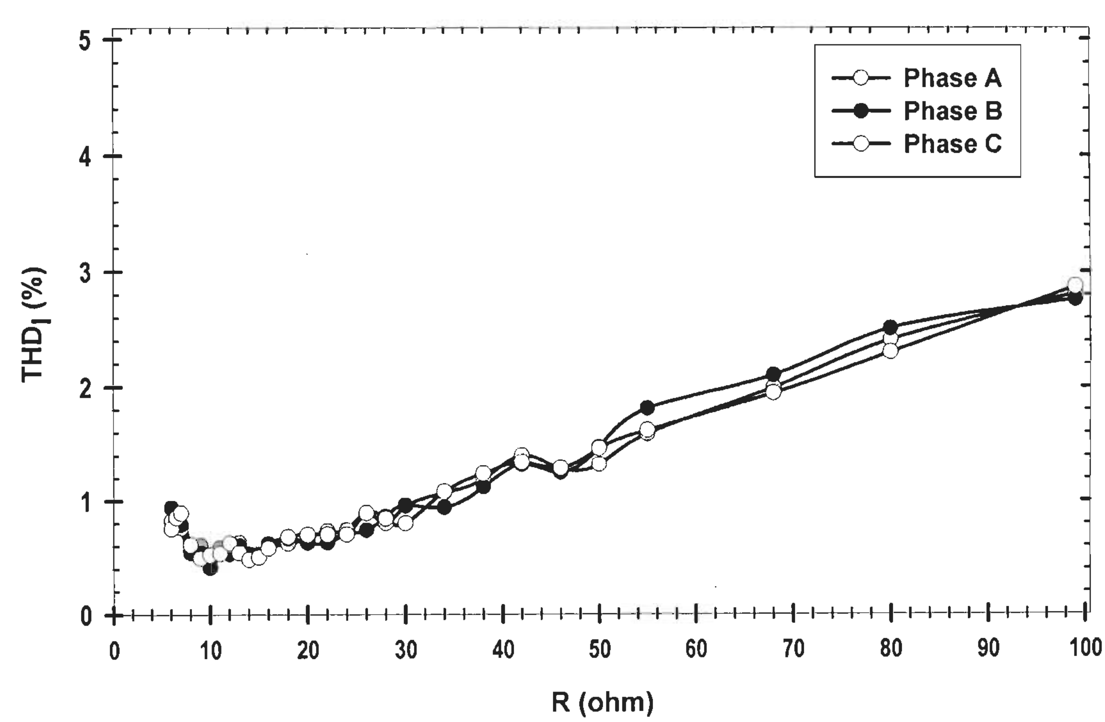

Fig. 5.57: Variation of THD$_I$ with "value of 'R' on DC side of non-linear load" after compensation (with APF), for case-3 of source voltage unbalance.

5.7 COMPARISON OF DC AND AC LOAD CURRENT SENSING METHODS

As the DC load current is sensed from the load side of rectifier while AC load current is sensed from utility side of rectifier, on making comparison between these two load current sensing methods it is observed that in technique-1 (DC load current sensing method) operating range is lesser than in technique-2 (AC load current sensing method) due to its known relation between AC load current and its equivalent DC load current. In case of AC load current sensing method the operating range is increased by a factor $\sqrt{2}$. Another advantage of AC load current sensing method is that in this method no additional arrangement is to be made for load current sensing for FLC, as the AC load current sensing is already being done for FLC with constant limiter, which is using the load current for hysteresis band (HB) current control method in pulse generation for inverter. There is not much difference in two methods as the performance is concerned except that at the points of load change (i.e. after every 10 cycles), the harmonic compensation is faster (i.e. takes lesser no. of cycles in bringing down the THD_I value below 5 %) for trapezoidal membership function than triangular membership function.

5.8 CONCLUDING REMARKS

The APF offers an unprecedented ability to clean the power system network from harmonics. This work demonstrate the validity of an APF controlled by fuzzy-expert system based variable limiter, which is found competent of handling a large range of variation in load current. The results of simulation study with proposed APF control techniques as discussed in this chapter are found quite acceptable to mitigate harmonics and eliminate reactive power components from the utility current. The proposed shunt APF is also found suitable in controlling the unbalanced distorted load currents caused by load unbalance and source voltage unbalance, and making them balanced and sinusoidal after compensation. These conclusions about the APF performance are authenticated by rigorous simulation study. It is evident from simulation results that the proposed topology is simple and robust as it is based on sensing load currents only, and is capable of providing compensation for random and dynamic load variations to meet the IEEE-519 standard requirements for harmonic limits. The proposed shunt APF enhances the system efficiency as it does not process the active power delivered to the load and results in sinusoidal, unity power factor and balanced utility currents.

CHAPTER VI

CONCLUSIONS

6.1 GENERAL

In the scope of this thesis a through and systematic study on power quality investigations is presented, through a series of steps. Power quality deterioration has two unusual aspects: one is transient disturbance (i.e. voltage sags, swells, impulses etc.) and another is steady state disturbances (i.e. harmonic distortion, unbalance, flicker etc.). This work is a discussion on the second aspect of power quality. In the first step, a wide background of these two attributes of power quality, in terms of causes and effects are presented.

The significance of harmonics in power systems has increased substantially due to their magnified impact on power systems caused by significantly increasing use of semiconductor based non-linear devices /power-electronic components. Power-electronic has provided a better management and control of electric power as the systems used for controlling different applications using power-electronics are more efficient, dynamic, faster in response, economical and smaller in size. But, ironically these also act as main perpetrator of harmonic pollution. The interest in harmonics (voltage or current distortion) involves all three parties concerned with the power industry i.e. utility companies, equipment manufacturers and electric power customers. Possibly due to this concern only, harmonic distortion has become most researched and most published among all the power quality disturbances, especially over the last few decades.

In second step, two different case studies are performed to quantify the harmonic contents in power system in case of single /multiple PC loads for different operating conditions and processing modes; and a variety of modern home appliances and equipments having different power levels. It is illustrated here that the parameters, which have an effect on harmonics produced in the line current are multiplicity of PC loads, mode of operation, and status of monitor. It is shown that presence of UPS also affects the harmonic distortion. Furthermore, it is also observed that attenuation and diversity are two important factors while studying the harmonic behavior of single-phase nonlinear loads, in particular for the higher order harmonic components.

Voltage unbalance in three phase electric system is a condition in which the three-phase voltages differ in magnitude and /or does not have its normal 120° phase relationship. While it is practically unfeasible to make available a perfectly balanced supply system to a customer, every attempt has to be taken to minimize the voltage unbalance to reduce its effects on customer loads, i.e. high dc distortion, over voltages and high currents, excessive losses in other rotating machines, KVAr inductive meter errors, protection relay malfunction, etc.

In third step, the effect of source voltage unbalance is studied with respect to the changes in magnitude as well as phase angles in individual phases, and in different possible combinations of phases for a rectifier load. In recent years, the three phase ac-dc rectifiers are finding great industrial utility. The static power converters are nonlinear in nature and consequently they generate harmonics into the supply. Unbalanced rectifier currents cause detrimental effects including: uneven current distribution over the legs of the rectifier bridge that increases the conduction loss and may cause failure of rectifying devices; increased rms ripple current in the smoothing capacitor; increased total rms line current and harmonics. Also, the input current harmonics are not restricted to the converter characteristic harmonics, and non-characteristic triplen harmonics appear which may make the power factor and system efficiency very low along with the undesirable harmonic distortion in the output.

In practical systems, the supply is usually unbalanced to a certain extent due to various unavoidable reasons, which aggravates the complications of harmonic generations. This work presents a detailed analytical study on the effect of voltage unbalance in the supply system on the performance of a three-phase AC-DC rectifier under various typical voltage unbalance cases. These different possible cases of unbalance have different noticeable impacts on the harmonic characteristics. Thus, it is not merely adequate to know the percentage of voltage unbalance, but it is equally significant to know the composition /type of unbalance. Four different definitions of source voltage unbalance are calculated for these unbalance cases and it is observed that relation between their numerical values varies for a variety of voltage unbalance cases. Even single-phase voltage unbalance influences the rms magnitude as well as THD_I of current waveforms of all three phases. The cases up to three-phase voltage unbalance have been considered to confirm the results.

An attempt has been made to recognize the responsibility of sequence voltage components in voltage unbalance analysis in existence of harmonics. It is found that the harmonic pattern is decided by the degree of voltage unbalance (VUF). Positive sequence voltage component (V_1) controls the magnitude of dc output parameters, while their distortion is found relative to negative sequence voltage component (V_2).

For a balanced three phase system with balanced operating conditions, the phase harmonic currents have equal magnitudes and a known phase sequence. Hence, analysis of only one phase is carried out. But in case of unbalanced system, harmonic content of each phase current differs with other phases and the difference in various phase harmonic component and their distortion levels can be significant. To simplify the harmonic current analysis in three different phases a new term "Phase Total Harmonic Distortion Unbalance Factor" (PTHDUF) is introduced. As the voltages become more unbalanced (i.e. % VUF increases), the PTHDUF increases in proportional to the degree of unbalance (%VUF). The variation of different characteristic and non-characteristic harmonics is investigated to understand the sensitivity of current harmonic components to different unbalance voltage operating conditions. A full understanding of sensitivity of the current harmonic components to different unbalance voltage operating conditions is also obtained.

A detailed analytical study gave the following results:

(i) Definitions of voltage unbalance for 1-Φ cases

- As for as single-phase voltage magnitude unbalance (either UV or OV) is concerned, the magnitudes of PVUR1, PVUR, LVUR and VUF are seen to be in the ratio of 3:2:1:1,
- For higher VUF (more than 10 %), LVUR happens to be little lower than VUF in case of single-phase under-voltage unbalance,
- For the single-phase over-voltage unbalance, the LVUR happens to be little higher than VUF,
- In case of single-phase angle variation (either CW or ACW), magnitudes of PVUR1 and PVUR are zero, and LVUR happens to be lower than VUF throughout the unbalance.

(ii) Definitions of voltage unbalance for eight different cases

It is clearly observable that for the same VUF,

- LVUR has lowest value for 1-Φ angle unbalance, and highest value for 1- Φ over-voltage (OV) unbalance,

- In case of phase angle movement unbalance, the LVUR is always higher for 2-Φ phase angle movement unbalance case in comparison to 1-phase angle movement unbalance case,

- Comparison between the1-Φ angle unbalance cases and 1-Φ UV (magnitude) unbalance cases, concludes that LVUR is always little lower than VUF,

- For the case of phase angle unbalance, change in value of V_1 is almost negligible, while the value of V_2 is almost comparable with other cases.

(iii) Effect on DC parameters of AC-DC rectifiers

- The existence of negative sequence voltage component (V_2) in power system indicates the presence of unbalance,

- Negative sequence voltage component (V_2) increases with the increase in VUF,

- The change in value of positive sequence voltage component (V_1) depends on the type of unbalance as the V_1 increases for OV unbalance and decreases for UV unbalance with increasing VUF,

- Positive sequence voltage component (V_1) regulates the magnitude of DC output parameters, while distortion in DC output parameters is proportional to negative sequence voltage component (V_2),

- For single-phase angle unbalance case the change in value of positive sequence voltage component (V_1) is very small, i.e. for 10% change in VUF, the V_1 changes by 1.0% and for 16% change in VUF, the V_1 changes by 2.5% only,

- The same pattern of variation is reflected in magnitudes of DC output parameters,
- Negative sequence voltage component (V_2) increases with the increase in degree of unbalance (VUF),
- Distortion of DC output parameters is found increasing with the increase in V_2,
- In a typical case where the VUF is regulated only by increasing the value of negative sequence voltage component (V_2) and keeping positive sequence voltage component (V_1) constant, it is found that magnitude of DC output parameters remains constant throughout the variation of VUF, while their distortion increases with increasing VUF,
- In a different condition, where two different cases are compared for unequal phase angle movements of two different phasors in opposite and similar direction, it is observed that in both cases, even with different three-phase source voltages, at every step of increasing VUF, the positive (V_1) and negative sequence voltage component (V_2) have similar values, and thus having identical DC output parameters and their distortion,
- As the VUF increases, the THD_I of three different phases also vary depending on the nature of unbalance. But degree of voltage unbalance (VUF) has no effect on the average THD_I of all three different phases, i.e. it remains almost constant.
- Phase Total Harmonic Distortion Unbalance Factor (PTHDUF) has been proposed as an effective measure of voltage source unbalance in presence of harmonic distortion, as it is found to be

  (a) Proportional to degree (VUF) of voltage unbalance

  (b) Reasonably characteristic for the type (voltage magnitude /phase angle movement) and degree (VUF) of voltage unbalance.

(iv) Effect on AC parameters of AC-DC rectifiers

- Even a single-phase supply voltage unbalance has its qualitative impact on AC current waveforms and its parameters (rms value and THD_I) of all three phases (I_A, I_B, and I_C),
- It is observed that for increasing value of rms current, the THD_I decreases and vice-versa,
- 'The change' in voltage magnitude (either UV or OV) 'most affects' the phase in which the supply voltage unbalance is taking place,
- THD_I decreases for the phase in which voltage value is increased and vice-versa,
- 'The change' in voltage phase angle (either CW or ACW) 'least affects' the phase in which the phase angle movement is taking place, and 'most affects' the phase towards which it is moving,
- For the CW movement of the phase in which the phase angle movement is taking place, the rms value of utility current and its THD_I are constant for any value of VUF,
- For ACW movement of the phase in which the phase angle movement is taking place, the THD_I slightly increases and accordingly, load current magnitude decreases, with increasing VUF,
- THD_I is found increasing for the phase towards which the voltage phasor (under movement) is approaching and decreasing for the phase from which it is moving away. This observation is valid for the single-phase voltage unbalance due to movement (CW or ACW) of any voltage phasor (*A*, *B* or *C*) considered individually at a time,
- If voltage unbalance is present in more than one phase, then the combination of unbalance voltages may nullify the detrimental effect of different individual voltage unbalances and the net effect (as the value of VUF) is very much reduced,

- For cases with voltage unbalance in two or three phases, analysis is done as the combination of two or three cases of single phase voltage unbalance. This analysis is presented for eight different possible cases of voltage unbalance with four distinctive values of VUF and it is observed that estimated values of THD_I (in three different phases) are found very close (almost equal) to the actual values,

- The data sheet developed can be used in analyzing any combination of source voltage unbalance, and finding the results for corresponding harmonic distortion. It can also be used in assessment of voltage unbalance (VUF) with the available knowledge of harmonic distortion.

In final step, the concept of an active power filter to control the harmonics under 'variable load' conditions is presented. A fuzzy-expert system to control the performance of shunt active power filter is developed. The suggested control strategy imparts the following special features:

- It is simple, cost-effective, efficient, and reliable.

- Easily adaptable for randomly, and dynamically varying nonlinear load currents.

- It provides harmonic current and reactive power compensation simultaneously.

- Furthermore, it is also compensating for unbalanced utility currents due to unbalance either in loads or in the three phase supply voltages.

The proposed APF control method results in almost sinusoidal, unity power factor, and balanced utility current operation of non-linear loads with harmonic current, reactive, and unbalanced components.

As the power quality issues are gaining the attention and concern of various researchers, because of large diffusion of non-linear and time varying single phase and three phase loads and their interactions with the distribution networks in residential, commercial and industrial areas, it has become very essential that unbalance phenomena in presence of harmonic distortion should also be well monitored, detected and corrected. The work presented here is an endeavor in this direction.

6.2 SCOPE FOR FUTURE WORK

Unbalanced supply conditions and unbalanced and /or nonlinear loads are the most common and realistic situations for most power conversions. It is, therefore, very important to know in advance how the power system will behave under new conditions. The data sheet developed can be used in analyzing any combination of source voltage unbalance, and finding the results for corresponding harmonic distortion. It can also be used in assessment of voltage unbalance (VUF) with the available knowledge of harmonic distortion.

In future, various possible cases of voltage unbalance, other than the cases studied so far, can also be taken up for further studies. These results for different voltage unbalance cases may be used to train the expert system, which could be helpful to investigate and characterize the type and quantity of voltage unbalance present in three-phase system. This information can help to identify threatening conditions in a power system and using this information the operator can use implement the corrective measures, in time.

A closer study on the case of multiple nonlinear devices under the influence of unbalance supply conditions can be the subject of future considerations, where a holistic approach combining statistical data of loads and network impedances with measurement based analytical methods can improve the thoroughness of the analysis.

[1] Bollen, M.H.J., *Understanding Power Quality Problems: Voltage Sags and Interruptions*, IEEE Press, New York, 1999.

[2] Dugan, R. C., McGranaghan, M. F., and Beaty, H. W., *Electrical Power Systems Quality*, McGraw-Hill, New York, 1996.

[3] Reeve, J., and Krishnayya P.C.S., "Unusual Current Harmonics Arising from HVDC Transmission," *IEEE Trans. Power App. System*, Vol. 87, 1968, pp.883-893.

[4] Reeve, J., Baron, J.A., and Krishnayya, P.C.S., "A General Approach to Harmonic Current Generation by HVDC Converters," *IEEE Trans. Power App. System*, Vol. PAS-88, July 1969, pp. 989-996.

[5] Phadke, A.G., and Harlow, J.H., "Generation of Abnormal Harmonics in High Voltage AC-DC Power Systems," *IEEE Trans. Power App. System*, Vol. 87, 1968, 873-883.

[6] Zheng, T., Makram, E.B., and Girgis, A.A., "Evaluating Power System Unbalance in the Presence of Harmonic Distortion," *IEEE Trans. Power Delivery*, Vol.18, 2003, pp. 393-397.

[7] Rashid, M.H., and Maswood, A.I., "Analysis of Three-Phase AC-DC Converters under Unbalanced Supply Conditions," *IEEE Trans. on Industrial Applications*, Vol. 24, 1988, pp.449-455.

[8] Sakui, N.M., Fujita, H., and Shioya, M., "A Method for Calculating Harmonic Currents of A Three-Phase Bridge Uncontrolled Rectifier with DC Filter," IEEE Trans. on Industrial Electronics, Vol. 36, 1989, pp. 434 -440.

[9] Maswood, A.I., Joos, G., Ziogas, P.D., and Lindsey, J.F., "Problems and Solutions Associated with the Operation of Phase-Controlled Rectifiers under Unbalanced Input Voltage Conditions," *IEEE Trans. Industry Applications*, Vol. 27, 1991, pp. 765-72.

[10] Yacamini, R., and Oliveira, J.C., "Harmonics in Multiple Converter Systems: A Generalized Approach," *IEE Proc-B*, Vol.127, 1980, pp. 96-106.

[11] Jouanne, V., and Banerjee, B., "Assessment of Voltage Unbalance," *IEEE Trans. on Power Delivery*, Vol. 16, 2001, pp. 782-790.

[12] Enjeti, P.N., and Ziogas, P.D., "Analysis of A Static Power Converter under Unbalance: A Novel Approach," *IEEE Trans. on Industrial Electronics*, Vol.37, 1990, pp. 91-93.

[13] Hu, L., "Sequence Impedance and Equivalent Circuit of A Converter System," *IEE Proceedings - Electrical Power Applications*, Vol.144, 1997, pp. 409-414.

[14] Ngandui, E., Olivier, G., April, G.E., and Guimaraes, C.A.M., "DC Harmonic Distortion Minimization of Thyristor Converters under Unbalanced Voltage Supply using Asymmetrical Firing Angle," IEEE *Trans on Power Electronics*, Vol.12, 1997, pp. 332-342.

[15] Manjure, D.P., and Makram, E.B., "Impact of Unbalance on Power System Harmonics," *Proc. of Tenth Int. Conf. on Harmonics and Quality of Power* 2002, pp. 328-333.

[16] Lee, C.Y., "Effects of Unbalanced Voltage on the Operation Performance of A Three-Phase Induction Motor," *IEEE Trans. Energy Conversion*, 1999, Vol. 14, 202-208.

[17] Grady, W. M., Samotyj, M. J., and Noyola, A. H., "Survey of Active Power Line Conditioning Methodologies," *IEEE Trans. on Power Delivery*, Vol. 5, No. 3, July 1990, pp. 1536-1542.

[18] Singh, B., Al-Haddad K., and Chandra, A. "A Review of Active Filters for Power Quality Improvement," *IEEE Trans. on Industrial Electronics*, Vol. 46, No. 5, Oct.1999, pp. 960-971.

[19] Akagi, H., "New Trends in Active Filters for Power Conditioning," *IEEE Trans. on Industry Applications*, Vol. 32, No. 6, Nov. /Dec. 1996, pp. 1312-1322.

[20] Peng F.Z., "Harmonic Sources and Filtering Approaches," *IEEE Industry Application Magazine*, Vol. 7, No.4, July /Aug. 2001, pp. 18-25.

[21] Green, T.C., and Marks, J.H., "Control Techniques for Active Power Filters," *IEE Proc.-Electr. Power Appl.*, Vol. 152, No.2, March 2005, pp. 369-381.

[22] Anis Ibrahim, W.R., and Morcos, M.M., "Artificial Intelligence and Advanced Mathematical Tools for Power Quality Applications: A Survey," *IEEE Trans. on Power Delivery*, Vol. 17, No. 2, April 2002, pp. 668-673.

[23] Moravej, Z., Vishwakarma, D. N., and Singh S. P., "ANN-Based Protection Scheme for Power Transformer," Electric Machines and Power Systems, Vol. 28, No. 9, Sep. 2000, pp. 875-884.

[24] Bose, B.K., "Expert System, Fuzzy Logic, and Neural Network Applications in Power Electronics and Motion Control," *Proc. IEEE PEMC'94*, 1994, pp. 1303-1323.

[25] Liao, Y., and Lee, J.B., "A Fuzzy Expert System for Classifying Power Quality Disturbances," *Electric Power and Energy Systems*, Vol. 26, No. 3, March, 2004, pp. 199-205.

[26] Zadeh L. A., "Fuzzy sets", *Information and Control*, Vol.8, 1965, pp. 38-53.

[27] Momoh, J.A., Ma, X.W. and Tomsovic, K., "Overview and Literature Survey of Fuzzy Set Theory in Power Systems" *IEEE Trans. on Power Systems*, Vol.10, No.3, Aug.1995, pp. 1676-1690.

[28] "Recommended Practices and Requirements for Harmonic Control in Electric Power Systems," IEEE Standard 519-1992, New York, 1993.

[29] Fourier, J. B. J., *Theorie Analytique De la Chaleur*, Paris.

[30] Owen, E. L., "A History of Harmonics in Power Systems," *IEEE Industry Applications Magazine*, Jan. /Feb. 1998, pp. 6-12.

[31] Emanuel, A. E., "Harmonics in Early Years of Electrical Engineering: A Brief Review of Events, People and Documents," in *Proc. IEEE ICHQP*, October 2000, pp. 1-7.

[32] Houston, E. J., and Kennelly, A. E., "The Harmonics of Electric Currents," *Electrical World*, June 2, 1894, pp. 735-741.

[33] Adams, C. A., "Fractional Pitch Winding for Induction Motor," *AIEE Trans.*, Vol. 26, 1907, pp. 1485-1492.

[34] Lincoln, P. M., "Choice of Frequency for Very Long Lines," *AIEE Trans.*, Vol. 22, 1903, pp. 373-384.

[35] Duddell, J. W., "Pressure Rises," *IEE Journal*, Vol. 52, 1913, pp. 1-16.

[36] Lincoln, P. M., "Waveform Distortion and Their Effects on Electrical Apparatus," *AIEE Trans.*, Feb. 1913 pp. 765-774.

[37] Rissik, H., *The Mercury Arc Current Converter*, Pitman, London, 1935.

[38] Read, J. C., "The Calculation of Rectifier and Inverter Performance Characteristics," *IEE Journal*, Vol. 92, Pt. 2, 1945, pp. 495-509.

[39] Kimbark, E. W., *Direct Current Transmission*, John Wiley & Sons, New York, 1971.

[40] "Bibliography of Power System Harmonics, Part I and II," *IEEE Papers* 84 *WM*214-3 and 84*WM*215-0, presented at the *Winter Power Meeting*, Dallas, Jan. 1984.

[41] Steinmetz, C. P., *Theory and Calculation of Alternating Current Phenomena*, McGraw-Hill Book Co. Inc., New York, 1916.

[42] Grady, W. M., and Santoso, S., "Understanding Power System Harmonics', *IEEE Power Engineering Review*, Vol. 21, No. 11, Nov. 2001, pp. 8-11.

[43] "Limits of Harmonic Current Emissions," *International Electrotechnical Commission Standard IEC* 1000-3-2, March 1996.

[44] Chu, R. F., and Burns, J. J., "Impact of Cycloconverter Harmonics," *IEEE Trans. Ind. Appl.*, Vol. 25, No. 3, May /June 1989, pp. 427-435.

[45] Dugan, R. C., "Simulation of Arc Furnace Power Systems', *IEEE Trans. Ind. Appl.*, Vol. 16, No. 6, Nov. /Dec. 1980, pp. 813-818.

[46] Delaney, E. J., and Morrison, R. E., "The Calculation of Harmonic and Interharmonic Distortion in Current Source Converter Systems', in *Proc. International conference on Harmonics in Power Systems*, *ICHPS V*, Sept. 22-25, 1992, pp. 251-255.

[47] Dugan, R. C., and Conrad, L. E., "Impact of Induction Furnace Interharmonics on Distribution Systems," in *Proc.* 1999 *IEEE Transmission and Distribution Conference*, Vol. 2, April 11-16, 1999, pp. 791-796,.

[48] Sharaf, A. M., and Abu-Azab, S. I. "Power Quality Enhancement of Time Dependent Interharmonic Loads," in *Proc. Ninth International Conference on Harmonics and Quality of Power*, Vol. 1, pp. 46-54, Oct. 1-4, 2000.

[49] Zhezhelenko, I., and Sayenko, Y., "Analysis Methods of Interharmonics Investigations in Power Supply Systems," in *Proc. Ninth International Conference on Harmonics and Quality of Power*, Vol. 1, Oct. 1-4, 2000, pp. 61-63.

[50] Beites, L. F., Mayordomo, J. G., Hernandez, A. and Asensi, R. "Harmonics, Interharmonics and Unbalances of Arc Furnaces: A New Frequency Domain Approach," *IEEE Trans. Power Delivery*, Vol. 16, No. 4, Oct. 2001, pp. 661-668.

[51] Barros, J. P. E., Pigazo, A., and Diego, R. I., "Simultaneous Measurement of Harmonics, Interharmonics and Flicker In A Power System for Power Quality Analysis', in *Proc. Fifth International Conference on Power System Management and Control*, *Conf. Publ.* No. 488, 17-19 April, 2002, pp. 100-105.

[52] Keaochantranond, T., and Boonseng, C., "Harmonics and Interharmonic Estimation using Wavelet Transform', in *Proc. IEEE /PES Transmission and Distribution Conference and Exhibition* 2002, Asia Pacific, Vol. 2, Oct. 6-10, 2002, pp. 775-779.

[53] Testa, A., Gallo, D., and Langella, R., "Interharmonic Measurements in IEC Standard Framework," in *Proc. IEEE Power Engineering Society Summer Meeting*, Vol. 2, July 21-25, 2002, pp. 935-940.

[54] Rosa, F. De, Langella, R., Solazzo, A., and Testa, A., "On the Interharmonic Components Generated by Adjustable Speed Drives," in *Proc.* 10th *International Conference on Harmonics and Quality of Power*, Vol. 1, October 6-9, 2002, pp. 183-188.

[55] Testa, A., "Issues Related to Interharmonics," in *Proc. IEEE Power Engineering Society General Meeting*, Vol. 2, July 13-17, 2003, pp. 1203-1208.

[56] Li, C., Xu, W. and Tayjasanant, "Interharmonics: Basic Concepts and Techniques for their Detection and Measurement," *Electric Power Systems Research*, Vol. 66, No. 1, July 2003, pp. 39-48.

[57] Hume, D. J., Wood, A. R., and Osauskas, C. M., "Frequency-domain Modeling of Interharmonics in HVDC Systems', *IEE Proc. Generation, Transmission and Distribution*, Vol. 150, No. 1, pp. 41-48, Jan. 2003.

[58] "IEC Standard Draft 61000-4-30: Power Quality Measurement Methods," Ed. 1999.

[59] "IEC Standard Draft 61000-4-7: General Guide on Harmonics and Interharmonic Measurements for Power Supply Systems and Equipment Connected Thereto," Ed. 2000.

[60] Wakileh, G. J., Power *System Harmonics: Fundamentals, Analysis, and Filter Design*, Spring Verlag, October 2001.

[61] Cristaldi, L., and Ferreso, A., "A Digital Method for the Identification of the Source of Distortion in Electric Power Systems," *IEEE Trans. Instrum. Meas.*, Vol. 44, February 1994, pp. 14-18.

[62] T. A. Timothy, A. George, and D. D. Bones, "Harmonic power flow determination using the fast Fourier transform," *IEEE Trans. Power Delivery*, Vol. 6, April 1991, pp. 530-535.

[63] Tanaka, T., and Akagi, H. "A New Method of Harmonic Power Detection based on the Instantaneous Active Power in Three-Phase Circuits," *IEEE Trans. Power Delivery*, Vol. 10, Oct. 1995, pp. 1737-1742.

[64] Tsukamoto, M., Kouda, I., Natsuda, Y., Minova, Y., and Nishimura, S., "Advanced Method to Identify Harmonic Characteristic between Utility Grid and Harmonic Current Sources," in *Proc. 8th Int. Conf. Harmonics Quality Power*, Athens, Greece, Oct. 1998, pp. 419-425.

[65] DeOliveira, A., DeOliveira, J. C., Resende, J. W., and Misskulin, M. S., "Practical Approaches for AC System Harmonic Impedance Measurements," *IEEE Trans. Power Delivery*, Vol. 6, Oct. 1991, pp. 1721-1726.

[66] Yang, H., Pirotte, P., and Robert, A., "Assessing the Harmonic Emission Level from One Particular Customer," in *Proc. 3rd Int. Conf. Power Quality: End Use Application Perspectives*, The Netherlands, 1994, B-2.08.

[67] Thunberg, and L. Soder, "A Norton Approach to Distribution Network Modeling for Harmonic Studies," *IEEE Trans. Power Delivery*, Vol. 14, Jan. 1999, pp. 272-277.

[68] Xu, W., and Liu, Y., "A Method for Determining Customer and Utility Harmonic Contributions at Point of Common Coupling," *IEEE Trans. Power Delivery*, Vol. 15, April 2000, pp. 804-811.

[69] Chen, C., Liu, X., Koval, D., Xu, W., and Tayjasanant, T., "Critical Impedance Method – A New Detecting Harmonic Sources Method in Distribution Systems," *IEEE Trans. Power Delivery*, Vol. 19, pp. 288-292, Jan. 2004.

[70] Li, C., Xu, W., and Tayjasant, T., "A Critical Impedance-based Method for Identifying Harmonic Sources," *IEEE Trans. Power Delivery*, Vol. 19, April 2004, pp. 671-678.

[71] Heydt, G. T., "Identification of Harmonic Sources by A State Estimation Technique," *IEEE Trans. Power Delivery*, Vol. 4, Jan. 1989, pp. 569-576.

[72] Xia, D. and Heydt, G., "Harmonic Power Flow Studies Part I – Formulation and Solution," *IEEE Trans. Power Apparatus and Systems*, Vol. 101, June 1982, pp. 1257-1265.

[73] Xia, D., and Heydt, G., "Harmonic Power Flow Studies Part II – Implementation and Practical Application," *IEEE Trans. Power Apparatus and Systems*, Vol. 101, June 1982, pp. 1266-1270.

[74] Gunthur, E., and Mc Granaghan, M., "A PC-based Simulation Program for Power System Harmonic Analysis," in *Proc. Second Int. Conf. Harmonics in Power Systems*, Manitoba HVDC Research Centre, Winnipeg, MB, pp. 175-183.

[75] Mahmoud, A., and Shultz, R., "A Method for Analysis of Harmonic Distribution in AC Power Systems," *IEEE Trans. Power Apparatus and Systems*, Vol. 101, April 1982, pp. 1815-1824.

[76] Kaprielian, S. R., Emanuel, A. E., Dwyer, R. V., and Mehta, H., "Predicting Voltage Distortion in a System with Multiple Random Harmonic Sources," *IEEE Trans. Power Delivery*, Vol. 9, July 1994, pp. 1632-1638.

[77] Xu, W., Liu, X., and Liu, Y., "An Investigation on the Validity of Power-direction Method for harmonic Source Determination," *IEEE Trans. Power Delivery*, Vol. 18, Jan. 2003, pp. 214-219.

[78] Ram, B. S., Forrest, J. A. C., and Swift, G. W., "Effects of Harmonics on Converter Transformer Load Losses," *IEEE Trans. Power Delivery*, Vol. 3, July 1988, pp. 1059-1066.

[79] IEEE Task Force on Effects of Harmonics on Equipment, "Effects of Harmonics on Equipment," *IEEE Trans. Power Delivery*, Vol. 8, April 1993, pp. 681-688.

[80] Massey, G. W., "Estimation Methods for Power System Harmonic Effects on Power Distribution Transformer," *IEEE Trans. Ind. Appl.*, Vol. 30, March /April 1994, pp. 485-489.

[81] Deliaiba, A. C., De-Oliveira, J. C., Vilaca, A. L. A., and Cardoso, J. R., "The Effect of Harmonics on Power Transformers Loss of Life," in *Proc.* 38 *Midwest Symposium on Circuits and Systems*, Vol. 2, Aug. 13-16, 1995, pp. 933-936.

[82] Pinato, P., and Zaninelli, D., "Harmonic Disturbances in Electric Traction System Overload Lines," in *Proc. 10th Int. Conf. Harmonics and Quality of Power*, 2002, Vol. 2, Oct. 6-9, 2002, pp. 748-753.

[83] Duarte, L. H. S., and Alves, M. F., "The Degradation of Power Capacitors under the Influence of Harmonics," in *Proc. 10th Int. Conf. Harmonics and Quality of Power*, 2002, Vol. 1, Oct. 6-9, 2002, pp. 334-339.

[84] Mahesh, G., Ganesan, R., and Das, S. K., "Effects of Power Harmonics and Its Control Techniques," in *Proc. Int. Conf. Electromagnetic Interference and Compatibilty*'99, Dec. 6-8, 1999, pp. 400-405.

[85] Watson, N. R., and Arrillaga, J. "Harmonics in Large Systems," *Electric Power Systems Research*, Vol. 66, July 2003, pp. 15-29.

[86] Li, J. C., and Wu, Y. P., "FFT Algorithms for the Harmonic Analysis of the Three-Phase Transformer Banks with Magnetic Saturation," *IEEE Trans. Power Delivery*, Vol. 6, Jan. 1991, pp. 158-165.

[87] Xu, W., Marti, J. R., and Dommel, H. W., "Harmonic Analysis of Systems with Static Compensators," *IEEE Trans. Power Systems*, Vol. 6, Feb. 1991, pp. 183-190.

[88] Xu, W., Marti, J. R., and Dommel, H. W., "A multi-phase harmonic load flow solution technique," *IEEE Trans. Power Systems*, Vol. 6, Feb. 1991, pp. 174-182.

[89] Arrillaga, J., and Callaghan, "Three-phase AC-DC Load and Harmonic Flows," *IEEE Trans. Power Delivery*, Vol. 6, Jan. 1991, pp. 238-244.

[90] Valcarcel, M., and Mayordomo, J. G., "Harmonic Power Flow for Unbalanced System," *IEEE Trans. Power Delivery*, Vol. 8, Oct. 1993, pp. 2052-2059.

[91] Lombard, X., Mahsevedjoan, J., Lefebvre, S., and Kieny, C., "Implementation of A New Harmonic Initialization Method in the EMTP," *IEEE Trans. Power Delivery*, Vol. 10, July 1995, pp. 1343-1352.

[92] Murere, G., Lefebvre, S., and Do, X. D., "A Generalized Harmonic Balance Method for EMTP Initialization," *IEEE Trans. Power Delivery*, Vol. 10, July 1995, pp. 1353-1359.

[93] Arrillaga, J., Medina, A., Lisboa, M. L. V., Cavia, M. A., and Sanchez, P., "The Harmonic Domain: A Frame of Reference for Power System Harmonic Analysis," *IEEE Trans. Power Systems*, Vol. 10, Feb. 1995, pp. 433-440.

[94] Vittek, J., and Najjar, M. Y., "Common Methodology for Steady-State Harmonic Analysis of Inverters," *IEEE Trans. Power Delivery*, Vol. 10, July 1995, pp. 1628-1634.

[95] Katic, V. A., Knezevic, J. M., and Graovac, D., "Application-oriented comparison of the Methods for AC /DC Converter Harmonic Analysis," *IEEE Trans. Ind.. Electronics*, Vol. 50, Dec.2003, pp.1100-1108.

[96] De Saa, M. A. L., and Garcia, U., "Three-phase Harmonic Load Flow in Frequency and Time Domain," *IEE Proc. Elect. Power Appl.*, Vol. 150, May 2003, pp. 295-300.

[97] Lordache, M., Mendes, E., Marchand, C., Belin, S., and Mickiewicz, V., "Harmonic Analysis Method for Traction Drives EMI Studies," *IEE Proc. Elect. Power Appl.*, Vol. 150, July 2003, pp. 431-438.

[98] Herraiz, S., Sainz, L., and Clua, J., "Review of Harmonic Load Flow Formulations," *IEEE Trans. Power Delivery*, Vol. 18, July 2003, pp. 1079-1087.

[99] Alonso, M. A. P., and Donsion, M. P., "An Improved Time Domain Arc Furnace Model for Harmonic Analysis," *IEEE Trans. Power Delivery*, Vol. 19, Jan. 2004, pp. 367-373.

[100] Bradley, D. A., "Measurement of Power System Harmonics," *IEE Colloquium on Electronics in Power Systems Measurement*, April 18, 1988, pp. 1/1-4/4.

[101] Bishop, M. T., Gilker, C., and Mendis, S. R., "PC-Controlled Hand-held Meter Measures Power System Harmonics," *IEEE Trans. Computer Applications in Power*, Vol. 4, Oct. 1991, pp. 17-21.

[102] Andrews, D., Bishop, M. T., and Witte, J. F., "Harmonic Measurements, Analysis, and Power Factor Correction in A Modern Steel Manufacturing Facility," *IEEE Trans. Ind. Applications*, Vol. 32, May /June 1996, pp. 617-624.

[103] Perkins, B. K., and Iravani, M. R., "Novel Calculation of HVDC Converter Harmonics by Linearization in the Time-Domain," *IEEE Trans. Power Delivery*, Vol. 12, April 1997, pp. 867-873.

[104] M. Nagpal, W. Xu, and J. Swada, "Harmonic Impedance Measurement using Three-Phase Transients," *IEEE Trans. Power Delivery*, Vol. 13, Jan. 1988, pp. 272-277.

[105] Driesen, J., Craenenbroeck, T. V., and Dommelen, D. V., "The Registration of Harmonic Power by Analog and Digital Power Meters," *IEEE Trans. Instr. and Meas.*, Vol. 47, Feb. 1998, pp. 195-198.

[106] DeLorenzi, A., Bettini, P., and Zanotto, L., "Harmonic Impedance Measurements and Calculations in the EHV Transmission Network," in *Proc. 10th Int. Conf. harmonics and Quality of Power*, Vol. 1, October 6-9, 2002, pp. 162-168.

[107] Eren, L., and Devaney, M. J., "Calculation of Power System Harmonics via Wavelet Packet Decomposition in Real Time Metering," in *Proc. 19th IEEE Conf. Instrumentation and Measurement Technology, IMTC*'2002, Vol. 2, May 21-23, 2002, pp. 1643-1647.

[108] Xiao, Y., Bin, H., and Chunnian, D., "Problems of Voltage Transducer in Harmonic Measurement," in *Proc. 10th Int. Conf. Harmonics and Quality of Power*, 2002, Vol. 1, Oct. 6-9, 2002, pp. 33-37.

[109] "IEC 61000-3-6, Electromagnetic Compatibility (EMC) Part 3: Limits - Section 6: Assessment of Emission Limits for Distorting Loads in MV and HV Power Systems - Basic EMC Publication. International Electrotechnical Commission," 1996.

[110] Arrillaga, J., and Watson, N. R. *Power System Harmonics*, Second Edition, John Wiley, London, October 2003.

[111] "IEC Standard 61000-2-2: Electromagnetic Compatibility (EMC), Part 2-2, Environment - Compatibility Levels for Low-Frequency Conducted Disturbances and Signaling in Public Low-Voltage Power Supply Systems."

[112] "IEC Standard 61000-2-4: Electromagnetic Compatibility (EMC), Part 2-4: Compatibility Levels in Industrial Plants for Low-Frequency Conducted Disturbances."

[113] Domijan Jr., A., and Embriz-Santander, E., "A Summary and Evaluation of Recent Developments on Harmonic Mitigation Techniques Useful to Adjustable Speed Drives," *IEEE Trans. Energy Conversion*, Vol. 7, March 1992, pp. 64-71.

[114] Degeneff, R. C., Ihara, S., and Lindh, C. B., *AC Filter Design for HVDC Converter Stations*, Tutorial Course, 84 EHO221-2-PWR, IEEE, New York, 1984.

[115] Arrillaga, J., *High Voltage Direct Current Transmission*, Peter Peregrinus Ltd., London, 1983.

[116] Padiyar, K. R., *HVDC Power Transmision Systems: Technology and System Interactions*, Wiley Eastern Limited, New Delhi, 1990.

[117] Phipps, J. K., "A Transfer Function Approach to Harmonic Filter Design," *IEEE Industry Appl. Magazine*, March 1997, pp. 68-82.

[118] Lin, K-P., Lin, M-H., and Lin, T-P., "An Advanced Computer Code for Single Tuned Harmonic Filter Design," *IEEE Trans. Industry Appl.*, Vol. 34, 1998, pp. 640-648.

[119] McGranaghan, M. F., and Mueller, D. R., "Designing Harmonic Filters for Adjustable-Speed Drives to Comply with IEEE-519 Harmonic Limits," *IEEE Trans. Industry Appl.*, Vol. 35, 1999, pp. 312-318.

[120] A. R. Prasad, P. D. Ziogas, and S. Manias, "An Active Power Factor Correction Technique for Three-Phase Diode Rectifiers," *IEEE Trans. Power Electronics*, Vol. 6, Jan. 1991, pp. 83-92.

[121] Massoud, A. M., Finney, S. J., and Williams, B. W., "Practical Issues of Three-Phase, Three-Wire, Voltage Source Inverter–Based Shunt Active Power Filters," in *Proc. 11th Int. Conf. on Harmonics and Quality of Power*, 2004, pp. 436-441.

[122] Duke, R. M., and Round, S. D., "The Steady State Performance of A Controlled Current Active Power Filter," *IEEE Trans. Power Electronics*, Vol. 8, April 1993, pp. 140-146.

[123] Chatterjee, K., Fernandes, B. G., and Dubey, G. K., "An Instantaneous Reactive Volt-Ampere Compensator and Harmonic Suppressor System," *IEEE Trans. Power Electronics*, vol14, March 1999, pp. 381-392.

[124] Huang, S-J., and Jinn-Chang, W., "A Control Algorithm for Three-phase Three Wired Active Power Filter under non-ideal Mains Voltages," *IEEE Trans. Power Electronics*, Vol. 14, July 1999, pp. 753-760.

[125] Chiang, S. J., and Chang, J. M., "Design and Implementation of Parallelable Active Power Filter," in *Proc. 30th Annual IEEE Power Electronics Specialists Conference*, (*PESC 99*), Vol. 1, June 27- July 1, 1999, pp. 406-411.

[126] Singh, G. K., Singh, A. K., and Mitra,R. "A Simple Fuzzy Logic Based Robust Active Power Filter for Harmonics Minimization Under Random Load Variation', *Electric Power Systems Research*, (in press).

[127] El-Habrouk, M., Darwish, M. K., and Mehta, P., "Active Power Filters: A Review," *IEE Proc. Electr. Power Appl.*, Vol. 147, September 2000, pp. 403-413.

[128] Chen, D., and Xie, S., "Review of the Control Strategies Applied to Active Power Filters," in *Proc. IEEE Int. Conf. on Electric Utility Deregulation, Restructuring and Power Technologies* (*DRPT-2004*), April 2004, pp. 666-670.

[129] Sasaki, H., and Machida, T., "A New Method to Eliminate AC Harmonic Currents by Magnetic Compensation-Consideration on Basic Design," *IEEE Trans. Power Appl. Syst.*, Vol. 90, 1971, pp. 2009-2019.

[130] Mansoor, A., Grady, W. M., Chowdury, A. H., and Samotyj, M. J. "An Investigation of Harmonics Attenuation and Diversity Among Distributed Single-Phase Power Electronic Loads," *IEEE Trans. Power Delivery*, Vol. 10, Jan. 1995, pp. 467–473.

[131] Koval, D. O., & Carter, C., "Power Quality Characteristics of Computer Loads" IEEE Transactions on Industry Applications, Vol.33, No. 3 , May-June 1997, pp. 613-621.

[132] Moore, P.J., and Portugues, I.E., "The Influence of Personal Computer Processing Modes on Line Current Harmonics," *IEEE Transactions on Power Delivery*, Vol.18, No. 4, Oct. 2003, pp. 1363– 1368.

[133] Grady, W.M., Mansoor, A., Fuchs, E.F., Verde, P., and Doyle, M., "Estimating the Net Harmonic Currents produced by Selected Distributed Single-Phase Loads: Computers, Televisions, and Incandescent Light Dimmers," *IEEE Power Engineering Society Winter Meeting*, 2002, Vol.2, Jan. 27-31, 2002, pp. 1090-1094.

[134] Wang, Y. J., Pierrat, L., and Feuillet, R., "An Analytical Method for Predicting Current Harmonics Produced by An AC/DC Converter Under Unbalanced Supply Voltage," European Transactions on Electrical Power Engineering, Vol. 2, 1992, pp. 237-244.

[135] Jouanne, A. V., and Banerjee, B. B., "Voltage Unbalance: Power Quality Issues, Related Standards and Mitigation Techniques," Electric Power Research Institute, Palo Alto, CA, EPRI Final Rep., May 2000.

[136] Woll, R. F., "Effect of Unbalanced Voltage on the Operation of Polyphase Induction Motors," *IEEE Trans. Industry Applications*, Vol. IA-11, No. 1, pp. 382, Jan./Feb. 1975.

[137] Paulilo, G., and Abreu, J.P.G., "Power Converters under Voltage Imbalance A Novel Solution," *IEEE Porto Power Tech. Conference (PPT-2001)*, Sept. 10-13, 2001, Porto, Portugal.

[138] Lee, C-Y, Chen, B-K, Lee, W-J, and Hsu, Y-F, "Effects of Various Unbalanced Voltages on the Operation Performance of an Induction Motor under the Same Voltage Unbalance Factor Condition," *Electric Power Systems Research*, Vol. 47, 1998, pp. 153–163.

[139] Pillay, P. and Manyage, M., "Definitions of Voltage Unbalance," *IEEE Power Eng. Review Mag.*, Vol. 5, May 2001, pp. 50-51.

[140] Bollen, M.H.J., "Definitions of voltage unbalance," *IEEE Power Eng. Review Mag.*, Vol. 22, No. 11, Nov. 2002, pp. 49-50.

[141] Kim, J-G, Lee, E-W, Lee, D-J, and Lee, J-H, "Comparison of Voltage Unbalance Factor by Line and Phase Voltage," *Proceedings of the Eighth Int. Conf. on Electrical Machines and Systems (ICEMS 2005)*, Sept. 27-29, 2005, Vol. 3, pp.1998-2001.

[142] CIGRE, "A New Simple and Effective Approximate Formulation for the Determination of Three-Phase Unbalances by Voltmeter Method," Belgique, CIGRE, 1986.

[143] Motors and Generators, ANSI7NEMA Standard MG1-1993.

[144] IEEE Standard Test Procedure for Polyphase Induction Motors and Generators, IEEE Standard 112, 1991.

[145] IEEE Standard Dictionary of Electrical and Electronics Terms, IEEE Std. 100-1996.

[146] IEC Standard 61000-4-27: Testing and Measurement Techniques – Unbalance, Immunity Test, August 2000.

[147] Ghijselen, J. A. L., and Van den Bossche, A. P. M., "Exact Voltage Unbalance Assessment without Phase Measurements," *IEEE Trans. on Power Systems*, Vol. 20, No. 1, February 2005, pp. 519-520.

[148] Jeong, S-G, "Representing Line Voltage Unbalance" *Proc. IEEE 37th IAS Annual Industry Applications Conference*, 2002, pp. 1724-1732.

[149] Faiz, J., Ebrahimpour, H., and Pillay, P., "Influence of Unbalanced Voltage on the Steady-State Performance of a Three-Phase Squirrel-Cage Induction Motor," *IEEE Trans. Energy Conversion*, Vol. 19, No. 4, December 2004, pp. 657- 662.

[150] Broadwater, R.P., Khan, A. H., Shaalan, H.E., and Lee, R. E., " Time Varying Load Analysis to Reduce Distribution Losses Through Reconfiguration," *IEEE Trans. Power Delivery*, Vol. 8, No. 1, Jan. 1993, pp. 294-300.

[151] Rice, D. E., "Adjustable Speed Drive and Power Rectifier Harmonics – Their Effect on power Systems Components" *IEEE Trans. on Industrial Application*, Vol. 22, No. 1, Jan/Feb 1986, pp. 161-177.

[152] Jeong, S.G., and Ju-Yeop Choi, J.Y., "Line Current Characteristics of Three Phase Uncontrolled Rectifiers under Line Voltage Unbalance Condition," *IEEE Trans. on Power Electronics*, Vol. 17, No. 6, November 2002, pp. 935-945.

[153] Dell'Aquila, Marinelli, Monopoli and Zanchetta, "New Power Quality Assessment criteria for Supply Systems under Unbalanced and Nonsinusoidal Conditions", *IEEE Trans. Power Delivery*, Vol. 19, No. 3, July 2004, pp. 1284-1290.

[154] Rice, D. E., "A Detailed Analysis of Six-Pulse Converter Harmonic Currents," *IEEE Trans. on Industry Applications*, Vol. 30, No. 2, March /April 1994, pp. 294-304.

[155] Taleb, M., and Ortmeyer, T.H., "Examination of the Current Examination Technique," IEEE Trans. on Power Delivery, Vol. 7, No. 1, January 1992, pp. 442-448.

[156] Manjure, D.P., and Makram, E.B., "Effect of Nonlinear Loads on Power Systems and on Other Customer Loads," Proc. of IEEE LESCOPE, June 20-22, 1999, Halifax, Nova-Scotia, Canada, pp. 165-169.

[157] Subjek, J. S., and Mcquilkin, J. S., "Harmonics-Causes, Effects, Measurements and Analysis," IEEE Trans. Ind. Appl., Vol. 26, No. 6, Nov. /Dec.1990, pp. 1034-1041.

[158] Dell'Aquila, A., Delvino, G., Liserre, M., and Zanchetta, P., "A New Fuzzy Logic Strategy for Active Power Filter," in Proc. Eighth Int. Conf. on Power Electronics and Variable Speed Drives, 2000,(IEE Conf. Publ. No. 475), Sept. 18-19, 2000, pp. 392-397.

[159] Shaosheng, F. and Yaonan, W. "Fuzzy Model Predictive Control for Active Power Filter," in *Proc. IEEE Int. Conf. on Electric Utility Deregulation, Restructuring and Power Technologies, 2004 (DRPT 2004)*. Vol. 1, April 5-8, 2004, pp. 295-300.

[160] Hamadi, A., Al-Haddad, K., Rahmani, S., and Kanaan, H., "Comparison of Fuzzy Logic and Proportional Integral Controller of Voltage Source Active Filter Compensating Current Harmonics and Power Factor," in *Proc. IEEE Int. Conf. on Industrial Technology, 2004 (IEEE ICIT '04)*, Vol. 2, Dec. 8-10, 2004, pp. 645-650.

[161] Farrokhi, M., Jamali, S., and Mousavi, S. A., "Fuzzy Logic based Indirect Current Control of the Shunt Active Power Filter," in *Proc. 39th Int. Universities Power Engineering Conference (UPEC 2004)*, Vol. 1, Sept. 6-8, 2004, pp. 489–493.

[162] Elmitwally, A., Kandil, M. S., and Elkateb, M. "A Fuzzy-Controlled Versatile System for Harmonics, Unbalance and Voltage Sag Compensation," *IEEE Power Engineering Society Summer Meeting, 2000*, Vol. 3, July 16-20, 2000, pp. 1439-1444.

[163] Gyugyi, L., and Strycula, E. C., "Active AC Power Filters," *IEEE Ind. Appl. Society Annual Meeting*, Atlanta, Georgia, USA, 1976, pp. 529-535.

[164] Peng, F. Z., Akagi, H., and Nabae, A., "A New Approach to Harmonic Compensation in Power Systems – A Combined System of Shunt Passive and Series Active Filters" *IEEE Trans. Ind. Appl.*, Vol. 26, No. 6, Nov. /Dec. 1990, pp. 983-989.

[165] Singh, B., Chandra, A., and Al-Haddad, K., "Computer Aided Modeling and Simulation of Active Power Filters," Electric Machines and Power Systems, Vol. 27, No. 11, 1999 pp. 1227-1241.

[166] Mohan, N., Undeland, T., and Robbins, W. P., *Power Electronics – Converters, Applications and Design*, John Wiley & Sons, 2003

[167] Bhattacharya, S., and Divan, D. M., "Active Filter Solutions for Utility Interface of Industrial Loads," in *Proc. IEEE Int. Conf. on Power Electronics, Drives and Energy Systems for Industrial Growth, PEDES-1996*, Vol. 2, January 8-11, 1996. pp. 1078-1084.

[168] Tzou, Y. and Lin, S., "Fuzzy-Tuning Current-Vector Control of A Three-Phase PWM Inverter for High-Performance AC Drives," *IEEE Trans. on Industrial Electronics*, Vol. 45, No. 5, October 1998, pp. 782-791.

[169] Tyagi, B., and Srivastava, S.C., "A Fuzzy Logic based Load Frequency Controller in A Competitive Electricity Environment," IEEE Power Engineering Society General Meeting, 2003, Vol. 2, July 13-17, 2003, pp.560-565.

[170] Bingul, Z., Cook, G. E., and Strauss, A. M., "Application of Fuzzy Logic to Spatial Thermal Control in Fusion Welding," *IEEE Transactions on Industry Applications*, Vol. 36, No. 6, November/December 2000, pp. 1523-1530.

[171] Picandet, L. "Temperature Control using Fuzzy Logic," *Application Note of SGG-Thomson Microelectronics*, 1994.

[172] Chaturvedi, D.K., Satsangi P.S., and Kalra, P.K., 'Fuzzy Simulation Model of Basic Commutating Electrical Machines,' Int. Journal of Engineering Intelligent Systems, Vol. 6, No. 4, 1998, pp. 225-236.

[173] Fonseca, J., Afonso, J. L., Martins, J. S. and Couto, C., "Fuzzy Logic Speed Control of an Induction Motor," *Journal of Microprocessors and Microsystems*, 1999, pp. 523-534.

[174] So, W., Tse, C. K. and Lee, Y., "Development of a Fuzzy Logic Controller for DC /DC Converters: Design, Computer Simulation, and Experimental Evaluation," *IEEE Trans. on Power Electronics*, Vol. 11, No. 1, January 1996, pp. 24-31.

[175] Satpathy, P. K., Das, D., and Dutta Gupta, P. B., "A Novel Fuzzy Index for Steady State Voltage Stability Analysis and Identification of Critical Busbars," Electric Power Systems Research, Vol. 63, No. 2, Sept. 2002, pp. 127-140.

[176] Yen, J. and Langari, R., *Fuzzy Logic: Intelligence, Control, and Information*, Upper Saddle River, NJ: Prentice Hall, 1998.

[177] Zadeh, L.A., "Outline of A New Approach to the Analysis of Complex Systems and Decision Processes," *IEEE Trans. on Systems, Man and Cybernetics*, Vol. SMC-3, No. 1, 1973, pp. 28-44.

[178] Driankov, D., Hellendoorn, H., and Reinfrank, M., *An Introduction to Fuzzy Control*, Springer-Verlag, New York, 1996

[179] Pedrycz, W., "Why Triangular Membership Functions?," *Fuzzy Sets and Systems*, Vol. 64, 1994, pp. 21-30.

[180] Ying, H., *Fuzzy Control and Modeling: Analytical Foundations and Applications*, IEEE press, 2000.

[181] Dounis, A. I. and Manolakis, D. E., "Design of a Fuzzy System for Living Space Thermal Comfort Regulation," *Elsevier, Applied Energy*, Vol. 69, No.2, 2001, pp. 119-144.

[182] Bilgic, T., and Türksen, I. B., "Measurement of Membership Functions: Theoretical and Empirical Work" in D. Dubois and H. Prade (Eds.), Handbook of Fuzzy Sets and Systems, Vol. 1, *Fundamentals of Fuzzy Sets*, Kluwer, 1995, pp. 195–232.

[183] Juuso, E.K., "Intelligent Systems Design with Linguistic Equations," *Ninth Workshop Fuzzy Control des GMA-FA*, Dortmund, Electrotecknik, 1999, pp. 177-196.

[184] Zhao, J., and Bose, B.K., "Evaluation of Membership Functions for Fuzzy Logic Controlled Induction Motor Drive," *28th Annual Conference of the IEEE Industrial Electronics Society, 2002, IECON 02*, Vol. 1, Nov. 5-8, 2002, pp.229 – 234.

[185] Donato, J.M., and Barbieri, E., "Mathematical Representation of Fuzzy Membership Functions," *Proc. of the Twenty-Seventh Southeastern Symposium on System Theory*, March 12-14, 1995, pp. 290 – 294.

[186] Sugeno, M., *Industrial Application of Fuzzy Control*, North Holland, Amsterdam, 1985.